In loving memory of my late father,

Anyanwu Nathan

and for all he stood for.

STUDIES OF MAGNETIC ALLOYS BY DIFFUSE NEUTRON SCATTERING

Thesis submitted for the Degree of
Doctor of Philosophy in the University of London

by

JOHN CHUKWUEMEKA ODODO

Imperial College of Science and Technology
The Blackett Laboratory
Prince Consort Road
London SW7 2BZ

April 1978

ABSTRACT

Diffuse elastic unpolarized neutron scattering measurements have been used to investigate the magnetic behaviour of four transition metal alloy systems namely, weakly ferromagnetic PtCo and PtFe alloys, the NiRh system from the strongly ferromagnetic alloys (dilute concentrations of Rh in Ni), to the critical concentration regime ($\simeq$ 63% Ni), and FeNi alloys in the Invar composition range.

To aid the interpretation of the neutron data a general theory of the onset of magnetism in transition metal alloys has been proposed to account for the succession of magnetic states as the concentration of the "magnetic" component is increased. It is suggested that the dilute alloy problem should indeed be seen as that of the stabilization, rather than formation, of local moments which exist, ab initio, as a result of intra atomic Coulomb and exchange interactions and that the concept of spin fluctuations, meaningfully reinterpreted within this framework, can be used to give a consistent explanation of the magnetic behaviour of dilute (transition metal) alloys. In fact, it is shown that the Kondo divergence problem is not relevant to the dilute alloy problem (i.e. the single impurity limit) but is simply a result of the neglect of inter-impurity interactions which must become important at some finite, even if very low, temperature. We also explore how the model carries over to a pure transition metal and suggest an alternative view of the "exchange enhancement" of transition metals. The possibility of paramagnon-induced attractive electran-electron interactions is

mentioned enabling us to conclude that all transition metals are either magnetic or superconducting.

The succession of magnetic states as interimpurity interactions become important is discussed and, in particular, we argue that local environment effects play a dominant role in the transition from the spin fluctuation regime to the ferromagnetic state (i.e. giant moment alloy systems). This transition, which occurs as a function of the impurity concentration ($T \simeq 0$ K), is a proper cooperative phase transition to which Landau's theory of phase transitions can be applied in spite of the unavoidable magnetic inhomogeneity of the transition. A thermodynamic theory of this transition is fully developed and it is shown that many properties of such alloy systems, including some Invar-like characteristics, are merely the consequences of the onset of ferromagnetism and not the peculiar attributes of any model of ferromagnetism such as that of weak itinerant ferromagnetism. In fact, the latter model is obviously incompatible with the intrinsic magnetic inhomogeneity of the phase transition.

The proposed model is then used to give a clear interpretation of the onset of magnetism in PtCo and PtFe alloys. While PtCo is a typical giant moment alloy system in which ferromagnetism sets in through the coupling of magnetic clusters whose concentration is less than the nominal impurity concentration it appears that PtFe resembles AuFe in which all the impurity atoms become magnetic long before ferromagnetism is stabilized. Thus, in spite of the polarization of the Pt matrix, PtFe is strictly a spin-glass alloy.

As a function of the scattering wave vector the neutron diffraction cross-sections for the Pt alloys are very similar to those of PdCo and PdFe alloys. The cross-sections at large angles when suitably combined with the available magnetization data give moments of $2.08 \pm 0.06\,\mu_B$ and $3.1 \pm 0.2\,\mu_B$, independent of concentration, for Co and Fe respectively, which values are about the same as observed in the Pd-based alloys. The Pt moment, however, is small and concentration dependent in this limit. Hitherto the sharp forward peaks observed in the neutron cross-sections of transition metal alloys has been taken as almost incontrovertible evidence for the inhomogeneous distribution of magnetization. However, it is shown that here the forward peaks are due to the critical scattering of neutrons at the critical concentration for the onset of ferromagnetism. The observation of this critical scattering serves to confirm that the onset of ferromagnetism, as a function of concentration, is a proper phase transition. The discussion highlights the need to distinguish between the spontaneous and saturation magnetizations of weakly ferromagnetic alloys and also between the polarization range of an isolated but otherwise magnetic perturbation centre and the correlation length of two or more such magnetic centres. The present results have also forced us to question the interpretation of the previous data for PdCo and PdFe and led us to suggest that the polarization range in both Pd and Pt matrices is probably of the order of the nearest neighbour distance only.

The magnetization, resistivity and other data for NiRh have been briefly reviewed and the critical concentration obtained by an analysis of the available data. It is suggested that the system is

suitable for observing Invar characteristics in a giant moment alloy system and that in fact some existing data support this conjecture. The neutron data show that

(i) for small additions of Rh ($\lesssim$ 4% Rh) the response of the system is similar to that reported for other transition and non-transition metal solutes in Ni thus suggesting that the response may be characteristic of the Ni matrix;

(ii) in this dilute concentration limit the Rh atom has a large moment ($\bar{\mu}_{Rh} \gtrsim 3\mu_B$) which is rapidly "destroyed" as the Rh concentration increases. For sufficiently high Rh concentrations ($\gtrsim$ 10% Rh) existing polarized neutron data show that $\bar{\mu}_{Rh}(c)$ decreases rather more slowly (and linearly). This behaviour of $\bar{\mu}_{Rh}(c)$ is attributed to a large but negative Rh-Rh exchange interaction;

(iii) The <u>local</u> Ni moment is also affected by local environment effects and appears to <u>decrease steadily</u> from its value ($\simeq 0.71\mu_B$) in pure Ni to zero near c_f;

(iv) for intermediate Rh concentrations ($10 \lesssim c \lesssim$ 20% Rh) the forward scattering cross-sections are in good agreement with the bulk magnetization values of $\frac{d\bar{\mu}}{dc}$ and can be adequately discussed within the framework of a magnetic-environment model;

(v) for $c \gtrsim$ 24% Rh the forward cross-sections are consistently and significantly larger than expected from magnetization values of $\frac{d\bar{\mu}}{dc}$, a discrepancy that is probably due partly to the increasing importance of the non-linear contributions to the observed cross-sections and partly to the fact that it may become necessary to consider the <u>explicit</u> role of magnetic clusters in the neutron scattering.

It is also suggested that in the critical concentration region the magnetic clusters consist of only those Rh and Ni atoms which have twelve Ni nearest neighbours. The Ni-centred clusters are probably stable up to the Curie temperature of pure Ni (as is the case for Cu Ni) but the Rh-centred clusters break up at $\sim$ 230 K showing that $J_{Rh-Ni} \simeq 0.37\ J_{Ni-Ni}$.

Neutron measurements have also been carried out on Fe 32.3, 35, 38 and 50% Ni alloys and a Rh-doped invar alloy ($Fe_{63}Ni_{33}Rh_4$) at both 4.2 K and room temperature using three different field geometries. The values of $\bar{\mu}_{Fe}$ and $\bar{\mu}_{Ni}$ determined from the low temperature data combined with existing data for other concentrations show that while $\bar{\mu}_{Fe}$ remains approximately constant at $\simeq 2.9 \mu_B$ up to the beginning of the invar region ($\lesssim$ 38% Ni) before it starts decreasing $\bar{\mu}_{Ni}$ begins to decrease at $\sim$ 50% Ni and is almost zero at $\sim$ 32% Ni. Thus local environment effects are even more severe for Ni than for Fe.

The use of different field geometries for measuring the neutron cross-sections at room temperature shows an additional small angle scattering which is attributed to paramagnetic scattering from magnetic clusters which have rather large moments but are located in low effective molecular fields. It is argued that the apparent broadening of the critical scattering at a ferromagnetic transition temperature of an alloy is due to such paramagnetic scattering which is made possible by the existence of a distribution of molecular fields.

Finally the Invar problem has been comprehensively reviewed

and it is explained that the prominent magnetovolume effects are due to a magnetic phase transition that occurs at low Ni concentrations ($\sim$ 25% Ni) and is driven by the antiferromagnetic exchange interactions between neighbouring Fe atoms. Thus the Invar properties proposed for giant moment alloys and already observed in fcc FeNi alloys are essentially similar in origin (being due to the onset of ferromagnetism). The peculiar properties of FeNi alloys namely the occurrence of antiferromagnetic ordering at low temperatures in small volume elements in an otherwise ferromagnetic matrix, the existence of short range atomic order (Fe_3Ni and/or $FeNi_3$) and (structural) martensitic transformations for low Ni concentrations are not essential for Invar behaviour although they modify this and probably result from the antiferromagnetic Fe-Fe interactions.

-----oOo-----

CONTENTS

CHAPTER 3 THE THEORY OF THERMAL NEUTRON SCATTERING

PREFACE

Diffuse elastic scattering of neutrons is a valuable technique for investigating the microscopic distribution of magnetization in magnetic alloys and thus is particularly useful for studying the magnetic behaviour of those alloy systems for which there exists a critical concentration for the onset of ferromagnetism. We have applied this technique to study four such alloy systems - PtCo, PtFe, NiRh and fcc FeNi (in the Invar composition range).

In writing a report of this type it is traditional to start with a brief (?) review of the current state of the art and this is what we have tried to do in Chapter 1. Having done this, however, we found ourselves asking certain questions such as whether it is really necessary for all the d-electrons of a transition metal solute atom to be completely itinerant and thus disregarding the intra-atomic Coulomb and exchange correlations. In an attempt to answer such questions we introduced, in Chapter 2, a model (which at this stage is still semi-phenomenological) that we believe can consistently (and simply) explain the apparently diverse behaviour of magnetic solute atoms in various hosts (both simple and transition metal). Some of the immediate consequences of this model have been explored and we then go on to discuss the succession of magnetic states (i.e. magnetic phase diagrams), the order of the phase transitions, and the thermodynamic theory of (including the effects associated with) the onset of ferromagnetism in giant moment alloys. Existing data on such systems are then used

to confirm the applicability of the thermodynamic theory outlined with particular emphasis on the determination of the critical concentration. The theory of weak itinerant ferromagnetism is critically reviewed and, of course, we could not end the discussion in this chapter without some reference to spin glasses.

Chapter 3 gives the theory of thermal neutron diffraction with emphasis on unpolarized neutron scattering from atomically disordered magnetic transition metal alloys while Chapter 4 is an account of the various experimental methods used in the investigations.

Chapters 5, 6 and 7 deal respectively with the onset of ferromagnetism in Pt alloys, the magnetic behaviour of the NiRh alloy system and the Invar problem. Each chapter is nearly self-contained in the sense that it contains a resume of the known properties of the system under discussion, the problem(s) to be investigated, the experimental results and their analysis, a discussion of these results and finally, a summary of any important conclusions.

The number of topics dealt with in Chapter 2 has been the major contributing factor to the length of this thesis but we have no doubt whatsoever that our understanding of some aspects of the magnetism of transition metals has been enormously increased and the relevance of the topics discussed cannot be questioned. For example our approach to the Invar problem derives almost wholly from the discussion in section 2.5. In retrospect some of our arguments in this chapter could have been presented more clearly and concisely; for example although we felt certain that the usual Kondo resistance minimum was not

relevant to the single impurity problem (section 2.2(3)) it was not until section 2.5(vii) that we could clearly state a criterion for observing a resistance minimum in the spin fluctuation region. Again it was not until after the discussion of the electrical resistivity of spin glasses that we could finally give the correct definition of the effective width of the impurity virtual bound state (eq.2.338) to be substituted in the formula for the spin fluctuation temperature (eq.2.8). Such shortcomings are unavoidable in the present circumstances and we shall beg to be excused.

-----oOo-----

CHAPTER 1

A Resume of the Theory of the Magnetism of Transition Metal Alloys

1.1. Introduction

One approach to the problem of satisfactorily understanding the microscopic origin of the bulk magnetism of certain metals has been through the study of metal alloys. The usual procedure is to introduce a magnetic impurity dilutely into a non-magnetic metal matrix and then to study the magnetic properties, where observable, of the almost isolated impurity in its metallic environment. One hopes that by gradually increasing the concentration of the magnetic impurity and simultaneously monitoring the concomitant changes in the properties of the combined system one may obtain a useful insight into the vexed question of the bulk magnetism of some pure metals. While such an approach has been successful in the case of the magnetic insulators the very nature of the metallic state itself not only severely limits the types of experimental probes that may be conveniently used to study the properties of the alloys but also makes any theoretical considerations much less tractable. In the latter case it is not at all clear that one can, ab initio, separate the problem of the formation or persistence of magnetic moments on the isolated impurity sites from the equally important one of the interaction between such moments. The local moment problem adopts the view that such a separation is feasible and then proceeds to consider under what conditions such a moment may be observed to exist. Thus the local moment approach seeks an answer to

the question: how and when may an isolated impurity atom be regarded as magnetic?

It is obvious that an answer to the above question demands an operational definition of a localized moment. An impurity is regarded as possessing a localized magnetic moment if its contribution to the magnetic susceptibility of the alloy system is significantly temperature-dependent in the form of a Curie Law:

$$\chi(T) = \frac{C}{T} \qquad 1.1$$

The absence of any strongly temperature-dependent susceptibility is taken therefore to imply the absence of any localized magnetic moment. We note that equation (1.1) subsumes the existence of an assembly of non-interacting spins of magnitude S say, each of which should have (2S+1) well-defined Zeeman energy levels in a uniform magnetic field. Such an assumption is clearly simplistic even if practical. Surely in any metal or metal alloy a localized moment will interact at least with the conduction electrons and indeed experimentally a wide spectrum is observed in the behaviour of the magnetic susceptibility of metal alloy systems, ranging from the weakly temperature-dependent susceptibility through the Curie Law form to a Curie-Weiss Law of the form

$$\chi(T) = \frac{C}{T+\theta} \qquad 1.2$$

where θ may be positive and often independent (apparently) of the impurity concentration.

It would appear that apart from any direct interactions between localized moments in metals and their alloys it is the interaction of the localized moments with the conduction electrons that is primarily responsible for any peculiarities of the phenomena of superconductivity and magnetism of the transition metals. This proposition assumes, a priori, the existence of localized magnetic moments in the favoured cases but maintains that the experimental observation of such moments is necessarily complicated by the dynamics introduced by the conduction electron - local moment interaction. Befor developing this theme further it is pertinent to discuss the theories that have hitherto been used to tackle the local moment problem. Excellent and fairly extensive reviews of both the theoretical and experimental aspects of the local moment problem have been given by Kondo (1), Heeger (2), Mills (3), Wohlleben and Coles (4) and more recently by Rizzuto (5) and Grüner and Zawadowski (6). In the following discussion of the local moment problem we shall, when necessary, draw heavily from the above references.

1.2. The Concept of a Virtual Bound State (VBS)

The first attempt at investigating the local moment problem was through the introduction of the concept of the virtual bould state (VBS) by Friedel (7). He noted that sinc conduction electron bands in metals were very broad the energy levels of an impurity atom would in general lie within the conduction band. Consequently, such impurity states cannot be truly localized since there is always a finite probability of the impurity state tunnelling into the conduction band. It is because of this fact that the impurity state is called a virtual bound state i.e. a strong hybridi-

zation of the local and conduction band states. It is characterized by a finite half-energy width Δ.

The impurity state can also be described in terms of a resonant bound state constructed from the conduction band states, a real bound state being a sharp undamped resonance whereas a VBS is a damped resonance. The energy width of a VBS, Δ , is greater the larger the distance of the resonance above the "top" of the conduction band but is smaller the larger the angular momentum of the original bound state (owing to the smaller admixture). Also since the overall electrical neutrality of the system must be maintained the excess charge, Ze, of the impurity is screened by the conduction electrons but produces an effective potential from which electrons are scattered. An analysis of the electron scattering caused by this effective potential, assumed to be spherically symmetric, leads to the Friedel sum-rule

$$Z = \frac{2}{\pi} \sum_{l} (2l+1)\, \eta_l(\varepsilon_F) \qquad 1.3$$

where $\eta_l(\varepsilon_F)$ is the phase shift, measured at the Fermi level ε_F , of the l^{th} partial wave component of the conduction electron wavefunction and the factor (2l+1) allows for the orbital degeneracy of the impurity atom. Equation (1.3) results from applying the self-consistency requirement that the total charge induced below the Fermi level by the effective perturbing potential should exactly annul the excess charge due to the impurity. In its derivation an oscillatory term which causes oscillations in the host local charge density has been neglected, since most of the screening charge is localized in the neighbourhood of the impurity

The total density of states is modified by the occurrence of the VBS. In terms of the phase shifts η_l the density of states at the Fermi level is given by

$$\rho(\varepsilon_F) = \rho_0(\varepsilon_F) + \frac{2}{\pi}\sum_l (2l+1)\frac{d\eta_l}{d\varepsilon} \qquad 1.4$$

where $\rho_0(\varepsilon_F)$ is the density of states at the Fermi level in the unperturbed system.

By analogy with the well-known Breit-Wigner formula for resonance scattering we have that

$$\eta_l = \cot^{-1}\frac{(\varepsilon_r - \varepsilon)}{\Delta} \qquad 1.5$$

where ε_r is the resonance energy corresponding to a VBS with angular momentum l and width Δ. For a transition metal impurity

$$\begin{aligned} \eta_l &= \eta_l^0 \qquad ; l \neq 2 \\ &= \eta_2^0 + \cot^{-1}\frac{(\varepsilon_d - \varepsilon)}{\Delta} \qquad ; l = 2, \end{aligned} \qquad 1.6$$

where η_l^0 are the non-resonant phase shifts.

Thus the additional electronic density of states associated with the VBS is given by

$$\rho_d(\varepsilon_F) \equiv \rho(\varepsilon_F) - \rho_0(\varepsilon_F) = \frac{10}{11}\frac{\Delta}{(\varepsilon-\varepsilon_d)^2+\Delta^2} \qquad 1.7$$

In this case equation (1.3) reduces to

$$Z = \frac{10}{11}\eta_2(\varepsilon_F) \qquad 1.8$$

The most direct way of determining the resonance energy is through electrical resistivity measurements. Using the partial wave analysis outlined above the impurity residual resistivity $\Delta\rho_0$ for a concentration c of impurity atom

is given by

$$\Delta\rho_0 = \frac{4\pi c\hbar}{\nu e^2 k_F} \sum_l l \sin^2(\eta_l - \eta_{l-1}) \qquad 1.9$$

where ν is the valency of the host metal, and k_F is its Fermi wavevector. Neglecting non-resonant phase shifts and using equation (1.8) for transition metal impurities equation (1.9) reduces to

$$\Delta\rho_0 = \frac{10\pi c\hbar}{\nu e^2 k_F} \sin^2\left(\frac{\pi Z}{10}\right) \qquad 1.10$$

The above equation predicts that the residual resistivity in a given host should show a peak as one goes across the 3d series say from Ti ($Z=2$) to Mn ($Z=5$) and then decrease as the 3d - shell fills. Such a behaviour has been observed (8) in the alloys of 3d impurities in Al and Zn. The peak occurs between Cr and Mn and is due to resonance scattering of the electrons at the Fermi level of Al (or Zn) when this level crosses the broadened VBS of the impurity. However, for 3d solutes in noble metals the residual resistivity at room temperature exhibits a double-peaked structure with a minimum in the middle of the series - see figure 4 in reference (2). The existence of this minimum was attributed to the exchange splitting of the VBS. Owing to exchange (J) and particularly the Coulomb (U) interactions between electrons in the d-shell the virtual states for up-spin are not equivalent to those of down-spin. Under these conditions the spin populations are unequal and a net magnetic moment then exists, localized on the impurity site. Instead of equations (1.8) and (1.10) we now have

$$Z_\uparrow = \frac{5}{\pi}\eta_{2\uparrow}(\varepsilon_F) \quad ; \quad Z_\downarrow = \frac{5}{\pi}\eta_{2\downarrow}(\varepsilon_F) \qquad 1.11$$

$$\Delta\rho_0 = \frac{4\pi c\hbar}{\nu e^2 k_F}\left\{\sin^2\eta_{2\uparrow}(\varepsilon_F) + \sin^2\eta_{2\downarrow}(\varepsilon_F)\right\}. \qquad 1.12$$

Thus the two spin directions could be considered essentially independent but additive in their effects. In this way it was possible to correlate the variation of the residual resistivity with the magnetic behaviour. In the non-magnetic case (3d impurities in Al or Zn) the maximum in the residual resistivity occurs near the middle of the series, whereas if the exchange splitting is large (i.e. the magnetic case) then two maxima are expected - the first being due to the up-spin resonance passing through the Fermi level and the second maximum due to a similar passing-through of the down-spin resonance. However, it has since been reported (10,11) that at sufficiently low temperatures the residual resistivit actually shows a single peak as in the "non-magnetic" case of 3d impurities in Al . To explain this single peak it was assumed that for the magnetic impurities the residual resistivity contains an additional logarithmically-increasing resistivity associated with the Kondo effect (see below - section 1.7).

Schrieffer (9) has proposed an alternative explanation of the residual resistivity data. He suggests that 3d impurities in Al have very high "Kondo temperatures" and so one gets the unitarity scattering for each of the $l = 2$ partial waves giving a resistivity which is proportional to the bare impurity spin S. The residual resistivity is obtained as

$$\frac{\Delta\rho_0}{c} = \frac{2mS}{\nu e^2\hbar\rho_s(\varepsilon_F)} \qquad 1.13$$

where S is assumed to be the free ion value, m is the electron mass and $\rho_s(\epsilon_F)$ is the host matrix density of states. The above prediction satisfactorily explains the experimental data also. This is not surprising because if S is the free ion value of the impurity spin then $S \propto Z$ for $Z \leq 5$; thus in our opinion equation (1.10) is more generally applicable than equation (1.13).

More importantly we reject the argument that the single peak observed at low temperatures in the residual resistivity of 3d impurities in noble metals is associated with the Kondo effect. In fact, as we shall discuss in the next chapter, the Kondo effect strictly cannot be observed in the ideal single impurity limit. Instead we shall regard the change from a double-peaked to a single-peaked structure as showing that some of the impurities which are "magnetic" at room temperature become "non-magnetic" at sufficiently low temperatures. Since the temperature change, equivalent to an energy change of only about 0.026 ev, is very unlikely to influence the exchange splitting of the VBS it follows that the apparent transition from 'magnetic' to 'non-magnetic' behaviour must be due to some other phenomenon not considered so far, which is the dynamics of the system. We believe that in the appropriate cases the VBS may really be exchange-split <u>irrespective of the host</u> but that the experimental observation of the resulting magnetic moment depends on the nature of the host since the latter greatly influences the dynamics of the system.

1.3. <u>The Anderson Model</u>

The qualitative ideas implicit in the concept of a

VBS were put into a quantitative form by Anderson (12). The transition metal impurity is regarded as an extra localized d-orbital in an otherwise free electron gas, so that the one-electron Hamiltonian of the system includes both localized and band states as well as a mixing term which couples the two. It is this mixing interaction which broadens the localized state thereby making it a VBS. The Hamiltonian of the system is written as

$$\mathcal{H} = \mathcal{H}_s + \mathcal{H}_d + \mathcal{H}_{sd} \qquad 1.14$$

where

$$\mathcal{H}_s = \sum_{K\sigma} \epsilon_K C^+_{K\sigma} C_{K\sigma} \qquad 1.15$$

$$\mathcal{H}_d = \sum_{m\sigma} \epsilon_m C^+_{m\sigma} C_{m\sigma} + \tfrac{1}{2}(U-J) \sum_{m\neq n} C^+_{m\sigma} C_{m\sigma} C^+_{n\sigma} C_{n\sigma} + U \sum_{m,n} C^+_{m\sigma} C_{m\sigma} C^+_{n,-\sigma} C_{n,-\sigma} \qquad 1.16$$

$$\mathcal{H}_{sd} = \sum_{Km\sigma} \{ V_{Km} C^+_{K\sigma} C_{m\sigma} + V_{mK} C^+_{m\sigma} C_{K\sigma} \} \qquad 1.17$$

$\mathcal{H}_s$ and $\mathcal{H}_d$ are the Hamiltonians for the conduction electrons and the d-electrons respectively and $\mathcal{H}_{sd}$ represents the s-d mixing interaction. C, C^+ are the annihilation and creation operators with subscripts σ for spin, K for the Bloch conduction-electron states, and m,n for the localized d-electron Wannier functions. ϵ_K, ϵ_m are respectively the conduction-electron and d-electron energies. U and J are the Coulomb and exchange integrals between two electrons localized on the impurity atom and V_{mK} is the admixture matrix elemen between d-states and conduction electrons.

The above Hamiltonian is approximate to the extent that

it neglects the following interations (i) electron - electron correlations except for electrons localized on the impurity site. This omission is not serious for simple metal hosts like Al , Zn or the noble metals but is thought to be so for the so-called exchange enhanced metals (Pd and Pt). However, as explained in the next chapter, we think that the incipient magnetism of Pd and Pt can be explained along the same general lines as used for the magnetism of several alloy systems. In other words the Anderson Hamiltonian (equation (1.14) to (1.17)) is sufficient to account for the electron - electron interactions in Pd and Pt.

(ii) Spin-orbit and orbit-orbit interactions. Although the effects due to these interactions are not sufficiently well known, they are not expected to be very significant. In any case, their neglect helps to keep the Hamiltonian less forbidding.

(iii) The direct ferromagnetic **S**-d interaction. This interaction is thought to be smaller (at least for transition metal impurities) than an antiferromagnetic covalent admixture local moment - conduction electron exchange interaction that is implicitly contained in the Anderson Hamiltonian.

(iv) Crystal-field splitting of d-orbital levels. Estimates of such splittings in the simple metals have shown that they are quite small.

As conceptually simple as the Anderson Hamiltonian is yet only an approximate solution can be given because of the electron - electron interaction term. The approximation used is the Hartree - Fock (HF) or self-consistent field approximation in which the number operator $n_{m\sigma}$ is replaced by

$$n_{m\sigma} = \langle n_{m\sigma} \rangle + \{ n_{m\sigma} - \langle n_{m\sigma} \rangle \} \qquad 1.18$$

and products such as $\{n_{m\sigma} - \langle n_{m\sigma}\rangle\}\{n_{n\sigma} - \langle n_{n\sigma}\rangle\}$

are neglected. Within this approximation the d-state energy becomes

$$\epsilon_{m\sigma} = \epsilon_d + (U-J)\sum_{n\neq m}\langle n_{n\sigma}\rangle + U\sum_n \langle n_{n,-\sigma}\rangle \qquad 1.19$$

while the additional density of states arising from the VBS is given by

$$\rho_{d\sigma}(\varepsilon) = \frac{2l+1}{\pi}\,\frac{\Delta}{(\varepsilon-\varepsilon_{d\sigma})^2+\Delta^2} \qquad 1.20$$

where $(2l+1)$ is the orbital degeneracy factor. The half-width of the virtual level, Δ , is given by

$$\Delta(\varepsilon) = \pi\langle V_{sd}\rangle^2 \rho_s(\varepsilon) \qquad 1.21$$

where $\langle V_{sd}\rangle^2$ is the mean square value of the admixture matrix element.

The self-consistency condition is satisfied by requirin that

$$\langle n_{d\sigma}\rangle = \int_0^{\varepsilon_F} \rho_{d\sigma}(\varepsilon)\, d\varepsilon$$

which gives

$$\langle n_{d\sigma}\rangle = \frac{2l+1}{\pi}\cot^{-1}\left\{\frac{\varepsilon_{d\sigma}-\varepsilon_F}{\Delta(\varepsilon_F)}\right\} \qquad 1.22$$

Implicitly the HF approximation requires that an electron remain on an impurity site only for such a time that it shoul not feel the presence of another spin state. Since the occupation time of an impurity site $\sim \frac{\hbar}{\Delta}$ and the one-electron lifetime due to the Coulomb interaction $\sim \frac{\hbar}{U}$. the HF theory therefore requires that $\frac{\hbar}{\Delta} < \frac{\hbar}{U}$

i.e. $$\frac{U}{\Delta} < 1 \qquad 1.23$$

In this limit, however, the only solution of equation (1.22) is that in which $\langle n_{d\uparrow} \rangle = \langle n_{d\downarrow} \rangle$ so that the impurity is non-magnetic (but in the sense that no time-averaged magnetic moment exists)

For given values of U, J and $(\varepsilon_d - \varepsilon_F)$ the limit of validity of the HF approximation is defined by the condition

$$(U + 4J)\rho_d^{\downarrow}(\varepsilon_F) = 1 \qquad 1.24$$

where $\rho_d^{\downarrow}(\varepsilon_F)$ is the added density of states per orbital (see equation (1.20)). Equation (1.24) is clearly similar to the Stoner criterion for band ferromagnetism. The most favourable case for magnetism occurs when the VBS lies self-consistently at the Fermi level; in this case the ferromagnetic instability condition (equation (1.24)) reduces to

$$\frac{U + 4J}{\pi\Delta} = 1 \qquad 1.25$$

This, however, is slightly beyond the limit of the HF solution of the Anderson Hamiltonian and strictly should not be used to discuss the exchange splitting of the VBS.

It is trivial to show that the HF solution of the Anderson model satisfies Friedel's sum rule since from equations (1.3) and (1.6)

$$Z = \frac{5}{\pi} \sum_{\sigma} \cot^{-1} \left\{ \frac{\varepsilon_{d\sigma} - \varepsilon_F}{\Delta(\varepsilon_F)} \right\}$$

$$= \frac{5}{\pi} \sum_{\sigma} N_{\sigma} \qquad 1.26$$

where the last equality follows on using equation (1.22).

N_σ is the occupation number common to each of the virtual levels of a given spin.

1.4. The Wolff-Clogston Model

Another quantitative analysis of the concept of the VBS was given by Wolff (13) and Clogston (14). Their approach treats the conduction electron - impurity system as a scattering problem in which the Bloch electrons scatter from a perturbing impurity potential. The impurity electrons are assumed to be part of the conduction band so that no extra d-orbital is assumed as in the Anderson model. The VBS appears as a scattering resonance which is a function of the energy of the incident electron. The question of local moment formation is then treated by including an electron-electron exchange potential. However, the only important matrix elements of this additional potential correspond to the Anderson form i.e. $U n_\downarrow n_\uparrow$. Thus apart from the different approaches towards obtaining the VBS the two models are essentially similar.

All the same, it is thought that Anderson's extra orbital approach is more suitable for transition metal (TM) impurities in simple hosts whereas the Wolff-Clogston model would be more appropriate for TM impurities in other TM hosts.

1.5. Effect of Correlation on the HF Criterion for Local Moment Instability

As with the band theory of ferromagnetism the HF solution of the Anderson model suffers from the disadvantage of over-estimating the tendency towards local moment formatio The repulsive potential which an up-spin electron feels when it is at an impurity site is proportional to the average

number of down-spin electrons on the site. Now as $\frac{U}{\Delta} \to \infty$ the repulsive potential would become so exceedingly large that one must consider the possibility that the up-spin electron will recede from the impurity orbit as a down-spin electron jumps onto it in order to avoid a simultaneous occupancy of the impurity orbital.

The effect of such correlated electron hopping has been considered by Schrieffer and Mattis (16,17) who showed that in the low-density limit (i.e. small number of electrons or holes in the VBS) the effective Coulomb interaction is given by

$$U_{eff} = \frac{U}{\left(1 + \frac{U}{\pi \varepsilon_d}\right) \tan^{-1} \frac{\varepsilon_d}{\Delta}} \qquad 1.27$$

which is less than U. Thus correlation effects suppress the tendency towards local moment formation. Since

$$\lim_{U \to \infty} U_{eff} = \frac{1}{\pi \varepsilon_d} \tan^{-1} \frac{\varepsilon_d}{\Delta} \ldots < \Delta$$

it is clear that the HF instability limit can never be attained i.e. no local moment would ever form. The existence of degenerate impurity orbitals would of course lessen the severe restrictions imposed by correlation effects but it does not alter the above conclusion for the low density limit.

1.6. Derivation of an antiferromagnetic s-d exchange Interaction from Anderson's Hamiltonian

Since the HF solution of the Anderson model is not valid in the magnetic limit (i.e. $\frac{U}{\Delta} \gg 1$) an alternative approach to this limit is clearly required. In the Friedel-Anderson model, a magnetic state consists of say a filled up-spin VBS lying below the Fermi level while the empty down-spin VBS lies well above it i.e.

$$\varepsilon_F - \varepsilon_{d\downarrow} \gg \Delta \quad \underline{\text{and}} \quad \varepsilon_{d\uparrow} + U - \varepsilon_F \gg \Delta . \qquad 1.28$$

According to Anderson and Clogston (18) the energy of a down-spin conduction electron can be lowered (in second order perturbation theory) by mixing-in a configuration in which a down-spin electron has simultaneously hopped into the impurity. The resulting energy shift is of the order

$$\Delta\varepsilon_d \sim -\frac{\langle V_{sd}\rangle^2}{U} \qquad 1.29$$

The resulting conduction-electron polarization is negative. This argument is similar to Anderson's superexchange mechanism in insulators and suggests that the conduction electron-local impurity interaction may be expressed as an antiferromagnetic (afm) s-d exchange integral of the form

$$\mathcal{H}_{sd} = -J\, \underline{S}_d \cdot \underline{s}_c \qquad 1.30$$

where $J < 0$ and Sd, sc are respectively the impurity and conduction electron spins. A more rigorous derivation of equation (1.30) from the Anderson Hamiltonian has been given by Schrieffer and Wolff (19) and by Bailyn (20) who performed a canonical transformation of the Anderson Hamiltonian in order to eliminate the mixing interaction Vsd to first order. By choosing an appropriate generating function the Anderson Hamiltonian was transformed into the expression

$$\mathcal{H}_{sd} = -\frac{J_{k_F k_F}}{N}\sum_{kk'}\left[\left(c^+_{k'\uparrow}c_{k\uparrow} - c^+_{k'\downarrow}c_{k\downarrow}\right)S^z + c^+_{k'\downarrow}c_{k\uparrow}S^+ + c^+_{k'\uparrow}c_{k\downarrow}S^-\right]$$

$$+\frac{V_{k_F k_F}}{N}\sum_{kk'}\left(c^+_{k'\uparrow}c_{k\uparrow} + c^+_{k\downarrow}c_{k\downarrow}\right) \qquad 1.31$$

where $$J_{k_c k_F} = \frac{-2\langle V_{sd}\rangle^2 U}{\epsilon_d(U-\epsilon_d)} \qquad 1.32$$

and $$V_{k_F k_F} = -\frac{\langle V_{sd}\rangle^2 U}{2\epsilon_d(U-\epsilon_d)} \qquad 1.33$$

$$\epsilon_d = \varepsilon_F - \varepsilon_d > 0$$ (see equation (1.28))

J and V have been evaluated at $k \simeq k' = k_F$ because clearly at absolute zero temperature only electrons near the Fermi level are effective. The above transformation is valid when equation (1.28) holds i.e. when the <u>virtual levels do not coincide with the Fermi level</u>. The first term in equation (1.31) represents an afm s-d exchange interaction while the second term represents an attractive potential scattering. We may note that Silverstein (21) has suggested that if one did not invoke the artificial distinction between direct and exchange terms then one finds that the Schrieffer-Wolff result above (equation (1.31)) is infact equivalent to an effective s-wave attractive interaction between the localized and conduction electrons. In particular for a homogeneous attractive s-wave interaction one of course finds that the ground-state of a 'normal' fermion system is unstable to the formation of time-reversed Cooper pairs leading to superconductivity. Even for the local attractive interaction the 'normal' ground state of the fermion system is still inappropriate but because the attraction is localized in configuration space any pairing is with a many-electron wave packet rather than with a single electron. The author, however, concludes that whether this configuration - space pairing represents some kind of phase

transition or not is a moot point.

1.7. The Kondo Effect

Having discussed some of the essentials of the problem of local moment formation we shall now briefly recall some of the effects associated with the existence of such local moments. The discussion is usually made in terms of an s-d model which assumes a well-defined localized impurity spin S coupled to the conduction electron spin **s** by an interaction of the form of equation (1.30). Historically the **s-d** model was first proposed by Zener (22) to explain the ferromagnetismof the 3d transition metals. Although it is generally suitable for the rare-earth (RE) elements there has been a persistent doubt as to its validity for the Fe-group metals. In practice the model has turned out to be extremely useful in explaining a wide variety of experimental phenomena, not least of all the Kondo effect which is discussed below. Within the framework of the Friedel-Anderson model the s-d model is valid only when $U \gg \Delta$, in which limit the s-d Hamiltonian is derivable from the Anderson Hamiltonian (see section 1.6)

The Kondo effect refers to a resistance minimum observe at sufficiently low temperatures in almost all alloys of the transition metals in which the impurity is known to be magnet (usually for simple metal hosts). The resistance minimum was first explained by Kondo (23) in terms of the scattering of conduction electrons from the magnetic impurities via the s-coupling. We write the Hamiltonian of the system as

$$\mathcal{H} = \mathcal{H}_s + \mathcal{H}_{sd}$$

where $\mathcal{H}_s$ and $\mathcal{H}_{sd}$ are given by equations (1.15) and (1.31)

respectively. Because $\mathcal{H}_{sd} \ll \mathcal{H}_s$ it is usually taken as weak perturbation on the kinetic energy of the conduction electrons. The scattering of conduction electrons by the exchange term in $\mathcal{H}_{sd}$ is usually called the spin-disorder scattering and can either be spin-flip (flipping both the impurity and conduction electron spins through the terms S^+s^- or S^-s^+) or non spin-flip (through the $S^z s^z$ term). To calculate the impurity contribution to the electrical resistivity of an alloy one considers the transition probability of scattering a conduction electron from state $\underline{k}$ to $\underline{k}'$ via the s-d interaction with the impurity. The total scattering probability will involve the probabilities of scattering through all distinguishable channels but we shall only consider the channel in which $\underline{k}\uparrow \rightarrow \underline{k}'\uparrow$ with the impurity spin state remaining the same in the initial and final states. We may write the total scattering amplitude as a sum

$$A_{\underline{k}\uparrow,\,\underline{k}'\uparrow} = \sum_p A^{(p)}_{\underline{k}\uparrow,\,\underline{k}'\uparrow} \qquad 1.34$$

where the suffix p denotes the contribution from the scattering which is to the p^{th} order in J. The lowest order (first Born approximation) calculation of the electrical resistivity has been made by Kasuya (24) and Yosida (25) and in particular the latter author was able to explain the negative magneto-resistance observed in some of the magnetic alloys. The significant step taken by Kondo was in extending the calculations to third order in J and thereby showing that (i) higher order terms in the perturbation theory could explain many of the experimental observations including the resistance minimum;

(ii) More importantly inspite of the fact that $\mathcal{H}_{sd} \ll \mathcal{H}$ its treatment by perturbation theory becomes invalid at sufficiently low temperatures.

In the second order approximation there are two distinguishable processes:-

(a) the direct process in which the incident electron, $\underline{k}$, is first scattered into an empty intermediate state $\underline{q}$ and then finally scattered into $\underline{k}'$;

(b) the exchange process in which an electron from a filled state $\underline{q}$ is scattered into the final state $\underline{k}'$ and subsequently the initial electron from $\underline{k}$ is scattered into the empty state $\underline{q}$. The intermediate state has an electron in $\underline{k}\uparrow$, another in $\underline{k}'\uparrow$ and a hole in $\underline{q}$. Equivalently we can say (6) that the first scattering creates an electron-hole pair while in the second scattering the created hole annihilates the electron with momentum $\underline{k}$ to create an electron in the final state $\underline{k}'$.

Owing to the exclusion principle restriction on the intermediate state the Fermi occupation or distribuition function is involved in the scattering amplitudes. In the case of the potential scattering term and the non spin-flip part of the exchange term in equation (1.31) the Fermi factor cancel out because of the coherent addition of the direct and exchange processes in the second order perturbation theory being considered. Thus in calculating the residual resistivity due to those terms the first Born approximation is sufficient. However, this cancellation does not occur for th spin-flip terms in the exchange part of $\mathcal{H}_{sd}$ and it is this non-cancellation that is responsible for the experimental anomalies observed. The contribution to the electrical resistivity due to these terms has been obtained as

$$\rho_m(T) = R_m \rho_s(\varepsilon_F) c J^2 S(S+1)\left\{1 + 4J\rho_s(\varepsilon_F) \ln \frac{K_B T}{W}\right\} \qquad 1.35$$

where the conduction band density of states $\rho_s(\varepsilon_F)$ is assumed to be constant over the band width $2W$. c is the impurity concentration and Rm is a constant involving atomic parameters. If we add the phonon resistivity ($\sim T^5$ at low temperatures) and the resistivity due to potential scattering then the total resistivity is given by

$$\rho(T) = R_m \rho_s(\varepsilon_F) c V^2 + R_m \rho_s(\varepsilon_F) c J^2 S(S+1)\left\{1 + 4J\rho_s(\varepsilon_F) \ln \frac{K_B T}{W}\right\} + bT^5 \qquad 1.36$$

We note that this equation does not strictly give the full temperature dependence of the total resistivity because we have not given the temperature-dependence of the resistivity due to the potential scattering term (the first term in equation (1.36) is simply the residual resistivity due to potential scattering).

For $J < 0$ the logarithmic term increases as the temperature is decreased; when this is combined with a decreasing phonon resistivity a resistance minimum is observed. The temperature of the minimum is given by

$$T_{min} = 4|J| \left\{\frac{\rho_s(\varepsilon_F) R_m}{5a} c\right\}^{1/5} \qquad 1.37$$

which shows that $T_{min} \propto c^{1/5}$ as is experimentally observed. For $T < T_{min}$

$$\rho(T) \sim A - Bc \ln T \qquad 1.38$$

where A and B are constants. The predicted logarithmic variation above the minimum has also been widely observed.

On the other hand, for $J > 0$ the resistivity is well behaved, decreasing continuously towards the residual value as the temperature decreases. The effect of similarly including higher order terms in the perturbation theoretic calculation of the properties of various other physical parameters has been extensively reviewed by Kondo (1), and so we shall be content to simply observe that such calculations do equally predict anomalies in the temperature variation of those parameters.

1.8. The Kondo Divergence

Although the logarithmic term in equation (1.35) gives a good account of the resistance minimum observed in a number of dilute magnetic alloys the fact that it diverges as the temperature decreases towards absolute zero is clearly undesirable and of course physically unacceptable. As T tends to zero, we must recover the unitarity limit in which the resistivity should attain a saturation value given by equation (1.13). Such a saturation of the electrical resistivity appears to have been observed for CuFe, CuCr and AuV alloys (see reference 2 for references to the individual papers).

However, the perturbation theory used in deriving equation (1.35) is not valid all the way down to absolute zero. It in fact ceases to be valid as soon as the second term in that equation becomes comparable with the first term. This happens for $T \approx T_K$ where T_K, called the Kondo temperature, is defined by

$$k_B T_K = W e^{-\frac{1}{4|J|\rho_s(\varepsilon_F)}} \qquad 1.39$$

Before continuing with the discussion we may mention that the logarithmic singularity of equation (1.35) may be suppressed by a sufficiently large magnetic field; for example, if $g\mu_B B \gg K_B T$ the ln T term is replaced by a ln $g\mu_B B$ term.

There has been a considerable number of attempts both to remove the divergence at $T = 0$ and to account for the physical properties of the systems below the Kondo temperature. A review of these attempts has been given by Kondo (1). Essentially the logarithmic singularity is assumed to occur because the perturbation theoretic treatment of the s-d exchange Hamiltonian will always break down at sufficiently low temperatures since the impurity -conduction electron system is in reality a many-body system. Consequently non-perturbative methods are sought which would describe the gradual transition of the alloy system to a highly correlated state for $T \lesssim T_k$. The transition must be gradual because no sharp phase transition can occur in a system with a small number of degrees of freedom. Heeger (2), by drawing an analogy between the phonon induced electron-electron interaction (which may lead to superconductivity) and the indirect electron-electron interaction via impurity-spin excitations, has been drawn to ponder whether the Kondo divergence does not signal the onset of a many-body condensed state, as is the case in superconductivity. As mentioned earlier, an excellent review of the theoretical descriptions of the quasibound state supposed to be formed by the impurity spin and the conduction electrons below T_k has been given by Kondo (1). A very concise but readable review has also been given by Phillips (26) and this includes a table summarizing the temperature dependence of some physical parameters as predicted by various theoretical models. Finally we may mention

that another explanation of the Kondo divergence which introduces some dynamics into the HF theory has been proposed by Mills (3). Recall that in the HF solution of the Anderson model (section 1.3) an up-spin electron feels only the average Coulomb repulsion $U\langle n_\downarrow \rangle$ due to down-spin electrons. Mills therefore suggests that to go beyond the HF approximation the up-spin electron must be allowed to feel the instantaneous Coulomb repulsion $U n_\downarrow$ i.e. the fluctuation in the interaction energy must be allowed for. One way of doing this would be to replace the intra-atomic Coulomb potential by a fluctuating effective magnetic field. Suppose that this effective field has an amplitude h and is 'frozen' at the time-independent value of h_0. Then in the non-magnetic limit $\left(\frac{U}{\Delta} \ll 1\right)$ the free energy, G, of the system sketched as a function of h_0 is as shown in figure 1.1(a)

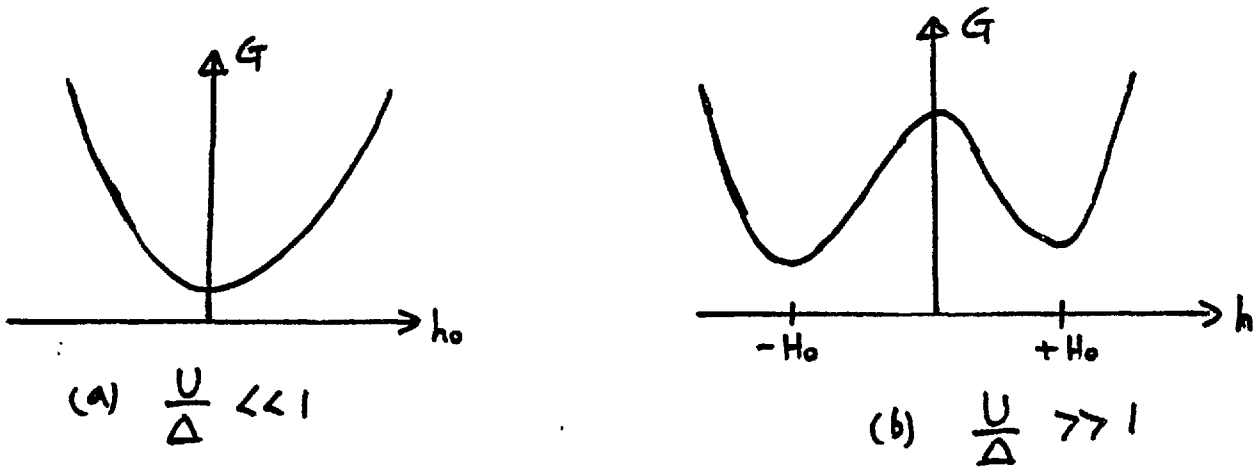

Fig. 1.1 Sketch of the free energy (G) as a function of the effective magnetic field (ho) in the non-magnetic and magnetic cases (after ref. 3)

G exhibits a nearly parabolic behaviour with a minimum at $h_0 = 0$. In the magnetic limit $\left(\frac{U}{\Delta} \gg 1\right)$ G has two minima, at $\pm H_0$ say. In the latter case it is possible that the effective field, apart from fluctuating about Ho can also change sign from $-H_0$ to $+H_0$ while the free energy still remains near the minimum value. This latter fluctuation corresponds to spin-flipping of the impurity spin.

However, for the impurity spin to be flipped it must tunnel through the energy barrier in figure 1.1(b). The contribution to the free energy by the repeated flips of the impurity spin is negative and is about $\Delta e^{-\frac{U}{\Delta}}$, which the authors suggests is $\sim k_B T_K$, if J is as given by equation (1.32) and $\Delta \sim W$. The only comment we wish to make here is that the suggestion that $\Delta \sim W$ seems unreasonable. For the relevant systems, experimental observations (see ref. 2 for details) give values of Δ of a few tenths of an electron-volt so that Δ is at least an order of magnitude smaller than W.

1.9.- Localized Spin Fluctuations

There are a few unsatisfactory features of the HF theory of local moment formation. One of them, already discussed in section 1.5, is the overestimation of the tendency towards local moment formation through the neglect of electron-electron correlations.

A second difficulty is that the HF model of a magnetic impurity requires the impurity spin to have a well-defined direction at all times, which would only be the case if there is a strong effective field acting on the spin i.e. either the alloy is automatically ferromagnetic or else a very strong external magnetic field is applied (3). Clearly no information can be obtained from this model about the temperature-dependence of the magnetic susceptibility. On the other hand, a proper theory must allow for the thermal fluctuations of the impurity spin.

An even more fundamental difficulty and one which is physically unacceptable is the fact that the HF solution of the Anderson Hamiltonian predicts a sharp boundary between

the magnetic and non-magnetic VBS. A magnetic VBS exists if $U \geq \Delta$ whereas the VBS is non-magnetic if $U < \Delta$. Such a sharp phase transition is reminiscent of a second or higher order thermodynamic phase transition. However, whereas a proper phase transition would involve the cooperative ordering of a large number of microsystems within a macroscopic volume the local moment formation transition is an entirely local phenomenon involving a small number of electrons within the impurity cell. Consequently fluctuations are bound to be very important since from statistics the amplitude of the fluctuation of any extensive thermodynamic variable pertaining to an assembly of N subsystems, is $\propto N^{\frac{1}{2}}$. Thus near the HF instability one should expect large amplitude spin fluctuations which would smear out any phase transition from the nonmagnetic to the magnetic VBS. Hence there is again the need to introduce some dynamics into the HF theory.

It was this need to introduce some dynamics into the HF theory that led a number of authors (15,27-31) to propose the replacement of the localized impurity spin by <u>localized spin fluctuations</u> (lsf).

In section 1.8 we mentioned that the Kondo divergence has been explained in terms of the formation of a many-body singlet state (often referred to as the Nagaoka condensed state). A simplistic way of viewing this is as follows (32): as $T \longrightarrow T_k$ the s-d mixing becomes stronger as more and more electrons hop per unit time into and out of the VBS. For $T < T_k$ the conduction electrons in the vicinity of the VBS become increasingly spin-polarized with their spins aligned predominantly antiferromagnetic to the impurity spin. Thus

the impurity spin becomes progressively surrounded by an extended cloud of antiparallel spin-polarized electrons which compensate its net magnetic moment and reduce its observable value. Eventually, for $T \ll T_k$ the impurity moment is completely compensated leaving an essentially non-magnetic impurity.

A localized spin fluctuation is defined as the repeated scattering between an electron and a hole of opposite spin on the impurity site (31). It has a certain lifetime denoted by τ_{sf}. Instead of regarding the disappearance of magnetism below T_k as due to a cloud of compensating electron spins the lsf model suggests that a magnetic impurity will appear to be non-magnetic if the thermal fluctuations are much slower than the spin fluctuations i.e. if $\frac{h}{k_B T} \ll \tau_{sf}$.

At higher temperatures $T \gtrsim \frac{h}{k_B \tau_{sf}}$ the spin fluctuations are slower than the thermal fluctuations of the temporary moment they describe so that there is then no observable difference between a spin fluctuation and a genuine spin. This description of a smooth transition clearly obviates the need for the sharp phase transition required by the HF theory.

The contribution to the static magnetic susceptibility by a non-magnetic impurity has been calculated (12) within the HF theory as

$$\chi_d(0) = \frac{g^2 \mu_B^2 \rho_d(\epsilon_F)}{1 - \frac{(U+4J)}{10} \rho_d(\epsilon_F)} \qquad 1.40$$

This is clearly an enhanced susceptibility which diverges at

the HF instability. However to characterize fully the magnetic response of the system we need the dynamic susceptibility and this has been obtained (15,31) as

$$\chi_d(\omega) = \frac{\chi_o(\omega)}{1 - U\chi_o(\omega)} \qquad 1.41$$

where $\chi_o(\omega)$ is the local susceptibility in the absence of enhancement effects. Rivier (15) has also shown that equatio (1.41) can be written in the form

$$\chi_d(\omega) = \frac{1}{\pi} \frac{g^2 \mu_B^2}{\tau_{sf}^{-1} + i\omega} \qquad 1.4$$

where

$$\tau_{sf}^{-1} = \frac{1 - U\rho_d(\varepsilon_F)}{\pi \rho_d(\varepsilon_F)} \qquad 1.4$$

Observe that (i) in the limit $\omega \to 0$ we recover the static susceptibility (equation (1.40))

(ii) as $\tau_{sf} \longrightarrow \infty$ $\chi_d(\omega)$ becomes

more sharply peaked so that the magnetization resulting from any applied field remains for a longer time.

As already explained for $\tau_{sf} < \frac{h}{K_B T}$ an impurity appears to be non-magnetic whereas for $\tau_{sf} > \frac{h}{K_B T}$ the impurity is magnetic. Rivier and Zuckermann (30) therefore defined a Kondo temperature T_k in the lsf model as

$$K_B T_K = h\tau_{sf}^{-1} \qquad 1.4$$

with the proviso that T_k merely indicates a change of regime and not the well-defined temperatures given in theories of the many-body singlet state.

Mills (3) however, disagrees with this idea that the Kondo effect and lsf are equivalent. His argument is essentially that the Kondo effect enters in the extremely magnetic limit $U\rho_d(\varepsilon_F) \gg 1$ whereas the lsf model applies in the limit $U\rho_d(\varepsilon_F) \lesssim 1$. In the magnetic limit the free energy is as sketched in figure 1.1(b) with two minima. The Kondo temperature is defined in this model as $\frac{h}{\tau}$ where τ is the time required for the local moment to tunnel from one minimum (say $\uparrow$) to the other ($\downarrow$). If $U\rho_d(\varepsilon_F) \gg 1$ the height of the barrier is large, and hence τ is large (i.e. low frequency spin fluctuations) giving a very small T_k.

On the other hand, for $U\rho_d(\varepsilon_F) \ll 1$ the free energy has only one minimum (fig. 1.1(a)) and Mills argues that fluctuations in the effective internal field are negligible.

As $U\rho_d(\varepsilon_F)$ increases towards unity large fluctuations may occur with little cost to the free energy because the curvature is proportional to $\{1 - U\rho_d(\varepsilon_F)\}$. The characteristic frequency is proportional to the curvature and is low near the HF instability limit. Thus according to Mills, although the Kondo and the lsf regimes are both characterised by the occurrence of low frequency fluctuations the two phenomena occur for different values of the quantity $U\rho_d(\varepsilon_F)$.

1.10 Exchange Enhancement in TM alloys:

Concept of Paramagnons

In the so-called incipient ferromagnets it has been assumed (33,34) that there exists a semi-phenomenological

short-range repulsion between the d-electrons which although not strong enough to give ferromagnetism outright, yet appreciably enhances the low-temperature paramagnetic susceptibility over the ordinary Pauli paramagnetism as calculated from the band structure density of states. In such a circumstance one attributes the susceptibility enhancement to the existence of spin fluctuations otherwise referred to as either paramagnons or critically damped spin waves.

Wolff (35) has shown that for a system of strongly interacting fermions the wave-vector and frequency-dependent susceptibility is given in the random phase approximation (RPA) by

$$\chi(q,\omega) = \frac{\chi_0 F(q,\omega)}{1 - U F(q,\omega) \rho(\varepsilon_F)} \qquad 1.45$$

where $\chi_0 \equiv \chi_{Pauli} = \frac{1}{2} g^2 \mu_B^2 \rho(\varepsilon_F)$ is the Pauli susceptibility; $\rho(\varepsilon_F)$ is the total density of states at the Fermi level. U is the screened (and hence short-ranged) Coulomb potential through which the electrons interact. $F(q,\omega)$ is the generalized Lindhard function.

As q , $\omega \to 0$, $F(q,\omega) \to 1$ so that we recover the HF criterion for ferromagnetic instability i.e. $U\rho(\varepsilon_F) = 1$.

The Stoner enhancement factor S is defined as

$$S = \frac{\chi_{obs}}{\chi_0} = \{1 - U\rho(\varepsilon_F)\}^{-1} \qquad 1.46$$

where χ_{obs} is the spin component of the observed susceptibility; for Pd $S \simeq 10$ so that $U\rho(\varepsilon_F) \simeq 0.9$

The electrons are expected to interact with the paramagnons much in the same way as electrons and phonons do. Conse-

quently there is a correction to the one-particle self-energy due to the virtual emission and reabsorption of paramagnons. The result is an increased effective electron mass with a mass enhancement factor given (36) by

$$\frac{m^*}{m} = 1 + \frac{9}{2} \ln \frac{5}{3} \qquad 1.47$$

where m is the bare-band electron mass and m^* is the enhanced mass. This mass enhancement clearly should be reflected in the electronic specific heat as an increase in γ, the coefficient of the linear term in the specific heat, since by definition

$$\gamma = \lim_{T \to 0} \frac{C_v(T)}{T} \qquad \propto m .$$

Hence if γ^* is the enhanced value then

$$\frac{\gamma^*}{\gamma} = \frac{m^*}{m} .$$

For Pd with $S = 10$ we therefore expect, from equation (1.47), that $\frac{m^*}{m} \sim 6$, which value should be compared to a value of 1.66 obtained from the experimentally determined γ and the calculated band structure density of states (37).

In addition to enhancing the value of γ the paramagnons are also predicted to contribute to higher order terms in the electronic specific heat. This contribution is calculated to be of the form $T^3 \ln \frac{T}{T_{sf}}$ where $T_{sf} = \frac{T_F}{S}$ and is called the spin-fluctuation temperature. T_F is of course the Fermi temperature. Thus for a strongly exchange-enhanced system like Pd the electronic heat capacity is expected to be of the form

$$C_v(T) = \gamma T \left\{1 + \frac{m^*}{m}\right\} + \beta T^3 + \delta \left(\frac{T}{T_{sf}}\right)^3 \ln \frac{T}{T_{sf}} \qquad 1.48$$

where the βT^3 term represents the phonon contribution at low temperatures, and $\delta \sim \gamma T_{sf}$. We may remark here that up to now the predicted $T^3 \ln T$ term in the heat capacity has not been observed in Pd or Pt.

The effect of electron-paramagnon interactions on the electrical resistivity will be discussed in a later section (2.5(vii)).

In applying the concept of paramagnons to the problem o nearly or weakly ferromagnetic alloys two models have so far been used. The first model (38) is the uniform exchange enhancement model which uses a concentration-dependent spatially-averaged exchange interaction between the d-electro so that the alloy is treated just like a pure metal as discussed above. This model predicts that (a) $\gamma^* \propto \ln \chi$ where χ is the uniform static susceptibility;
(b) the coefficient of the T^2 term in the impurity electrical resistivity should vary as χ^2 ;
(c) the specific heat at low temperatures should vary as

$$\frac{C_v}{T} = \gamma^* + \beta T^2 + \frac{2\pi^2}{5}\frac{(S-1)^2}{S}\left(\frac{T}{T_{sf}}\right)\ln\left(\frac{T}{T_{sf}}\right) \qquad 1.49$$

where γ^*, χ, C_v, S and T_{sf} are all concentration-dependent, and in particular

$$T_{sf} \simeq \left[\pi/4\,(S-1)\,\rho(\varepsilon_F)\right]^{-1}$$

$$\chi = \tfrac{1}{2} g^2 \mu_B^2 S \rho(\varepsilon_F) \qquad 1.50$$

$$S = \left\{1 - U(c)\,\rho(\varepsilon_F)\right\}^{-1}$$

where $U(c)$ is the spatially averaged intra-atomic Coulomb interaction.

For $S \gg 1$ equation (1.49) reduces to

$$\frac{C_v}{T} \simeq \gamma^* + \beta T^2 + \frac{2\pi^2}{5} S_0 \left(\frac{\chi}{\chi_0}\right)^3 \left(\frac{T}{T_{sf}^0}\right)^2 \left\{ \ln \frac{T}{T_{sf}^0} - \ln \frac{\chi}{\chi_0} \right\} \qquad 1.51$$

where S_0, χ_0 and T_{sf}^0 refer to the host matrix.

The second model is the <u>local exchange enhancement model</u> (39-41) which assumes that the main effect of the impurity is to change the local intra-atomic Coulomb interaction. This model was orginally proposed to explain those properties of <u>Pd</u>Ni alloys which could not be accounted for on the uniform exchange model (42) and in general for dilute alloys of 3d impurities in <u>isoelectronic</u> 4d or 5d hosts with negligible exchange enhancement (40). An increase in the linear term in the specific heat was obtained and also a correction term proportional to T^3 but the model did not give any $T^3 \ln T$ term as obtained with the uniform enhancement model. The model was later extended (41) to the case where the matrix has significant exchange enhancement. In the single impurity limit there exists a strong mass enhancement and a $T^3 \ln T$ term; the T^3 correction term obtained by Lederer and Mills (40) was found to be small. The main predictions of the local exchange enhancement model are as follows:-

(a) γ, χ , and the coefficient of the T^2 term in the electrical resistivity are all <u>linear</u> functions of the impurity concentration, and hence are proportional to one another;

(b) the quantity $\frac{1}{\gamma}\frac{d\gamma}{dc}$ depends on the characteristics of the host metal and on the change in local intra-atomic Coulomb interaction; it is also proportional to $\frac{1}{\chi}\frac{d\chi}{dc}$; specifically

$$\frac{1}{\gamma}\frac{d\gamma}{dc} = 3\,\frac{\rho(\varepsilon_F)}{\rho^*(\varepsilon_F)}\,\frac{1}{\chi}\,\frac{d\chi}{dc} \qquad 1.52$$

where $\rho(\varepsilon_F)$ and $\rho^*(\varepsilon_F)$ are respectively the bare-band structu and the observed specific heat density of states.

(c) at low temperatures the specific heat is given by

$$\frac{C_v}{T} = \gamma\left\{1 + C\,\frac{\Delta\gamma}{\gamma}\right\} + \beta T^2\left[1 + C\,\frac{\Delta\gamma}{\beta}\left\{\frac{10^3 \ln\frac{T}{T_{sf}^0}}{\lambda T_{sf}^0} - \frac{8}{T_{sf}^2}\right\}\right] \qquad 1.53$$

where $\lambda \sim \frac{1}{2} S_0$.

The above equation shows up another difference between the localized and uniform exchange-enhancement models. The $T^3 \ln T$ terms have different concentration-dependences and also different values of Tsf. (see reference 41 for the relation giving Tsf on the localized model).

Equation (1.53) also shows that on the local enhancement model the low-temperature specific heat data may be analysed in the form

$$\frac{C_v}{T} \simeq \gamma^* + (\beta - \Delta\beta)\,T^2 \qquad 1.5$$

where $\Delta\beta \propto C$. This follows because $T^3 \ln\frac{T}{T_{sf}^0} \sim T^3$ if $T_{sf}^0 \gtrsim 20\,K$. From their specific heat measurements Chouteau et al (43) estimated that for the Pd-Ni system

$T_{sf}^0 \sim 400 \pm 80\,K$ and $T_{sf} \sim 20 \pm 4\,K$.

Other contributors (44,45) to the theory of paramagnons obtain essentially similar results for the specific heat. Differences and refinements of course occur with respect to the details, especially of the concentration-dependence and the temperature range of validity of the $T^3 \ln T$ term.

For instance Fulde and Luther (45) show that the $T^3 \ln T$ term should, at low temperatures, be replaced by the term

$$\left(\frac{T}{T_{sf}}\right)^3 \ln\left(\frac{T + T_{imp}}{T_{sf}}\right)$$

where Timp characterizes the impurity scattering.

For temperatures sufficiently low that $T < T_{imp}$ the above term becomes practically indistinguishable from an ordinary T^3 term. In conclusion we note that a very recent review of the paramagnon theory has been given by Mills et al (46).

1.11 Local Environment Effects

Within the last decade or so it has become clear from experimental observations that the magnetic properties of atoms depend strongly on their local environment especially for TM impurities in a metallic host. This dependence has been observed for a variety of alloy systems by varying the temperature, alloy composition and the thermal and mechanical treatment of the alloy. Historically the first local environment effects to be studied related to order-disorder effects (47), although some observable effect of atomic ordering on the saturation magnetization and magnetic anisotropy of Ni_3Fe was reported (48) some ten years earlier. However, the first detailed experimental analysis of the local environment effect was made on a dilute alloy of a magnetic impurity in a binary disordered non-magnetic host. By studying the Pd concentration dependence of the NMR measurements of the Co^{59} resonance of dilute concentrations of Co in $Pd_x Rh_{1-x}$ alloys

Jaccarino and Walker (49) concluded that the magnetization of a Co impurity takes place discontinuously. A Co

atom is magnetic with its maximum value of 1.7 μ_B only if it has at least two Pd atoms as near-neighbours; otherwise it is non-magnetic. This local environment model was also used to explain the observed average magnetic moment of Fe atoms in the Nb_xMo_{1-x} matrix. An Fe atom assumes the full moment of 2.1 μ_B if it has at least seven Mo atoms as near-neighbours. Local environment effects have also been observed in AuV alloys (50,51) where a V atom is magnetic if and only if it has no other V atom as a nearest neighbour (but see reference 52). However the most interesting examples of local environment effects occur for binary TM alloys in which there exists a critical concentration for the onset of ferromagnetism. Magnetization heat capacity and neutron diffraction measurements have severally or jointly demonstrat unequivocally the inhomogeneous nature of the onset of ferromagnetism in CuNi, RhNi and PdNi alloys. Specifically near their respective critical concentrations these systems are now known to contain magnetic clusters and it is the interaction between these clusters that is believed to give rise to ferromagnetism. We shall not attempt to catalogue all the careful experiments that have finally led to the above conclusion. A good review of the local environment effect has been given by Garland and Gonis (53) and this contains references to many of the original papers.

Because of the many factors that have to be considered atomic clustering or short range order, statistical fluctuations in local environment, interactions between magnetic clusters or between individual local moments in clusters - it is hardly surprising that very few microscopic theoretical

treatments of the local environment effect exist. We shall consider the work of Kim (54) and of Garland and Gonis (55) since only these bear directly on the problem of the local environment effect.

Kim (54) was the first author to attempt a microscopic theoretical treatment of the local environment effect. He generalized Anderson's Hamiltonian (equation (1.14)) to include the interactions between impurity atoms and also the Coulomb interaction between conduction electrons of the host metal. The latter was to allow for a possible exchange enhancement of the metal host (see section 1.10). For this purpose the orbitally degenerate 3d (or 4d) electrons of the TM host were regarded as conduction electrons! The interaction between the solute atoms is given in the form of a direct transfer integral

$$\mathcal{H}_t = \sum_{i,j,\sigma} T_{ij}\, d_{i\sigma}^{+} d_{i\sigma} \qquad 1.55$$

where $d_{i\sigma}^{+}$, $d_{i\sigma}$ are the usual fermion creation and annihilation operators for a σ spin at the i^{th} solute atom. The matrix element is a function of the species of the i^{th} and j^{th} impurities as well as their separation. T_{ij} is real and T_{ii} is of course zero. The local environment effect is introduced by assuming that the effect of the presence of the j^{th} impurity near the i^{th} impurity is to modify the width of the i^{th} VBS, say through a change of the density of states at the Fermi level. Suppose the width of the i^{th} VBS changes from Δ_i^0 to $\Delta_i = \Delta_i^0 + \delta\Delta_i$ as a result of a change in the density of states from $\rho_i^0(\epsilon_F)$

to $\rho_i(\varepsilon_F)$ owing to an interaction between the i^{th} and j^{th} impurities. The following two possibilities can then arise:-

$$\text{(a)}\quad U_i \rho_i^{\circ}(\varepsilon_F) < 1 \qquad \text{but} \qquad U_i \rho_i(\varepsilon_F) \geq 1 \qquad 1.56$$

corresponding to the situation in say CuNi where the presence of Ni near neighbours enhances moment formation, and

$$\text{(b)}\quad U_i \rho_i^{\circ}(\varepsilon_F) \geq 1 \qquad \text{but} \qquad U_i \rho_i(\varepsilon_F) < 1 \qquad 1.57$$

as may be the case for AuV .

If the position of the VBS is near ε_F equation (1.56) can be rewritten as

$$\frac{U_i}{\pi \Delta_i^{\circ}} < 1 \quad \text{but} \quad \frac{U_i}{\pi(\Delta_i^{\circ} + \delta\Delta_i)} \geq 1 \qquad 1.56a$$

and similarly for equation (1.57).

Avoiding the Green's functions and operators we finally obtain that $\delta\Delta_i$ can be expressed as the sum

$$\delta\Delta_i = \delta\Delta_i^{(1)} + \delta\Delta_i^{(2)} + \delta\Delta_i^{(3)} \qquad 1.58$$

$\delta\Delta_i^{(1)}$ comes from indirect impurity-impurity interactions via the host metal conduction electrons and is given by

$$\delta\Delta_i^{(1)} \simeq \pi \langle V_{sd} \rangle^2 \Delta\rho_s(\varepsilon_F) \qquad 1.59$$

where $\Delta\rho_s(\varepsilon_F)$ is the change of the Fermi level density of states of the host metal conduction electrons at the i^{th}

impurity site due to the presence of other surrounding impurities. Since $\Delta\rho_s(\varepsilon_F)$ can be positive or negative $\delta\Delta_i^{(1)} \gtrless 0$. Using a number of simplifying assumptions one further obtains

$$\frac{\delta\Delta_i^{(1)}}{\Delta_i^0} \simeq \frac{1}{K_F^2} \sum_{j(\neq i)} \frac{\cos(2K_F r_{ij})}{r_{ij}^2} \qquad 1.60$$

where r_{ij} is the distance between the two impurities. The oscillatory behaviour of $\delta\Delta_i^{(1)}$ has the same origin as the R K K Y interaction (see section 1.12 below). If we consider only the nearest neighbours of which there are say z_0 then

$$\frac{\delta\Delta_i^{(1)}}{\Delta_i^0} = 4 z_0 \frac{\cos(2K_F r_0)}{(2K_F r_0)^2} \qquad 1.61$$

where r_0 is the near-neighbour distance. Since $-1 \leq \cos(2K_F r_0) \leq 1$ it is quite possible for $|\delta\Delta_i^{(1)}| \sim 0.1\,\Delta_i^0$ for a single other impurity in a near-neighbour site.

$\delta\Delta_i^{(2)}$ is due to the direct transfer interaction between impurities and is always positive. Again using some simplifying assumptions

$$\delta\Delta_i^{(2)} = \sum_{j(\neq i)} \frac{T_{ij}^2}{\Delta_j^0} \qquad 1.62$$

and if we consider only nearest neighbours for which $T_{ij} = T$ we get

$$\frac{\delta\Delta_i^{(2)}}{\Delta^0} \simeq z_0 \left(\frac{T}{\Delta^0}\right)^2 \qquad 1.63$$

where $\Delta_j^0 = \Delta^0$ for all j.

$\delta\Delta_i^{(3)}$ is some sort of cross term involving both V_{sd} and T_{ij}. Its magnitude is assumed to lie between those of $\delta\Delta_i^{(1)}$ and

$\delta\Delta_i^{(2)}$. It is not always easy to determine, a priori, which of $\delta\Delta_i^{(1)}$ and $\delta\Delta_i^{(2)}$ is more important for transition metals; but for RE metals $\delta\Delta_i^{(1)}$ clearly should dominate $\delta\Delta_i^{(2)}$. Nonetheless, using plausible values of the relevant parameter Kim was able to show that it is possible for

$$|\delta\Delta_i^{(1)}| \gg \ll \delta\Delta_i^{(2)}$$

In either case $\delta\Delta_i^{(3)}$ may be neglected compared to the dominant term. For $|\delta\Delta_i^{(1)}| \gg \delta\Delta_i^{(2)}$ equations (1.56) and (1.57) may be satisfied since $\delta\Delta_i^{(1)} \lesssim 0$ But for $|\delta\Delta_i^{(1)}| \ll \delta\Delta_i^{(2)}$ only equation (1.57) can be satisfied. We thus have a fairly straightforward explanation of the local environment effect.

The author then goes on to discuss the onset of ferromagnetism at the critical concentration. He starts off by assuming that in the single impurity limit the impurity does not have a localized moment and then calculates the total (i.e. including both impurity and host metal electrons) magnetic susceptibility in the "paramagnetic" state, including the effect of interactions between the impurities, between the impurity and the host, and among the host-metal electrons. These interactions have to be taken account of because the magnetic susceptibilities of the impurity and host metal electrons cannot be independent of each other. The procedure yields a set of coupled equations for the impurity and host susceptibilities which are then solved using a mean field approximation to give the result that the condition for the occurrence of a localized magnetic moment is exactly the same as the condition for the onset of ferromagnetism in the entire system.

Finally the author discusses a number of critical concentration systems and in particular for CuNi alloys he suggests that the polarization clouds observed in neutron diffraction measurements(204) arise from critical exchange enhancement of the matrix surrounding a single magnetic Ni atom just as in PdFe, rather than from a coupling of local moments induced by cooperative effects.

Garland and Gonis (53) while accepting the validity of Kim's treatment of the environment effect in local moment formation, however, rightly criticize the unphysical result regarding the onset of ferromagnetism. They attribute Kim's result to the mean field approximation used in evaluating the matrix susceptibility because such an approximation essentially reduces to a collective electron model of band ferromagnetism. On the other hand we must note Kim's argument that it is impossible for the impurity susceptibility to diverge (corresponding to local moment formation) without the matrix susceptibility diverging if all the interactions within the alloy system are considered. In view of this an obvious conclusion is that something is not quite right with the Friedel-Anderson-Wolff theory of local moment formation.

Garland and Gonis also criticize Kim's view of the polarization clouds in CuNi. In our view this criticism may be unfounded because as will be shown in subsequent chapters the onset of ferromagnetism in those systems which are known to exhibit "giant moment" or "polarization cloud" characteristics is essentially the same. These characteristics arise from the occurrence of a phase transition at the critical concentration.

More importantly Garland and Gonis discuss an addition effect which may arise from the hopping (or direct transfer) integral which Kim (54) did not consider. The hopping integral Tij may split the localenergy levels and give rise to structure and broadening of the d-band. The additional effec refers to this possible splitting of the initially degenerate localized levels (into bonding and antibonding states) and to the change of their occupancies. This is essentially equivalent to some crystal field effect since the covalent admixture (through Tij) is equivalent to a strong crystal field.

Garland and Gonis then give a qualitative discussion of the local environment effect as it applies to TM impurities in non-magnetic hosts. We shall comment only on CUNi alloys in view of what has been said above. Photoemission data (56) in Cu-rich ($\geq$ 77 at % Cu) CuNi alloys show that $\epsilon_d \sim -1$ ev and $\Delta \sim 0.4$ ev. But the authors conclude that an isolated Ni impurity atom cannot support a local moment, which is rather puzzling. Using the above values in equation (1.20) gives $\rho_d(\epsilon_F) \simeq 0.54$ state / ev. atom; also the effective (i.e. allowing for electron-electron correlations as discussed in section 1.5) value of $(U + 4J) \sim 6\text{-}7$ ev for Ni in Cu (see reference 2 for details). It is therefore clear that the HF instability limit is well exceeded! Nevertheless let us assume that for some other reason the Ni atom does not develop a local moment. We then have to consider the effect of the transfer integral $T \sim 0.15$ ev for nearest-neighbour Ni atoms. For a particular Ni atom with z nearest neighbours

the highest antibonding level energy $\varepsilon_d \geq 0.15Z - 1$ ev; it therefore follows that a given Ni atom requires $Z \geq 7$ Ni nearest-neighbours to support a moment.

Garland and Gonis then go on to argue, rather tenuously, that all these neighbouring Ni atoms must also carry local moments, so that their view of a polarization cloud in CuNi alloys is that of a group more than 7Ni atoms all carrying (presumably the same!) local moments.

The importance of the study of local environment effects lies in the fact that such a study could yield the essential features necessary to formulate a proper theory of the magnetism of the transition metals. The pros and cons of the two extreme models of ferromagnetism - the purely localized Heisenberg model and the completely itinerant-electron model - are sufficiently well known (53,57,58). However, it is now generally accepted that any plausible theory of ferromagnetism must contain attributes of both the localized and itinerant models and one step in this direction is the introduction of local correlations into the itinerant-electron picture. Though this is a step in the right direction it probably has not gone far enough. In particular, the local environment effects suggest a local-moment point of view and this cannot readily be described within a collective-electron model. In the same way the existence of a spin-glass magnetic state (see chapter 2) clearly falls outside the limits of the itinerant electron model. These notwithstanding we share the sentiment expressed by Waber (59) that the present tug-of-war between the localized and collective electron models of ferromagnetism may be an action replay of a similar one that occurred many years ago

in another branch of Physics, namely, the wave-particle duality of light. As is now history, there was no victor in that contest. The same situation is envisaged for ferromagnetism and in fact it does not seem to us, in the light of all the available experimental data, that the localized and band aspects of magnetism are mutually exclusive. They, in fact, are necessarily complementary!

1.12 Interactions within an Alloy System

We shall now consider some of the interactions that may occur within a given alloy. These are taken to include

(a) the spin polarization of the host matrix;

(b) direct inter-impurity interactions;

(c) indirect inter-impurity interactions via the conduction electrons of the host matrix.

The Moriya Rules

Using the s-d exchange model Moriya (60) has discussed both the spin polarization of the host matrix by a magnetic impurity and the direct impurity-impurity interactions and obtained a number of semi-empirical rules which govern the sign of these interactions. The rules may be summarised as follows:

(a) Spin Polarization of the host matrix

For simple metal hosts

(i) when the impurity atom has a nearly half-filled d shell the induced moments are mostly antiparallel to the impurity moment.

(ii) when the number of electrons in the impurity atom increases there is an increasing tendency towards parallel spin polarization.

For transition metal hosts

(iii) when the d-band of the host metal is nearly half-filled the induced moments are mostly negative;

(iv) when the number of electrons in the d-band increases there is an increasing tendency towards parallel spin polarization.

In addition there is also the usually positive contribution arising from the direct exchange interaction between the impurity atom and the conduction electrons of the host matrix. Thus with the above rules one expects that in say a Pd matrix Fe, Co, and Ni impurities will give ferromagnetic coupling with the Pd atoms while Cr will give an antiferromagnetic coupling; Mn however will probably give a small but positive spin polarization because of the positive contribution from the direct exchange coupling.

(b) Direct Interaction between Impurity Atoms

The direct inter-impurity interactions comprise crystalline field effects and some covalent admixture of the impurity states. Their effect is to split the VBS orbitals of energy $\varepsilon_{i\sigma}$ into bonding and antibonding orbitals $\varepsilon_{i\sigma}^{-}$ and $\varepsilon_{i\sigma}^{+}$ respectively. For transition metals the crystalline field splitting of orbitally degenerate d-levels is usually much smaller than the width of the VBS and so the effect may be neglected. In the case of the covalent admixture of impurity states (which, as stated above, may be regarded as a strong crystal field effect) further discussion by Moriya (66) leads to the following conclusions:-

(v) the localized magnetic moment already on an impurity atom is not greatly influenced by that on a neighbouring impurity atom provided that the former is sufficiently large

and is in the "saturation range". (N.B. Moriya had already shown that when a localized moment appears it usually has fairly large value or a substantial fraction of its saturation value).

(vi) however where an impurity is just above the HF instability limit then its moment be significantly changed by the covalent admixture;

(vii) A moment may be induced on a non-magnetic impurity atom which is a near-neighbour of a magnetic atom. The induced moment is negative for atoms with nearly half-filled d-shells and positive for atoms with nearly filled d-shells;

(viii) if all the neighbouring impurity atoms are magnetic then there is a tendency for antiferromagnetic coupling for atoms with nearly half-filled d-shells and ferromagnetic coupling for atoms with nearly filled d-shells.

The last two rules have also been obtained by Kim (54) and it is pertinent to recall that Zener (22) had in fact used such rules to explain some of the lattice structures of the transition metals.

(c) Indirect Inter-impurity Interactions

(i) The RKKY Interaction

The idea that the exchange interaction between a localized impurity magnetic moment and the conduction electrons can lead to an indirect coupling between the localized moment derived from a similar problem involving nuclear magnetic moments. Fröhlich and Nabarro (61) first suggested that the contact hyperfine interaction between s-state electrons and nuclear magnetic moments could lead to a coupling between the nuclear moments. This suggestion was later put on a quantitative basis by Rudermann and Kittel

(62)who also showed that it led to a broadening of the NMR absorption. With respect to the magnetism of metals Vonsovskii (63) and later Zener (22) proposed this indirect mechanism as the cause of the ferromagnetism of some of the transition metals. The Zener model involved an antiferromagnetic direct exchange interaction between nearest neighbours which is outweighed by a ferromagnetic indirect exchange interaction. The conduction electrons were assumed to be uniformly polarized with spin parallel to that of the impurity and, as it was shown later, the indirect ferromagnetic coupling turned out to be independent of the separation of the interacting moments, a clearly physically unreasonable result. More detailed investigations of the indirect exchange interaction were carried out by Kasuya (24,64) and Yosida (65). The former investigated the effect of the interaction on magnons and on the electrical resistivity while the latter used it to explain the magnetic properties of the CuMn system. Consequently the indirect coupling of magnetic moments by conduction electrons is usually called the Ruderman-Kittel-Kasuya-Yosida (or RKKY for short) interaction.

To obtain an expression giving the form of this interaction we follow the method outlined by White (66) which is both elegant and fairly straightforward.

On the s-d model the interaction between an impurity spin S_d located at say the origin of the coordinate axes and a conduction electron spin $\underline{s_i}$ at r_i is given by

$$\mathcal{H} = -J \sum_i \underline{S_d} \cdot \underline{s_i}\, \delta(r_i) \qquad 1.64$$

Therefore each conduction electron spin experiences an effective field

$$B_{eff}(\underline{r}) = \frac{-J}{g\mu_B} S_d \, \delta(\underline{r}). \qquad 1.6$$

On a linear response theory the response of the electron gas to such a perturbing field is given by the magnetization $M(\underline{r})$ defined as

$$M(\underline{r}) = \sum_q \chi(q) e^{i\underline{q}\cdot\underline{r}} B_{eff}(q) \qquad 1.66$$

where $\chi(q)$ and Beff (q) are the Fourier transforms respectively of the magnetic susceptibility and effective field. From equation (1.65)

$$B_{eff}(q) = \frac{-J}{g\mu_B} S_d \qquad 1.67$$

Defining the conduction electron spin density $s(r)$ by

$$M_\sigma(\underline{r}) = g\mu_B s_\sigma(r)$$

it follows that

$$s_\downarrow(\underline{r}) - s_\uparrow(\underline{r}) \equiv s(\underline{r}) = \frac{2JS_d}{g^2\mu_B^2} \sum_q \chi(q) e^{i\underline{q}\cdot\underline{r}} \qquad 1.68$$

For a free electron gas

$$\chi(q) = \chi_{Pauli} \, F(q/2k_F) \qquad 1.69$$

where

$$F(x) = \frac{1}{2} + \frac{1}{4x}(1-x^2)\ln\left(\frac{1+x}{1-x}\right) \qquad 1.70$$

is the Lindhard function: Evaluating the sum over q_z in equation (1.68) one obtains

$$s(r) = \frac{3JS_d}{8\varepsilon_F} \frac{nK_F^3}{16\pi} \left\{ \frac{\sin 2K_F r - 2K_F r \cos(2K_F r)}{(K_F r)^4} \right\} \qquad 1.71$$

where n is the number of conduction electrons per unit volume. Equation (1.71) shows that the presence of an impurity spin sets up an oscillating spin polarization in its neighbourhood. These spin-density oscillations have the same form as Friedel's charge-density oscillations which result when an electron gas screens a charged impurity. Another impurity spin $S_{d'}$ at r interacts with this induced spin density leading to an effective coupling between the impurity spins given by

$$\mathcal{H}_{RKKY} = \frac{3nK_F^3 J^2 f(2K_F r)}{128\pi\varepsilon_F} \underline{S}_d \cdot \underline{S}_{d'} \qquad 1.72$$

where

$$f(y) = \frac{y\cos y - \sin y}{y^4} \qquad 1.73$$

is called the Ruderman-Kittel function. For y small $f(y) \to -\frac{1}{6y}$ and since $f(y) = 0$ first for $y = 4.49$ it follows that for $r < \frac{4.49}{2K_F}$ the impurity spins are coupled ferromagnetically and for greater distances the coupling becomes antiferromagnetic and so on.

This oscillatory nature of the RKKY interaction results from the infinite slope of $\chi(q)$ at $q = 2K_F$. Thus finite temperatures or finite conduction electron mean free paths which tend to smear out this singularity will also smear out the oscillations in $J(r)$ at sufficiently large

r . De Gennes (67) has shown that for a finite electron mean free path λ the RKKY function is multiplied by a fact $e^{-r/\lambda}$.

The RKKY interaction is very important not only beca it is responsible for the magnetism of RE metals where its oscillatory nature leads to helimagnetism but also because it is probably the only interimpurity interaction that exist for dilute concentrations of magnetic impurities in non-magnetic hosts. In the latter case it does lead to the now well-known spin-glass state, at sufficiently low temperatures, in which the oscillatory nature of the interaction ensures a nearly random freezing of the impurity spins.

For $k_F r >> \pi$, $\mathcal{H}_{RKKY} \propto r^{-3}$

which shows that the interaction is very long-ranged. This, o course, means that irrespective of the diluteness of the magnetic impurity concentration there will always be a spin-glass type ordering of any existing magnetic centres at sufficiently low temperatures. Another important consequence of the inverse r^3 -dependence of the RKKY interaction is the existence of <u>scaling laws</u> for spin-glasses, according to which the spin-glass ordering temperature, Tsg, is a linear function of the impurity concentration while the reduced magnetization, $\frac{M}{C}$, and the susceptibility, χ , are functions of T/c , the reduced temperature, and B/c, the reduced field i.e.

$$M/c = F(T/c, B/c) \qquad 1.74$$

and

$$\chi = f(T/c) \qquad 1.75$$

We may point out that the above outline of the derivation of the RKKY interaction involves some rather extreme approximations which include:

(a) using a free-electron band structure for the conduction-electrons and hence also the free electron approximation for $\chi(q)$;

(b) assuming that localized electrons on the impurity sites do not overlap;

(c) letting the exchange interaction parameter, J, be wave vector - independent i.e. a delta-function interaction is assumed.

The generalization of the RKKY interaction to non-spherical Fermi surfaces has been discussed by Roth et al (68) and by Rivier (15). They find that in general $\mathcal{H}_{RKKY}$ falls off as r^{-3} and oscillates with a period corresponding to a calipering of the Fermi surface in the direction of r. For the special cases of parallel or cylindrical regions of the Fermi surface a slower fall off, going respectively as r^{-1} and r^{-2}, is obtained thereby considerably increasing the range of interaction. However for Pd with its scaffolded Fermi surface Rivier (15) has attempted to show that the r^{-3} law is still valid. Further discussion of this problem including some other relevant references is given in the review article by Freeman (69).

The use of a free-electron gas approximation for $\chi(q)$ clearly ignores the effects of correlation and exchange which are thought to be important particularly for the incipient ferromagnets (see section 1.10). Various authors (35,70, see also 69) have shown that the effect of any electron-

electron interactions is to increase the range of polarization. For a Stoner enhancement factor of about 10 the spati range of polarization could be increased by up to 50%.

Finally we observe that the fact that J in the Hamiltonian of equation (1.64) is assumed wave-vector independent results in a spin-density oscillation whose asymptotic form $\sim \frac{1}{r^3}\cos(2k_F r)$; this form however diverges at the origin. Several attempts have been made to remove this unphysical result (see reference 69 for details).

(ii) Zener's double Exchange Mechanism

The double exchange mechanism was first proposed by Zener (71) as providing a ferromagnetic coupling between two cations of the same element in an ionic solid through the exchange of valence states via the intervening anion. Suppo C^{+} and C^{2+} represent two valence states of a cation in a given ionic solid. Then the exchange mechanism can be though of as a process in which an electron jumps from say the C^{+} ion to the intervening anion and simultaneously a second electron jumps from the anion to the C^{2+} ion. That this coupling is ferromagnetic may be seen from the simple argumen given by Zener and Heikes (72).

The relevance of this double exchange mechanism to the ferromagnetism of the transition metals is its possible applicability to Ni, especially when we consider the s-d exchange interaction in conjunction with Van Vleck's minimum polarity model (73) involving mainly $3d^{10}$ and $3d^{9}$ Ni atoms. In this case it is obvious that the conduction electron gas would fulfil the role of the intervening anion.

CHAPTER 2

The Phenomenology of the Onset of Magnetism in Transition Metal Alloys

2.1. Introduction

In the preceding Chapter we outlined the Friedel-Anderson-Wolff(FAW) theory of local moment formation according to which an impurity introduced dilutely into a non-magnetic matrix can carry a local moment only if $\frac{U+4J}{\pi\Delta} > 1$, where the parameters have already been defined. We also discussed some of the difficulties inherent in this approach the most pertinent being the absence of any dynamics in the theory, a defect which was partially corrected by the introduction of the concept of a localized spin fluctuations (lsf). The lsf model provided an alternative explanation of the apparent disappearance of a local moment below a certain temperature T_k (the Kondo temperature), an effect that had hitherto been attributed to the formation of a many-body singlet state (the Nagaoka spin-compensated or condensed state). Following this theoretical approach the experimentally observed properties of dilute binary alloy systems consisting of a solute element (which is usually magnetic in the pure state) and a non-magnetic metal host have led to a rather broad classification of solutes as either "good moment solutes", "Kondo solutes" or simply "no-moment Solutes" according as whether the solute is observed to be magnetic, magnetic only above T_k or simply not magnetic at all - within the temperature range of measurement. Likewise the solvents have been classified as

simple metal, simple transition metal and enhanced transition metal solvents (74). In general "good moment solutes" in simple metal solvents are observed to lead to spin-glass ordering in the dilute concentration limit, with the possibility of long-range magnetic ordering setting in at higher concentrations. On the other hand, for either the "kondo moment" or "no moment" solutes apparently the first magnetic state that sets in is the ferromagnetic state (e.g. CuNi). In such cases the onset of ferromagnetism has hitherto been discussed (75-79) as a transition from a strongly exchange-enhanced paramagnetic region (also labelled "nearly ferromagnetic") to a weakly ferromagnetic regime, oftentimes identified as weak itinerant ferromagnetism. The transition occurs at a certain concentration, called the critical concentration, of the magnetic impurity.

Our aim in this Chapter is to show that only a single concentration-dependent parameter is necessary to specify the magnetic behaviour of a given alloy and, following from this, to present a unified, albeit semi-phenomenological, model for the succession of magnetic states as the impurity concentration is varied within the given alloy system. Specifically we propose that the onset of magnetism in these alloys is essentially a phase transition from a non-magnetic region (non-magnetic in the sense described below but certainly distinguishable from the paramagnetic region) to a magnetically ordered state at a well-defined (at least in principle) critical concentration, Cm, of the magnetic impurity. For this purpose, we shall regard

the spin-glass state as a magnetically ordered state even though ideally the individual spins are randomly oriented throughout the system. This is because, as mentioned below, we can define an order parameter for the spin-glass state. Thus magnetic ordering should not necessarily be taken to imply long-range magnetic order. In particular we shall fully explore the thermodynamic consequences in the case where a transition occurs from the non-magnetic region straight into a ferromagnetic regime, deriving in the process, some relations which enable a fairly precise determination of the critical concentration to be made. We may remark here that owing to the difficulty of understanding some of the complex phenomena that accompany this phase transition the concept of a well-defined critical concentration has been recently questioned(80). As will be shown for the CuNi and PdNi systems, without a proper quantitative analysis the determination of the critical concentration from a consideration of the experimental data becomes somewhat subjective in the sense that ad hoc criteria are often used. Such a process has at least, in the case of the afore-mentioned alloy systems, led to wrong values of the critical concentration which is something that is not particularly helpful towards a better and fuller understanding of the behaviour of these systems.

In the section immediately following we critically discuss the Friedel-Anderson-Wolff theory of local moment formation and suggest an alternative and probably more helpful model. We then go on to discuss how this model bears on such important problems as the Kondo effect and

and the magnetism and superconductivity of the transition metals. In section 2.3 we discuss the succession of magnetic states as a function of the impurity concentration while section 2.4 deals with the corresponding order of the phase transitions. In section 2.5 we explore many of the attendant phenomena involved in the non-magnetic-ferromagnetic phase transition. In section 2.6 we analyse some of the available data on a number of alloy systems in the light of the theory developed in the previous section. Section 2.7 criticizes the applicability of the model of weak itinerant ferromagnetism to these systems and finally in section 2.8 we outline a simple qualitative theory of spin-glasses.

2.2.(1) A Critique of the Friedel-Anderson-Wolff Theory of Local Moment Formation

There are two main short-comings of the Friedel-Anderson-Wolff (FAW) theory of local moment formation, one of which is the absence of any dynamics in the theory as previously discussed. Many properties of a large number of alloy systems can be easily understood on the assumption that as the temperature tends to zero the electrical and magnetic properties resemble those of a non-magnetic VBS whereas above some characteristic temperature the properties correspond to those of a magnetic VBS. The FAW model clearly does not allow for this kind of transition which was why the concept of localized spin fluctuations was very welcome. The other defect of the FAW model is the fact that the intraionic correlations are completely neglected. An impurity atom is first stripped of all its electrons outside closed shells (i.e. of its s- and d- electrons)

and then the impurity potential is allowed to interact with the host conduction electrons without any consideration of the Hund's rules correlation. Such an approach has been criticized in the excellent review article by Wohlleben and Coles (4) who maintain that the traditional models could be producing qualitatively wrong trends because of the tendency to overemphasize the itineracy of the impurity d-electrons. They suggest that for real magnetic impurities ionic Hund's rule correlations may be more important than conduction electron - local electron correlations. In other words, theory should have concerned itself with the problem of the <u>persistence</u> of local moments rather than that of their formation. The other main points stressed by the authors may be summarised as follows:-

(i) Redefinition of a local moment: "A local magnetic moment exists if the expectation value of the $\hat{z}$-component of the moment operator over a volume of the order of the lattice cell has a finite value in the limit $B_0 \longrightarrow 0$, $T \longrightarrow 0$". (B_0 is the magnetic induction). The $\hat{z}$-component is chosen because it is the quantity measured in observations in an externally applied magnetic field; moreover, in such measurements one cannot distinguish fluctuations of magnitude of the magnetic moment from the fluctuations of the $\hat{z}$-component.

(ii) With respect to the above definition a local moment can exist in metals only in magnetically ordered state which of course implies the existence of a sufficient concentration of magnetic centres. In the dilute limit no such moment can exist even if an effective moment is

observed in the form of a Curie-Weiss law at higher temperatures because as $T \rightarrow 0$ the ground state of the system consisting of the local moment interacting at least residuall with the conduction electrons must become a singlet state. Apart from the expected Coulomb and exchange interactions between the impurity and host electrons there could exist residual crystal field interactions and residual spin-orbit coupling, the latter resulting from the incomplete quenching of the orbital moment.

(iii) Consequently there must exist a temperature, T^* say, below which the motion of the axis of the local moment is dominated by the intrinsic fluctuations due to these residual interactions with conduction electrons rather than by thermal fluctuations (which give the Curie-Weiss behaviour). The magnetic susceptibility of the impurity in a finite field will be less than without the residual interactions and the zero-field susceptibility cannot diverge at absolute zero because

$$\lim_{\substack{B_0 \rightarrow 0 \\ T << T^*}} \chi = \frac{\mu_{eff}^2}{k_B T^*}$$

(iv) For an ordinary electron gas the effective moment is in principle measureable above the degeneracy temperature T_F, where the static susceptibility should obey a Curie law. Nevertheless, even below T_F the z-component of the moment can be observed provided measurements are done on a sufficiently short time-scale $t < \frac{h}{k_B T_F}$ and over a sufficiently small volume. Therefore, it may be useful

to regard the z-component of the magnetic moment (μ_z) as fluctuating intrinsically with a frequency

$$\nu_s = \frac{K_B T_F}{h}$$

In the same way the <u>isolated</u> local moment which has a characteristic temperature T* may be observed if measurements are done in a time $t < \frac{h}{K_B T^*}$.

T* is given by the Kondo-Suhl-Abrikosov formula

$$T^* = T_F e^{-\frac{1}{|J_{sd}|\rho_s(\epsilon_F)}} \qquad 2.1$$

where J_{sd} is the (negative) effective s-d exchange integral which may be written as

$$J_{sd} = J_0 S \;;$$

S is the impurity spin and Jo depends only on the matrix. This approach ties in with the lsf model proposed by Rivier and Zuckermann (30) among others, but the authors suggest that these spin fluctuations are different from those that are thought to occur in alloy systems where the host is exchange-enhanced e.g. <u>Pd</u>Ni.

(v) In some RE metals and intermetallic compounds intermediate valence phases are known to exist in which there is a continuously reversible variation of the proportion of the valence phases with either pressure or composition of the system. Other features of the phenomena associated with "soft" RE moments include the absence of magnetic order, a constant susceptibility as $T \rightarrow 0$, and an "intermediate" susceptibility at higher temperatures. The basic ingredients of the intermediate valence state seem to be

only the occurrence of two ionic states and a conduction band. Physically it is more reasonable to imagine that the intermediate state is spatially homogeneous i.e. the time average is identical on each ion ('temporal mixture') rather than being a "spatial mixture" - a static spatial distribution of ions with different integral valences. The occurrence of a temporal mixture is of course, in line with the hybridization (or mixing-in) between the 4f and conduction-electron states as required by the FAW theory. In the magnetic state little or no mixing apparently occurs. The authors then conclude that at least non-magnetic rare-earths and possibly also TM impurities may have well-preserved Hund's rules correlations even in the non-magnetic limit.

(vi) Finally the authors give a brief discussion of the Hirst ionic model (81) which can explain many of the experimental features observed for RE metals and their compounds. In this model ionic many-electron states are assumed to exist. Hund's rules correlations result in an integral occupation of the magnetic shells. Consequently the ionic states may be perturbed but cannot be broken up by interactions with the conduction electrons. The relative positions of the ionic energy levels are given by

$$\mathcal{E}_n = \frac{1}{2} n(n-1)\epsilon_0 + nV_0 + \text{constant}$$

where ϵ_0 is the electron-electron interaction energy within the magnetic shell; V_0 is the nuclear potential energy and n is the occupation number of the shell.

$$\therefore \quad \varepsilon_n = \tfrac{1}{2}(n-n_{min})^2 \epsilon_0 \quad + \text{ constant} \qquad 2.2$$

The value of n_{min} is continuously variable being affected by pressure (via the band structure) and local environment. The interaction of the conduction electrons with the local electrons results potentially in an effective width Δ given by equation (1.21). However, the mixing can occur only if the excitation energy $\varepsilon_{exc} \sim |\varepsilon_n - \varepsilon_{n+1}|$; thus there exists an effective energy gap for mixing whose value depends on n_{min}. Effective mixing can only occur if

$$\Delta \gtrsim \varepsilon_{exc} \qquad 2.3$$

which condition replaces Anderson's Stoner-type criterion for the HF instability.

The above points have been dealt with at some length because we agree with these general points raised by those authors even if not in their exact details. However, before expanding these points we would like to examine exactly how the Anderson theory applies to real alloy systems. We recall that on this theory an impurity atom should carry a localized moment if

$$\frac{(U+4J)_{eff}}{\pi\Delta} \geq 1 .$$

(equation 1.25)

We shall therefore discuss how the experimentally determined values of the effective Coulomb and exchange integrals compare with the measured widths of the virtual bound states.

Such a comparison has already been made by Heeger (2) and once again we shall be content with just a summary of the relevant points.

(a) The free atom values of U range from 13-20 eV while $J \sim 1$ ev. (82). If these values applied to metals then all impurities would be magnetic since Δ is expected to be about 1 ev. However, the value of U in metals is reduced owing to screening by conduction electrons and to d-electron many-body correlation effects. According to Herring (82b) for Ni $U_{eff} \sim 0.5$ ev and $J_{eff} \sim 0.1$ ev; if these values are taken as being representative of the TM group with respect to the dilute impurity problem then no impurity atom would be magnetic. The existence of magnetic impurities with effective moments nearly equal to the maximum possible suggests that $(U + 4J)$ eff is of the order of a few electron volts.

(b) Spectroscopic and photoemission experiments on alloys of Cu, Ag and Au with Pd, Mn, and Ni (56, 83-85) clearly confirm the existence of VBS. For AuNi, AgPd and CuNi only a single VBS was observed but for AgMn both the up-spin and down-spin VBS were observed, at +1.6 ev. and -3.25 ev. respectively, with respect to the Fermi level. Thus for AgMn $(U + 4J)_{eff} \simeq 5$ ev. The CuMn data indicate a similar value. Since the splitting is due to intra-atomic Coulomb and exchange interactions one would expect this result to be independent of the matrix.

(c) Values of $(U + 4J)$ eff can also be indirectly obtained from an analysis of the enhanced susceptibility data for "non-magnetic" impurities. Such analyses for

CuNi and BeNi systems gave $(U + 4J)$ eff $\sim$ 6 - 7 ev. almost independent of the matrix. The apparent constancy of the deduced values of $(U + 4J)$ eff shows that metallic screening is not overly sensitive to the details of the host.

(d) In addition to the condition for the existence of a spin magnetic moment (equation (1.24)) Anderson (12) also derived a condition for the formation of orbital moments which is that

$$(U - J)_{eff}\ \rho_{dl}(\varepsilon_F) = 1 \qquad 2.4$$

where $\rho_{dl}(\varepsilon_F)$ is the impurity density of states per orbital at the Fermi level. The nearly complete quenching of orbital moments of Fe-group atoms in noble metals sets an upper limit on (U-J) eff whereas the existence of spin moments for Cr and Mn in these hosts gives a lower bound to the value of (U +4J) eff. Using such arguments Yosida et al (86) deduced that for TM Ueff $\sim$ 3.5 ev and Jeff $\sim$ 1 ev almost independent of the host matrix. We see from the foregoing that estimates of $(U + 4J)$ eff from the optical and magnetic susceptibility measurements are about the same showing that d-electron correlations are also not very effective in reducing the Coulomb and exchange interactions in the dilute alloy problem in clear contrast to the situation suggested by Herring (82b) for the pure transition metals.

(e) The width, Δ , of the VBS is expected to be host dependent, since it depends on the density of states of the conduction electrons at the d-level resonance. However

estimates of this parameter for TM impurities in simple metals from a wide variety of experiments give values of Δ lying between 0.2 — 0.6 ev.

From the above values of Ueff, Jeff and Δ it is clear that for TM impurities in simple metal hosts

$$\frac{(U+4J)_{eff}}{\pi\Delta} > 1$$

which is well above the HF instability and hence these impurities should in all cases be observed to magnetic. The fact that experimentally this is not so shows up a basic defect of Anderson's theory of local moment formation.

Having noted (i) some of the valid points raised by Wohlle ben and Coles (4) as outlined above, and (ii) the fact that the experimentally determined values of U, J and Δ require that, according to the HF instability criterion, TM impurities in simple metal hosts should always be magnetic and, above all, recognizing the basic defects of the FAW theory as already discussed we now suggest the following model to explain the magnetic behaviour of TM alloys.

(2) Outline of Model

(a) We accept the experimentally proven (and physically plausible) existence of virtual bound states.

(b) In the FAW model there exists initially only a single impurity d-level resonance which is then broadened by interaction with conduction electrons into a VBS. This VBS may or may not be spin-split depending on whether the local moment instability limit is exceeded or not. In contrast we shall assume that in the favourable cases (i.e. with the possible exception of Sc, Y and La

whose free atom d-shells contain only a single electron) the intraionic Coulomb and exchange correlations are sufficiently strong to give <u>two</u> resonance d-levels corresponding to $\varepsilon_{d\uparrow}$ and $\varepsilon_{d\downarrow}$. In other words, the d-level resonance is exchange-split <u>ab initio</u>. The splitting is such that the resulting magnetic moment is <u>almost</u> the same as would be expected on the basis of Hund's rules correlations for the d-electrons in a free atom. The implicit assumption is made here that the impurity atom **S**-electrons merge into the host conduction band. The exact form of the exchange splitting may depend on a number of other factors such as crystalline field effects but we shall ignore such fine details for now. We take it that the exchange splitting, which will be denoted by Δ_o, is of the order of the intraionic Coulomb interaction, U.

(c) The effect of the conduction electrons is, as before, to broaden the exchange-split resonance levels into spin-up and spin-down virtual bound states via the s-d mixing interaction (but note the discussion below). Each resonance level now acquires a width Δ given by equation (1.21) with the proviso that $\rho_s(\varepsilon_F)$ is now the density of states <u>per spin index</u> of the host conduction electrons at the Fermi surface. Thus owing to the s-d mixing interaction the localized moment now acquires and intrinsic fluctuating frequency, or to put this in another way, there exists now a characteristic temperature, T* for the local moment-conduction electron system. The lifetime, τ_{sf}, of the localized spin fluctuations is defined by

$$h\tau_{sf}^{-1} = k_B T^* \qquad 2.5$$

which is the same as equation (1.44) except that we have replaced T_k by T^*. This replacement is considered necessary because T_k was first introduced as a result of the Kondo divergence problem (vide section 1.8) which we shall later show to have no general bearing on the local moment problem. T^*, which will also be called the local effective degeneracy temperature, is given by the Kondo-Suhl-Abrikosov formula - equation (2.1) - which however is modified as follows:- instead of equation (1.32) for Jsd, which strictly is valid only in the limit $\epsilon_d \gg \Delta$, we propose that

$$J_{sd} = \frac{-2\langle V_{sd}\rangle^2}{\Delta_o} \sim \frac{-2\langle V_{sd}\rangle^2}{U} \qquad 2.6$$

In the Anderson formulation this relation is approximately valid in the case where the impurity atom is fully spin-polarized with say the up-spin VBS full and lying below ε_F while the down-spin VBS lies at an energy $\sim$ U above ε_F (see reference 87 and also section 1.6, equation (1.29) above). However equation (2,6) may actually be more valid than is immediately apparent. Hitherto, we have used s-d hybridization synonymously with s-d exchange interaction. There is however a subtle difference between the two, as clearly expressed by Ziman (87). In principle the s-d hybridization only links s- and d- states of the same spin whereas the

s-d exchange mixing interaction involves s- and d-electrons of opposite spins. Applying perturbation theory to the latter situation gives an expression of the form of equation (2.6). From equations (1.21) and (2.6) we obtain that

$$J_{sd}\, \rho_s(\varepsilon_F) = -\frac{2\Delta}{\pi\Delta_o} \qquad 2.7$$

and so

$$T^*_{imp} = T_F\, e^{-\frac{\pi\Delta_o}{2\Delta}} \qquad 2.8$$

where T_f is the effective degeneracy temperature of the host. For example, for AgMn $\Delta_o \simeq 5$ ev, $T_f \sim T_F = 6.36 \times 10^4$ K and with $\Delta \sim 0.5$ ev one gets $T^*_{Mn} \sim 10$ mK, which is of the right order of magnitude (74). Similar values would be expected for Cu and Au matrices. However we shall emphasize that even though we believe the functional form of equation (2.8) is correct its method of "derivation" is certainly less than rigorous.

Equation (2.8) shows that if $\Delta_o = 0$, which either implies complete s-d hybridization or a full d-shell, then $T^*_{imp} = T_f$, as should be expected. For a finite Δ_o it follows that T^*_{imp} is always less than T_f. On the other hand, for $\Delta = 0$ i.e. an infinitely sharp resonance level, $T^* = 0$. This situation is however impossible because for an isolated impurity atom there will always exist residual local moment-conduction electron interactions (4) so that T^* may be extremely small but certainly finite. Note that the important parameter is the

ratio of $\frac{\Delta_o}{\Delta}$. If this is small then the system has a high characteristic temperature. Physically, we could say that the s-d mixing interaction broadens the resonance levels so much that they nearly merge into a single VBS which would appear to be non-magnetic. But if $\frac{\Delta_o}{\Delta} \gg 1$, then the system would have a very low characteristic temperature and would be readily observed to be magnetic.

A comparison of our approach to the local moment problem with the traditional Anderson model is illustrated in figures 2.1 and 2.2. The diagrams are self-explanatory.

In retrospect it does seem that Ziman (87) actually did not fully agree with the details of the FAW theory. For one thing, he started off with the exchange-split d-level resonances as we have done but then failed to consider the dynamics of the system.

(d) If the orbital angular momentum is not completely quenched there will exist a residual spin-orbit coupling of the form

$$\mathcal{H}_{so} = \lambda \underline{L} \cdot \underline{S} \equiv \lambda \left[L_z S_z + \tfrac{1}{2} \{ L^+ S^- + L^- S^+ \} \right] \qquad 2.9$$

where λ is the spin-orbit coupling constant and the other symbols have their usual meaning. The first term in equation (2.9) splits the impurity d-levels and the corresponding VBS. It is this term which is responsible for the left-right asymmetry in conduction electron scattering and hence also for the Hall effect (88), because the phase shifts are dependent on the eigenvalues of S_z. The second and third terms mix the spin-up and

Schematic Illustration of Local Moment Formation in a Simple Metal Host

Fig.2.1: The FAW Model (after ref.3)

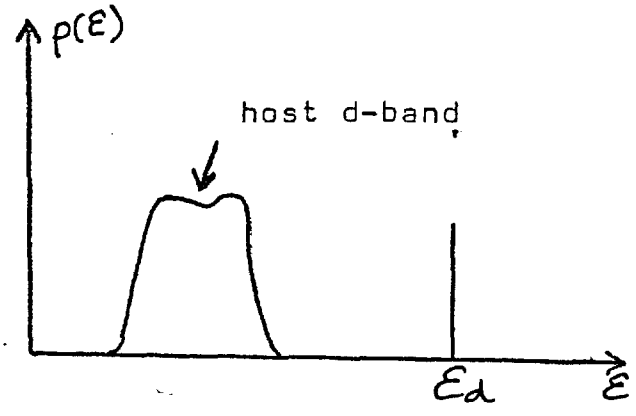

(a) no s-band; single sharp d-resonance.

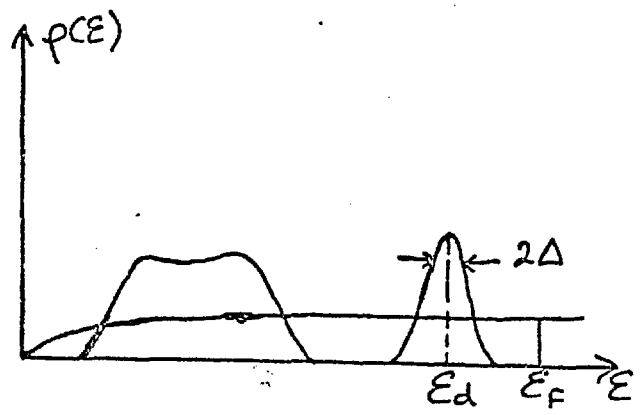

(b) s-band broadens resonance into a VBS: here the VBS is non-magnetic i.e. $\frac{U+4J}{\pi\Delta} < 1$

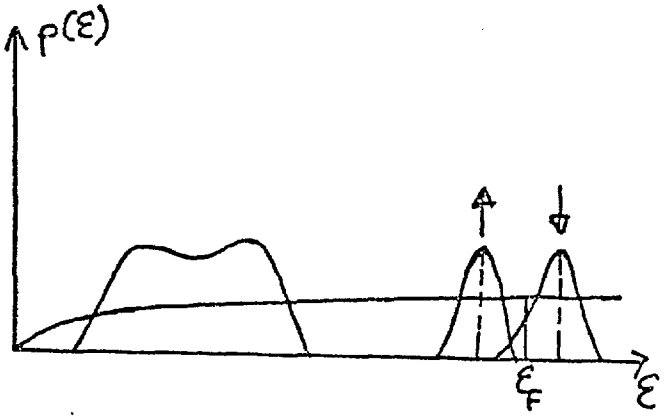

(c) VBS magnetic; $\frac{U+4J}{\pi\Delta} \geq 1$

Fig.2.2: Proposed Model

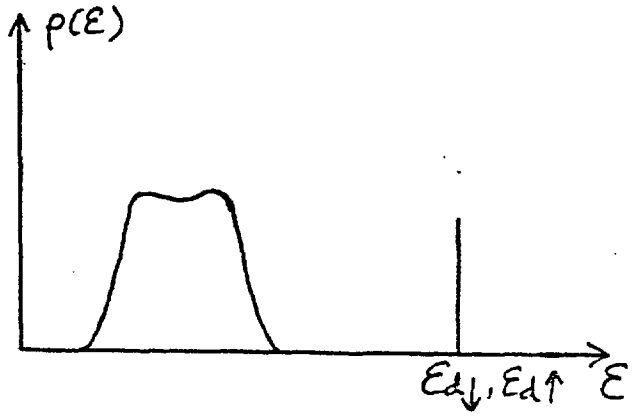

(a) d-resonance exchange-split ab initio but levels degenerate in the absence of the s-band.

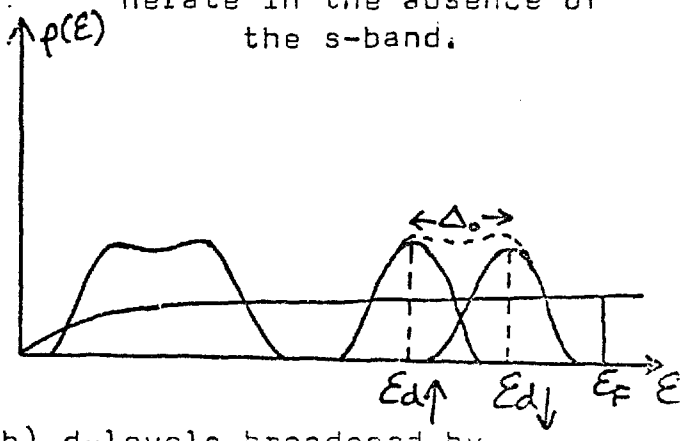

(b) d-levels broadened by s-band; here $\Delta \sim \Delta_o$ so that $T_o^* = T_f e^{-\frac{\pi\Delta_o}{2\Delta}}$ is high.

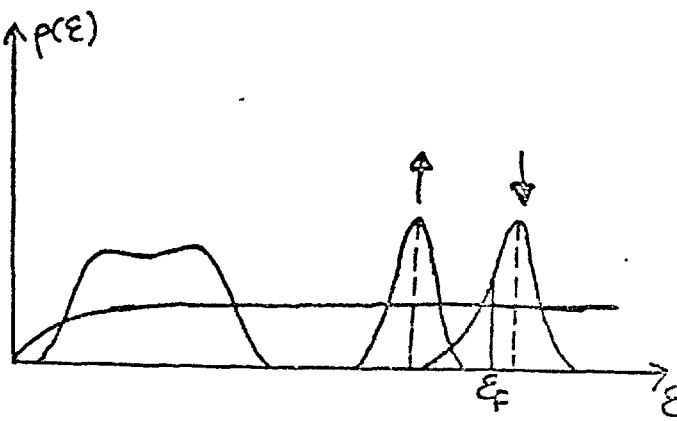

$\Delta \ll \Delta_o$

(c) Small T_o^*

spin-down VBS. This splitting is usually weak since $\lambda \underline{L}.\underline{S}$ is much smaller than the exchange splitting. However Yafet (89) has shown that when the VBS is spin-split λ may be enhanced owing to what he calls "the lowering of the correlation energy". He obtained that

$$\lambda_\sigma = \frac{\lambda_o}{1-(U-J)\rho_\sigma(\varepsilon_f)} \qquad 2.10$$

where λ_o is the unenhanced spin-orbit coupling constant. Observe that if both equation (2.4) and (2.10) are correct the appearance of an orbital moment would be accompanied by an infinite spin-orbit coupling constant. Ignoring this aside one can see that any intra-ionic spin-orbit coupling would give the resonance levels a finite width Δ_{so}, even in the absence of the s-d exchange mixing interaction. In general therefore, we should write

$$\Delta = \Delta_{sd} + \Delta_{so} \qquad 2.11$$

where Δ_{sd} is the width arising from s-d mixing interactions and Δ_{so} will be taken to include the effects of both the intraionic spin-orbit coupling and also that between the residual impurity orbital moment and the conduction electron spin. Δ_{so} Should be particularly important for elements at the beginning and end of each transition series.

(3) Having outlined the essential details of the model we can now discuss some of its immediate consequences:

(i) Local Environment Effects

As defined by equation (2.8) T^*_{imp} applies to only an isolated impurity atom. This, of course, is an ideal since it is not practicable to put only a single impurity atom into a given matrix. In practice one therefore has to consider a finite concentration of impurities and hence the concomitant interactions amongst them. As discussed in section 1.11 the effect of interimpurity interactions may be taken as a change in the effective width of the VBS. This proposal is in line with suggestions made by Caroli (90) and Tournier (91) that Friedel oscillations of charge density, induced by other impurities, generate a local variation of the density of the VBS at ε_F and so are able to influence the magnetic behaviour. Instead of equation (2.11) we should now write

$$\Delta = \Delta_{sd} + \Delta_{so} + \Delta_{dd} \qquad 2.12$$

where Δ_{dd} is the contribution to the effective width of the VBS arising from interimpurity interactions. The resultant effect is that Δ becomes concentration dependent so that

$$T^*_{imp} = T^*_{imp}(c)$$

Table 2.1 shows the variation of the width of the VBS with impurity concentration for the AuNi system (85).

Table 2.1 Variation of Δ with impurity concentration C for AuNi system

C at % Ni	Δ ev.	ϵ_d ev.
1.2	0.129	0.495
1.8	0.102	0.457
4.7	0.059	0.534

The authors cautioned against determining VBS parameters from transport properties alone.

According to equation (1.58) Δ_{dd} consists of three terms

$$\Delta_{dd} = \delta\Delta^{(1)} + \delta\Delta^{(2)} + \delta\Delta^{(3)} ;$$

$\delta\Delta^{(1)}$ comes from <u>indirect</u> interimpurity interactions mediated by the host matrix conduction electrons. Not surprisingly it has an oscillatory behaviour similar to the RKKY interaction and so it may be positive or negative; $\delta\Delta^{(2)}$ is due to a <u>direct</u> transfer interaction between the impurities and is always positive; Lastly $\delta\Delta^{(3)}$ is a cross-term between $\delta\Delta^{(1)}$ and $\delta\Delta^{(2)}$ As mentioned in section 1.11 it is not always possible to determine, ab initio, which of $\delta\Delta^{(1)}$ and $\delta\Delta^{(2)}$ is the dominant term. The possibility exists that $|\delta\Delta^{(1)}|$ could be much larger or much smaller than $\delta\Delta^{(2)}$. In either case we may neglect $\delta\Delta^{(3)}$ compared with the dominant term. Thus for the ith impurity

$$\Delta_{dd}{}^{(i)} = \sum_{j \neq i}^{Nc} \left\{ \delta\Delta_j^{(1)} + \delta\Delta_j^{(2)} \right\} \qquad 2.13$$

but if we consider only the nearest neighbours of a given impurity atom then

$$\Delta = \Delta_{sd} + \Delta_{so} + z_o c\left\{\delta\Delta^{(1)} + \delta\Delta^{(2)}\right\} \qquad 2.14$$

where Z_o is the coordination number of the lattice. Since $\delta\Delta^{(2)}$ is always positive we should perhaps rule out the possibility that $|\delta\Delta^{(1)}| \lll \delta\Delta^{(2)}$ because

this would imply that in all cases T*imp will increase as the impurity concentration increases. It is more physically plausible to suppose that in all cases $|\delta\Delta^{(1)}| \gtrsim \delta\Delta^{(2)}$. In fact, Kim (54) has shown that

$$\frac{|\delta\Delta^{(1)}|}{\delta\Delta^{(2)}} \simeq \frac{4}{(2K_F r_0)^2}\left(\frac{\Delta}{T}\right)^2 \qquad 2.15$$

where r_0 is the nearest neighbour distance and T is the direct transfer integral between impurities. In the tight-binding approximation the bandwidth $W \sim 2Tz_0$. Therefore, for transition metals $T \sim \frac{W_d}{2z_0}$ where W_d is the bandwidth of the d-electrons. For the host metal $\rho_s(\epsilon_F) \sim \frac{N}{W_c}$ where W_c is the bandwidth of the conduction electrons and N is the number of atoms per unit volume. Thus

$$\Delta \sim \pi \langle V_{sd}\rangle^2 \frac{N}{W_c} \qquad 2.16$$

If we take $2K_F r_0 \sim \pi$, then

$$\frac{|\delta\Delta^{(1)}|}{\delta\Delta^{(2)}} \sim 16 z_0^2 \left\{\frac{N\langle V_{sd}\rangle^2}{W_c W_d}\right\}^2 \qquad 2.17$$

Now $N^{\frac{1}{2}}\langle V_{sd}\rangle$ is of the order of one particle energy, $\sim$ 1-2 ev say while $W_c \sim 5$ ev and $W_d \sim 3$ ev. Since the smallest value of z_0 is 8 (lattice structures are either bcc, fcc or hcp) it immediately follows that at least $|\delta\Delta^{(1)}| \gtrsim \delta\Delta^{(2)}$. Equation (2.14) gives an approximate relation for the variation of the width of the VBS with the impurity concentration. Let us suppose that, in fact, $|\delta\Delta^{(1)}| > \delta\Delta^{(2)}$; then since $\delta\Delta^{(1)}$ could

be positive or negative there exists the possibility of interimpurity interactions increasing or decreasing the width of the VBS. In the latter case T*imp decreases as the impurity concentration increases and we can immediately define a critical concentration, Cm, above which all impurity atoms should be observed to be magnetic by stipulating that

$$T^*_{imp}(C_m) = 0 \quad . \qquad 2.18$$

As Δ_o, the exchange splitting, depends mainly on the intraionic Coulomb and exchange interactions and possibly also on the lattice structure (via any crystalline field effects) it is not much affected by the interimpurity interactions. Therefore $T^*(Cm)=0$ implies that $\Delta(Cm)=0$, and hence we obtain that

$$C_m \geq \frac{\Delta_{sd} + \Delta_{so}}{z_o\left\{|\delta\Delta^{(1)}| - \delta\Delta^{(2)}\right\}} \qquad 2.19$$

It is obvious that the above scheme allows the formation of magnetic clusters and so provides a ready explanation of local environment effects. For, if owing to statistical fluctuations in the impurity concentration, a given impurity atom finds itself with z nearest neighbours of its own kind (where $z_o \geq z \geq z_o c$), then the width of its VBS will be less than the average width for the impurity atoms so that its local characteristic temperature will be less than T*imp. Denoting the characteristic temperature of an impurity atom surrounded by z other atoms of its own species by T^*_z we then have that

$$T^*_{zo} < T^*_{zo-1} < \cdots\cdots < T^*_z < \cdots\cdots < T^*_{imp} \qquad 2.20$$

If an observation is made at a temperature, T exp, only clusters containing at least z impurity atoms will be classified as magnetic if T exp $\geq$ T*z. A cluster containing (z-1) impurity atoms may be observed to be nearly magnetic because T*z-1 may just be greater than T exp. Thus we have an explanation of why it is possible for pairs, triplets, etc. of impurity atoms to appear to be magnetic whilst individual impurity atoms do not. In the same way if $\delta\Delta^{(1)}$ is positive then

$$T^*_{zo} > T^*_{zo-1} > \cdots\cdots > T^*_z > \cdots\cdots > T^*_{imp} \qquad 2.21$$

but, of course, in this case no critical concentration would exist for the truly <u>disordered</u> alloy; however, the system can still be magnetic if for some impurity concentration there exists an <u>ordered</u> structure of the alloy in which an impurity atom has no nearest neighbours of its own species, as in Au_4V. Observe that because of the oscillatory nature of $\delta\Delta^{(1)}$ it is possible for the first and second nearest neighbour impurity atoms to affect a given impurity atom in opposing ways.

(ii) <u>The Kondo Problem</u>

The magnetic phase diagram that emerges from our model is sketched in part in figure 2.3

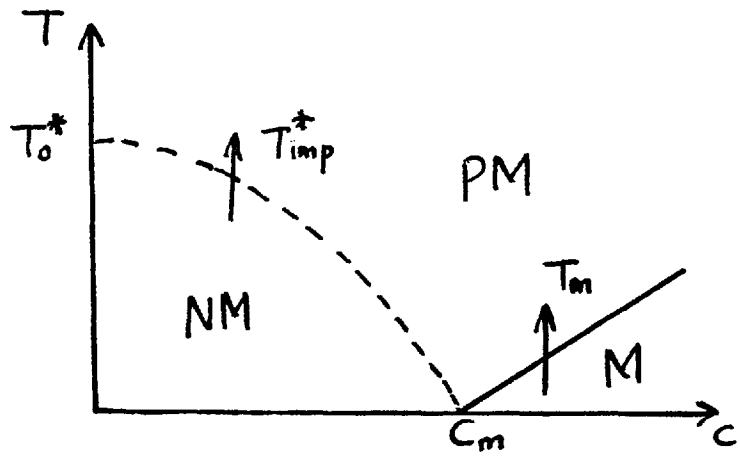

Fig. 2.3

Sketch of part of a general magnetic phase diagram.

As the impurity concentration is increased the characteristic temperature decreases from a value T^*_o appropriate for the single impurity limit (equation (2.8)) to zero at the critical concentration c_m above which a magnetically ordered state exists. The magnetic region (M) is separated from the paramagnetic region (PM) by a normal phase boundary. The PM region is also demarcated from the non-magnetic region (NM) by the boundary traced by the locus of T^*_{imp} as a function of the impurity concentration. As already mentioned (section 1.9) and as will be further discussed below (sections 2.3 and 2.4) the transition from the NM region to the PM region cannot be a proper phase transition. It is dominated by spin fluctuation effects.

Usually the onset of a magnetically ordered state is preceded by a cluster-region. The magnetically ordered state could either be ferromagnetic or spin-glass, but in the latter case there is the possibility of long-range magnetic order setting in at higher impurity concentrations. Only in a few cases (RuFe and MoCr) does it appear that no such cluster regions exist there being a straight transition from the non-magnetic region to a

spin density wave region (otherwise referred to as "itinerant antiferromagnetism").

We wish to consider the origin of the Kondo divergence which, in various ways, has been primarily associated with the existence of the non-magnetic region. Let us take an alloy with an impurity concentration which is slightly greater than c_m. Such an alloy will clearly have a fairly low magnetic ordering temperature, T_m say. Sufficiently above T_m the system consists of a collection of very weakly interacting spins from which conduction electrons may scatter. We recall that the effective impurity - conduction electron exchange integral consists of two terms - a direct positive (i.e. ferromagnetic) term and an indirect negative term. For the 3d transition metal impurities the indirect term generally dominates giving an effective negative exchange integral Jsd. The possible exception is Mn which may give a slightly positive nett polarization (see section 1.12(a)). For rare-earth impurities, however, the opposite appears to be the case (except for Ce) there resulting generally a positive effective exchange integral. This difference in the behaviour of 3d transition metals and the rare-earths is important when we realise that the explanation of the Kondo resistance minimum requires an s-d Hamiltonian with a negative Jsd whereas the Abrikosov-Gor'Kov theory (92) of paramagnetic impurities in superconductors uses an s-d Hamiltonian with a positive Jsd. Not surprisingly the latter theory works particularly well for superconductors doped with Gd.

For an s-d Hamiltonian with a negative exchange integral we have seen (section 1.7) that carrying out perturbation theory calculations beyond the first Born approximation can explain the occurrence of a resistance minimum. At temperatures below that corresponding to this minimum the resistivity varies as lnT. The perturbation theoretic calculation unfortunately ceases to be valid at a temperature, T_k, defined in equation (1.39), and it is this temperature that has so far been taken to signal the onset of the non-magnetic regime. It is this assumption that we wish to clarify and in doing so to also point out two aspects of the Kondo effect that appear to have been confused with each other. The two aspects of the Kondo resistance minimum refer to two different regions of the phase diagram sketched in figure 2.3. In the region to the right of c_m the impurity spins are well-defined <u>at all temperatures</u> and interact with one another. Above T_m the interimpurity interaction energy is smaller than the thermal fluctuation energy and one is justified in considering the s-d Hamiltonian as the only perturbation on the electron energies, thus deriving equation (1.35) as outlined. However, this perturbation calculation ceases to be valid at about the temperature corresponding to the energy of the inter-impurity interactions. In other words, in this case the divergence of the lnT term in the resistivity is not due to the onset of the non-magnetic regime ($T < T^*_{imp}$) but is the result of the neglect of interimpurity interactions in the original Hamiltonian. In most cases of interest (excluding <u>Pd</u>-based alloys of Mn, Fe and Co) the magnetic

ordering that sets in is a spin-glass type for which both experiment (93) and theory (94) appear to indicate a resistivity varying as

$$\rho(T) = DT^{3/2} \qquad 2.22$$

where D is a weak function of the concentration. Experimentally (93) D is found to vary as $c^{-1/5}$ or equally as $\ln c$. In a hand-waving sort of way one may expect the resistivity for $T \lesssim T_m$ to vary as the sum of eq.(1.38) and (2.22) i.e.

$$\rho(T) = A - Bc\ln T + DT^{3/2} \,. \qquad 2.23$$

Consequently a resistivity maximum occurs at a temperature $To \sim (\frac{2Bc}{3D})^{\frac{2}{3}}$; if we take it that $D \sim c^{-1/5}$ then $To \sim c^{0.8}$. This concentration dependence is nearly the same as that expected for T_m ($\equiv T_{sg}$) in a spin-glass system for which the scaling laws are applicable i.e. $T_m \propto c$. In fact, near T_{sg} and above, the resistivity does not vary as $T^{3/2}$ but rather as T. This would give $To \sim c$. However, eq.(2.23) should not be taken too seriously because we are not certain that both the $\ln T$ and the $T^{3/2}$ terms should be <u>simultaneously</u> present for a <u>spin-glass alloy</u>. What we wish to point out is that the maximum in the resistivity of a "dilute" TM alloy is closely related to the onset of spin-glass freezing.

At sufficiently low temperatures the excitations of the spin-glass state should be frozen out and $\rho(T)$ should then tend to its residual value, ρ_0. Thus we expect the electrical resistivity of alloys in the region $c > c_m$ to vary with temperature as sketched in Fig.2.4

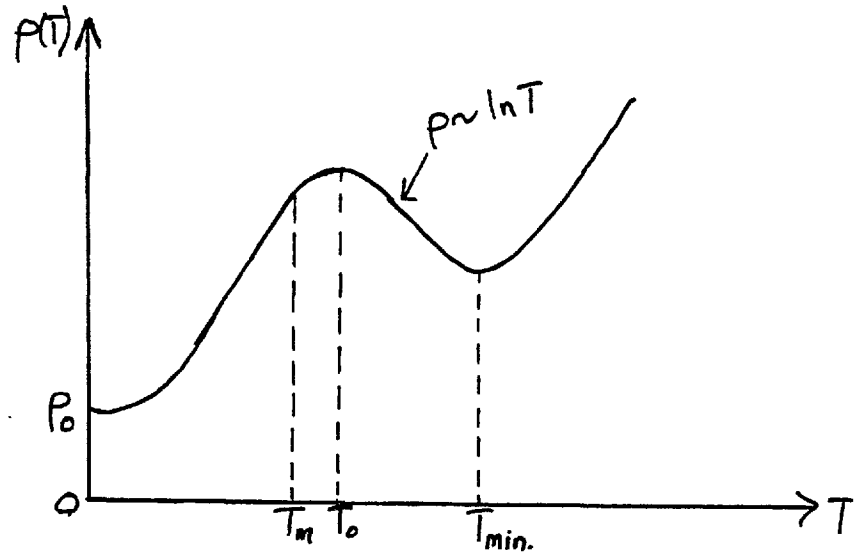

Fig. 2.4

ρ(T) for an alloy exhibiting a Kondo resistivity minimum

Suitable examples of alloys to which preceding discussion should apply are alloys of Mn with the noble metals and also with Zn and Cd. For these alloys c_m is only a few ppm as previously mentioned and even for such concentrations interimpurity interactions are bound to become important at some finite temperature. This has been clearly shown in the ultra-low temperature susceptibility measurements of Hirschkoff et al. (96) - interaction effects were observed down to concentrations of about 9 ppm!

In the special case of Pt Mn a minimum occurs near the spin-glass freezing temperature (95) and has been attributed to the fact that the electrostatic potential due to the difference between the core charges of Pt and Mn is larger than the Pt bandwidth (530).

We should compare the above explanation of the resistivity maximum observed in some alloys exhibiting the Kondo resistance minimum with that proposed by Beal-Monod (97) and Matho and Beal-Monod (98). These authors considered a pair of spins S_1, S_2, coupled by an exchange energy

$$\mathcal{H}_{MBM} = -W_0 \underline{S}_1 \cdot \underline{S}_2 \qquad 2.24$$

where the spin-coupling energy W_0 has the spatial dependence

of the RKKY interaction. The eigenstates $|j,m\rangle$ of the above Hamiltonian are characterized by the total spin quantum number $j=0,1\ldots,2S$ and the magnetic quantum number $m_1 + m_2 = -j, \ldots\ldots, +j$. The energy levels $\mathcal{E}_j$ are given by

$$\mathcal{E}_j = \text{constant} - \tfrac{1}{2} W_0 j(j+1) \qquad 2.25$$

and are $(2j+1)$ - fold degenerate in m. Inelastic transitions are assumed to occur from a given level j to neighbouring levels $j \pm 1$. Using a perturbing Hamiltonian consisting of a potential scattering term and $\mathcal{H}_{MBM}$ and carrying out the perturbation calculation to the third order in W_0 the authors derived that the additional resistivity due to a single pair of interacting impurity atoms is given by

$$\rho_p = 2R_m \rho(\mathcal{E}_F) \left\{ V^2 + \rho_{ps} \right\} \qquad 2.26$$

V is the potential scattering term, and Rm is an atomic constant first introduced in section 1.7 ($\equiv \frac{2\pi m^*}{\nu \hbar e^2 N}$ where m^* is the effective electron mass, ν is the valency of the host matrix and N is the number of atoms per unit volume). ρ_{ps} is the spin-part of the pair resistivity. It is given by

$$\rho_{ps} = \frac{\Gamma^2}{8\rho^2(\mathcal{E}_F)} S^2_{eff}\left(\frac{W_0}{k_B T}\right) \begin{cases} 1 + \Gamma \ln \frac{T}{T_F} + \Gamma \ln \frac{(T^2 + T_{W_0}^2)^{1/2}}{T_F} ; & W_0 > 0 \\ 1 + 2\Gamma \ln \frac{(T^2 + T_{W_0}^2)^{1/2}}{T_F} ; & W_0 < 0 \end{cases} \qquad 2.27$$

where

$$\Gamma \sim 2 |W_0| \rho(\mathcal{E}_F),$$

and $S^2_{eff}\left(\frac{W_0}{k_B T}\right)$ is the effective spin amplitude i.e. the factor S(S+1) modified by the exchange coupling W_0

For $W_0 \neq 0$, $\lim_{T \to 0} S^2_{eff} = \begin{cases} S(S+1) & ; W_0 > 0 \\ 0 & ; W_0 < 0 \end{cases}$

It is the thermal variation of S^2_{eff} which is the dominant effect of the pair interaction on the resistivity. A consequence of the interaction is a modification of the "Kondo temperature" of the pair, T_{pk}, as a function of the coupling strength W_0. For antiferromagnetic coupling T_{pk} tends to zero at some value of W_0 whereas for ferromagnetic coupling T_{pk} decreases less rapidly and does not tend to zero.

The calculation was then extended statistically to cover all pairs in a random dilute alloy, the resistivity $\rho(c,T)$ being developed as a function of the impurity concentration up to the c^2 term. The resulting expression was then used to analyse the experimental data on a number of alloys of Mn with Au, Ag, Zn and Cd. Satisfactory agreement was obtained for two AuMn alloys (containing 500 and 1000 ppm Mn) and on AgMn (558 ppm Mn). For higher and lower concentrations agreement was poor. It is fortunate that the systems selected were those that have extremely low critical concentrations. Consequently no "Kondo divergence problem" really exists because the concentrations whose data were analysed are well above the critical values so that the impurity spins are well-defined at all temperatures. Therefore the fact that a satisfactory fit was obtained for "moderate" concentrations is a welcome development because it does indicate another method for

calculating the electrical resistivity of spin-glasses as will be briefly discussed later (section 2.8)

The other aspect of the Kondo problem refers to the region of the magnetic phase diagram where the impurity spins are not well-defined at all temperatures i.e.for concentrations $c << c_m$. In this case we have to consider the gradual transition from the paramagnetic region to the non-magnetic region (see figure 2.3), a "transition" that is dominated by spin fluctuations. It is this particular phenomenon that has been incorrectly described as the formation of a magnetic singlet state and to which, consequently, a great deal of theoretical effort has been directed (or misdirected!). A review of these theoretical efforts has been given by Kondo (1) and Grüner and Zawadowski (6). Tables summarising the predictions of the temperature dependence of various physical parameters according to different theories of the singlet state are given in references 2 and 26. We briefly review the situation as it applies to the electrical resistivity. An exact solution of Nagaoka's equations of motion (99) derived by using Green's function techniques was obtained by Hamann (100). His relation for the resistivity was

$$\rho(T) = R_m \rho(\varepsilon_F) c \left\{ 1 - \frac{\ln T/T_K}{\left[\ln\left(\frac{T}{T_K}\right)^2 + \pi^2 S(S+1) \right]^{1/2}} \right\} \qquad 2.28$$

This curve has an inflection point at $T = T_k$ where $\rho(T)$ is linear on a logarithmic temperature-scale. For $\ln T >> \ln T_K$ one obtains

$$\rho(T) \sim \left\{ 1 + 2J\rho_s(\varepsilon_F) \ln \frac{K_B T}{W} \right\} \qquad 2.29$$

which is of the same form as Kondo's result (equation (1.35)), while at sufficiently low temperatures that $\ln\left(\frac{T}{T_K}\right) > \pi S$ equation (2.28) reduces to

$$\rho(T) \approx R_m \rho(\xi_F) c \left\{ 1 - \frac{\pi^2 S(S+1)}{4 \ln^2 (T/T_K)} \right\} \qquad 2.30$$

Appelbaum and Kondo (101) developed the variational ground state model first proposed by Kondo. For the resistivity they obtained

$$\rho(T) = \rho_0 \left\{ \cos^2 \eta_v - \frac{16}{5} \cos 2\eta_v \left(\frac{T}{T_K} \ln \frac{T}{T_K} \right)^2 \right\} \qquad 2.31$$

where η_v is the phase-shift due to potential scattering. Equations (2.28) and (2.31) have been fitted with varying degrees of success to a number of systems. Heeger (2) has shown that Hamann's equation (equation (2.28)) fits the resistivity data on CuCr ($\lesssim 28$ ppm Cr) very well at temperatures above T_K (~ 2K) but below this temperature the fit is very poor. On the other hand, the Appelbaum-Kondo formula (equation (2.31)) fits the same data over a narrow range in the low temperature region ($\lesssim 0.8$ K). The latter formula has also been fitted to resistivity data on AuV (0.8 and 2% V) and CuFe (13, 80 and 400 ppm Fe) (10). These fits however, have been criticized by Star (102) who attributed the apparent agreement between the data and the Appelbaum-Kondo (AK) theory to either poor experimental accuracy or very high impurity concentrations. For example in CuFe he found that for impurity concentrations of about 50 ppm Fe the resistivity showed a temperature dependence

of the form

$$\rho(T) = \rho_0(1 - aT^2) \qquad 2.32$$

where $a \sim T_K^{-2}$.

But for a CuFe alloy with an impurity concentration of 500 ppm the AK formula fitted the data well with Tk = 50K. Star also found a T^2- dependence in dilute PdCr, PtCr and AuV alloys, as had been earlier observed in AlMn and AlCr alloys (103). It is now being gradually accepted that the general behaviour of the temperature dependence of the electrical resistivity of alloys in the region of the magnetic phase being discussed is as follows (104): at very low temperatures ($T \ll T^*_{imp}$) the resistivity decreases as in equation (2.32). This low temperature quadratic behaviour then gives way to a region in which the resistivity decreases linearly with temperature and this in turn is succeeded by a higher-temperature region which is closely logarithmic. It would appear that the linear region is merely a consequence of the crossover from a T^2 to a lnT behaviour. None of the very sophisticated theories of the singlet state has so far suggested this behaviour. On the other hand, the spin fluctuation theories of Zuckermann (105) and particularly Rivier and Zlatic (106) tend to reproduce this behaviour. Neither this nor the experimentally observed behaviour is surprising. The Kondo problem is really nothing other than a manifestation of the spin fluctuations of the magnetic system (localized moment + conduction electrons). Well below the spin fluctuation temperature, T*imp, one should observe behaviour

resembling that of a Fermion gas, with simple power laws for various physical parameters. Well above the spin fluctuation temperature the s-d Hamiltonian of Kasuya (24) and Yosida (25) as used in Kondo's theory (23) is appropriate and one gets the logarithmic behaviour observed in the resistivity. Spin fluctuation theories redeveloped along the lines of our model (which would mean restructuring the Anderson Hamiltonian or introducing a completely new Hamiltonian to reflect the existence of a localized impurity moment) will be able to successfully bridge the gap between the very low and very high temperatures (i.e. relative to T^{*}_{imp}). In this connection one would question the validity of Wilson's recent phenomenological theory (107) which, in essence, is a theory of the singlet state. The theory assumes an effective afm coupling between an impurity atom and a conduction electron which is temperature dependent. In the non-magnetic limit this coupling is infinite (or much greater than the bandwidth, $K_B T_F$) so that the conduction electron is locked with the impurity giving rise to a singlet state. On the other hand at high temperatures the coupling becomes weak ($\ll K_B T_F$) and the impurity spin fluctuates freely. Thus as one moves along the temperature axis from the paramagnetic regime to non-magnetic limit the coupling changes from being weak to intermediate (near Tk) and finally to very strong at low temperatures. A very readable account of the theory is given by Nozieres (108). This model of a temperature-dependent effective coupling should be contrasted with the spin fluctuation model in which the coupling is constant

but the different regimes are determined by the ratio of the interaction energy to the thermal energy. One good thing though about the Wilson theory is that the impurity atom is always magnetic even if its spin is supposed to be locked in with that of a conduction electron at very low temperatures. Before concluding this discussion of the Kondo problem we shall comment briefly on the resistance minimum that occurs in the second aspect of the problem. We have mentioned that for alloy systems in the relevant concentration region the resistivity decreases logarithmically at sufficiently high temperatures. When this decrease is combined with the phonon resistivity a minimum results. However the temperature of this minimum is not necessarily restricted to low temperatures where the phonon resistivity $\sim T^5$ so that one should not expect that $T_{min} \sim C^{1/5}$ (equation (1.37)).

In fact experimentally the resistance minimum almost always occurs at temperatures greater than about $\frac{\theta_D}{20}$ where θ_D is the Debye temperature; for example for CuCr (109) the minimum occurs at about 30 - 40 K, compared with a Debye temperature of 325K for Cu (calculated from tabulated elastic constants (110)). In this temperature region the phonon resistivity could vary either as T^3 or as $AT^2 + BT^4$.

It might be pertinent to mention that it would appear that not all resistance minima are Kondo-like. A good example is the resistivity of a Pd 4% Rh alloy which exhibits a minimum at about 7.5K (111).

We have thus shown that Kondo-like resistance minima

may be observed in two different regions of the magnetic phase diagram. One minimum occurs in the magnetic region ($c > c_m$) and it is to this minimum that Kondo's original theory (23) is fully applicable, as outlined in section 1.7 (particularly equations (1.35)-(1.37)). The Kondo divergence in such a case is due to the phase transition at T_m, marking the onset of magnetic ordering (usually spin-glass type). The resistance minimum is accompanied by a maximum at still lower temperatures. The other resistance minimum occurs in the non-magnetic region ($c << c_m$); here the Kondo divergence is due to the transition into the non-magnetic state, an event dominated by spin fluctuations. In this case below the temperature of the resistance minimum the resistivity varies as $\ln T$, T, and finally tends to the unitarity limit as T^2. It was the failure to recognize these two aspects of the Kondo problem that led Mills (3) to conclude that the Kondo effect occurs only in the magnetic limit (HF criterion) whereas localized spin fluctuations occur in the non-magnetic limit.

We should however, sound a note of caution by recallin that in the non-magnetic region there is the possibility of magnetic clusters forming say through statistical fluctuations in concentration. Such clusters (mostly pairs for dilute impurity concentrations) are bound to affect the resistivity of such systems, e.g. Star (102) has observed that in CuFe

$$\rho(T) = \rho_0 - f(c)T^2 - g(c)\ln T \qquad 2.33$$

where $f(c) = 2.5c + 9000c^2 \quad (\mu\Omega\,cm/K^2)$

and $g(c) \sim 3000\, c^2$ ($\mu\Omega$-cm)

The effect of clusters will also be observed in the magnetic susceptibility; one has to consider nearly magnetic and magnetic clusters in addition to the non-magnetic single impurity atoms. Tournier (91) has given a short discussion of the observed phenomena.

(iii) Exchange Enhanced Hosts

Since the ultimate aim of studying the properties of magnetic alloys is to be able to explain the magnetic behaviour of metals it is only logical that we should explore how our model for a dilute alloy carries over to a pure metal. The central feature of the dilute alloy problem is the occurrence of VBS for both spin directions. It is the magnitude of the width of the VBS relative to the exchange splitting that essentially determines the characteristic temperature of an impurity in the metal host. For binary alloys we had considered three contributions to the width, Δ, of the VBS (equation (2.12)) these being the s-d exchange mixing interaction, the spin-orbit coupling and the inter-impurity interactions. In the single impurity limit one could neglect the contribution from the last mentioned interaction and thus obtain the limiting value of the characteristic temperature, T_o^*, for a given solute atom. As the impurity concentration increases so does the importance of the inter-impurity interactions and, as discussed, it is the main cause of the concentration-dependence of Δ and hence of T_{imp}^*. It is clear that in the limiting case of a pure metal one should consider the effect of d-d interactions as being dominant, with any s-d

interactions and spin-orbit coupling effects being "perturbations". It is also clear that in the same limit we cannot strictly talk of virtual bound states. We therefore propose that for a pure transition metal there is a de facto broadening of the former atomic d-levels into a d-band caused by interatomic d-d electron interactions but that this d-band is exchange-split by the intratomic Coulomb and exchange interactions. In view of the procedure adopted for the alloy problem it may perhaps be more consistent to start off with exchange-split atomic d-levels which are then broadened into bands. However, the order in which the exchange-splitting and broadening occur is largely irrelevant, as what matters to us is the end result which is the existence of up-spin and down-spin d-bands. It is pertinent to mention here that the overlap integrals between near-neighbour d states (equivalent to crystal field effects) lead to different energies for d-wavefunction of symmetry t_{2g} or e_g. We shall now take Δ to represent the additional width of the d-bands due to s-d exchange mixing and spin-orbit coupling i.e. equation (2.11) holds. Thus one can correspondingly define a characteristic temperature T_h^* (or an effective magnetic degeneracy temperature) for a pure metal as in equation (2.8) i.e.

$$T_h^* = T_F \, e^{-\frac{\pi \Delta_o}{2\Delta}} \qquad 2.34$$

where T_F is the Fermi temperature of the metal. For the simple metals in which the d-band is either full or non-existent clearly Δ_o is zero so that $T_h^* = T_F$.

On the other hand, for the transition metals Δ_o is expected to be finite so that T*h should always be less than T_F.

We may now rewrite equation (2.8), replacing T_f by T*h to give

$$T^*_{imp} = T^*_h e^{-\frac{\pi}{2}\left(\frac{\Delta_o}{\Delta}\right)_i} \qquad 2.35$$

$$\equiv T_F e^{-\pi/2\left\{\left(\frac{\Delta_o}{\Delta}\right)_h + \left(\frac{\Delta_o}{\Delta}\right)_i\right\}} \qquad 2.36$$

where the subscripts i and h imply that the appropriate parameters refer to the impurity and host matrix respectively. The addition of an impurity to a metal host may alter the value of Δ_h and this may increase or decrease T*h. In our previous discussion we had tacitly assumed that Δ_h was constant and so only considered the concentration-dependence of Δ_i thereby deriving an expression for the critical concentration (equation (2.19)). This procedure will be approximately valid only for simple metal hosts for which T*h $\sim$ T_F and in which the impurity VBS lies sufficiently below the Fermi level. Thus for say CuMn T*h and T*imp vary as sketched in figure 2.5 •

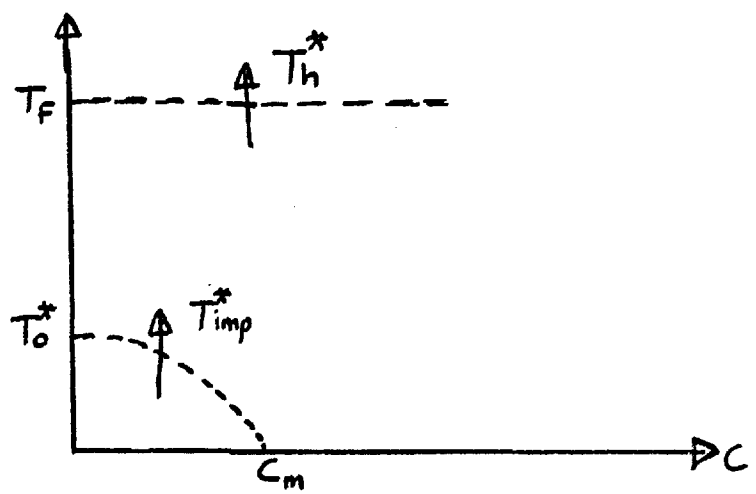

Fig. 2.5
Concentration dependence of T*h and T*imp in CuMn.
($T^*_o \sim 10mK$; $T_F \sim 10^5 K$)

For transition metal hosts the situation is no longer simpl and one would have to consider how a particular impurity affects Δ_h especially through its effect on the density of states at the Fermi level since both s- and d- states are present. The position of the VBS with respect to the Fermi level then becomes important. Thus for say a Pd host the Fe VBS may lie below the Fermi level while those of V lie above it, as is known to be the case for dilute Ni-based alloys. Consequently, one can expect Fe and V impurities to affect a Pd host differently, the former decreasing T*h or at worst leaving it unaltered while the latter will increase it (because its electrons are emptied into the host band).

It is in the context of an effective degeneracy temperature that one should view the properties of the so-called incipient ferromagnets Pd and Pt. They should simply be regarded as having very low characteristic temperatures. It has been known for a long time that the susceptibility of Pd exhibits a maximum at about 85K (112-118). Above the temperature of the maximum the susceptibility can be fitted to a Curie-Weiss law with an effective Curie constant that has been reported to be almost the same as in pure Ni (119). Foner et al (115) reported observing a small maximum in the temperature dependence of the susceptibility of Pt but in the data of Hoare and Mathews (112) and Budworth et al (113) only a change of curvature is seen. Consequently we shall confine most of our discussion to Pd especially, as briefly mentioned below, the temperature dependence of the susceptibility

of Pt could be more interesting than hitherto imagined.

In the dilute alloy problem it is expected that for $T > T^*_{imp}$ a Curie-Weiss law should be observed. One may, by analogy, identify the temperature of the susceptibility maximum in Pd as its characteristic temperature i.e. $T^*_h \simeq 85K$. Since $T_F = 8.13\times10^4 K$ (37), using equation (2.34) we estimate that for Pd

$$\frac{\Delta_o}{\Delta} \simeq 4.37 .$$

If we take Δ_o for Pd to be the same as in Ni i.e. $\sim$ 0.4 ev (120), then $\Delta \sim 0.09$ ev. Now suppose for the sake of argument that we neglect spin-orbit coupling and put $\Delta = \Delta_{sd}$ only; then an estimate of J_{sd} may be obtained by using equation (2.7). This however, requires a value for $\rho_s(\varepsilon_F)$ and so we shall assume that $\rho_d(\varepsilon_F) \sim 30\,\rho_s(\varepsilon_F)$. Band structure calculations (37) give $\rho(\varepsilon_F) = 1.20$ states / ev atom per spin index; thus $\rho_s(\varepsilon_F) \sim 0.04$ state / ev atom per spin index giving J_{sd} (Pd) $\sim$ -3.7 ev. This value is not unreasonable although it is certainly larger than it should be because of the neglect of spin-orbit coupling. The g-factor for Pd has been estimated at 2.6 (121) which would mean that the orbital contribution to any Pd moment could amount to as much as 30%, as compared with about 10% generally for Fe, Co and Ni. The relative orbital contribution would even be higher than 30% in the case of Pt since it is the heaviest transition metal.

Alternatively, suppose $\frac{\Delta_o}{\Delta}$ is constant for Ni, Pd and Pt. Then for Pt with $T_F = 11.27\times10^4 K$ (37) $T^*_h \sim 118K$ which is about the temperature at which Foner et al (115)

report observing a maximum in the temperature variation of the susceptibility; for Ni with $T_F = 6.7 \times 10^4$K we obtain $T^*_h \sim 70$K. It would mean that it is the ferromagnetic interactions between Ni atoms (leading to a Curie temperature of 631K) which stabilize the moments on the Ni atoms at low temperatures. A further discussion of this point will be given elsewhere.

It will be pertinent here to note the following two observations which may have a bearing on the interpretation of the magnetic behaviour of Pd and Pt. These are that -

(a) thermopower measurements on "pure" Pd (122,123) showed the existence of a maximum around 60K, an effect that was attributed to phonon drag. We should however recall that well-defined maxima have been observed in the temperature dependence of the thermopower of dilute AuFe, AuCo, AuV and CuFe alloys (10) at temperatures correspondin to their characteristic temperatures. The fact that the maximum in the thermopower of the Pd specimen occurred around 60K instead of near 85K is most probably attributable to the impurity of the "pure" specimen. Fairly low concentrations of magnetic solutes like Fe or Mn could cause T^*_h to decrease. No thermopower measurements on pure Pt seem to be reported in the literature.

(b) the temperature dependence of the shear modulus C_{44} (in standard notation) of both Pd and Pt shows an anomalous variation near the corresponding characteristic temperatures (124-126). This time the anomalies have been interpreted as reflecting the temperature variation of the electron

contribution to the shear moduli resulting from the overlap of the Fermi surface across the faces of the Brillouin zone.

It could well be that the occurrence of the anomalies in the magnetic susceptibility, thermopower and shear modulus at about the same temperature is merely coincidental but the chances are that these anomalies have the same origin which, it would appear, is magnetic.

We recall that the large magnetic susceptibility of Pd has been attributed to a strong uniform exchange enhancement caused by "critical spin fluctuations" or paramagnons. In an earlier discussion (vide section 1.10) we mentioned some of the expected consequences of the existence of paramagnons but we shall now briefly review these in the light of the experimental evidence.

(i) An enhancement of the magnetic susceptibility relative to the Pauli value as calculated from the band structure density of states at the Fermi level is expected. The enhancement factor, S, is defined by equation (1.46). For Pd Chouteau et al (127) have estimated that $S \simeq 10$. On our model of an effective degeneracy temperature for Pd one would also expect an enhancement of the normal Pauli susceptibility. Using equation (2.5) to define the lifetime of the spin fluctuations in Pd and assuming the validity of equation (1.42) one is led to expect that

$$\chi_{obs} \simeq \frac{g^2\mu_B^2 \tau_{sf}}{\pi} \equiv \frac{g^2\mu_B^2 h}{\pi K_B T_h^*}$$

Since $\chi_{Pauli} = g^2\mu_B^2 h/\pi K_B T_F$ it follows that

$S \simeq \frac{T_F}{T^*_h} \sim 10^3$ which is about

two orders of magnitude larger than the estimate of Choutea et al (127). However, as discussed shortly below, it seems that equation (1.42) is not valid so that putting $S \sim \frac{T_F}{T^*_h}$ is a bit simplistic. In this connection it is of interest to point out the similarity between the susceptibility calculated on the lsf model (equation (1.41) and that calculated on the exchange enhancement model (equation 1.45)). An obvious conclusion would be that paramagnons are not really different from localized spin fluctuations which is, of course, our viewpoint although Heeger (2) disagrees. He instead suggests that two important differences exist between localized spin fluctuations and paramagnons namely-that the impurity problem is localized so that there can be no explicit wave-vector dependence of the susceptibility and secondly, that the paramagnon approximation provides a good description of the exchange enhancement model up to the Stoner instability limit while the HF approximation (Anderson model) is only applicable well away from the HF instability limit. Both points are incorrect. The paramagnon approximation in its present form has been shown to be good only for sufficiently dilute PdNi and PtNi alloys and even then a localized exchange enhancement model has to be used. Also it is now very well-known that the paramagnon theory has not yet provided a satisfactory quantitative description of the critical concentration region of any alloy system. In fact, one may ask how would paramagnon theory explain the experimentally proven (128, 186) inhomogeneity of the onset of ferromagnetism in the PdNi alloy system?

(ii) A second effect of the existence of paramagnons is the enhancement of the d-electron mass. The mass enhancement, $\frac{m^*}{m}$, is given by equation (1.47) and should be reflected in an enhancement of the coefficient, γ, of the linear term in the specific heat. From the observed and calculated values of this linear term it was determined (37) that $\frac{m^*}{m} = 1.66$, which value should be compared with that ($\sim$ 6.4) expected from equation (1.47) using $S \simeq 10$. No reasonable explanation of this glaring discrepancy seems to have been advanced apart from suggestions that attribute it to approximations in the theory such as the use of a single spherical band, the inadequacy of the random phase approximation etc.

(iii) A further contribution, $\sim T^3 \ln \frac{T}{T_{sf}}$, to the specific heat is also expected, with $T_{sf} \sim \frac{T_F}{S}$ (see equation (1.48)). This T^3 term is supposed to give rise to an upturn, at low temperatures, in the plot of $\frac{C_v}{T}$ against T^2, as sketched in figure 2.6 •

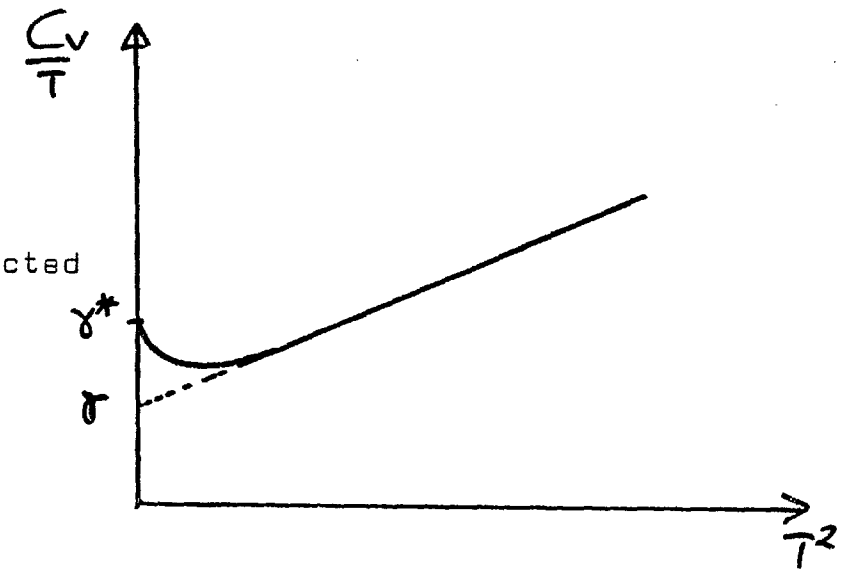

Fig. 2.6
Sketch of $\frac{C_v}{T}$ as predicted by current paramagnetic theory.

$\left(\frac{\gamma^*}{\gamma} = \frac{M^*}{m}\right)$

Such an upturn has not yet been observed for either pure Pd or Pt and even for dilute PdNi and PtNi alloys. In some other systems where such an upturn has been observe detailed investigations have decisively shown it to be due to the presence of magnetic clusters (see section 2.5(xi) below). The presence of the $T^3 \ln \frac{T}{T_{sf}}$ term is also expected to modify the coefficient of the phonon contributi to the specific heat (equation (1.54)). Although such a modification appears to have been observed in PdNi alloys (43) the effect is not peculiar to this system since it is observed in all other alloy systems where such measurements have been carried out and, more importantly, there certainly seems to be a definite correlation between this behaviour and the critical concentration for the onset of ferromagnetism. An alternative explanation of this correlation is also offerred in section 2.5(xi) in terms of the effect of the magnetic clusters.

(iv) A contribution of a T^2 term to the electrical resistivity of the alloys. Such a T^2 term has been widely observed but then such behaviour is also expected on the lsf model of Rivier (15) and others (27-31). In fact, as Lederer and Mills (39) have remarked the T^2 law simply reflects inelastic electron-electron scattering processes and indicates that the magnetic fluctuations have a temperature-dependent amplitude. Both Kaiser and Doniach (129) and Rivier and Zlatic (130) have predicted a particular pattern for the temperature dependence of the resistivity of such alloys. For $T/T_{sf} \ll 1$ the resistivity increases as $\left\{\frac{T}{T_{sf}}\right\}^2$ changing to a T/T_{sf} dependence in the high

temperature limit (see section 2.5(vii)). The latter authors (130) however, also insist that this pattern would hold for the resistivity due to any quantum scattering involving the internal structure of the scattering object.

From the above comparison of experimental observations with the theoretical predictions of paramagnon theory it would appear that the latter is not well founded. Such a conclusion requires an objective re-examination of the concept of paramagnons. As mentioned earlier paramagnons have been primarily associated with inter-atomic d-electron interactions or correlations and their occurrence restricted to the so-called nearly ferromagnetic metals or alloys. It would, however, appear to be more correct to identify paramagnons with localized spin fluctuations or, in keeping with current jargon, to call paramagnons the quasi-particles of localized spin fluctuations. In other words, paramagnons are a direct consequence of the s-d exchange mixing interaction and therefore are expected to occur in a wide variety of systems where magnetic behaviour is expected. Thus paramagnons occur as much in AlMn (103), AuV (102), IrFe (131), PtFe (132), MoCo (133), AuTi (134) as in the pure metals Rh, Pt and Ru etc. The only difference is in the excitation energy of the paramagnons i.e. the frequency of the localized spin fluctuations which is determined by the appropriate characteristic temperature as in equation (2.5). The existence of low frequency paramagnons (low T^*_h or T^*_{imp}) would mean that a given metal or impurity atom is nearly magnetic but in the case of a pure metal it would not necessarily imply being nearly ferromagnetic as

well. Thus the fact that Pd (and Pt?) has a low effective degeneracy temperature does not imply that it is nearly ferromagnetic. We should bear this in mind. Identifying paramagnons as localized spin fluctuations is, however, only part of the problem. It does, of course, mean that the susceptibility of the systems in question can be worked out with the same formalism as used for the Kondo problem. Unfortunately it does not appear that an equivalent amount of effort has been devoted to an exact calculation of the susceptibility in the Kondo problem as was devoted to the electrical resistivity. The susceptibility of a free spin is expected to obey a Curie law (equation (1.1)) while that of a free electron gas comes from the Pauli paramagnetism. For an alloy system in which an impurity spin interacts with the conduction electrons the total susceptibility will generally be different from the sum of the local (impurity) susceptibility and Pauli paramagnetism. It is therefore, assumed that

$$\chi_{total} \simeq \chi_{impurity} + \chi_{Pauli} + \Delta\chi \qquad 2.3$$

where $\Delta\chi$ is the change in the Pauli susceptibility due to the s-d interactions. These interactions also cause a deviation of the impurity spin susceptibility from a Curie law. For example, Yosida and Okiji (135) have obtained that

$$\chi_{impurity} \simeq \frac{\mu_{eff}^2}{3K_B T_K} \frac{\left\{1 + 4J^2\rho^2(\varepsilon_F)\ln\frac{K_B T}{W}\right\}}{\left\{1 - 2J\rho(\varepsilon_F)\ln\frac{K_B T}{W}\right\}} \qquad 2.38$$

with

$$\mu_{eff}^2 = g^2\mu_B^2 S(S+1).$$

There is apparently no consensus on the magnitude or form of the correction $\Delta\chi$ to χ_{Pauli} (2).

An expression for the susceptibility has also been obtained using some sophisticated theories of the singlet state. Thus according to Iche (136)

$$\chi \simeq \frac{1}{\pi\Delta} e^{\frac{U}{\pi\Delta}} \qquad 2.39$$

while Menyhard (137) derived that

$$\chi \simeq \frac{\mu_B^2}{2\pi\Delta}\left\{1 + \frac{U}{\pi\Delta} + 0.54\left(\frac{U}{\pi\Delta}\right)^2 + \cdots\cdots\right\} \qquad 2.40$$

where the parameters Δ and U are as defined in Chapter 1. Equations (2.39) and (2.40) have been compared (6) with a similar expression obtained in the lsf model:

$$\chi_{lsf} = \frac{\mu_B^2}{2\pi\Delta}\left\{1 - \frac{U}{\pi\Delta}\right\}^{-1} \qquad 2.41$$

The above expressions do not give any guide about the temperature dependence of the susceptibility so that we have to resort to physical intuition. At temperatures well below the characteristic temperature we should expect a temperature dependence similar to that of a Fermion gas i.e.

$$\chi(T) \sim \chi(0)\left\{1 - \left(\frac{T}{T^*}\right)^2\right\} \qquad 2.42$$

as obtains for the electrical resistivity (equation (2.32)). $\chi(0)$ is an effective susceptibility at absolute zero. Such a temperature dependence of the magnetic susceptibility

of course, been predicted by the spin-fluctuation theories of Rivier and Zuckermann (30), Beal-Monod et al (138), Beal-Monod and Mills (139) and even by some theories of the singlet state (140,141) where in many of these theorie

$$\chi(0) \sim \frac{q^2 \mu_B^2}{\pi K_B T^*} . \qquad 2.43$$

Equation (2.42) has been reported to be approximately obeyed by a number of alloys such as AlMn (142), CuFe (143) and AuV (144). The question then arises - will a logarithmic term also be observed at higher temperatures? There is no obvious direct answer to this question but we shall note that Misawa (145) has shown that at low temperatures the susceptibility of a nearly ferromagnetic Fermi liquid obeys the relation

$$\chi(T) = \chi(0) - A T^2 \ln \frac{T}{T_0} \qquad 2.44$$

where $A > 0$ and T_0 is some characteristic temperature. From equation (2.44) one can easily deduce that $\chi(T)$ has a maximum at temperature

$$T_{max} = T_0 e^{-1/2} . \qquad 2.45$$

Noting that Pd has been known to have a susceptibility maximum which has not been previously satisfactorily explained Misawa (146) suggested that equation (2.44) may well apply to it, as verified later by Jamieson and Manchester (146). A similar analysis has been applied to

α-Mn and some of its alloys with Fe and Cr (148) and recently to YCo_2, $LuCO_2$ and YNi_2 (149). However, Kojima and Isihara (150) have questioned the applicability of Fermi liquid theory to metals with prominent d-band characteristics. Instead from their many-body theory of the susceptibility of metals at finite temperatures they have proposed the relation

$$\frac{\chi(T)}{\chi(0)} = 1 - \frac{\pi^2}{12}\left(\frac{T}{T_F^*}\right)^2\left\{1 - \frac{S^2}{2}\left(\ln\frac{T}{T_F^*}\right)^2 + 0.01325S^2\ln\frac{T}{T_F^*}\right\} \qquad 2.46$$

where S is a parameter related to an effective electron density and T_F^* is an effective degeneracy temperature. An attractive feature of equation (2.46) is that at low temperatures it reduces to the form of equation (2.42). A logarithmic term may also be inferred from the paramagnon theories outlined in section 1.10. It is therefore apparent that a proper treatment of the magnetic susceptibility within the context of localized spin fluctuations should reproduce the logarithmic behaviour observed in the intermediate temperature range for Pd and the other alloys mentioned above while reducing to equation (2.42) at low temperatures.

It will be useful at this juncture to comment briefly on the temperature dependence of the susceptibility of the transition metals. Most of these metals have a positive temperature coefficient of susceptibility while V, Nb, Ta, Pd and Pt (which have some of the highest density of states at the Fermi level) have a negative coefficient, at least

at low temperatures (151). The usual explanation for this behaviour based on the rigid-band model is in terms of the energy dependence of the density of states as expressed by the Stoner relation (152)

$$\chi(T) = 2\mu_B^2 \rho(\varepsilon_F)\left[1 + \frac{(\pi k_B T)^2}{6}\left\{\frac{1}{\rho(\varepsilon)}\frac{\partial^2 \rho(\varepsilon)}{\partial \varepsilon^2} - \left(\frac{1}{\rho(\varepsilon)}\frac{\partial \rho(\varepsilon)}{\partial \varepsilon}\right)^2\right\}_{\varepsilon=\varepsilon_F}\right] \qquad 2.47$$

A sharp peak in the density of states at ε_F would then give a negative temperature coefficient of susceptibility while a relative minimum would have the opposite effect. Also depending on the "fine structure" in $\rho(\varepsilon)$ a number of extrema may occur successively. However, it has been pointed out that at least in the case of Ti (153) the temperature dependence of the susceptibility would require a curvature that is several orders of magnitude greater than that provided by the rigid-band curve. It is thought that this comment could well apply in general to many of the transition metals whose susceptibility increases with temperature. In other words some alternative explanation must be sought for the observed behaviour. We have already mentioned that the susceptibility maximum in Pd has been explained (116) in terms of a logarithmic term deduced from the theory of Fermi liquids (145). However, it is suggested that the logarithmic term arises from spin fluctuations, in which case it should be observed for many of the transition metals. This conjecture appears to be confirmed by the fact that Rh also has a susceptibility maximum (151). The susceptibility has been similarly analysed and it is

found (154) that in fact,

$$\chi(0) \simeq 8.26 \times 10^{-7} \text{ emu g}^{-1}$$

$$A \simeq 5.86 \times 10^{-13} \text{ emu g}^{-1}$$

and

$$T_o = 2720 \text{ K}; \quad T_h^* \sim T_{max} = 1650 \text{ K}.$$

A preliminary analysis of the susceptibility data of Ir (151) has also been carried out (154) giving

$$\chi(0) \simeq 1.36 \times 10^{-7} \text{ emu g}^{-1}$$

$$A \simeq 2.21 \times 10^{-14} \text{ emu g}^{-1}$$

and

$$T_o \simeq 1.68 \times 10^4 \text{K},$$

which would give a maximum at $T_{max} \simeq 10^4$K. It is planned to extend the analysis to the other transition metals*. It is also interesting to note that the susceptibility data on V, Nb and Ta (151) appear to satisfy equation (2.42) with $T_h^* \simeq$ 4300, 3354 and 4260 K respectively. These values should be slightly less than the true effective degeneracy temperatures of these metals, particularly in the case of Nb, because the specimens used were reported to contain appreciable amounts of Fe impurity ($\sim$ 400, 700 and 30 ppm respectively). We are unable to get out the Fermi temperatures of these metals in order to obtain an idea of the enhancement effects.

Returning to the particular probelm of the magnetic behaviour of Pd we show in fig.2.7 its Curie-Weiss plot. The figure clearly shows that the Curie-Weiss law is obeyed quite well at sufficiently high temperatures with

$$\chi_{Pd} \simeq \frac{\mu_{eff}^2}{3K_B(T-85)} \qquad 2.48$$

---

* Such an analysis has been subsequently reported by Misawa and Kanematsu (753) and Misawa (754).

where $\mu_{eff} \simeq 1.12 \mu_B$ which should be compared with a value of $1.60 \mu_B$ for Ni (177) within the same temperature range ($T \gtrsim 600K$). It may be highly significant that the Curie-Weiss constant corresponds to the temperature of the maximum in the susceptibility, which we have assumed is equal to T^*_h for Pd. Could it then be that Pd is not magnetic because its apparent Curie temperature ($\approx$ Curie-Weiss constant) coincides with its spin fluctuation temperature? We shall attempt to answer this question elsewhere but we shall point out here that for Pdfe (and PdCo) a plot of the Curie temperature against the impurity concentration extrapolates to a value of about 80K for Pd from the high temperature side (see section 2.6). For Pt a Curie-Weiss law is also observed - figure 2.8.

$$\chi_{Pt} \simeq \frac{\mu^2_{eff}}{3K_B(T+920)} \qquad 2.49$$

with $\mu_{eff} \approx 1.35 \mu_B$. The negative Curie-Weiss constant indicates antiferromagnetic interactions between Pt atoms. However, it should be noted that a more than cursory examination of the data of Kojima et al (151) reveals that below about 900K the susceptibility of Pt appears to vary linearly with T down to a temperature of about 150K. Details of this behaviour and of the temperature dependence of the susceptibility of transition metals in general will be discussed elsewhere.

The discussion will also include recent attempts to explain the Curie-Weiss behaviour observed for Ni, Pd, Pt and the so-called "weak itinerant ferromagnets" in terms of

FIG.2.7: THE TEMPERATURE DEPENDENCE OF THE SUSCEPTIBILITY OF PURE Pd.

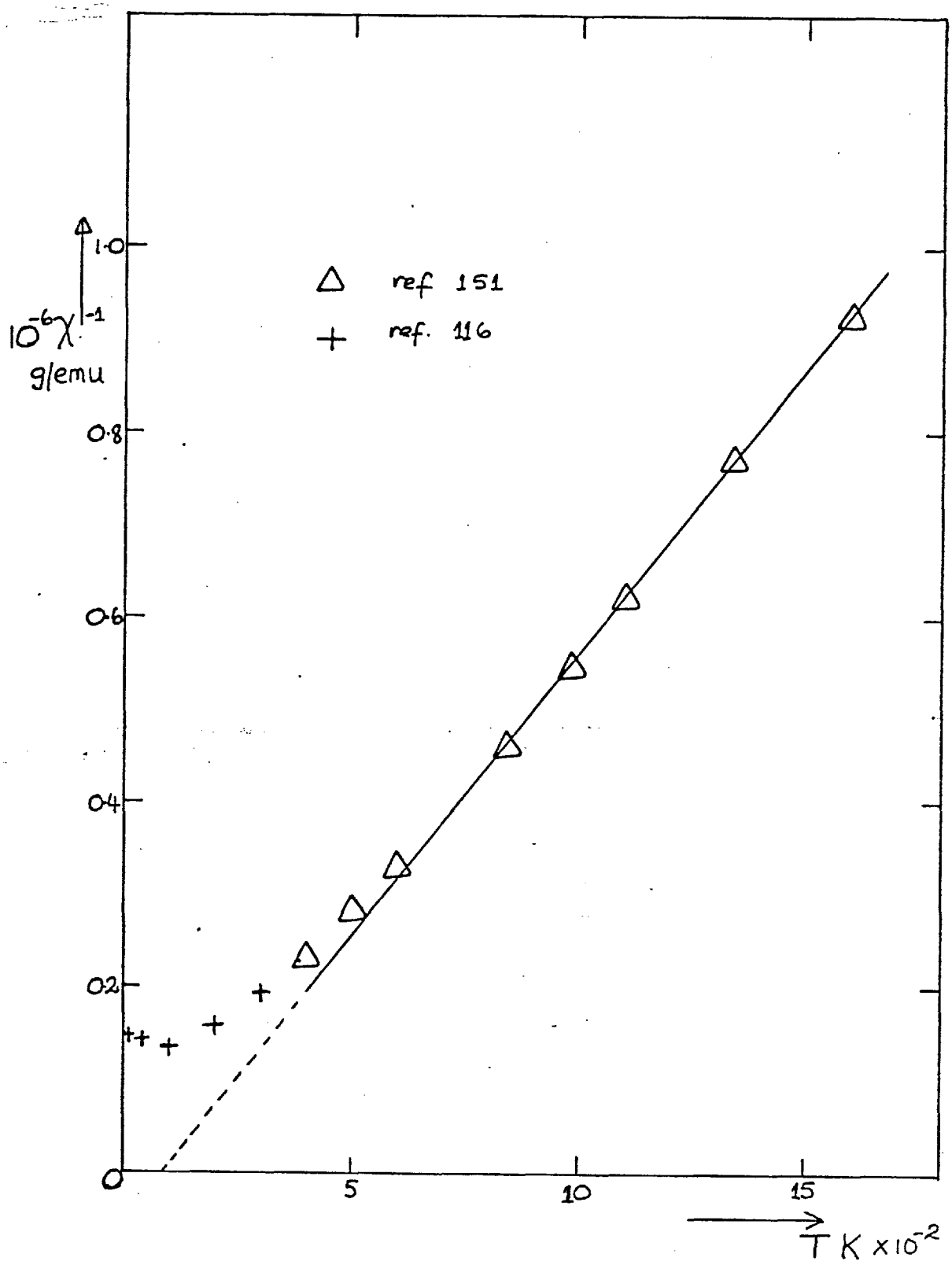

FIG.2.8: THE TEMPERATURE DEPENDENCE OF THE SUSCEPTIBILITY OF PURE Pt.

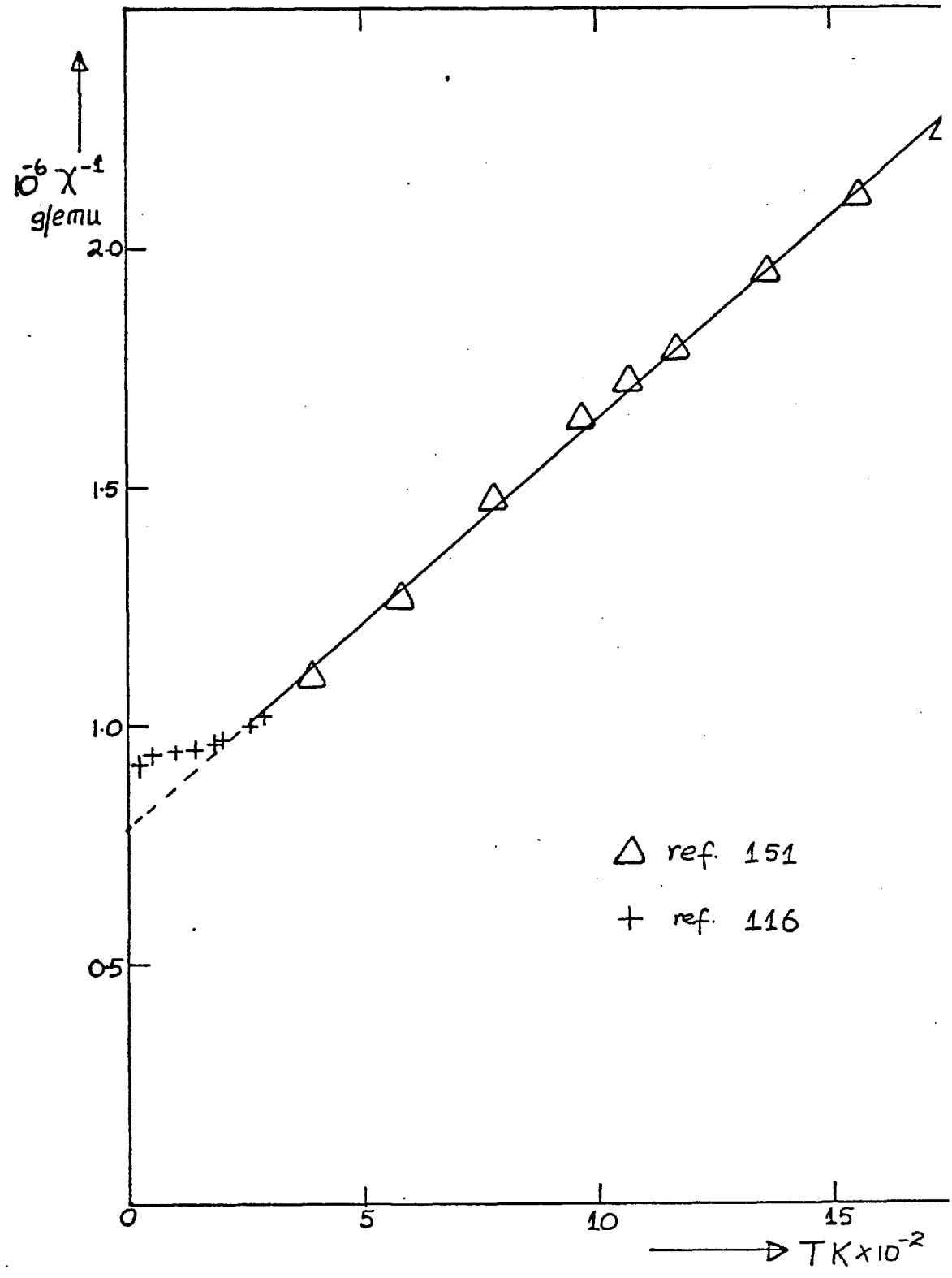

either spin fluctuations (178-181) or some peculiarities of the band structure (182).

It is trivial to point out that the localized exchange enhancement model for magnetic impurities follows very naturally from our interpretation of exchange enhancement effects in general. An impurity atom has its own spin fluctuation temperature which is determined by its own values of the parameters Δ_o and Δ. This characteristic temperature is, of course, different from that of the host (T^*_h) which may or may not be greatly affected by the presence of the impurity. Another important point is that the condition for an impurity atom to appear magnetic is not identical with the condition for the onset of ferromagnetism. This particular point is emphasized in view of current theories of the magnetism of PdNi and PtNi alloys.

To end this discussion of exchange enhanced hosts we remark that proponents of the original concept of paramagnons as a manifestation of inter-atomic d-d electron correlations could easily argue that the suggestion that paramagnons are really localized spin fluctuations due to s-d interactions is nothing different. This is because the s-electrons can always be imagined to sample the d-d correlations via the s-d interactions; certainly transport measurements alone cannot distinguish between the two viewpoints. However, such an argument is largely unnecessary because our suggestion is a logical development of the dilute alloy problem in which inter-atomic electron correlations do not play the crucial role assigned to them in the usual paramagnon theories; moreover one can always devise gedanken

experiments to aid the distinction. What is required is a proper redevelopment of spin fluctuation theory to reflect the fact that an impurity TM atom would always appear magnetic if there were no s-d or other residual interactions which give the moment a finite fluctuation frequency. Among other things such a theory should produce equation (2.42) at very low temperatures, give a logarithmic term in the intermediate temperature range ($T \lesssim T^*$) and reduce to a Curie-Weiss law at high temperatures ($T \gg T^*$) - i.e. where any magnetic interactions occurring above T^* are not sufficient to stabilize the moments below it.

(iv) Superconductivity in Transition Metals

According to the BCS theory (155) the phenomenon of superconductivity is due to an attractive electron-electron interaction induced by electron-phonon coupling. The superconducting transition temperature, Tsc, is obtained as

$$T_{sc} = 1.14\,\theta_D\, e^{-\frac{1}{V\rho(\xi_F)}} \equiv 1.14\,\theta_D\, e^{-\frac{1}{\lambda_{ph}}} \qquad 2.50$$

where θ_D is the Debye temperature, $\rho(\xi_F)$ the density of states per spin index at the Fermi level and V is the pairing potential arising from electron-phonon interaction; $\lambda_{ph} = V\rho(\xi_F)$ is called the electron-phonon coupling constant. An immediate consequence of equation (2.50) is the dependence of Tsc on θ_D which leads us to expect an isotope effect according to which

$$T_{sc}\, M^{1/2} = \text{constant} \qquad 2.51$$

for a given atomic species, where M is the isotopic mass. However, it is now known that the isotope effect in the form of equation (2.51) is more of an exception rather than the rule. A host of superconducting elements, especially the

superconducting transition metals, do exhibit a variety of power laws other than the $M^{-\frac{1}{2}}$ law required by the BCS theory. Specifically the failure to observe any isotope effect in the superconductivity of both Ru and Os has, amongst other factors, led to the suggestion that their superconductivity is caused by spin-exchange interactions (156). But for Mo say, where $T_{sc} \sim M^{-\frac{1}{3}}$ the same authors (156) suggested that electron-phonon and spin-exchange interaction effects may be jointly responsible for the superconductivity. A good deal of significant, even if circumstantial, evidence exists in the literature linking superconductivity and magnetism.

Overhauser (157) in discussing the theory of spin density waves (SDW) noted the striking similarity between some of the equations which occurred in his theory and those that occur in the BCS theory of superconductivity. One can also observe the similarity between the Kondo-Suhl-Abrikosov formula for the Kondo temperature T_k (equation (2.1)) and the BCS formula for Tsc (equation (2.50)). Other arguments in favour of a correlation between magnetism and superconductivity have been advanced notably by Matthias (158) and others (156, 159). Unfortunately more attention has hitherto been paid to the problem of the destructive influence of magnetic impurities on superconductivity rather than the equally important one (in our opinion) of exploring any possible common origin of magnetism and superconductivity especially for the transition metals.

Garland (160) in discussing the possible mechanisms for superconductivity in transition metals has outlined the experimental evidence which suggest that superconductivity in TM does not arise primarily from the electron-phonon interaction. These include the absence or considerable reduction of the isotope effect in superconducting TM, the pressure dependence of T_{sc}, observations relating T_{sc} to the position in the periodic table and the total density of states at the Fermi level, and the effects of (especially magnetic) impurities. According to the author the attractive interaction between the Landau quasi-particles (i.e. an approximate representation of the interacting electrons) which causes superconductivity derives from the following interactions:-

(a) V_{ph}, due to the virtual exchange of phonons, it is attractive for small energy transfers between the quasi-particles. Since for TM $\rho_s(\epsilon_F) \ll \rho_d(\epsilon_F)$, the quasi-particles involved here are primarily d-like so that any superconductivity would arise essentially from d-d interactions.

(b) V_c, a screened Coulomb interaction between the electrons. Since the heavy d-electrons cannot follow the motion of the s-electrons during s-s interactions they tend to "antishield" them and the possibility therefore exists of an attractive screened Coulomb interaction between the s-electrons. On the other hand, both the s- and d- electrons follow the motion of the d-electrons the Coulomb interaction between the d-electrons is always repulsive. Therefore we can put $V_c = V_{ss}$. There is thus the possibility of at

least two energy gaps existing for clean (i.e. very pure) TM superconductors, one due to primarily d-like quasi-particles (V_{ph}) and the other due to primarily s-like (V_{ss}) quasi-particles. An attractive effective interaction arising from some coupling terms between s- and d-band gap equations is neglected. However, for dirty TM superconductors only one gap is thought to exist - that due to V_{ph}.

In a companion paper (161) Garland then goes on to discuss the isotope effect in dirty TM superconductors. Writing

$$T_{sc} \propto M^{-\frac{1}{2}(1-\xi)} \qquad 2.52$$

where ξ is the deviation from the expected isotope effect, ie. the inverse square root of equation (2.51), the author attempts to account for the observed difference between the reduced isotope effect ($\xi \geq 0.3$) of the TM and the nearly complete isotope effect ($\xi \sim 0.1$) of simple metals in terms of band structure effects. He obtained that

$$\xi = \left\{ \frac{K_c^*}{K_{eff}} \right\}^2 \qquad 2.53$$

where $$K_{eff} = K_c^* + \langle K_{ph} \rangle$$

and K^*_c, $\langle K_{ph} \rangle$ are parameters that characterize the net Coulomb and average phonon contributions respectively to the electron-electron interaction. It follows that the "deviation parameter" ξ is significant only when $K_c^* \sim \langle K_{ph} \rangle$. Numerical values of ξ were deduced

which, although subject to very large errors ($\sim$ 25-40%) nevertheless appeared to agree with experimental values.

McMillan (162) has considered the problem of the transition temperatures of superconductors in the strong-coupling limit ($\lambda_{ph} \gtrsim 1$). He assumed that the BCS theory is so <u>accurate and sufficiently well-developed</u> that given the relevant parameters of the normal state of a metal, namely the electron energy bands near ε_F , the phonon dispersion curves, the screened electron-phonon and screened Coulomb electron-electron interaction matrices, one could readily calculate T_{sc} very accurately (say to about 1%!). The effect of the (repulsive) Coulomb interaction between the d-electrons is given in terms of the Coulomb pseudopotential, μ^* first introduced by Morel and Anderson (163).

$$\mu^* = \frac{V_c \rho(\varepsilon_F)}{1 + V_c \rho(\varepsilon_F) \ln \frac{\varepsilon_F}{\hbar \omega_m}} \qquad 2.54$$

$$\equiv \frac{\mu}{1 + \mu \ln \frac{\varepsilon_F}{\hbar \omega_m}} \qquad 2.55$$

where ω_m is the maximum phonon frequency, and the Coulomb repulsion $\mu = V_c \rho(\varepsilon_F)$; V_c is the matrix element of the screened Coulomb interaction averaged over the Fermi surface. The transition temperature was obtained as

$$T_{sc} = 1.14 \hbar \omega_m \, e^{\frac{-(1+\lambda)}{\lambda_{ph} - \mu^* - \frac{\langle \omega \rangle}{\omega_m} \lambda_{ph} \mu^*}} \qquad 2.56$$

where $\langle \omega \rangle$ in the average phonon frequency. After some numerical analysis equation (2.56) is reduced to

$$T_{sc} = \frac{\theta_D}{1.45} e^{\frac{-1.04(1+\lambda_{ph})}{\lambda_{ph} - \mu^*(1+0.62\lambda_{ph})}} \qquad 2.57$$

In the weak-coupling limit ($\lambda_{ph} << 1$) equation (2.56) reduces to the usual BCS equation with λ_{ph} replaced by ($\lambda_{ph} - \mu^*$). Equation (2.56) shows that the effect of the Coulomb interaction is to change the energy gap function in such a way that the phonon contribution is reduced from λ_{ph} to $\lambda_{ph}\{1 - \frac{\langle w \rangle}{w_m}\mu^*\} \simeq \lambda_{ph}(1 - 0.62\mu^*)$. T_{sc} depends on the isotopic mass directly through the presence of θ_D and implicitly through the w_m dependence of μ^*. From equations (2.54) and (2.57) the author obtained

$$\xi = \left\{\mu^* \ln \frac{\theta_D}{1.45 T_{sc}}\right\}^2 \frac{1 + 0.62\lambda_{ph}}{1 + \lambda_{ph}} \qquad 2.58$$

and hence that

$$\mu^* \simeq \frac{\xi^{1/2}}{\ln \frac{\theta_D}{1.45 T_{sc}}} \qquad 2.59$$

Using the observed values of ξ , T_{sc} and θ_D he estimated that $\mu^* \sim 0.1$ for the transition metals. The author concludes that λ_{ph} depends mainly on the phonon frequencies and is insensitive to large variations in electronic properties like the band-structure density of states. The above treatment neglects any spin fluctuation effects although the author suggested that their nett effect might be to increase the value of μ^* .

Riblet (164) has explicitly considered the effect of localized spin fluctuations in Ir-based alloys of

Fe, Co and Ni. He argued that the screened Coulomb interaction cannot be expected to be responsible for the destruction of superconductivity in these alloys since the electrons can always correlate their motion to be sufficiently far apart to avoid the Coulomb interaction while still taking advantage of the phonon induced attraction. In other words the Coulomb interaction must be cut off at energies $\sim \mathcal{E}_F >> K_B\theta_D$, resulting in the replacement of μ^* by μ. He suggested that spin fluctuations will give rise to an additional contribution to the Coulomb interaction; Such a contribution can be pictured to arise from the emission of a virtual paramagnon by one electron and its absorption by a second electron. This additional term should be cut off at energies $\sim h\nu_{sf}$ where $\nu_{sf} = \tau_{sf}^{-1}$.

If $h\nu_{sf} << \mathcal{E}_F$ and $h\nu_{sf} \sim K_B\theta_D$ then the spin fluctuations will have the dominant effect in suppressing superconductivity. Representing the coupling constant for the spatially averaged electron-paramagnon interaction by λ_{sf} then

$$\frac{\gamma^*}{\gamma} = 1 + \lambda_{ph} + \lambda_{sf} \qquad 2.60$$

and provided $h\nu_{sf} \sim K_B\theta_D$ Riblet assumed that the McMillan formula (equation (2.57)) could be modified to read

$$T_{sc} = \frac{\theta_D}{1.45}\, e^{-\frac{1.04(1+\lambda_{ph}+\lambda_{sf})}{\lambda_{ph}-\lambda_{sf}-\mu^*(1+0.62\lambda_{ph})}} \qquad 2.61$$

In the dilute impurity concentration limit μ^*, $\rho(\mathcal{E}_F)$ and λ_{ph} may be taken to remain constant while λ_{sf}

increases linearly say with c so that $\lambda_{sf} = ac$; a being a constant. Thus

$$\ln \frac{T_{sc}(c)}{T_{sc}(0)} \simeq \left\{ \ln \frac{1.45\, T_{sc}(0)}{\theta_D} - 1 \right\} \sum_{p=1}^{\infty} A_0^p \qquad 2.62$$

with $$A_0 = \frac{ac}{\lambda_{ph} - \mu^*(1 + 0.62\lambda_{ph})}$$

For $c \ll 1$, $-\ln T_{sc}(c) \propto c$, as was observed experimentally. Riblet was also able to fit equation (2.61) to the data of Maple et al (165) on ThU . We must mention though that Maple et al (165) had fitted their data to a formula given by Kaiser (166) namely

$$\ln \frac{T_{sc}(c)}{T_{sc}(0)} = - \frac{(A+B)c}{(1 - Bc)\lambda_{ph}} \qquad 2.63$$

where $$A = \frac{\rho_d(\varepsilon_F)}{\rho_s(\varepsilon_F)}$$

$$B = \frac{\rho_d^2(\varepsilon_F)\, U_{eff}}{\rho_s(\varepsilon_F)(2l+1)\lambda_{ph}}$$

and $\rho_d(\varepsilon_F)$ is the impurity density of states (equation (1.20)). For rare-earths $\rho_d(\varepsilon_F)$ is replaced by $\rho_f(\varepsilon_F)$. Equation (2.63) readily gives the critical concentration, Co, for the disappearance of superconductivity as

$$C_o = \frac{\rho_s(\varepsilon_F)(2l+1)\lambda_{ph}}{\rho_d^2(\varepsilon_F)\, U_{eff}} \qquad 2.64$$

However, the applicability of Kaiser's formula to the system is suspect because according to Maple (167) the density of states $\rho_f(\varepsilon_F)$ derived by using the formula is

much smaller than the value deduced from low temperature normal specific heat data.

Almost simultaneously with Riblet's work Bennemann and Garland (168) discussed the occurrence of magnetism in superconductors. They observed that the role of spin fluctuations in suppressing superconductivity must be dominant because (i) the initial slope of T_{sc} as a function of the magnetic impurity concentration is usually much larger for magnetic TM impurities than for magnetic RE impurities owing to the larger s-d exchange interaction as compared with the s-f interaction and (ii) in Laves-phase crystals such as V_3X, Nb_3X, $CeRu_2$, etc. with chains of TM atoms the suppression of superconductivity depends strongly on whether the magnetic atoms are substituted into lattice positions belonging to the chain or not. Starting with a Hamiltonian consisting of the Anderson Hamiltonian (equation (1.14)) and the phonon-induced electron-electron interaction Bennemann and Garland derived what was termed the generalized McMillan equation:

$$T_{sc}(c) = 1.14\,\theta_D\, e^{-\frac{m^*/m}{\lambda_{ph} - \lambda_{sp} - \mu^* - \frac{c\rho_d^2(\varepsilon_f) V_{eff}}{\rho_s(\varepsilon_f)}}} \qquad 2.65$$

where $\lambda_{sp} = c\,\rho_d(\varepsilon_f)\, V_{sp}$ is the coupling constant for the interaction between electrons at the Fermi level and the localized spin fluctuations. An analysis of the ratio of the fractional increase in the linear heat capacity to the fractional increase

in the magnetic susceptibility for various superconductors doped with TM impurities led the authors to suggest that strong Hund's rule coupling exists for most TM impurities. Equation (2.65) is more general than Kaiser's formula (equation (2.63)) because the latter can be re-written in the form

$$T_{sc}(c) \sim e^{-\frac{m^*/m}{\lambda_{ph} - c\,\frac{\rho_d^2(\varepsilon_F)\,U_{eff}}{\rho_s(\varepsilon_F)}}} \qquad 2.66$$

Most of the above discussion has been restricted to the influence of localized spin fluctuations on superconductivity. As we do not intend to discuss the whole problem of the correlation between superconductivity and magnetism in all relevant systems we shall not bother about the merits and demerits of the well-known Abrikosov-Gorkov theory (92) of paramagnetic impurities in superconductors. Excellent reviews of the experimental and theoretical situations have been given by Maple (167) and Müller-Hartmann (169) while Fischer and Peter (170) discuss the possible coexistence of ferromagnetism and superconductivity. We should however, point out that the Abrikosov-Gorkov theory can only be valid for impurity concentrations such that $T^*_{imp}(c) < T_{sc}$. For smaller concentrations one would have to deal with localized spin fluctuations. It is therefore not surprising that superconductors containing RE impurities, particularly Gd, offer the best testing grounds for the Abrikosov-Gorkov theory. These impurities should clearly have very low values of T^*_{imp} owing to the very small

s-f exchange mixing. Thus our preoccupation with lsf effects in superconductors is not totally injudicious.

We wish to suggest that spin fluctuations arising from the s-d exchange mixing interaction do provide a mechanism that may be partly responsible for the superconductivity of the transition metals. The mechanism is identical in most respects to that provided by electron-phonon interactions. An effective electron-electron interaction is engendered through the virtual emission and absorption of paramagnons in processes similar to the direct and exchange processes invoked in the discussion of the Kondo effect (section 1.7). However, we do not agree with Riblet (164) that the induced electron-electron interaction is necessarily repulsive. Following the standard treatment of the effective phonon-induced electron-electron interaction (171) we may represent the paramagnon induced electron-electron interaction by the matrix element of the form

$$\langle \underline{k}-\underline{K}, \underline{k}'+\underline{K} | V | \underline{K}, \underline{k}' \rangle \sim \frac{|W_{\underline{k},\underline{k}-\underline{K}}|^2 \hbar\nu_{sf}}{[\mathcal{E}(\underline{k})-\mathcal{E}(\underline{k}-\underline{K})]^2-(\hbar\nu_{sf})^2} \quad 2.67$$

where ν_{sf} is the paramagnon frequency and $W_{\underline{k},\underline{k}-\underline{K}}$ is the matrix element of the electron-paramagnon interaction. Equation (2.67) clearly shows that there exists the possibility of the effective electron-electron interaction being repulsive or attractive. The latter obtains if

$$|\mathcal{E}(\underline{k}) - \mathcal{E}(\underline{k}-\underline{K})| < \hbar\nu_{sf}$$

which is satisfied if ν_{sf} is sufficiently large i.e. if the TM has a sufficiently high effective degeneracy temperature. We note that Sólyom and Zawadowski (172) had in fact shown theoretically that the inelastic part of the electron-electron interaction induced by spin fluctuations is attractive if the s-d exchange coupling is antiferromagnetic. We also observe that it was the analogy between the phonon-induced and paramagnon-induced electron-electron interactions that led Heeger (2) to ponder whether the Kondo divergence signalled that onset of a many-body condensed state, as in superconductivity.

In analogy with the BCS formula (equation (2.50)) we therefore propose that the superconducting transition temperature is given by

$$T_{sc} = 1.14\, T_h^{*}\, e^{-\frac{1}{\lambda_{sf}-\mu^{*}}} \qquad 2.68$$

where λ_{sf} is an electron-paramagnon coupling coefficient given by

$$\lambda_{sf} \sim \langle V_{sd} \rangle \rho(\varepsilon_F) \qquad 2.69$$

$\rho(\varepsilon_F)$ being the total density of states per spin index at the Fermi level ($\frac{1}{2}\rho_d(\varepsilon_F)$ for the TM in question) and μ^{*} is, as before, the Coulomb pseudopotential. There are thus two almost independent parameters which determine the magnitude of T_{sc} - the characteristic temperature, T^{*}_{h}, of the TM which depends on the value of $\frac{\Delta_0}{\Delta}$ (see equation (2.34)) and the coupling constant

λ_{sf} which depends on both the matrix element of the s-d mixing interaction and the density of states at the Fermi level. To get an order of magnitude estimate let us consider Ir for which $\rho(\epsilon_F)$ = 0.51 state / ev. atom per spin index (37); from a crude analysis of the temperature dependence of the magnetic susceptibility (see above) $T^*_h \sim T_{max} = T_{oe}{}^{-\frac{1}{2}} \approx 10^4$K; T_{sc} = 140 mK (173). Neglecting μ^* these parameters give $\lambda_{sf} \sim 0.09$ and hence that $\langle V_{sd} \rangle \sim 0.17$ev.

From equation (2.68) one may immediately make the following observations:

(i) $T_{sc} \propto T^*_h$, so that if $T^*_h \neq 0$, then the transition metal in principle, must have a finite superconducting transition temperature. Thus for Rh with $T^*_h \sim$ 1650K (see above) and $\lambda_{sf} \sim 0.1$ (as estimated for Ir) one obtains $T_{sc} \sim$ 85mK; experimentally, however, no superconductivity has been observed in Rh down to at least 86 mK (174) but then it must be borne in mind that equation (2.68) applies to an <u>ultrapure</u> sample. Impurities, especially if magnetic, may reduce T_{sc} below measurable values. Also as equations (2.8), (2.11), (1.21) and (2.69) clearly show a large value of T^*_h would not necessarily imply a correspondingly large λ_{sf} and conversely. Similarly very pure Pd should be superconducting with a transition temperature of about 1.4 mK again using $\lambda_{sf} \sim 0.09$ (but see equation (2.71) below)

(ii) There is no <u>explicit</u> dependence on the mass of the atomic species so that the absence of an isotope effect would not require any additional postulates.

However, some isotope effect may be expected because of the renormalization of the total density of states by electron-phonon interactions. If $\Theta_D < T^*_h$, as happens to be the case for many pure TM, then one can incorporate the effect of electron-phonon interactions easily into equation (2.68) by using the electron-phonon coupling constant. One obtains

$$T_{sc} = 1.14\, T^* \, e^{-\frac{1}{\lambda_{sf} + \lambda_{ph} - \mu^*}} \qquad 2.70$$

with the possibility of λ_{ph} actually being negative! On the other hand, if $\Theta_D > T^*_h$, as for Pd, then

$$T_{sc} = 1.14\, \Theta_D \, e^{-\frac{1}{\lambda_{ph} + \lambda_{sf} - \mu^*}} \qquad 2.71$$

with the proviso that λ_{sf} can be negative. In this case spin fluctuations may suppress the tendency towards superconductivity.

(iii) The effect of impurities is readily taken into account through their modification of T^*_h and λ_{sf}. There exists, in principle, the possibility that T^*_h may be increased or decreased. A non-magnetic impurity may, however, increase the value of λ_{sf} through the additional contribution to the density of states, $\rho(\varepsilon_F)$, without significantly altering T^*_h. Usually, though the decrease of T^*_h caused by the presence of a magnetic impurity far outweighs the concomitant small increase in the value of λ_{sf} so that T_{sc} decreases. If we neglect the concentration dependence of the exponential factor in equation (2.70) then we expect that

$$\frac{dT_{sc}}{dc} = -\frac{dT^*}{dc} \qquad 2.72$$

(iv) From equations (2.34) and (2.70)

$$T_{sc} = 1.14\,T_F\, e^{-\left\{\frac{\pi\Delta_0}{2\Delta} + (\lambda_{sf} + \lambda_{ph} - \mu^*)^{-1}\right\}} \qquad 2.73$$

If for a given column of superconducting TM the exponential factor in equation (2.73) remains approximately constant then since $T_F \propto \gamma$ we get that

$$\gamma T_{sc} \simeq \text{constant} \qquad 2.74$$

as noticed by Matthias et al (156). Table 2.2 lists some values of T_{sc} for some superconducting TM groups.

Table 2.2 γT_{sc} values for some TM groups

Element	γ (mJ/mole K^2)	T_{sc}(K)	γT_{sc}(mJ/mole K
Ti	3.35	0.45$^+$	1.51
Zr	2.80	0.546	1.53
Hf	2.16	0.16	0.34^{+++}
Ru	3.1	0.51	1.58
Os	2.4	0.66	1.58
Rh	4.7	0.085^{++}	0.40
Ir	3.2	0.14	0.45

Notes:

+ Values in the literature (see reference 118) range from 0.39 to 0.49K, so an average value has been taken.

++ Estimated value (see text)

+++ Based on the γT_{sc} values of Ti and Zr one would expect a much higher T_{sc} for Hf than quoted, say about 0.7K. We emphasize again that specimen purity is an important factor because the theory outlined above strictly applies to very clean superconductors.

For those elements with a large density of states at the Fermi level (particularly V, Nb and Ta) the effect of electron-phonon interactions will be important so that equation (2.74) is not expected to be valid.

(v) We should perhaps mention that since $T_{sc} \propto T^*_h$ and since a low T^*_h indicates a tendency towards magnetic behaviour it is then obvious that for the transition metals superconductivity and magnetism appear to be mutually exclusive.

In conclusion we will like to state that a consistent explanation of the superconducting properties of the transition metals and alloys of one member with another (see references 156 and 175 for a summary of these properties) can be given in terms of the variations of T^*_h and λ_{sf}, with λ_{ph} coming in whenever $\rho(E_F)$ is especially large.

Summary

The main points discussed in the foregoing subsection may be summarized thus:-

(i) The "magnetic state" of a transition metal impurity in a non-magnetic metal host is characterized by just one parameter - its characteristic (or spin fluctuation) temperature, T^*_{imp}. It is defined by equation (2.8)

or more generally by equation (2.36). As the latter equation shows the magnitude of T^*_{imp} is determined by the effective degeneracy (magnetic) temperature of the host matrix, the exchange splitting, Δ_o, of the d-level resonance and the width, Δ, of the impurity VBS. Δ_o results from intra-atomic correlations and so varies only slightly, if at all, with either host matrix or impurity concentration. On the other hand, Δ contains contributions from spin-orbit coupling, s-d exchange mixing interactions and inter-impurity interactions. Owing to the latter interactions, Δ, and hence T^*_{imp}, is concentration-dependent, decreasing from a value appropriate in the single impurity limit (giving T^*_o) to zero at some critical concentration, c_m, of the magnetic solute. Thus $T^*_{imp}(c_m) = 0$, a condition which ensures that all impurity atoms would be observed to be magnetic at all temperatures even in the absence of any form of magnetic ordering. The concentration-dependence of T^*_{imp} also allows one to readily account for the existence of local environment effects. Also, although not discussed, it is expected that Δ will be affected by an applied pressure P so that $T^*_{imp} = T^*_{imp}(c,P)$

(i) It was also pointed out that there are two aspects of the Kondo problem, a fact which becomes immediately obvious from figure 2.3. The two aspects refer to the transition from the paramagnetic region to either the magnetic region $c \gtrsim c_m$ or to the non-magnetic region, $c \ll c_m$. In the first case, the Kondo divergence results from the neglect of inter-impurity magnetic interactions

which lead to magnetic ordering at a temperature T_m. We must caution that it is strictly incorrect to assume that in general magnetic ordering will help to stabilize the impurity spins. In this particular case, the impurity spins will still be well-defined at all temperatures as just mentioned above. The resistance minimum in this case should always be accompanied by a resistance maximum at some lower temperature. It is to this case that Kondo's original theory applies fully, with its predicted concentration dependence of T_{min} etc.

In the second case the impurity spins are not well-defined at all temperatures. As discussed the s-d interactions and spin-orbit coupling endow an impurity spin with a finite characteristic temperature (or a finite spin fluctuation frequency). The Kondo divergence in this case is then the result of the "transition" into a non-magnetic state, a not-particularly-apt description because any experimental probe with frequency $\nu >> \nu_{sf}$ $(= \frac{k_B}{h} T_{imp}^{*})$ would observe the local magnetic moment of the impurity atom. In deference to Kondo and also to correct the above terminology, we should call this region the Kondo region. It should be emphasized that the transition into the Kondo state is governed entirely by localized spin fluctuations so that all theories relating to the supposed existence of a magnetic singlet state are clearly inappropriate. It is clearly high time "the less and less fruitful staggering in the jungle of traditional Kondoism" (4) was stopped.

(iii) The concept of a spin fluctuation temperature in the dilute alloy problem can easily be extended to the

pure transition metals by the obvious modification that inter-atomic interactions broaden the d-levels into bands. Therefore, the exchange-split virtual bound states of the dilute alloy problem now give way to exchange-split d-bands in a pure transition metal, with Δ now representing the additional broadening due to s-d interactions and spin-orbi coupling. Consequently every transition metal has an effective magnetic degeneracy temperature, T^*_h, which, in general, is less than the Fermi temperature, T_F, as is apparent from equation (2.34). In this respect every transition metal is intrinsically "exchange enhanced" and it is also in this context that one ought to consider the magnetic behaviour of Pd and Pt. However, we have to treat the case of Pt with some caution because there appears to be some similarity between its magnetic behaviour and that of Cr. This similarity will be considered elsewhere but it will be mentioned here that it could significantly modify the current view of the stabilization of spin density waves in pure Cr.

It has also been argued that paramagnons are, in fact, localized spin fluctuations arising from the s-d interaction It is clear from all the foregoing discussion that any itineracy of the d-electrons is limited to their presence at the Fermi level and consequently inter-atomic electron-electron correlations do not figure as prominently as in the current paramagnon theories. We have suggested that a redevelopment of these theories to reflect this view of paramagnons would bring the predictions of the paramagnon theories into better agreement with experiment.

(iv) It is also suggested that paramagnon-induced attractive electron-electron interactions could be primarily responsible for the superconductivity of the transition metals, with electron-phonon interactions being significant only in cases where $\rho(E_F)$ is especially large. In fact, since for many transition metals $T^*_h >> \Theta_D$, the possibility exists that electron-phonon interactions can in some cases actually tend to suppress superconductivity. However, for $\Theta_D >> T^*_h$ the relative importance of spin-fluctuations and electron-phonon interactions is reversed. Both the electron-paramagnon and electron-phonon mechanisms for superconductivity could lead to two separate energy gaps for superconducting transition metals, each of which involves all electrons at the Fermi surface (i.e. <u>both</u> s- and d- electrons. This suggestion contrasts that of Garland (160) who has suggested two energy gaps with one being predominantly d-like and the other predominantly s-like. It should also be mentioned that in a recent publication Kim (176) showed that exchange interactions could significantly enhance the electron-phonon coupling constant and so increase T_{sc}. This, at least, supports our contention that spin fluctuations do not <u>always</u> suppress superconductivity as has been hitherto widely believed.

(v) An apparently trivial point which was omitted in the main body of our discussion is the temperature-dependence of the observed effective moment, μ_{eff}, of an impurity atom. We wish to correct any impression that may have developed to the effect that $\mu_{eff}(T)$ is zero for

$T < T^*$ and then boostraps to its maximum value for $T \geq T^*$ a kind of step-function behaviour. This is, of course, unphysical. We should instead expect that

$$\mu_{eff}(T) \sim \mu_{max} f\left(\frac{T}{T^*}\right) \qquad 2.75$$

where μ_{max} is the maximum magnetic moment determined by the exchange splitting and $f\left(\frac{T}{T^*}\right)$ is a function that tends asymptotically to unity for $T \gg T^*$ and to zero for $T \ll T^*$.

We regret that it has not been possible to throw the full weight of Green's functions, Feynman diagrams, etc. behind some of our arguments. However, we cannot be too apologetic because the one or two crucial assumptions which we have made are those that usually would be introduced ad hoc in any formal mathematical treatment. Nonetheless, we have tried, wherever possible, to incorporate any new ideas (or our interpretation of existing ones) withi the currently accepted mathematical framework. Where such a framework has been found wanting suggestions for improvement have been given. The overriding concern has been to ensure a coherent, consistent and easily readable (i.e. understandable) explanation of the Physics involved in the phenomena so far discussed (and to be discussed). As for the lack of mathematical rigour we can either take solace in Heeger's observation (2) that very often the significance and meaning of the approximations made in the formal treatment of the local moment problem are unclear even to the experts in the field! or gladly accept Nozieres' view (108)

that "a simple qualitative theory is worth more than a complicated quantitative theory". Having said this, we must not, of course, fail to recognize the importance of a suitable mathematical theory and it would appear that the way is now clear for such a theory of the magnetism of transition metals to be correctly developed.

2.3 The Magnetic Phase Diagram

In the preceding section we explained how and when the local moment on an impurity transition metal atom introduced dilutely into a non-magnetic matrix may be observed. We saw that the observation of this moment depended essentially on the characteristic temperature (or "spin fluctuation temperature"), T^*_{imp}, of the impurity atom. Within the context of our operational definition of a local moment (section 1.1.) no local moment would be observed for $T < T^*_{imp}$ because no Curie or Curie-Weiss law is expected in this range. More generally, however, we can state that any experimental probe whose 'frequency' is less than $\frac{K_B T^*_{imp}}{h}$ cannot detect the local moment on an impurity atom which, we have assumed, exists ab initio in favourable cases.

We have also seen that the characteristic temperature depends on the nature of both the host matrix and the impurity and also, owing to inter-impurity interactions, on the impurity concentration. For some species of impurity atoms T^*_{imp} decreases continuously from a value T^*_o appropriate in the single impurity limit, as the impurity concentration is increased and we were thus able to define a critical concentration, c_m, for which $T^*(c_m) = 0$. For concentrations

$c \gg c_m$ all impurity atoms should have well-defined spins at all temperatures irrespective of whether or not some form of magnetic order sets in at some finite temperature. This is because the mutual inter-impurity interactions which over come the destabilizing effects of the s-d interactions and spin-orbit coupling are not necessarily magnetic in origin. On the other hand, in the concentration region $c < c_m$, which region we call the Kondo region, the spin on a single impurity atom is not well-defined at temperatures $T < T^*_{imp}$ and in this region magnetic ordering may help stabilize the individual spins especially if the effective field acting on a spin $B_{eff} \sim \frac{K_B T^*_{imp}}{g\mu_B}$. It is only in the case of ferromagnetic ordering that we expect any significant interna fields.

It has also been mentioned that in the Kondo region it is possible for clusters of impurity atoms (pairs, triplets etc) to have a lower local characteristic temperature, T^*_{cl}, than an isolated impurity atom and such a cluster can be classified as "non-magnetic","nearly magnetic" or "magnetic" according as T^*_{cl} ($< T^*_{imp}$) is much greater than, of the order of, or less than the temperature at which the observation is made. Unless otherwise stated it will be assumed that the binary alloy under discussion is completely disordered so that any clusters present are due solely to statistical concentration fluctuations; in these circumstances the concentration of a particular cluster is exactly calculable by standard probability theory. For a lattice structure with a coordination number z_0 the probability of an impurity atom having at least n nearest neighbours of its own species at an impurity concentration c is given by

$$P_n = \sum_{p=n}^{z_o} C_p^{z_o} c^p (1-c)^{z_o - p} \qquad 2.76$$

where $$C_p^{z_o} = \frac{z_o!}{p!(z_o-p)!} .$$

If n_o is the minimum number of nearest neighbour impurity atoms required in order that a cluster be observed to be magnetic at a given temperature then the total number of "magnetic" clusters is simply $c P_{n_o}$. Note that as defined n_o would be a function of temperature so that the number of such "magnetic" clusters would increase as the temperature of observation is increased. Also since T^*_{imp} depends on the impurity concentration, n_o will similarly do so. In general

$$n_o = n_o(T, c, B, P) \qquad 2.77$$

where B is the effective field acting on the cluster (internal and external) and P is the pressure. It is therefore clear that no simple behaviour can be predicted. Fortunately though any variation in cluster concentration and size can only be important for systems with large critical concentrations, and even then it does appear that it is only in the critical concentration range that the difference between $T^*_{n_o}$ and $T^*_{n_o-1}$ is sufficiently small as to affect the magnetic properties of the system significantly. For low impurity concentrations only pairs and triplets of impurity atoms occur in significant concentrations. If the impurity concentration is c then the concentration of impurity pairs is

$$C_{pairs} = z_0 c^2 (1-c)^{z_0-1} \approx 100 c^2 z_0 \text{ ppm}, \qquad 2.78$$

if c is given in atomic percent; similarly

$$C_{triplets} = \tfrac{1}{2} z_0 (z_0-1) c^3 (1-c)^{z_0-2} \simeq \tfrac{1}{2} z_0 (z_0-1) c^3 \text{ ppm} \qquad 2.79$$

again with c in at. %.

In systems where there exists a natural tendency towards atomic clustering, as in AuFe and CuNi alloy systems it is clear that the concentration of a particular cluster will be higher than the statistical estimate. While it is not our intention to discuss the exact detials of how the presence of such pairs or triplets, etc, affects the magneti and transport properties of dilute non-magnetic alloys, we can expect a certain pattern of behaviour - contributions to the magnetic susceptibility and electrical resistivity which vary as c^{no} (i.e. as c^2 or c^3, etc). A satisfactory account of some of these contributions has been given by Tournier (91) although we do not agree with a few of his conclusions or suggestions. One of these concerns the possible existence of "antiferromagnetic regions in the non-magnetic - antiferromagnetic transition". As discussed below it is doubtful whether such a transition actually exists as no system has yet been found to exhibit it.

We can now turn our attention to the magnetic region as labelled in figure 2.3. Our aim in this section is to

discuss the succession of magnetic states as the impurity concentration is increased. So let us consider an alloy system for which T^*_o is very low - say alloys of Mn with the noble metals, with $T^*_o \sim 10$ mK as mentioned several times earlier. The critical concentration will consequently be very small, a few ppm at most. At such low concentrations the only important magnetic interaction is clearly the indirect RKKY coupling which leads to the well-known spin-glass magnetic order below some transition temperature T_{sg}. The magnetic properties of the spin-glass state will, of course, depend on the nature of the RKKY interaction and, as mentioned in section 1.12, the inverse r^3 - dependence of the RKKY interaction gives rise to the existence of scaling-laws (equations (1.74) and (1.75)). Thus the spin-glass ordering temperature, T_{sg}, increases linearly with the impurity concentration. However, inspite of the overall dominance of the RKKY interaction in this low impurity concentration region there is still a finite statistical probability that some impurity atoms could find themselves as near neighbours and subsequently couple their moments through some magnetic interaction. The nature of this magnetic interaction may be determined from the "Moriya rules" quoted in section 1.12. Thus for impurity atoms with nearly half-filled d-shells the magnetic coupling is anti-ferromagnetic whereas for impurity atoms with nearly-filled d-shells the coupling is ferromagnetic. Therefore it is expected that near neighbour Mn or Cr spins would tend to couple antiferromagnetically whilst near neighbour Co spins would couple ferromagnetically. We must however, caution against an injudicious application of this particular Moriya

rule, especially with respect to Fe whose d-shell is just more than half-filled. It does appear that the effective interaction between Fe atoms depends sensitively on their separation, being antiferromagnetic if the separation is less than a critical distance. This point is well illustrated by the behaviour of the RhFe system in which first order ferromagnetic - antiferromagnetic phase transitions occur in alloys containing about 50% Rh (183). At room temperature the magnetic phase changes from ferromagnetism to antiferromagnetism as the Rh concentration increases from 49% to 50%. The lattice constant of the 49%Rh alloy is 2.993 Å while that of the 50%Rh alloy is 2.986 Å . Also a 53% Rh alloy is antiferromagnetic at 288K (lattice constant = 2.987 Å) but is ferromagnetic at 338 K (lattice constant = 2.997 Å)

For sufficiently low impurity concentrations the concentration of the spin clusters is negligible; for example, if c = 0.1%, the concentration of pairs of impurity spins is about $z_0 p p_m$ (see equation (2.78)). The concentration of larger clusters is even much less. As the impurity concentration increases the concentration of these clusters increases even more rapidly: for an fcc lattice $c_{pairs} \sim 0.12\%$ and 0.48% for impurity concentrations of 1 and 2% respectively. Much more important, however, is that fact that there is a rapidly increasing probability of large clusters forming, extending say over several lattice spacings. Such large clusters with their large moments are bound to significantly affect the physical properties of the alloy in question. The increasing significance of these clusters as the impurity concentration increases would imply that the scaling laws can only apply in the low impurity concentration region

($c_m \leq c \lesssim$ 5% say). Before continuing with the discussion of the succession of magnetic states we shall briefly return to the Kondo region. It has been discussed already how near neighbour impurity atoms can in some cases help to stabilize their local spins. This stabilization process is not magnetic in origin but is due to <u>charge density oscillations</u> which affect the host density of states at the Fermi level (see equation (1.59) and also reference 91). It is, of course, possible that the fact that the stabilized spins would then couple magnetically may "catalyze" the stabilization process. The resulting magnetic clusters interact via the RKKY coupling to give what we shall term a <u>cluster-glass</u> below an appropriate transition temperature, T_{cg}. This phenomenon is often termed <u>residual magnetism</u>. A cluster-glass will be taken to refer to spin-glass type ordering in which the magnetic entities involved are <u>clusters</u> of impurity atoms only, the single impurity atoms still remaining "non-magnetic". Thus, by our definition, a cluster-glass exists only in the Kondo region, $c < c_m$. We shall restate that any magnetic ordering can only significantly affect single impurity atoms if the resulting internal field $\sim \frac{k_B T_{imp}^*}{g\mu_B}$. Again for low impurity concentrations only pairs or triplets of impurity atoms will be important and if these are taken as the magnetic units then the scaling laws would equally be valid. Thus for <u>Au</u>Co $T_{cg} \sim c^3$ (91) whereas for <u>Cu</u>Fe (91) and <u>Au</u>Fe (184) $T_{cg} \sim c^2$.

In the magnetic region we have seen that as the impurity concentration increases one would have to consider both the 'direct' inter-impurity interaction and the RKKY coupling.

In AuFe near-neighbour Fe atoms couple ferromagnetically whereas in AuMn or CuMn near neighbour Mn atoms couple anti-ferromagnetically.

However, the fm coupling in AuFe must be viewed in the context of the comment made above in the case of RhFe).

An alloy in which there are single impurity atoms with well-defined spins and in which some of these spins couple ferromagnetically to give large moment clusters will be called a mictomagnet. The only example that has been extensively studied is of course, AuFe. A second example could be the MoFe system (212). The more general term of superparamagnetism will be taken to include both cluster-glasses and mictomagnets. In view of the prevalent lax usage of these terms it is necessary to clearly define the exact circumstances under which a given terminology is most appropriate. This is done shortly below.

Irrespective of whether mictomagnetism occurs or not if the near neighbour impurity coupling is ferromagnetic then long-range ferromagnetic order is expected to set in when the percolation limit is reached i.e. when there is a sufficient concentration of impurity spins which can link up to form an infinite ferromagnetic chain. In the special case where the fm coupling is restricted to just nearest neighbour sites then the percolation concentration is reached when at least two of the nearest neighbour positions of a given impurity site are occupied by impurity atoms (185); it is given simply by

$$c_p = \frac{2}{z_o} \qquad 2.80$$

which works out at 33.3, 25 and 16.7% for sc, bcc and fcc (or hcp) lattices respectively. Other estimates of this concentration have been given using various approximations. For example, Elliot (187) has obtained

$$c_p = \frac{S+1}{S(z_0-1)} \qquad 2.81$$

where S is the spin moment. By means of small angle neutron scattering Murani et al (188) have determined that for AuFe the percolation concentration lies between 15 and 17% Fe, which is in good agreement with the values given by equations (2.80) and (2.81) (with $S \simeq 1.5$ as observed for Fe in fcc lattices).

Observe that if the range of fm coupling is less than the nearest neighbour distance or more generally, if the range is always smaller than the average impurity - impurity distance, then ferromagnetism may never set in. On the other hand, if the range spans several lattice spacings, then the effective percolation concentration will be small.

Ferromagnetism is obviously not the only form of long range magnetic order that exists. Other forms include helimagnetism, antiferromagnetism and spin density waves (SDW), otherwise called "itinerant antiferromagnetism".

(a) Helical ordering (or helimagnetism) can be stabilized from the spin-glass regime at an impurity concentration determined by the nature of the host matrix (specifically by the nature of the Fermi surface of the host, which influences the range of the RKKY coupling - see section 1.12). The impurity spins involved are usually the rare-earths; for example, alloys of $\left\{\begin{matrix} Y \\ Sc \end{matrix}\right\}$ with $\left\{\begin{matrix} Gd \\ Tb \end{matrix}\right.$ (189).

While we shall strive to restrict our discussion to transition metal impurities only, we shall point out that some of the discussion can be carried over to the case of RE impurities with only minor modifications (to allow for say cryst field effects). An important point is that such systems in which helical ordering is stabilized from a spin-glass regime are usually not "bedevilled" by clustering and are therefore, the most suitable candidates for studying the properties of a true spin-glass, particularly the dynamics.

(b) Antiferromagnetism in the conventional form where a well defined spin exists on a particular sub-lattice cannot obviously occur in our alloy systems which are presumed to be randomly disordered. Therefore there is no possibility that this form of antiferromagnetism can be stabilized from the spin-glass regime. What would happen in say CuMn as the Mn concentration increases, is that an increasing number of nearest neighbour Mn atoms couple antiferromagnetically, giving local regions with practically no internal field. The system, of course, still behaves as a spin glass but its transition temperature T_{sg} will slowly increase to a maximum and then decrease as the number of 'voids' (i.e. afm-coupled Mn atoms) dominates the uncoupled spins. The effect should be more clearly reflected in the effective moment or Curie constant obtained by fitting the susceptibility to a Curie-Weiss law at temperatures sufficiently above the corresponding transition temperatures. The Curie constant should exhibit a gentle maximum while the magnitude of the (negative) Curie-Weiss constant should increase continuously. However, the above picture is a

rather simplified one of the actual situation that may obtain. As the Mn concentration increases a given Mn atom will eventually find itself surrounded by more than just a single nearest neighbour Mn atom. In such an event one of three things may happen:-

(i) the Mn atoms adjust their spin directions in such a way as to accommodate their mutual "dislike" of one another say by the "canting" of their spins;

(ii) the lattice structure changes to a form that may allow the mutual antiparallelism of the spins - probably some sort of layered cubic structure;

(iii) both (i) and (ii) occur simultaneously.

(Note that a change of lattice structure could bring about a change in the observed magnitude of the local spin).

For want of a better descriptive name we will refer to this type of system as a disordered intrinsic antiferromagnet (DAF).

(c) Among the transition metals it is only Cr that has been unequivocally shown to possess spin density waves. This fact has been attributed to the particular nature of its Fermi surface which through some god-effect happens to be just right (a perfect matching of the electron and hole portions of the Fermi surface) for the stabilization of spin density waves (157, 190). However, it seems to us that the essential conditions favourable for the stabilization of SDW include (i) existence of a small localized moment, $\lesssim 0.4\ \mu_B$ / atom, (ii) an intrinsic afm coupling between such moments and (iii) a fairly large s-d exchange coupling. These conditions are clearly satisfied for Cr,*

[* see also Ref. 755]

and possibly for Pt.

Among the transition metal alloys only MoCr is known to exhibit a transition from the Kondo state to SDW at about 76% Cr (191, 192). This is not in the least unexpected - not only are Mo and Cr isoelectronic but also they have the same bcc lattice structure with lattice constants that diffe by less than 10%. A largely Cr matrix exhibiting magnetic properties that are similar to those of pure Cr is not surprising.

One other system suspected of such behaviour is yet another isoelectronic pair RuFe (193) with a critical composition of about 50% Fe. The reason for the apparent restriction of the occurrence of SDW to isoelectronic alloys seems to be obvious - the need to avoid large potential scattering effects. Accordingly, it is possible that in TcMn SDW will be stabilized from the Kondo region at about 65% Mn if there are no metallurgical complications. One important point about the transition from the Kondo region to the SDW region is that apparently no magnetic clusters occur at all. It would not, of course, be experimentally easy to detect a cluster of say two antiferromagnetically-coupled spins each of moment $\lesssim 0.4 \mu_B$, so that the absenc of magnetic clusters is a moot point. It does not appear that the rather tenuous link between the occurrence of spin density waves and the superconductivity of one of the constituent elements is of any great significance but it should be further investigated especially in the light of our suggestion concerning the superconductivity of transition metals.

So far we have considered two classes of alloys; one in which the first magnetic state that occurs is a spin-glass which may or may not give way to long range magnetic order at higher impurity concentrations. In the other class of alloys a straight transition occurs from the Kondo region into a SDW region, apparently without any magnetic clusters ever forming. Owing to the variety of magnetic behaviour observed in the first class of alloys an equally varied terminology has been used. This includes cluster-glass, spin-glass, superparamagnetism, mictomagnetism and lately disordered intrinsic antiferromagnet (DAF). In order to clarify the situation and especially to specify the magnetic behaviour to be expected, we suggest the following scheme. The term spin-glass should continue to be used to specify the magnetic ordering in a system where the dominant exchange interaction is the RKKY interaction.

A cluster-glass refers to the ordering that may occur in the Kondo region between clusters of impurity atoms, giving rise to the so-called residual magnetism. Individual impurity atoms still remain non-magnetic (in the sense already described) because the internal field that ensues with the magnetic ordering is usually not effective (i.e. $<< \frac{K_B T^*_{imp}}{g \mu_B}$).

Above the critical concentration all impurity spins are magnetic and the magnetic properties obey the scaling laws. We suggest that this particular spin-glass state be called speromagnetism, in analogy with a similar phenomenon that occurs in some amorphous magnetic materials (194). Of all the spin-glass states it is only the speromagnetic state that can lend itself to theoretical calculations

because the concentration of magnetic units is known exactly and also because, ideally, the conditions at all the impurit sites are identical. Unfortunately, the concentration range over which speromagnetism occurs is restricted to fairly low impurity concentrations ($\lesssim$ 5%).

From the speromagnetic state, long range magnetic order may be stabilized in two cases: helimagnetism for RE impurities and ferromagnetism for some alloys of Fe and Co (the only proven examples to-date are AuFe and RhCo, although as discussed below the exact succession of magnetic states in the latter system is not very clear). The onset of ferromagnetism in AuFe alloys is preceded by mictomagnetism in which there exist large Fe clusters with their spins coupled to give large moments. One cannot easily predict the exact behaviour of a mictomagnet because owing to the existence of both single and cluster spins one has to consider the interactions between the single spins, between the single spins and clusters and also the inter-cluster and intra-cluster interactions. It is clearly conceivable that a mictomagnet would have a number of characteristic temperatures corresponding to these various interactions, but we shall consider only two of these. One is the transition temperature, T_{sg}, characterizing the spin-glass ordering. This will have to be an average value because the transition from the spin glass state to the paramagnetic state is considerably broadened owing to a distribution of local fields. The other characteristic temperature is the temperature T_{cl}, at which clusters of the most probable size are formed, i.e. T_{cl} is a measure of the interaction energy between the spins in a given cluster. Murani (195) has

reported observing these two temperatures for Au 15% Fe. Finally, a speromagnet can give way to disordered intrinsic antiferromagnetism in alloys where the effective interaction between neighbouring impurity atoms is afm. This applies mostly to Mn alloys.

We shall stress again that the above classification scheme helps to give useful information about the type of spin-glass ordering and especially about the relevant concentration regime. The main distinction between the various types lies in the distribution of local fields. With the exception of the speromagnetic state where the local fields are expected to be uniform all other spin-glass states have local staggered fields whose different characteristics serve to distinguish them - the presence of strong fields amidst an otherwise uniform distribution of local fields would indicate a mictomagnet, etc. That the distribution of local fields in a speromagnet is nearly uniform may be deduced from the muon-spin depolarization experiments on Cu 0.7% Mn and Au 1.5% Fe by Murnick et al (196) who showed that the distribution of the dipolar fields on the impurity sites had no strong peaks or singularities. To summarize the succession of magnetic states in "spin-glass alloys" is as follows:

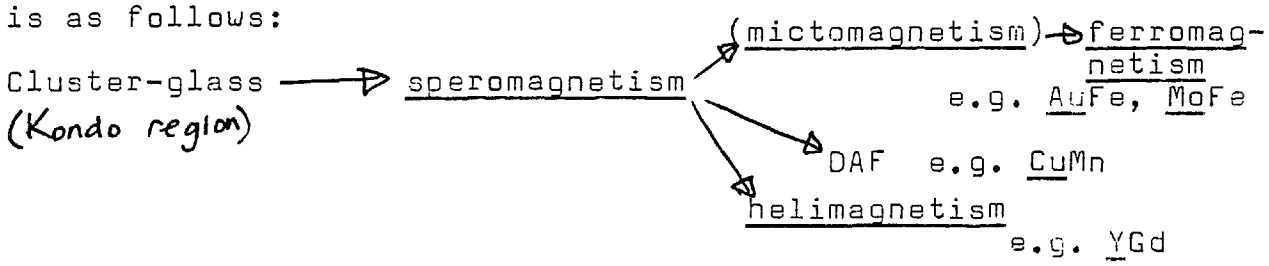

Since cluster-glasses and mictomagnets contain magnetic entities with fairly large moments they may also be referred to as superparamagnets.

There is yet a third class of alloys for which there appears to be a straight transition from the Kondo region to ferromagnetism, again with a cluster-glass regime existin just below the critical concentration. The alloys exhibitin this kind of behaviour include -

(a) Pd based alloys of Mn, Fe and Co and PtCo ;

(b) Alloys of Ni with non-magnetic metals ;

(c) a few other alloys of Fe such as VFe and possibly NbFe.

The list is not exhaustive but probably contains all the alloys at present known to show the particular behaviour mentioned. The most extensively studied are the Ni and Pd alloys.

The onset of magnetism in these alloys is essentially the same as in the spin-glass alloys, the importance of local environment effects depending on the peculiarities of a given host and a given solute. In the Pd-based alloys of Mn, Fe and Co ferromagnetism sets in at very low impurity concentrations ($\sim$ 0.1%), with each magnetic unit seeding a polarization cloud and so giving rise to "giant moments". Both the low critical concentration and the onset of ferro-magnetism (instead of speromagnetism as in say Au-based alloys) are a direct consequence of the fact that Pd is not just nearly magnetic ($T^*_h \simeq$ 85K) but nearly ferromagnetic, as compared with Pt which is also nearly magnetic but with a tendency towards antiferromagnetism (see preceding section) Thus Pt based alloys of the same impurities exhibit some of the properties of the archetypal spin-glass alloys. The difference in the behaviour of various solutes - from Co and Fe for which the Curie temperature T_c increases at the rate

of about 52K/ at %, to Mn for which $\frac{dTc}{dc}$ is a leisurely 4.1K/ at %, to Cr for which a spin-glass state sets in at about 7 at % Cr - can be understood either in terms of the spin polarization of the host matrix as given by the Moriya rules (section 1.12a) or, more consistently, in terms of the position of the impurity VBS with respect to the Fermi level of the Pd host, and the concomitant mutual effect on the characteristic temperatures of the impurity and host. The characteristic temperature, T^*_o, of Cr in Pd has been estimated (102) at about 200K which would imply that T^*_h for Pd was considerably increased from its value of 85K for the pure matrix (see equation (2.35)). This would not be unlikely if, by analogy with NiCr, the Cr VBS were to lie above the Fermi level of Pd.

In PdFe and PdCo neutron diffraction measurements (197, 198) have established that the spin polarization of the matrix is of the form

$$\chi(r) \sim \frac{1}{r} e^{-K_o r} \qquad 2.82$$

where r is the radial distance from a solute atom and K_o is the inverse polarization range which has a value of about 0.2Å^{-1}. Now for an impurity concentration c the average distance between the impurity atoms is given by (199)

$$r_{av} = 0.554 c^{-1/3} a_o \qquad 2.83$$

where a_o is the lattice constant; thus for $c \sim 0.1\%$, $r_{av} \sim 5.54 a_o$ and for Pd this gives an average separation of about 22Å between the centres of the polarization clouds.

Since the polarization range (= $^1/K_o$) is about 5Å it is just conceivable that the ferromagnetism of dilute PdFe and PdCo alloys arises through the overlap of the polarization clouds seeded by the impurity atoms. While a great deal of attention (perhaps too much!) has been focused on the "Special" properties of Pd, less notice has been taken of the fact that a critical concentration exists for the onset of ferromagnetism. Chouteau and Tournier (200) have investigated the magnetic properties of very dilute PdFe alloys and have shown that residual magnetism exists in the concentration region below the critical concentration (0.1%Fe) just as in AuFe or CuFe. Thus a cluster-glass region also exists in the PdFe system.

The behaviour of the other alloys in the group being presently considered is simply explained in terms of local environment effects which, although present in any given alloy system, are most important for end members of the transition metal series. This is especially true of Ni impurities in non-magnetic matrices. Extensive studies (magnetization (201-203), neutron diffraction (204), NMR (205), heat capacity measurements (201, 206) etc) have clearly shown that in CuNi alloys only clusters of eight or more Ni atoms are magnetic in the critical concentration region ($\lesssim$ 48%Ni) These clusters become ferromagnetically coupled (either through RKKY interactions or through the overlap of the clusters themselves) when their concentration reaches a few tenths of an atomic percent. The existence of such clusters has also been shown in many other alloy systems - VNi, CrNi, RhNi, VFe, etc and there is no longer any doubt about

the inhomogeneity of the onset of ferromagnetism in these alloys. In fact, it would seem that inhomogeneity is a necessary feature of the onset of ferromagnetism in disordered transition metal alloys since even in spin-glass alloys the ferromagnetic region is preceded by mictomagnetism. The inherent inhomogeneity of this ferromagnetic transition has made the exact determination of the critical concentration difficult, partly speculative and partly subjective through the use of ad hoc criteria which sometimes have no sound physical basis. It is in recognition of this problem that we shall devote the whole of section 2.5 to either deriving some relations that may be used to quantitatively analyse the data or else to explain the physical basis of any extrapolation procedures.

The presence of the magnetic clusters is reflected in their effect on the physical properties of the alloy systems. Thus one can either observe a resistance minimum as in CuNi (207), VFe (208), a change of slope in the plot of the residual resistivity against the impurity concentration (208) or a magnetic cluster-glass. The culpable failure to recognise the existence of such cluster-glass regions in these systems, particularly CuNi, PdNi and PtNi, has not in the least helped towards a better understanding of their properties. Well above the ferromagnetic Curie point, the magnetic clusters continue to exist as superparamagnetic entities until a temperature, T_{cl}, is reached at which the thermal fluctuation energy is equal to the intra-cluster interaction energy and the clusters therefore break up. We recall that Murani (195) reported observing $T_{cl} \lesssim 110K$

for a mictomagnetic AuFe alloy (15% Fe). For VFe $T_{cl} \lesssim 100$ K (208) while for Cu Ni $T_{cl} \gtrsim 600$ K (207), quite close to the Curie temperature of pure Ni. The interpretation of the observed behaviour in Cu Ni has, however, been questioned by Ahmad and Greig (209) who found similar anomalies in the temperature dependence of the electrical resistivity of a Pd 40% Ag alloy as found in several Cu Ni alloys (207)*.

Thus in general the succession of magnetic states in binary alloys follows three main patterns:

(i) "Spin glass" alloys

(ii) "SDW" alloys

(iii) "Giant moment" alloys.

In spin-glass alloys a speromagnetic (SPM) state is stabilized before any long-range magnetic order ensues whereas in SDW alloys and "giant moment" systems there appears to be a straight transition from the non-magnetic (Kondo) region into long-range magnetic order. Also in (i) and (iii) the magnetic state is preceded by a cluster-glass region which occurs in the Kondo region just below the critical concentration: this cluster region is apparently absent in (ii). Finally in (i) the fm state is preceded by mictomagnetism so that one can assume that the onset of ferromagnetism in disordered alloys is always inhomogeneous.

The magnetic phase diagrams corresponding to the above three patterns are sketched below.

---

* The resistivity of PdAg alloys (including Pd 40% Ag) has been recently remeasured by Arajs et al.(756). The minimum observed by Ahmad and Greig, which was not confirmed in these recent measurements, was attributed to strain effects rather than being an intrinsic characteristic of the PdAg alloy system.

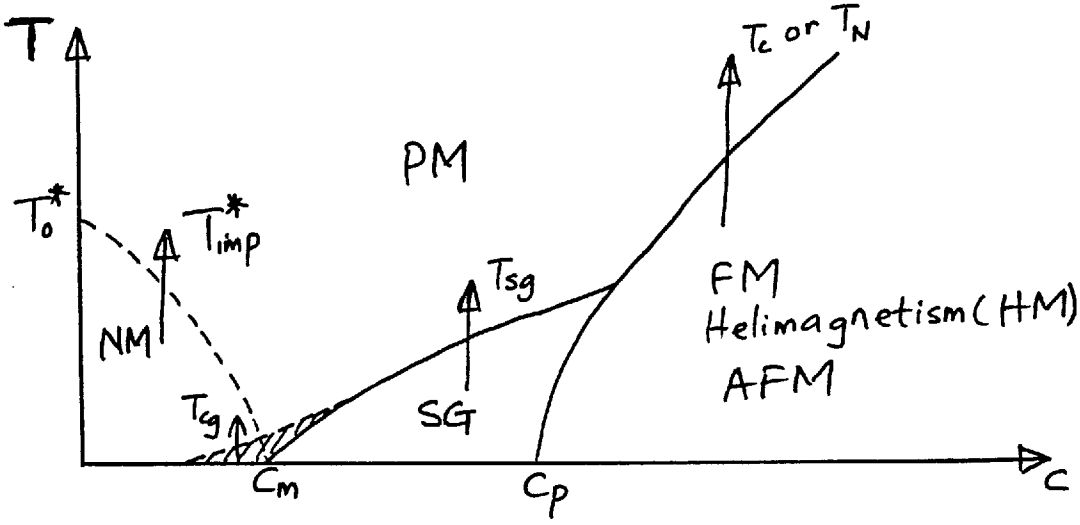

Fig.2.9

Magnetic "phase diagram" of a spin-glass alloy.

Figure 2.9 represents the general magnetic phase diagram for a spin-glass alloy. The letters NM, PM, SG, FM and AFM refer to the non-magnetic (Kondo region), paramagnetic, spin-glass, ferromagnetic and antiferromagnetic regions. c_p is the percolation concentration already defined, and applies only to FM and HM, since at the moment we are not sure how such a concentration would apply in the case of a transition to AFM. The other symbols have their usual meanings. The shaded area around c_m denotes the cluster-glass region; one should be extremely careful in interpreting the properties of a system within this concentration region because c_m is a sort of <u>triple point</u> and a complex behaviour may be expected. We have emphasized several times that cluster-glass ordering in the Kondo region can only affect individual impurity spins if the resulting internal field acting on an impurity atom $\sim \frac{k_B T^*_{imp}}{g\mu_B}$. Close to c_m where $T^*_{imp} \sim 0$ this condition may be satisfied so that individual impurity spins become well defined below T_{cg}. The small overlap of the cluster-glass region

into the true magnetic region implies that in this region the cluster-glass temperature, T_{cg}, is larger than the spin-glass temperature, T_{sg}.

The above sketch neglects the complications introduced by inter-impurity interactions which become important beyond the speromagnetic region and which may lead to ferromagnetic or antiferromagnetic impurity clusters. Let us consider some of the details in the case where ferromagnetic clustering occurs, i.e. where mictomagnetism is observed, as in AuFe or MoFe. Firstly, we have to delineate the speromagnetic region, (SPM) which is a small concentration region above c_m. As stated already the only reason for doing this is that this is the only region in the phase diagram where the concentration of magnetic units is exactly known, a priori. This concentration is equal to the impurity concentration. Neglecting any statistical concentration fluctuations the situation at a given magnetic unit site is the same as at any other site, i.e. the magnetic moment, the local field (dipolar + RKKY) etc are the same. This fact coupled with the inverse r^3 -dependence of both the dipolar and RKKY interactions essentially account for the scaling laws observed in this concentration regime. The scaling laws may also apply in the cluster-glass region because the magnetic units are probably predominantly of a particular cluster size— either pairs or triplets, etc. If the concentration of such clusters is known, say from an analysis of their paramagnetic behaviour, then there is no reason why the scaling laws should not apply. Beyond the SPM region is the mictomagnetic region whose characteristics

have also been defined. Here we have a broad transition temperature region whose upper bound is T_{cl}, (measuring the intra-cluster interaction energy of clusters of the most probable size) and whose lower bound is the actual T_{sg} which, it would appear characterizes the impurity spins not grouped within any clusters.

We think that as the impurity concentration increases T_{cl} also increases because the size of the most probable cluster may increase and, at the percolation concentration, T_{cl}, should coincide with the Curie temperature, T_c, since here the ferromagnet is essentially (and by definition) an infinite cluster. In AuFe this occurs near 16%Fe which is about the critical concentration. Accordingly, for such an alloy we sketch a typical phase diagram as in fig. 2.10

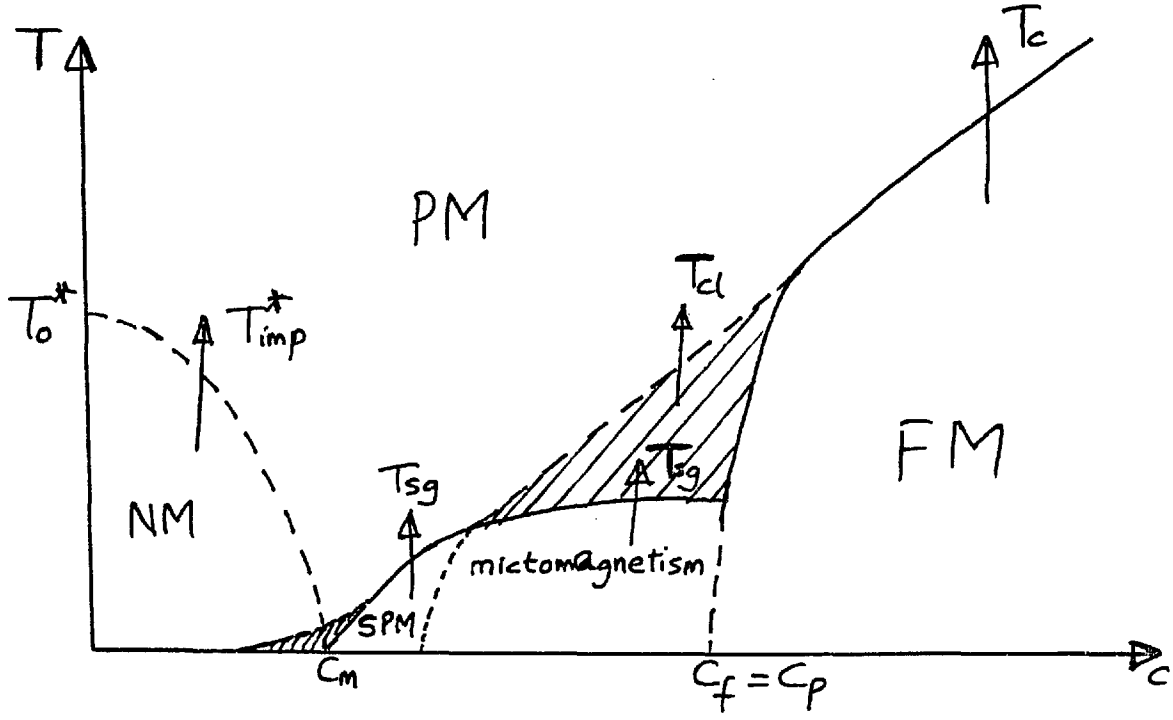

Fig.2.10: Magnetic phase diagram of a mictomagnetic spin-glass alloy, e.g. AuFe, MoFe.

The above phase diagram closely resembles that given by Murani et al (188) who labelled the shaded region as superparamagnetic.

We should perhaps make the following two comments. The first one refers to the variation of T_{sg} with impurity concentration. As observed for AuFe T_{sg} increases relatively slowly with impurity concentration instead of a rather rapid variation expected because of the fm clustering. One explanation of this behaviour is to assume that T_{sg} is proportional to the number of magnetic units. As the impurity concentration increases so does the number of impurity atoms grouped into clusters; therefore the effective number of magnetic units is smaller than the impurity concentration and in fact, is only marginally bigger than the number of spins not grouped into clusters. This is the rationale behind our earlier statement that in the mictomagnetic region T_{sg} refers to the "loners" i.e. ungrouped spins. The other comment applies to only AuFe and then well into the ferromagnetic regime. As the Fe concentration increases the lattice constant decreases and at some point the near neighbour distance decreases below a critical value so that neighbouring Fe atoms now interact antiferromagnetically. Beyond this limit the comments we made earlier about the possible canting of spins and/or lattice distortion in Mn rich spin-glass alloys such as CuMn would equally apply. This explains the remark made above that the fm coupling between impurity Fe atoms in AuFe must be viewed in the same way as in RhFe. It is not unlikely that the metallurgical problems encountered at the Fe rich end of the AuFe system are related to the magnetic properties in this

region.

In a DAF spin-glass alloy afm clusters exist, so that the susceptibility of the alloy becomes increasingly <u>smaller</u> as the impurity concentration increases. As in the case of mictomagnetic alloys T_{sg} here increases slowly with **c** as well and will actually attain a <u>maximum</u>, albeit a gentle one. With the exception of little differences the phase diagram for a DAF spin-glass alloy, sketched in figure 2.11 below, is essentially as for a mictomagnetic alloy (fig 2.10). A cluster temperature exists and in this case corresponds to the afm intra-cluster coupling energy. For <u>Cu</u> 65% Mn the susceptibility and electrical resistivity data (219) indicate that $T_{sg} \sim$ 135K while $T_{cl} \sim$ 240K. Again T_{cl} should join up smoothly with T_N at the concentration where long-range afm order is established.

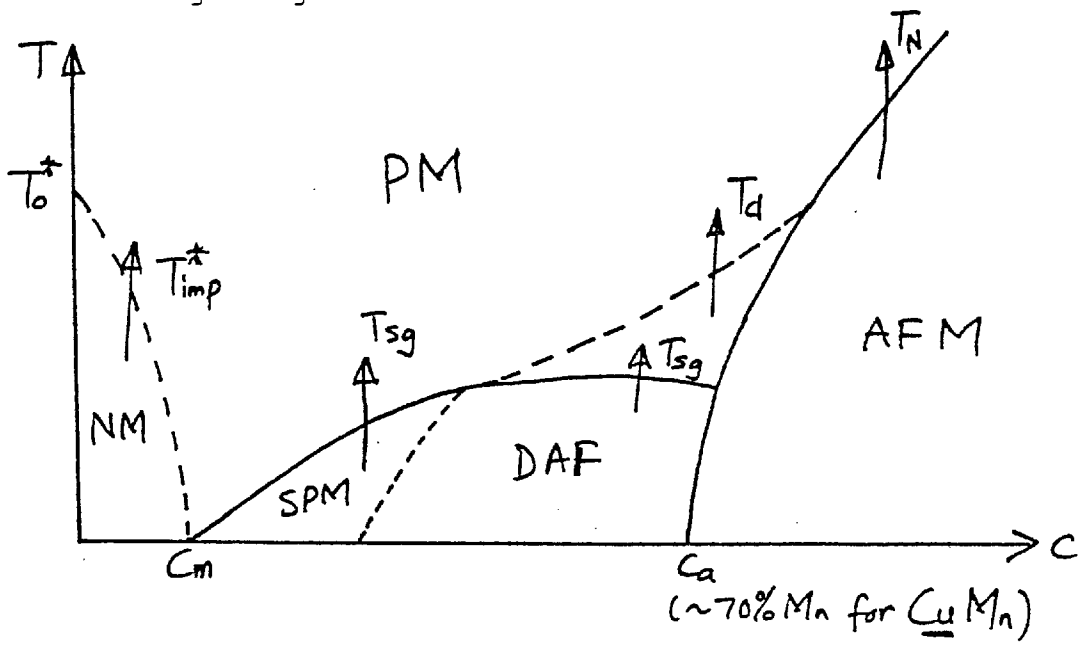

<u>Fig.2.11</u>: Magnetic phase diagram for a DAF spin-glass alloy (cf Fig. 2.10)

Note that as in the <u>AuFe</u> case, close to the concentration for spin-glass $\longrightarrow$ afm transition ($\sim$ 70% Mn in <u>CuMn</u>) $T_{cl} \backsimeq 2T_{sg}$. It is not known now what significance, if any, this observation has.

Figure 2.12 is the phase diagram for "SDW alloys" and "giant moment alloys" in which long-range magnetic order is stabilised from the Kondo region.

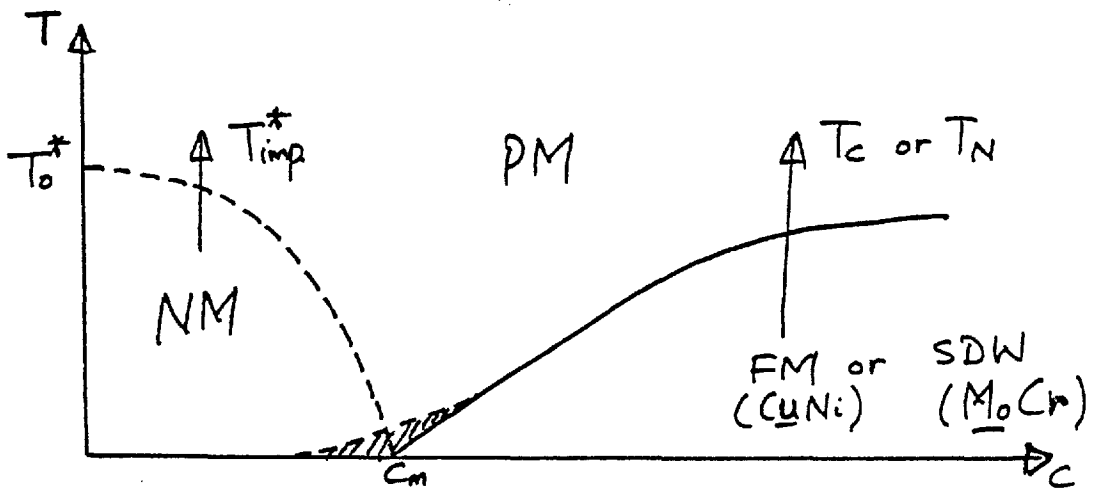

Fig.2.12: Magnetic phase diagram of "SDW" and "giant moment" alloys.

Again the shaded region is the cluster-glass region which is observed only in the case of "giant moment" alloys.

The above phase diagrams should be compared with those in current literature, such as the phase diagram of Sherrington and Mihill (210) - figure 2.13.

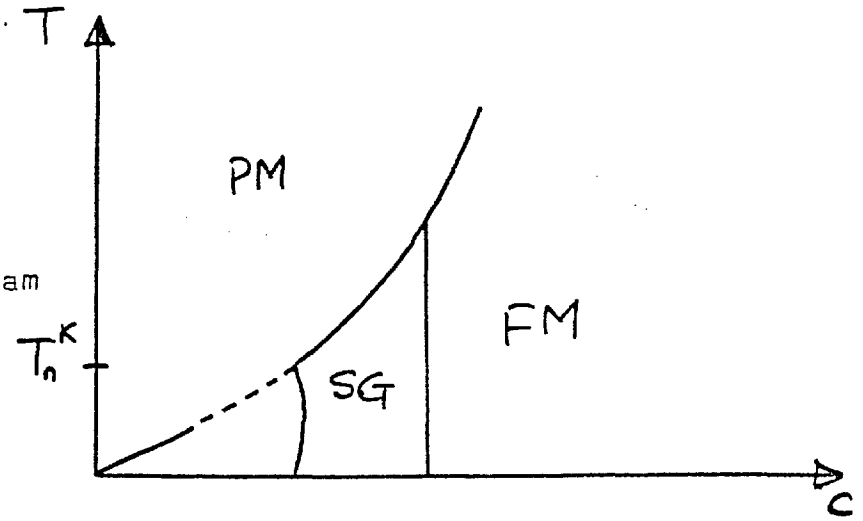

Fig.2.13: Magnetic phase diagram in ref.210.

One important difference is the clear delineation of the Kondo region.

In conclusion let us consider the magnetic behaviour of the solid solutions of the isoelectronic 4d-3d transition metals:

Y + Sc : The properties of the alloy system are not known, but since Y is superconducting under pressure it may be expected that dilute Y-Sc alloys have a similar property.

Zr + Ti : Alloys are superconducting for all compositions; T_{sc} is minimum at the equiatomic composition.

Nb + V : Same as for Zr-Ti

Mo + Cr : Dilute MoCr alloys ($\lesssim$ 5%Cr) are probably superconducting but not in the cubic phase (211); the system becomes magnetic (SDW) at about 76%Cr.

Tc + Mn : No data on the alloys are available; possibly very dilute TcMn alloys may be superconducting. A magnetic state, presumably SDW in the hcp phase, may set in at about 65%Mn.

Ru + Fe : As already mentioned RuFe becomes magnetic at about 50% Fe, and it is suggested that SDW occur.

Rh + Co : It is currently thought that a spin-glass state occurs at about 20% Co and ferromagnetism at about 36%; but it would appear that what occurs at about 20% Co

is a cluster glass which goes over into ferromagnetism at about 44% Co. Thus RhCo is a giant moment alloy, like CuNi. (See immediately below).

Pd + Ni : Magnetic clusters form at about 0.7% Ni but ferromagnetism does not set in until close to 2.8% Ni (see below - section 2.6).

It is clear from above that as one moves across the periodic table from left to right the isoelectronic alloys change gradually from being superconducting to magnetic; SDW occur in the middle of the table and give way to "spin-glass alloy " behaviour in RhCo and finally to the "giant monent" ferromagnetism of PdNi. Perhaps a similar variation occurs along a column e.g. from indications of antiferromagnetism in Pt to nearly fm Pd to fm Ni.

Comment on the RhCo System

Finally a brief discussion of the RhCo system is necessary in order to identify the class of alloys to which it properly belongs, since the current account (213, 214) of the succession of magnetic states does not appear to be very satisfactory. As expected local environment effects are operative since in the dilute limit the Co atom does not appear to carry any local moment (215). Electrical resistivity measurements (213, 214) exhibited in the form of a plot of $\Delta\rho\left(=\rho_{4.2}-\rho_{1.7}\right.$, where ρ_T is the resistivity at a temperature T$\left.\right)$ against impurity concentration showed two anomalies - a rather prominent maximum at $\sim$ 20% Co and a kink at $\sim$ 36% Co. The anomaly at 20% Co was assumed to signal the onset of a spin-glass state which then went over to a ferromagnetic state at about 36% Co.

A recent study (216) of the magnetic properties of the system attempted to further substantiate the above conclusion. However, after a careful study of the resistivity and magnetic data we are forced to conclude that instead of being a spin-glass alloy the RhCo system is really another giant moment system in the mould of CuNi or RhNi (which is to be discussed later). In fact, Jamieson (216) did notice that the temperature dependence of the susceptibility of the RhCo alloys resembled that of RhNi alloys. Unlike in the CuNi or RhNi system where no structural changes occur, ferromagnetism apparently does not set in in RhCo alloys before the martensitic fcc → hcp transformation becomes unavoidable. Certainly the Rh 42% Co alloy is a cluster-glass whereas the ferromagnetism reported (216) for Rh 44% Co must be viewed in relation to the structural transformation that was suspected to have occurred. The apparent saturation of the magnetization of this alloy in small fields (~ 100 oe) is similar to that observed by Acker and Huguenin (220) for some CuNi alloys with concentrations just below the critical concentration (~ 47.5% Ni). A fuller discussion will be given elsewhere. Our immediate interest, in the light of our reclassification of the RhCo system, is in the significance of the anomalies observed in the resistivity plot mentioned above. The phase diagram of the RhCo system, as given by Hansen (217), indicates that a martensitic fcc → hcp transformation may occur at low temperatures at about 40% Co. Recent hardness studies (218), however, have shown that hardness-sensitive structural changes probably occur in two ranges of composition,

namely from about 13-20% Co and from 35% Co upwards. While acknowledging the difficulty in assessing the evidence for structural changes in the lower Co concentration range the author (218) nevertheless suggests that the observed hardness changes indicate the presence of a dome-shaped phase field with a maximum at about 320K ($\sim$16% Co) and which widens to between 7 and 25% Co at nitrogen temperature. For the higher Co contents it was suggested that the maximum probability line for the fcc $\longrightarrow$ hcp transformation runs from $\sim$360K at 50% Co to $\sim$76K at 40% Co; it is therefore possible that at helium temperatures the transformation could begin at about 36% Co! Skipping the relevant arguments, for the moment, we shall just conclude that the observed anomalies in the resistivity difference plot do in fact, represent structural changes and so open up the possibility of using such measurements to study martensitic transformations.

Perhaps we should caution that as an indicator of a change in magnetic regimes the resistivity difference plot ($\rho_{4.2} - \rho_{1.5}$ versus c) should be used with extreme caution. It should only be used as a last resort after all attempts to fit resistivity data in the relevant temperature range to physically meaningful laws (power laws, lnT terms, etc) have proved abortive. With a clearer pattern of the evolution of magnetism in binary alloy systems gradually emerging the use of such plots as "magnetic indicators" will be rendered largely unnecessary.

2.4. The Order Of The Phase Transitions

Typical magnetic phase diagrams for the three main groups of transition metal alloys have been sketched in

figures 2.9 and 2.12. As the diagrams show we can distinguish four main regions namely - the Kondo region, the spin-glass region, the long-range magnetically ordered region (ferromagnetic, antiferromagnetic, SDW or helical) and of course, the ubiquitous paramagnetic region.

The first three regions go over into the paramagnetic region at various concentration-dependent temperatures. We shall therefore consider the following transitions:-

(a) Kondo region ⟶ paramagnetic region

(b) Spin-glass ⟶ paramagnetic region

(c) Long-range magnetically ordered state ⟶ paramagnetic region

In addition there are also transitions which occur as a function of concentration at a constant temperature (which for convenience will be taken as absolute zero). The latter transitions are -

(d) the transition from the Kondo region to a magnetic state (either spin-glass, ferromagnetic or SDW);

(e) the transition from a spin-glass state (random magnetic order) to magnetic long-range order.

Our first task is to clarify the orders of these phase transitions and to do this it will be appropriate to recall the distinctions between the various types of phase transitions. In a phase transition the thermodynamic potential (or the Gibbs free energy), G, remains constant whilst its derivatives may change. For a first order phase transition the first order derivatives of G (entropy and volume) change discontinuously at the transition point whereas the second-order derivatives (heat capacity, thermal expansivity and the isothermal compressibility) diverge at

the transition point. Familiar examples include -

(i) fusion, vaporization and suolimation;

(ii) onset of ferroelectricity in displacive ferroelectrics;

(iii) order - disorder transition of AB_3 alloys.

In a <u>second-order</u> transition the first-order derivatives of G change <u>continuously</u> but the <u>second-order</u> derivatives undergo <u>finite</u> changes at the transition temperature. This finiteness of the discontinuity of the second-order derivatives is extremely important because it rules out most of the phase transitions usually classified as second-order phase transitions. To date it appears that the only genuine second-order phase transition is the transition from normal to superconductivity at the superconducting transition temperature T_{sc}. If, however, the second-order derivatives <u>diverge</u> at the transition point instead of undergoing <u>finite</u> discontinuities then we have a <u>λ (lambda) - transition</u> (221, 222), a name that arises from the shape of the heat capacity curve near the transition point (the same shape as for a first-order transition). To be consistent a λ-transition, should be called a <u>third-order</u> phase transition, since the third-order derivatives of G would undergo finite discontinuities at the transition point. This distinction between second-order and third-order phase transitions is best illustrated by the variation of the heat capacity curve in the critical region - figure 2.14. Examples of third-order phase transitions include -

(i) onset of ferroelectricity in order-disorder ferroelectrics;

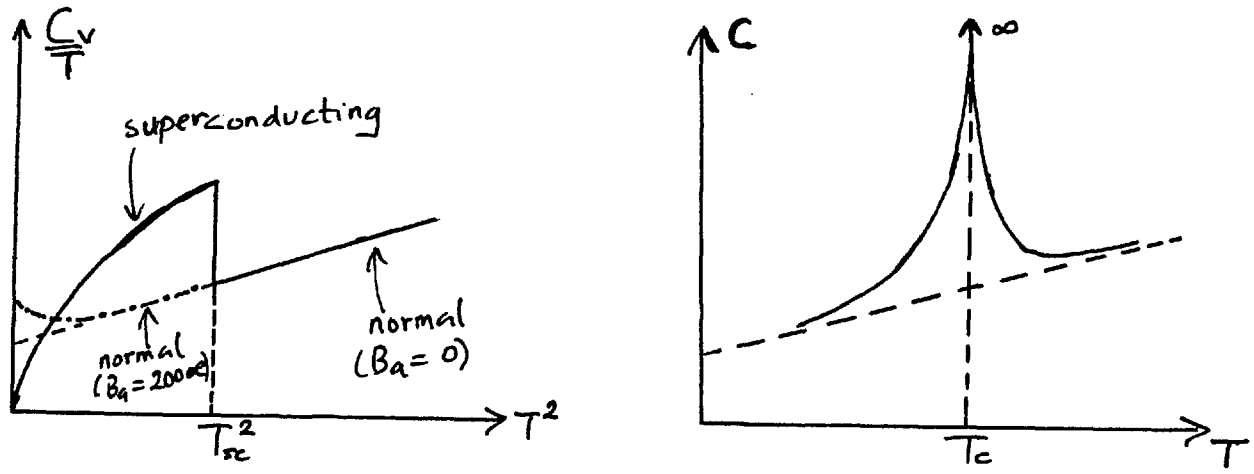

(a) Ga; 2nd order

(b) CuZn (β -brass): 3rd order

Fig.2.14: Variation of the heat capacity curve near a phase transition point.

(ii) order-disorder transition in AB alloys:

(iii) the transition from long-range magnetic order to the paramagnetic state;

(iv) the He_I^4 (liquid) $\longrightarrow$ He_{II}^4 (liquid) transition.

Hitherto it has been the practice to lump all co-operative phenomena as phase transitions of the second order but it is clear that the kind of cooperation envisaged in superconductivity (i.e. a Bose gas condensation) is very different from the cooperation involved in say long range magnetic ordering.

We may also remark that if a would-be third-order transition involves an appreciable volume striction then it becomes a first-order phase transition instead. The volume striction could either be caused by primary structural changes as in displacive ferroelectrics, or by changes in

the magnetic interactions (spontaneous magnetostriction). As an example of the latter case we mention the nickel arsenide structure compounds, like MnAs and MnBi, which lose their spontaneous magnetization abruptly at some temperature. This is taken as a first-order ferromagnetic-antiferromagnetic transition caused by "exchange-inversion" (223). Finally, we note that a phase transition can be of one order according to one variable and of another order for a different variable e.g. metamagnets undergo a first-order afm-fm transition under the action of a strong magnetic field (but this is not equivalent to spin-flopping in an ordinary afm) while with temperature as the variable the transition becomes a third-order transition.

In view of the foregoing, we can now classify the transitions (a) - (e) as follows:

(a) The transition from the Kondo region to the paramagnetic region is not a true phase transition as already explained (see section 1.9). The boundary between these two regions in the magnetic phase diagrams merely indicates a change of regime from the Kondo region where spin fluctuations are dominant to the paramagentic region where thermal fluctuations are more important. This change of regime is reflected in the temperature-dependence of various physical properties of the magnetic system such as the thermopower (224), electrical resistivity (106, 129, 130), magnetic susceptibility (see section 2.2), heat capacity (11, 225) etc. In order to maintain some form of consistency in the order of phase transitions it may be perhaps appropriate to call this change of regime a zero-order phase transition which, of course, implies that the thermodynamic potential is not

conserved during the transition.

(b) We propose that the transition from the spin-glass state to the paramagnetic state is a proper second-order phase transition which occurs at the well-defined transition temperature T_{sg}, the spin-glass temperature. This is because (i) one can define an order parameter in terms of the local magnetization whereas no such order parameter can be defined in the paramagnetic state;

(ii) Numerous measurements of the AC or very low fied DC susceptibility exhibit a very sharp peak at T_{sg} (226, 227);

(iii) The usual argument against the existence of a proper phase transition has been the rather broad maximum observed in the heat capacity near T_{sg} (228) instead of a λ-shaped curve. This argument is, however, incorrect since we have shown above that there is a clear definitive distinction between second-order and third-order phase transitions and this distinction is also reflected in the variation of the heat capacity across the transition temperature (see fig. 2.14). The broad specific heat maximum may, in fact, confirm that the transition at T_{sg} is truly second-order. A further discussion of this will be given elsewhere although the heat capacity of spin-glasses will be mentioned briefly in section 2.8.

(c) The transition from the long-range magnetically ordered states to the paramagnetic region is, of course, an example of the well-known cooperative transition which we have shown should be a third-order phase transition (or a λ-transition). We should, of course, add the proviso that where there esists a spontaneous volume magnetostriction the transition reverts to first-order.

(d) The transition from the Kondo region to the spin-glass state clearly involves a change of magnetic symmetry. Since the critical concentration point is a triple-point, the transition to the spin-glass state must be of the same order as that occurring at T_{sg}, i.e. it must be a second-order phase transition. By a similar argument the transition from the Kondo region to either ferromagnetism or SDW must be third-order.

(e) We finally consider the transition from a spin-glass state to long-range magnetically ordered states. Such a transition does not involve any change of symmetry since clearly we can define the same order parameter for the two regimes (the local magnetization). Therefore, it cannot be either a second- or third-order phase transition; so by elimination it must be first-order. If this is the case, the transition must be accompanied by a significant spontaneous volume magnetostriction probably leading to structural transformations. We recall that two of the most studied spin-glass alloys AuFe and CuMn are metallurgically problematic, the former being subject to atomic clustering while in the latter several allotropic forms may coexist. In particular, in AuFe where small angle neutron scattering measurements have confirmed the existence of the spin-glass - ferromagnetic transition (188) the observed properties for impurity concentrations greater than a few atomic percent are those of a metallurgically metastable system, since the true equilibrium states consist of two phases. The single phase fcc structure in which the ferromagnetism is observed is only retained at the temperatures at which observations are made by quenching from high temperatures. The quenching

merely slows down the segregation of the phases so that the details of the magnetic behaviour depend on ageing, annealing, cold-work, etc. Some "giant moment" alloys such as VFe also are metallurgically difficult, there being a tendency towards atomic ordering in a CsCl structure which would keep the Fe atoms separate. The martensitic fcc ⟶ hcp transformation in RhCo near the critical concentration for the onset of ferromagnetism has been previously mentioned. We shall not pursue this particular problem any further.

The above discussions on the order of the phase transitions are best summarised in figure 2.15.

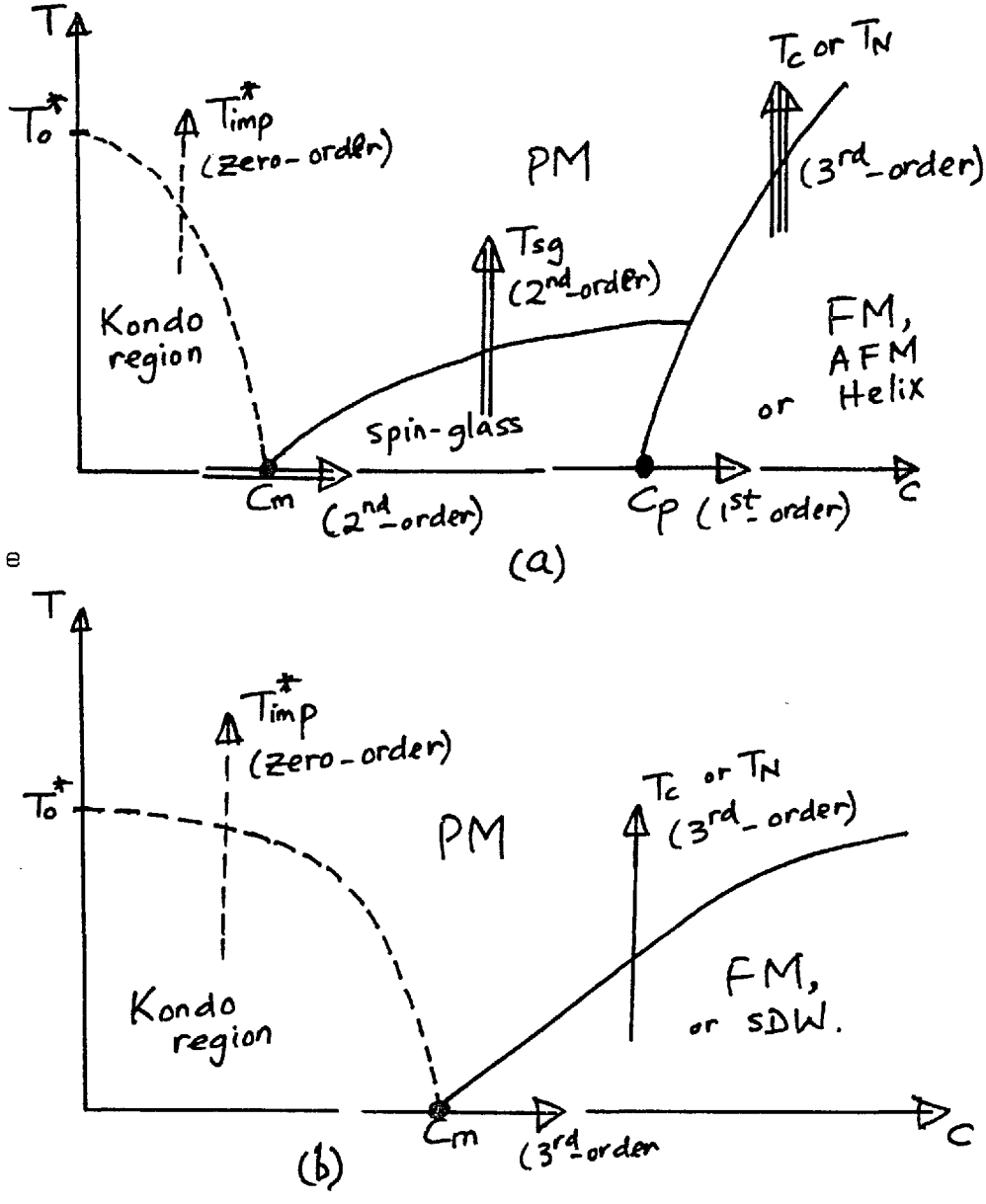

Fig.2.15: Summary of types of phase transitions.

We observe that in the above diagrams the order of the phase transitions appears to be conserved!

An important consequence of the distinction between second-order and third-order phase transitions is the thermodynamic improbability of the coexistence of superconductivity and ferromagnetism, but superconductivity and spin-glass magnetism can certainly coexist. The neutron diffraction measurements of Roth et al (230) on $Ce_{1-x}Tb_xRu_2$ compounds have clearly shown that only short-range magnetic order exists in samples that are superconducting while samples which exhibit some long-range magnetic order (those containing more than about 40% Tb) are not superconducting. Further comments on "ferromagnetic superconductors" will be made elsewhere.

2.5. A Thermodynamic Theory Of The Onset Of Ferromagnetism In Some Transition Metal Alloys

2.5(i) Introduction

Having dealt at great length with phenomenology of the onset of magnetism in transition metal alloys in general we shall now restrict further discussion to "giant moment alloys" where a transition occurs from the Kondo region to the ferromagnetic state. We have already considered the magnetic phase diagram for such systems (fig. 2.12) and also explained in the preceding section why this transition is a third-order phase transition. Our primary aim in this section is to fully consider the thermodynamics of this transition and for this purpose we shall apply Landau's theory of cooperative phase transitions (231) especially in the form extensively developed by Belov (232). Some of the

properties of a number of these alloy systems have been explained in terms of a transition from a strongly exchange-enhanced paramagnet to a weak itinerant ferromagnet (75-79, 233-236). However, in what follows we shall attempt to show that a wide range of experimental results is easily explicable only by the thermodynamics of the phase transition so that these results are independent of any particular model of ferromagnetism - a fact that has been previously pointed out (237, 238) but apparently generally ignored by the so-called cognoscenti. Furthermore, for all the binary alloys in question, we have already shown that the onset of ferromagnetism is necessarily inhomogeneous, the ferromagnetism arising from the interaction between magnetic clusters. These clusters also give rise to a cluster-glass region below the critical concentration for the onset of ferromagnetism. Many of the apparently complex properties of these alloy sytems which do not follow from elementary thermodynamics alone may be attributable to the existence of magnetic clusters; the failure to take a proper account of the effect of these clusters has, in a few cases, led to a gross misinterpretation of the observed data.

The applicability of Landau's theory follows naturally from the fact that near the critical composition both the spontaneous magnetization, M, and the Curie temperature, T_c are inevitably small. Consequently, the theory developed here should be valid for all temperatures from absolute zero up to, and above, the Curie temperature, in contrast to the usual Landau theory which is only valid in a small temperature range near the transition point. Also since the

magnetic moments are observed on favoured clusters only whose concentration near the critical composition is usually small (about a few tenths of an atomic percent) the saturation moment per atom would clearly be small (less than a Bohr magneton) and so non-integral. That this is so therefore, cannot be taken to automatically imply the itineracy of the magnetic electrons; on the contrary, the very existenc of such magnetic clusters does rule out the appropriateness of any simplistic model of itinerant ferromagnetism. Even for those ferromagnetic intermetallic compounds where clusters have not yet been shown to exist - specifically Sc_3In, UGe_2 and $PuGe_2$ - a little care should be exercised in labelling them as itinerant ferromagnets, especially in the light of our comment on the relation between superconductivity and ferromagnetism in transition metals (section 2.2), i.e., spin fluctuations could be of decisive importance. However, our terms of reference do not, for the moment, include the intermetallic compounds. Their properties will, therefore, be discussed elsewhere.

To be able to use Landau's theory, we need to define an order parameter. This comes in naturally as the spontaneous magnetization in terms of which we can uniquely define a critical concentration for the onset of ferromagnetism. We denote this concentration by c_f. As discussed below, the magnetic behaviour of these systems is significantly affected by an externally applied pressure. Consequently, it is important to specify the external pressure in the definition of c_f. Ideally we would have required a zero external pressure but it is perhaps more convenient to use the normal atmospheric pressure as standard since it may not always be

possible, ab initio, to know the exact variation, with pressure, of the specific property being investigated to enable a precise extrapolation to be made. Thus we shall define the critical concentration as follows:-

$$\lim_{\substack{B_0,T\to 0 \\ c\to c_f^-}} M(B_0,T) = 0 \qquad 2.84$$

for a given temperature T and at normal atmospheric pressure. $M(B_0,T)$ is the observed magnetization for a magnetic induction B_0 and at a temperature T; c_f^- is a concentration which is infinitesimally smaller than the critical concentration. A direct determination of c_f by bulk magnetization measurements is rather difficult because the existence of magnetic clusters in the critical composition region implies that there will always be some measureable response in a finite field. In particular, one cannot know, a priori, that this response is linear so that the validity of determining M by extrapolating high field measurements to zero field is questionable. Our objective includes deriving expressions which would enable a quantitative analysis of the magnetization data to be made and hence allow for a proper extrapolation to the critical concentration. Such a procedure should stop the rather prevalent use of ad hoc criteria some of which are subjective while others have no sound physical basis other than the fact that they appeared to work in a previous example.

Other methods of obtaining c_f^- depend on the secondary effects of the onset of ferromagnetism. The most important of these include the concentration dependence of the initial susceptibility, the coefficient of the T term in the specific heat and the coefficient of the T^2 term in the electrical resistivity. These methods and others are described in greater detail in what follows.

2.5(ii) The Magnetization and Susceptibility

Following the procedure in reference 232 we define the thermodynamic potential G as

$$G = G(P,T,B_o,c,M) \qquad 2.8$$

where in addition to the usual thermodynamic variables P,T and B_o we have now explicitly included the concentration, c, of the magnetic impurity. M is the spontaneous magnetization which has been defined as the order parameter. Within the framework of the Landau theory the order paramete is not a state variable but just a parameter that has to be introduced in the theory. Near the critical concentration M has extremely small values and hence G can be expanded in even powers of M thus:-

$$G = G_o + aM^2 + bM^4 + \ldots\ldots\ldots \qquad 2.86$$

where G_o is the value of G in the non-ferromagnetic state an the coefficients a and b are, in general, functions of P,T and **c.** The expansion in equation (2.86) is possible because the decisive criteria for third-order phase transitions are that both G and the order parameter should remain continuous through the transition point but with the order parameter vanishing at the transition point itself. Consequently G may be regarded as an analytic function of the order parameter. The restriction to only even powers of M is, of cours due to the fact that G is a scalar function whereas M is a vector quantity. For P,T constant G will be stationary (i.e. $\delta G=0$) if one or more parameters are varied. In thermodynamic equilibrium G must be a minimum with respect to the order parameter. Thus the equilibrium is determined by requiring that $\left(\frac{\partial G}{\partial M}\right)_{P,T} = 0$ thus giving that either

$$M = 0 \qquad 2.87$$

or

$$M = \left(-\frac{a}{2b}\right)^{1/2} . \qquad 2.88$$

It is trivial to show that for M=0 the free energy is minimized if and only if a is positive definite which corresponds to the non-magnetic state $c < c_f$; similarly equation (2.88) minimizes G if $a < 0$ corresponding to the ferromagnetic state $c > c_f$. At $c=c_f$, a is zero. However, the coefficient b(P,T,c) must be positive definite as otherwise the non-magnetic state would become unstable when $c < c_f$. However b is not a critical function of c and may therefore be considered a constant near c_f. Further we assume that near c_f a(P,0,c) is small and can therefore be expanded in powers of $(c_f - c)$ i.e.

$$a(P,T,c) = \alpha_0(P,0)\,(c_f - c) \qquad 2.89$$

Thus $$G = G_0 + \alpha_0(c_f - c)M_0^2 + bM_0^4 + \cdots$$

and in the equilibrium state we then have that

$$M_{00}^2 = \frac{\alpha_0}{2b}(c - c_f) \qquad 2.90$$

NB: The following notation will be used:-

$$M = M(B_0, T, c)$$

$$M_0 = M(0, T, c);\ M_{00} = M(0, 0, c)$$

$$M^* = M(P) \equiv M(B_0, T, c, P) \text{ etc}$$

Suppose we now apply a magnetic field B_0; we shall then get

$$G(B_0, T, c, M) = G_0 + aM^2 + bM^4 + \cdots - MB_0 \qquad 2.91$$

Minimizing G with respect to M as before we obtain the equation of state for the system near c_f as

$$2aM + 4bM^3 = B_o \qquad 2.92$$

which form is very familiar when we recall the Belov-Arrott plots for the ferromagnetic Curie point. We reiterate, however, that equation (2.92) is valid at <u>all</u> temperatures, up to and above the Curie temperature.

In principle a and b may be determined by doing corresponding Belov-Arrott plots near c_f and hence c_f may be found. Wohlfarth (76) refers to such plots as "Mathon plots".

Note that the observed magnetization in the presence of an applied field is

$$M = M_s + M_p(B_o) \qquad 2.93$$

where M_s is the spontaneous magnetization and $M_p(B_o)$ is the true magnetization induced by the applied field. One may write

$$M_p(B_o) = \chi_v B_o$$

where χ_v is the volume susceptibility. We define the initial susceptibility in the usual way, i.e.

$$\chi_v^o = \lim_{B_o \to 0} \left(\frac{\partial M}{\partial B_o}\right)_T \qquad 2.94$$

It is then straightforward to show that in the non-magnetic state

$$\chi_{nm}^o \equiv \chi_v^o (c < c_f) = \frac{1}{2a_o}\{c_f - c\}^{-1} \qquad 2.95$$

and in the ferromagnetic state

$$\chi_f^\circ \equiv \chi_V^\circ (c > c_f) = \frac{1}{4\alpha_0}\{c - c_f\}^{-1} . \qquad 2.96$$

Thus as is usually obtained for the ferromagnetic - paramagnetic transition at the Curie point,

$$\frac{\chi_V^\circ (P, T, c < c_f)}{\chi_V^\circ (P, T, c > c_f)} = -2 . \qquad 2.97$$

We stress that this relation is strictly valid for only the initial susceptibility, and not either the high field (or paraprocess) susceptibility.

According to equations (2.95) and (2.96) the initial susceptibility should diverge at c_f, thus providing one convenient method for determining the critical concentration. From equation (2.96),

$$a = -\frac{1}{4\chi_f^\circ} \qquad 2.98$$

and since from equation (2.88) $b = -\frac{a}{2M^2 c_0}$ it follows that

$$b = \{8\chi_f^\circ M_\infty^2\}^{-1} \qquad 2.99$$

Thus b, the slope of the Belov-Arrott plots, is, within the approximations made, independent of both the temperature and the impurity concentration. By substituting equations (2.98) and (2.99) into equation (2.92) the magnetic isotherms can be rewritten in the alternative form

$$\frac{M^2}{M_0^2} = 2\chi_f^\circ \frac{B_0}{M} + 1 \qquad 2.100$$

which may be compared with Mathon's expression (75)

$$\frac{M^2}{M_0^2} = 2\chi_0 \frac{B_0}{M} \frac{M_{00}^2}{M_0^2} + 1 \qquad 2.101$$

or the equivalent formula derived by Edwards and Wohlfarth (235) namely

$$\frac{M^2}{M_{00}^2} = 2\chi_0 \frac{B_0}{M} + \left\{1 - \left(\frac{T}{T_c}\right)^2\right\} \qquad 2.10$$

since the latter authors assume that

$$M_0^2 = M_{00}^2 \left\{1 - \left(\frac{T}{T_c}\right)^2\right\} \qquad 2.103$$

Observe that in equations (2.101) and (2.102) we have used χ_0 instead of χ_f^0 appearing in equation (2.100). This is because there is apparently some confusion as to the exact meaning attached to χ_0 in the context of weak itinerant ferromagnetism. The initial susceptibility (or the static zero field susceptibility (75, 237)) was correctl defined (234,236) as in equation (2.94) but then it has been wrongly called the <u>high field susceptibility</u> (76, 234, 236, 239, 240) and consequently identified as the <u>enhanced Pauli</u> paramagnetic susceptibility (233, 235) given by

$$\chi_p(T) = \frac{N\rho(\varepsilon_F)\mu_B^2}{\gamma_b \varepsilon_0^2} \equiv \frac{N\mu_B^2 T_F^2 \rho(\varepsilon_F)}{T_c^2} \qquad 2.104$$

where N is the number of atoms per unit volume, γ_b, ε_0 are parameters that occur in the theory of itinerant ferromagnetism and T_f is taken as an effective degeneracy temperatur

Needless to say, there is an obvious and important distinction between the initial susceptibility and the high field susceptibility which becomes apparent when one considers a typical magnetization-induction curve for a ferromagnet, as sketched in figure 2.16.

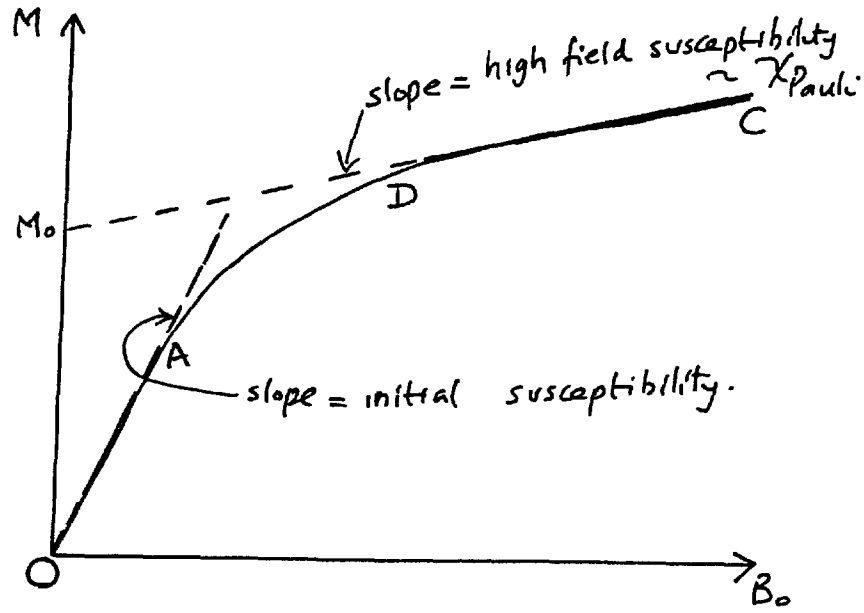

Fig.2.16:

$M-B_0$ curve for a ferromagnet

Clearly the initial susceptibility is only equal to the high field susceptibility for paramagnets and then only at temperatures sufficiently removed from the transition temperature, where linear $M-B_0$ curves should obtain. Part of the confusion between the initial and high field susceptibilities is directly attributable to the failure to recognise the onset of ferromagnetism for what it is - a proper phase transition. If this had been realised it would have become clear that the initial susceptibility would necessarily diverge asymmetrically at the critical concentration c_f, whereas the high field susceptibility remains nearly constant across the critical region. Also the alloys with impurity concentrations less than c_f have been referred

to as strongly exchange-enhanced <u>paramagnets</u>; they may well be "exchange-enhanced" but as explained already they certainly are not paramagnets.

It may be relevant to mention that the experimentally determined value of the initial susceptibility does depend on the measuring field. From equation (2.92) we see that near the critical concentration

$$M \simeq \frac{B_0^{1/3}}{(4b)^{1/3}}$$

$$\therefore \chi_f^0 = \left(\frac{\partial M}{\partial B_0}\right) = \frac{1}{3}\frac{B_0^{-2/3}}{(4b)^{1/3}} \qquad 2.105$$

It is clear from equation (2.105) that the magnitude of the measured initial susceptibility depends greatly on B_0. Ideally B_0 should be zero in which case $\chi_f^0 \rightarrow \infty$, as required by theory. The smearing out of the maximum in the initial susceptibility by large fields should, of course, occur at any relevant transition point - say at the ferromagnetic Curie point, T_c or at the spin-glass transition temperature T_{sg}.

2.5(iii) <u>The Effect of Pressure</u>

The effect of pressure can be most simply discussed by adding two other terms to the expression already given for the thermodynamic potential in equation (2.91). Again following Belov (232) we may write

$$G = G_0 + a(T,c)M^2 + bM^4 + \gamma P M^2 - \tfrac{1}{2}\kappa P^2 - MB_0 \qquad 2.10$$

where $\gamma P M^2$ represents the magnetoelastic energy and $-\frac{1}{2}\kappa P$ is the elastic deformation energy, (the sign of the latter

has been chosen to make it positive for a lattice contraction); γ represents a magnetoelastic coupling coefficient and κ is the isothermal compressibility (strictly at constant magnetization; as explained below in 2.5(iv) it may be sometimes necessary to distinguish between the compressibility at constant magnetization and at constant magnetic induction).

From the condition that $\frac{\partial G}{\partial M} = 0$, we determine the equation of state as

$$2(a+\gamma P) + 4bM^{*2} = \frac{B_0}{M^*} \qquad 2.107$$

On comparing this with equation (2.92) we see that the effect of the pressure, to a first approximation is to shift the Belov-Arrott plots parallel to themselves. Clearly, this means an increase (or decrease, depending on the sign of γ) of the spontaneous magnetization which is equivalent to a shift of the critical concentration. Such a shift of the Belov-Arrott plots following the application of pressure is well illustrated by the data on Ni_3Al (241) and PtNi (242).

From equation (2.107) we get the analogue of equation (2.90) as

$$M_{oo}^{*2} = \frac{1}{2b}\{\alpha_0(c-c_f) - \gamma P\}. \qquad 2.108$$

For $B_0 = 0$ we easily obtain the change ΔM_{oo} in the spontaneous magnetization as

$$\Delta M_{oo} \equiv \{M_{oo}^* - M_{oo}\} = \frac{-\gamma P}{2b\{M_{oo}^* + M_{oo}\}} \qquad 2.109$$

Thus $\Delta M_{oo} \propto P$, as shown by the above mentioned data on Ni_3Al and PtNi. Near c_f, $M_{oo} \propto (c-c_f)^{\frac{1}{2}}$ (equation (2.90)), therefore, it follows from equation (2.109) that $|\Delta M_{oo}|$ should reach a maximum value as $c \rightarrow c_f$.

However, to obtain the true magnetoelastic effect (sometimes referred to as the "Villari effect" (243)) we have to consider the case where $B_o \neq 0$. Using equation (2.107) we easily get

$$\Delta M(P) \equiv M^* - M = \frac{-2\gamma M^* P}{2a + 4b\{M^{*2} + M^* M + M^2\}} \qquad 2.110$$

which again shows that $\Delta M(P) \propto P$. Also equation (2.110)) suggests one way of determining the critical concentration. Near c_f,

$$a \sim \alpha_\theta (c_f - c) \quad \text{and} \quad M_{oo}^2 \sim (c - c_f)$$

; thus as $c \rightarrow c_f^+$ the denominator in equation (2.110) decreases faster than the numerator, so that $|\Delta M|$ increases attaining its maximum value at c_f. For $c < c_f$ $|\Delta M(P)|$ decreases rapidly .

Next we consider the dependence of $\Delta M(P)$ on the applied field B_o. We take the special case where $c=c_f^+$; then $a \simeq 0$ and $M \simeq M^*$; since $M^3 \simeq \frac{B_o}{4b}$,

$$\{\Delta M(P)\}_{c=c_f^+} = \left\{\frac{-\gamma(2b)^{2/3}}{6}\right\} \frac{P}{B_o^{1/3}} \qquad 2.111$$

so that $|\Delta M(P)|$ should decrease as the applied field increases.

For $c < c_f$, a is rather large compared

to the other term in the denominator of equation (2.110), since both M and M* are small. We therefore, obtain

$$\{\Delta M(P)\}_{c<c_f} = -\frac{\gamma}{a} PM \simeq -\frac{\gamma P}{2a^2} B_0 \quad (2.112)$$

using the fact that $M \simeq \frac{B_0}{2a}$.

Hence below the critical concentration the absolute value of ΔM increases with the field, showing the opposite behaviour to that which obtains above the critical concentration. The recent experiments on PdNi (244) are at least in qualitative agreement with this analysis - refer to their figures 2(a) - (c). In addition, the data show that the true critical concentration for the onset of ferromagnetism is at least above 2.5 at %Ni and not 2.3%Ni, a point which has already been mentioned.

The same data (fig 3(a)) also justify the earlier conclusion that $|\Delta M_{oo}|$ should reach a maximum at the critical concentration (equation (2.109)).

It will be useful to estimate the dependence of the critical concentration on the applied pressure. To do this we use the already noted observation that the effect of pressure on the magnetization is equivalent to a change of the coefficient a to a new value a(P) given by

$$a(P) = a + \gamma P \simeq \alpha_0 (c_f - c) + \gamma P \quad 2.113$$

The condition for the critical concentration under the pressure P is that a(P) should vanish for small values of $(c_f - c)$. If c^*_f is the critical concentration for a

pressure P then clearly

$$\alpha_0(c_f - c_f^*) + \gamma\Delta P = 0$$

writing $\Delta c_f \equiv c^*_f - c_f$ we then get that

$$\frac{\Delta c_f}{\Delta P} = \frac{\gamma}{\alpha_0} \qquad 2.114$$

Differentiating equation (2.108) with respect to P for small P gives

$$2M_\infty \frac{\partial M_\infty}{\partial P} = -\frac{\alpha_0}{2b}\frac{\partial c_f}{\partial P}$$

$$\equiv \frac{-M_{\infty}^2}{(c-c_f)}\frac{\partial c_f}{\partial P}, \text{ since } M_0 \simeq M^*.$$

$$\therefore \quad -\frac{2}{M_\infty}\frac{\partial M_\infty}{\partial P} = \frac{1}{c-c_f}\frac{\partial c_f}{\partial P} \qquad 2.115$$

Similarly from equation (2.96)

$$\frac{\partial \chi_f^\circ}{\partial P} = \frac{1}{4\alpha_0}(c-c_f)^{-2}\frac{\partial c_f}{\partial P}$$

giving

$$\frac{1}{\chi_f^\circ}\frac{\partial \chi_f^\circ}{\partial P} = \frac{1}{c-c_f}\frac{\partial c_f}{\partial P} \qquad 2.116$$

Combining equations (2.114) and (2.115) gives

$$\frac{1}{\chi_f^\circ}\frac{\partial \chi_f^\circ}{\partial P} = \frac{1}{c-c_f}\frac{\partial c_f}{\partial P} = -\frac{2}{M_\infty}\frac{\partial M_\infty}{\partial P} \qquad 2.117$$

The relations in equation (2.117) are, of course, valid at only at $T=0$. Similarly we may consider the transition from the ferromagnetic state to the paramagnetic state at the Curie temperature T_c. We again use the Landau theory as already outlined to obtain

$$M_0^2(T_1) = \frac{A}{2B}(T_c - T_1) \qquad 2.118$$

and

$$\chi_f^\circ(T_1) = \frac{1}{4A}(T_c - T_1)^{-1} \qquad 2.119$$

where $A = A(c, P)$ and T_1 is less than but close to T_c.

In the limit $P \longrightarrow 0$ we easily obtain from equations (2.118) and (2.119) that

$$-\frac{1}{\chi_f^\circ}\frac{\partial \chi_f^\circ}{\partial P} = \frac{1}{T_c - T_1}\frac{\partial T_c}{\partial P} = \frac{2}{M_0}\frac{\partial M_0}{\partial P} \qquad 2.120$$

On combining equations (2.117) and (2.120) we have that for alloys close to the critical concentration for ferromagnetism (with $T_1 \simeq 0$)

$$\frac{1}{\chi_f^\circ}\frac{\partial \chi_f^\circ}{\partial P} = \frac{1}{c - c_f}\frac{\partial c_f}{\partial P} = \frac{-2}{M_{00}}\frac{\partial M_{00}}{\partial P} = \frac{-1}{T_c}\frac{\partial T_c}{\partial P} \qquad 2.121$$

These equalities may be compared with those given by Beille et al (242) namely

$$\frac{1}{\chi_0}\frac{\partial \chi_0}{\partial P} = \frac{1}{c - c_f}\frac{\partial c_f}{\partial P} = \frac{-2}{M_0}\frac{\partial M_{00}}{\partial P} = -\frac{2}{T_c}\frac{\partial T_c}{\partial P} \qquad 2.122$$

As simple test of these relations we calculate

$$\frac{dc_f}{dP} = \frac{-(c - c_f)}{T_c}\frac{\partial T_c}{\partial P} \qquad \text{from equation (2.121)}$$

$$= \frac{-2(c - c_f)}{T_c}\frac{\partial T_c}{\partial P} \qquad \text{from equation (2.122)}$$

For PtNi alloys c_f = 41.7% Ni and for c = 42.9% Ni T_c = 14.6 K (see fig.2.34 in section 2.6) while for this alloy

$$\frac{dT_c}{dP} = -1.52\text{K/k bar at } T = 4.2\text{ K (242).}$$

Equation (2.121) then gives $\frac{dc_f}{dP} = 0.12\%\ (\text{k bar})^{-1}$ whereas equation (2.122) gives $\frac{dc_f}{dP} = 0.25\%\ (\text{k bar})^{-1}$, as compared with the experimental value of 0.1/k bar (242). In passing we note that the authors in reference (242) take the critical concentration as 42.1% Ni but in the same paper a Curie temperature of 12 K is quoted for a 41.4% Ni alloy!

Finally from equation (2.121)

$$\frac{dT_c}{dP} = -\frac{T_c}{c-c_f}\frac{dc_f}{dP} \quad . \qquad 2.123$$

Using equation (2.114) for $\frac{dc_f}{dP}$ gives

$$\frac{dT_c}{dP} \simeq -\frac{T_c}{c-c_f}\frac{\gamma}{\alpha_o} \quad . \qquad 2.124$$

Since α_o is positive definite the sign of $\frac{dT_c}{dP}$ depends on that of γ. Also the behaviour of $\frac{dT_c(c)}{dP}$ is essentially determined by that of $T_c(c)$. If, as is found for most of the alloys to be discussed here,

$$T_c \propto (c-c_f) \qquad 2.125$$

then equation (2.124) predicts that

$$\frac{dT_c}{dP} = \text{constant} \times \frac{\gamma}{\alpha_o}$$

$$\simeq \text{constant} \ ;$$

in practice $\frac{dT_c}{dP}$ may be expected to decrease slowly as c increases,

since T_c may increase less rapidly than implied by the proportionality to $(c-c_f)$; however, $T_c \frac{dT_c}{dP}$ should <u>systematically increase</u> as the concentration c increases. On the other hand, if

$$T_c^2 \propto (c - c_f) \qquad 2.126$$

as claimed for weak itinerant ferromagnets (75, 233), then $T_c \frac{dT_c}{dP}$ will be expected to remain constant and $\frac{dT_c}{dP} \propto T_c^{-1}$. As shown in Table 2.3 the data on Ni_3Al seem to confirm the earlier conclusion that $T_c \frac{dT_c}{dP}$ does indeed increase regularly with T_c. This is in spite of the fact that the published values of T_c appear to satisfy equation (2.126). As mentioned later equation (2.126) appears to hold only for alloys where <u>atomic ordering</u> is unavoidably present as in Ni_3Fe, Ni_3Al, etc. For truly <u>disordered</u> alloys equation (2.125) is generally valid. It is therefore, very striking that for Ni_3Al $T_c \frac{dT_c}{dP}$ increases with T_c.

TABLE 2.3

Magneto-Volume Paramaters for $Ni_{75+x}Al_{25-x}$ Alloys

x	T_c K	$\frac{-dT_c}{dP}$ K/kbar	$-T_c \frac{dT_c}{dP}$ K^2/kbar	γ (=KC)[c] $(g/emu)^2 \times 10^6$	M_{oo}[b,c] emu/g	$w(=\gamma M_{oo}^2)$ $\times 10^6$
-0.2	30[a]	0.58[a]	17.4	0.59[a]	-	-
0	43[a] 39[b] 41.5[d]	0.50[a] 0.51[c]	20.7[e]	0.47[e]	6.2	18
0.5	59[a] 58[b] 58.1[d]	0.42[a] 0.48[c]	26.4[e]	0.51[c]	8.6	38
1.0	72[a] 71[b] 71.5[d]	0.36[a] 0.50[c]	30.8[e]	0.49[c]	10.4	53

a: ref. 245

b: ref. 246

c: ref. 247

d: ref. 241

e: Average of minimum and maximum values.

2.5(iv) Volume Magnetostriction and Expansivity

Near a ferromagnetic Curie point only the exchange magnetostriction is important and this is necessarily a volume effect since the exchange is isotropic. However for the giant moment alloy systems we have been discussing the onset of ferromagnetism involves the ferromagnetic coupling of a relatively small number of magnetic clusters. Owing to the usually low Curie temperatures of these alloys the exchange interactions involved must be very weak and hence it will be necessary to consider the magnetic interactions as well, specifically the dipolar and/or pseudo-dipolar interactions, the latter arising from spin-orbit coupling effects. We suggest that these dipolar interactions are the dominant cause of any anisotropy, and hence of magnetostriction, in the relevant alloys in the critical concentration region. It may be recalled that the relatively large magnetostriction of the rare-earth metals is usually associated with large spin-orbit coupling effects.

If dipolar interactions are involved then one ought to strictly consider only the linear magnetostriction along the directions specified by the spontaneous magnetization. Fortunately, however, the alloys are usually in the form of polycrystals so that owing to the averaging effect one can safely deal with the volume magnetostriction. This will be done using the general thermodynamic approach already developed to establish relations for the dependence of the magnetostriction near the critical concentration on the magnetization and the applied magnetic induction. To proceed we note that it will be more straightforward to

rewrite equation (2.106) in terms of the volume magnetostriction which will be denoted by w. We now have

$$G = G_0 + aM^2 + bM^4 - \frac{\gamma w}{\kappa} M^2 - \frac{w^2}{2\kappa} - MB_0 \qquad 2.127$$

Minimizing G with respect to w easily gives

$$w(B_0, T, c) = \gamma M^2 \qquad 2.128$$

In general the spontaneous magnetostriction is defined by

$$w(0, T, c) = \gamma M_0^2 \qquad 2.129$$

However, it will be necessary to distinguish between the <u>concentration-dependent</u> spontaneous magnetostriction at the absolute zero of temperature which follows the onset of ferromagnetism at the critical concentration and the spontaneous magnetostriction which usually occurs at a ferromagnetic transition point, T_c. The former which we denote by $\omega(c)$ may be tentatively attributed to magnetic forces while the latter denoted by $\omega(c, T_c)$ is due to exchange forces. From equation (2.129)

$$w(c) = \gamma M_{00}^2 \qquad 2.130$$

which implies a <u>lattice expansion</u> since $\gamma > 0$. Also $\omega(c)$ has the same concentration dependence as M^2_{00} i.e.

$$w(c) = \frac{\alpha_0 \gamma}{2b} (c - c_f) \qquad 2.131$$

on substituting for M^2_{oo} from equation (2.90).

Table 2.3 above shows some values of $\omega(c)$ for the Ni_3Al system.

The temperature-dependent part of the magnetostriction $\omega(T)$ is given by

$$w(T) = \gamma(M_o^2 - M_{oo}^2) \qquad 2.132$$

which will clearly depend on the temperature dependence of the magnetization, M_o. Thus

$$w(c, T) \equiv w(c) + w(T) = \gamma M_o^2 \qquad 2.133$$

The forced magnetostriction is defined as

$$w(B_o, T, c) - w(T, c) = \gamma\{M^2 - M_o^2\} \qquad 2.134$$

Near c_f, $M_o \simeq M_{oo} \sim 0$ and $M \sim \left(\frac{B_o}{4b}\right)^{\frac{1}{3}}$

$$\therefore \quad w(B_o) \simeq \gamma\left(\frac{B_o}{4b}\right)^{2/3} \qquad 2.135$$

giving the field dependence of the forced magnetostriction. The data for $ZrZn_2$ (248) appear to obey the above relation - see figure 2.17

The forced magnetostriction coefficient, h_o', is easily derived from equation (2.134); by definition

$$h_o' = \lim_{B_o \to o} \frac{\partial w(B_o)}{\partial B_o}$$

$$= 2\gamma M_o \chi_f^o \qquad 2.136$$

Fig:2.17: Variation of $\frac{\Delta l}{l}$ with $H^{2}/3$ for $ZrZn_2$ (data taken from ref.248).

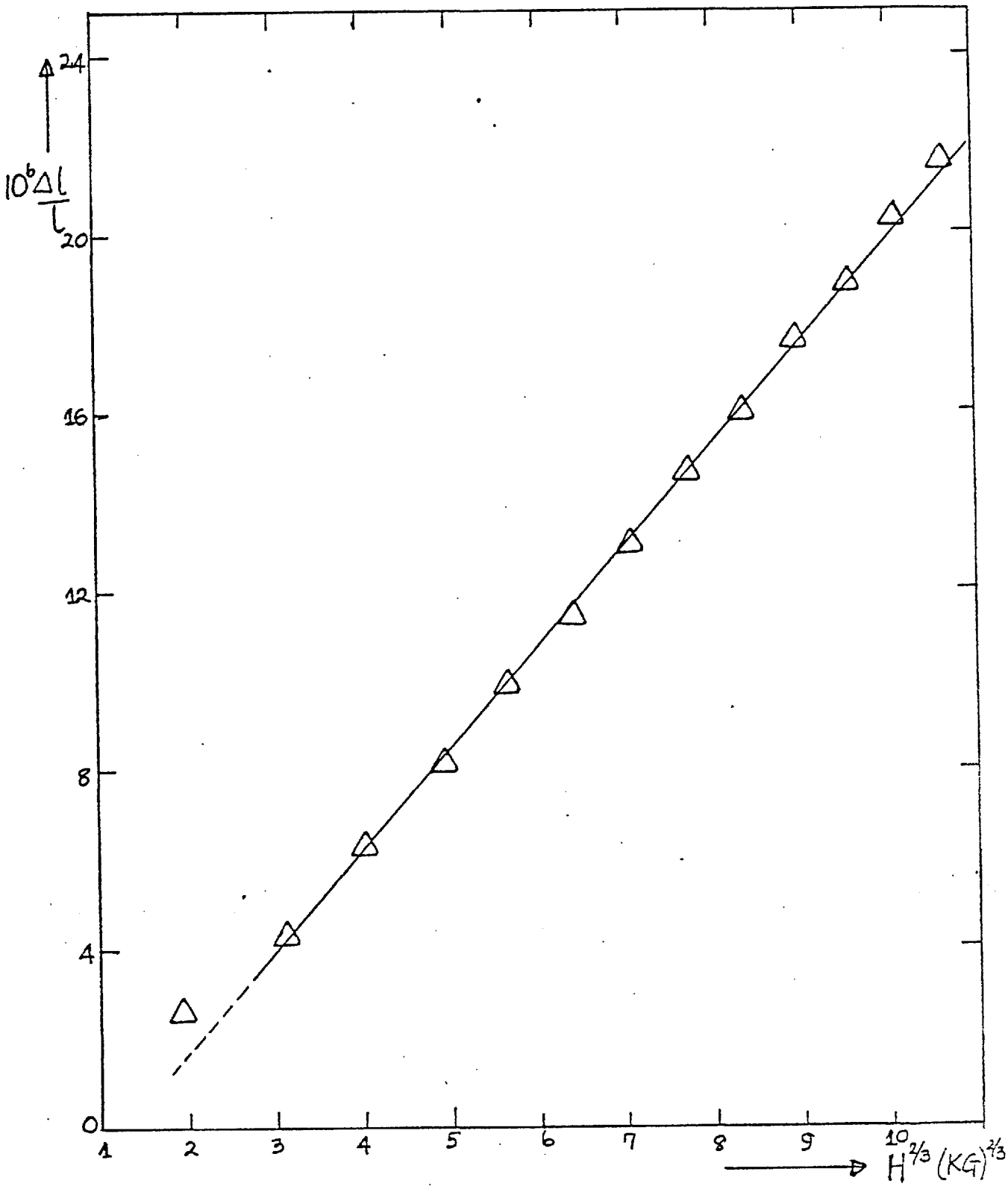

and hence from equations (2.90) and (2.96),

$$h_0' \propto (c - c_f)^{-1/2} \quad ; \qquad 2.137$$

thus the forced magnetostriction coefficient is positive and increases very rapidly near the critical concentration, in fact, more rapidly than the initial susceptibility (which increases as $|c-c_f|^{-1}$). It is possible that the magnetostriction measurements reported for NiRh (249) in which the above conclusion was observed may, in fact, refer to the forced magnetostriction coeeficient.

It will be pertinent to make the following remarks:-

(a) The magnetoelastic coupling constant γ used here is equivalent to the constant K_C used by Wohlfarth (233, 234, 239, 240) and others in discussing the volume magnetostriction.

(b) The relation given by equation (2.128) for $w(B_0, T, c)$ is strictly valid only when the applied pressure, P (or more precisely the pressure difference, ΔP) tends to zero. Otherwise we have to obtain the magnetostriction by differentiating equation (2.106) with respect to P. This gives

$$w(B_0, c, T) = -\frac{\partial G}{\partial P} = \gamma M^2 + K_M P \qquad 2.138$$

Here K_M is the isothermal compressibility under constant magnetization defined as

$$K_M = -\frac{1}{V}\left(\frac{\partial V}{\partial P}\right)_{M,T} \qquad 2.139$$

Hitherto we have used both the susceptibility and compressibility without defining them rigorously; since volume changes are also involved, we ought to distinguish between the susceptibility at constant pressure defined as

$$\chi_p = \left(\frac{\partial M}{\partial B_0}\right)_{p,T} \qquad 2.140$$

and the susceptibility at constant volume,

$$\chi_V = \left(\frac{\partial M}{\partial B_0}\right)_{V,T} . \qquad 2.141$$

Similarly we should distinguish between the isothermal compressibility at constant magnetization defined already in equation (2.139) and the isothermal compressibility at constant magnetic induction

$$\kappa_{B_0} = -\frac{1}{V}\left(\frac{\partial V}{\partial P}\right)_{B_0,T} . \qquad 2.142$$

The four quantities defined in equations(2.139)-(2.142) are related by (250)

$$\chi_p \kappa_M = \chi_V \kappa_{B_0} ; \qquad 2.143$$

$$\chi_p = \chi_V \left\{1 - \frac{\chi_V}{V\kappa_M}\left(\frac{\partial V}{\partial M}\right)^2_{p,T}\right\}^{-1} \qquad 2.144$$

and

$$\kappa_{B_0} = \kappa_M \left\{1 - \frac{\chi_V}{V\kappa_M}\left(\frac{\partial V}{\partial M}\right)^2_{p,T}\right\}^{-1} \qquad 2.145$$

As an example the initial susceptibility used in many of the foregoing equations should refer to the initial susceptibility at constant pressure $\chi^0_{p_f}$, which is usually,

and more conveniently, measured.

The Volume Expansivity

The volume expansivity, β , is usually defined as

$$\beta = \frac{1}{V}\left(\frac{\partial V}{\partial T}\right)_P$$

For ferromagnetic substances we may write

$$\beta = \beta_0 + \beta_M \qquad 2.146$$

where β_0 is the volume expansivity in the absence of any magnetization i.e. β_0 consists of the electron and lattice contributions, while β_M is the contribution due to the temperature-dependence of the spontaneous volume magnetostriction i.e.

$$\beta_M = \frac{dw}{dT} \qquad 2.147$$

For Ni, near the Curie temperature T_c, $\frac{dw}{dT}$ is positive, leading to a positive anomaly in the thermal expansion; but for the Fe invars say, $\frac{dw}{dT}$ is large and negative thereby giving rise to a net negative thermal expansivity.

Writing $w = w(B_0, T, c)$, we have that

$$dw = \left(\frac{\partial w}{\partial T}\right)_{B_0} dT + \left(\frac{\partial w}{\partial B_0}\right)_T dB_0$$

and so $$dw = \left(\frac{\partial w}{\partial T}\right)_{B_0} dT + \left(\frac{\partial w}{\partial B_0}\right)_T \left\{\left(\frac{\partial B_0}{\partial M}\right)_T dM + \left(\frac{\partial B_0}{\partial T}\right)_M dT\right\} \qquad 2.148$$

$$\therefore \quad \left(\frac{\partial w}{\partial T}\right)_M = \left(\frac{\partial w}{\partial T}\right)_{B_0} + \left(\frac{\partial w}{\partial B_0}\right)_T \left(\frac{\partial B_0}{\partial T}\right)_M \qquad 2.149$$

In equation (2.149) $\left(\frac{\partial w}{\partial T}\right)_M \simeq \beta_0$, the "normal" volume expansivity; $\left(\frac{\partial w}{\partial T}\right)_{B_0}$ gives the observed volume

expansivity, β , including the magnetic contribution $\beta_M = -\left(\frac{\partial w}{\partial B_0}\right)_T \left(\frac{\partial B_0}{\partial T}\right)_M$. Thus

$$\begin{aligned}\beta &= \beta_0 - \left(\frac{\partial w}{\partial B_0}\right)_T \left(\frac{\partial B_0}{\partial T}\right)_M \\ &= \beta_0 + \left(\frac{\partial M}{\partial P}\right)_T \left(\frac{\partial B_0}{\partial T}\right)_M .\end{aligned} \qquad 2.150$$

Using equations (2.117), (2.114) and (2.90) this becomes

$$\beta \simeq \beta_0 - \frac{\gamma}{4b(c-c_f)^{1/2}} \left(\frac{\partial B_0}{\partial T}\right)_M \qquad 2.151$$

The quantity $\left(\frac{\partial B_0}{\partial T}\right)_M$ can be determined from the magnetization curves and is always positive. For the alloys being discussed $\gamma > 0$ (giving $\frac{dT_c}{dP} < 0$); consequently the magnetic contribution is negative and could well be so large near c_f as to overcome β_0 and thereby give an overall negative thermal expansion. If however, $\gamma < 0 \left(\Rightarrow \frac{dT_c}{dP} > 0\right)$ then there is a positive magnetic contribution to the thermal expansion.

Alternatively one can immediately determine the sign of the magnetic contribution to the volume expansivity by using the Ehrenfest's relations for a third-order phase transition:-

$$-\frac{\Delta c_f}{\Delta P} = \frac{c_f \Delta \beta}{\Delta C_p} = \frac{\Delta \kappa_{B_0}}{\Delta \beta} \qquad 2.152$$

where Δc_f represents the change in the critical concentration resulting from the application of the pressure P, and the other increments refer to the difference in the values of the various parameters in the non-magnetic and ferromagnetic phases respectively.

We show below (section 2.5(x)) that $\Delta\kappa_{B_o} = \frac{\gamma^2}{2b} > 0$ so that $\Delta\beta$ has the opposite sign to $\frac{\Delta C_f}{\Delta P}$.

In discussing the magnetic contribution to the thermal expansion we shall restrict ourselves to considering the temperature dependence of only the spontaneous magnetostriction w(c,T). But firstly we note the temperature dependence of β_o . The electronic term is given by

$$\beta_{el} = \frac{\gamma_{el}\,\kappa\, C_{el}}{V} \qquad 2.153$$

where γ_{el} is the electronic Gruneison parameter defined (251) as

$$\gamma_{el} = 1 + \left\{ \frac{\partial \ln \rho(\varepsilon_F)}{\partial \ln V} \right\}_T \qquad 2.154$$

and C_{el}, the electronic heat capacity, is

$$C_{el} = \frac{\pi^2}{3} \rho(\varepsilon_F)\, K_B^2\, T \ . \qquad 2.155$$

The lattice term is similarly given by

$$\beta_{ph} = \frac{\gamma_{ph}\,\kappa\, C_V}{V} \qquad 2.156$$

where γ_{ph} is the lattice Gruneison-Debye constant and C_v is the lattice heat capacity given by

$$C_V(T) = \frac{12\pi^4}{5V} N K_B \left(\frac{T}{\theta_D}\right)^3 \qquad 2.157$$

which is valid for low temperatures ($T \lesssim \frac{\theta_D}{50}$); θ_D is the

Debye temperature of the solid. Thus for normal metals at sufficiently low temperatures

$$\beta_o = a_o T + b_o T^3 + \cdots\cdots \qquad 2.15$$

or in terms of the linear magnetostriction

$$\frac{\Delta l}{l} = a_o' T^2 + b_o' T^4 + \cdots\cdots \qquad 2.159$$

where a_o, a_o', b_o and b_o' are arbitrary constants. The magnetic contribution to the volume expansivity has been defined in equation (2.147) i.e.

$$\beta_M = \frac{d}{dT} w(c, T)$$
$$= \frac{d}{dT} (\gamma M_o^2)$$

using equation (2.133). If we assume that γ is independent of temperature (or at most depends only very weakly) then

$$\beta_M = \gamma \frac{d}{dT} M_o^2 \qquad 2.160$$

Further we assume a temperature dependence of the magnetization of the form

$$M_o^2 = M_{oo}^2 \left\{ 1 - \frac{T^2}{T_c^2} \right\} \qquad 2.161$$

usually taken to represent the magnetization due to <u>single particle excitations</u> in the limit of very weak itinerant ferromagnetism (235). Thus

$$w(c, T) = \gamma M_{oo}^2 \left\{ 1 - \frac{T^2}{T_c^2} \right\} \qquad 2.162$$

as compared with the relation given by Wohlfarth (236) namely

$$w(c,T) = -\frac{\gamma M_{00}^2}{T_c^2} T^2 \quad . \qquad 2.163$$

However, in either case

$$\beta_M = -\frac{2\gamma M_{00}^2}{T_c^2} T \quad . \qquad 2.164$$

Since $\gamma > 0$ one immediately sees that the magnetic contribution to the volume expansivity is negative. We shall again pause to make a few observations:-

(i) On the model of itinerant ferromagnetism it is stated that $M_{00} \sim T_c$ (252) - hence equation (2.126) -; then from equation (2.164)

$$\beta_M = - \text{ constant x } T \qquad 2.165a$$

Thus one would expect a <u>concentration-independent</u> magnetic contribution to the linear term in the volume expansivity. As already hinted, it does appear that $M_{00} \sim T_c$ only for alloys in which atomic ordering occurs near stoichiometry (e.g. Ni_3Al). For all other alloys which can be <u>completely</u> disordered $T_c \sim M_{00}^2$ (and hence equation (2.125)) so that the magnetic contribution to the volume expansivity decreases in magnitude as T_c increases (i.e. as the concentration increases) because

$$\beta_M \simeq -\frac{2\gamma}{T_c} T \qquad 2.165b$$

Thus as T_c increases the magnitude of the negative magnetic contribution to the thermal expansivity is reduced.

(ii) Also equation (2.163) shows that Wohlfarth and others (see for example ref. 248) have hitherto not rigorousl defined the spontaneous magnetostriction for they obtain

$$w(c,0) = 0 \qquad 2.166a$$

and

$$w(c,T_c) = -\gamma M_{00}^2 \qquad 2.166b$$

These results imply the absence of any spontaneous magnetostriction at absolute zero and also a <u>lattice contraction</u> ($\gamma > 0$) at the ferromagnetic transition point. We should contrast these conclusions with those given by equation (2.162) according to which

$$w(c) = \gamma M_{00}^2 \qquad \text{(as in equation (2.130)}$$

which thus implies a <u>lattice expansion</u> and

$$w(c,T_c) = 0 \qquad 2.167$$

The latter results, of course, make more sense if the magnetostriction arises from magnetic, instead of exchange, forces as we have already suggested.

Equation (2.163) always gives a lattice <u>contraction</u> whose magnitude <u>increases</u> as the Curie temperature is approached while equation (2.162) always gives a lattice <u>expansion</u> whose magnitude <u>decreases</u> towards T_c. The two

variations are sketched in figure 2.18 below.

In this connection we note that Hayase et al. (253) appear to be the only authors to have used the correct form of $w(c,T)$ as given by equation (2.162), although judging from the references these authors quoted as sources (ref. 248 and 254) it would appear that their use of the equation was merely ad hoc. More interestingly their data on the $Fe_{65}(Ni_{1-c}\ Mn_c)_{35}$ alloys confirm very nicely the fact that $w(c) \propto (c - c_f)$ as given by equation (2.131). Figure 2.19 shows that equation (2.131) is valid for both the ferromagnetic ($c_f \simeq 0.243$) and antiferromagnetic ($c_{af} \simeq 0.295$) alloys. It is possible that a spin glass regime exists between c_f and c_{af}.

We may also comment on the usual practice of exhibiting magnetostriction or thermal expansion data in the form of $\frac{\Delta l}{l}$ vs T^2 plots where

$$\frac{\Delta l}{l} = \frac{l(T) - l(T_o)}{l(T_o)} \quad ; \quad T_o \neq 0 \ . \qquad 2.168$$

$l(T_o)$ is the length measured at a chosen reference temperature T_o. $l(T) = l_o + \frac{1}{3}\, l(0)\, w(T)$. It is easily shown that

$$\frac{\Delta l}{l} \simeq \frac{1}{3}\left\{ w(T) - w(T_o) \right\} \qquad 2.169$$

and hence using equation (2.162) this becomes

$$\frac{\Delta l}{l} = \frac{\gamma M_{oo}^2 A}{3}\left\{ T_o^2 - T^2 \right\} \ . \qquad 2.170$$

Equation (2.170) shows that plots of $\frac{\Delta l}{l}$ against T^2 should give <u>finite positive intercepts</u> of magnitude $\frac{1}{3}\gamma M_{oo}^2 A T_o^2$

$$\simeq \frac{\gamma M_{oo}^2 T_o^2}{3 T_c^2} \ .$$

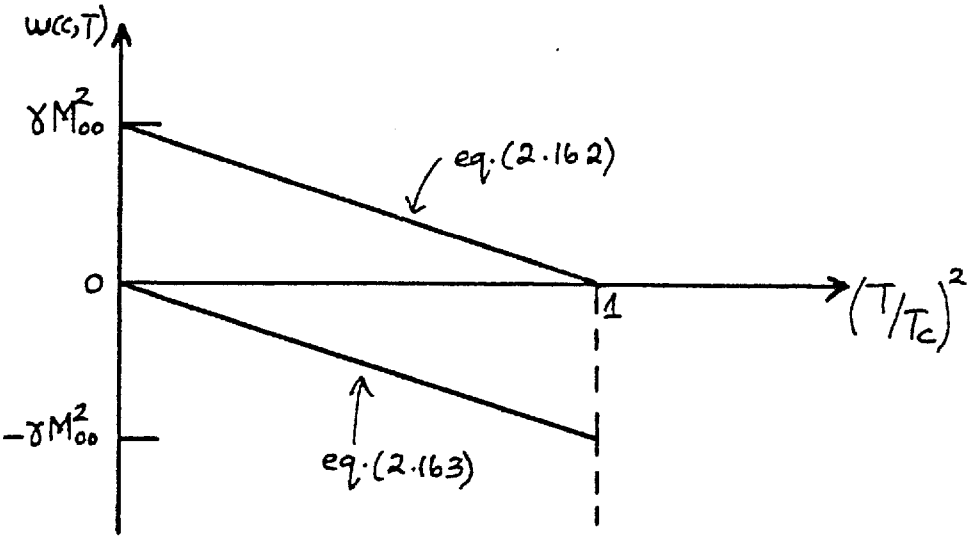

Fig. 2.18

Variation of w(c,T) with temperature as given by eq. (2.162) and (2.163)

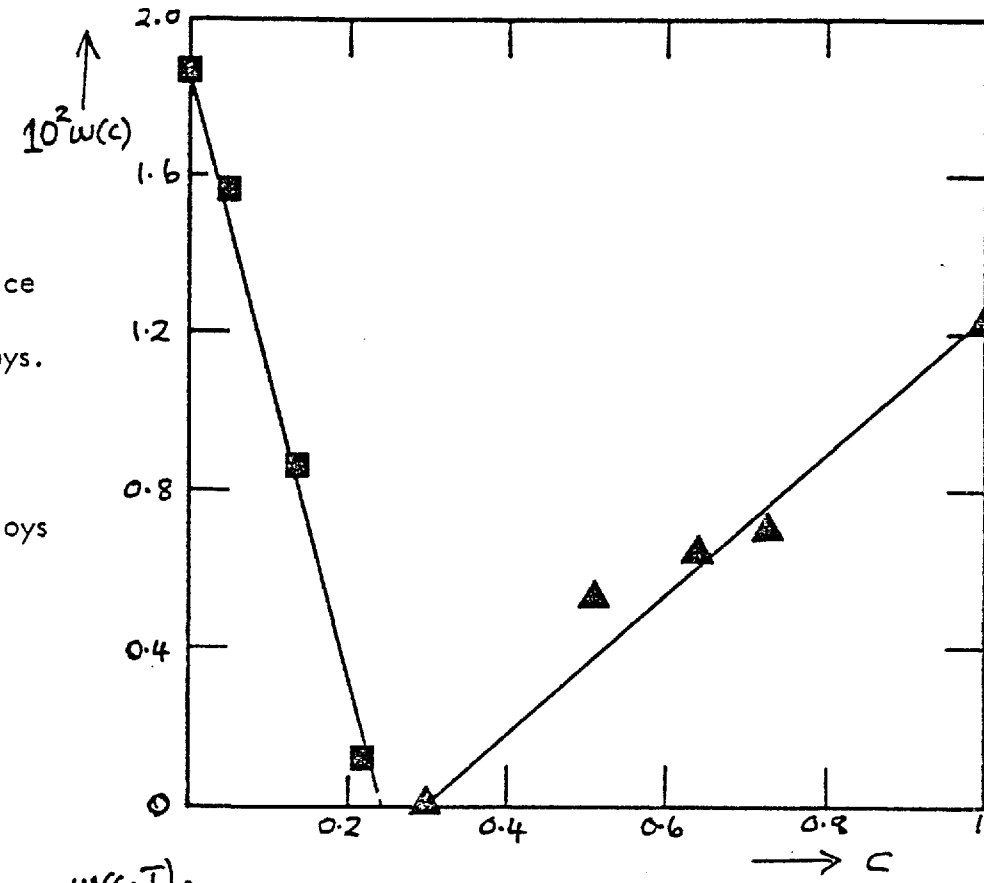

Fig. 2.19

The linear dependence of w(c) on c for $Fe_{65}(Ni_{1-c}Mn_c)$ alloys. The squares and triangles refer to ferromagnetic and antiferromagnetic alloys respectively. Data from Ref.253.

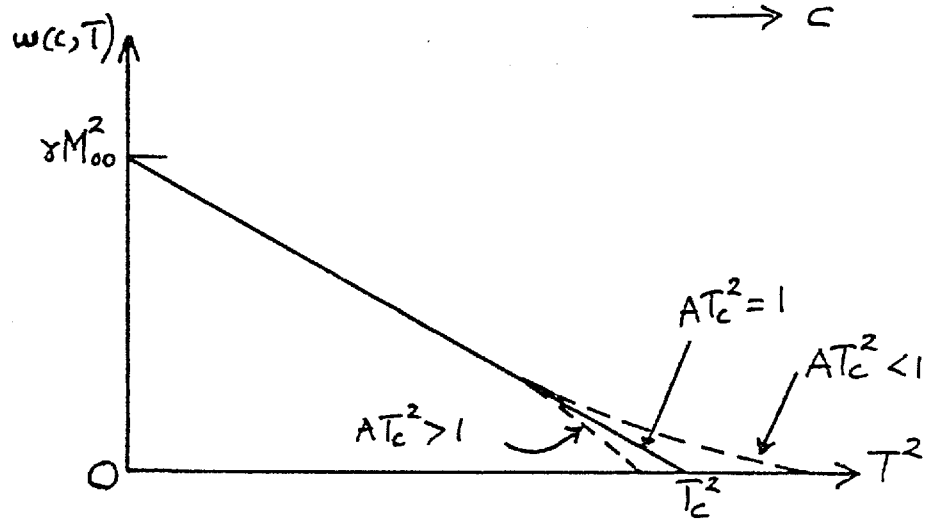

Fig. 2.20

The variation of w(c,T) with T^2 as given by eq. (2.173).

To illustrate this fact let us use the data on $ZrZn_2$ (248);

$\gamma = 1.80 \times 10^{-10}$ (mole/emu)^2 (the magnetostriction value);

$M_{oo} = 720$ emu/mole;

$T_c = 25$ K and $T_o = 1.8$ K. Therefore, we should expect a positive intercept of $\sim 1.1 \times 10^{-7}$, which the authors (248) referred to as an "unusual feature". As shown here it is perfectly normal and in fact, the true spontaneous magnetostriction at $T = 0$ is given by

$$w(c) = \gamma M_{oo}^2 \simeq 64.3 \times 10^{-6} .$$

The thermal expansion data are therefore really given by

$$10^6 w(T) \simeq 64.3 - 0.106\, T^2 . \qquad 2.171$$

So far we have used the temperature dependence of the spontaneous magnetization as given by the model of itinerant ferromagnetism. Suppose that instead, we have

$$M_o = M_{oo}\{1 - AT^2\} \qquad 2.172$$

as observed for Ni_3Al (241, 255) with $A \sim T_c^{-2}$. Then

$$w(c,T) = \gamma M_{oo}^2 \{1 - 2AT^2 + A^2T^4\} \qquad 2.173$$

and

$$\beta_m = -4\gamma M_{oo}^2 \{AT - A^2T^3\} . \qquad 2.174$$

Equation (2.174) shows that there now exists both a negative contribution to the linear term and a positive contribution to the T^3 term. Moreover, if $AT_c^2 \neq 1$, then $w(c, T_c) \neq 0$. Specifically, if $AT_c^2 > 1$, then $w(c, T_a) = 0$ for $T_a = A^{-\frac{1}{2}}T_c$ ($< T_c$), but if $AT_c^2 < 1$, then $w(c, T_a) = 0$ for

$T_a > T_c$. These cases are sketched in figure 2.20 which also shows the case for which $AT_c^2 = 1$. The magnetostriction data for the $Fe_{65}(NiMn)_{35}$ alloys (253) appear to correspond to the case $AT_c^2 < 1$. Equation (2.174) also shows that in some cases, the negative magnetic contribution to the T term in the thermal expansivity may be enhanced. For example, the data on the Ni_3Al system (241,255) show that $A \simeq 0.63 T_c^{-2}$, so that the magnetic contribution to the T term is $\frac{2.52\,\gamma M_{oo}^2 T}{T_c^2}$ which is 26% larger than the value given by equation (2.164). It therefore, follows that values of γ deduced from thermal expansion measurements by using equation (2.164) will be systematically higher than the values obtained from direct magnetostriction measurements by about 26%. Published data (256) show that the thermal expansion values of γ are larger than the magnetostriction values by an average of 18%.

2.5(v) Magnetothermal and Galvomagnetic Effects

(a) The Magnetocaloric Effect

If we neglect volume changes then for a magnetic system we may write

$$T dS = C_B dT + \frac{T}{\rho_o}\left(\frac{\partial M}{\partial T}\right)_B dB \qquad 2.175$$

where S is the entropy, C_B is the specific heat at constant field (and constant pressure) and ρ_o is the density of the system, introduced here because the magnetization M is per unit volume. At constant pressure, the adiabatic temperature change resulting from a change in the magnetic

induction is

$$\Delta T \simeq -\frac{T}{\rho_0 C_B}\int \left(\frac{\partial M}{\partial T}\right)_B dB$$

$$= -\frac{T}{\rho_0 C_B}\left(\frac{\partial M}{\partial T}\right)_B \Delta B \,. \qquad 2.176$$

Near the critical concentration $\left(\frac{dM}{dT}\right)_B$ is expected to be large, and so there should be a large magnetocaloric effect. In fact, using equation (2.172) we easily obtain

$$\Delta T \simeq \frac{2 M_{00} T^2}{\rho_0 C_B T_c^2} \Delta B \,. \qquad 2.177$$

Further with $T_c \sim (c - c_f)$ and $M_{00} \sim (c - c_f)^{\frac{1}{2}}$,

$$\Delta T \sim \frac{\Delta B}{(c - c_f)^{3/2}} \qquad 2.178$$

so that by measuring ΔT (for a given ΔB) as a function of concentration the critical concentration may be obtained. Alternatively, we may rewrite equation (2.175) in the form

$$T dS = C_M dT - \frac{B}{\rho_0} dM \qquad 2.179$$

where C_M is now the specific heat at constant magnetization. It immediately follows that

$$\left(\frac{\partial T}{\partial M}\right)_{S,P} = \frac{B}{\rho_0 C_M} \,. \qquad 2.180$$

In a molecular field approach, $B = B_0 + \lambda M$ where λ is a molecular field constant.

$$\therefore \left(\frac{\partial T}{\partial M}\right)_{S,P} = \frac{B_0 + \lambda M}{\rho_0 C_M} \,. \qquad 2.181$$

For $c < c_f$, $\frac{M}{B_o} \simeq$ constant at a given temperature so that

$$(\Delta T)_{S,P} \simeq \frac{(B_o/M + \lambda)}{2\rho_o C_M} \Delta(M^2) \qquad 2.182$$

but for $c > c_f$, we may take $B_o \ll \lambda M$, giving correspondingly

$$(\Delta T)_{S,P} \simeq \frac{\lambda}{2\rho_o C_M} \Delta(M^2) \qquad 2.183$$

or

$$(\Delta T)_{S,P} = \frac{\lambda}{2\rho_o C_M} \{M^2 - M_o^2\} \qquad 2.184$$

From equation (2.184) we may deduce a relation governing the field dependence of the magnetocaloric effect near the critical concentration; for we can take $M_o \sim 0$ and $M \simeq (\frac{B_o}{4b})^{\frac{1}{3}}$ so that

$$(\Delta T)_{S,P,c} = \frac{\lambda}{2\rho_o C_M} \left(\frac{1}{4b}\right)^{2/3} B_o^{2/3} \qquad 2.185$$

More generally, we can substitute M from equation (2.184) into equation (2.107) to give

$$2(a+\gamma P) + \frac{8b\rho_o C_M}{\lambda} (\Delta T)_S = \left(\frac{\lambda}{2\rho_o C_M}\right)^{1/2} \frac{B_o}{(\Delta T)_S^{1/2}} \qquad 2.186$$

so that a plot of $(\Delta T)_S$ against $\frac{B_o}{(\Delta T)_S^{1/2}}$ should give a straight line. Also since $\gamma > 0$ for the alloys concerned, equation (2.186) shows that a decrease of pressure should lead to an increase in the magnitude of $(\Delta T)_S$ at a constant applied field and conversely.

(b) Magnetoresistance and the Hall Effect

It is not proposed to give a general review of the Hall Effect and magnetoresistance phenomena in ferromagnets. An excellent discussion of these has already been given (257). Our interest lies mainly in the conjectured behaviour of these quantities in the region of the critical concentration for the onset of ferromagnetism and we shall discuss these by drawing a suitable analogy with the observed behaviour at the ferromagnetic Curie point. The analogy is justified since the onset of ferromagnetism as either a function of concentration or temperature is a critical phenomenon.

Let us define the magnetoresistance as

$$\frac{\Delta\rho}{\rho} \equiv \frac{\rho(B,T) - \rho(T)}{\rho(T)}$$

where $\rho(B,T)$ is the electrical resistivity of a sample in a magnetic induction B and temperature T K. It is known that well below T_c and for sufficiently high fields $\frac{\Delta\rho}{\rho}$ is positive and increases as the square of the applied magnetic induction. This positive conventional magnetoresistance is, of course, due to the Lorentz force acting on the conduction electrons in a magnetic field.

However, for a number of ferromagnetic metals and alloys it has been shown that near T_c the magnetoresistance is large and negative in relatively small applied magnetic fields (258). At temperatures sufficiently above T_c ($\frac{T-T_c}{T_c} \sim 10^{-2}$) $\frac{\Delta\rho}{\rho} \propto B_o^2$; very close to T_c $\Delta\rho/\rho$ varies a little less rapidly than B_o, while below T_c $\frac{\Delta\rho}{\rho} \propto B_o$. More importantly a direct proportionality between the magnetoresistance and the magnetocaloric effect was observed

near the Curie point (258) as shown in fig. 2.21. It was possible to write

$$\frac{\Delta\rho}{\rho} = A C_M (\Delta T)_{S,P} \qquad 2.187$$

where A is a constant for a given material.

The close correspondence between these two quantities is very remarkable considering the fact that $\frac{\Delta\rho}{\rho}$ is determined isothermally while $(\Delta T)_{S,P}$ is measured adiabatically. It does imply that near T_c those effects are governed essentially by the critical nature of the transition. We shall, therefore, assume that the same correspondence exists between the above quantities near the critical concentration for the onset of ferromagnetism.

Accordingly (i) from equation (2.178) we should expect that

$$\frac{\Delta\rho}{\rho} = \frac{\text{constant}}{(C-C_f)^{3/2}} \qquad 2.188$$

and so the magnetoresistance should reach a minimum at the critical concentration;

(ii) from equation(2.183) we also expect that

$$\frac{\Delta\rho}{\rho} \propto \Delta(M^2) \qquad 2.189$$

and therefore, near the critical concentration

$$\frac{\Delta\rho}{\rho} \propto B_o^{2/3} \qquad 2.190$$

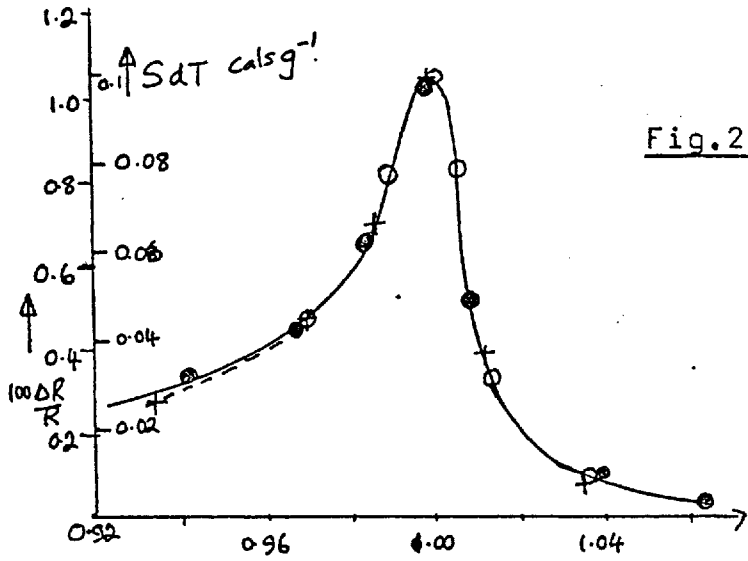

Fig.2.21: Magnetoresistance and magnetocaloric effects as a function of temperature.

+ : magnetocaloric effect

● : ΔR in longitudinal field

○ : ΔR in transverse field (after ref.258)

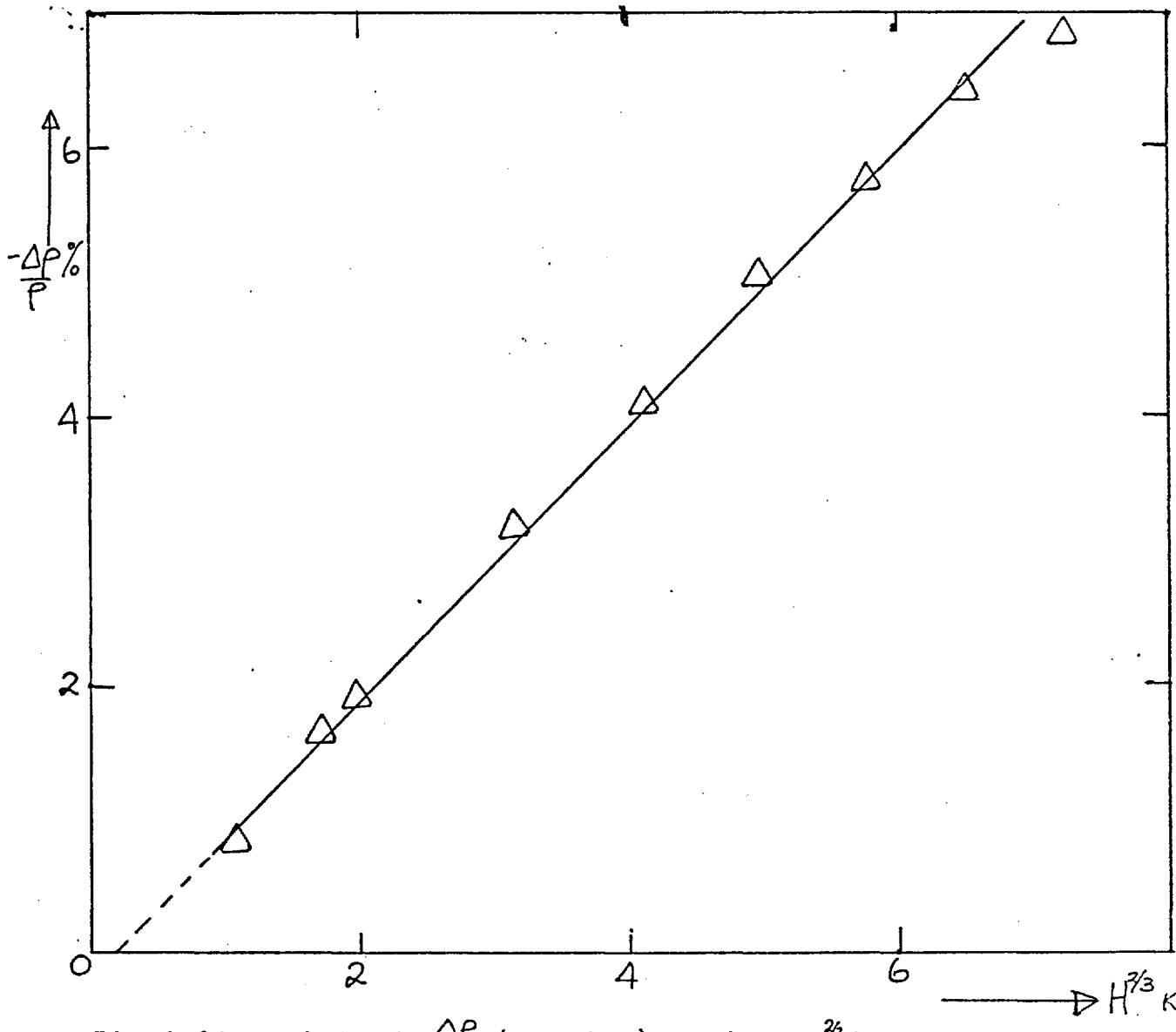

Fig.2.22: Plot of $\frac{\Delta\rho}{\rho}$ (T = 25K) against $H^{2/3}$ for Ni_3Al. Data taken from ref.259.

valid at <u>all</u> temperatures; the published data for Ni_3Al (259) appear to satisfy the above relation for moderate fields ($\lesssim$ 2T) as shown in fig 2.22. A deviation at high fields may be expected owing to the increasing importance of the conventional positive magnetoresistance;

(iii) by analogy with equation (2.186)

$$2(a+\gamma P) + C\,\frac{\Delta\rho}{\rho} = \frac{D\,B_0}{\left|\frac{\Delta\rho}{\rho}\right|^{1/2}} \qquad (2.191$$

where C and D are constants. It is also possible to define a "<u>magnetoelastic resistance</u>" (or simply elastoresistance) as

$$\frac{\Delta\rho(P)}{\rho} = \frac{\rho(B,B,T) - \rho(B,T)}{\rho(B,T)} \qquad 2.192$$

For f.c.c. <u>Ni</u>Fe alloys (260) it has been observed that there is a correlation between the sign of the elastoresistance and that of the magnetostriction. It will be interesting to see if the same correlation exists for alloys in the critical concentration region. Since $\gamma > 0$, we should expect a **positive** elastoresistance.

In the case of the Hall effect, we may write (261)

$$\mathcal{E}_H = R_0 B_0 + \mu_0 R_s M \qquad 2.193$$

where for convenience, we consider a unit current density so that $\mathcal{E}_H$ is identical with the Hall resistivity. R_0 is called the ordinary Hall coefficient and R_s the spontaneous Hall coefficient.

Near c_f we have shown that $M_o^2 \sim (c-c_f)$ and $2a + 4bM^2 = B_o/M$ (equations (2.90) and (2.92) respectively). Equation (2.193) shows that $\varepsilon_H \propto M$ and so it follows that

$$\varepsilon_H \propto (c-c_f)^{\frac{1}{2}} \qquad 2.194$$

and

$$2a' + 4b' \varepsilon_H^2 = \frac{B_o}{\varepsilon_H} \qquad 2.195$$

where a' and b' are constants. From equation (2.195),

$$\varepsilon_H \sim B_o^{\frac{1}{3}} \qquad 2.196$$

Finally, it has been shown both experimentally and theoretically (257) that

$$R_s = a_o + b_o M^2 \qquad 2.197$$

where a_o, b_o are constants. In the critical concentration region, we may therefore, expect also that

$$R_s \sim (c-c_f) \qquad 2.198$$

In this section (2.5(v)) we have obtained a number of relations which could be tested experimentally in order to assess the suitability of using magnetothermal and galvomagnetic effects to determine the critical concentration for the onset of ferromagnetism.

2.5(vi) Critical Fluctuations of Magnetization and Critical Scattering:

It is well known that condensing gases and binary

liquid mixtures exhibit the phenomenon of critical opalescence which is a marked increase in the scattering of light above the condensation point and the point of demixtion respectively (262). According to the Smoluchowski-Einstein theory ordinary light scattering (Rayleigh scattering) may be attributed to statistically independent fluctuations in the local density. Near the critical point there is a rapid increase of the local density fluctuations and, more importantly, these fluctuations are no longer independent but have a correlation length which tends to infinity at the critical point itself. Identical phenomena are also known to occur in solids. Pertinently, it has been experimentally demonstrated that near a ferromagnetic Curie point the thermal neutron cross-section for magnetic scattering increases very rapidly, peaking at the Curie temperature T_c (263). Van Hove (264) explained the peak at T_c by assuming only a strongly increasing correlation range for the fluctuations of the local magnetization, in analogy with the Ornstein-Zernicke theory for fluids.

Now we have proposed that the onset of ferromagnetism in many alloy systems is a phase transition. Consequently we should expect the transition to be characterized by strongly increasing spontaneous local fluctuations of magnetization whose correlation range should tend to infinity at the critical concentration, c_f. Therefore, we should expect critical scattering, of say thermal neutrons, to occur near the critical concentration.

The Initial Susceptibility and the Mean Square Magnetization Fluctuation:

The response of a given system to a small perturbation

is characterized by its generalized susceptibility $\chi(q, \omega)$. Specifically if we consider a magnetic medium subjected to a small perturbing magnetic induction B, the 'output' of this system is, of course, given by the magnetization M whereas the response is measured by the magnetic susceptibility. If the magnetic medium is linear and has translational invariance it may be shown (66, 265-267) that the susceptibility satisfies two very general relations viz

(i) the Kramers-Kronig relations which are simply dispersion relations connecting the real and imaginary parts of the susceptibility; they follow essentially from the principle of causality i.e. that the response of a system should be causally related to the perturbation producing it.

(ii) the fluctuation-dissipation theorem which relates the Fourier spectrum of the (thermal) fluctuations of the magnetization to the imaginary (i.e. dissipative) part of the susceptibility.

By combining the Kramers-Kronig relations with the fluctuation - dissipation theorem and taking the classical limit ($\hbar\omega \ll K_B T$) one obtains the classical fluctuation theorem (268)

$$\chi(0,0) = \frac{1}{K_B T}\left\{\langle M^2\rangle - \langle M\rangle^2\right\} \qquad 2.199a$$

$$\equiv \frac{1}{K_B T}\left\{M - \langle M\rangle\right\}^2 . \qquad 2.199b$$

We thus see that the isothermal static susceptibility is proportional to the mean square fluctuation of the magne-

tization. The above result may also be obtained by a direct calculation of the magnetic susceptibility as the response to a perturbing static field (269) or from a general theory of the fluctuations of extensive parameters (262).

More generally near the critical point we may write, in the quasi-static approximation (266,269), that

$$\chi(q,0) = \frac{1}{K_B T}\left\{\langle M_q^2\rangle - \langle M_q\rangle^2\right\} \qquad 2.200$$

where $\chi(q)$ is the Fourier transform of the static susceptibility $\chi(r)$ and the right hand side of equation (2.200) represents the Fourier spatial transform of the magnetic correlation function. Instead of equation (2.86) it may be more useful to write

$$G = G_0 + aM^2 + \delta(\nabla M)^2 + ... \qquad 2.201$$

where δ is a positive definite constant. The additional term allows for the spatial fluctuations of magnetization. This is because at the critical concentration the terms in M^2 and M^4 are negligible ($a=0$ at $c=c_f$) and so the $\delta(\nabla M)$ term becomes dominant. From equation (2.201) it has been shown (267) that for sufficiently small wavevectors q,

$$\langle M_q^2\rangle - \langle M_q\rangle^2 = \frac{\frac{1}{4}K_B T}{a + \delta q^2} \qquad 2.202$$

which is of the well-known Ornstein-Zernicke form.

Combining equations (2.200) and (2.202) we obtain

$$\chi(q) = \frac{A_0}{K_0^2 + q^2} \qquad 2.203$$

where $K_0^2 = \frac{|a|}{\delta}$ and $A_0 = \frac{1}{4\delta}$.

If $G(r) = \langle M(\underline{r}), M(o) \rangle$ is the magnetic pair correlation function, then equation (2.203) gives that

$$G(r) \sim \frac{e^{-K_0 r}}{r} \qquad 2.204$$

which clearly shows that K_0 is an <u>inverse correlation range</u>. It will be shown later that $\chi(q)$ is proportional to the elastic diffuse thermal neutron cross-section and consequently equation (2.203) suggests that the forward neutron cross-section for alloys near the critical concentration should be Lorentzian.

Also from equation (2.203) as $q \longrightarrow 0$ $\chi(q)$ tends to K_0^{-2}; but we have shown that as $c \longrightarrow c_f^{\pm}$, $\chi \longrightarrow \infty$ so that K_0 must tend to zero as $c \longrightarrow c_f^{\pm}$. Thus as we approach the critical concentration from <u>either</u> side the correlation between the net spins of the magnetic clusters becomes extremely long-ranged falling off as $1/r$. If the variation of K_0 with concentration is as

$$K_0 \sim (c - c_f)^{\nu} \qquad 2.205$$

as $c \longrightarrow c_f$ then by comparison with equations (2.95) and (2.96) we would expect $\nu = \frac{1}{2}$ on the model which has so far been used. (Actually it is not necessary to invoke the concentration dependence of χ to obtain equation (2.205)

since $K_0^2 = \frac{|a|}{\delta} \sim \frac{\alpha_0}{\delta}(c-c_f)$, and in general, $K_0 = K_0(c,T)$.

Experimentally it has been found (270) that for CuNi and CrNi alloys on which fairly extensive neutron measurement have been made $\nu \simeq 0.31$ ($\simeq 5/16$). This observed concentration dependence of the inverse correlation range clearly illustrates the critical nature of the onset of ferromagnetis We would like to mention that even though $T_c \rightarrow 0$ as $c \rightarrow c_f$ (by definition) so that one can consider the fluctuations of magnetization as being thermally induced such an interpretation may not be correct. This is because the critical diffuse neutron cross-section at a ferromagnetic Curie point $\propto K_B T$ (see eq.(3.132) below) and would vanish as $T \rightarrow 0$. The fluctuations of magnetization that occur near c_f are those caused by concentration fluctuations only. To illustrate the difference between thermal and concentration fluctuations let us consider a Cu 52% Ni alloy whose $T_c \simeq 68K$. Neutron diffraction measurements at $\sim 68K$ would give the critical scattering caused by thermally induced magnetization fluctuations but similar measurements at $\sim$ 4.2K should give the scattering due to concentration fluctuations.

Although the value of the critical exponent in equation (2.205) is not of immediate importance it is useful to comment on the value obtained. A discussion of the phenomenon of the transition at a ferromagnetic Curie point yields the following power laws:-

$$\chi^o(T) \sim \epsilon^{-\alpha_t} \; ; \; T \rightarrow T_c^+ \qquad 2.206$$

$$M_o(T) \sim \epsilon^{\beta} \; ; \; T \rightarrow T_c^- \qquad 2.207$$

$$M(T_c, B_i) \sim B_i^{1/\delta} \qquad 2.208$$

where $\epsilon = \left|1 - \frac{T}{T_c}\right|$, Bi is the internal field and γ_t, β, and δ are the critical exponents. These exponents have been shown (271) to satisfy the scaling law

$$\gamma_t = \beta(\delta - 1) \quad . \tag{2.209}$$

In the mean field approximation (MFA) $\gamma_t = 1$, $\beta = \frac{1}{2}$ and $\delta = 3$ which values satisfy the scaling law. However, recent theoretical and experimental results have shown that $\gamma_t \simeq {}^4/_3$; for example for Fe $\gamma_t = 1.333$ (272) and for Ni $\gamma_t = 1.35$ (273). Values of γ_t higher than ${}^4/_3$ could result from the neglect of magnetic dipolar interactions at the Curie point (274). For the magnetic isotherm values of $\delta = 4.22$ for Ni (273) and 4.35 for Fe (275) have been obtained, in good agreement with the density-pressure isotherm of simple gases at their critical temperatures. In the case of the coexistence curve some magnetic measurements indicate that $\beta = \frac{1}{3}$ as observed for gases but for Fe $\beta = 0.389$ (275). In fact, the use of the Padé approximant in the numerical analysis of the three-dimensional Ising model gives $\beta \simeq 0.313 \pm 0.004$ (276). If we make the adhoc assumption that a similar relation applies to the onset of ferromagnetism at the critical concentration then

$$M_o \sim (c - c_f)^{5/16} \tag{2.210}$$

instead of the MFA result given by equation (2.90). Since $\chi_f^o \sim M^{-2}$ and $K_o^2 \sim \chi_f^{o\,-1}$, it follows that

$$K_0 \sim (c - c_f)^{5/16} \qquad 2.211$$

as observed (270). It will be interesting to check if

$$\chi_f^0 \sim (c - c_f)^{-10/16} \qquad 2.212$$

In concluding the discussion in this subsection we briefly comment on the expression for the Fourier transform of the static correlation function. In deriving equation (2.202) the term in M^4 in the expression for the thermodynamic potential was neglected. It has been shown (277) that

$$bM^4 \equiv 4b \langle M^2 \rangle M^2$$

so that instead of equation (2.202) we should now have (278)

$$\langle M_q^2 \rangle - \langle M_q \rangle^2 = \frac{K_B T}{\{a + 4b\langle M^2 \rangle\} + \delta q^2} \qquad 2.213$$

This relation, however, can only alter the details of the main conclusions already reached - the existence of some critical scattering in the critical concentration region and the concentration-dependence of the inverse correlation range.

2.5(vii) <u>The Electrical and Thermal Resistivities</u>

<u>The Electricial Resistivity</u>

The low temperature behaviour of the electrical resistivity of both the nearly magnetic metals and dilute alloys of the magnetic metals has been extensively discussed by a number of authors, (38,39,279). All consider the contribution to the electrical resistivity arising from the

spin-flip scattering of conduction electrons by spin-fluctuations in either the d-band of a pure metal or at the site of a nearly magnetic transition metal impurity. In calculating this resistance a number of important assumptions is usually made, namely,

(a) that the effective mass of the d-electrons is much larger than that of s-electrons and consequently only the latter are involved in the transport processes;

(b) for alloys potential scattering and the effects of any VBS are ignored; accordingly the results are restricted to isoelectronic alloys. In addition, inter-impurity interactions are neglected so that the theory is further restricted to relatively very dilute impurity concentrations.

Using a uniform exchange enhancement model which, for an alloy, implies that a magnetic impurity merely increases the average exchange enhancement factor Schindler and Rice (38) derived that at sufficiently low temperatures

$$\rho_{sf}(T) \sim A(c)\left(\frac{T}{T_{sf}}\right)^2 \qquad 2.214$$

valid for $T \lesssim 0.1\ T_{sf}$, where $\rho_{sf}(T)$ is the spin-fluctuation resistivity. It was also deduced that $A(c) \propto \chi^2(c)$, where $\chi(c)$ is the magnetic susceptibility of the alloy. The authors then tried to use the theory to explain their experimental data on pure Pd and three PdNi alloys containing 0.5, 1.0 and 1.66% Ni. From the upper limit of the temperature range over which the T^2 low was valid they estimated $T_{sf} \sim$ 80K for Pd and 140, 100 and 30 K respectively for the alloys. The latter values

would imply that T_{sf} attains a maximum value at some Ni concentration less than 0.5%. However, the fit of their data to equation (2.214) is far from being satisfactory so that the meaningfulness of the estimates of T_{sf} for the alloys is questionable. A more glaring discrepancy between theory and experiment concerns the variation of A with χ. Experimentally $A \propto \chi$, in contrast to the quadratic dependence predicted by theory.

On the other hand, Lederer and Mills (39) used a localized exchange enhancement model in which a magnetic impurity increases the exchange enhancement only in the unit cell containing it. Their theory again predicts a quadratic increase of the spin fluctuation resistivity with temperature and more importantly, that the coefficient of the T^2 term should vary linearly with both the impurity concentration, c, and with χ, in agreement with the results obtained by Schindler and Rice (38).

Kaiser and Doniach (129) extended the theoretical calculations of Lederer and Mills (39) to higher temperatures and were able to show that (i) $\rho_{sf}(T)$ changes from a T^2 to a T dependence at $T \sim 0.25\ T_{sf}$; (ii) the data for various alloys should all fit a plot of $\tilde{\rho}$ versus $\frac{T}{T_{sf}}$, where $\tilde{\rho}$ is some normalised resistivity (per impurity atom). The quantities $\tilde{\rho}$ and T/T_{sf} are dimensionless so that the above plot is referred to as a "universal curve" The curve varies as $(T/T_{sf})^2$ in the low temperature limit ($T \ll T_{sf}$), in agreement with equation (2.214), and as (T/T_{sf}) in the high temperature limit. In order to analyse the data for some alloy systems it was assumed that one could write

$$\rho_{imp} \equiv \rho_{alloy} - \rho_{host} = \rho_{sf}(T) + \rho_{non\text{-}mag} \qquad 2.215$$

where $\rho_{non\text{-}mag}$ is a temperature-independent resistivity due to non-magnetic impurity scattering. For dilute impurity concentrations this procedure nearly eliminates the phonon resistivity. An examination of the fit of the universal curve to the PdNi data of Schindler and Rice (38) shows that the agreement with theory for the 1.0 and 1.66% alloys is definitely much better than for the 0.5% alloy. For the latter a marked deviation from the curve is observed for temperatures as low as 5K whereas no significant deviation is observed for the more concentrated alloys up to $\sim$ 20K. Clearly this is paradoxical because in view of the assumptions mentioned at the beginning of this subsection it is the more dilute alloy for which the theory is expected to be most valid. However, for Ir 0.5% Fe the fit to the universal curve is excellent, at least up to 30K; the T^2 law changes to a T law at T $\sim$ 7K giving $T_{sf} \sim$ 28K for this alloy. Above 30K the increase of ρ_{sf} with T is slower than a T-law and this was attributed to a temperature dependence of the exchange parameter.

An attempt was also made to fit the resistance data on Rh 0.5% Fe (280) but only a linear portion between 0.3 - 3K was identifiable. Owing to the absence of the T^2 regime Kaiser and Doniach (129) expressed strong reservations about the applicability of their model to highly exchange enhanced systems (with enhancement factors $\gtrsim$ 100). Since then the T^2 regime in RhFe has been found (281,282) so that the model certainly has a wider applicability than originally envisaged.

A more comprehensive discussion of the resistivity

of alloys has been given by Rivier and Zlatic (106, 130). They have grouped alloys into two classes namely

(a) "Kondo Alloys" such as AuMn, AlMn, etc, which are supposed to exhibit a resistance minimum and

(b) "Coles' Alloys" in which both constituents are transition metals e.g. RhFe, PdNi, etc.

For a "Kondo alloy" the authors calculated the resistivity due to conduction electrons scattered by a VBS undergoing spin fluctuations. The scattered conduction electrons are assumed to be those that form the impurity VBS and hence are already at the unitarity limit so that the additional scattering by the localized spin fluctuations can only cause the resistivity to decrease. A universal curve was again obtained according to which the resistivity decreases as $(T/T_{sf})^2$ at low temperatures ($T \ll T_{sf}$) and as $\ln(T/T_{sf})$ for $T > T_{sf}$; between these two regions there exists an intermediate or changeover regime where the resistivity varies linearly with temperature.

For a "Coles' alloy" the resistivity was assumed to be due to the scattering of conduction electrons by localized spin fluctuations with no VBS being formed i.e. the electrons do not have to be scattered into an extra orbital (VBS) before seeing the lsf as for a "Kondo alloy". The resistivity obtained turned out to be a mirror image of that for a "Kondo alloy" i.e. it increases as $(T/T_{sf})^2$ at low temperatures, then as (T/T_{sf}) for $T \gtrsim 0.14\ T_{sf}$, as $\ln(\frac{T}{T_{sf}})$ for $T > T_{sf}$ and finally tends to the unitarity limit (identified with the Yosida spin-disorder limit) as $(1 - \frac{T_{sf}}{T})$. Thus there exists both lnT and $1/T$ dependences in addition to the T^2 and T regimes already obtained by

Kaiser and Doniach (129). The lnT regime has been shown to exist in RhFe, IrFe and PtFe alloys. It was this region that Kaiser and Doniach (129) attempted to explain in terms of a temperature-dependent exchange enhancement.

Following the above resume of the present state of the theory of the electrical resistivity of metal alloys we will make the following comments:

(1) The stated distinction between "Kondo alloys" and "Coles' alloys" is not very meaningful or useful. We have already discussed at great length (vide section 2.2) under what conditions a resistance minimum may be observed. The resistance minimum hitherto observed in AuMn, CuMn etc. is different in character from the resistance minimum observed in CuCr, AlMn, PdCr, PtMo, etc. The latter minima are due to spin fluctuation effects involved in the magnetic — non-magnetic changeover whereas the former are caused by the spin-flip scattering of conduction electrons from well-defined spins and in these cases the minima should always be accompanied by maxima at sufficiently lower temperatures. Also these minima are necessarily restricted to low temperatures only ($T \lesssim 0.05\ \theta_D$). A decisive criterion for observing resistance minima due to spin-fluctuations is given shortly below (equation (2.226)).

(2) Whereas the Rivier-Zlatic theory uses only a single band for "Coles' alloys" our approach to the general problem of the magnetism of the transition metals and their alloys involves identifiable sp- and d- orbitals, even for a pure TM host; thus it is always a two-band model. One can then consider the combined effects of s-d hybridization and s-d exchange mixing interactions, the latter being responsible

for the existence of localized spin fluctuations since it has been stated that the d-band in a TM is exchange-split. This exchange-splitting of the d-band is the main differenc between a simple metal host and a non-magnetic TM host; the latter is, ab initio, "exchange-enhanced" owing to the occurrence of paramagnons and thus has an effective magneti degeneracy temperature, T^*_h, which, in most cases, is much less than T_F (see equation (2.34)). Otherwise impurity VBS exist in TM hosts just as much as in simple metal hosts, the observed magnetic behaviour of an impurity being determined in either case by the relative value of T^*_{imp} to the observation temperature. We may recall that the magnetic properties of dilute Ni-based alloys have been explained using the concept of VBS (7). If Cr VBS exist in Ni, there is no a priori reason why they should not exist in say Pd.

(3) We have already discussed how spin-fluctuations can give rise to superconductivity in some TM especially those with high characteristic temperatures (see equation (2.68)). Otherwise a non-magnetic TM should exhibit a spin fluctuation resistivity which varies as $(\gamma T^*_h)^2$ at low temperatures ($T \ll T^*_h$) as predicted by the various spin fluctuation theories (38,39,129,130). The upper limit of this T^2 regime is as given by Schindler and Rice (38) or by Rivier and Zlatic (130) i.e. $T \sim 0.1\ T^*_h$. (The uniform exchange enhancement model (38) may be applied to a pure TM even though the spin fluctuations are still localized). It would appear that the Kaiser-Doniach theory (129) underestimates the range of validity of the T^2 law.

For Pd where the T^2 law has been observed up to about 8K (38) $T^*_h \simeq$ 80K as already suggested (see section 2.2). A T^2 law has also been observed in a large number of TM (283) but neither has the upper limit of the T^2 regime been clearly identified nor are we sure that there are no other processes (e.g. Baber's electron-electron scattering process) which contribute to the T^2 term. However, for those metals whose T^*_h can be estimated from $\chi(T)$ we can readily state the approximate upper limit of the T^2 regime. Thus for Pt with $T^*_h \sim$ 150K, the upper limit is about 15K while for Rh with $T^*_h \sim$ 1650K the upper limit is about 165K.

In general, at low temperatures, the resistivity of a non-magnetic TM may be written as

$$\rho_{TM} = \rho_o + \rho_{sf} + \rho_{bss} + \rho_{sd} + \rho_{ss} \qquad 2.216$$

where ρ_o is the residual resistivity; ρ_{sf} is the spin fluctuation resistivity which varies as $(\frac{T}{T^*_h})^2$; ρ_{bss} represents Baber's electron-electron scattering i.e. the scattering of s-electrons from the heavier d-holes through a screened Coulomb interaction ($s \longrightarrow s^I$; $d \longrightarrow d^I$) and it varies as T^2 also. ρ_{sd} is the resistivity arising from the phonon-induced scattering of s-electrons <u>into</u> the d-band (i.e. $s \longrightarrow d$; $d^I \longrightarrow d^{II}$); at low temperatures it varies as T^3 (284). Finally ρ_{ss} is the more familiar resistivity due to phonon-induced scattering of conduction electrons within a single-band (the s-band) and is given by the Bloch-Grüneison formula which predicts a T^5 dependence

at low temperatures. Thus at low temperatures

$$\rho_{TM} \sim \rho_0 + aT^2 + bT^3 + cT^5 \qquad 2.217$$

where a,b, and c are arbitrary constants. The purpose of writing equation (2.217) is two-fold: firstly, to show how simplistic it is to analyse the low temperature resistivity of a TM in the form

$$\rho_{TM} = \rho_0 + aT^n \qquad 2.218$$

where n is often non-integral e.g. for Ru $n \simeq 4.75$ (283,285); secondly, and more importantly, to highlight the difficulty of identifying the T^2 term due to spin fluctuations especially for those metals with very high characteristic temperatures (the coefficient of the T^2 term $\propto (T^*_h)^{-2}$ e.g. the superconducting TM. The difficulty is further compounded by the fact that we cannot think of a way of separating the Baber term from the spin-fluctuation term. However, we shall hope that a fit of the low temperature resistivity of a TM to equation (2.217) will show which terms are important and also that for those metals with $T^*_h \lesssim 10^3$K the spin-fluctuation resistivity will dominate the Baber term. Incidentally, we will note that for those TM which are superconducting a lower limit of T^2 regime is obviously the superconducting transition temperature, T_{sc}.

(4) A TM impurity in a given host matrix has a

spin fluctuation temperature given by equation (2.36). The presence of the impurity also affects T^*_h through its effect on the host density of states at the Fermi level. The concentration-dependence of T^*_h is particularly important for a TM host. We shall suppose that we can write

$$\rho_{imp} \equiv \rho_{alloy} - \rho_{host} = \rho_V + \rho_{sf}^{(T)} + \rho_{band}^{(T)} \qquad 2.219$$

where the terms contributing to ρ_{imp} are as follows:-

(a) ρ_V is the resistivity due to the impurity potential scattering, i.e. the impurity residual resistivity. It is given by equation (1.12) i.e.

$$\rho_V = \frac{2\pi\hbar c}{\nu e^2 k_F}\left\{\sin^2\eta_{2\uparrow} + \sin^2\eta_{2\downarrow}\right\} \qquad 1.12$$

or in the alternative form (286, 287)

$$\rho_V = \frac{2\pi\hbar c}{\nu e^2 k_F}\left\{1 - \cos 2\delta_V \cos 2\delta_M\right\} \qquad 2.220$$

where

$$2\delta_V = \eta_{l\uparrow} + \eta_{l\downarrow} = \frac{\pi Z}{2l+1}\,, \qquad 2.221$$

(cf equation (1.11))

$$2\delta_M = \eta_{l\uparrow} - \eta_{l\uparrow} = \frac{2\pi S}{2l+1}\,, \qquad 2.222$$

$$\delta_M = \lim_{T\to\infty} \delta_m(T)\,. \qquad 2.223$$

S is the effective spin of the impurity atom which, in the ideal single impurity limit, is temperature-dependent (see section 2.2 - summary). Strictly Z, the impurity-host charge difference, should be replaced by an effective

value that allows for any distortion of the lattice by the impurity. According to Blatt (288)

$$Z_{eff} \simeq Z - \frac{\delta\Omega}{\Omega} \qquad 2.224$$

where $\frac{\delta\Omega}{\Omega}$ is the relative change in the volume of the unit cell containing the impurity and is given by

$$\frac{d\ell}{\ell} = \frac{1+\sigma}{1-\sigma}\,\frac{\delta a_0}{a_0} \,. \qquad 2.225$$

$\frac{\delta a_0}{a_0}$ is the fractional change in the lattice parameter in percent per atomic percent impurity and σ is Poisson's ratio.

For a given host, say Cu, and in the <u>ideal single impurity limit</u> ρ_V should give a peak in the middle of the transition series, near Cr. We shall take the single impurity limit to denote impurity concentrations less than about 0.1 c_m, where c_m is the critical concentration for the onset of magnetism. In <u>addition</u>, the resistivity must be measured at temperatures much lower than T^*_0 (the spin fluctuation temperature in the single impurity limit). Thus for <u>Cu</u>Mn where $T^*_0 \sim$ 10 mK and $c_m \sim$ a few ppm, ρ_V can only be properly determined for $T \lesssim$ 10 mK and for Mn concentrations $\sim 10^{-5}$%. When this prescription is consistently carried out only a <u>single peak</u> should be observed. Otherwise a double peak may result. This point is clearly illustrated by the data of Kedves et al (292) on Al-based 3d alloys.

(b) $\rho_{sf}(T)$ is the temperature-dependent resistivity

due to spin fluctuations at the impurity sites. Again in the dilute impurity concentration region ($c \lesssim 0.1\ c_m$) we suggest that this resistivity is given by

$$\rho_{sf}(T) = A \cos 2\delta_V f(B_o, T) \qquad 2.226$$

where $A \simeq \frac{20\pi\hbar c}{\nu e^2 K_F}$. The temperature-dependence of the spin-fluctuation resistivity is as derived by Rivier and Zlatic (130) i.e

$$f(0,T) \sim \left(\frac{T}{T^*_{imp}}\right)^2 \quad \text{for } T \ll T^*_{imp},$$

$$\sim \frac{T}{T^*_{imp}} \quad \text{for } 0.1\,T^*_{imp} \lesssim T \lesssim T^*_{imp}$$

$$\sim \ln\left(\frac{T}{T^*_{imp}}\right) \quad \text{for } T > T^*_{imp}$$

and tends to the Yosida spin-disorder limit as T^{-1} as $T \longrightarrow \infty$. Laborde and Souletie (287) have proposed that

$$\rho_{sf}(T) = \frac{20\pi\hbar c}{\nu e^2 K_F} \cos 2\delta_V f(B_o, T)\, G\left(\frac{W_o c}{T}\right) \qquad 2.227$$

where $f(T) = \cos 2\delta_M - \cos 2\delta_m(T)$

and $G(\frac{W_o c}{T})$ allows for RKKY interactions between impurities. Since spin fluctuations are important only for concentrations below c_m we do not think it is advisable to include the effect of inter-impurity interactions because we cannot determine, a priori, what the magnetic units are i.e. whether these are pairs, triplets etc. In other words, it will be more useful to restrict the discussion to the dilute impurity limit. Also in Laborde and Souletie's

scheme (287) $f(T)$ is determined essentially from the temperature dependence of the magnetic susceptibility. What we wish to stress in equation (2.226) is that the sign of the spin fluctuation resistivity is determined only by the phase shift due to potential scattering. If $Z_{eff} \geq 2.5$, $2\delta_V > \pi/2$ so that ρ_{sf} is negative and a resistance minimum is observed. This is the only criterion for observing a resistance minimum due to spin-fluctuation effects. Any other resistance minima have nothing to do with the magnetic $\longrightarrow$ non-magnetic changeover. For a given host matrix the T^2 term changes sign as Z_{eff} increases, as is well illustrated by the resistivity of Rh-based 3d alloys (289) or of Pd-based alloys. Since the coefficient of the T^2 term $\propto (T^*_{imp})^{-2}$ it is clear that PdCr say will show a more pronounced resistance minimum than either PtCr or RhCr. It should by now be much clearer why any classification of alloys into "Kondo" or "Coles" alloys is not very relevant. CuMn will exhibit a spin-fluctuation resistance minimum provided we worked in the appropriate concentration and temperature regimes ($C < 10^{-5}$% Mn; $T < 10$ mK). We observe that the phase factor in equation (2.226) occurs in the Appelbaum-Kondo expression (equation (2.31)) and has also been introduced phenomenologically by Loram et al (132).

We should caution that care has to be exercised in obtaining ρ_{imp}. The definition of this quantity as ($\rho_{alloy} - \rho_{host}$) assumes that ρ_{host} is essentially unaltered by the presence of the impurity. However, we have already mentioned that $T^*_h = T^*_h(c)$ and for TM hosts where there is an intrinsic spin fluctuation resistivity the concentration dependence of T^*_h will surely alter

both the magnitude of the T^2 term in the resistivity of the host and the upper limit of its range of validity. Thus in PdCo, for example, T^*_h decreases as the Co concentration increases so that the magnitude of the T^2 term in the resistivity of the host itself increases but its range of validity is decreased. It would appear therefore that, as defined, ρ_{imp} contains an additional term

$$\Delta\rho_{imp} \sim \frac{\bar{T}_h^*(0)^2 - \bar{T}_h^*(c)^2}{\left\{\bar{T}_h^*(0)\,\bar{T}_h^*(c)\right\}^2} \qquad 2.228a$$

$$\simeq \frac{2\,\delta\bar{T}_h^*}{\bar{T}_h^*(0)^3} \qquad 2.228b$$

where $$\delta\bar{T}_h^* = \bar{T}_h^*(0) - \bar{T}_h^*(c) \qquad 2.229$$

resulting from a change in the spin fluctuation temperature of the host. For PdCo δT^*_h is positive so that ρ_{imp} as obtained from the experimental data is larger than its true value whilst the converse is true for PdCr. It is to be hoped that in the dilute limit ($c \leq 0.1$cm) the effect may become negligible particularly for those hosts with high T^*_h values.

Another problem that can be validly raised is whether paramagnon-paramagnon interactions in a dilute alloy can occur. As proposed there are at least two types of paramagnons in a dilute alloy - those of frequency $\frac{K_B \bar{T}_h^*}{h}$ corresponding to the spin fluctuations of the host matrix and those of frequency $\frac{K_B \bar{T}^*_{imp}}{h}$ representing the spin

fluctuations at the impurity sites. It will be noted that because of the exponential factor in equation (2.35) T^*_h is at least an order of magnitude greater than T^*_{imp} so that, to a first approximation, any interactions between the paramagnons may be neglected.

(5) So far we have discussed two mechanisms that lead to resistance minima namely

(a) The spin fluctuations associated with the change from a magnetic to a non-magnetic regime at T^*_{imp}, but only when the impurity-host charge difference is such that the phase shift, $\delta_V > \pi/4$.

(b) The spin-flip scattering of conduction electrons from <u>well-defined</u> but non-interacting magnetic units (individual spins or clusters). As already discussed (section 1.7) this scattering gives rise to a lnT term (equation (1.35)). If, in addition, the exchange coupling between the conduction electrons and the magnetic units is negative, then a resistance minimum results at a temperature given by equation (1.37). The "Kondo divergence" merely reflects the neglect of the interactions between the magnetic units which, as mentioned several times earlier, leads to a resistance maximum at a still lower temperature.

We shall now mention a third mechanism that could conceivably give rise to a resistance minimum. This refers to a reduction of the phonon-induced interband s-d scatterin resulting from the energy dependence of the density of states at the Fermi level. This dependence modifies the resistivity by a factor $(1-AT^2)$ where A is given by the

second term in the brackets in equation (2.47). It has been suggested (291) that this factor is also important for s-d impurity processes so that in alloys where A is appreciable, the decreasing "s-d resistivity" when combined with the ideal resistivity (increasing as T^5 at low temperatures) leads to a resistance minimum. This explanation has been advanced to account for the minima observed in PdRh (111) and PdAg (209). However, in the case of PdAg alloys, the resistance minima were originally explained in terms of scattering from "exchange-enhanced localized pockets" of holes (294), a viewpoint that has recently been supported by Murani (295).

The resistance minimum observed in a Pd 4% Rh alloy (111) was not observed in a later investigation by Purwins et al (296). If the presence of this minimum is confirmed then the explanation in terms of a reduced s-d scattering is certainly plausible but then a resistance minimum should also be observed in Pt $\sim$ 4% Rh and Pd- and Pt- based alloys of Ru, Ir, Os, etc of similar concentrations. On the other hand the possibility of a Rh atom bearing a local moment in a Pd- rich environment should not be discounted (557), so that case (b) above may still apply. NMR measurements at low temperatures (558) show that the local Rh susceptibility $\chi_{Rh} >> \chi_{Pd}$ and is extremely sensitive to statistical fluctuations of the local environment. Also perturbed angular correlation studies (559) indicate that at low temperatures the Rh atoms are nearly magnetic with $T^* \sim 100K$. As discussed in Chapter 6, in RhNi a Rh atom surrounded by 12 Ni nearest neighbours has a fairly large moment ($\simeq 2.6 \mu_B$) but this moment "disappears" as soon

as there is a Rh nearest neighbour. A similar effect could exist for PdRh and, in fact, Gersdorf and Muller (560) have suggested that a Rh atom surrounded by 12 Pd atoms has a very high paramagnetic susceptibility.

Having discussed the nature of the spin fluctuation resistivity which occurs in the dilute impurity concentration region where inter-impurity interactions may be presumed to be negligible we shall once more return to the critical concentration region for the onset of ferromagnetis where inter-impurity interactions must be considered. Specifically, we need to consider the effect of the magnetic clusters which we have shown to be necessarily present in the transition region. As mentioned above (see comment 5(b)) and also by Beck (297) the spin-flip scattering of conduction electrons from these clusters should lead to resistance minima and indeed such minima have been observed in CuNi (207, 293) and VFe (208) alloys. In the latter case an abrupt increase in the slope of the plot of the residual resistivity against impurity concentration is also observed at the same concentration at which the resistance minimum first occurs. This correlation confirms that the resistance minimum is due to the pres ence of magnetic clusters. For CuNi no residual resistivity measurements in the relevant concentration region ($\lesssim$ 30%Ni) have been reported but a similar change of slope should be expected. If the magnetic clusters interact to form a cluster-glass then the resistance minimum will be accompanied by a maximum. This is the explanation for the resistance maximum and minimum observed at low temperatures

for Cu 46% Ni (207). This alloy is not ferromagnetic as generally assumed because, as shown below (section 2.6) the critical concentration is $\simeq$ 47.6% Ni.

Also near the critical concentration, c_f, we should consider the scattering of conduction electrons by critical fluctuations of magnetization. In the ferromagnetic regime ($c > c_f$) these critical fluctuations are similar to the spatial fluctuations of magnetization that usually occur near a ferromagnetic Curie point with the modification that in the present case $T_c \sim 0K$. In the non-magnetic regime ($c < c_f$) spin fluctuations do occur.

In both cases the scattering of conduction electrons gives rise to a T^2 term in the electrical resistivity whose coefficient is proportional to the initial susceptibility. In the dilute concentration region the initial susceptibility is, of course, identical with the high field susceptibility and is proportional to the impurity concentration (39); however, close to the critical composition the initial susceptibility varies as $|c - c_f|^{-1}$ (equations (2.95) and (2.96)) so that the coefficient of the T^2 term in the electrical resistivity peaks at the critical concentration. This is not surprising because at the critical concentration the fluctuations of magnetization are greatest. Thus we can give a physical explanation of the now standard procedure for obtaining c_f by plotting the coefficient of the T^2 term in the resistivity as a function of concentration (193, 298, 299). We note that as in the case of the initial susceptibility the peak in the coefficient of the T^2 term should be asymmetric. It has often been the practice to analyse the low temperature resistivity of an alloy in the

critical concentration region in terms of the phenomenological relation (cf eq.(2.218))

$$\rho(T) = \rho_0 + a(c)T^n \quad . \qquad 2.230$$

The exponent n is determined from the best fit of eq.(2.230) to the measured resistivity over a selected temperature range - 1.6 to 5K (214a,300) or 4.2-300K (301,302) and the coefficient a(c) thereby determined. The critical concentration is then estimated from the maximum in a(c). This procedure is incorrect because there is no theoretical or physical explanation of why n should vary smoothly from abou 1 to 2 through the critical concentration; alternatively, what meaning should be attached to the coefficient of a term whose exponent is continuously varying as a function of the impurity concentration? Mathon (75) has attempted to obtain the temperature dependence of the resistivity in the critical concentration region. Using the concept of a uniform exchange enhancement of spin fluctuations he predicted that away from the critical region $\rho(T) \propto T^2$ while near the critical region $\rho(T) \propto T^5/3$, i.e. n is never less than 1.5. The model upon which Mathon's theory is based is clearly unsuitable and, in any case, the $T^5/3$ law has not been observed in any of the relevant alloy systems. However, such a $T^5/3$ dependence has been reported for $ZrZn_2$ (303) over a temperature region spanning the ferromagnetic Curie point. Firstly, we suggest that since we are concerned with a phase transition as a function of the impurity concentration any analysis of the electrical resistivity data should be restricted to the lowest temperatures only (about 0-5K). Secondly, since magnetic clusters are present in the critical region their contribu-

tion to the temperature dependence of the electrical resistivity must also be considered. It has already been mentioned that the clusters could give rise to a resistance minimum to be followed by a maximum just above the temperature, T_{cg}, at which the clusters "freeze in" to form a cluster-glass. We consider two specific cases:-

(i) Where T_{cg} is well <u>below</u> the lowest temperature of observation. In such a case the observed resistivity may be represented by

$$\rho(T) = \rho_0 + a(c)T^2 - b\ln T \qquad 2.231$$

The origin of the lnT term is obvious.

(ii) Where T_{cg} is well <u>above</u> the highest temperature of observation. In this case, the observed resistivity will include that of a cluster-glass which we can take to vary as $T^3/2$ (but see below - section 2.8). Thus we can write

$$\rho(T) = \rho_0 + a(c)T^2 + d\,T^{3/2} \qquad 2.232$$

It is interesting to note that the above temperature dependence has been predicted for the ferromagnetic metals (315). The above are the two simplest cases that may be considered. A wide variety of intermediate cases clearly exists so that various forms of T-dependence are possible. While we have stated that the coefficient of the T^2 term, i.e. a(c), should peak at the critical concentration we cannot, a priori, predict the concentration dependence of b or d except to suggest that either coefficient could exhibit a peak at a concentration lower than c_f where there exists a maximum number of <u>uncoupled</u> clusters. Leaving these details aside what we wish to stress is that the critical concentration determined by fitting the resistivity measurements

to a single power law (equation (2.230)) in an alloy system where magnetic clusters are known to exist is more than likely to be different from the true value. In this context we should also note that plotting $\Delta\rho\{= \rho(4.2) - \rho(1.7)\}$ as a function of concentration may not always be very helpful, if at all. This is because if no magnetic clusters appear to be present (as say in the transition from a non-magnetic state to SDW) then

$$\rho(T) \simeq \rho_0 + a(c)T^2 \qquad 2.233$$

and $$\rho(4.2) - \rho(1.7) = 14.75\, a(c)$$

so that no extra information is gained by plotting $\Delta\rho$ as well as a(c) as a function of concentration except that $\Delta\rho$ is an order of magnitude larger than the corresponding value of a and probably less accurate. A glance at figure 4 of reference 193 clearly shows this to be true. If clusters are present then the procedure may give a wrong interpretation of the data as has been mentioned in the case of RhCo; for PdNi it gives a wrong value of the critical concentration (2.3% Ni as compared with the true value of 2.8% Ni). Other systems where the method has so far been applied (AuFe, RhFe) have not been equally scrutinized. It may well be that the usefulness of the plot ($\Delta\rho$ vs c) lies in correlating magnetic changes with structural transformations and atomic ordering; but whether this is true or not we suggest that a plot of $\Delta\rho$ versus c should always be accompanied by a plot of the resistivity at the lower temperature as a function of c as well.

The Residual Resistivity

The presence of magnetic clusters in an alloy system should be reflected in their contribution to the residual resistivity. If we assume that all the magnetic clusters are identical, each with a net spin S, and if their concentration is C^*, then their contribution to the residual resistivity is

$$\Delta\rho_o = \frac{4\pi\hbar C^*}{\nu e^2 k_F} J_o^2 S(S+1) \qquad 2.234$$

where J_o is the exchange integral between a conduction electron and a magnetic cluster. It is this contribution that is probably responsible for the increased slope of the residual resistivity versus impurity concentration curve observed for VFe (208). With the onset of long range ferromagnetic order this magnetic contribution disappears so that as a function of the impurity concentration the magnetic contribution to the residual resistivity peaks at C_f. Another way of looking at this is to note that, in general, the impurity residual resistivity is proportional to the differential scattering cross-section per impurity atom (304). For the magnetic contribution to the residual resistivity the scattering cross-section is, of course, related to the fluctuations of magnetization which are maximum at the critical concentration. The obvious limitation to the use of this procedure to determine C_f is that it would be difficult to obtain the magnetic contribution to the residual resistivity especially in situations where magnetic changes are inextricably linked with structural

transformations.

We may remark that the onset of a spin-glass state does not seriously reduce the magnitude of the magnetic residual resistivity. Instead of equation (2.234) we now have

$$\Delta\rho_0 = \frac{4\pi\hbar c^*}{\nu e^2 k_f} J_0^2 S^2 \qquad 2.235$$

Magnetoresistance

Since the effect of an applied magnetic field would be to suppress the fluctuations of magnetization in the critical region it is expected that the impurity magnetic residual resistivity will increase while the coefficient of the T^2 term will decrease in an applied field; thus there should be a negative temperature-dependent magnetoresistance A decrease in the coefficient of the T^2 has been observed for several PdNi alloys (305,306). A discussion of the concentration - and field-dependence of the magnetoresistance in the critical concentration region has already been given (section 2.5(v)).

It should be noted that a negative magnetoresistance may also be observed in spin-glasses.. In the absence of an applied field there is no magnetization even below the ordering temperature. When a field is applied some net magnetization results. It has been shown (304,307) that the resulting magnetoresistance is negative and is proportional to the square of the magnetization (cf equation (2.189)). For a spin-glass we may take $M \propto B_0$ so that

$$-\frac{\Delta\rho}{\rho} \propto B_0^2 \qquad 2.236$$

as compared with a $B_0^{2/3}$ dependence in the critical concentration region (equation (2.190)). The above behaviour (i.e. for $C <, =, > C_f$) parallels that observed near the Curie temperature T_C.

The Thermal Conductivity

Corresponding to the T^2 term in the electrical resistivity there should be a term, linear in T, in the thermal resistivity. Therefore at the critical concentration the coefficient of this linear term should exhibit a maximum. From elementary kinetic theory it is known that the thermal conductivity, $\mathfrak{K}$, is given by $\mathfrak{K} \sim C_v v \Lambda$ where C_v is the heat capacity per unit volume, v is the velocity of the particles and Λ is the mean free path. It is thus apparent that the predicted maximum in the coefficient of the linear term in the thermal conductivity is related to the maximum observed in the linear term in the heat capacity (see below section 2.5(ix)).

We should also discuss the possible contribution of the phonon term to the thermal conductivity. Although in pure metals this contribution is much smaller than the electronic term in alloys the two terms may be of the same order of magnitude. Now thermal phonon resistivity results from only umklapp-processes which are frozen out at very low temperatures so that usually in metals and alloys the low temperature phonon conductivity is mainly due to geometrical scattering i.e. scattering by lattice imperfections, boundaries, randomness of isotopic distribution, degree of atomic disorder, etc. However, in the critical concentration region we would expect some phonon thermal resistivity arising from the interaction of phonons with

magnetization fluctuations via the magnetoelastic coupling. This effect leads to the renormalization of the velocity of sound and an increase in sound attenuation as discussed below (see section 2.5(x)). There we derive that the relaxation time, τ, is given by $\tau \sim \{8\Gamma b M_o^2\}^{-1}$ where Γ is a coefficient that appears in the kinetic equation of motion for the interaction process (see section 2.5(x)) and the parameters b and M_{oo} have already been defined (section 2.5(ii)). Since $b = (8\chi_f^o M_{oo}^2)^{-1}$ (equation (2.99)), it follows that $\tau \sim \chi_f^o/\Gamma$ so that

$$K_{ph} \sim \frac{C_v}{\Gamma} v_s^2 \chi_f^o \qquad 2.237$$

where v_s is the velocity of sound. At low temperatures the phonon heat capacity $\sim T^3$; consequently

$$K_{ph} \sim \frac{v_s^2 \chi_f^o}{\Gamma} T^3 \qquad 2.238$$

Now χ_f^o diverges at the critical concentration and so we should expect that the coefficient of the T^3 term in the thermal conductivity will peak at the critical concentration. In fact, since both the electron and phonon contributions to the thermal conductivity increase in the same way near c_f it follows that another sensitive way of determining c_f would be to measure the thermal conductivity at a given low temperature as a function of concentration.

2.5(viii) The Thermopower

It is known that the thermopower, Q, is the most sensitive electronic transport property of a metal (304),

being sensitive to the type of electron scattering mechanism and the shape of the Fermi surface. It is also affected by phonon drag which refers to the fact that owing to electron-phonon interactions a displacement of the electron system (say through the flow of an electric current) leads to a displacement of the phonon system as well, since the latter must come to equilibrium with the electrons (308). In other words a displaced electron system "drags" the phonon system along with it.

Owing to the resulting complexity of the thermopower it is not usually easy to explain its observed characteristics in terms of the simple theories developed for it. The thermopower of a metal or alloy has been shown (309) to be given by

$$Q = -\frac{\pi^2}{3}\frac{K_B^2 T}{|e|}\left\{\frac{\partial}{\partial \varepsilon}\ln \sigma(\varepsilon)\right\}_{\varepsilon_F} \qquad 2.239$$

where $\sigma(\varepsilon)$ is the value the electrical conductivity would have if the Fermi energy were ε ; $|e|$ is clearly the absolute value of the electronic charge. A simple theory (304) shows that

$$\sigma = \frac{e^2 \Lambda A_F}{12\pi^3 \hbar} \qquad 2.240$$

where Λ is the electron mean free path (mfp) and A_F is the area of the Fermi surface. Thus

$$\frac{\partial}{\partial \varepsilon}\ln \sigma(\varepsilon) \simeq \frac{\partial}{\partial \varepsilon}\ln \Lambda + \frac{\partial}{\partial \varepsilon}\ln A_F \qquad 2.241$$

showing that, as a first approximation, the thermopower

depends on the electron mfp and on the effective mass of the electrons. Since the latter depends on the details of the Brillouin zone it is not possible to predict, a priori, the sign of the thermopower.

[The first term in equation (2.241) is, however, positive because the greater the energy of an electron is the less likely it is to be scattered i.e. the greater its mfp]. All the same equation (2.239) has been useful in explaining at least qualitatively the variations in the thermopower of the noble metals ($Q > 0$) and the bismuth group (large Q but of variable sign). The transition metals which are of interest to us have fairly large but usually negative thermopowers. This is believed (304,309) to be due to the same mechanism that is responsible for the relatively high resistivity of these metals - the scatterin of s-electrons into the d-band. Clearly then

$$\Lambda \propto \rho_d(\varepsilon_F)$$

thereby giving a contribution to the thermopower of magnitu

$$\frac{-\pi^2 K_B^2 T}{3|e|} \left\{ \frac{\partial}{\partial \varepsilon} (n\, \rho_d(\varepsilon)) \right\}_{\varepsilon_F}$$

This shows that Q depends on the variation of the density of states with ε. For example for the Ni group of metals $\rho_d(\varepsilon)$ decreases rapidly with ε so that Q can be expected to be large and negative. More quantitatively if we assume a parabolic band of the form

$$\rho_d(\varepsilon) \sim (\varepsilon_0 - \varepsilon)^{1/2}$$

then $$Q = -\frac{\pi^2 K_B^2 T}{6|e|} (\varepsilon_0 - \varepsilon_F)^{-1} \cdot \qquad 2.242$$

The addition of say a noble metal to the transition metal leads to a decrease of ($\varepsilon_0 - \varepsilon_F$), (since the d-holes are being filled) and hence Q should increase continuously until all the holes are filled up (at about 55% of the noble metal). Thereafter Q should decrease rapidly to a value comparable to that of the noble metal (309). The observed thermopower data on AgPd and AuPd alloys (310) follow the trend predicted by theory although a detailed examination reveals marked discrepancies. The maximum value of Q occurs at about 40% Ag and 50% Au respectively in AgPd and AuPd alloys. The value for AgPd is nearer the experimentally determined number of d-holes in Pd, about 0.364/atom (311). In addition, the drop in the thermopower when the concentration of Ag or Au exceeds the "critical value" is not as sharp as the theory leads us to expect. The discrepancy between theory and experiment is even worse for CuNi alloys (312). Significantly, however, the variation of the thermopower with composition for both AgPd and CuNi is somewhat similar to the corresponding resistance - composition curves; this again shows that there exists some correlation between resistance and thermopower.

More pertinently it has been shown that near both the order-disorder phase transition in β-brass (313) and the ferromagnetic critical region in $GdNi_2$ (314) the variation of the temperature derivatives of the resistance and thermopower are essentially identical. This identity shows the common origin, at least in the critical region, of the

mechanism governing both phenomena, which is clearly the scattering of conduction electrons by critical fluctuations. We may therefore expect that near the critical concentration for the onset of ferromagnetism where fluctuations of magnetization occur the thermopower measured at low temperatures (strictly $\frac{Q}{\zeta}$ at $T = 0$) should peak at the critical concentration - in the same way as the magnetic contribution to the residual resistivity. Alternatively, since near the critical concentration $\rho(T) \propto T^2$ at low temperatures a similar temperature dependence should obtain for Q(T) and the coefficient of such a T^2 term should peak at c_f.

2.5(ix) The Specific Heat**

If we substitute equation (2.88) into equation (2.86) we get

$$G = G_o - bM_o^4 + \text{---------} \qquad 2.243$$

By definition the magnetic specific heat at constant pressure, C^m_p, is

$$C^m_p \equiv C_{p,B_o} - C_{p,M} = -\frac{T}{\rho_o}\frac{\partial^2 G}{\partial T^2} \qquad 2.244$$

where C_p, B_o and C_p, M are respectively the specific heat at constant field and constant magnetization and ρ_o is the density of the system. Thus in the magnetic state

$$C^m_p = \frac{T}{\rho_o}\frac{\partial^2}{\partial T^2}\left\{bM_o^4\right\}. \qquad 2.245$$

** A more comprehensive discussion of the "electronic" heat coefficient of nearly and weakly ferromagnetic alloys has been given elsewhere (Ododo 1978: J.Phys. Chem. Solids (to be published)).

It is clear from equation (2.244) that the specific heat is determined by the temperature dependence of the spontaneous magnetization. As in the case of the volume magnetostriction (section 2.4(iv)) we shall consider two forms of the temperature dependence of the spontaneous magnetization. The first is given by equation (2.161) on the model of weak itinerant ferromagnetism. Assuming that b is at worst weakly dependent on temperature it is easily derived that

$$C_p^m = -\frac{4bM_{oo}^4}{\rho_o T_c^2} T + \frac{12bM_{oo}^4}{\rho_o T_c^4} T^3 \qquad 2.246$$

as originally obtained by Mathon (75). If we substitute for M^2_{oo} from equation (2.90) we finally get that

$$C_p^m = -\frac{2M_{oo}^2 \alpha(c-c_f)}{\rho_o T_c^2} T + \frac{6M_{oo}^2 \alpha(c-c_f)}{\rho_o T_c^4} T^3 \qquad 2.247$$

Writing $$C_o = \gamma_o^s T + \beta_o^s T^3$$

and $$C_p = C_o + C_p^m \equiv \gamma^s T + \beta^s T^3$$

where C_o is the specific heat in the absence of any magnetic effects then

$$\gamma^s = \gamma_o^s - \frac{2M_{oo}^2 \alpha(c-c_f)}{\rho_o T_c^2} \qquad 2.248$$

and

$$\beta^s = \beta_o^s + \frac{6M_{oo}^2 \alpha(c-c_f)}{\rho_o T_c^4} \qquad 2.249$$

Furthermore if equation (2.126) is valid i.e. $T_c \simeq k M_{oo}$, then equations (2.248) and (2.249) reduce to

$$\gamma^s = \gamma_0^s - \frac{2\alpha}{\rho_0 K}(c - c_f) \qquad 2.250a$$

$$\beta^s = \beta_0^s + \frac{12b}{\rho_0 K^2} \qquad 2.250b$$

These equations predict that the coefficient of the linear term in the specific heat should decrease continuously in the ferromagnetic region while that of the T^3 term should undergo a finite discontinuity at the critical concentration. The expected variations are sketched in figure 2.23

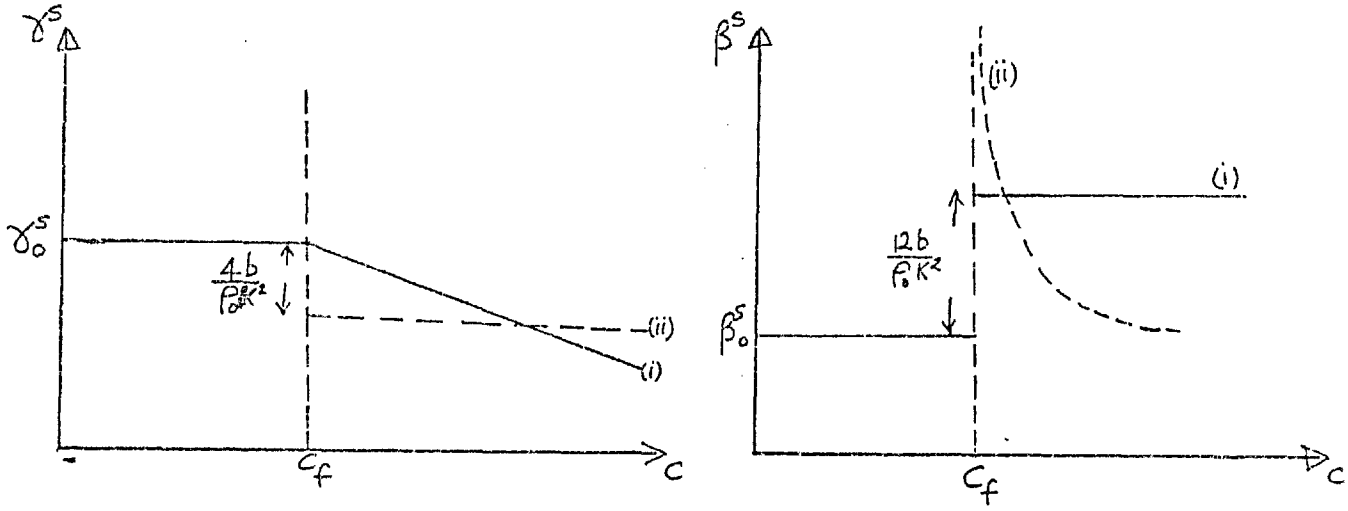

Fig.2.23: Variation of γ^s, β^s with impurity concentration:

(i) equations (2.250)

(ii) equations (2.251)

On the other hand, for <u>disordered</u> ferromagnetic alloys equation (2.125) appears to be valid i.e. $T_c \simeq K M_{00}^2$, so that instead of equations (2.250) we now have

$$\gamma^s = \gamma_0^s - \frac{4b}{\rho_0 K^2} \qquad 2.251a$$

and $$\beta^s = \beta_0^s + \frac{12b}{\rho_0 K^2 T_c^2} \qquad 2.251b$$

These equations are also sketched in figure 2.23 (dotted lines).

Another form of the temperature dependence of the spontaneous magnetization is that given by equation (2.172). This form gives

$$C_p^m = \frac{2bM_{00}^4}{\rho_0}\left\{-4AT + 36\,A^2T^3 - 60\,A^3T^5 + 28\,A^4T^7\right\} \qquad 2.252$$

which, if we disregard terms of higher order than A^2 (since $A \sim T_c^{-2}$), is essentially of the same form as equation (2.246) so that the discussion leading to equations (2.250) and (2.251) also applies. Although the two forms of the temperature dependence of the spontaneous magnetization may often be practically equivalent in the temperature region of interest ($T \ll T_c$) there appears to be an important fundamental difference. The difference is that at low temperatures the expression

$$M_0 = M_{00}\left\{1 - AT^{3/2}e^{-\Delta/k_BT}\right\} \qquad 2.253$$

may be represented by a quadratic temperature variation of the form of equation (2.172). This behaviour was first pointed out by Niira (316) and Mackintosh (317) in connection with the magnetization of a number of rare-earth metals and has also been recently confirmed for Fe and Ni (147). The usual interpretation of equation (2.253) is in terms of a spin-wave term modified by the presence of a

magnetic anisotropy factor. We shall comment on this in a little more detail in a later section (section 2.7) but we note meanwhile that whichever form of the temperature dependence of M_0 is subsequently ascertained to be valid cannot account for the observed variation of γ^S and β^S with concentration. γ^S is found to show a slightly asymmetric but otherwise smooth maximum at the critical concentration whereas in many cases β^S appears to exhibit a minimum which is nearly zero and sometimes negative! We sketch below a derivation of the magnetic contribution to the coefficient of the linear term in the specific heat of an alloy system which gives a plausible explanation of the maximum observed at the critical concentration in terms of the critical fluctuations of magnetization.

In the critical region and in the absence of any externally applied magnetic field

$$M_\nu \simeq 0 \quad ; \quad \nu = x, y, z$$

so that $\delta M \sim M$, where δM is the fluctuation in the magnetization. The probability, $P(\delta M)$, of such a fluctuation occurring is given by the usual Boltzmann factor $e^{-\frac{\Delta G}{k_B T}}$, where ΔG is the concomitant change in the thermodynamic potential. From equation (2.86)

$$\Delta G \equiv G - G_0 \simeq a (\delta M)^2$$

$$\therefore P(\delta M) = C e^{-\frac{a(\delta M)^2}{k_B T}}$$

where C is a normalising constant determined from the condition that

$$\int_{-\infty}^{\infty} P(\delta M)\, d(\delta M) = 1$$

giving $$C = \left(\frac{a}{\pi k_B T}\right)^{1/2} .$$

Therefore the mean square fluctuation, $\langle(\delta M)^2\rangle$, is given by

$$\langle(\delta M)^2\rangle = C\int_{-\infty}^{\infty}(\delta M)^2 P(\delta M)\, d(\delta M) = \frac{K_B T}{2a} \qquad 2.254$$

More concisely we may obtain the same expression by using the classical fluctuation theorem already stated (equation (2.199)). This gives immediately that

$$\langle(\delta M)^2\rangle = K_B T \chi^o$$

where χ^o is the initial susceptibility as given by equations (2.95) and (2.96). To obtain the contribution to the specific heat, ΔC^m_p, arising from such magnetization fluctuations near the critical concentration we first calculate the magnetic entropy S^m:

$$S^m \equiv -\frac{\partial}{\partial T}(\Delta G) = -\frac{1}{P_o^2}\frac{\partial a}{\partial T}\langle(\delta M)^2\rangle$$

since the term containing the temperature derivative of M is zero because $\frac{\partial G}{\partial M} = 0$. We now make the plausible assumption that a is a linear function of temperature say

$$a = \alpha_c (T_c - T) \qquad 2.255$$

as used in the Landau theory of the ferromagnetic transition at T_c. Such a temperature dependence has actually been experimentally observed for some Fe-Ni invars (238). Thus

$$\Delta C_p^m = T\left(\frac{\partial S^m}{\partial T}\right)_p = \frac{\alpha_c}{P_o^2} T \frac{\partial}{\partial T}\langle(\delta M)^2\rangle$$

i.e.

$$\Delta C_p^m = \frac{\alpha_c}{P_o^2} K_B \chi^o T \qquad 2.256$$

which shows that there is an extra contribution to the linear term in the specific heat which correlates with the initial susceptibility. It is therefore to be expected that the coefficient of the temperature linear term in the specific heat would peak asymmetrically at the critical concentration. We thus have an explanation of the observed maximum in γ^s i.e.

$$\gamma^s = \gamma_0^s + \frac{\alpha_c K_B \chi^0}{p_0^2} \qquad 2.257$$

- a problem that so far has not been suitably explained in any other way (318-320). We make the following remarks:-

(i) The simple discussion given above leaves out two important terms in the expansion of the thermodynamic potential - the quartic term, bM^4, and the term $\sim \delta(\Delta M)^2$. The latter term may be neglected if we consider only long wavelength fluctuations but the quartic term is important because it limits the amplitude of the magnetization fluctuations to

$$\langle(\delta M)^2\rangle_{c=c_f} \sim \left(\frac{K_B T}{b}\right)^{1/2} \qquad 2.258$$

instead of the apparent divergence suggested by equation (2.254). Also an exact solution for $\langle(\delta M)^2\rangle$ can be obtained when this quartic term is included but this is now in terms of the error function. It is not necessary to give here the messy details of the integration since some of the parameters needed for a numerical estimate have to be determined experimentally in which case equation (2.257)

will be adequate.

(ii) Since we know that clusters exist in the critical concentration we ought to consider their possible contribution to the specific heat. It is sufficiently well known that the upturn observed at low temperatures in the plot of C_p/T against T^2 for a number of alloy systems is due to the presence of clusters. A discussion of this is given in section 2.5(xi) but in anticipation of that we note that the specific heat of the clusters should be considered over two temperature regions - below T_{cg} (the cluster-glass temperature) and above T_{cg}. Below T_{cg} the specific heat of the cluster-glass is <u>linear in temperature and concentration-independent</u>. This rules out clusters as being responsible for the maximum in γ^s (see also reference 318). Above T_{cg} we, of course, have a random array of clusters and the dynamics and statics of individual spins <u>within</u> the clusters must be considered. A contribution to the temperature linear term in the specific heat has also been predicted by Hahn and Wohlfarth (321) as resulting from the anisotropy energy of the "superparamagnetic" clusters. Surely such a contribution can only be meaningfully discussed below T_{cg} and therefore can be included in the effective field distribution used to derive the linear temperature dependence of spin-glasses.

(iii) It would appear that the apparent minimum observed in the coefficient of the T^3 term is as a result of an improper procedure adopted in analysing the specific heat data. This point is also discussed in section 2.5(xi) but we can state quite simply here that there is no physical basis for the apparently large variation of the Debye

temperatures (obtained from the experimental values of β^s) within the narrow concentration ranges involved nor can there be any obvious meaningful interpretation of the negative values of β^s sometimes observed (322).

(iv) The effect of an applied magnetic field would be to reduce the fluctuations of magnetization and hence dimini γ^s slightly, as observed by Gupta et al (206) and also by Robbins et al (201). A magnetic field will also effectivel increase the cluster-glass temperature, Tcg, and hence extend the temperature range over which the cluster specific heat is linear in temperature. This point should be borne in mind when considering the suppression of the upturn in the C_p/T versus T^2 plot when a magnetic field is applied.

(v) It is known that at the ferromagnetic Curie point a correlation exists between the temperature derivatives of both the electrical resistivity and thermopower and the elec tronic heat capacity (313, 314, 323 - 325). Specifically for $T \sim Tc$

$$\frac{d\rho}{dT} = -\frac{dQ}{dT} = \frac{C_p^m}{eT} \quad ; \qquad 2.259$$

the correlation between these quantities obviously stems from the fact that near the transition point electrons are scattered by fluctuations of magnetization. We may expect a similar correlation between parameters that may be usefully and meaningfully defined at $T=\theta$ in the critical concentration region. It is therefore relevant that we have suggested a similarity in the concentration - dependence of the coefficients of the T^2 terms in the electrical resistivity and thermopower at low temperatures and the coefficient of the linear term in the specific heat. The similarity again

arises from the occurrence of critical fluctuations of magnetization at the critical concentration.

In concluding the discussion in this section we shall again emphasize that the magnetization fluctuations considered arise primarily from statistical concentration fluctuations but obviously these fluctuations can also be thermally dependent (e.g. because of the temperature dependence of the average projection of the cluster moments in a given direction).

2.5(x) Renormalization of sound velocity and ultrasonic absorption in the critical region

It has long been known that the dispersion and attenuation of sound can be very useful in studying both the statics and dynamics of cooperative (i.e. third-order) phase transitions. It is therefore relevant to consider similar effects in the critical concentration region for the onset of ferromagnetism. We shall discuss only the interaction between long wavelength acoustic phonon modes with the magnetization fluctuations that occur in the critical region. The interaction occurs via the magnetoelastic coupling and leads to a renormalization of both the sound velocity and the attenuation coefficient. Near c_f the magnetization fluctuations increase anomalously so that their effects on the sound velocity and attenuation are maximal. Specifically the sound velocity is decreased while the attenuation coefficient is increased. An excellent treatment of these effects has been given by Levanyuk (327) and by Young and Bienenstock (328). They considered essentially the expansion of the thermodynamic potential as given by equation (2.106) but in the absence of an applied field i.e.

$$G = G_0 + aM^2 + \delta(\nabla M)^2 - \frac{\gamma w}{\kappa} M^2 - \frac{w^2}{2\kappa} \qquad 2.260$$

in which the quartic term in M has been omitted but the term $\delta(\nabla M)^2$ included to allow for the spatial fluctuations of magnetization (see section 2.5(vi)). Equation (2.260) is then substituted into a general kinetic equation of motion to obtain the equation of motion of the spontaneous magnetization as

$$\Gamma^{-1}\frac{\partial M}{\partial t} + 2aM - 2\delta\nabla^2 M - \frac{2\gamma}{K}\omega M = f(r,t) \qquad 2.261$$

where f(r,t) is a random fluctuating force and Γ^{-1} is the kinetic coefficient. In addition to the above equation we also have the linearized equation of motion of longitudinal acoustic waves

$$\rho_0 K\frac{d^2\omega}{dt^2} + \nabla^2\omega + \gamma\nabla^2(M^2) = 0 \qquad 2.262$$

where ρ_0 is the density of the system. Equations (2.261) and (2.262) are two coupled equations for the spontaneous magnetization and the sound wave. In the low-frequency lon wave-length region the sound velocity V, and the attenuation coefficient, α_s, are obtained as (328)

$$V^2 \doteq V_0^2\left\{1 - \frac{9K_BT(\gamma/K)^2}{64\pi V_0^4\rho_0(\delta^3 a)^{1/2}}\right\} \qquad 2.263$$

$$\alpha_s = \frac{27K_BT(2\pi\nu)^2(\gamma/K)^2}{2048\,\Gamma V_0^6\rho_0\pi(\delta a)^{3/2}} \qquad 2.264$$

where ν is the frequency and $V_0 = \left(\frac{3}{2\rho_0 K}\right)^{\frac{1}{2}}$. In section 2.5(vi) it was derived that $a = \delta K_0^2$, where K_0 is the invers correlation range. In the critical concentration region $K_0 \sim |c-c_f|^{1/2}$ so that

$$(\delta^3 a)^{1/2} = \frac{a^2}{K_0^3} \sim |c-c_f|^{1/2}$$

and

$$(\delta a)^{3/2} = \left(\frac{a}{K_0}\right)^3 \sim |c-c_f|^{3/2}$$

Hence near the critical concentration both the attenuation coefficient and the decrease in the sound velocity attain their maximum values. Observe that

$$\alpha_s \sim \frac{\nu^2}{(c-c_f)^{3/2}} \sim \nu^2 (\chi^0)^{3/2} \qquad 2.265$$

which compares with a similar relationship near the ferromagnetic Curie point. However, the above formulae are not very suitable for order of magnitude estimates of either the reduction in the velocity of sound or of the attenuation coefficient since the value of δ is required. In order to to obtain a more readily usable equation we shall adopt the phenomenological approach of Belov et al (329,330) as used in their discussion of similar phenomena at the ferromagnetic Curie point. This approach also allows us to include the effect of an applied field. We shall go back to equation (2.106) which excludes the $\delta(\nabla M)^2$ term - justified since we shall restrict discussion to the long wavelength limit only. The equilibrium magnetization is given by equation (2.107) i.e

$$2(a + \gamma P) + 4b M^{*2} = \frac{B_o}{M^*}$$

(recall that $M^* = M(Bo, T, c, P)$; $M = M(Bo, T, c)$)

If P=o, then

$$2a + 4bM^2 = Bo/M \quad \text{(equation 2.92))} .$$

Suppose a varying hydrostatic stress $P \sim e^{i2\pi\nu t}$ is applied; this induces an alternating component of the magnetization

$$M_p(t) = M_p e^{i2\pi\nu t}$$

so that the total magnetization is

$$M^* = M + M_p(t) \quad ; \quad M >> M_p .$$

The equilibrium conditions are now determined by the kinetic equation

$$-\frac{\partial M}{\partial t} = \Gamma \frac{\partial G}{\partial M} \qquad 2.266$$

which, after suitable manipulation, is reduced to

$$-i2\pi\nu M_p \simeq \Gamma\left\{\frac{B_0}{M} + 8bM^2\right\}M_p + 2\gamma\Gamma PM \quad . \qquad 2.267$$

We recall, from equation (2.138), that

$$w = \gamma M^{*2} + \kappa P$$

$$\simeq \kappa P + 2\gamma M M_p + \gamma M^2 \qquad 2.268$$

The last term on the right hand side of equation (2.268) is the volume magnetostriction in the absence of an applied stress which has been earlier discussed (section 2.5(iv)). Thus the additional volume magnetostriction produced by the varying hydrostatic pressure is given by

$$w(P) = w - \gamma M^2$$

$$= \kappa P + 2\gamma M M_p \qquad 2.269$$

Substituting for Mp from equation (2.267) gives

$$\frac{w(P)}{P} = \kappa + \frac{4\Gamma^2\gamma^2M^2\left(\frac{B_0}{M} + 8bM^2\right) - i4(2\pi\nu)\Gamma\gamma^2M^2}{\Gamma^2\left(B_0/M + 8bM^2\right) + (2\pi\nu)^2} \; . \qquad 2.270$$

Define a relaxation time τ as

$$\tau^{-1} = \Gamma\left(\frac{B_0}{M} + 8bM^2\right) \qquad 2.271$$

then

$$\frac{w(P)}{P} = \kappa + \frac{4\Gamma\gamma^2M^2\tau\{1 - i2\pi\nu\tau\}}{1 + (2\pi\nu\tau)^2} \qquad 2.272$$

Thus near the critical concentration we obtain for the compressibility, κ_c, and the logarithmic decrement, δ_c, the following expressions:

$$\kappa_c = \kappa\left\{1 + \frac{\Delta\kappa/\kappa}{1+(2\pi\nu\tau)^2}\right\} \qquad 2.273$$

$$\delta_c = \frac{\pi(2\pi\nu\tau)\,\frac{\Delta\kappa}{\kappa}}{1+(2\pi\nu\tau)^2} \qquad 2.274$$

where

$$\Delta\kappa = \frac{4\gamma^2 M^2}{B_0/M + 8bM^2} \qquad 2.275$$

In the absence of a magnetic field ($M \longrightarrow M_0$) and also in the static limit ($\nu \sim 0$)

$$\Delta\kappa = \frac{\gamma^2}{2b} \qquad 2.276$$

Thus in going through the critical concentration the fractional <u>increase</u> in the static compressibility is

$$\frac{\Delta\kappa}{\kappa} = \frac{\gamma^2}{2b\kappa} \qquad 2.277$$

which, as shown, is determined essentially by the square of the magnetoelastic coupling coefficient and the slope of the Belov-Arrott plots. Substituting for b from equation (2.99) gives

$$\frac{\Delta\kappa}{\kappa} = \frac{4\gamma^2 M_{00}^2 \chi_f^0}{\kappa} \qquad 2.278$$

This equation resembles that which may be obtained from Döring's formula (331) for the anomaly in the elastic modulus

of Fe-Ni invars, namely

$$\frac{\Delta E}{E^2} = -\tfrac{1}{9}\frac{\left(\frac{\partial \omega}{\partial B_0}\right)^2}{\frac{\partial M}{\partial B_0}} \qquad 2.279$$

where $\left(\frac{\partial \omega}{\partial B_0}\right)$ is the forced volume magnetostriction, E is Young's modulus and $\left(\frac{\partial M}{\partial B_0}\right)$ is stated to be the high field susceptibility. For alloys near the critical concentration

$$\frac{\partial \omega}{\partial B_0} = 2\gamma M_0 \chi_f^0 \qquad \text{(equation (2.136))}$$

and if we substitute the initial susceptibility for $\left(\frac{\partial M}{\partial B_0}\right)$ equation (2.279) becomes

$$\frac{\Delta E}{E^2} = -\frac{4}{9}\gamma^2 M_0^2 \chi_f^0 \qquad 2.280$$

as has been obtained by Wohlfarth (332) (though χ_f^0 is still referred to as the high-field susceptibility). A comparison of equations (2.278) and (2.280) shows that

$$\frac{\Delta E}{E^2} = -\frac{1}{9}\Delta\kappa = \frac{1}{9}\frac{\Delta B}{B^2} \qquad 2.281$$

where $B=\kappa^{-1}$ in the bulk modulus.

Equation (2.277) predicts a step jump (of $\Delta\kappa$) in the value of the compressibility at the critical concentration. Such a discontinuity is of course implicit in the mean field approximation used here. In practice the increase will be smaller than the predicted value and probably spread out over a finite concentration range. To obtain an idea of the magnitude of this relative increase in the compressibility

let us consider the Pt Ni system for which the values of the relevant parameters have been measured (256, 333, 334). For Pt 42.9% Ni (which is about 1% above the critical concentration)

$$\gamma = 3.6 \times 10^{-6} \text{ (g/emu)}^2 \quad (256, 333)$$

M_{oo} = 1.32 emu/g and $\chi_f^o = 30.6 \times 10^{-5}$ emu/g (333).

Using $\kappa_{Ni} = 0.538 \times 10^{-12}$ cm^2/dyne and $\kappa_{Pt} = 0.359 \times 10^{-12}$ cm^2/dyne we interpolate to obtain $\kappa_{alloy} = 0.45 \times 10^{-12}$ cm^2/dyne.

Thus from eq.(2.278) $\frac{\Delta\kappa}{\kappa} = 6.1\% = -\frac{\Delta B}{B}$.

The values of M_{oo} (= 2.072 emu/g) and χ_f (=14.5 $\times 10^{-5}$ emu/g) given by Alberts et al. (334) give a similar value of $\frac{\Delta\kappa}{\kappa}$ ($\simeq$ 7.2%).

Since $E = \frac{9BG}{3B+G}$, where G here is the shear modulus it is easy to show that for a Poisson's ratio of $\frac{1}{3}$

$$\frac{\Delta E}{E} = \frac{1}{9}\frac{\Delta B}{B} + \frac{8}{9}\frac{\Delta G}{G} \qquad 2.282$$

so that a fractional change of 6% in the bulk modulus can only lead to a 0.7% change in Young's modulus. Since in the critical region no large changes in the bonding of electrons is envisaged only a small change, if at all, in the shear modulus can occur. Thus the onset of ferromagnetism is not expected to cause any large changes in Young's modulus.

Similarly for Ni_3Al (333)

$\gamma = 0.47 \times 10^{-6}$ (g/emu)^2 (from pressure experiments)

$M_{oo} = 6.58$ emu/g

$\chi_f^o = 5.7 \times 10^{-5}$ emu/g

and $\kappa = 0.42 \times 10^{-12}$ cm/dyne,

giving $\frac{\Delta K}{K} = 0.52\%$ and $\frac{\Delta E}{E} \sim 0.06\%$.

These small relative changes in either the compressibility of Young's modulus are in reasonable agreement with the observed values (see note added in proof in reference 320).

For measurements at non-zero frequencies relaxation effects must be taken into account. For $B_0 = 0$ the relaxation time is given by

$$\tau = \frac{1}{8b\Gamma M_{00}^2} \equiv \frac{1}{4\alpha_0\Gamma(c-c_f)} \quad ; \quad c > c_f \qquad 2.283a$$

$$= \infty \quad ; \quad c \leq c_f \qquad 2.283b$$

So as $c \rightarrow c_f$, $K_c \rightarrow K$ because of the increasing relaxation time. This effect leads to some spreading out of the predicted increase in K. From eq.(2.274) it is easy to show that the internal friction is maximum when

$$2\pi\nu\tau = 1 \quad . \qquad 2.284$$

This will occur at a concentration c* given by

$$c^* = c_f + \frac{2\pi\nu}{4\alpha_0\Gamma} \qquad 2.285$$

using equations (2.283a) and (2.284).

Next we consider the influence of a magnetic field on the compressibility and the internal friction. Near the critical concentration.

$$M_0 \sim \left(\frac{B_0}{4b}\right)^{1/3} .$$

Thus from equation (2.275),

$$\Delta K = \frac{\gamma^2}{3b} \qquad 2.286$$

which is independent of the field in the static limit. Observe though that the fractional increase in the compressibility is reduced by 16.7%.

At a finite frequency ν we may still take $M \sim B_0^{\frac{1}{3}}$, so that

$$\tau \simeq \frac{B_0^{-2/3}}{(108\, b)^{1/3}\, \Gamma} \qquad 2.287$$

and

$$(\kappa_c - \kappa)^{-1} \simeq \frac{3b}{\gamma^2}\left\{1 + \left(\frac{2\pi\nu}{\Gamma}\right)^2 \frac{B_0^{-4/3}}{(108\, b)^{2/3}}\right\} . \qquad 2.288$$

From equations (2.271), (2.274) and (2.275) we see that near the critical concentration an applied magnetic field decreases the relaxation time and hence increases the frequency for which maximum sound absorption occurs. Thus the concentration c* for which this maximum occurs (eq. (2.285)) is further increased beyond the critical concentration. Also the applied field reduces the magnitude of the sound absorption (eq. (2.274)).

In conclusion we note that it is not necessary to consider the temperature dependence of $\Delta\kappa$ simply because the derivation is strictly valid at T = 0 only. However, on the model of itinerant ferromagnetism $\Delta\kappa$ is temperature independent because if at a finite temperature we write

$$\Delta\kappa \simeq 4\gamma M_0^2 \chi_f^0(T)$$

then M_0^2 is given by eq.(2.161) while

$$\chi_f^0(T) = \chi_f^0(0)\left\{1 - \frac{T^2}{T_c^2}\right\}^{-1} \qquad 2.289$$

so that the product $M_0^2 \chi_f^0(T)$ remains independent of temperature.

2.5(xi) The specific heat of magnetic clusters and the " ΔG effect"

In a previous subsection (2.5(ix)) we attempted to explain why the coefficient of the temperature linear term in the specific heat of an alloy should attain a maximum at the critical concentration, an experimental observation which had hitherto not been properly accounted for especially with respect to the large values obtained. In this section we shall be primarily concerned with another effect that is observed in the specific heat of alloys within the critical concentration region. This refers to an upturn in the plot of $\frac{C_v}{T}$ against T^2 at sufficiently low temperatures as seen in the data for V Fe (335), Ti Fe (336), Cu Ni (206), Rh Ni (337), Pd Ni (42), Pd Fe (125), etc and even in the intermetallic compounds Ni_3Al and Ni_3Ga (318).

We recall that for a normal metal such a plot should give a straight line from which γ^s and β^s may be deduced. From this point of view the observed upturn was anomalous. An initial explanation of this effect was advanced in terms of the electron - paramagnon interaction. This interaction, which has been discussed earlier on (see sections 1.10 and 2.2), was thought to lead to an enhancement of the electronic specific heat through the renormalization of the d-electron mass and also to contribute a term, $\sim T^3 \ln \frac{T}{T_{sf}}$, to the lattice term (eq.(1.54)). It was this term that was supposed to give an upturn in the curve of $\frac{C_v}{T}$ versus T^2 at low temperatures - see figure 2.6. Consequently the rather pronounced anomalies in the specific heat data of Cu Ni (206) and Rh Ni (337) were cited as supporting evidence for the theory

of electron - paramagnon interactions. However no anomaly has yet been reported for both pure Pd and Pt or for some of their alloys in which exchange enhancement effects are expected to be pronounced. On the other hand the upturn observed for a TiFe sample (336) was explained in terms of magnetic clusters, the specific heat data between 1.4 and 4K being shown to fit an expression of the form

$$C_v = A + \gamma^S T + \beta^S T^3 \qquad 2.290$$

where A is a temperature independent parameter attributed to the presence of the magnetic clusters. Equation (2.290) has since been used in the attempt to explain the observed anomalies in VFe (338), CuNi (201, 338) and RhNi (321) alloys. In the latter two cases it was shown that the cluster model gave a more consistent description of the experimental data than the paramagnon model. It is not our intention to weigh the pros and cons of both the cluster and paramagnon models for the simple reason that it is not necessary to do so. Paramagnons, as the quasi-particles of localized spin fluctuations, and magnetic clusters both occur within a given alloy system but their effects are predominant in different concentration regions. Paramagnon effects are dominant in the dilute impurity region ($\lesssim 0.1$ at.%); we have already suggested a "renormalization" of the existing paramagnon theories so as to reflect the proposed clearer physical explanation of their origin and to bring the theories into better quantitative accord with experiment,

especially as regards the d-electron mass renormalization and the specific heat anomaly currently under discussion. However, in the critical concentration region where a transition from a non-magnetic to a ferromagnetic state occurs it has been shown that magnetic clusters necessarily exist and it is therefore logical that the physical properties of alloys in this region be greatly influenced by the presence of these clusters. It is pertinent to mention that a number of experiments have been carried out in the attempt to establish whether paramagnons or clusters are responsible for the specific heat anomaly. The experiments were of three types namely (i) effect of an applied magnetic field:- A sufficiently large magnetic field will clearly freeze out contributions to the specific heat due to either paramagnons or clusters, so that it is only the magnitude of the field necessary to produce observable effects that is important. It was estimated (339) that magnetic fields less than about 10T(= 100 KG) should not freeze out the paramagnon contribution so that any effects observed for much lower fields would have to be attributed to the presence of clusters. Measurements in applied magnetic fields have been carried out on some Cu Ni (201, 206), V-Fe (340), RhNi (341) and Ni_3Ga (342) alloys. In these cases the experimental results appeared to favour the cluster model although for Ni_3Ga alloys the authors (342) felt that the evidence was inconclusive. (ii) measurements of the specific heat down to sufficiently low temperatures:- as explained below the upturn in the C/T vs T^2 plots at low temperatures is actually the rising portion of a Schottky

function. It was thought that by extending the measurements to very low temperatures it would be possible to map out the peak of the Schottky function. Such measurements have been made on V Fe (343) Ni_3Ga (318) ond Cu Ni; the data were approximately fitted by Einstein functions but for Ni_3Ga a peak resembling that for o Schottky function wos clearly observed. (iii) Effects of cold work and heat treatment: such experiments will only be useful in systems where atomic clustering or short range order is known to occur, os in Cu Ni, because these processes will affect the size and number of the mognetic clusters. In such cases onnealing moy increose the susceptibility of the system without increasing the number of clusters so that the cluster specific heat will be unchonged; on the other hand plastic deformation, by breaking up the magnetic clusters into smoller entities, will increose the cluster specific heat but decrease the averoge magnetic moment (345). The results of the experiments carried out on CuNi (201, 345) unequivocally fovour the cluster model. Thus, on balance, the experimentol evidence is in favour of the cluster model. However, irrespective of these, our earlier conclusion remoins valid, i.e. in the critical concentration region magnetic clusters exist ond probably dominote the mognetic and other physical properties of the system. We shall now proceed to consider the form of the specific heat of these mognetic clusters; in doing this we shall bear in mind thot the clusters will interoct magnetically. Very close to c_f the interoction is presumably through the overlop of the "polorization clouds" based on the cluster units ond this overlap is necessarily ferromognetic os

otherwise it would not occur at all. Below the critical concentration a possible coupling mechanism between the clusters is clearly the RKKY interaction. This interaction will lead to the formation of a cluster glass at a characteristic temperature, T_{cg}. Another characteristic temperature exists but this refers to intra-cluster interactions. If B_a is the effective anisotropic magnetic induction acting on the net spin of a cluster then we can define a temperature T_a given by

$$K_B T_a = g \mu_B B_a \qquad 2.291$$

At the moment it seems that the effective anisotropy field can only result from magnetostatic interactions (true dipole-dipole and pseudodipolar interactions). It is not possible to know, a priori, which of T_{cg} and T_a is greater. T_{cg} can, of course, be easily determined by the now well known procedure of measuring the temperature-dependence of the initial susceptibility. For simplicity we shall consider the case where $T_{cg} > T_a$, although the cases $T_{cg} \sim T_a$ and $T_{cg} \ll T_a$ are equally interesting. Needless to say, B_a is not the effective internal molecular field which would characterize the intracluster exchange energy. It is presumed that the clusters remain stable up to fairly high temperatures (much larger than both T_{cg} and T_a). Also the two temperatures T_{cg} and T_a are not related (at least there is no obvious relation). This is in contrast to the two characteristic temperatures (ta, T_a) introduced by Hahn and Wohlfarth (321) because $St_a = T_a$, S being the net cluster spin.

Consider the temperature range $T > T_{cg}$. The specific heat of a magnetic cluster is as a result of the fact that the

cluster spin has a preferred orientation determined by the magnetic anisotropy and so can undergo thermal excitations from the easy direction of magnetization. As already mentioned, in the case of uniaxial anisotropy the anisotropy can be replaced by an effective field B_a. We can then consider the motion of the magnetic clusters, each of spin S say, in this effective field. Under these circumstances the clusters are equivalent to a system of harmonic oscillators whose energies are quantized. The energy of a cluster, $\mathcal{E}_{cl}$, is given by

$$\mathcal{E}_{cl} = \mathcal{E}_o + g\mu_B m B_a \qquad 2.292$$

where $\mathcal{E}_o$ is the ground state energy and $0 \leq m \leq 2S$.

The average energy of a cluster is therefore given by

$$\bar{\mathcal{E}}(T) = \frac{1}{Z} \sum_{m=0}^{2S} \{\mathcal{E}_o + g\mu_B m B_a\} e^{-\mathcal{E}_{cl}/K_B T}$$

where the partition function

$$Z = \sum_{m=0}^{2S} e^{-\mathcal{E}_{cl}/K_B T}$$

On working at the algebra in the usual way we find that for $S \longrightarrow \infty$

$$\bar{\mathcal{E}}(T) \longrightarrow \mathcal{E}_o + \frac{K_B T x}{1 - e^{-x}} \qquad 2.293$$

where $x = \frac{Ta}{T}$. Hence the specific heat per cluster in this limit is

$$C_V^{cl} = \frac{\partial \bar{\mathcal{E}}(T)}{\partial T} = \frac{K_B x^2 e^x}{(e^x - 1)^2} \equiv K_B E(x) \qquad 2.294$$

where E(x) is called the Einstein function (and Ta the Einstein temperature). At sufficiently high temperatures $(T_a \ll T)$ $E(x) \longrightarrow 1$ so that $C_V^{cl} \longrightarrow K_B$.

If the atomic concentration of such clusters is c* then the contribution of the clusters to the specific heat of alloy is $c^* C_V^{cl}$. Thus the parameter A in equation (2.290) is given by

$$A = c^* C_V^{cl} \qquad 2.295$$

Thus for an infinitely large cluster spin

$$C_V = c^* K_B E(x) + \gamma^S T + \beta^S T^3 \qquad 2.296$$

which, in the limit $T_a << T$, reduces to

$$C_V = c^* K_B + \gamma^S T + \beta^S T^3 \qquad 2.297$$

This latter form may be used to <u>estimate</u> c*.

However, in the case of a <u>finite</u> spin the cluster specific heat has been obtained (318,346) as the Schottky-type function

$$C_V^{cl} = K_B \left[E(x) - E(\{2S+1\}x) \right] \qquad 2.298$$

which is sketched in figure 2.23 below for S = 2.5

<u>Fig.2.23</u>: Sketch of C_V^a/T versus T^2. T is in units of T_a. (from ref.318).

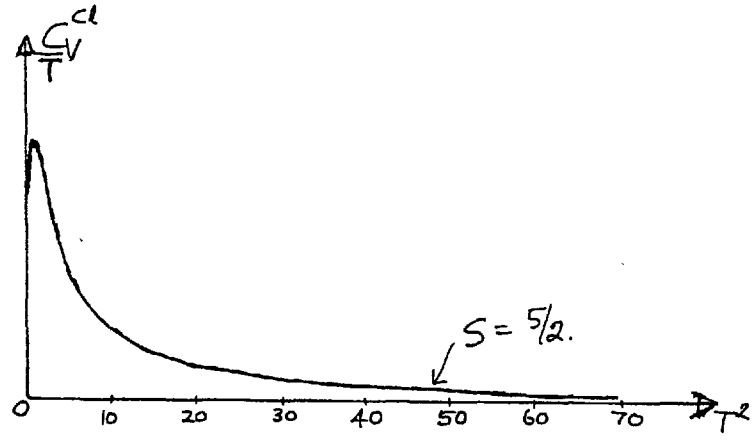

It is apparent from the above diagram that the anomalous upturn observed is in reality the rising portion of a Schottky anomaly peak. Also from equation (2.298) one can deduce that a "constant" cluster specific heat is observable only for

$$T_a << T << (2S+1)T_a \qquad 2.299$$

So that to obtain an approximately constant cluster specific heat over a decade of temperature a very large cluster spin is required. This point should be borne in mind when considering PtNi alloys where in the critical concentration region the specific heat data (347) apparently do not show up the existence of clusters in the expected manner. Falge and Wolcott (346) have been able to show that a Schottky function for the cluster specific gives a better fit to their specific heat data for some CuNi and CuNi Fe specimens than either an Einstein function or a constant term.

It should be noted that the above derivation is approximate in the sense that in a real situation one may expect a distribution of spins and effective anisotropy fields. For example Acker and Huguenin (220) estimate that in CuNi about 90% of the clusters have a small moment varying from $8\mu_B$ in Cu 40% Ni to about $12\mu_B$ in Cu 50% Ni. The remaining 10% of the clusters have much larger moments lying between 40 and 220 μ_B. However both S and Ta should be taken to refer to the most probable cluster size which in CuNi would refer to the clusters with moments of about $8\mu_B$.

Below the cluster-glass temperature Tcg the cluster specific heat is determined by the inter-cluster interactions which are presumed to be of the RKKY form. One now has to consider the probable distribution of the molecular fields acting on the cluster units. The normalized probability density distribution, P(Bi), of the molecular fields, Bi, has been considered in an Ising model by Marshall (348), Klein and Brout (349) and Klein (350). A readable and concise description of these calculations is given in reference 26 (pp 483 - 487).

P(Bi) is approximately Lorentzian (199) but exhibits a shallow minimum at Bi = 0. The important result, however, is that in this temperature range ($T < T_{cg}$) the cluster specific heat is linear in temperature and concentration - independent. Souletie and Tournier (352) have extended the argument to a three-dimensional model and shown that in general

$$c^* P(B_i, T, B_o) = f\left(\frac{B_i}{c^*}, \frac{T}{c^*}, \frac{B_o}{c^*}\right) \qquad 2.300$$

and hence that

$$C_V^{cl} = F\left(\frac{T}{c^*}, \frac{B_o}{c^*}\right) \qquad 2.301$$

where f, F are universal functions independent of the cluster concentration. From the Marshall-Klein theories

$$F\left(\frac{T}{c^*}\right) \sim T/c^*$$

so that the specific heat of the clusters is

$$c^* C_V^{cl} = \gamma_{cg} T \qquad 2.302$$

where γ_{cg} is concentration-independent. Physically the contribution of each cluster unit to the specific heat is a Schottky function (with a characteristic temperature $T_a = \frac{g\mu_B B_i}{k_B}$) but averaging over the values of Bi gives a linear temperature dependence. This implies that γ_{cg} can be obtained by averaging equation (2.298) over fields $0 \leq B_i \leq \frac{k_B T_{cg}}{g\mu_B}$. This has been done by de Dood and de Chatel (318) who obtained

$$\gamma_{cg} = \frac{\pi^2 k_B}{3 t_{cg}} \frac{2S}{2S+1} \qquad 2.303$$

where $T_{cg} = c^* t_{cg}$.

From the foregoing the cluster specific heat is expected to vary with temperature as sketched in figure 2.24. Below Tcg

it is linear in T while above Tcg it varies like the Schottky function.

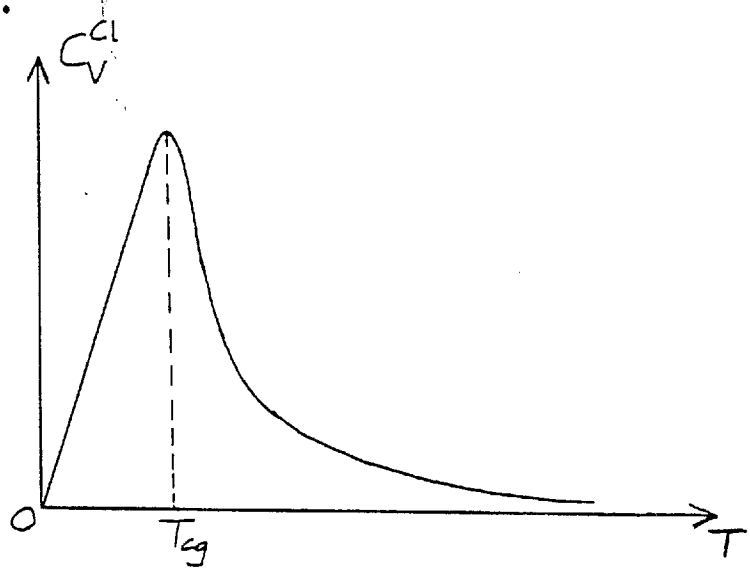

Fig.2.24: Temperature dependence of C_V^{cl}

We should note the following two observations:- (i) the concentration dependence of the number of magnetic clusters:- Most analyses of the specific heat data of alloys in the critical concentration region have made use of equation (2.297) in which the parameter A is temperature-independent and hence directly proportional to the number of magnetic clusters. The resulting values of A show a strong concentration dependence attaining a maximum value at an impurity concentration that is lower than the true critical concentration given by the concentration at which the coefficient of the temperature linear term peaks. The maximum in the value of A is clearly shown in the data for CuNi (201,353), VFe (343,353), $(CuNi)_{90}$ Al_{10} and $(VFe)_{90}$ Al_{10} (353). The concentration at which A peaks ($\sim$ 43%Ni in CuNi) has usually been assumed to be the critical concentration. Consequently for CuNi there arose the problem of explaining why in the "ferromagnetic region" ($>$ 43% Ni) the number of clusters, C_{nd}^{*}, determined by diffuse neutron diffraction experiments (204) is greater than the

number obtained from the cluster specific heat, C^*_{sh} ; also it was necessary to explain why $C^*_{sh} \rightarrow 0$ at the critical concentration. An ingenious explanation (354) was that the cluster specific heat parameter is a measure of the number of "thermally excitable" magnetic clusters i.e. the "uncoupled" clusters, while neutron diffraction measurements sample those clusters which are ferromagnetically coupled. This explanation is, of course, unacceptable. The determination of c* by fitting equation (2.297) to specific heat data is improper for the reasons already given. The cluster specific heat should be fitted to a Schottky function (equation (2.298) for $T > T_{cg}$ in order to obtain c*. Extracting the cluster specific heat is, unfortunately, a difficult problem because it requires a precise knowledge of both the true electronic and lattice contributions. As discussed shortly below the latter contribution can only be correctly obtained from elastic moduli constants for the alloy at low temperatures as done by Falge and Wolcott (346). However, their values of c* do not, as expected, show any strong concentration dependence. On the other hand, c^*_{nd} tends to zero at the critical concentration simply because the spontaneous magnetization is used in conjunction with the neutron data to obtain it. The spontaneous magnetization clearly vanishes at the critical concentration but the total magnetic moment of the clusters, which may only be obtained at very low temperatures and high fields, decreases smoothly across c_f. The paramagnetic susceptibility measurements of Kouvel and Comly (202) confirm the expected smooth variation of the number of magnetic clusters across the critical

region. In conclusion we shall state quite categorically that the reported strong concentration dependence of the number of magnetic clusters is unreal being an artifact of the improper analysis of either the specific heat or neutron diffraction data. In fact it would appear that the only correct method of obtaining C^* is through magnetic measurements — determination of the saturation magnetization at low temperatures and high fields (if at all feasible, because of the formation of a cluster-glass) and of the slope of the Curie-Weiss plot at sufficiently high temperatures. We shall have more to say on the neutron diffraction data in a later chapter.

(ii) The second observation refers to the upturn observed in the plots of $\frac{C_V}{T}$ against T^2 for some intermetallic compounds. Castaing et al (355) have reported that in the $V_{1-c}Cr_cB_2$ metallic compounds antiferromagnetic ordering is observed for $c > 77\%$ but no long-range magnetic ordering occurs for lower concentrations. The coefficient of the temperature linear term in the specific heat, γ^s, also peaks at this critical concentration, but the peak was explained in terms of "quasi-particle dressing with spin fluctuations". More interestingly in the non-magnetic compounds an upturn was observed in the specific heat data plotted in the usual way. Similar observations had been reported earlier for the $Mo_{1-c}Cr_cB_2$ series (356). The peaking of γ^s at the critical concentration for the onset of long range magnetic order is, of course, not surprising. We have shown that this is related to the critical fluctuations of the order parameter. Thus in MoCr γ^s attains its maximum value at 76% Cr

where a transition into the SDW state occurs (191, 192). A maximum in γ^s at about 19% Fe is seen in the specific heat data of Cheng et al (335) for CrFe and would have to be appropriately interpreted, the existence of "super-paramagnetic clusters" (357) notwithstanding. On the other hand an upturn is observed in the $\frac{C_v}{T}$ versus T^2 plots of the specific heat of Ni_3Al and Ni_3Ga (318) and these have been shown to be due to the existence of clusters. A peak in γ^s is also observed for these alloys. It would therefore appear that the specific heat data of the $V_{1-c}Cr_cB_2$ compounds can be consistently interpreted in terms of magnetic clusters. We shall not, however, pursue this matter any further here.

Lastly we shall consider the anomalous concentration-dependence of β^s, the coefficient of the T^3 term in the specific heat. Values of β^s deduced by simply fitting the experimental data to equation (2.290) tend, almost linearly, to a deep minimum at the critical concentration and in a few cases such as CrNi (322), VNi (358), CrFe (335), RhNi (321) negative values of β^s are actually obtained. Now in the Debye theory of the lattice specific heat β^s is related to the Debye temperature, θ_D, as in equation (2.157) i.e.

$$\beta^s = \frac{12\pi^4 N K_B}{5\theta_D^3} \qquad 2.304a$$

$$\equiv \frac{1943.74}{\theta_D^3}\ J\,mole^{-1}\,K^{-4} \qquad 2.304b$$

Figure 2.25 shows the variation of θ_D with concentration for a number of Ni alloys. An estimate of θ_D may also be made

FIG.2.25: CONCENTRATION DEPENDENCE OF θ_D (SPECIFIC HEAT) FOR SOME Ni ALLOYS

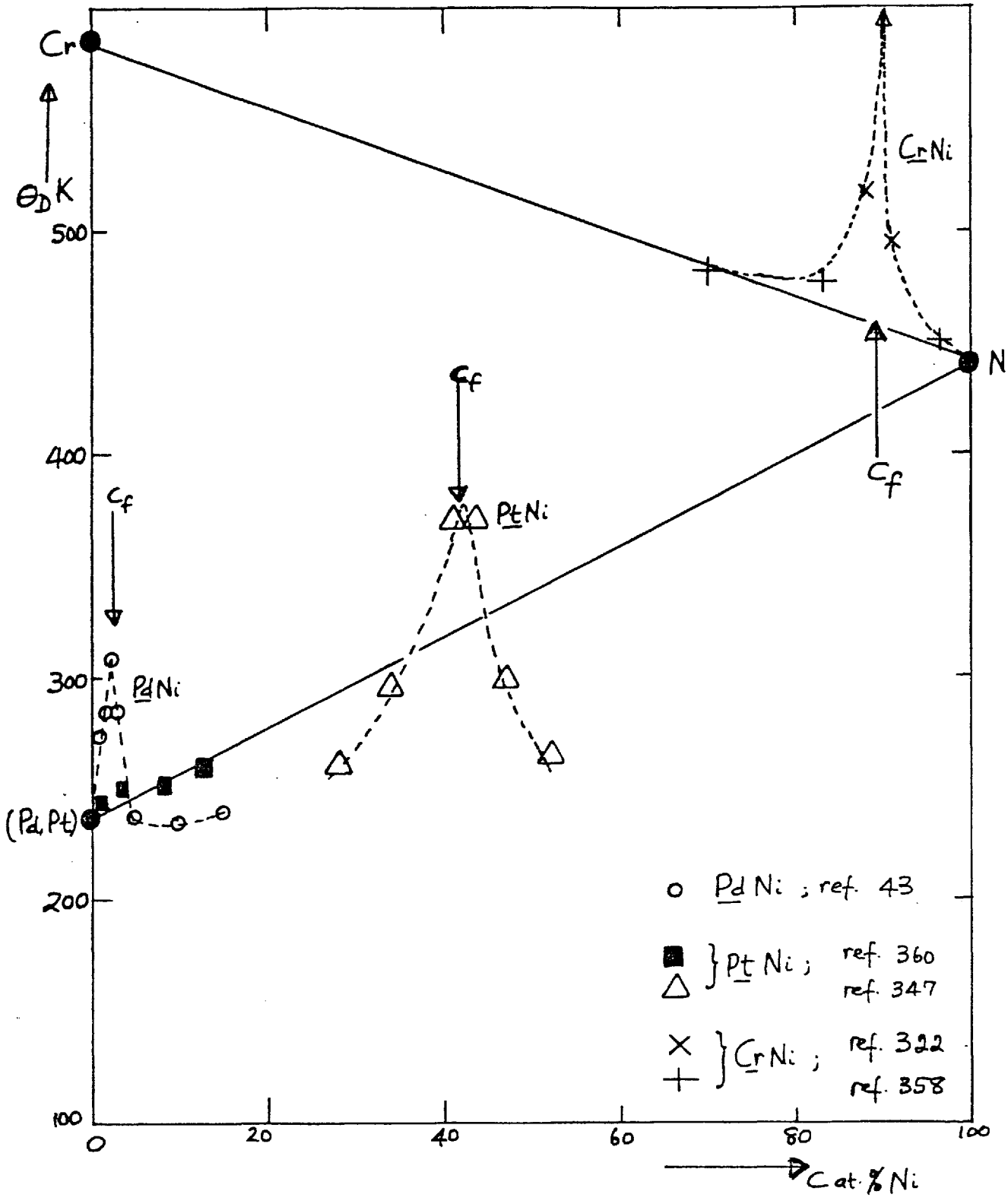

from a knowledge of the elastic constants. We have

$$\theta_D(\text{elastic}) = \frac{h}{K_B}\left(\frac{3}{4\pi\Omega_0}\right)^{1/3} v_m \qquad 2.305$$

where h is Planck's constant, Ω_0 is the atomic volume and v_m is the mean velocity of acoustic phonons. If v_l and v_t are respectively the longitudinal and transverse accoustic phonon velocities then

$$\frac{3}{v_m^3} = \frac{2}{v_t^3} + \frac{1}{v_t^3} \simeq \frac{9}{4v_t^3}$$

since usually $v_l \simeq 2v_t$.

Thus $$v_m \simeq 1.1 v_t \equiv 1.1 \left\{\frac{G}{\rho_0}\right\}^{1/2}$$

and $$\theta_D(\text{elastic}) \simeq 1.1 \frac{h}{K_B}\left(\frac{3}{4\pi\Omega_0}\right)^{1/3}\left\{\frac{G}{\rho_0}\right\}^{1/2}. \qquad 2.306$$

Usually θ_D(elastic) $\simeq \theta_D$(low temperature specific heat) to within 1%. It therefore follows that an anomalous variation of β^S implies an equally anomalous variation of θ_D which, in turn, implies rather large changes in the shear modulus. Such a large change in the shear modulus would reflect a large change in the bonding of the alloy system and, in particular, the apparently large increase in the value of G at the critical concentration would mean a marked weakening of the next nearest neighbour bonding (359). In the PdNi system (with c_f=2.8%Ni) the anomalous peaking of θ_D in such a narrow concentration range is surely unjustifiable especially as Pd and Ni are isoelectronic. The situation is even less satisfactory for PdFe ($c_f \simeq$ 0.1%F Moreover as Gregory and Moody (358) have clearly pointed out the negative values of β^S that have been obtained for some systems can hardly be associated with the lattice specific heat. In the preceding subsection (2.5(x)) we showed that at the critical concentration there should be

some reduction in the velocity of sound. Although the analysis applies strictly to the longitudinal velocity V_L we can take it as giving an order of magnitude estimate of the corresponding change (if any) in the transverse velocity especially for a polycrystalline solid which may be regarded as elastically isotropic. Thus for Ni_3Al the fractional decrease in the value of $G \sim 0.5\%$ while for Pt Ni the maximum change $\sim 7\%$. The apparent change observed for most alloys is often greater than 50% (see fig. 2.25) so that it became necessary to find other explanations. For Pd Ni alloys Chouteau et al. (43) argued that the observed reduction in β^S was in accord with the predictions of the localized exchange enhancement model in the theory of paramagnons (eq. (1.54)), provided a spin fluctuation temperature of more than 20K was accepted. This explanation was however advanced before the neutron diffraction experiments of Aldred et al. (128) confirmed the existence of magnetic clusters. On the other hand, the similar variation observed for Pt Ni (347) has been interpreted by Wohlfarth (32) as being a real effect i.e. that the shear modulus, G, of PtNi alloys actually increases by over 50% in the critical concentration region - hence the so-called "ΔG effect" by analogy with the well-known anomaly that occurs, as a function of temperature, in FeNi and FePt invars. Wohlfarth's proposal stems from the observations that (i) the magnetic and other properties of the Pt Ni system appear to be well-explained in terms of the model of weak itinerant ferromagnetism (334); and (ii) no upturn was observed in the $\frac{C_V}{T}$ versus T^2 plots of the specific heat (347). Both observations are in error. There is no a priori reason why the on set of ferromagnetism in PtNi alloys should be basically different from that in all other alloy systems where the

ferromagnetic state sets in directly from the non-magnetic state. We have been at great pains to explain why this transition is unavoidably inhomogeneous. We must therefore conclude that magnetic clusters exist in the PtNi system at least within the critical region. In this respect it is of interest to note that both Alberts et al. (334) and Kortekaas (333) report clustering effects in the "low-field" ($\sim$ 25KG!) magnetization data. It is also significant that despite its apparent "exchange enhancement" the critical concentrations for the onset of ferromagnetism in PtNi and CuNi are similar ($\simeq$ 42% and 47.6% Ni respectively). The rather large value for PtNi is probably due to the intrinsic antiferromagnetism of pure Pt as mentioned earlier (section 2.2). The apparent absence of an upturn in the $\frac{C_v}{T}$ versus T^2 plot of the specific heat of the PtNi is not conclusively indicative of the absence of magnetic clusters. In the PdNi system where neutron diffraction (128) has clearly shown the existence of magnetic clusters the specific heat data do not convincingly show them up. Schindler and Mackliet (42) had to really convince themselves that a slight upturn near 1.15 K in the specific heat data for Pd 1.95% Ni was a real effect. An even smaller anomaly was also reported for the 1.66% Ni alloy. Also a small anomaly occurs in the data of Fawcett et al. (381) for Pd 1.89% Ni. However, Chouteau et al. (43) did not observe any anomalies whatsoever between 0.3 K and 3 K and for concentrations up to 10% Ni. So which experimental probe is right - neutron diffraction or specific heat measurements? The clue to the answer lies in the observation by Chouteau et al. (43) that Pd 2% Ni was ferromagnetic! with $T_c \gtrsim 4$ K. Since, as shown below (section 2.6), $c_f = 2.8\%$ Ni it is not unlikely that the failure to observe the

expected specific heat anomaly is connected with the formation of a cluster-glass. Presumably $T_{cg} \geq 4$ K for Pd 2% Ni. Below T_{cg} the cluster specific heat is linear in temperature and so only adds to the value of γ^s . Thus we can suggest that the absence of the expected anomaly in the specific heat data of both PdNi and PtNi is due to the fact that a cluster-glass already exists in the temperature range of measurement.

There is, of course, no reason why the anomalous variation of Θ_D at c_f in PdNi and PtNi systems should be explained individually and differently while similar anomalies, also at c_f, in CuNi, CrNi, PdFe etc are generally ignored. It is thought that the anomaly in all these systems have a common origin which derives from the presence of the magnetic clusters. The apparent Θ_D anomaly arises from the fact that in determining β^s no proper correction is made for the cluster specific heat. In some analyses no correction has been made at all while in others equation (2.290) has been used. We have already explained that an Einstein function (which gives a constant term at high temperatures) is not an appropriate representation for the cluster specific heat; a Schottky function is better but only for $T_{cg} \ll T$. However, the parameters needed for the Schottky function fit cannot be obtained independently without knowing the value of Θ_D . The conclusion therefore is that specific heat data are not very useful for obtaining the Debye temperatures of alloys whose compositions lie within the critical region for the onset of ferromagnetism. A better idea would be to assume that β^s (or Θ_D) varies smoothly (or nearly so) with concentration and hence to use the data to obtain the actual concentration of the magnetic clusters in the system and the magnitude of the

intracluster effective anisotropy field. The electronic heat capacity should be determined in the usual way by extrapolation from sufficiently high temperatures in order to exclude the possible contribution from the clusters below T_{cg}. The procedure has already been used for CuNi and CuNiFe alloys (346) but should be more widely adopted. It is encouraging, however, to note that Einstein functions have recently been used in the case of CrNi and VNi alloys (358). The assumption of a smooth variation of β^S with concentration is reasonable especially for isoelectronic alloy systems like PdNi and PtNi. We have also shown that the onset of ferromagnetism by itself should not lead to any large abrupt changes in the bonding energy of the alloy series. In fact, for the CuNi system where elastic constants data are available over the whole concentration range the calculated values of Θ_D show an almost linear dependence on the concentration of Ni - see fig. 2.26. A slight kink is just discernible near c_f (= 47.6% Ni) as would be expected. This smooth variation of Θ_D is in marked contrast to the sharp peak in Θ_D deduced from the specific heat data.

Note Added in Proof

By considering the temperature dependence of the initial susceptibility a negative contribution to the T^3 term in the heat capacity (i.e β^S) may be obtained. From the discussion in section 2.5(ix)

$$\langle (\delta M)^2 \rangle \sim K_B T \chi^0(T) \simeq K_B T \chi^0(0) \left\{ 1 - \frac{T^2}{T^{*2}} \right\},$$

where T^* is a temperature that characterizes the critical fluctuations of the order parameter and is minimum at c_f. It is then easy to show that there is an additional contribution to $\beta^S \sim -\frac{3\alpha K_B \chi^0(0)}{\rho_0 T^{*2}}$ which, for $c \simeq c_f$, can overcome the positive phonon and magnetic contributions. Details will be discussed elsewhere.

FIG.2.26: VARIATION OF θ_D WITH COMPOSITION FOR CuNi ALLOYS

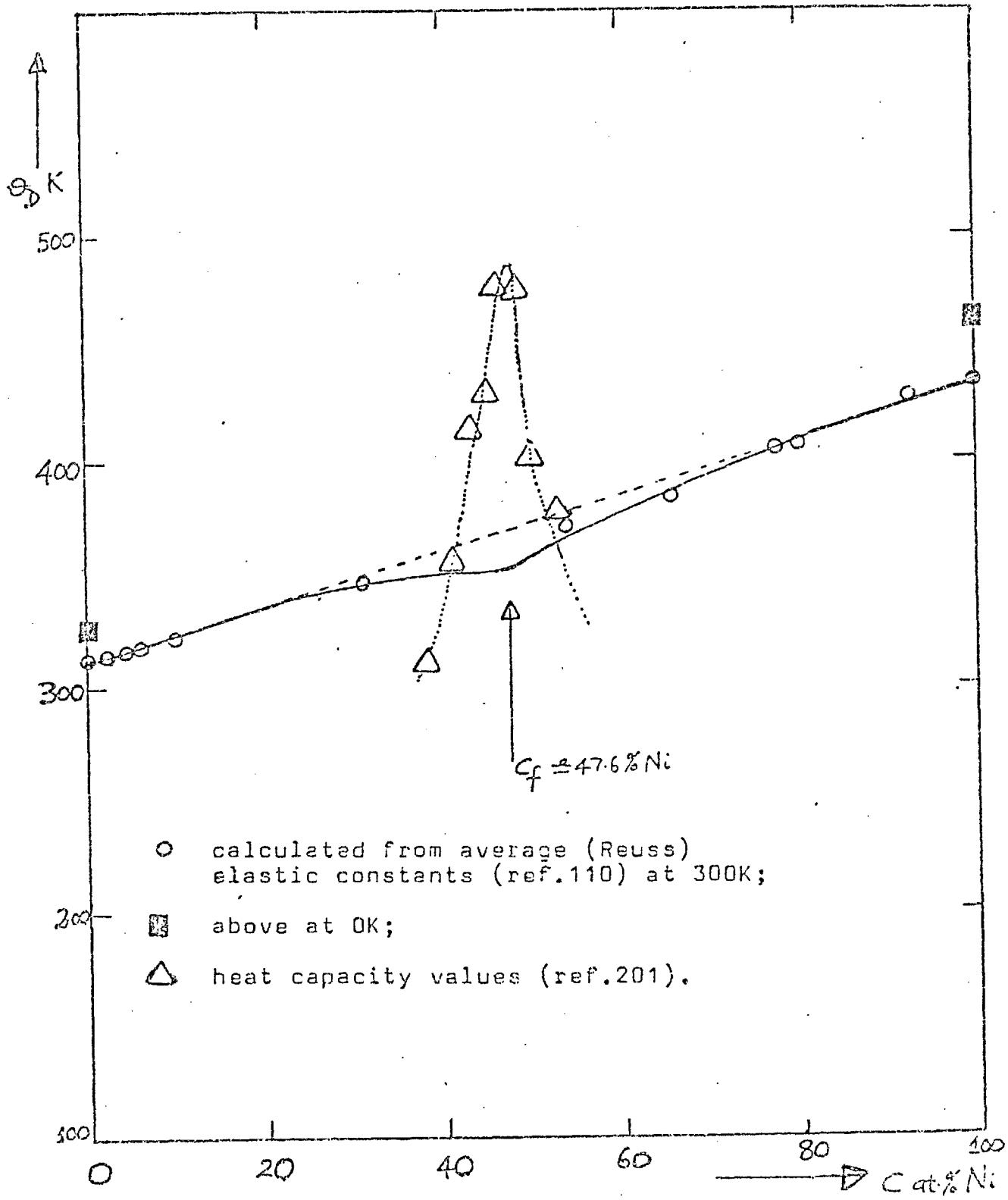

2.6 A Discussion of some representative transition metal alloy systems

In the preceding subsection we attempted to explain the concentration dependence of some of the physical properties of transition metal alloys in the critical region for the onset of ferromagnetism and, in some cases, we were able to derive quantitative expressions which may allow for a proper determination of the critical concentration. The parameters discussed include the spontaneous magnetization (M_{oo}), the initial susceptibility (χ^{o}_{nm} and χ^{o}_{f}), the coefficients of both the T and T^3 terms in the thermal conductivity and the coefficient of T term in the specific heat (γ^{s}). A notable omission was the concentration dependence of T_c, the ferromagnetic Curie temperature. We shall assume that just above the critical concentration the parameters c and T_c are interchangeable so that equation (2.125) is valid

$$\text{i.e.} \quad T_c \propto (c - c_f)$$

but only for a truly disordered alloy.

Using the derived relations we have reanalysed the existing data on a number of alloy systems in order to test the applicability of the relations. In doing this we note that we have only been able to show that the parameters γ^{s} and A attain their maximum values at the critical concentration and that the approach to this maximum is asymmetric. The location of the exact critical concentration is still dependent, to a certain extent, on the judgement of the observer. This uncertainty is removed however, by the predicted linear dependence of M^2_{oo}, T_c and the inverse of the initial susceptibility. Unfortunately, great caution must be exercised in

treating the published susceptibility data because these are not always the initial suceptibilities required. Many supposedly "low field" measurements really imply applied fields of 10-25KG!; also care must be taken to avoid measuring the susceptibility of cluster-glasses since this would be expected to be considerably less than the true initial susceptibility. Consequently in some cases such data for concnetrations close to c_f have been neglected.

One other point is that all the relevant parameters must be expressed per atom unit (or per mole or Kg atom, etc). This could be important in cases where the two constituent metals of an alloy system have widely differing atomic weights. From experience the differences introduced are small but the advantage is that some of the parameters occurring in the equations which are supposed to be concentration-independent remain so. In what follows we shall only state the deduced critical concentration and make only those comments which are of relevance to what has been discussed or to what would be of interest in later chapters. A detailed examination of each system will be considered elsewhere.

(a) <u>CuNi</u>

Figure 2.27 shows the concentration dependence γ^s, $(\chi^o_{nm})^{-1}$, M^2_{oo} and T_c and we obtain that c_f=47.6± 0.1% Ni. A <u>cluster glass region</u> extends from about 40% Ni up to the critical concentration. Close to c_f and even above it some of the magnetic properties of this system are expected to resemble those of a mictomagnet. The above critical concentration is much higher than the value previously generally assumed (~ 44% Ni) but it appears to be in better agreement with the experimental data

Fig. 2.27

CuNi: The Concentration Dependence of γ^s, M_{oo}^2 $(\chi^o_{nm})^{-1}$ and T_c against Ni Concentration

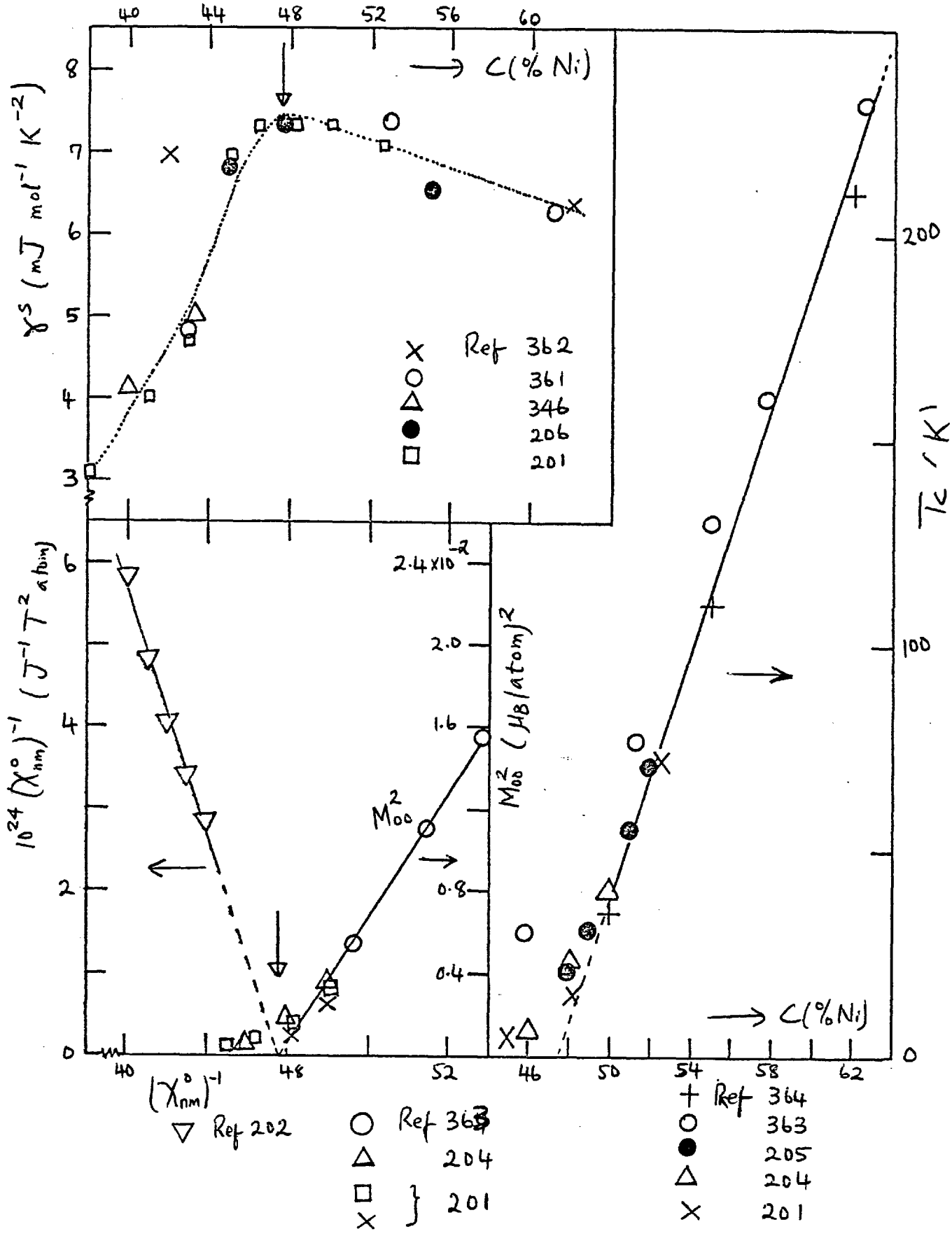

Fig. 2.28: CuNi; Plots of Residual Resistivity (ρ_0) and Absolute Thermopower (Q) against Ni Concentration.

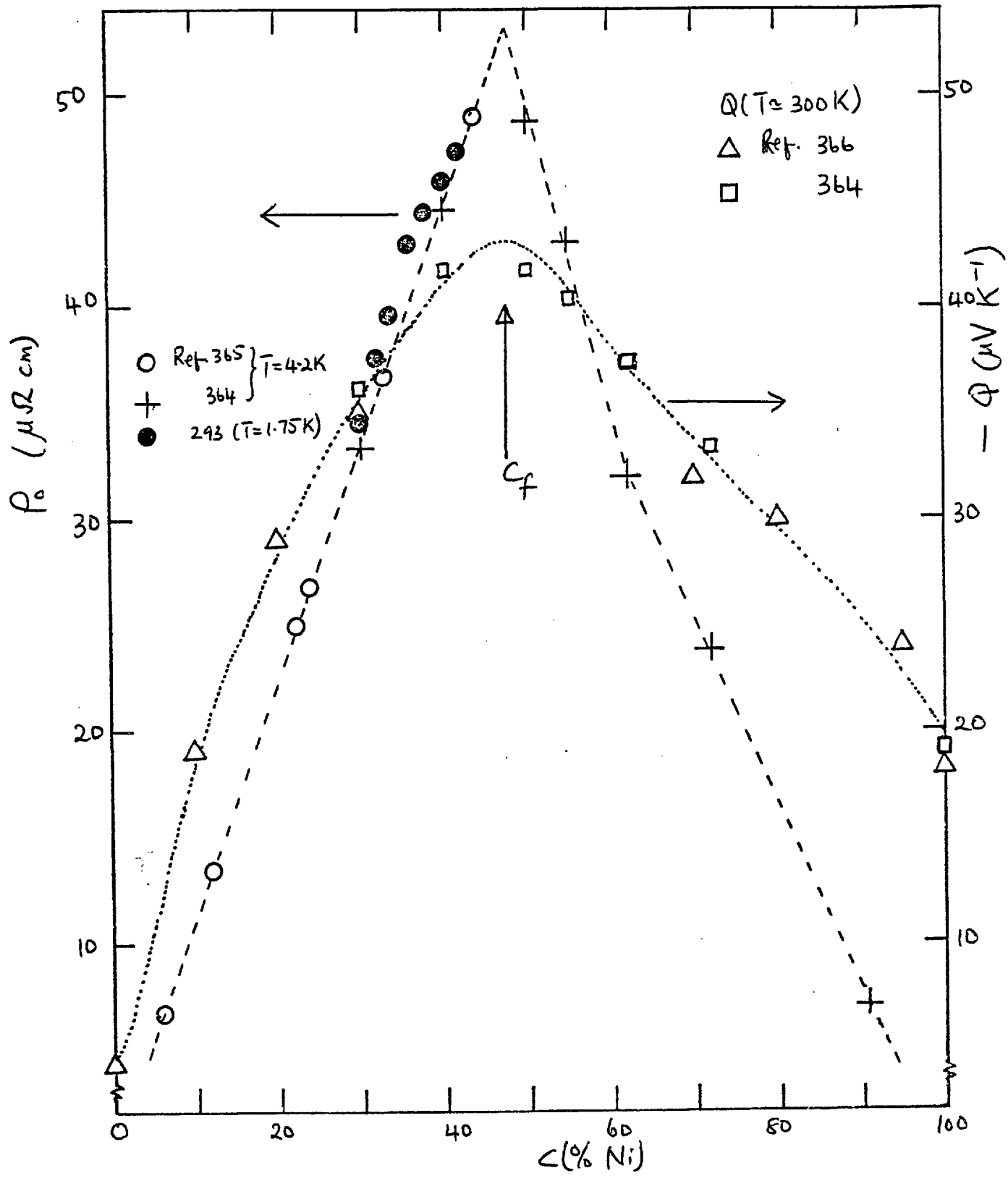

(as it should!). As an example we note that the low temperature ($T < 100K$) resistivity of the 46% Ni alloy (207) is typical of a spin-glass - a resistance minimum followed by a maximum at a lower temperature that was labelled as T_c. This "Curie temperature" is, in fact, just slightly larger than the cluster-glass temperature of this alloy.

In figure 2.28 the residual resistivity and the absolute thermopower at room temperature have been plotted against the Ni concentration. These quantities also exhibit a maximum near the critical concentration (arrowed in the diagram) but this must be regarded as just a bonus. Strictly only the magnetic contribution to either ρ_o or Q must be considered and, in particular, only values of Q at low temperatures ought to be used. The coincidence may not be unconnected with the fact that in a rigid band model the d-band in Ni should be full at about 60% Cu.

(b) CrNi

From the variation of γ^s and M_{oo}^2 with concentration (figure 2.29) we deduce that c_f = 89.4 ± 0.1% Ni. However, the T_c data give a lower critical concentration ($c_f \simeq$ 88.3% Ni) but this is because the observed T_c values are probably too large. The importance of an accurate determination of T_c in the critical concentration region cannot be over-emphasised. For example Marian (371) obtained T_c = 158K for Cr 88.81% Ni while Sadron (372) got T_c = 130K, which values should be compared with that of Besnus et al (367) which is 28K. Similar discrepancies exist in the published T_c values in the critical concentration regions of many

Fig. 2.29: Cr Ni; Plots of γ^s, M_{oo}^2 and T_c against Ni Concentration.

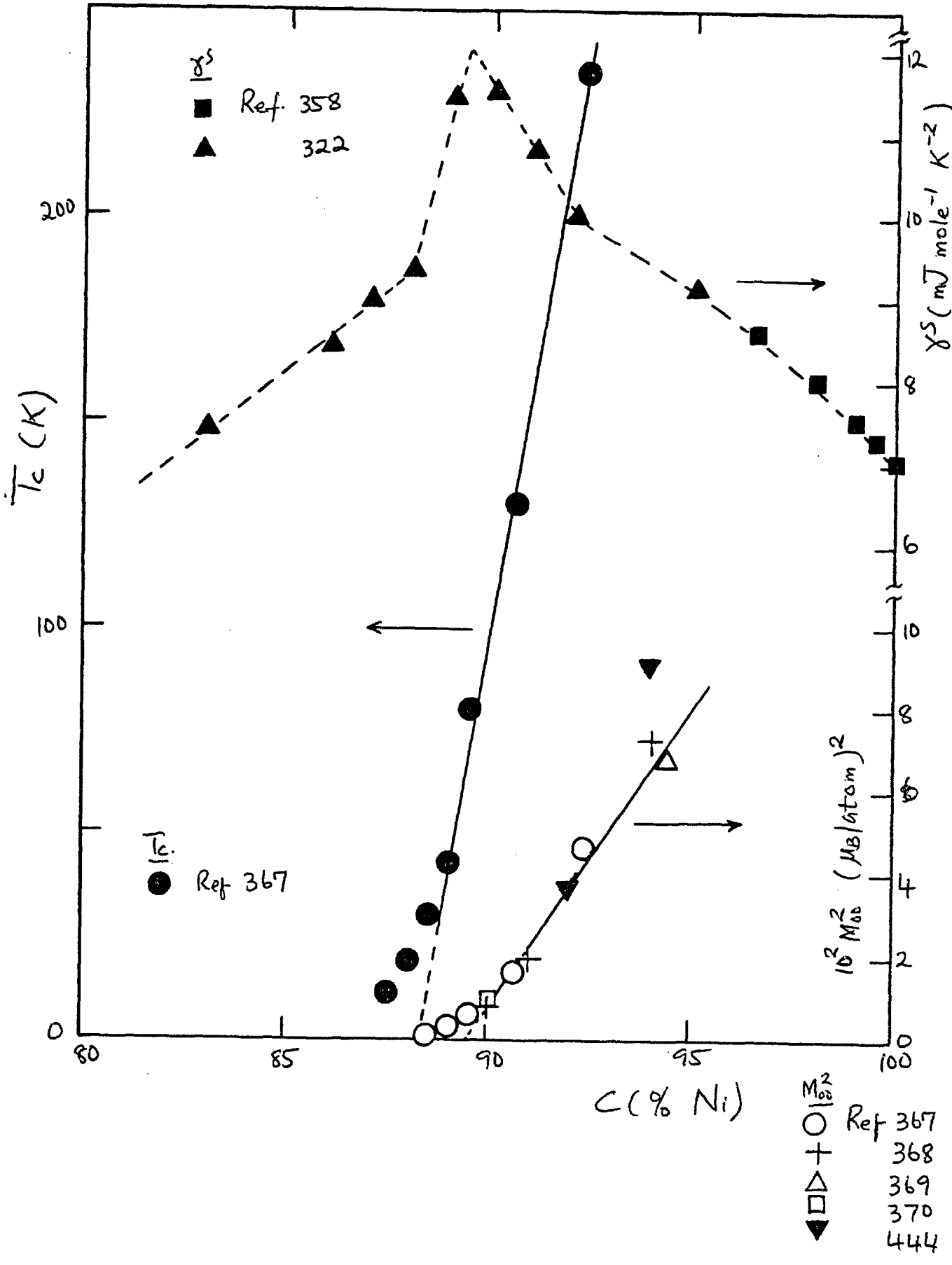

alloy systems. It is suggested that only low fields ($\lesssim$ 10 oe) should be used in such measurements, and the values obtained then checked by doing the Belov-Arrott plots in the temperature regions of interest (see also reference 392).

(c) PdFe:

The data for M_{oo}^2 , γ^s and T_c for PdFe have been plotted in figure 2.30. A critical concentration c_f = 0.12 $\pm$0.01% Fe is obtained. The considerable scatter in the data for γ^s (c < 1% Fe) results from the fact that the values were read off from the published graphs without a proper correction for the effect of magnetic clusters whose presence was clearly shown in the specific heat data of Veal and Rayne (125). The authors in both references 125 and 375 ignored the affected concentration region probably because no explanation could be offered for the anomalous variation of γ^s (and also β^s) in such a small concentration region. It is important that PdFe should be seen to resemble CuNi in its approach to ferromagnetism except for the much lower critical concentration. Whereas in CuNi the polarization clouds are seeded by clusters of eight or more Ni atoms in PdFe the clouds are probably seed by pairs of Fe atoms. The latter conjecture follows from the observation by Chouteau and Tournier (200) that below 0.1% Fe (i.e. below the critical concentration) the "Curie temperature" vary as c^2. The much lower critical concentration for the onset of ferromagnetism in Pd based alloys of Mn, Fe and Co is of course due to the very low spin fluctuation temperature of the Pd matrix and the intrinsic

Fig. 2.30

PdFe: Variation of M_{oo}^2, γ^s and T_c with Fe Concentration.

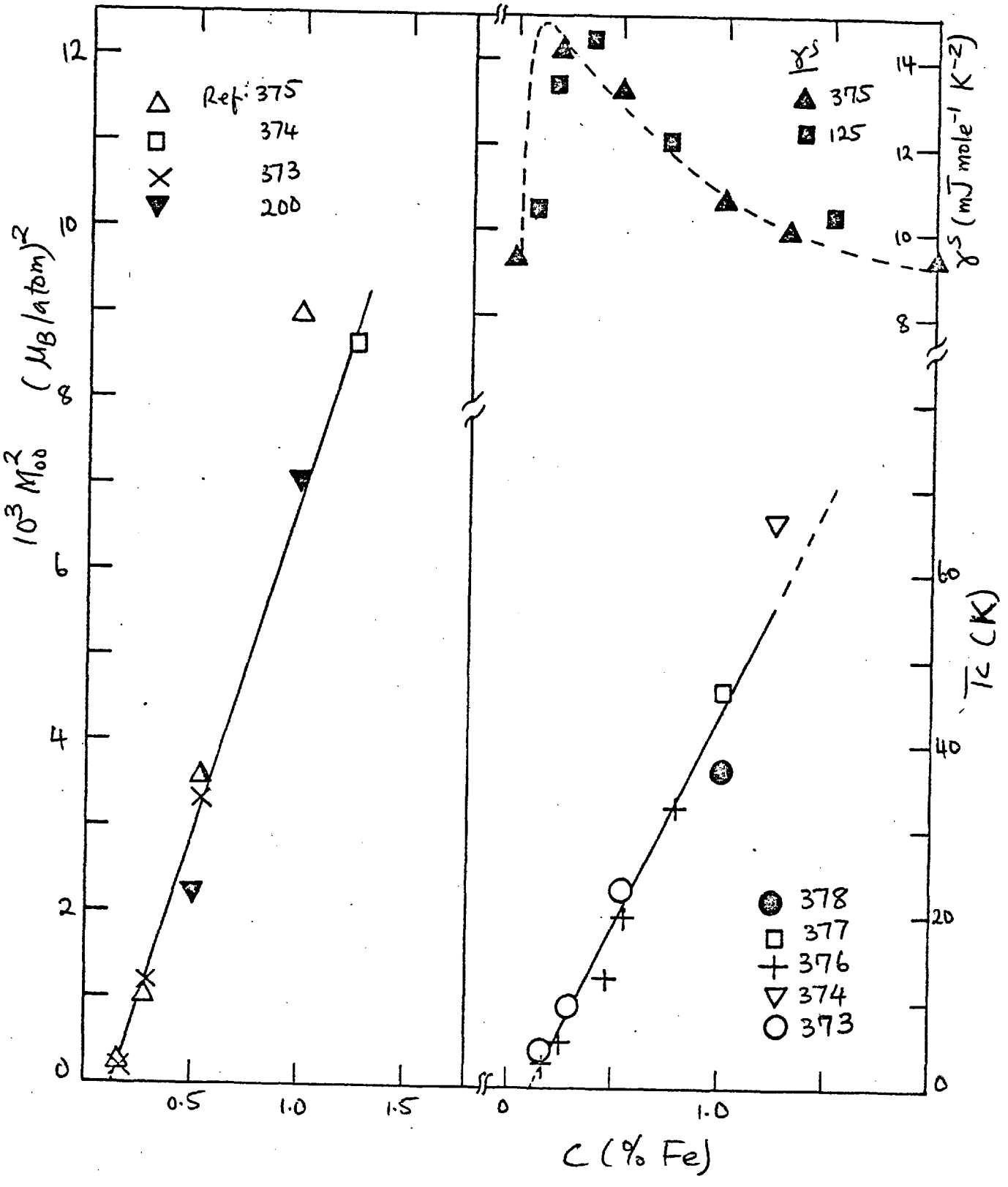

Fig. 2.31: PdFe; Concentration Dependence of the Curie Temperature.

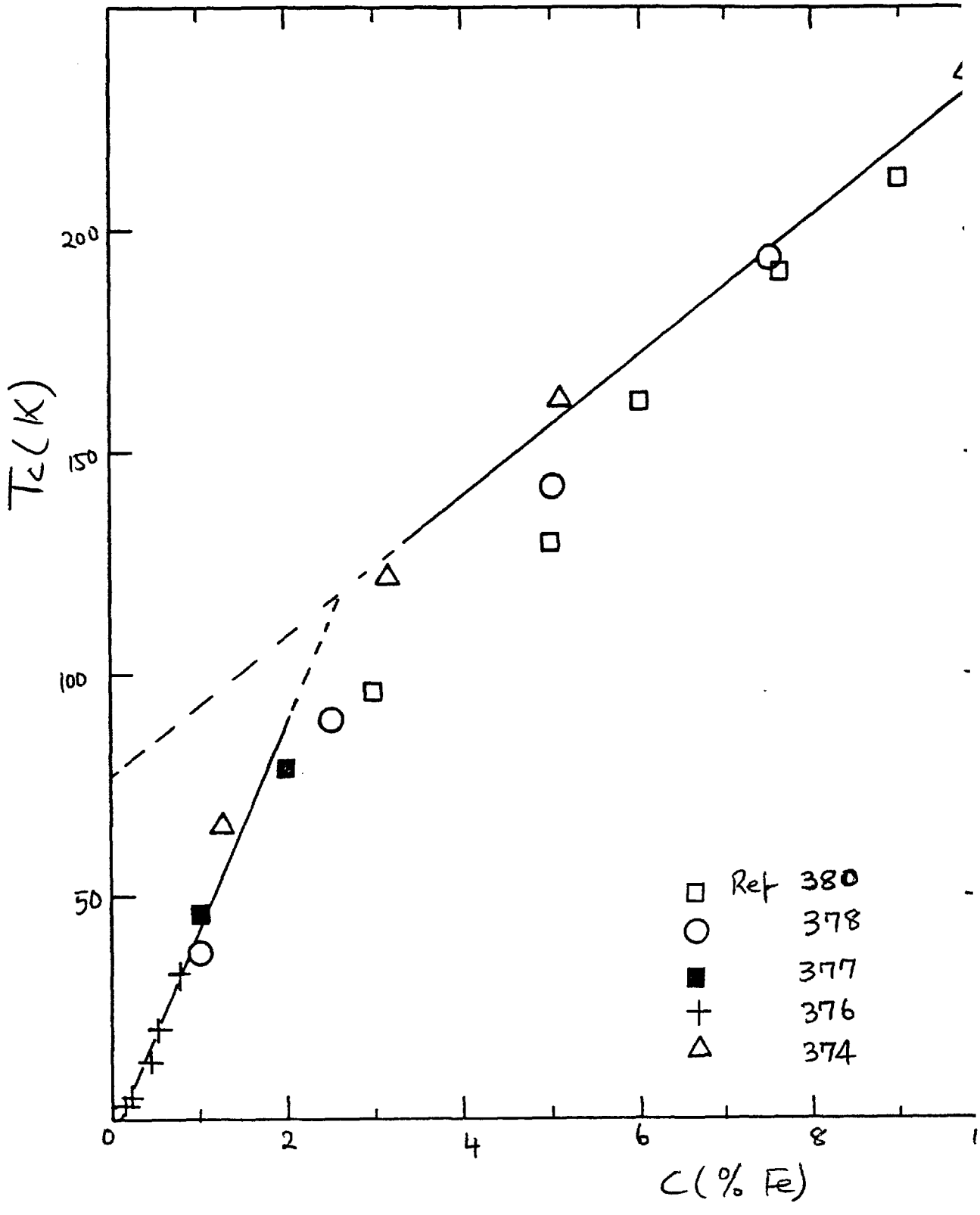

ferromagnetic interactions between the Pd atoms. These points were extensively discussed in section 2.2 where we say that the susceptibility of pure Pd obeys a Curie-Weiss law over a large temperature range (see figure 2.7 and equation (2.48)). It was suggested that Pd was not ferromagnetic only because its supposed Curie temperature is less than the spin fluctuation temperature ($\sim$ 85K). We observe that in figure 2.31 where the Curie temperatures of PdFe alloys (with c $\leq$ 10%Fe) have been plotted T_c extrapolates to a value of about 77K for pure Pd from the high temperature side. This observation was first made by Mydosh et al (380) and is also apparent in similar data for PdNi (figure 2.33). The implication of the above observation is that for $T_c \gtrsim$ 80K (i.e. c $\gtrsim$ 2%Fe) all Pd atoms should carry the same moment (of about 0.4μ_B/atom). It is to this extent that one should consider the "saturation" of the response of the Pd host to a driving magnetic impurity. A fuller discussion of this and the other points raised above will be given elsewhere. A pertinent point that should be mentioned here is that in the "saturation region" between 2-7% Fe the T_c values obtained from the maximum in the temperature coefficient of the resistivity (378,380) are always smaller than the T_c values determined by magnetization measurements. A similar effect has been also observed in CuNi (391) and it would appear to be related to the inhomogeneity of the magnetization in these alloys. In all cases the T_c value from magnetization measurements corresponds to the point of inflexion on the $\frac{d\rho}{dT}$ curve rather than to the temperature of the maximum. It is of interest to note however that the magnetization values of Tc agree well with the temperatures

at which a change of slope is observed in the $\rho(T)$ curve (380). The recent discussion of the determination of T_c by AC susceptibility measurements on the PdCo system (392) should also be carefully noted.

(d) PdNi

This is another system that has been extensively studied. Van Dam (144) by considering his specific heat and other data deduced a critical concentration of 2.6% Ni while Murani et al (351) have suggested a critical concentration of $2.32 \pm 0.01\%$ Ni. As shown in figure 2.32 the variation of $M^2_{oo}, \left(\chi^o_{nm}\right)^{-1}$, and T_c extrapolate to a critical concentration of $2.8 \pm 0.1\%$ Ni, as confirmed by the peak in γ^s. Additional evidence in support of this value of the critical concentration is provided by the effect of pressure on the magnetization. As discussed in section 2.5(iii) the "Villar effect" is maximum at the critical concentration and also above the critical concentration it decreases as an applied field increases (in fact as $B_o^{-\frac{1}{3}}$) while below the critical concentration it increases linearly with the applied field These conclusions are borne out by the recent observations of Beille and Chouteau (244). Figure 2.33 shows that the M^2_{oo} dependence on (c-cf) extends up to 30% Ni which is very remarkable. The same figure also shows that the ferromagnetic Curie temperatures again extrapolate to 77K for pure Pd from the high temperature side, as observed for PdFe. The same is true for PdCo but the graph is not shown here.

(3) PtNi

The concentration dependence of γ^s, T_c and M^2_{oo} are shown in figure 2.34 from which we obtain that $c_f = 41.7\%$ Ni.

Fig. 2.32: Concentration Dependence of γ^s, M_{oo}^2, χ_{nm}^{-1} and T_c for Pd Ni

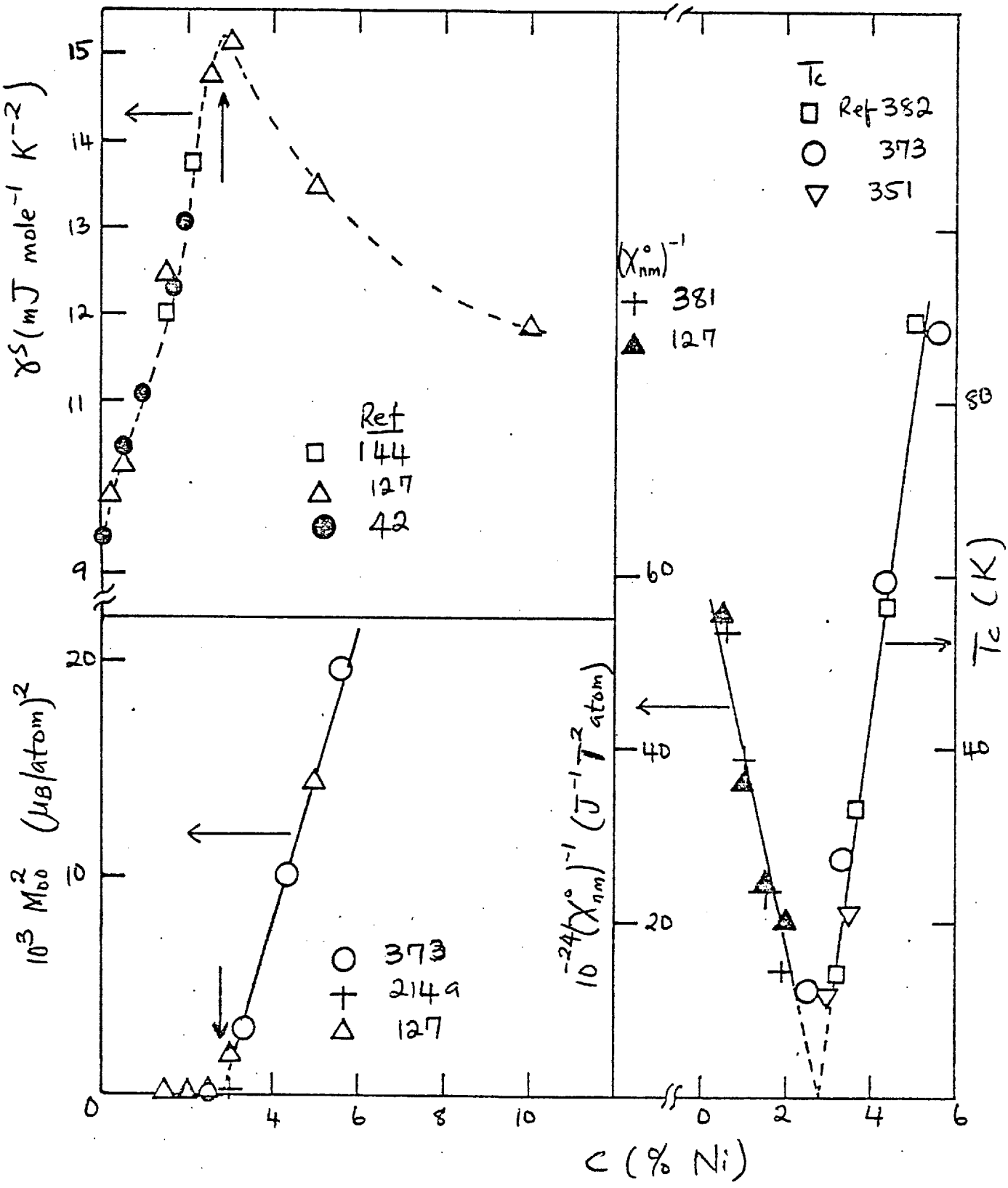

Fig. 2.33: Concentration Dependence of T_c and M_{oo}^2 for Pd Ni.

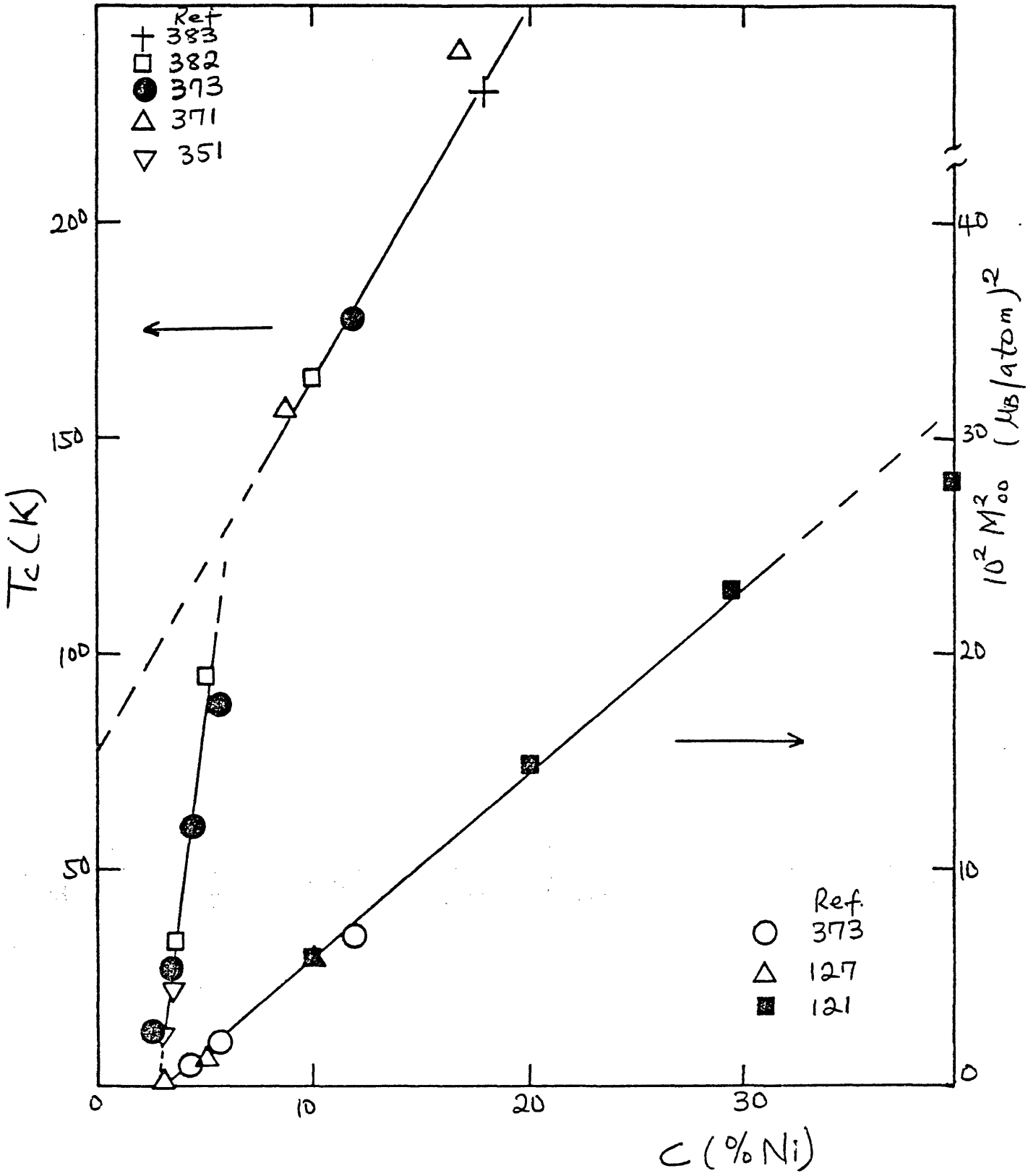

Fig. 2.34: Concentration Dependence of γ^s, T_c and M_{oo}^2 for Pt Ni.

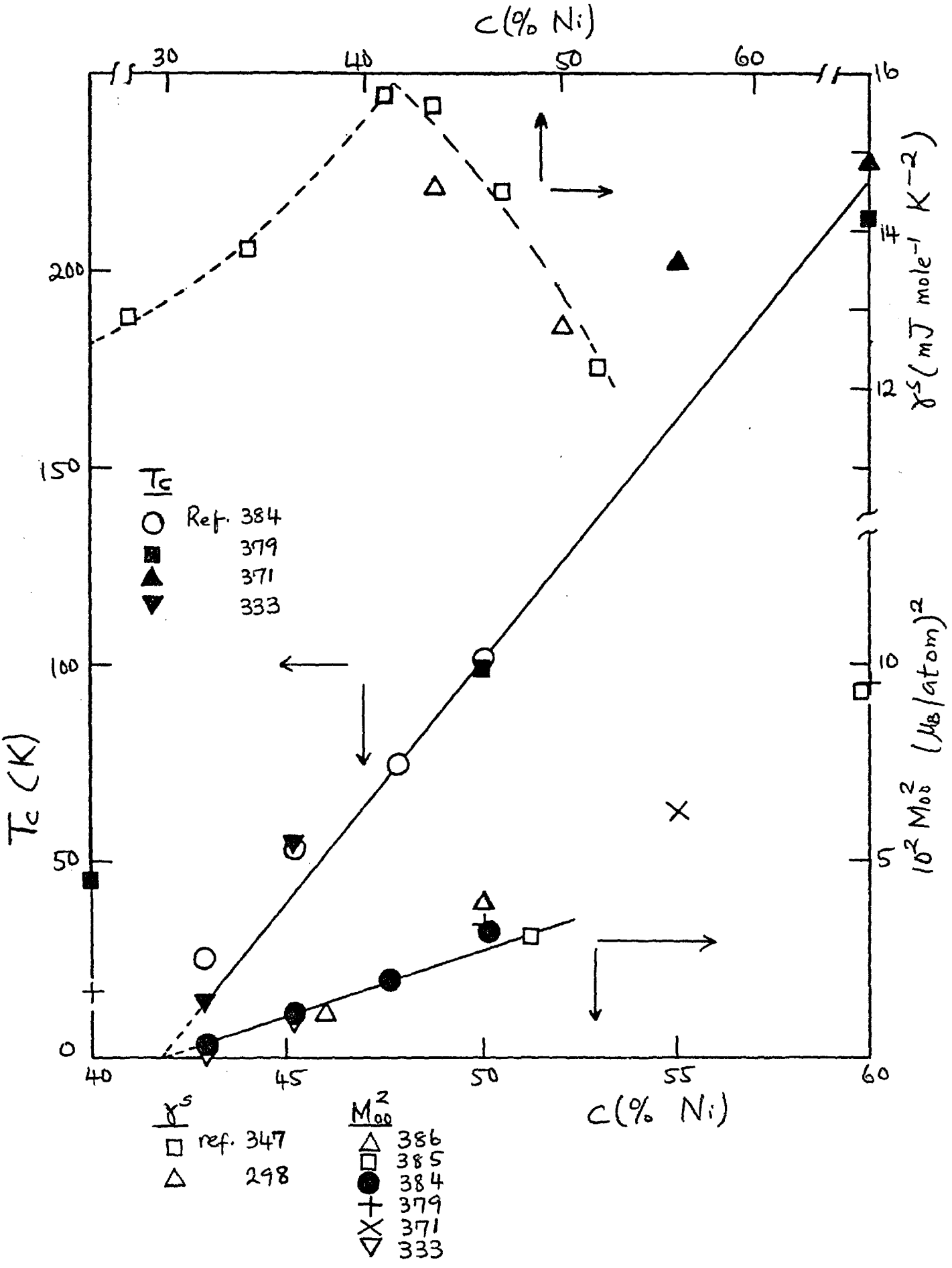

The inverse susceptibility in both the non-magnetic and ferromagnetic regimes also appear to extrapolate to this concentration (figure 2.35). The same figure also shows the anomalous variation of β^s which was mentioned in section 2.5 (xi). β^s exhibits an apparent minimum near the critical concentration. However, it must be mentioned that extrapolation to the above value of the critical concentration was largely determined by the position of the maximum in γ^s . We observe that from figure 2.36 which shows the concentration dependence of M_{oo}^2 up to 80% Ni values of c_f equal to 41.7, 44.5 and 49.5% Ni may be obtained by varying the concentration range from which the extrapolation is made. This problem is not at all helped by the concentration dependence of T_c - figure 2.37. One observes two almost parallel straight lines extrapolating to about 41% and 49% Ni respectively. The origin of the difficulty in interpreting uniquely the data on PtNi lies in the structural changes that occur in the system. A simple discussion of the metallurgical problems involved has been given by Gillespie et al (298) who observed that changes in the duration of the homogenising anneal caused significant changes in the magnetic behaviour of the system. One puzzling phenomenon is the resistance minimum observed in the supposedly ferromagnetic samples (298, 386). A resistance minimum involving a lnT term is of course characteristic of spin-glasses (i.e. including cluster-glasses). In the systems already described such resistance minima are not observed in the ferromagnetic regime.

A resistance minimum has also been observed (504) in

Fig. 2.35

PtNi: Concentration Dependence of χ^{-1} and β^s .

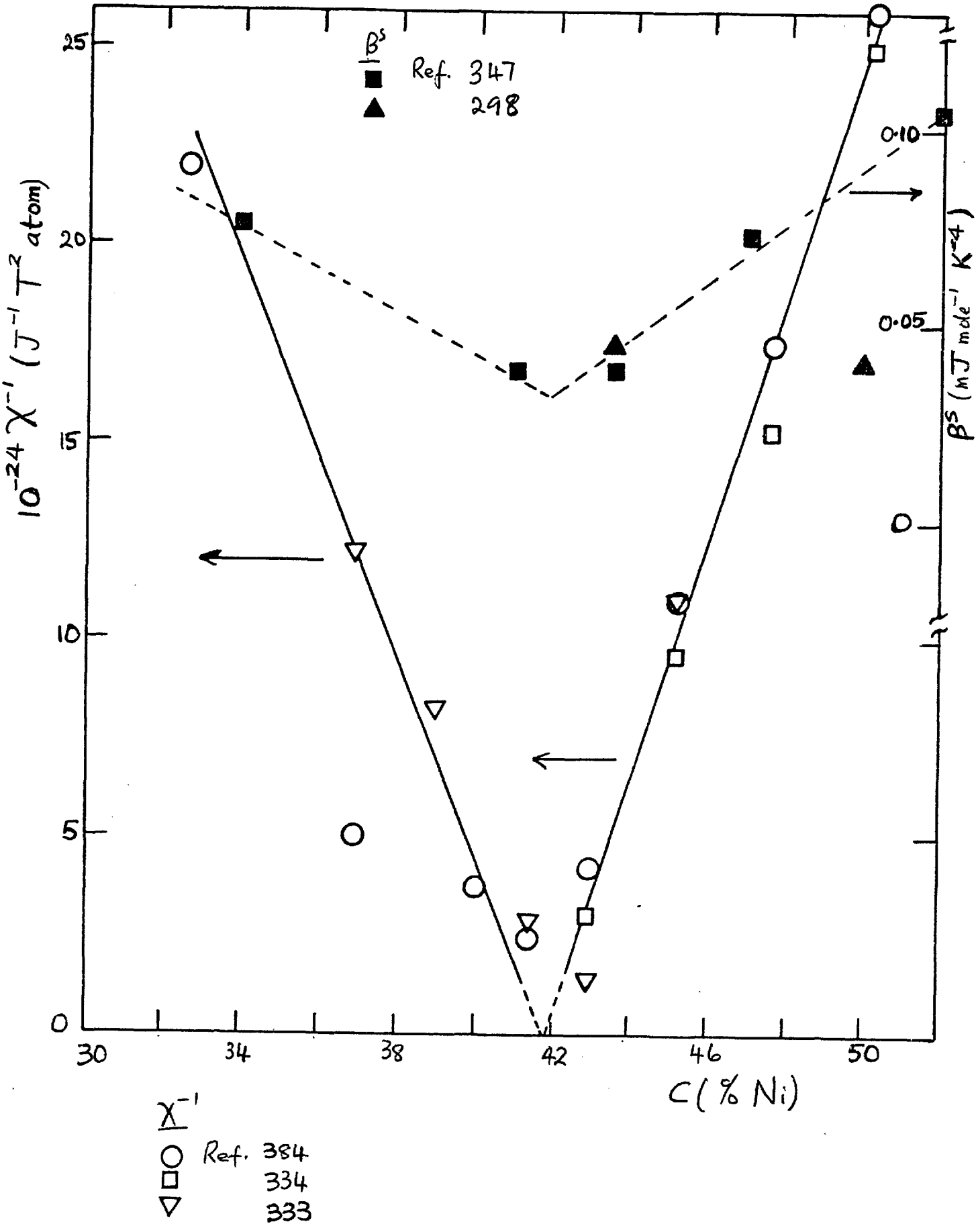

Fig. 2.36

PtNi: Concentration Dependence of M_{oo}^2 .

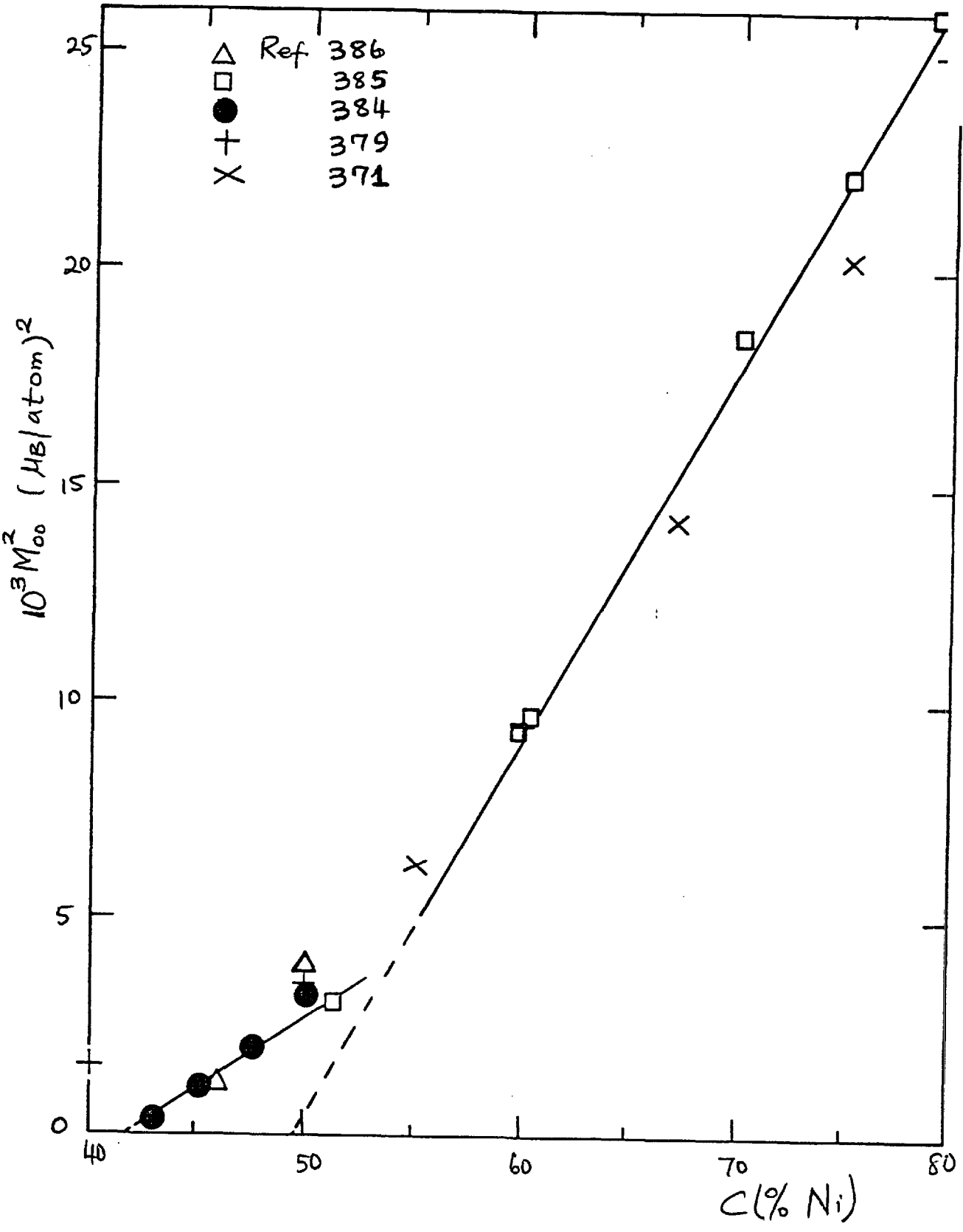

Fig. 2.37

PtNi: Concentration Dependence of T_c .

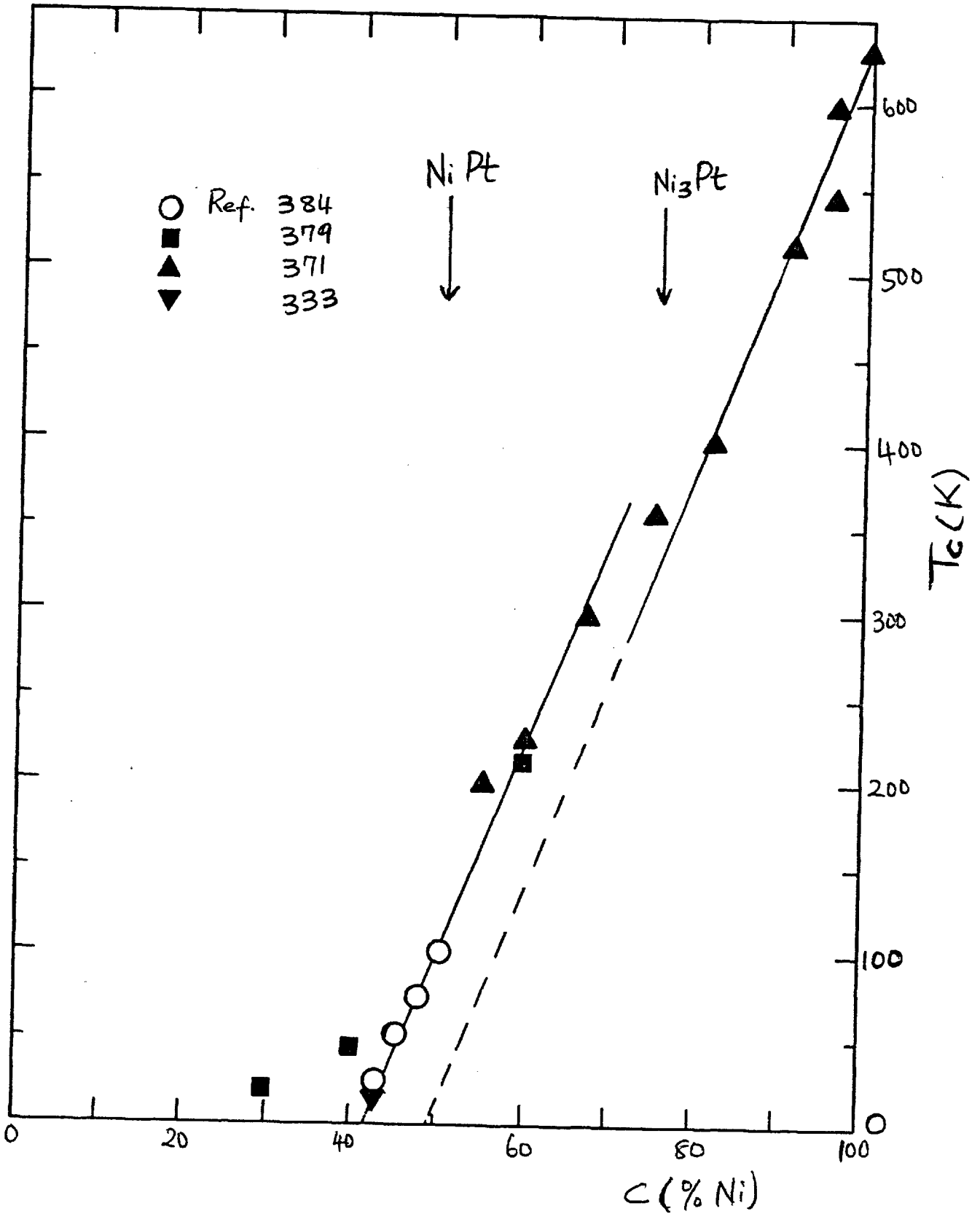

Pt 5% Co at a temperature which is well below the ferromagnetic ordering temperature of this alloy ($\triangleq$ 96 K). An attempt by Beal-Monod (428) to account for this resistance minimum is not very plausible because the resistance minimum is predicted to occur <u>just below</u> T_c. It is presently not clear what causes this resistance minimum in <u>ferromagnetic</u> alloys but it has been suggested (524) that in these alloys the effective molecular field acting on the magnetic units is very low, as the low Curie temperatures indicate, so that the magnetic units remain essentially free to participate in the spin-flip scattering of conduction electrons. However, our immediate interest lies in the approach to ferromagnetism in this system. We believe that magnetic clusters occur in this system just as much as in isoelectronic PdNi. Several reasons can be immediately adduced in favour of this contention but we will discuss these elsewhere although we have tried to explain why the presence of magnetic clusters may not show up in the expected way in the specific heat data (see section 2.5(xi)).

(f) <u>VFe</u>

Figure 2.38 shows the variation of γ^S, M_{oo}^2 and A with concentration. M_{oo}^2 extrapolates to a critical concentration c_f=29.3%Fe which is near the concentrations where the values of γ^S and A peak. Resistivity (208,299), specific heat (335,338,343), EPR(389), and magnetization (387) measurements have confirmed the existence of magnetic clusters so that we may expect cluster-glass behaviour below the critical concentration. The existence of cluster is also responsible for the widely differing "Curie temperatures" determined by Claus (299,388) and by Pataud

Fig. 2.38

VFe: Concentration Dependence of A, γ^s and M_{oo}^2.

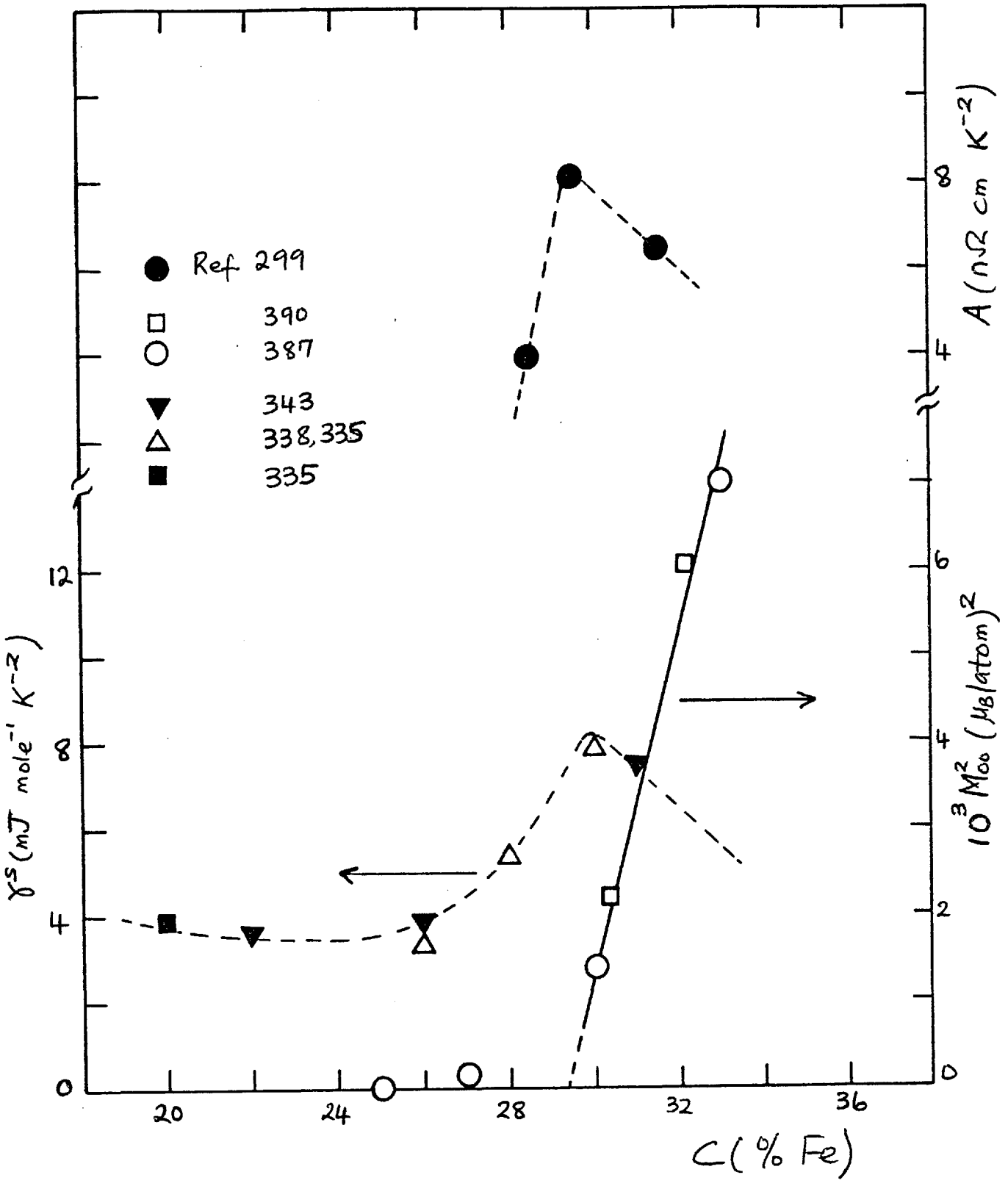

Fig. 2.39

VFe: Concentration Dependence of T_c.

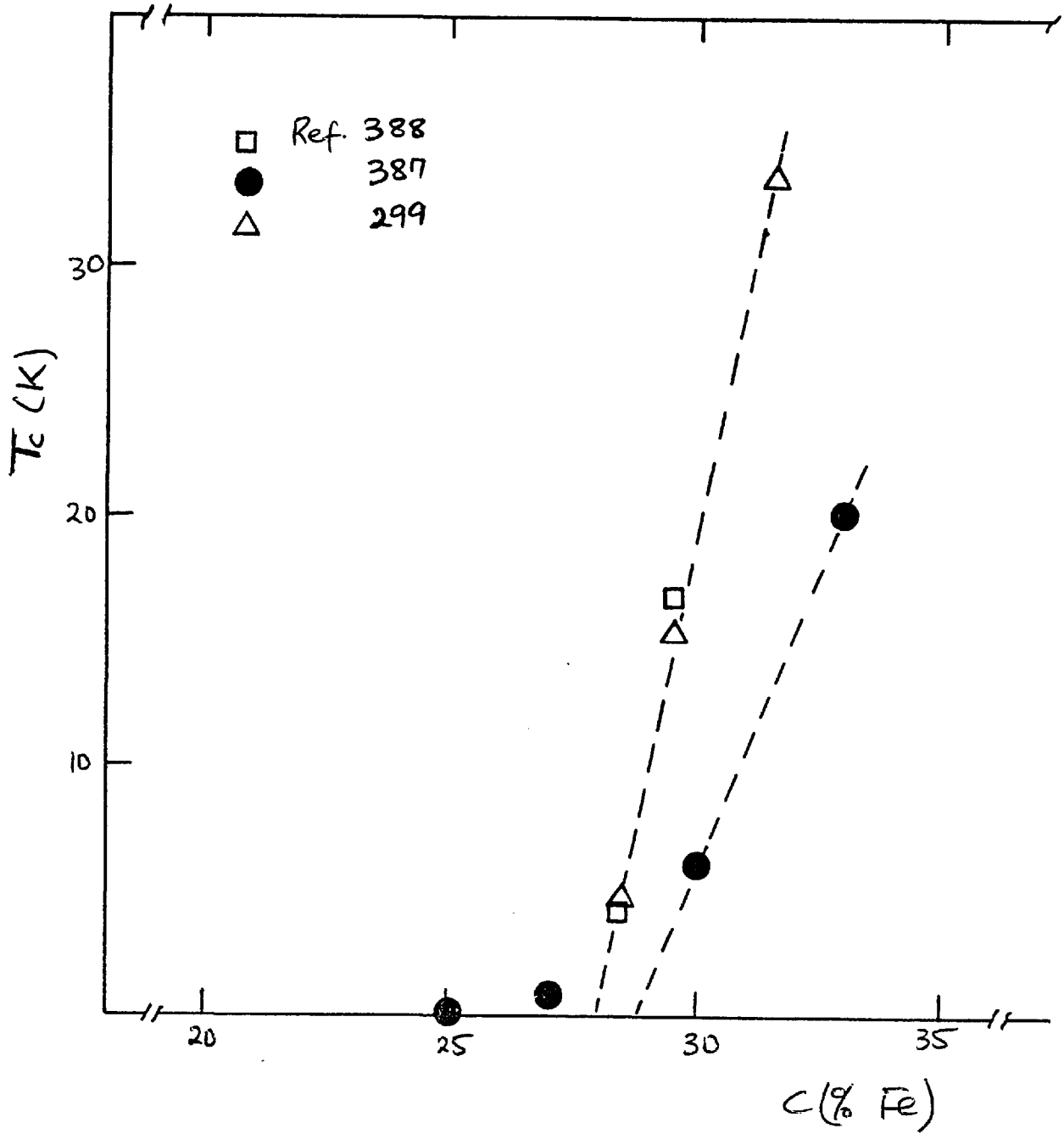

et al (387) as shown in figure 2.39. It would appear that the values obtained by Pataud et al (387) using very low dc fields are more accurate. On the other hand, it is probable that the temperatures determined by Claus (299, 388) refer to the cluster-temperature (T_{cl}) which are distinct from the cluster-glass temperatures (Tcg) (see section 2.3). T_{cl} refers to the temperature at which the thermal fluctuation energy becomes equal to the intra-cluster interaction energy i.e. the correlation energy of spins in a given cluster. In the mictomagnetic Au 15% Fe alloy $T_{cl} \triangleq 110K$ (195) but for VFe alloys an upper limit of 100K for T_{cl} has been suggested (208). The formation of a cluster is also of importance with respect to electrical resistivity because below Tc a conduction electron is scattered by cluster of spins acting as one magnetic unit. It is therefore not surprising that $\frac{d\rho}{dT}$ shows a maximum at this temperature. As suggested by Claus (388) the formation of a cluster leads to some anisotropy which is measured by T_a (equation (2.291)). However, we expect that T_a is about one or two orders of magnitude smaller than T_{cl} since an upturn is observed in the low temperature plot of $\frac{C_v}{T}$ against T^2 for the specific heat. As explained in section 2.5(xi) this upturn can only be observed if $Tcg < T$ and $Ta \ll T$. A further study of this system is continuing.

(g) AlNi

This system becomes ferromagnetic near the stoichiometric composition Ni_3Al. The variation of γ^s, $(\chi^o_{nm})^{-1}$, M^2_{oo} and Tc^2 with composition is shown in figure 2.40. The general behaviour is as in the systems already mentioned with the

Fig. 2.40

Ni_3Al: Concentration Dependence of γ^s, χ_{nm}^{-1}, M_{oo}^2 and T_c^2.

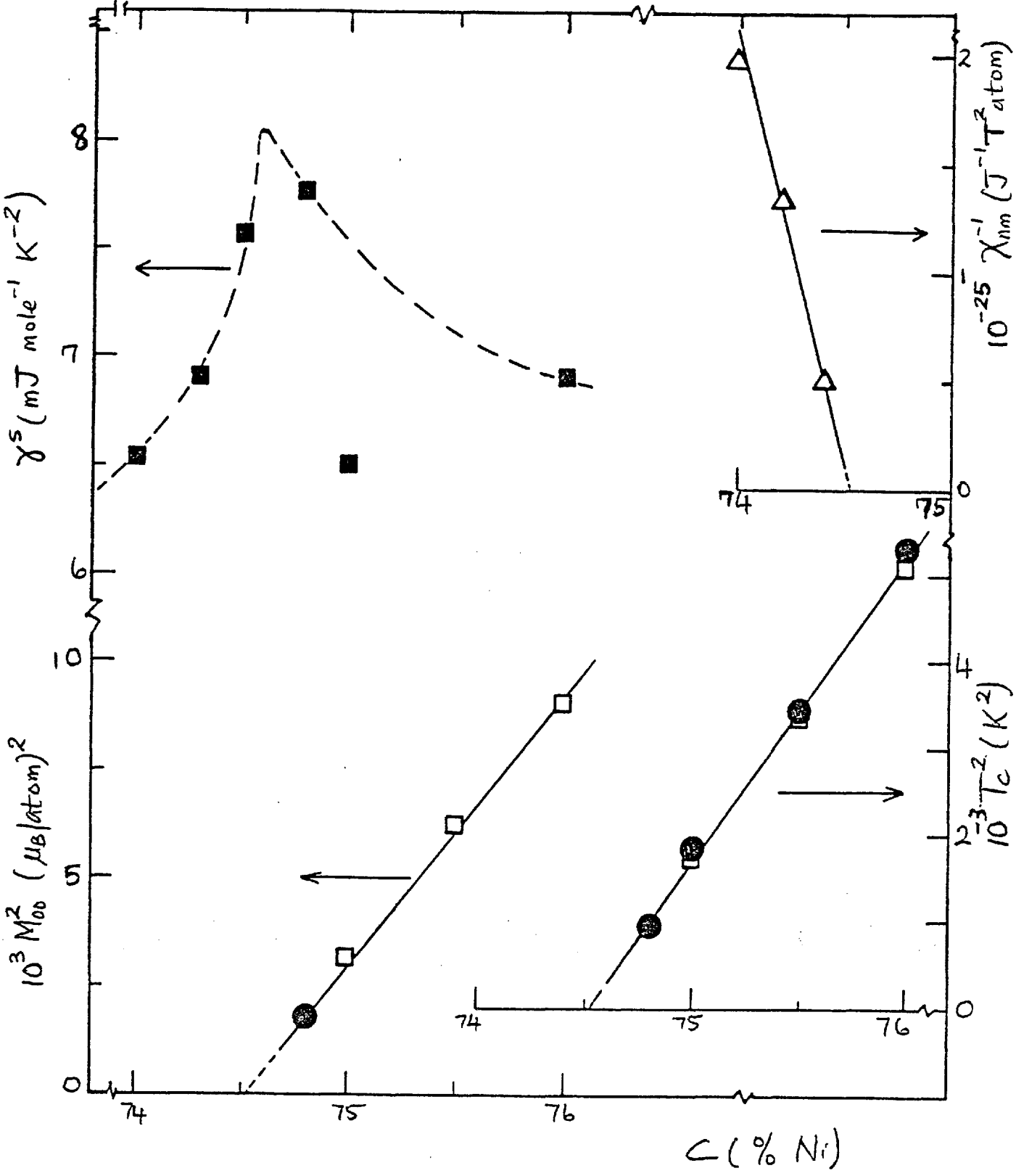

△ ● Ref 333
■ 318
□ 255, 241

exception that $T_c \propto (c - c_f)^{\frac{1}{2}}$. A critical concentration of 74.52% Ni is obtained which is below exact stoichiometry. However, the peak in γ^s appears to occur at a slightly higher concentration ($\simeq$ 74.6% Ni) but it will be noticed that above c_f the variation of γ^s is anomalous. We cannot understand why the value of γ^s should decrease abruptly at stoichiometry or, if this effect is real, why this anomaly is not reflected in the magnetization and Curie temperatures.

It will be recalled that this system has been cited as an example of a weak itinerant ferromagnet (241, 255), but an interpretation of both the influence of plastic deformation on the magnetic properties (393) and of the specific heat (318) requires the existence of magnetic clusters. In general, the properties of the AlNi system follow the general pattern described in section 2.5 with the exception of the concentration dependence of T_c. For completely disordered transition metal alloys where magnetic clusters are presumed to occur only through statistical concentration fluctuations $T_c \propto (c-c_f)$. It is therefore very likely that the observed dependence ($T_c \propto (c-c_f)^{\frac{1}{2}}$) is connected with the existence of the Ni_3Al structure near the critical concentration. In this regard it is interesting to note that the initial slope of the T_c versus c plot extrapolates to the critical concentration (see figure 2.41). The points used in the extrapolation are outside the concentration region ($\sim$ 77 - 90% Ni) where both the fcc NiAl and the Ni_3Al phases coexist. Observe, however, that the initial slope of the magnetic

Fig. 2.41

AlNi: Concentration Dependence of M_{oo} and T_c.

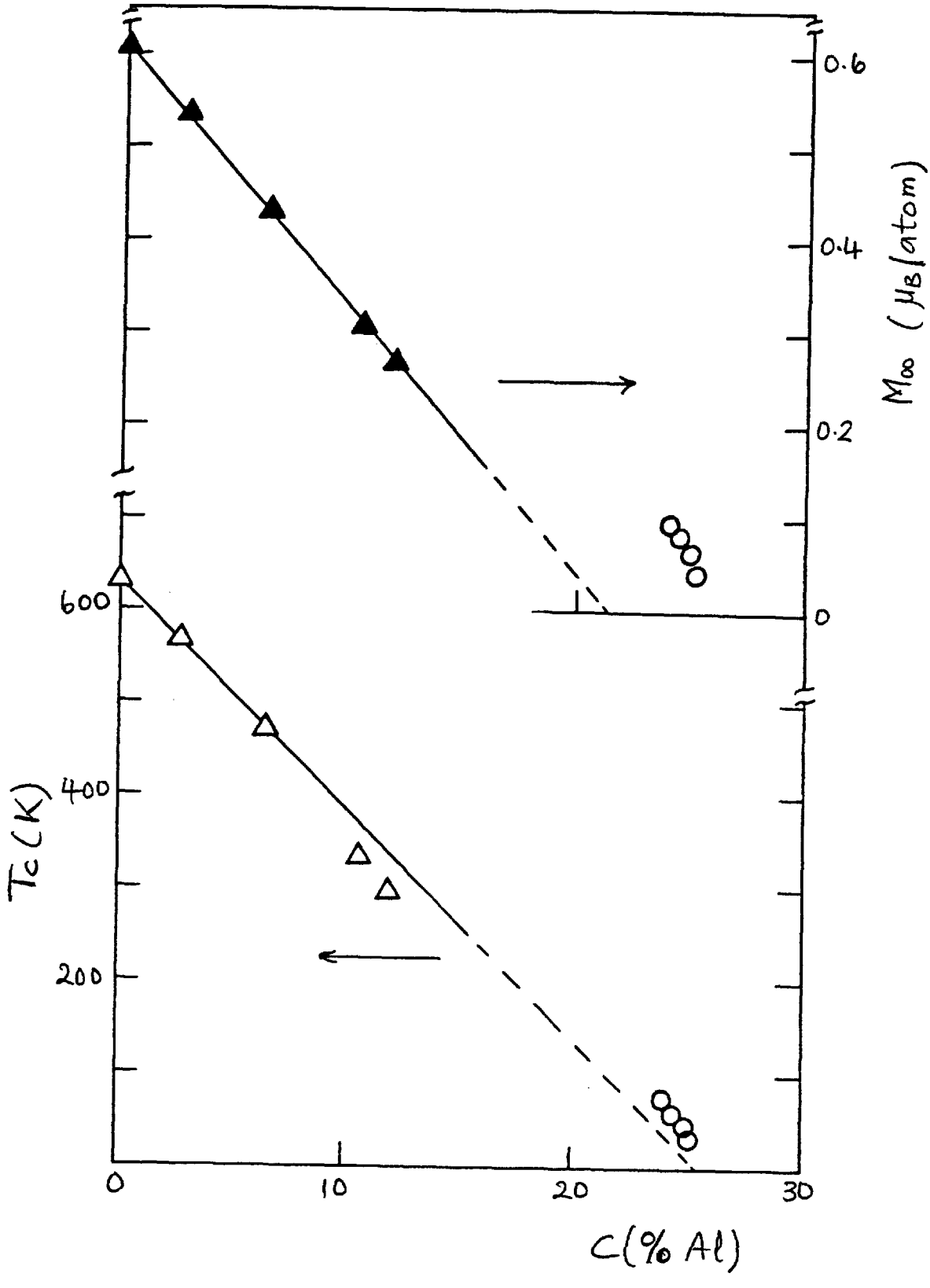

▲ } Ref. 395
△
○ 333

moment extrapolates to a higher critical concentration ($\sim$ 78.6% Ni) although we cannot rule out the possibility of some error in the quoted value of the spontaneous magnetization of the 93.6% Ni alloy. Such an error could arise from the occurrence of some Ni_3Al phase at the low temperatures where M_{oo} is determined (see the Ni-Al phase diagram given in reference 241).

In conclusion, we can state that the various properties of transition metal alloys in the critical region for the onset of ferromagnetism follow the predictions of the usual thermodynamic theory of a cooperative phase transition. Once again we shall emphasize that the basic mechanism of the onset of ferromagnetism in these alloys is essentially the same, namely, the overlap of adjacent polarization clouds seeded by clusters of magnetic impurity atoms. The clusters could be pairs, triplets, octuplets, etc, of impurity atoms as in PdFe (200), PdNi (394) and CuNi (203) respectively.

2.7 A critique of the theory of weak itinerant ferromagnetism

Weak itinerant ferromagnets (WIF) have been defined (240, 395) as magnetic metals, compounds or alloys which possess the following characteristics:-

(i) Metallurgical homogeneity which, on the itinerant model of ferromagnetism, implies a state of magnetic homogeneity..

(ii) Low Curie temperatures, small values of the spontaneous magnetization and large high fields susceptibilities, these quantities being related as

$$M_{oo}^2 \sim T_c^2 \sim \chi_o^{-1} \sim (c - c_f)$$

where c_f is the critical concentration for the onset of ferromagnetism.

(iii) the pressure derivatives of the above quantities are related as in equation (2.122) i.e.

$$\frac{1}{\chi_o}\frac{\partial \chi_o}{\partial P} = \frac{1}{c-c_f}\frac{\partial c_f}{\partial P} = -\frac{2}{M_{oo}}\frac{\partial M_{oo}}{\partial P} = -\frac{2}{T_c}\frac{\partial T_c}{\partial P} .$$

Using the proposition that $T_c^2 \sim (c - c_f)$ it then follows that

$$T_c \frac{\partial T_c}{\partial P} \sim -\frac{dc_f}{dP} = -\alpha$$

where α is a constant. Since the quantity $\frac{dc_f}{dP}$ is experimentally found to be positive one obtains that the pressure derivatives of M_{oo} and T_c are negative.

(iv) the volume magnetostriction, $w(B_o, T)$, is given by

$$w(B_o, T) = \kappa C \{ M^2 - M_o^2 \}$$

where κ is the compressibility and C the magnetoelastic coupling constant; following from the above a forced magnetostriction coefficient is defined as

$$\lim_{B_o \to 0} \left(\frac{\partial w}{\partial B_o} \right) = 2 \kappa C \chi M_o .$$

(v) A negative temperature-linear contribution to the thermal expansivity which in some cases outweighs the positive electron and phonon contributions thereby giving a net negative thermal expansivity. It has been suggested (240) that the fact that this contribution is observed over a very narrow range of concentrations confirms that the alloys concerned are rather magnetically homogeneous.

(vi) exhibit the "Δ E effect", which normally refers to a change of Young's modulus with magnetization at a constant temperature but the terminology has been generalized to include the temperature-dependence of this effect as well. WIF are expected to show a large "Δ E effect" and the apparent observation of this anomaly in Pt Ni has let to its being dubbed the " ΔG effect" (320).

Owing to the fact that these properties were first observed for the traditional invars (FeNi, FePd and FePt in certain concentration regions) it was proposed (395) that invar-type materials should be classified as weak itinerant ferromagnets. However, we argue below that the above mentioned properties are not peculiar to Ni_3Al, Pt Ni, Fe-invars, etc but are the general properties accompanying the onset of ferromagnetism at c_f. The reason why they have not been observed in Cu Ni, Pd Ni, etc is simply because they have not been looked for. Therefore instead of labelling say Pt Ni an invar-type material we should explore whether some magnetic phase transition occurs in the Fe-invars either as a function of temperature for a given composition or as a function of concentration at a given temperature or both. This is the approach we will adopt in a later discussion of invar alloys. We shall limit our criticism of the WIF

model to a few comments. A full account will be given elsewhere. The comments are as follows:-

(1) We have shown that the onset of ferromagnetism in what we have called "giant moment" alloy systems (vide section 2.3) is a proper third-order phase transition i.e. a cooperative transition. Consequently it is justified to apply Landau's theory of such phase transitions to the critical concentration region. The identification of the phase transition is the only important factor and it does, in effect provide some justification for Mathon's ad hoc use of an analogy between c_f and T_c (75). We shall, however, reiterate that the transition concerned is not from a paramagnetic state but from a non-magnetic state (in the sense already explained) to a ferromagnetic state. The true paramagnetic state is delineated from the non-magnetic state by a spin-fluctuation regime. Since the spontaneous magnetization and Curie temperature decrease uniformly and continuously to zero at the critical concentration and since therefore in this critical region both M_o and T_c are evidently small one can expand the Gibb's free energy (or the thermodynamic potential) as a function of the magnetization (equations (2.85) and (2.86)). By including the effects of an applied magnetic field and also of pressure (and hence the magnetoelastic energy) in the expression for the thermodynamic potential (equation (2.106)) it has been possible to discuss the general behaviour of alloy systems in the critical concentration region (section 2.5). It is therefore seen that all those properties which are regarded as characterising weak itinerant ferromagnets are merely the thermodynamic consequences of

the cooperative phase transition that sets in at c_f and, as such are strictly independent of any model of ferromagnetism. Consequently one has to consider some other aspects of the observed behaviour - for example the temperature-dependence - in any attempt to justify the applicability of any particular model of ferromagnetism.

(2) An important requirement of the WIF model is the metallurgical homogeneity of the alloy which is taken as implying magnetic homogeneity as well. The converse is also assumed to hold. It is thus apparent that the very existence of magnetic clusters is incompatible with a fundamental assumption of the WIF model. However, in section 2.2 we saw why and how magnetic clusters occur and we have stated that ferromagnetism sets in through the overlap of the polarization clouds seeded by these clusters. Hence, as also already noted, the phase transition is necessarily magnetically inhomogeneous. It is assumed that the alloys under consideration are truly randomly disordered so that only the unavoidable statistical fluctuations of concentration can occur. It is such concentration fluctuations which are responsible for the existence of magnetic clusters. It is, of course, true that the number of magnetic clusters may be enhanced (as in CuNi) or diminished (as in PtNi) by atomic ordering or clustering but this complication is not an essential part of the theory. Therefore, it is evident that magnetic inhomogeneity does not necessarily imply metallurgical inhomogeneity. In Ni_3Al which is highly ordered the magnetic clusters do not arise from statistical concentration fluctuations but from either misplaced Ni atoms (318) or from small regions of the NiAl phase (241). As noted in section 2.6 the concentration dependence of T_c in Ni_3Al is different from that of the disordered alloys.

The inhomogeneity of the magnetization may be allowed for by including a term $\sim(\nabla M)^2$ in the thermodynamic potential (see equation (2.201)). This additional term does not affect the basic deductions from Landau's theory because essentially only long wavelength fluctuations are considered; however, for critical scattering, say of neutrons, the additional term is important and its coefficient partly determines the inverse correlation range (see section 2.5(vi)). We therefore contend that the validity of equation (2.92) i.e.

$$2a + 4bM^2 = \frac{B_o}{M}$$

is not a proof of the magnetic homogeneity or otherwise of the alloy concerned. Incidentally below the critical concentration in PtNi and AlNi systems, which are supposed to be weak itinerant ferromagnets, clustering effects have been observed in the "low-field" magnetization data (333, 334) but these have been simply ignored. However, clusters have definitely been shown to exist in Ni_3Al (318) and if looked for properly will also be found in PtNi*.

(3) Apparently the only other system for which $T_c^2 \sim (c - c_f)$, apart from Ni_3Al, is the Fe-Ni system in the invar composition range (396). In this system atomic ordering based on Ni_3Fe (or possibly Fe_3Ni) is known to exist and it is also sufficiently well-established that the Fe-Ni invars are magnetically inhomogeneous (see reference 397 for a list of appropriate references).

(4) The form of the temperature dependence of the spontaneous magnetization is important because it governs the temperature dependence of the volume magnetostriction and hence of the magnetic contribution to

---

*Recent magnetization and neutron scattering experiments (757) have clearly shown the magnetic inhomogeneity of the PtNi system and very low field DC susceptibility measurements have also confirmed the existence of a cluster-glass at low temperatures (758).

the thermal expansivity (equation (2.160)). In section 2.5(iv) we considered two forms of the temperature dependence of M_o namely

$$M_o^2 = M_{oo}^2 \left\{ 1 - \frac{T^2}{T_c^2} \right\} \qquad \text{(equation (2.161))}$$

resulting from single particle excitations in very weak itinerant ferromagnets (235) and

$$M_o = M_{oo} \left\{ 1 - A T^2 \right\} \qquad \text{(equation (2.172))}$$

as observed for Ni_3Al (241, 255) and Pd 3% Ni (214a). This latter form, with A exactly equal to T_c^{-2}, has also been proposed (252) as arising from single particle excitations in weak ferromagnets, but is in addition to a spin-wave term which must exist. However, for Ni_3Al $A \simeq 0.63\ T_c^{-2}$ while for the Pd 3% Ni (214a) $A \simeq 0.43\ T_c^{-2}$ (with T_c = 8.9K, a value deduced from the intercepts of the Belov-Arrott plots). It has also been found (147) that equation (2.172) appears to be valid for both pure Fe and Ni in the temperature range $0 < T \leq 0.4\, T_c$ with A approximately equal to $0.27\ T_c^{-2}$ and $0.26\ T_c^{-2}$ respectively, although Schlosser (398) has shown that equation (2.161) was approximately valid but with the coefficient of the T^2 term different from T_c^{-2}. This is not surprising because if A in equation (2.172) is very small (i.e. T_c large) then

$$M_o^2 \simeq M_{oo}^2 \left\{ 1 - 2AT^2 \right\} .$$

It thus appears that equation (2.172) may be of general validity. If this is so then what happens to the spin-wave term which must surely exist at low temperatures? Spin-waves have been observed for Fe and Ni and there is no reason why they should not exist in PdNi or Ni_3Al. A clue to the answer to this question is provided by a similar behaviour observed for a number of rare-earth metals (Dy, Tb, Er and Ho) which was explained (316, 317) in terms of the usual $T^{3/2}$ spin-wave term modified

by an exponential factor involving the intrinsic energy-gap in the spin-wave excitation spectrum. It was proposed that

$$\frac{\Delta M}{M_{oo}} \equiv \frac{M_{oo} - M_o}{M_{oo}} = a T^{3/2} e^{-\Delta/T} \qquad 2.307$$

where Δ is the energy gap in the spin-wave spectrum. Over a certain temperature range equation (2.307) gives a similar temperature dependence as equation (2.172). Such a functional form has been tried out (147) for Fe and Ni and it was pleasantly surprising to find that the low temperature data are exactly fitted by equation (2.307). For Ni

$$\frac{\Delta M}{M_{oo}} \simeq 7.58 \times 10^{-6} T^{3/2} e^{-\frac{5.79}{T}} \qquad 2.308$$

valid up to 120 K, while for Fe

$$\frac{\Delta M}{M_{oo}} \simeq 4.2 \times 10^{-6} T^{3/2} e^{-\frac{53.5}{T}} \qquad 2.309a$$

valid up to 300 K!

As evident in eq.(2.308) and (2.309a) the coefficients of the $T^{3/2}$ terms are the same as those obtained by several investigators (252, 399-406). The energy-gap in Ni is only a factor of two larger than the estimate previously given by Pugh and Argyle (400) and Argyle et al. (402) but is significantly larger than the value estimated from very recent hyperfine field measurements (406b). On the other hand, the energy gap for Fe appears to be unreasonably large but this is probably due to the inaccuracy of the analysed data (759). At low temperatures the values of $\frac{\Delta M}{M_{oo}}$ derived from the data in Ref. 759 are significantly smaller than those of other authors (402, 404, 406a). If we use the hyperfine field data of Riedi (406a) which are probably the most accurate for $T \lesssim 50$ K we obtain that

$$\frac{\Delta M}{M_{oo}} \simeq 3.35 \times 10^{-6}\, T^{3/2}\, e^{-\frac{2.58}{T}} \,, \qquad 2.309b$$

the resulting energy gap of 2.58 K being close to a value of 1.6 K obtained from neutron diffraction measurements at room temperature (760). (It must be pointed out that there is a great difficulty in obtaining a sufficiently large single phase single crystal of pure Fe for use in neutron diffraction experiments so that the difference between the values of 2.58 K and 1.6 K for the energy gap should not be viewed with great concern).

It has, in fact, been found possible to fit the magnetization data for $0 \leq T \lesssim 0.98\, T_c$ with the expression

$$\frac{\Delta M}{M_{oo}} = T^{3/2} \sum_{\nu=1}^{3} A_\nu\, e^{-\frac{\Delta_\nu}{T}} \qquad 2.310$$

with the following values of the parameters A_ν (in $K^{-3/2}$) and Δ_ν (in K).

Ni (T_c = 631 K)

$A_1 = 7.58 \times 10^{-6}$; $\Delta_1 = 5.79$

$A_2 = 40.7 \times 10^{-6}$; $\Delta_2 = 635$

$A_3 = 0.100$; $\Delta_3 = 5260$

Fe (T_c = 1044 K)

$A_1 = 3.35 \times 10^{-6}$; $\Delta_1 = 2.58$

$A_2 = 29.8 \times 10^{-6}$; $\Delta_2 = 1500$

$A_3 = 0.800$; $\Delta_3 = 11800$.

The values of these parameters suggest that we can rewrite eq.(2.310) as

$$\frac{\Delta M}{M_{oo}} \simeq T^{3/2}\left\{A_1 e^{-\frac{\Delta_1}{T}} + A_2\, e^{-\frac{3ST_c}{(S+1)T}} + A_3\, e^{-\frac{\Delta_o}{T}}\right\} \qquad 2.311$$

where S is approximately equal to 1 for Fe and $\frac{1}{2}$ for Ni and Δ_o is the exchange splitting. It is interesting to note that it is the second term

in eq.(2.311) which has been mistaken for the contribution due to single particle excitations; for example Thomson et al. (252) obtained $A_2 = 62 \times 10^{-6}$ and $\Delta_2 = 743$ K from an analysis of some NMR data for Ni given in Ref.(400). We shall pursue the discussion of the temperature dependence of Mo elsewhere but meanwhile we suggest that eq.(2.172) which appears to be valid for weak (Fe) and strong (Ni) ferromagnets alike, for Pd Ni (a giant moment alloy) and Ni_3Al (a WIF?) is an approximation to the actual expression which involves a spin wave term modified by an anisotropy factor.

(5) As with the itinerant model of ferromagnetism itself the WIF model has a large compliance - any discrepancies between theory and experiment are readily attributed to effects which are neither easily quantifiable nor readily susceptible to a direct experimental verification e.g. the existence of very fine structures in the density of states.

More importantly we question the physical basis of the itinerant model of ferromagnetism and reject the automatic association of "band magnetism" with complete itineracy of the d-electrons. We saw in section 2.2, how the dilute alloy problem carries over to a pure transition metal. The essence of the discussion there is that every transition metal is intrinsically magnetic because there always exist exchange - split spin-up and spin-down levels but these levels are broadened into bands by the s-d hybridization (involving same spins), the d-d interactions (covalent admixture) and spin-orbit interactions. The main difference between a pure metal and a dilute alloy is in the relative importance of the d-d overlap integrals. Thus we propose a localized form of "band magnetism" in which any itineracy of d-electrons

is strictly limited to the accident of the presence of the d-band at the Fermi level and to s-d hybridization. One can easily see that as the d-level fills up not only will the exchange splitting decrease but also the Fermi surface will at some point no longer intersect both sub-bands. Thus there is a natural progression from the "weak" ferromagnetism of Fe to the "strong" ferromagnetism of Ni.

In conclusion there does not seem to be any particular justification for the applicability of the model of weak itinerant ferromagnetism to transition metal alloys and, in our view, it is even doubtful whether any ferromagnetism can be essentially itinerant. Any plausible model of magnetism should be able to provide the basic guidelines for discussing the magnetism of dilute alloys as well as pure metals and, at the moment, it does not seem that spin-glass alloys can be fitted into the itinerant model of magnetism.

2.8 Comments on the theory of spin-glasses

As extensively discussed in section 2.3 some form of a spin-glass state occurs in the magnetic phase diagram of most transition metal alloys, the only apparent exception being alloy systems where a SDW is stabilized from the non-magnetic regime. In an effort to characterize the various spin-glass states we proposed a nomenclature scheme based essentially on the effective number of magnetic units in the system and on the nature of inter-impurity interactions. Denoting the effective number of magnetic entities by c* then one has either a cluster-glass, mictomagnet or disordered intrinsic antiferromagnet (DAF) if $c^* < c$ and a speromagnet if $c^* = c$. In a cluster-glass only the impurity atoms grouped into favoured clusters are magnetic while in a mictomagnet or DAF all impurity atoms have well-defined spins but in addition some of these may be grouped into either ferromagnetic or antiferromagnetic clusters depending on the nature of the inter-impurity interaction. Thus the cluster-glass is simply some residual magnetism existing below the critical concentration for the onset of magnetism. It also exists just below the critical concentration for the onset of ferromagnetism in "giant moment alloys" e.g. in PdNi a cluster-glass state exists for $0.5\% \lesssim c < c_f$ (= 2.8% Ni).

It is only for speromagnets that not only is the exact number of magnetic units known, ab initio, but also the units may be regarded as essentially identical except for the usual statistical fluctuations in concentration. Therefore it is this system which is the most easily amenable to a theoretical description although a cluster-glass may be equally suitable if there is a predominant cluster-size whose concentration

c* is known (say from susceptibility measurements). On the other hand a complete theoretical description of either micto-magnets or DAFs looks forbidding because the properties of these systems depend on factors that are not easily quantifiable - heat treatment, cold work etc, but a qualitative description is possible. We shall thus restrict our comments to the speromagnetic state.

(a) The speromagnetic state is a well-defined magnetic state which in the absence of applied field and in the equilibrium state, has no net magnetization averaged over a macroscopic volume. This is believed to result from a spatially random orientation of otherwise well-defined spins which are exchange coupled solely via RKKY interactions.

(b) The speromagnetic state sets in at a given temperature called the spin-glass temperature, Tsg. That this temperature is well-defined is shown by the sharp CUSP observed in the initial susceptibility (226,407), the sharp collapse of the Mössbauer hyperfine spectra (408) and more recently by the sharp onset of the relaxation of the muon's polarization in the muon spin precession experiment (196). The sharpness of the onset of the speromagnetic state does suggest a phase transition at Tsg and indeed we suggested earlier (see section 2.4) that it is a second order phase transition, of which apparently the only other known example is the superconducting transition in zero field. Adkins (222), however, lists the superfluid transition in liquid belium and the order-disorder transition in AB alloys (such as β-brass) as second-order phase transitions whereas we classified these as third-order. For the speromagnetic-paramagnetic phase transition the order parameter was defined (section 2.4) as the local magnetization

(or local molecular field), Bi, at an impurity site. Its magnitude is uniform but its direction is random so that in effect one has a distribution P(Bi) of local molecular fields In general this distribution is affected by both temperature and an applied magnetic field (Bo) i.e. $P(B_i) = P(B_i, T, B_o)$ A theoretical justification of the existence of such a local molecular field has been recently provided by Edwards and Anderson (409). They showed that the spin auto-correlation function, q(T), defined as

$$q(T) = \lim_{t\to\infty} \langle S_i(0) \cdot S_i(t) \rangle \qquad 2.312$$

has a finite value for $T \leq T_{sg}$ but vanishes for $T > T_{sg}$. Thus we can consider the local molecular field as being of the order of the root mean square of S_i^2 averaged over the system and over a sufficiently long time interval. It is our considered opinion that the demonstration of the existence of the order parameter is the only useful result of the recent theories (409,412) of the spin-glass state. This is because below Tsg there is an additional field that acts on the impurity spins due to magnetic forces (dipolar and pseudo-dipolar interactions) and provides some form of random uniaxial anisotropy. (For an obvious reason this anisotropy field cannot be present in the paramagnetic phase). Consequently a discussion of the thermodynamic properties of a spin-glass is best given in terms of a distribution of local fields as in the random molecular field theories of Marshall (348) and others (349-352). The main fault of these early theoretical treatments was that they predicted a <u>gradual</u> onset of local ordering in contrast to the sharp phase transition observed and now proved theoretically. We note that Adkins and Rivier (413) also used the

local magnetization as the order parameter in their treatment of the susceptibility of a spin-glass. The local magnetization is, however, assumed to be due to magnetic short range order. This assumption is now clearly unnecessary. In fact magnetic short range order may occur because of magnetic forces in a spin-glass state. Observe that in both a speromagnet and a superconductor the order parameter is microscopic (the local molecular field and the Cooper pair potential respectively) whereas in a ferromagnet the order parameter is macroscopic (the spontaneous magnetization).

(c) The sharp cusp in the initial susceptibility at Tsg is extremely sensitive to an applied magnetic field (407), the effect of the field being to flatten the maximum. Such an effect would be expected for such phase transitions but there appears to be a difference (not unexpected though) in the behaviour of a speromagnet and a ferromagnet at their transition points. For a ferromagnet mean field theory predicts that the initial susceptibility should diverge at the transition point and that in the presence of an applied field the peak value of the susceptibility should vary as in equation (2.105) i.e $\chi_f^0 \sim B_0^{-2/3}$

Strictly, however, the susceptibility does not diverge at the transition point because the fluctuations are limited to a finite amplitude by the quartic term in M in the expression for the thermodynamic potential (see equation (2.258)). However, for a spin-glass the data of Cannella and Mydosh (407) for some AuFe alloys show that for the low fields used ($\lesssim 300$G) the field dependence of the susceptibility

κ at Tsg is <u>linear</u>. Specifically at Tsg

$$\chi^{o}_{max}(B_o) \simeq \chi^{o}(0) - a B_o \qquad 2.313$$

e.g. for Au 2% Fe

$$10^5 \chi_{max}(H) \simeq 23.16 - 3.3 \times 10^{-3} H \qquad 2.314$$

and for Au 8% Fe.

$$10^5 \chi_{max}(H) = 233.4 - 7.09 \times 10^{-2} H \qquad 2.315$$

where χ_{max} is in emu/cm^3 and H is in gauss. In a simple way $\chi^{o}(0)$ would represent the paramagnetic susceptibility at Tsg ($\sim \frac{C}{Tsg}$, where C is some constant) while the field dependent term allows for some demagnetization due to an anisotropy field Another interesting observation made by Cannella and Mydosh (40 was that an external field of about 100G can shift upwards the apparent spin-glass temperature by as much as 1K. This observation may be due to the effect of the applied field on any ferromagnetic clusters present in the alloy.

(d) As mentioned above once it has been agreed that a shar phase transition occurs at Tsg one can then go on to discuss many properties of the spin-glass in terms of a distribution of molecular fields. This distribution has been shown (352) to be a universal function of the reduced parameters T/c, Bo/c and Bc/c (see equation 2.300). Thus the initial susceptibilit the magnetization, and the magnetic heat capacity are universal functions of the above reduced parameters. The distribution function has also been successfully used (199) to account for the decrease in resistance at low temperatures for some dilute Au - based alloys of Fe and Mn, as well as the decrease in the thermopower and the field dependence of the latter at low

temperatures. Since no acceptable theoretical proof is presently available we shall merely accept the experimentally observed relation that

$$Tsg \propto c^{*}. \qquad 2.316$$

Thus the concentration dependence of Tsg depends on the manner in which the number of magnetic units varies with the impurity concentration. In the cluster-glass region for AuCo $c^{*} \sim c^{3}$ (91), so that $Tcg \sim c^{3}$ while in CuFe (91) and AuFe (184) $c^{*} \sim c^{2}$ so that $Tcg \sim c^{2}$ etc. For speromagnets $c^{*} = c$ and hence $Tsg \sim c$ if we neglect statistical fluctuations of concentration. The relation obtained by Sherrington and Southern (410) namely that

$$Tsg \propto c^{\frac{1}{2}} \qquad 2.317$$

is only fortuitously (and even then only approximately) valid for AuFe containing 1-8%Fe. What the empirical relationships found by Cannella and Mydosh (407) ($Tsg \sim c^{0.58}$) and by Violet and Borg (408) ($Tsg \sim c^{0.45}$) actually imply is that $c^{*} \simeq c^{\frac{1}{2}}$. In fact the data in figure 1 of reference 407 would appear to suggest that $c^{*} \sim (c-co)^{\frac{1}{2}}$ for $1 \lesssim c \lesssim 10\%$. On the other hand Tholence and Tournier (414) have shown that between about 0.03-1%Fe $Tsg \sim c$, which would mean that ferromagnetic clustering (i.e. the mictomagnetic region) becomes important for concentrations as low as about 2% Fe. This is confirmed by the positive values of the paramagnetic Curie temperature and the increasingly large values of the magneton number (see Table II of ref.407). Note that the lower bound of the linear regime determines c_m which from reference 414 would be 0.03% Fe (identified in the reference as c_K. Incidentally also there is a nagging suspicion that inspite of the small angle neutron measurements (188) the

critical concentration for the onset of ferromagnetism in Au Fe is actually less than the percolation concentration. Some evidence, such as the concentration dependence of the residual resistivity and the almost linear variation of T_c with c for c ≳ 17% Fe extrapolated to $T_c = 0$ (cf CuNi), certainly indicate that the critical concentration for ferromagnetism in Au Fe may be nearer 12% Fe than the 15-17% Fe suggested by the neutron results. We shall review the evidence elsewhere.

(e) The main argument against recognising the onset of spin-glass state as a proper phase transition is the fact that no cusp or marked discontinuity at T_{sg} has been observed in the magnetic specific heat (228, 415, 416). The expectation was engendered by the cusp observed in the initial susceptibility and by the known behaviour of the magnetic specific heat at the ferromagnetic Curie point. The observed specific heat for a spin-glass, however, has a broad maximum at a temperature that coincides with T_{sg}. Below this temperature the specific heat is linear in temperature and concentration-independent (417). Such a magnetic specific heat has been derived from the random molecular field theories of Marshall, Klein and Brout (348-350) in a two-dimensional Ising model but has been extended to a three-dimensional lattice by Souletie and Tournier (352). A detailed rederivation has also been given by Rivier (418). We have already used the results in section 2.5(xi) - see equations (2.300) to (2.302). We may write that

$$C_p^m = \gamma_{sg} T \qquad 2.318$$

where in general γ_{sg} is given (352) by

$$\gamma_{sg} = \frac{\pi^2}{6} N_c P(B_i=0) \frac{K_B^2}{\mu_B} \frac{2S}{2S+1} \qquad 2.319$$

with Nc P(Bi = 0) representing the number of spins in zero molecular field. By averaging over internal fields $0 \leq B_i \leq \frac{K_B T_{sg}}{g\mu_B}$ equation (2.319) may be reduced to equation (2.303) (318). Above Tsg we have the paramagnetic state so that one should expect the specific heat to vary as sketched in figure 2.42. The heat capacity increases

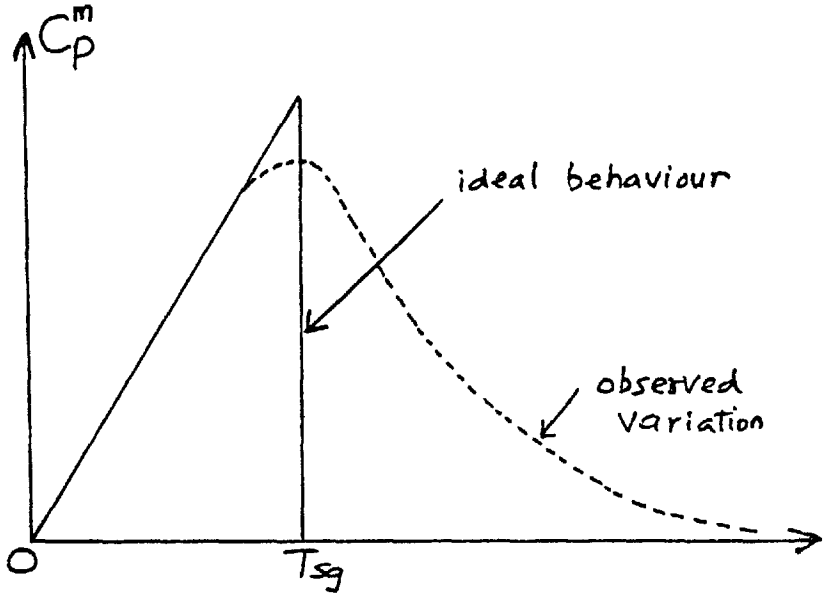

Fig. 2.42: Sketch of the temperature - dependence the heat capacity of a spin-glass

linearly with temperature up to Tsg and then <u>ideally</u> drops discontinuously to zero. The discontinuity at the transition point is

$$\Delta C_p^m = \gamma_{sg} T_{sg} \qquad 2.320$$

This is, of course, the sort of discontinuity expected for a second order phase transition - compare with figure 2.14a illustrating that of a superconductor. For the latter the discontinuity at the transition point is

$$\Delta C = 1.43 \gamma_{el} T_{sc} \qquad 2.321$$

The variation sketched in figure 2.42 is a mean field result and the precipitate drop at Tsg is clearly characteristic of such a theory. In a real spin glass one would have to consider some

magnetic short range order arising either through direct near-neighbour impurity - impurity coupling (in say statistically impurity rich regions) or simply through the action of magnetic dipolar forces creating what has been called "monodomains" (414). Whatever the mechanism is the important point is that some clusters exist just beyond Tsg and would contribute to the specific heat. Thus the sharp corners in figure 2.42 become rounded off and the heat capacity gradually falls to zero at some temperature above Tsg (see dotted curve in figure 2.42). We shall not attempt any inspired guess as to the form of the temperature variation of the heat capacity above Tsg. In the case of only clusters of the same size we showed that above the cluster-glass temperature the heat capacity is given by the Schottky function (equation (2.298)). While such a possibility cannot be totally ruled out for a speromagnet it would be more plausible to expect much smaller clusters - pairs, triplets etc. Thus for LaGd Bonnerot et al. (419) observed that for $T > Tsg$

$$\Delta C_p^m \sim \frac{A(c^2)}{T^2} \qquad 2.322$$

while for some PdFe alloys ($c \leq 0.115\%$ Fe; recall that $c_f = 0.12\%$Fe as in figure 2.30) Chouteau et al. (420) observed that

$$\Delta C_p^m (T > "T_c") \sim \frac{A(c^2)}{T} - \frac{B(c^3)}{T^2} \qquad 2.323$$

but this was only over a very limited range (about 1 - 2.5K) so that we should treat the equation with some caution. However, Smith (416) also observed that $\Delta C_p^m \sim \frac{A(c^2)}{T}$ for $T > Tsg$ in ZnMn alloys. We shall therefore conclude that it may not be possible to observe the discontinuity at Tsg

(certainly no cusp is to be expected) but the failure to do so should not be construed to mean an absence of a proper phase transition. In this connection it is significant that a maximum occurs in the temperature derivative of the impurity resistivity at a temperature coinciding with that of the maximum in the heat capacity. As discussed towards the end of section 2.5 (ix) such behaviour is expected at a phase transition point.

(f) The electrical resistivity of spin-glasses has been discussed by a number of investigators (93, 94, 421). The experimental results (93, 421) show that at the lowest temperatures the impurity resistivity has a $T^{3/2}$ dependence which is followed by a T- dependence in the region near Tsg while at higher temperatures a resistance m aximum occurs. Apparently the $T^{3/2}$ regime at low temperatures has a lower bound below which the resistivity goes as T^2 (93, 422). A theoretical explanation of the observed $T^{3/2}$ dependence has been proposed by Rivier and Adkins (94) in terms of the scattering of conduction electrons by highly damped spin-wave modes otherwise referred to as spin diffusion modes. The explanation, especially in the absence of any other, seems plausible enough although it suffers the very serious handicap of not being able to reproduce the resistivity maximum that is observed in a wide range of alloys. In AuFe the resistivity maximum is observed over more than two decades of the impurity concentration from about 0.04% Fe (423) to at least 5% Fe (421). Clearly any theory of the electrical resistivity of alloys must give a resistance maximum at least for a certain impurity concentration range. However, in order to aid the search for a satisfactory

theory of the resistivity of spin glasses it must first be shown beyond all reasonable doubt that the $T^{3/2}$ low observed is not a cross-over regime between a T^2 region at very low temperatures and a T regime just below the resistance maximum. Ford and Mydosh (93) did recognise the possibility of the $T^{3/2}$ law being replaceable by $(aT + bT^2)$ dependence. Such a polynomial will not be unusual. The resistivity of pure Fe and Ni appear to obey such an expression at very low temperatures $(\lesssim 4K)$(424). Once this doubt is cleared the next problem would be to establish the validity of the $T^{3/2}$ law in the speromagnetic region. In AuFe this region extends from C_m ($\sim 0.03\%$) to about 1% as already mentioned above. Unfortunately even though suitable data exist in this concentration region no discussion of the temperature dependence of the resistivity appears to have been given. A preliminary examination of these data shows that below the resistance maximum the resistivity is again linear in T; the measurements did not extend to sufficiently low temperatures for any deviation from linearity to be observed. We can thus take it that a linear region always exists at least just below the resistance maximum. (This would confirm the statement made in section 2.2 that the temperature of the resistance maximum would be proportional to the impurity concentration).

Spin diffusion is, of course, the simplest form of an excitation that can occur in a magnetic system without long range magnetic order. Its theory in the region just above the ferromagnetic Curie point has long been known, and it is essentially a hydrodynamic description of the magnetization in the system. Consequently it is valid over large distances and for long time

intervals. One should thus expect the spin diffusion concept to remain valid at least up to Tsg especially when the latter is small. It is therefore paradoxical, in our view, that the range of validity of the $T^{3/2}$ law is smallest for the lowest Fe concentrations e.g. for Au 1% Fe the $T^{3/2}$ law is strictly valid between $\sim 0.5 - 1.6\,K$! whereas Tsg $\simeq$ 8.5K. More interestingly the range of validity increases rather rapidly beyond about 2% (the approximate upper limit of the speromagnetic regime) and in fact at 12% Fe the range extends to 1.1Tsg as one would expect. This observation tends to confirm our suspicion that, as formulated, the spin diffusion concept is only applicable in the mictomagnetic region where magnetic short range order exists (in the ferromagnetic clusters). Another way of looking at this problem is to consider the diffusion equation itself i.e.

$$\frac{\partial}{\partial t} G(\underline{r},t) = \Lambda \nabla^2 G(\underline{r},t) \qquad 2.324$$

where

$$G(\underline{r},t) = \langle S^{\alpha}(0)\, S^{\alpha}_{r}(t) \rangle \qquad 2.325$$

is the spin pair correlation function, and Λ is the diffusion constant.

In an ideal spin-glass $G(\underline{r},t)$ is zero, by definition at least, so that equation (2.324) vanishes trivially. A non-trivial solution is only possible if $G(\underline{r},t)$ is non- zero which clearly requires some magnetic order even if short range. But then the question arises - is the existence of only short range order compatible with the hydrodynamic description of the magnetization required by the spin diffusion concept? We shall not pursue this question any further here. It will be sufficient to merely state that the spin diffusion modes approximation will

get better as the alloy becomes more mictomagnetic, with ferromagnetic clusters spanning tens of lattice spacings. In this limit, however, one could equally use the theory proposed by Long and Turner (425) and Mills et al (426) in which a similar $T^{3/2}$ law is obtained by assuming the non-conservation of momentum in the scattering of conduction electrons by spin-waves in a random alloy. The similarity is not surprising because to conduction electrons ferromagnetic clusters or polarization clouds are equivalent as long as their spatial extent is much larger than the electron mean free path. The spin diffusion concept could apply also to the cluster-glass region preceding the onset of ferromagnetism in "giant moment alloys".

In order to calculate the resistivity of speromagnets we need to consider the Hamiltonian

$$\mathcal{H} = \mathcal{H}_s + \mathcal{H}_{sd} + \mathcal{H}_v \qquad 2.326$$

where $\mathcal{H}_s$ is the Hamiltonaian for the conduction electrons (equation (1.15)), $\mathcal{H}_{sd}$ is the Hamiltonain for the scattering of conduction electrons by localized impurity spins and $\mathcal{H}_v$ is the potential scattering term. $\mathcal{H}_{sd} + \mathcal{H}_v$ constitute the perturbation on $\mathcal{H}_s$ and in the usual electron operators are given by

$$\mathcal{H}_{sd} = -\frac{1}{N}\sum_{\substack{k,k'\\ q,l}} J(q)\, e^{iq\cdot l}\left\{\left[c^+_{k'\uparrow}c_{k\uparrow} - c^+_{k'\downarrow}c_{k\downarrow}\right]S^z_l + c^+_{k'\downarrow}c_{k\uparrow}S^+_l + c^+_{k'\uparrow}c_{k\downarrow}S^-_l\right\} \qquad 2.327$$

$$\mathcal{H}_v = \frac{1}{N}\sum_{\substack{k,k'\\ q,l}} V e^{iq\cdot l}\left\{c^+_{k'\uparrow}c_{k\uparrow} + c^+_{k'\downarrow}c_{k\downarrow}\right\} \qquad 2.328$$

with $q_v = k' - k$. These equations are, of course, identical to equation (1.31) except that J and V have nothing to do with the parameters $\langle V_{sd} \rangle$, U and ϵ_d . The perturbation calculation has been worked out in the first Born approximation (i.e. second order perturbation theory expansion in J) by Kasuya (24) and Yosida (25) and in this limit the impurity resistivity $\Delta\rho_{KY}$ is given by

$$\Delta\rho_{KY} = R_m \rho_s(\varepsilon_F) c\{V^2 + J^2 S(S+1)\} \qquad 2.329$$

where Rm and $\rho_s(\varepsilon_F)$ have been defined earlier (see section 1.7). The first term in equation (2.329) can be expressed in terms of the phase shifts η_d as in equation (1.12) or (2.220).

Also in this first Born approximation one derives the indirect coupling between the impurity spins i.e. the RKKY interaction (equation (1.72)). As explained in section 1.7 Kondo extended the calculation to the second Born approximation and was able to obtain a temperature-dependent contribution to the resistivity. Thus to the third order in J we can write

$$\Delta\rho(T) = \Delta\rho_{KY} + \Delta\rho_{Kondo} \qquad 2.330$$

$$= R_m \rho_s(\varepsilon_F) c\{V^2 + J^2 S(S+1)\} + 4R_m \rho_s^2(\varepsilon_F) c J^3 S(S+1) \ln \frac{K_B T}{W} \qquad 2.331$$

where clearly $\Delta\rho_{Kondo}$ refers to the second term in equation (1.35). When J is negative (afm coupling) the above expression gives an increasing resistivity at low temperatures which when combined with the decreasing phonon resistivity gives rise to a resistance minimum. The temperature of this minimum has a characteristic dependence on the impurity concentration

($\propto C^{1/5}$). As T $\longrightarrow$ 0 the expression however diverges (the "Kondo divergence") and this had been previously taken to indicate the loss of the magnetic moment of the impurity atoms, thus necessitating the use of expressions such as "spin-compensated state", strong impurity spin - conduction electron coupling" etc . However as explained in section 2.2 and particularly in section 2.5 (Vii) the Kondo divergence has nothing to do with the magnetic - non magnetic transition. The latter is essentially a <u>single impurity effect</u> and as such one should not expect the concentration dependence found for the temperature of the resistance minimum and, in any case, the moment on the impurity spin never really disappears. What happens is that the magnetic moment becomes observable only under special conditions once the observation temperature becomes smaller than the characteristic temperature of the spin (the spin fluctuation temperature). Kondo's expression diverges simply because the perturbation theory leading to it becomes invalid at a temperature, T_o, such that the thermal energy is of the order of the interaction energy between the impurity spins i.e.

$$K_B T_o \sim \mathcal{H}_{RKKY} \quad . \qquad 2.332$$

We shall again remind ourselves that summing the perturbation expansion to infinite order does not remove the Kondo divergence. For example Abrikosov (430) obtained

$$\Delta\rho_{Kondo} \sim \left\{ V^2 + \frac{J^2 S(S+1)}{\left[1 - 2J\rho_s(\varepsilon_F) \ln \frac{T}{T_F}\right]^2} \right\} \qquad 2.333$$

which again diverges at $T_k \simeq T_F \exp\left(-\frac{1}{2J\rho_s(\varepsilon_F)}\right)$ (see also equation (1.39)). It will be useful to check if To relates

to Tk as given above. Meanwhile we can perhaps take To to correspond to the temperature of the resistance maximum (see figure 2.4) and, for an order of magnitude estimate, let it be the interaction energy between neighbouring impurity spins. Writing

$$J(r) \sim \frac{A \cos 2K_F r}{(2K_F r)^3}$$

then

$$K_B T_o \sim \frac{AS}{(2K_F r_{av})^3} \qquad 2.334$$

where r_{av} is given by equation (2.83) i.e.

$$r_{av} = 0.554\, c^{-\frac{1}{3}} a_o$$

For AgMn, $\frac{A}{K_B}\{2K_F a_o\}^{-3} \simeq$ 220K (429);

thus $T_o \sim 12.94\, cS$, 2.335

with c in atomic percent. For Mn S $\simeq$ 2.5 giving

$$T_o = 32.4\ cK\ .$$

It will be of interest to see if T_o correlates with the temperature at which the tail in the heat capacity of spin-glasses vanishes. We note that Chouteau et al (420) used such a pair interaction in an attempt to derive the form of the specific heat (equation (2.323)) observed in PdFe below the critical concentration in the temperature range $T_{cg} < T < 3K$. It would mean that the maximum value of T_o for these alloys is about 3K. At some temperature T_{sg} below T_o the spin-glass state sets in. According to the cluster-model of spin-glasses propounded by Smith (429) this temperature corresponds to the formation of a colli-near infinite cluster and is given by

$$K_B T_{sg} \simeq \frac{A S_c}{18\pi \delta_o \gamma x} \qquad 2.336$$

where $\delta_0 = 2.7$ and $x \sim 1$. ν is the valency of the host metal. Again for AgMn $\frac{A}{K_B} \simeq 7.6 \times 10^4$ K giving

$$T_{sg} = 4.98 c\, S \text{ K (c in at.\%)}$$
$$\approx 12.44 c \text{ K}$$

with $S = 2.5$.

Hence $$T_0 \sim 2.6\, T_{sg}. \qquad 2.337$$

In the spin-glass state one ought to discuss the electrical resistivity in terms of the scattering of conduction electrons by impurity spins which are subject to internal, albeit, random exchange fields. Clearly such a consideration must alter the nature of the conduction electron scattering because hitherto it has been tacitly assumed that both the auto- and pair- spin correlation functions vanish.

$$G_s(0,t) \equiv \langle S_i^\alpha(0)\, S_i^\alpha(t) \rangle = 0$$
$$G(r,t) \equiv \langle S_i^\alpha(0,0)\, S_j^\alpha(r_{ij},t) \rangle = 0$$
$$\alpha = x, y, z.$$

However in the spin glass state we have seen that

$$q(T) \equiv \lim_{t\to\infty} \langle S_i^\alpha(0)\, S_i^\alpha(t) \rangle \neq 0 \; ; \; T \leq T_{sg}$$
$$= 0 \; ; \; T > T_{sg}$$

(equation (2.312)). $G(r,t)$ may still be presumed zero if there is no magnetic short range order. The question then follows:- does the finiteness of $q(T)$ imply that one has to consider only the $s^z S^z$ term in $\mathcal{H}_{sd}$? The answer is a qualified no because $q(T)$ is only finite if we average over a sufficiently long time interval. For shorter time intervals $q(T)$ may be zero for $T < T_{sg}$. Thus one can still consider scattering processes in which the impurity spin is

flipped but only for a short time interval, in fact, short enough that before another scattering event the impurity spin must have lost all memory of the previous one. Hence once again we have the ubiquitous spin fluctuations!; the temperature dependence of the resulting resistivity is already well-known. In this case the spin-fluctuation temperature is simply T_{sg} so that if $\Delta\rho_{sg}(T)$ is the impurity resistivity in the spin-glass regime then

$$\Delta\rho_{sg}(T) \sim \left(\frac{T}{T_{sg}}\right)^2 \quad \text{for } T \ll T_{sg},$$

$$\sim \frac{T}{T_{sg}} \quad \text{for } 0.1T_{sg} \lesssim T \lesssim T_{sg} \text{ (or } T_0).$$

For $T > T_{sg}$ we should of course get the usual Kondo resistivity, $\sim J^3 \ln T$. For $J < 0$ this $\ln T$ term is negative and a resistance maximum may be obtained. ν_{sg} $\left(\equiv \frac{K_B T_{sg}}{h}\right)$ is thus a measure of the inverse lifetime of the components of the localized and well-defined spin. It is trivial to stress that these spin fluctuations are different (in energy and origin) from those involved in the magnetic-nonmagnetic transition in the magnetic phase diagram. Recall from equation (2.12) that the width of the VBS is given by

$$\Delta = \Delta_{sd} + \Delta_{so} + \Delta_{dd}$$

which can be rewritten as

$$\Delta = \Delta_{s\uparrow d\uparrow} + \Delta_{s\uparrow d\downarrow} + \Delta_{so} + \Delta_{dd} \qquad 2.338$$

where the first term represents the broadening due to the s-d hybridization and the second term gives the broadening due to s-d exchange mixing. The other terms have already been defined. It is $\Delta_{s\uparrow d\downarrow}$ which may be represented by

$\mathcal{H}_{sd}$ in which J_{sd} is necessarily afm, irrespective of either the host or the impurity. The spin fluctuation temperature is, in the case of the VBS, given by equation (2.8) i.e. $T^*_{imp} = T_f e^{-\frac{\pi \Delta_0}{2\Delta}}$ and thus involves the intra-atomic exchange splitting. Strictly, Δ in the above formula should be replaced by $\{\Delta - \Delta_{s\uparrow d\uparrow}\}$. In the case of the thermally induced spin fluctuations in a spin-glass J may be positive or negative depending on both the impurity and host.

It therefore would appear that the $T^{3/2}$ law observed at low temperatures for speromagnets is the transition region between the T^2 and T regimes. Since $T_{sg} \propto C$, the coefficient of the T^2 term is inversely proportional to C while that of the T term is independent of C. One can thus expect a slow decrease in the coefficient of the pseudo $T^{3/2}$ term as the impurity concentration increases. However, in mictomagnets and in giant moment alloys near the critical concentration where ferromagnetic clusters and polarization clouds respectively are known to exist one can use the spin diffusion model of Adkins and Rivier (94) and in such cases the $T^{3/2}$ law should be valid over a relatively large temperature range.

It should be noted that Harrison and Klein (427) used the random molecular field model to calculate $\rho_{sg}(T)$. They obtained the linear temperature dependence below T_0 with a slope which was independent of concentration. Also we recall that Laborde and Souletie (287) had proposed a form of the spin fluctuation resistivity in AuFe alloys which explicitly took into account the impurity-impurity interactions namely

$$\rho_{sf}(T) \sim \cos 2\delta_V f(T) G\left(\frac{W_{oc}}{T}\right) \qquad \text{(equation 2.227)}$$

where $G(\frac{W_{oc}}{T})$ allows for RKKY interactions ($W_o \equiv (\frac{A}{2k_F})^3$ used above). They obtained that $G(\frac{W_{oc}}{T}) \sim \exp\{-D/T \sin^2 2\delta_m(T)\}$ with $D \propto C$, but this expression is apparently only valid in the cluster-glass region where residual magnetism occurs. However, inspite of all the foregoing discussion it would still be useful to investigate how the RKKY coupling is modified in the second Born approximation—perhaps an explicit expression for an s-d Hamiltonian appropriate to the spin-glass regime may be obtained. We had earlier (section 2.2) mentioned that Matho and Beal-Monod (98) considered RKKY pair interactions and by carrying out the calculation to the third order in J they were able to reproduce the resistivity maximum for some alloys. However, their calculation was done in the context of a Kondo effect (i.e. the magnetic-nonmagnetic transition) but we did suggest that a suitable modification of that approach could be usefully applied to spin-glasses.

(g) The preceding section shows that it may not be necessary to assume that the linear heat capacity of a spin-glass is due to those spins sitting in a zero molecular field (see sections 2.5(xi) and 2.8(e)). Below T_{sg} the thermal fluctuation energy at a temperature T is "renormalized" to $K_B \frac{T}{T_{sg}}$ so that the heat capacity of a spin-glass containing a concentration, c*, of almost identical magnetic units is given by

$$C_V^m = 3c^* K_B \frac{T}{T_{sg}} \qquad 2.339$$

which should be compared with

$$C_V^m = \frac{2S}{2S+1} \frac{\pi^2}{3} c^* K_B \frac{T}{T_{cg}} \quad . \qquad 2.340$$

obtained from equations (2.302) and (2.303). Since in all known cases $S > 1$ equations (2.339) and (2.340) are nearly equivalent. Equation (2.339) is useful because it shows that the coefficient of this temperature-linear heat capacity may also be used to obtain c*, in addition to magnetization measurements already outlined in section 2.5(xi).

(h) A final comment refers to our first one, i.e. the fact that a spin-glass state is well-defined, meaning that it has a <u>unique</u> equilibrium state. Any time-dependent effects are non-equilibrium properties and are observable only because a spin-glass can be considered to be extremely "magnetically" viscous, with a very long relaxation time. The true equilibrium properties can only be determined when the observation time tends to infinity - something that might task the patience of a Job.

CHAPTER 3

The Theory of Thermal Neutron Scattering

3.1 A General Theory of Magnetic Neutron Scattering

We consider the scattering cross-section due to the magnetic interaction between a neutron and the magnetic field of unpaired electrons in an atom. In doing so we shall follow the treatment given by Marshall and Lovesey (431) and by Squires (432).

A typical scattering set-up is as sketched in figure 3.1. A fairly uniform beam of thermal neutrons (i.e. with energy in the range 1-200 meV) is incident on a scatterer which may be regarded as a collection of electrons and nuclei. The scattered neutrons are monitored by a suitable neutron detector.

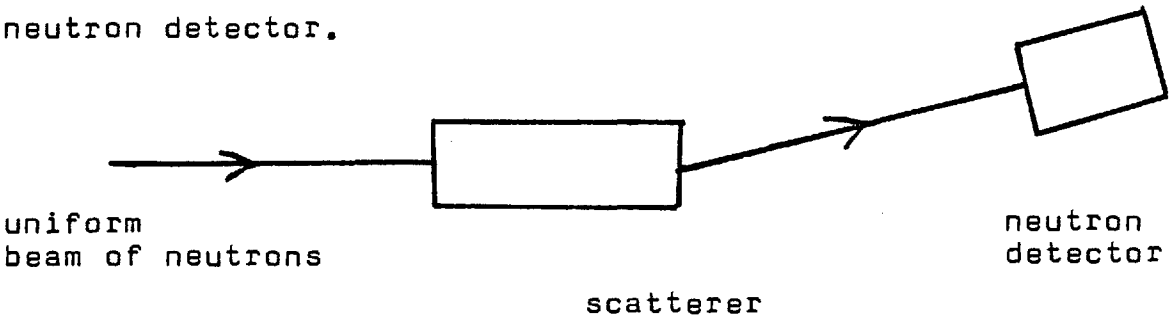

Fig.3.1: A Typical Scattering Problem

The problem is then to relate the observed intensity and distribution of the scattered neutrons, usually expressed as a cross-section, to the properties of the scatterer. In the particular case of magnetic scattering where the fact that a neutron possesses a magnetic moment is utilized we seek to obtain some information about the magnetic structure and dynamics of the scatterer.

If E, E' denote the energies of an incident and a

scattered neutron respectively and $d\Omega$ is an element of a solid angle we can define the following cross-sections:-

(a) the partial differential cross-section, $\frac{d^2\sigma}{d\Omega\, dE'}$;

$$\frac{d^2\sigma}{d\Omega\, dE'} \equiv \frac{\text{number of neutrons scattered per second into } d\Omega \text{ with energy between } E^1 \text{ and } E^1+dE^1}{d\Omega \times dE^1 \times \text{incident flux.}} \qquad 3.1$$

(b) the differential cross-section, $\frac{d\sigma}{d\Omega}$;

$$\frac{d\sigma}{d\Omega} \equiv \int_0^\infty \left\{\frac{d^2\sigma}{d\Omega\, dE'}\right\} dE' \qquad 3.2$$

$$= \frac{\text{number of neutrons scattered per second into } d\Omega}{d\Omega \times \text{incident flux}}$$

(c) the total cross-section, σ_{tot}

$$\sigma_{tot} = \int \frac{d\sigma}{d\Omega}\, d\Omega \qquad 3.3$$

= total number of neutrons scattered in all directions per second per unit incident flux.

We shall be chiefly interested in the differential cross-section; the partial differential cross-section gives the most information about a target system but correspondingly it is the most difficult to measure.

Next we specify the initial and final states of the neutron and target system as follows:

$$\left.\begin{array}{l}\underline{\text{initial state}}: P \\ \text{neutron } \underline{K}, E \\ \text{target system } \lambda, E_\lambda\end{array}\right\} + \text{interaction potential, } \hat{V} \longrightarrow \left\{\begin{array}{l}\underline{\text{final state}}: P' \\ \underline{K}', E' \\ \lambda', E_{\lambda'}\end{array}\right.$$

$\underline{K}$, $\underline{K}'$ are the initial and final wavevectors respectively of

the neutron; λ and λ' denote all parameters necessary to completely specify the initial and final states of the target system. The combined state $|\underline{K},\lambda\rangle$ of the neutron and target system may for convenience be denoted by P. Similarly for $|\underline{K}',\lambda'\rangle = P'$. The probability of transitions $P \longrightarrow P'$ is given by Fermi's golden rule (first Born approximation)

$$W_{P\to P'} = \frac{2\pi}{\hbar} \rho_{K'} \left| \langle P'|\hat{V}|P\rangle \right|^2 \qquad 3.4$$

where $\rho_{K'}$ is the density of final scattering states per unit energy range. The differential cross-section is then given by

$$\left(\frac{d\sigma}{d\Omega}\right)_{P\to P'} = \frac{W_{P\to P'}}{d\Omega \times \text{incident flux}}$$

$$= \frac{2\pi}{\hbar} \frac{\rho_{K'}}{d\Omega} \frac{\left|\langle P'|\hat{V}|P\rangle\right|^2}{\text{incident flux}} \qquad 3.5$$

Assuming the target system is enclosed in a box it is trivial to show that equation(3.5) reduces to

$$\left(\frac{d\sigma}{d\Omega}\right)_{P\to P'} = \frac{K'}{K}\left(\frac{M}{2\pi\hbar^2}\right)^2 \left|\langle P'|\hat{V}|P\rangle\right|^2 \qquad 3.6$$

where M is the neutron mass.

The conservation of energy is now built into the cross-section by introducing a delta-function

$$\delta(E_\lambda - E_{\lambda'} + E - E') \equiv \delta(\hbar\omega + E_\lambda - E_{\lambda'})$$

where $\hbar\omega = \frac{\hbar^2}{2M}(K^2 - K'^2)$

Finally equation (3.6) is summed over all the final states, λ', of the target and averaged over all the initial states,

λ , which occur with a probability P_λ . We also average over the spin states σ, σ' of the neutron, with P_σ representing the probability distribution of the incident neutrons We then obtain the expression

$$\frac{d^2\sigma}{d\Omega dE'} = \sum_{\lambda\sigma} P_\lambda P_\sigma \sum_{\lambda',\sigma'} \left(\frac{d^2\sigma}{d\Omega dE'}\right)_{\substack{\lambda\\\sigma}} \Big\} \rightarrow \Big\{ \begin{matrix}\lambda'\\ \sigma'\end{matrix} \qquad 3.7$$

where

$$\left(\frac{d^2\sigma}{d\Omega dE'}\right)_{\substack{\lambda\to\lambda'\\ \sigma\to\sigma'}} = \left(\frac{M}{2\pi\hbar^2}\right)^2 \frac{k'}{k} \left| \langle \lambda'\sigma' k' | \hat{V} | k\sigma\lambda \rangle \right|^2 \delta(\hbar\omega + E_\lambda - E_{\lambda'}) \qquad 3.8$$

The interaction potential, $\hat{V}$, is given by

$$\hat{V} = -\underline{\mu}_n \cdot \sum_i \underline{B}_i \quad ;$$

$\underline{\mu}_n \ (= -\gamma \mu_N \underline{\sigma})$ is the magnetic moment of the neutron; μ_N is the nuclear magneton and $\gamma = 1.91$. B_i is the magnetic induction due to the spin and orbital current of the i^{th} electron. It is given by

$$\underline{B} = -\frac{\mu_0}{4\pi} 2\mu_B \left[\nabla \wedge \left\{ \frac{\underline{s} \wedge \underline{R}}{R^3} \right\} + \frac{1}{\hbar} \frac{\underline{p} \wedge \underline{R}}{R^3} \right] \qquad 3.9$$

where $\underline{p}$ is the orbital angular momentum and $\underline{s}$ is the spin angular momentum in units of $\hbar$. μ_0 is the permeability of free space. Thus

$$\hat{V} = -\frac{\gamma \mu_0 \mu_B \mu_N}{2\pi} \underline{\sigma} \cdot \sum_i \underline{B}_i \qquad 3.10$$

Now it may be shown that

$$\sum_i \langle k' \left| \left\{ \nabla \wedge \frac{(\underline{s}_i \wedge \underline{R})}{R^3} + \frac{1}{\hbar} \frac{\underline{p}_i \wedge \underline{R}}{R^3} \right\} \right| k \rangle \equiv 4\pi \underline{Q}_\perp$$

where the operator $\underset{\sim}{Q}_\perp$ is defined as

$$\underset{\sim}{Q}_\perp = \sum_i e^{i\underline{\kappa}\cdot\underline{r}_i}\left\{\hat{\underline{\kappa}}\wedge[\underline{\sigma}_i\wedge\hat{\underline{\kappa}}] + \frac{i}{\hbar\kappa}[\underline{p}_i\wedge\hat{\underline{\kappa}}]\right\} \qquad 3.11$$

where $\underline{\kappa} = \underline{k} - \underline{k}'$, the change in the wave-vector of the incident neutron, is called the scattering vector. $\hat{\underline{\kappa}}$ is a unit vector in the direction of $\underline{\kappa}$, while $\underline{r}_i$ is the position vector of the i^{th} electron. In terms of $\underline{Q}_\perp$ equation (3.8) becomes

$$\left(\frac{d^2\sigma}{d\Omega dE'}\right)_{\lambda\sigma\to\lambda'\sigma'} = (\gamma r_0)^2\frac{k'}{k}\left|\langle\lambda'\sigma'|\underline{\sigma}\cdot\underline{Q}_\perp|\sigma\lambda\rangle\right|^2\delta(\hbar\omega + E_\lambda - E_{\lambda'}) \qquad 3.12$$

where $r_0 = \frac{\mu_0}{4\pi}\frac{e^2}{m}$ is the classical radius of an electron ($=2.818\times10^{-15}$m). Equation (3.11) can be further developed to show that $\underline{Q}_\perp$ is related to the <u>total magnetization</u> of the scattering system. It is found that

$$\underline{Q}_\perp = \hat{\underline{\kappa}}\wedge\{\underline{Q}\wedge\hat{\underline{\kappa}}\} \qquad 3.13$$

where $\underline{Q} = -\frac{1}{2\mu_B}M(\underline{\kappa})$ 3.14

and $M(\underline{\kappa})$ is the Fourier transform of the total magnetization.

The neutron spin coordinates $\underline{\sigma}$ are clearly independent of the coordinates (space and spin) of the target. Therefore we can factorize the matrix element in equation (3.12) as follows:-

$$\langle\lambda'\sigma'|\underline{\sigma}\cdot\underline{Q}_\perp|\sigma\lambda\rangle = \sum_\alpha\langle\lambda'\sigma'|\sigma_\alpha Q_{\perp\alpha}|\sigma\lambda\rangle\ ;\ \alpha = x,y,z$$
$$= \sum_\alpha\langle\sigma'|\sigma_\alpha|\sigma\rangle\langle\lambda'|Q_{\perp\alpha}|\lambda\rangle\ ;$$

for <u>unpolarized</u> neutrons

$$\sum_\sigma p_\sigma\langle\sigma|\sigma_\alpha\sigma_\beta|\sigma\rangle = \delta_{\alpha\beta}$$

so that

$$\left(\frac{d^2\sigma}{d\Omega dE'}\right)_{\substack{\lambda\sigma\to\lambda'\sigma'}} = (\gamma r_0)^2 \frac{\kappa'}{\kappa} \left|\langle\lambda'|\underset{\sim}{Q}_\perp|\lambda\rangle\right|^2 \delta(\hbar\omega + E_\lambda - E_{\lambda'})$$

$$= (\gamma r_0)^2 \frac{\kappa'}{\kappa} \langle\lambda|\, \underset{\sim}{Q}_\perp^+ |\lambda'\rangle \cdot \langle\lambda'|\, \underset{\sim}{Q}_\perp |\lambda\rangle \delta(\hbar\omega + E_\lambda - E_{\lambda'})$$

where $\underset{\sim}{Q}^+_1$ is the complex conjugate of $\underset{\sim}{Q}_1$.

$$\underset{\sim}{Q}_\perp^+ \cdot \underset{\sim}{Q}_\perp = \sum_{\alpha,\beta} \{\delta_{\alpha\beta} - \hat{\kappa}_\alpha \hat{\kappa}_\beta\} \tilde{Q}_\alpha^+ Q_\beta \,.$$

Therefore

$$\left(\frac{d^2\sigma}{\lambda\, d\Omega dE'}\right)_{\substack{\lambda\sigma\to\lambda'\sigma'}} = (\gamma r_0)^2 \frac{\kappa'}{\kappa} \sum_{\alpha,\beta} \{\delta_{\alpha\beta} - \hat{\kappa}_\alpha \hat{\kappa}_\beta\} \times$$

$$\langle\lambda|Q_\alpha^+|\lambda'\rangle\langle\lambda'|Q_\beta|\lambda\rangle \delta(\hbar\omega + E_\lambda - E_{\lambda'}) \qquad 3.15$$

and

$$\frac{d^2\sigma}{d\Omega dE'} = \sum_{\lambda,\lambda'} P_\lambda \left(\frac{d^2\sigma}{d\Omega dE'}\right)_{\substack{\lambda\to\lambda'\\ \sigma\to\sigma'}} \qquad 3.16$$

For spin scattering only $\underset{\sim}{Q} = \sum_i e^{i\underset{\sim}{\kappa}\cdot\underset{\sim}{r}_i} s_i$

In order to keep the notation simple we shall consider only the special case of a Bravais lattice with identical magnetic atoms. In such a case

$$\langle\lambda'|\underset{\sim}{Q}|\lambda\rangle = \sum_l e^{i\underset{\sim}{\kappa}\cdot\underset{\sim}{R}_l} \sum_\nu \langle\lambda'|\, e^{i\underset{\sim}{\kappa}\cdot\underset{\sim}{r}_\nu} s_\nu |\lambda\rangle$$

where the summation over ν refers to the electrons in a given unit cell. The above matrix element may be evaluated by using the Wigner-Eckart theorem. We obtain

$$\langle\lambda'|\underset{\sim}{Q}|\lambda\rangle = \sum_l e^{i\underset{\sim}{\kappa}\cdot\underset{\sim}{R}_l} F(\underset{\sim}{\kappa}) \langle\lambda'|\underset{\sim}{S}_l|\lambda\rangle \qquad 3.17$$

where

$$F(\underset{\sim}{\kappa}) = \int \rho_s(r)\, e^{i\underset{\sim}{\kappa}\cdot\underset{\sim}{r}}\, dr \qquad 3.18$$

$F(\kappa)$ is the Fourier transform of the normalized spin density in an atom and is called the atomic form factor. $\rho_s(r)$ is the normalized spin density i.e. if there are n unpaired electrons in the atom, $n\rho_s(r)\,dr$ gives the probability of finding any one of them in a volume dr at r. $S = \sum_\nu s_\nu$ is the net spin of an atom. Hence we finally obtain the expression

$$\frac{d^2\sigma}{d\Omega dE'} = (\gamma r_0)^2 \frac{\kappa'}{\kappa} |F(\kappa)|^2 \sum_{\alpha\beta} (\delta_{\alpha\beta} - \hat{\kappa}_\alpha \hat{\kappa}_\beta) \sum_{l,l'} e^{i\kappa\cdot(R_l - R_{l'})} \times \sum_{\lambda\lambda'} p_\lambda \langle\lambda| S_{l'}^\alpha |\lambda'\rangle\langle\lambda'| S_l^\beta |\lambda\rangle \delta(\hbar\omega + E_\lambda - E_{\lambda'}) \qquad 3.19$$

Although equation (3.19) has been derived in the case of spin scattering only it may be generalized to the case where an atom possesses both spin and orbital angular momentum. The generalization is made in the so-called "dipole approximation" in which it is assumed that the wavelength of the incident neutron is much greater than the mean radius of the orbital wavefunction of the unpaired electrons. In this limit equation (3.19) may still be considered as being valid but with the following modifications:-

(a) instead of equation (3.18) the atomic form factor is now given by

$$\frac{1}{2} g F(\kappa) = \frac{1}{2} g_s \langle j_0 \rangle + \frac{1}{2} g_L \left(\langle j_0 \rangle + \langle j_2 \rangle \right) \qquad 3.20$$

where

$$g_L = \frac{1}{2} - \frac{\{S(S+1) - L(L+1)\}}{2J(J+1)}$$

$$g_s = 1 + \frac{S(S+1) - L(L+1)}{J(J+1)}$$

and $g_L + g_S = g$, the Landé g-factor.

$$f_n(\kappa) = 4\pi \int_0^\infty j_n(\kappa r)\,\rho(r)\,r^2\,dr \qquad 3.21$$

and $j_n(\kappa r)$ is a spherical Bessel function of order n. For spin only $L=0$, $J=S$, $g_L=0$ and $g_S=2$, so that $F(\kappa) = f_0$. Using $j_0(\kappa r) = \frac{\sin \kappa r}{\kappa r}$ we recover equation (3.18).

(b) the operator $\underline{S}$ is regarded as the effective angular momentum operator, i.e. $\underline{S}$ may be either the actual spin (for atoms with $\underline{L}=0$), the total angular momentum $\underline{J}$ (for RE ions) or some effective spin operator in the case of partially quenched orbital angular momenta. With the above modifications equation (3.19) can now be written in the form

$$\frac{d^2\sigma}{d\Omega dE'} = \frac{1}{4}(\gamma r_0)^2 \frac{k'}{k} |g F(\kappa)|^2 \sum_{\alpha,\beta} (\delta_{\alpha\beta} - \hat{\kappa}_\alpha \hat{\kappa}_\beta) \sum_{l,l'} e^{i\underline{\kappa}\cdot(\underline{R}_l - \underline{R}_{l'})} \times \sum_{\lambda,\lambda'} p_\lambda \langle\lambda|S_{l'}^\alpha|\lambda'\rangle\langle\lambda'|S_l^\beta|\lambda\rangle\, \delta(\hbar\omega + E_\lambda - E_{\lambda'}) \qquad 3.22$$

3.2 Scattering Cross-section for a Paramagnet

(a) Zero Magnetic Field

In an ideal paramagnet the spins of the atoms are randomly oriented so that if the orientation of a particular spin changes there is no change in the energy of the system, i.e. $E_\lambda = E_{\lambda'}$, hence the scattering is elastic. The argument of the δ-function in equation (3.22) does not depend on λ' and the sum over λ' can be done immediately by closure:

$$\sum_{\lambda,\lambda'} p_\lambda \langle\lambda|S_{l'}^\alpha|\lambda'\rangle\langle\lambda'|S_l^\beta|\lambda\rangle = \sum_\lambda p_\lambda \langle\lambda|S_{l'}^\alpha S_l^\beta|\lambda\rangle$$

$$\equiv \langle S_{l'}^\alpha S_l^\beta \rangle_T \qquad 3.23$$

where $\langle\ \rangle_T$ denotes the thermal average at a temperature T. Thus

$$\frac{d\sigma}{d\Omega} = \frac{1}{4}(\gamma r_0)^2 |g F(K)|^2 \sum_{\alpha,\beta} (\delta_{\alpha\beta} - \hat{K}_\alpha \hat{K}_\beta) \sum_{l,l'} e^{i\underline{K}\cdot(\underline{R}_l - \underline{R}_{l'})} \langle S_{l'}^\alpha S_l^\beta \rangle_T \qquad 3.24$$

To evaluate the matrix elements we note that for a paramagnet there is, by definition, no correlation between the spins of different atoms so that

$$\langle S_{l'}^\alpha\ S_l^\beta \rangle = \langle S_{l'}^\alpha \rangle \langle S_l^\beta \rangle = 0.$$

For $l = l'$, $\langle S_l^\alpha S_l^\beta \rangle = \delta_{\alpha\beta} \langle (S_l^\alpha)^2 \rangle$

$$= \frac{1}{3}\langle S^2 \rangle = \frac{1}{3} S(S+1)$$

Equation (3.24) therefore becomes

$$\frac{d\sigma}{d\Omega} = \frac{1}{4}(\gamma r_0)^2 |g F(K)|^2 \sum_{\alpha,\beta} (\delta_{\alpha\beta} - \hat{K}_\alpha \hat{K}_\beta)\, N \frac{1}{3} \delta_{\alpha\beta} S(S+1)$$

where N is the total number of spins.

$$\therefore \left(\frac{d\sigma}{d\Omega}\right)_{B_0=0} = \frac{N}{4}(\gamma r_0)^2 |g F(K)|^2 \frac{2}{3} S(S+1) \qquad 3.25$$

Thus the cross-section is <u>isotropic</u> (as expected) and is large for large values of S. There is no coherent scattering because of the random orientation of the spins and any dependence on K arises through $F(K)$ only.

(b) <u>Finite Magnetic Field</u>

Suppose a magnetic field, Bo, is applied along the Z-axis say. The energy change when a spin state changes

$\sim \mu_B B_0$

$\sim 9\times10^{-24}$ J | for $B_0 = 1$ T;

this should be compared with the energy of the thermal neutrons $\sim K_B T$

$\sim 4\times10^{-21}$ J for $T \sim 300$ K.

Hence even in quite a large magnetic field the energy changes in the system are small compared with the energy of an incident thermal neutron. Any such changes are therefore ignored (equivalent to a static approximation); so we put $E_\lambda = E_{\lambda'}$ in the argument of the δ-function. We sum over λ' and integrate with respect to E' and again obtain equation (3.24) as in case (a) above. However the matrix elements $\langle S_{l'}^\alpha S_l^\beta \rangle_T$ are not the same.

$$\langle S_{l'}^x S_l^y \rangle = \langle S_{l'}^x S_l^z \rangle = \langle S_{l'}^y S_l^z \rangle = 0 ;$$

but

$$\langle S_{l'}^x S_l^x \rangle = \langle S_{l'}^y S_l^y \rangle = \begin{cases} 0 ; & l \neq l' \\ \frac{1}{2}\left[S(S+1) - \langle (S^z)^2 \rangle\right] ; & l = l' \end{cases}$$

and

$$\langle S_{l'}^z S_l^z \rangle = \langle S^z \rangle^2 + \delta_{l'l} \left\{ \langle (S^z)^2 \rangle - \langle S^z \rangle^2 \right\}$$

Therefore

$$\sum_{\alpha,\beta} (\delta_{\alpha\beta} - \hat{K}_\alpha \hat{K}_\beta) \langle S_{l'}^\alpha S_l^\beta \rangle_T = (1 + \hat{K}_z^2) \langle S_{l'}^x S_l^x \rangle_T + (1 - \hat{K}_z^2) \langle S_{l'}^z S_l^z \rangle_T \qquad 3.26$$

and

$$\sum_{\alpha,\beta}(\delta_{\alpha\beta}-\hat{K}_\alpha\hat{K}_\beta)\sum_{l,l'}e^{i\underline{K}\cdot(\underline{R}_l-\underline{R}_{l'})}\langle S_{l'}^{\alpha}S_l^{\beta}\rangle_T$$
$$= N(1+\hat{K}_z^2)\tfrac{1}{2}\{S(S+1)-\langle(S^z)^2\rangle\}$$
$$+N(1-\hat{K}_z^2)\left[\frac{(2\pi)^3}{V_0}\langle S^z\rangle^2\sum_{\underline{G}}\delta(\underline{K}-\underline{G})+\{\langle(S^z)^2\rangle-\langle S^z\rangle^2\}\right] \quad 3.27$$

V_0 is the volume of a unit cell and $\underline{G}$ is a reciprocal lattice vector. Equation (3.27) shows that the differential cross-section consists of two terms - a coherent term and and incoherent term.

$$\left(\frac{d\sigma}{d\Omega}\right)^{coh}_{B_0\neq 0}=\frac{N}{4}(\gamma r_0)^2|gF(K)|^2(1-\hat{K}_z^2)\langle S^z\rangle^2\frac{(2\pi)^3}{V_0}\sum_{\underline{G}}\delta(\underline{K}-\underline{G}) \quad 3.28$$

This term is proportional to the square of the average value of the z-component of the spin and is zero when $\underline{K}$ is in the direction of $\underline{B}o$. The incoherent (or diffuse) scattering cross-section is given by

$$\left(\frac{d\sigma}{d\Omega}\right)^{inc}_{B_0\neq 0}=\frac{N}{4}(\gamma r_0)^2|gF(K)|^2\left\{\tfrac{1}{2}S(S+1)+\tfrac{1}{2}\langle(S^z)^2\rangle-\langle S^z\rangle^2\right.$$
$$\left.+\hat{K}_z^2\left[\tfrac{1}{2}S(S+1)-\tfrac{3}{2}\langle(S^z)^2\rangle+\langle S^z\rangle^2\right]\right\} \quad 3.29$$

which shows that it is proportional to the square of the fluctuations of both the transverse and the z-components of the spin. A part of this scattering is isotropic while the other part is anisotropic ($\propto \hat{K}_z^2$). If θ is the angle between the directions of the scattering vector and the magnetic field measured in a plane perpendicular to the direction of the beam then $\hat{K}_z^2=\cos^2\theta$, and we can write equation (3.29) in the simple form

$$\left(\frac{d\sigma}{d\Omega}\right)^{inc}_{B_0\neq 0}=a+b\cos^2\theta \quad 3.30$$

$\langle S^z \rangle$ and $\langle (S^z)^2 \rangle$ may be evaluated in the usual manner to give

$$\langle S^z \rangle = (S+1/2)\coth(S+1/2)u - \tfrac{1}{2}\coth\tfrac{1}{2}u \qquad 3.31$$

and

$$\langle (S^z)^2 \rangle = S(S+1) - \coth\tfrac{1}{2}u \langle S^z \rangle$$
$$\equiv \frac{1}{4}\frac{\cosh u+3}{\cosh u-1} + (S+1/2)^2 - (S+1/2)\coth(S+1/2)u \coth\tfrac{1}{2}u \qquad 3.32$$

where $u = \dfrac{g\mu_B B_0}{K_B T}$.

At high fields and low temperatures $u \to \infty$ and both $\coth(S+1/2)u$ and $\coth\frac{1}{2}u$ tend to unity so that $\langle S^z \rangle = S$ and $\langle (S^z)^2 \rangle = S^2$, as may be expected.

On the other hand at low fields and high temperatures i.e. $u \to 0$, $\coth u \to \frac{1}{u} + \frac{u}{3}$ and thus

$$\langle S^z \rangle \longrightarrow \tfrac{1}{3}S(S+1)u$$

$$\langle (S^z)^2 \rangle \longrightarrow \tfrac{1}{3}S(S+1) .$$

In the limit Bo=0 ($\Rightarrow u=0$) the cross-section given by equation (3.29) becomes identical to that given by equation (3.25), as it should.

3.3 Elastic Diffuse Scattering From Binary Alloys

(a) Derivation of Essential Equations:

We go back to equation (3.22) and use

$$\delta(\hbar\omega + E_\lambda - E_{\lambda'}) = \frac{1}{2\pi\hbar}\int_{-\infty}^{\infty} dt\, e^{-i\omega t} e^{-i/\hbar(E_\lambda - E_{\lambda'})t} \quad ;$$

Thus

$$\langle\lambda|S_{l'}^{\alpha}|\lambda'\rangle\langle\lambda'|S_{l}^{\beta}|\lambda\rangle\,\delta(\hbar\omega+E_\lambda-E_{\lambda'})$$
$$=\frac{1}{2\pi\hbar}\int_{-\infty}^{\infty}dt\,e^{-i\omega t}\langle\lambda|S_{l'}^{\alpha}\,e^{\frac{i}{\hbar}\mathcal{H}t}|\lambda'\rangle\langle\lambda'|S_{l}^{\beta}\,e^{-\frac{i}{\hbar}\mathcal{H}t}|\lambda\rangle$$

where $\mathcal{H}$ is the Hamiltonian of the target system. By closure

$$\sum_{\lambda'}\langle\lambda|S_{l'}^{\alpha}\,e^{i\mathcal{H}t/\hbar}|\lambda'\rangle\langle\lambda'|S_{l}^{\beta}\,e^{i\mathcal{H}t/\hbar}|\lambda\rangle$$
$$=\langle\lambda|S_{l'}^{\alpha}\,e^{i\mathcal{H}t/\hbar}\,S_{l}^{\beta}\,e^{-i\mathcal{H}t/\hbar}|\lambda\rangle$$
$$\equiv\langle\lambda|\,S_{l'}^{\alpha}\;S_{l}^{\beta}(t)|\lambda\rangle$$

where $S_l^{\beta}(t)$ is the Heisenberg operator for S_l^{β}.

Further

$$\sum_{\lambda}p_\lambda\langle\lambda|\,S_{l'}^{\alpha}\;S_{l}^{\beta}(t)\,|\lambda\rangle=\langle S_{l'}^{\alpha}\;S_{l}^{\beta}(t)\rangle_T$$

as already used in equation (3.23). Equation (3.22) thus reduces to

$$\frac{d^2\sigma}{d\Omega dE'}=\frac{1}{4}(\gamma r_0)^2\frac{K'}{K}|gF(K)|^2\sum_{\alpha,\beta}(\delta_{\alpha\beta}-\hat{K}_\alpha\hat{K}_\beta)$$
$$\times\frac{1}{2\pi\hbar}\sum_{l,l'}\int_{-\infty}^{\infty}dt\,e^{-i\omega t}\,e^{i\underline{K}\cdot(\underline{R}_l-\underline{R}_{l'})}\langle S_{l'}^{\alpha}\,S_{l}^{\beta}(t)\rangle_T$$

3.33

or more compactly,

$$\frac{d^2\sigma}{d\Omega dE'}=\frac{1}{4}(\gamma r_0)^2\frac{K'}{K}|gF(K)|^2\sum_{\alpha,\beta}(\delta_{\alpha\beta}-\hat{K}_\alpha\hat{K}_\beta)\,S^{\alpha\beta}(K,\omega)$$

3.34

with

$$S^{\alpha\beta}(\underline{K},\omega)=\frac{1}{2\pi\hbar}\sum_{l,l'}\int_{-\infty}^{\infty}dt\,e^{-i\omega t}\,e^{i\underline{K}_\alpha(\underline{R}_l-\underline{R}_{l'})}\langle S_{l'}^{\alpha}\,S_{l}^{\beta}(t)\rangle_T$$

3.35

or

$$S^{\alpha\beta}(\kappa,\omega) = \frac{1}{2\pi\hbar}\int_{-\infty}^{\infty} dt\, e^{-i\omega t} \langle S^{\alpha}(-\kappa,0)\, S^{\beta}(\kappa,t)\rangle_T \qquad 3.36$$

where

$$S(\kappa,t) = \sum_m e^{i\underline{\kappa}\cdot\underline{R}_m} S_m(t) \qquad 3.37$$

$S^{\alpha\beta}(\kappa,\omega)$ is, of course, the scattering function which is the spatial and time Fourier transform of the time-dependent spin pair correlation function.

For systems with only exchange coupling equation (3.34) becomes (269)

$$\frac{d^2\sigma}{d\Omega dE'} = \frac{1}{4}(\gamma r_0)^2 \frac{\kappa'}{\kappa} |gF(\kappa)|^2 \sum_{\alpha} (1-\hat{\kappa}_\alpha^2)\, S^{\alpha\alpha}(\kappa,\omega) \qquad 3.38$$

The elastic part of this cross-section is

$$\left(\frac{d\sigma}{d\Omega}\right)_{el} = \frac{1}{4}(\gamma r_0)^2 |gF(\kappa)|^2 \sum_{\alpha} (1-\hat{\kappa}_\alpha^2)\, S^{\alpha\alpha}(\kappa) \qquad 3.39$$

with

$$S^{\alpha\alpha}(\kappa) = \langle S^{\alpha}(-\kappa)\, S^{\alpha}(\kappa)\rangle \qquad 3.40a$$

$$\equiv \sum_{l,l'} e^{i\underline{\kappa}\cdot(\underline{R}_l - \underline{R}_{l'})} \langle S_{l'}^{\alpha} S_l^{\alpha}\rangle \qquad 3.40b$$

In applying equation (3.39) to binary alloys we shall make the following modifications;

(i) only a <u>collinear</u> system will be considered i.e. one in which the time-averaged magnetic moments are parallel to a given direction which will be chosen as the z-axis.

(ii) the magnetogyric ratios and form factors for the two constituents of an alloy will be assumed to be different;

(iii) for convenience we replace

$g_n \langle S_n^z \rangle$ by μ_n, and $\underline{R}_l$ by just $\underline{l}$.

With these modifications we now have that

$$\left(\frac{d\sigma}{d\Omega}\right)_{el} = \frac{1}{4}(\gamma r_0)^2 (1-\hat{K}_z^2) \sum_{l,l'} e^{i\underline{K}\cdot(\underline{l}-\underline{l}')} F_l \mu_l F_{l'} \mu_{l'} \qquad 3.41$$

Equation (3.41) shows that the cross-section depends upon the precise distribution of the magnetic moments. If we <u>assume</u> that this distribution is <u>random</u> then we can define an average cross-section for the system as

$$\left(\frac{d\sigma}{d\Omega}\right)_{el} = \frac{1}{4}(\gamma r_0)^2 (1-\hat{K}_z^2) \sum_{l,l'} e^{i\underline{K}\cdot(\underline{l}-\underline{l}')} \langle F_l \mu_l F_{l'} \mu_{l'} \rangle \qquad 3.42$$

For a ferromagnetic alloy we can separate equation (3.42) into the coherent (Bragg) scattering and incoherent (diffuse) scattering.

$$\left(\frac{d\sigma}{d\Omega}\right)_{el}^{coh} = \frac{N}{4}(\gamma r_0)^2 (1-\hat{K}_z^2) \langle F(K)\mu \rangle^2 \frac{(2\pi)^3}{V_0} \sum_{G} \delta(\underline{K}-\underline{G}) \qquad 3.43$$

where $$\langle F(K)\mu \rangle = \frac{1}{N} \sum_n F_n(K) \mu_n \qquad 3.44$$

The diffuse magnetic cross-section which is of interest to us is

$$\left(\frac{d\sigma}{d\Omega}\right)_{el}^{inc} = \frac{N}{4}(\gamma r_0)^2 (1-\hat{K}_z^2) T(K) \qquad 3.45$$

where $$T(K) = \frac{1}{N} \sum_{l,l'} e^{-i\underline{K}\cdot(\underline{l}'-\underline{l})} \left\{ \langle \mu_l F_l \mu_{l'} F_{l'} \rangle - \langle \mu F(K) \rangle^2 \right\}$$

$$\text{i.e. } T(K) = \frac{1}{N}\sum_{l,l'} e^{iK\cdot(l-l')}\langle\{F_l\mu_l - \langle F\mu\rangle\}\{F_{l'}\mu_{l'} - \langle F\mu\rangle\}\rangle \qquad 3.46$$

Equation (3.46) clearly shows that the diffuse scattering arises from the spatial fluctuations of the magnetic moment about its mean value. This is an exact result and we shall later consider what drives these spatial fluctuations. In the forward direction ($K=0$), $F_l = F_{l'} = 1$ (by definition) and

$$T(0) = \frac{1}{N}\sum_{l,l'}\{\langle\mu_l\mu_{l'}\rangle - \langle\mu\rangle^2\}$$

$$= \frac{1}{N}\{\langle M^2\rangle - \langle M\rangle^2\} \qquad 3.47$$

where $M = \sum_n \mu_n$

Writing $\delta M = M - \langle M\rangle$ then

$$T(0) = \frac{1}{N}\langle(\delta M)^2\rangle \qquad 3.48$$

Therefore the forward cross-section is proportional to the mean-square spatial fluctuation of the total magnetic moment.

(b) Strongly Ferromagnetic Binary Alloys

By strongly ferromagnetic binary alloys we mean ferromagnetic metals doped with magnetic or non-magnetic impurities; more strictly instead of magnetic or non-magnetic impurities we should say transition or non-transition metal impurities in view of our earlier discussions in section 2.2. In such alloys the any fluctuations of magnetization result primarily from concentration fluctuations. Again

following the discussion already given by Marshall (431,434) it will be assumed that the disturbance in the magnetic moment of either the host or impurity atom is a linear function of the number and type of its neighbours, the principal effect being due to the nearest neighbours. It will also be assumed that the mean short range order parameter is zero. Thus if a host atom is at site m then by definition it has a moment given by

$$\mu_m = \bar{\mu}_h + \sum_r g(r)\{P_{m+r} - c\} \qquad 3.49$$

whereas if an impurity is at m then

$$\mu_m = \bar{\mu}_i + \sum_r h(r)\{P_{m+r} - c\} \; . \qquad 3.50$$

$\bar{\mu}_i$ and $\bar{\mu}_h$ are the average moments of the impurity and host atoms respectively and h(r), g(r) are the disturbances in the values of μ_i and μ_h produced by fluctuations in the number of impurity atoms at a distance r. By definition

$$g(o) = 0 = h(o) \; .$$

P_m is a probability operator which is unity if an impurity atom is at m but is zero if a host atom is at m. Its average value is equal to the impurity concentration i.e.

$$\langle P_m \rangle = c$$

Equations (3.49) and (3.50) may be combined to give the general relations

$$\mu_m = \bar{\mu}_h + (\bar{\mu}_i - \bar{\mu}_h)P_m + \sum_r g(r)(P_{m+r} - c) + \sum_r P_m\{P_{m+r} - c\}\{h(r) - g(r)\} \qquad 3.51$$

and

$$F_m \mu_m = F_h \bar{\mu}_h + (F_i \bar{\mu}_i - F_h \bar{\mu}_h) p_m + F_h \sum_r g(r)(p_{m+r} - c) + \sum_r p_m (p_{m+r} - c)\{F_i h(r) - F_h g(r)\} \quad 3.52$$

We also define the following functions and their Fourier transforms:

$$G(\underline{k}) = \sum_r e^{i \underline{k} \cdot \underline{r}} \; g(\underline{r}) \quad 3.53$$

$$H(\underline{k}) = \sum_r e^{i \underline{k} \cdot \underline{r}} \; h(\underline{r}) \quad 3.54$$

$$W(\underline{r}) = h(\underline{r}) - g(\underline{r}) \quad 3.55a$$

$$W(\underline{k}) = H(\underline{k}) - G(\underline{k}) \quad 3.55b$$

$$W(\underline{k}, \underline{Q}) = F_i(\underline{k}) H(\underline{Q}) - F_h(\underline{k}) G(\underline{Q}) \quad 3.56a$$

$$= \sum_r e^{i \underline{Q} \cdot \underline{r}} \{F_i(\underline{k}) h(\underline{r}) - F_h(\underline{k}) g(\underline{r})\} \quad 3.56b$$

$$U(\underline{r}) = W^2(\underline{r}) \; ; \; U(\underline{k}) = \sum_r e^{i \underline{k} \cdot \underline{r}} \; W^2(\underline{r}) \quad 3.57$$

$$U(\underline{k}, \underline{Q}) = \sum_r e^{i \underline{Q} \cdot \underline{r}} \{F_i(\underline{k}) h(\underline{r}) - F_h(\underline{k}) g(\underline{r})\}^2 \quad 3.58$$

If $F_i(K) = F_h(K) = F(K)$, as is approximately true for alloys within a given period, then the functions $W(K,Q)$ and $U(K,Q)$ become unnecessary because

$$W(K,Q) = F(K)\,W(Q)$$

and similarly for $U(K,Q)$.

Equation (3.51) gives the full variation of the moments with concentration fluctuations about the mean value of c and with short-range order fluctuations about the mean value of zero. From the definitions given above it follows that

$$\frac{\partial \bar{\mu}_i}{\partial c} = H(0) \qquad 3.59$$

$$\frac{\partial \bar{\mu}_h}{\partial c} = G(0) \qquad 3.60$$

$$\begin{aligned}\frac{\partial \mu}{\partial c} &= \bar{\mu}_i - \bar{\mu}_h + (1-c)\,G(0) + c\,H(0) \\ &= \bar{\mu}_i - \bar{\mu}_h + G(0) + c\,W(0)\end{aligned} \qquad 3.61$$

$$\frac{\partial^2 \mu}{\partial c^2} = 2\,W(0) \qquad 3.62$$

and

$$\frac{\partial \mu}{\partial s(\underline{r})} = W(\underline{r}) \qquad 3.63$$

In the last equation s(r) is the short-range order parameter defined by

$$P_{ii} = c^2 + s(\underline{r}) \quad ; (r \neq 0) \qquad 3.64$$

where P_{ii} is the probability of finding pairs of impurity

atoms separated by a distance $\underline{r}$. From equations (3.46) and (3.52) it may be shown that

$$T(K) = c(1-c)\{F_i\bar{\mu}_i - F_h\bar{\mu}_h + F_h G(K) + c\,W(K,K)\}^2 + c^2(1-c)^2\{U(K,0) + U(K,K)\} \qquad 3.65$$

In the forward direction equation (3.65) reduces to

$$T(0) = c(1-c)\{\bar{\mu}_i - \bar{\mu}_h + G(0) + c\,W(0)\}^2 + 2c^2(1-c)^2\,U(0) \qquad 3.66$$

$$\equiv c(1-c)\left(\frac{\partial\mu}{\partial c}\right)^2 + 2c^2(1-c)^2\,U(0) \qquad 3.67$$

Observe that from equations (3.57) and (3.63)

$$U(0) \equiv \sum_r W^2(\underline{r}) \equiv \sum_r \left\{\frac{\partial\mu}{\partial s(\underline{r})}\right\}^2$$

so that

$$T(0) = c(1-c)\left(\frac{\partial\mu}{\partial c}\right)^2 + 2c^2(1-c)^2\sum_r\left\{\frac{\partial\mu}{\partial s(\underline{r})}\right\}^2 \qquad 3.68$$

If we make the further approximation that the magnetization varies only with the nearest-neighbour short-range order parameter i.e. $W(\underline{r})$ is zero beyond the nearest neighbours then we can write

$$W(\underline{r}) \simeq W\sum_{\rho_0}\delta(\underline{r}-\rho_0)$$

where ρ_0 is the nearest-neighbour distance. Thus

$$W(0) \simeq z_0 W$$

and $$U(0) = z_0 W^2 = \frac{1}{z_0} W^2(0)$$

$$= \frac{1}{4z_0} \left\{ \frac{\partial^2 \mu}{\partial c^2} \right\}^2$$

Therefore

$$T(0) \leq c(1-c)\left(\frac{\partial \mu}{\partial c}\right)^2 + \frac{c^2(1-c)^2}{2z_0}\left(\frac{\partial^2 \mu}{\partial c^2}\right)^2 \qquad 3.69$$

At either end of the concentration range the factor $c^2(1-c)^2$ is small; also $1/z_0 \sim 0.1$ so that in general the second term in equation (3.69) is usually smaller than the first term except when $\left(\frac{\partial \bar{\mu}}{\partial c}\right)$ is about zero, as would be the case if the magnetization curve exhibits a maximum as a function of concentration.

Let us now consider the specific case of dilute impurity concentrations. The immediate environment of each impurity atom would be the same and therefore it is very plausible to suppose that all impurity atoms have the same magnetic moment μ_i. Equations (3.51) and (3.52) now become

$$\mu_m = \bar{\mu}_h + (\bar{\mu}_i - \bar{\mu}_h) p_m + \sum_r g(\underline{r})\, p_{m+\underline{r}} \qquad 3.70$$

and

$$F_m \mu_m = F_h \bar{\mu}_h + (F_i \bar{\mu}_i - F_h \bar{\mu}_h) p_m + \sum_r F_h g(\underline{r})\, p_{m+\underline{r}} \qquad 3.71$$

Hence

$$\bar{\mu} = \bar{\mu}_h + c\{\bar{\mu}_i - \bar{\mu}_h + G(0)\} \qquad 3.72$$

and

$$\frac{d\bar{\mu}}{dc} = \mu_i - \mu_h + G(0) \qquad 3.73$$

Also it may be shown that in this limit (of dilute concentrations)

$$T(K) = c(1-c)\left\{F_i\bar{\mu}_i - F_h\bar{\mu}_h + F_h G(K)\right\}^2 \qquad 3.74$$

which in the forward direction becomes

$$T(0) = c(1-c)\left(\frac{\partial\bar{\mu}}{\partial c}\right)^2 \qquad 3.75$$

Suppose that the disturbance $g(\underline{r})$ extends to only the nearest-neighbours ($r = \rho_0$ say) and that $g(\rho_0) = g_0$; then near the forward direction and for a polycrystalline sample we can write

$$T(K) \simeq c(1-c)\left\{\bar{\mu}_i - \bar{\mu}_h + z_0 g_0 \frac{\sin K\rho_0}{K\rho_0}\right\}^2 \qquad 3.76$$

where the third term in equation (3.76) is the spherical average of $G(K)$. The following possibilities may arise:-

(i) Both $(\bar{\mu}_i - \bar{\mu}_h)$ and $G(0)$ have the same sign, which is the same as that of $\frac{d\bar{\mu}}{dc}$; then the cross-section exhibits a peak in the forward direction, and falls rapidly to a value oscillating about $(\bar{\mu}_i - \bar{\mu}_h)$ for large K. The width of the peak is about π/ρ, where ρ measures the range of the disturbance $g(\underline{r})$.

(ii) $(\bar{\mu}_i - \bar{\mu}_h)$ and $G(0)$ have opposite signs; then if $|\bar{\mu}_i - \bar{\mu}_h| > |G(0)|$ the cross-section will dip in the forward direction and will have a maximum at some $K \neq 0$.

However if $|\bar{\mu}_i - \bar{\mu}_h| < |G(0)|$ then the cross-section will be zero at some value of κ for which $|\bar{\mu}_i - \bar{\mu}_h| = |G(\kappa)|$.

At large values of κ the oscillations of $G(\kappa)$ become relatively unimportant and one obtains

$$T(\kappa) \simeq c(1-c)\left\{F_i\bar{\mu}_i - F_h\bar{\mu}_h\right\}^2 \qquad 3.77$$

which is a result first derived by Shull and Wilkinson (435). From the cross-section at large κ a value of $|\bar{\mu}_i - \bar{\mu}_h|$ can be obtained. By combining this with the average moment determined from bulk magnetization measurements i.e.

$$\bar{\mu} = c\mu_i + (1-c)\bar{\mu}_h \qquad 3.78$$

values of $\bar{\mu}_i$ and $\bar{\mu}_h$ may be found.

(c) Contribution from the Second Moment of the Fluctuation of the Local Moments

The diffuse scattering cross-section at large κ given by equation (3.77) involves only the fluctuations in the average values of the impurity and host atom magnetic moments. However an inspection of equation (3.46) shows that we should also allow for the fluctuations in the magnetic moments of both the impurity atoms and the host atoms. We thus have the additional terms

$$\delta T(\kappa) = \frac{1}{N}\sum_{ll'} e^{i\underline{\kappa}.(l-l')}\left\{F_i^2\langle(\delta\mu_i)^2\rangle + F_h^2\langle(\delta\mu_h)^2\rangle\right\}\delta_{ll'}$$

$$= cF_i^2\langle(\delta\mu_i)^2\rangle + (1-c)F_h^2\langle(\delta\mu_h)^2\rangle \qquad 3.79$$

Thus, more generally, at large κ

$$T(K) = c(1-c)\{f_i\bar{\mu}_i - f_h\bar{\mu}_h\}^2 + c\,F_i^2\langle(\delta\mu_i)^2\rangle + (1-c)F_h^2\langle(\delta\mu_h)^2\rangle \qquad 3.80$$

These additional contributions were first pointed out by Felcher et al (436) although their method of derivation is equivalent to obtaining equation (3.46) using a different notation.

The contribution of the second moments of the fluctuation of the magnetic moments of the impurity and host atoms to the scattering cross-section particularly at large K makes it impossible to obtain $\bar{\mu}_i$ and $\bar{\mu}_h$ from bulk magnetization and unpolarized neutron diffuse scattering data only. As shown later it is often more accurate to use polarized neutron diffuse scattering data.

(d) Effect of Chemical Short-range Order

The effect of a small but finite chemical short-range order has been considered by Marshall (434. Defining $s(K)$ as

$$s(K) = \sum_r e^{i\underline{K}\cdot\underline{r}}\, s(\underline{r}) \qquad 3.81$$

and re-defining the functions $w'(\underline{r})$, $U'(\underline{r})$, $W'(K,Q)$ and $U'(K,Q)$ as

$$w(\underline{r}) = s(\underline{r})\{h(\underline{r}) - g(\underline{r})\} \qquad 3.82$$

$$u(\underline{r}) = s(\underline{r})\,w^2(\underline{r}) \qquad 3.83$$

$$W(K,Q) = \sum_r e^{i\underline{Q}\cdot\underline{r}}\, s(\underline{r})\{f_i(K)h(\underline{r}) - f_h(K)g(\underline{r})\} \qquad 3.84$$

$$U(\underline{k},\underline{Q}) = \sum_{\underline{r}} e^{i\underline{Q}\cdot\underline{r}}\, s(\underline{r})\left\{F_i(\underline{k})\,h(\underline{r}) - F_h(\underline{k})\,g(\underline{r})\right\}^2 \qquad 3.85$$

Marshall showed that instead of equation (3.65) we should now have, correct to the first order in $S(\underline{r})$,

$$T(\underline{k}) = \{c(1-c) + sc(\underline{k})\}\left[F_i\bar{\mu}_i - F_h\bar{\mu}_h + F_h G(\underline{k}) + c\,W(\underline{k},\underline{k}) + \frac{1-2c}{c(1-c)}\left\{W'(\underline{k},0) + W'(\underline{k},\underline{k})\right\}\right]^2$$
$$+ c^2(1-c)^2\left\{U(\underline{k},0) + U(\underline{k},\underline{k})\right\}$$
$$+ (1-2c)^2\left\{U'(\underline{k},0) + U'(\underline{k},\underline{k})\right\}$$
$$+ c(1-c)\frac{1}{N}\sum_{\underline{Q}} sc(\underline{Q})\left\{W(\underline{k},\underline{Q}) + W(\underline{k},\underline{Q}+\underline{k})\right\}^2 \qquad 3.86$$

Clearly such an expression involving many parameters is not very convenient for analysing experimental data. Fortunately only the first set of terms in equation (3.86) is of importance and therefore further discussion will be restricted to it. However in the cases where $\left(\frac{d\bar{\mu}}{dc}\right) \sim 0$ the second term becomes important (see equation (3.69)). Also following usage (437 -9) we will write

$$S(\underline{k}) = 1 + \frac{sc(\underline{k})}{c(1-c)}$$

$$w(\underline{k},0) = \frac{W'(\underline{k},0)}{c(1-c)}$$

and similarly for $w(\underline{k},\underline{k})$.

With these modifications equation (3.86) reduces to

$$T(\underline{k}) \simeq c(1-c)S(\underline{k})\left[F_i\bar{\mu}_i - F_h\bar{\mu}_h + F_h G(\underline{k}) + c\,W(\underline{k},\underline{k}) + (1-2c)\left\{w(\underline{k},0) + w(\underline{k},\underline{k})\right\}\right]^2 \qquad 3.87$$

Further if $F_i \simeq F_h = F(\underline{k})$ then

$$T(K) \simeq c(1-c)S(K)F^2(K)\left[\tilde{\mu}_i - \tilde{\mu}_h + G(K) + cW(K) + (1-2c)\{w(0) + w(K)\}\right]^2 \quad 3.88$$

which can also be written as

$$T(K) \simeq c(1-c)S(K)F^2(K)\left[\tilde{\mu}_i - \tilde{\mu}_h + (1-c)G(K) + cH(K) + (1-2c)\{w(0) + w(K)\}\right]^2 \quad 3.89$$

$S(K)$ may be determined from the nuclear diffuse scattering cross-section of the alloy. This cross-section is given by

$$\left(\frac{d\sigma}{d\Omega}\right)^{inc}_{nuc} = c\sigma_i + (1-c)\sigma_h + c(1-c)(b_i - b_h)^2 S(K) \quad 3.9$$

where the σ's are the incoherent cross-sections and the b's are the coherent scattering lengths.

(e) The Temperature-dependence of the Diffuse Scattering Cross-section

Using a Heisenberg model Lovesey and Marshall (440) and Lovesey (441) have considered the temperature dependence of the elastic diffuse scattering cross-section for small impurity concentrations in ferromagnetic or antiferromagneti hosts. Since we are not interested specifically in such a temperature dependence we shall be content with just a summary of the relevant points. These are that

(i) for $T \lesssim 0.6T_c$ the forward cross-section increases with temperature only by about 10% for both bcc and fcc host lattices;

(ii) in the critical region

$$T(K)^{1/2} \sim \frac{M}{K_0^2 + K^2} \quad 3.9$$

where M is the magnetization of the pure host and κ_0 is an inverse correlation range (cf eq.(2.204)). Thus

$$T(0) \sim \frac{M}{\kappa_0^2} \; ; \qquad 3.92$$

in a mean field approximation both M and κ_0 vary as $(T_c - T)^{\frac{1}{2}}$ so that

$$T(0)^{1/2} \propto (T_c - T)^{-1/2} \qquad 3.93$$

while at large κ ,

$$T(\kappa)^{1/2} \sim (T_c - T)^{1/2} \; . \qquad 3.94$$

However, experimental observation shows that $M \propto (T_c - T)^{\frac{1}{3}}$ (see discussion on critical exponents towards the end of section 2.5(vi)); also from the theory of Gammel et al. (442) $\kappa_0 \propto (T_c - T)^{2/3}$ and thus

$$T(0)^{1/2} \propto (T_c - T)^{-1} \qquad 3.95$$

and, $T(\kappa \text{ large})^{\frac{1}{2}} \propto (T_c - T)^{1/3} \; . \qquad 3.96$

Many of the measurements to be reported later have been carried out at 4.2 K only with the exception of two Fe-Ni invar alloys and one Rh-doped Fe-Ni invar alloy for which measurements were made at both 4.2 K and at room temperature (see chapter 7). Since equations (3.93) - (3.96) strictly apply in a small region round the Curie temperature they cannot be used to test if the observed forward cross-sections follow the predicted temperature dependence of the magnetic scattering

(f) Inclusion of Non-linear Effects

The various expressions for $T(\kappa)$ obtained above have

all been based on the assumption that the change of an atomic magnetic moment is due to a linear superposition of the effects of all neighbouring atoms taken separately. This linear superposition approximation has been relaxed by Balcar and Marshall (443) by considering second-order changes of magnetization arising from the arrangements of neighbourhood atoms. Thus if the disturbance produced on a host atom by an impurity atom at $\underline{r}$ is $g(\underline{r})$ the presence of impurit atoms at both $\underline{r}$ and $\underline{R}$ ($\underline{r} \neq \underline{R}$) will give rise to an extra influence on the magnetic moment which may be described by the function $a(\underline{r},\underline{R})$. Therefore for a host atom one may write

$$\mu_n = \bar{\mu}_h + \sum_{\underline{r}}' g(\underline{r})(P_{n+\underline{r}} - c) + \sum_{\underline{r},\underline{R}}' a(\underline{r},\underline{R})(P_{n+\underline{r}} - c)(P_{n+\underline{R}} - c) \qquad 3.97$$

while for an impurity atom

$$\mu_n = \bar{\mu}_i + \sum_{\underline{r}}' h(\underline{r})(P_{n+\underline{r}} - c) + \sum_{\underline{r},\underline{R}}' b(\underline{r},\underline{R})(P_{n+\underline{r}} - c)(P_{n+\underline{R}} - c) \qquad 3.98$$

where $h(\underline{r})$ and $b(\underline{r},\underline{R})$ describe the effects of impurity atoms on other impurity atoms. $a(\underline{r},\underline{R})$ is by definition taken to be symmetric and also is such that

$$a(\underline{r},\underline{r}) = a(0,\underline{R}) = a(\underline{r},0) = 0$$

Similarly for $b(\underline{r},\underline{R})$. Defining

$$d(\underline{r},\underline{R}) = b(\underline{r},\underline{R}) - a(\underline{r},\underline{R}) \qquad 3.99$$

equations (3.97) and (3.98) can be combined to give

$$\mu_n = \bar{\mu}_h + \sum_{\underline{r}}' g(\underline{r})(P_{n+\underline{r}} - c) + \sum_{\underline{r},\underline{R}}' a(\underline{r},\underline{R})(P_{n+\underline{r}} - c)(P_{n+\underline{R}} - c)$$
$$+ P_n(\bar{\mu}_i - \bar{\mu}_h) + \sum_{\underline{r}}' W(\underline{r}) P_n (P_{n+\underline{r}} - c)$$
$$+ \sum_{\underline{r},\underline{R}}' d(\underline{r},\underline{R})\, P_n (P_{n+\underline{r}} - c)(P_{n+\underline{R}} - c) \qquad 3.100$$

Also we define the Fourier transforms

$$A(k,q) = \sum_{r,R} a(\underline{r},\underline{R})\, e^{i\underline{k}\cdot\underline{r} - i\underline{q}\cdot\underline{R}} \qquad 3.101$$

and D(k,q) in an obvious way.

With these definitions it is shown (443) that in the case where $F_i = F_h = F(\underline{k})$, $T(\underline{k})$ is now given by

$$\begin{aligned}\frac{T(\underline{k})}{F^2(\underline{k})} &= c(1-c)\{\bar{\mu}_i - \bar{\mu}_h + G(\underline{k}) + c\,W(\underline{k})\}^2 \\ &+ 2c^2(1-c)^2\frac{1}{N}\sum_{\underline{K}}'\{W(\underline{K}) + A(\underline{k}+\underline{K},\underline{K}) + c\,D(\underline{k}+\underline{K},\underline{K})\}^2 \\ &+ c^2(1-c)^2\frac{1}{N}\sum_{\underline{K}}'[W(\underline{K})\{W(\underline{k}+\underline{K}) - W(\underline{K})\}] \\ &+ 2c^3(1-c)^3\frac{1}{N^2}\sum_{K,q}'\{D^2(K,q) + 2D(K,q)\,D(\underline{k}+K-q,K)\}\end{aligned} \qquad 3.102$$

The above equation shows that corrections for second-order effects as introduced into the model used so far first appear in the second term in (3.102) with a factor of $c^2(1-c)^2$! In order to estimate the order of magnitude of the correction terms one can consider a nearest-neighbour approximation in which $g(\underline{r})$, $a(\underline{r},\underline{R})$ vanish beyond the nearest-neighbour distance. One then obtains

$$T(0) \simeq c(1-c)\left(\frac{\partial\bar{\mu}}{\partial c}\right)^2 + \frac{c^2(1-c)^2}{2z_0}\left(\frac{\partial^2\bar{\mu}}{\partial c^2}\right)^2 + \frac{c^3(1-c)^3}{6z_0^2}\left(\frac{\partial^3\bar{\mu}}{\partial c^3}\right)^2 \qquad 3.103$$

Since z_0 = 8 or 12 for bcc and fcc lattices and since the correction terms appear with factors $c^2(1-c)^2$ and $c^3(1-c)^3$, these terms may be neglected except when $\frac{\partial\bar{\mu}}{\partial c} = 0$. This non-linear model has been used by Cable and Medina (370) for NiCr where it was assumed that $\bar{\mu}_{Cr}$ is zero so that $h(\underline{r})$

and $b(\underline{r},\underline{R})$ are also zero.

3.4 Diffuse Magnetic Scattering in "Giant Moment" Systems

(a) A Short Review of Previous Neutron Studies of Such Systems

We now wish to consider the interpretation of the results of neutron scattering measurements on a group of TM alloys which we have dubbed "giant moment alloys". As fully discussed in section 2.3 these are alloy systems in which there exists a non-magnetic - ferromagnetic phase transition at a critical concentration, cf, of the magnetic impurity. The onset of ferromagnetism has been shown to be necessarily inhomogeneous arising through the overlap of polarization clouds seeded by clusters of impurity atoms. A common feature of the magnetic diffuse scattering cross-section of these alloys is the occurrence of a forward peak as first observed for PdFe and PdCo (197). In order to discuss the analysis of the neutron data equation (3.46) is written in the form

$$T(\underline{K}) = c(1-c)\left| \int_{V_s} d\underline{r}\ \Delta\rho(\underline{r})\, e^{i\underline{K}\cdot\underline{r}} \right|^2 \qquad 3.104$$

as used by Law and Collins (445, 446). In the above equation $\Delta\rho(\underline{r})$ is the disturbance in the magnetic moment density due to the presence of a single impurity and Vs is the volume of the sample. We recall that this equation is strictly valid for a ferromagnetic host doped with magnetic or non-magnetic impurities of concentration c. Therefore in order to use equation (3.104) in the case of a weakly ferromagnetic system (i.e. a non-magnetic matrix containing a sufficient concentration of a magnetic impurity to render

the whole ferromagnetic) it becomes necessary to interpret $\Delta\rho(r)$ as the ferromagnetic polarization density associated with a single solute atom at $r = 0$. The polarization is assumed to consist of two parts:

(i) a moment, μ_i, due to electrons in 3d orbitals at the impurity atom site itself;

(ii) the remaining moment which is mainly distributed in the Pd host but may include any moments in the s-orbitals at the solute site. Associating these two contributions with form factors $F_i(K)$ and $F_h(K)$ respectively then

$$T(K) = c(1-c)\{\mu_i F_i(K) + M_h F_h(K)\}^2 \qquad 3.105$$

Since $F_i(K)$ is a d-orbital form factor and $F_h(K)$ corresponds to a much more widespread distribution $F_h(K)$ falls to zero with increasing K much more rapidly than $F_i(K)$ so that at sufficiently large K all the scattering is due to 3d-orbital moments. $M_hF_h(K)$ can thus be obtained from the experimental values and the resulting data Fourier-inverted to give the distribution of M_h in real space. For polycrystalline specimens $M_hF_h(K)$ may be assumed to be spherically symmetric so that one writes

$$M_h F_h(K) = \int_0^\infty dr\, \Delta\rho(r)\, 4\pi r^2\, \frac{\sin Kr}{Kr} \qquad 3.106$$

where r is the radial distance from an impurity. Results of such an analysis for PdFe and PdCo (197) showed the existence of a long range polarization in the Pd matrix, extending to about 10A and hence affecting a large number ($\sim$ 200) of Pd atoms.

To explain the origin of the long-range polarization

in the Pd matrix, it was noted that Pd is supposed to be strongly uniformly exchange-enhanced, with a susceptibility given by equation (1.45) i.e.

$$\chi(K) = \frac{\chi_{Pauli}\, F(K/2K_F)}{1 - U\, F(K/2K_F)\, \rho(\varepsilon_F)}$$

where the symbols have all been previously defined (vide section 1.10). For very small wavevectors

$$F\left(\frac{K}{2K_F}\right) \approx 1 - \tfrac{1}{3}\left(\frac{K}{2K_F}\right)^2$$

so that one obtains (36, 57, 447)

$$\chi(K) \simeq \frac{\frac{12}{\epsilon} K_F^2 \;\chi_{Pauli}}{K_0^2 + K^2} \qquad 3.107$$

where

$$K_0^2 = 12 K_F^2 \frac{(1-\epsilon)}{\epsilon} \qquad 3.108$$

and $\epsilon = U\rho(\varepsilon_F)$ and $(1-\epsilon)^{-1}$ is the Stoner enhancement factor of the Pd matrix. Thus again we have a function $\chi(K)$ which is of the Ornstein-Zernicke form for small wavevectors (N.B. only such small values are important since we are interested in the long-range nature of the susceptibility). It is further supposed that <u>each</u> impurity atom gives rise to a driving field $B(K)$ so that

$$\Delta\rho(r) = \int d\underline{K}\, B(K)\, \chi(K)\, e^{i\underline{K}\cdot\underline{r}} \qquad 3.109$$

If each impurity is spatially well localized then

$B(\underline{r}) \simeq b_o S(r) \Longrightarrow B(\kappa) = b_o$, a constant. Substituting for $\chi(\kappa)$ from equation (3.107) gives that

$$\Delta\rho(r) = \frac{b_o}{\epsilon}\chi_{Pauli}\frac{3K_F^2}{\pi r}e^{-\kappa_o r} \qquad 3.110$$

Equation (3.110) shows that κ_o is a measure of the polarization range in the matrix. A large enhancement factor implies a small κ_o and therefore a large polarization range and conversely (see equation (3.108)). For Pd susceptibility measurements (127) give an enhancement factor $S \simeq 10$. Also $k_F \sim 0.8\text{Å}^{-1}$ (197). These values give $\kappa_o \simeq 0.9\text{Å}^{-1}$ and hence a polarization range of about 1 Å only. On the other hand if we use the measured value of $\kappa_o \sim 0.2 - 0.3\text{A}^{o-1}$ (197,198) then $S \sim 100\text{-}240$, which is an order of magnitude greater than the estimated value. However there have been attempts (448) to explain the discrepancy between the values of κ_o obtained from neutron diffraction measurements and from the exchange enhancement factor in terms of a momentum-dependent interaction parameter, $U(\kappa)$. For small wave-vectors $\chi(\kappa)$ is still Lorentzian as in equation (3.107) but with

$$\kappa_o^{-2} \simeq -\frac{S}{2}\left\{U(0)\frac{d^2\chi(\kappa)}{d\kappa^2} + \chi_{Pauli}\frac{d^2U(\kappa)}{d\kappa^2}\right\}_{\kappa=0} \qquad 3.111$$

instead of equation (3.108). By assuming an appropriate form for $U(\kappa)$ the calculated value of κ_o may be brought into agreement with the observed value. For example Clogston (449) has suggested that

$$U(\kappa) = U_o + U_1\sum_{z_o} e^{i\underline{\kappa}\cdot z_o} \qquad 3.112a$$

$$= U_0 + 12 U_1 \left\{ 1 - \frac{z_0^2 K^2}{6} \right\} \qquad 3.112b$$

where U_0 and U_1 are respectively the intraatomic and interatomic exchange parameters and z_0 is the number of nearest-neighbours. Agreement with the experimental value of κ_0 is achieved if there is an appreciable nearest-neighbour exchange interaction which clearly will depend on the d-band structure assumed.

The value of κ_0 given above ($0.9 A^{o-1}$) has been obtained on a spherical band model i.e. using free-electron-like band structures for Pd. Diamond (450) has proposed a theory of the susceptibility of the strongly exchange-enhanced transition metals so as to include, ab initio, the effects of band structure. Using a tight-binding model for the Pd d-bands with overlap parameters adjusted to fit Fermi-surface data he calculated the wave-vector-dependent susceptibility which, at long wavelenghts, corresponded to a Yukawa form (equation (3.110)) for the spin polarization around a localized perturbation. For a Stoner enhancement factor of 10 the range parameter is found to be $3\mathring{A}$ which is a great improvement on the value given by a spherical band model although it is still smaller than the experimental value. Interestingly this value is just greater than the nearest-neighbour distance in Pd(=2.75A). As with the spherical band model agreement with the experimental value can be further improved by including some interatomic exchange. For $\frac{U_1}{U_0} \sim 0.3$ and with S=10, $\kappa_0 \simeq 0.23 A^{o-1}$, while if S is increased to about 14 the experimental value of $\kappa_0 \simeq 0.2 A^{o-1}$ is reproduced. However, it is our opinion

that the assumed magnitude of the interatomic exchange is unreasonable even if we take U_o to be only 1ev. Now

$$M_h F_h(\kappa) = B(\kappa)\chi(\kappa) = b_o \chi(\kappa) . \qquad 3.113$$

By definition $F_h(0) = 1$ so that

$$M_h = b_o \chi(0) = \frac{b_o}{\kappa_o^2} \frac{12}{\epsilon} K_F^2 \chi_{Pauli} \qquad 3.114a$$

$$\equiv b_o S \chi_{Pauli} \qquad 3.114b$$

From equations (3.107), 3.113) and (3.114) it follows that

$$F_h(\kappa) = \left\{ 1 + \frac{\kappa^2}{\kappa_o^2} \right\}^{-1} \qquad 3.115$$

For more concentrated alloys it has been suggested (198, 448) that the response of the Pd host to the exchange field of any additional impurity should vanish when all the holes of one spin direction are filled. Since the number of holes in Pd is 0.36/atom it is expected that $M_h \sim 0$ when $\bar{\mu}_{Pd} \simeq 0.36\mu_B$. Therefore for a concentrated Pd alloy

$$\frac{d\bar{\mu}}{dc} = \bar{\mu}_i - \bar{\mu}_{Pd} + M_h . \qquad 3.116$$

Using the bulk magnetization values of $\frac{d\bar{\mu}}{dc}$ and values of $\bar{\mu}_i$ from the large angle neutron data the variation of M_h with $\bar{\mu}_{Pd}$ has been obtained (198). This showed a rapid decrease of M_h with $\bar{\mu}_{Pd}$ and indeed it appeared that M_h would vanish for $\bar{\mu}_{Pd} \sim 0.3 - 0.4\mu_B$. However, the behaviour of PdCo and PdFe appeared to be different in this context

and no explanation of this has yet been advanced. The observed neutron cross-section for Pd4% Fe gave $M_h \sim 0$ as compared with a value of $\sim 2.5 \mu_B$ expected on the basis of the predicted variation of M_h with $\bar{\mu}_{Pd}$.

The above discussion of the PdFe and PdCo alloys has been given on a model in which the polarization in the Pd host is assumed to be continuously distributed. Hicks et al (198) have given an essentially equivalent treatment in terms of a discrete model in which the magnetic moment at a lattice site $\underline{r}$ in the Pd matrix is given by

$$M_h(\underline{r}) = \sum_{\underline{r}'} \chi(\underline{r}-\underline{r}')\,\phi(\underline{r}') \qquad 3.117$$

where $\chi(\underline{r}-\underline{r}')$ is a non-local unenhanced susceptibility and

$$\phi(\underline{r}') = b_0\,\delta(\underline{r}') + U M_h(\underline{r}').$$

$b_0\delta(\underline{r}')$ is as before, the driving field of an impurity atom and $UM_h(\underline{r}')$ is an exchange enhancement term. Fourier-transforming equation (3.117) and re-arranging gives

$$M_h(K) = \frac{b_0 \chi_0(K)}{1 - U\chi_0(K)} \equiv b_0 \chi(K) \qquad 3.118$$

where

$$\chi_0(K) = \chi_{Pauli}\, F\left(\frac{K}{2k_F}\right)$$

Further discussion follows along the same lines as for the continuum model.

Diffuse magnetic neutron scattering experiments have also been carried out in the critical concentration region for CuNi (204), PdNi (128) and CrNi (368) alloy systems. For these systems it had been well-established that there

exists a critical concentration for the onset of ferromagnetism. The observed neutron scattering cross-sections for these alloys shows a marked forward peak similar to that observed for PdFe and PdCo (197). However the neutron data have been analysed in slightly different ways. For PdFe and PdCo each magnetic impurity was regarded as a perturbation centre driving an essentially paramagnetic Pd matrix. For the other alloys it has been necessary to assume a model in which the forward scattering is wholly attributed to the presence of identical but nearly independent moment disturbances (also called polarization clouds) whose concentration, c* say, is less than the concentration of the magnetic impurity. The cluster concentration c* is assumed to increase steadily from zero (at the critical concentration) as the impurity concentration increases. Thus on this model the scattering cross-section will still be given by equations (3.46) and (3.104) if we replace c by c* i.e.

$$\frac{d\sigma}{d\Omega} = \frac{N}{4}(\gamma r_0)^2(1-\hat{K}_z^2)\,c^*(1-c^*)\{M(K)\}^2 \qquad 3.119$$

where

$$M(K) = T(K)^{1/2} \equiv \int d\underline{r}\,\rho(r)\,e^{i\underline{K}\cdot\underline{r}} \qquad 3.120$$

is the Fourier transform of the average moment density within a polarization cloud. At $K = 0$

$$M(0) = \int \rho(r)\,d\underline{r} \qquad 3.121$$

giving the average total integrated moment per cloud. Thus

in the forward direction

$$\left(\frac{d\sigma}{d\Omega}\right)_{K=0} = \frac{N}{4}(\gamma r_0)^2(1-\hat{K}_z^2)c^*(1-c^*)\{M(0)\}^2 \qquad 3.122$$

This forward scattering is determined by assuming that

$$\rho(\underline{r}) \propto \frac{e^{-K_0 r}}{r} \qquad 3.123$$

where K_0 again is a range parameter which characterizes the extent or spread of the polarization cloud. Hence

$$\left(\frac{d\sigma}{d\Omega}\right)^{1/2} \propto M(K) = \frac{M(0)K_0^2}{K_0^2+K^2} \qquad 3.124$$

The experimental data at low K are therefore plotted as $\left(\frac{d\sigma}{d\Omega}\right)^{-1/2}$ versus K^2 to determine both K_0 and $\left(\frac{d\sigma}{d\Omega}\right)_{K=0}$. Furthermore the polarization clouds are assumed to contribute <u>additively</u> to the spontaneous magnetization of the system so that

$$\bar{\mu} = c^* M(0) \qquad 3.125$$

The values of $\left(\frac{d\sigma}{d\Omega}\right)_0$ and $\bar{\mu}$ are then used to obtain c* and M(0).

(b) <u>A Critical Discussion of the Above Models</u>

At the time of observation of the neutron diffuse magnetic scattering from <u>Pd</u>Fe and <u>Pd</u>Co by Low and his colleagues the interpretation of the data in terms of the extended polarization of an essentially paramagnetic Pd matrix by magnetic Fe or Co atoms was probably the most meaningful that could have been given. However since then it has been shown that there exists a critical concentration

for the onset of ferromagnetism in these and a number of other alloy systems. Our approach so far has been that the onset of ferromagnetism in these "giant moment systems", Pd Fe, Pd Co, V Ni, Rh Co, Cu Ni, etc, is essentially the same, the process being governed by local environment effects. Thus, as already explained (see section 2.3), the onset of ferromagnetism is necessarily inhomogeneous, arising from the ferromagnetic "overlap" of clusters of impurity atoms. The brief analysis reported in section 2.6 showed the similarity in the behaviour of various physical properties of the alloy systems. Some of these physical properties were found to obey quite general relations that were derived in section 2.5. Thus for Pd Fe for $0.12 \leq c < 1.3\%$ Fe

$$M_{oo}^2 = 7.75 \times 10^{-3} \{c - 0.12\} \quad (\mu_B/\text{atom})^2; \qquad 3.126a$$

$$T_c = 49.56 (c - 0.12) \quad K \qquad 3.126b$$

as shown in fig. 2.30. Now the most dilute Pd Fe alloy on which neutron diffraction measurements were carried out was Pd 0.26% Fe. It is obvious that the Fe concentration in this "dilute" Pd Fe alloy is already more than twice the critical concentration. Therefore it is not surprising that at this concentration all the impurity Fe atoms are magnetic and "drive" polarization clouds around themselves. However, near the critical concentration we do not expect that isolated Fe atoms will be observed to be "magnetic" (at $T \sim 0$) in the usual sense. Indeed magnetization (200, 461) and heat capacity (420) data indicate that close to c_f only pairs of Fe atoms are magnetic. Moreover, well below c_f (say $c \lesssim 0.1\ c_f$) spin fluctuation phenomena more commonly associated with dilute Pd Ni and Pt Ni alloys should be observed.

Although such spin fluctuations have been reported for dilute PdCo alloys (460) the evidence is not very convincing. Measurements on samples of much lower impurity concentrations than 0.05% Co would be very useful**

Clearly the model used by Low and Holden (197) or by Hicks et al. (198) cannot be used to account for the behaviour of Fe or Co atoms in the single impurity limit. In this regard we would like to question the procedure used in "correcting" the observed susceptibility of pure Pd for Fe impurity content (114-5). It is assumed that the "upturn" at low temperatures in the $\chi(T)$ vs T curve for Pd is due to the polarization clouds of Fe impurities with effective moments of $\sim 12\,\mu_B$ (per Fe atom); the contribution of such Fe clusters is then subtracted from the measured susceptibility. This procedure is incorrect because even if at such very low impurity concentrations (a few ppm) the Fe atoms are still magnetic (especially if $T^*_{Fe}(0) \ll 1$ K) the large cluster moments ($\sim 8\,\mu_B$ /Fe atom - see chapter 5) will ensure that the clusters are fully aligned in relatively small magnetic fields (~ 5 KOe). Consequently such impurity clusters will not contribute to the measured susceptibility. However, the Fe impurities affect the Pd susceptibility because their presence should lead to a decrease of the host spin fluctuation temperature (T^*_h) and since at low temperatures

$$\chi(T) \sim \chi(0)\left\{1 - \frac{T^2}{T_h^{*2}}\right\} \quad \text{and} \quad \chi(0) \sim \frac{g^2\mu_B^2}{\pi K_B T_h^*}$$

one can easily see why an upturn in the $\chi(T)$ vs T plot occurs at low

---

** Very recent measurements have confirmed the existence of spin fluctuations in sufficiently dilute PdCo with $T^* \sim 100$ mK (761 - 2).

temperatures and also why this upturn should be "sharper" for increasing Fe impurity concentrations. A number of other alloy systems are also known to exhibit this upturn at low temperatures (451 - 3).

Furthermore the Curie temperature of Pd 0.26% Fe is $\simeq$ 6.9K (see eq. (3.126b)). Since the neutron diffraction experiments were carried out at 4.2K it is surprising that no critical scattering effects were seen in the observed data. This point has been raised by de Pater et al. (454) while considering their own neutron data for Pd 0.23% Mn.

Finally as seen in fig. 2.31 some change occurs in the concentration dependence of the Curie temperature of Pd Fe alloys between 1.5 - 3% Fe. A similar change is evident in the concentration dependence of the spontaneous magnetization (not shown here). One can attribute such a change to "saturation effects" i.e. within this concentration region many Pd atoms would begin to carry the maximum allowed magnetic moment. Generalizing local environment effects to include both local chemical (i.e. number and type of near-neighbours) and local magnetic (i.e. type and strength of exchange interaction) effects the magnetic moment on a Pd atom can be written as

$$\mu_{Pd}(r) = \frac{\chi_o(r)\, B(r)}{1 + \beta\, B(r)} \qquad 3.127$$

a form recently proposed by Hicks (455) for the Ni moment in Cu Ni alloys. In eq.(3.127) $\chi_o(r)$ is the initial susceptibility at a Pd site while B(r) is the effective exchange field acting on the site. β is a constant and clearly χ_o/β is the maximum value of the magnetic moment of a Pd atom. At large Fe concentrations the exchange or molecular field acting on the Pd sites no longer increases and each Pd atom appears to have attained its maximum moment. Thus for c $\geq$ 10 % Fe

$$\bar{\mu} = c\,\bar{\mu}_{Fe} + (1-c)\,\bar{\mu}_{Pd}$$

with $\bar{\mu}_{Fe} \simeq 3\,\mu_B$ and $\bar{\mu}_{Pd} \sim 0.36\,\mu_B$; hence

$$\frac{d\bar{\mu}}{dc} \simeq \bar{\mu}_{Fe} - \bar{\mu}_{Pd}$$ (cf equation (3.116)).

Therefore for sufficiently large Fe impurity concentrations the neutron diffuse scattering cross-section should be nearly α -independent. At all concentrations, excluding clustering effects, we do not see any reason why the extrapolated forward cross-section should be less than a value corresponding to $\frac{d\bar{\mu}}{dc}$. Consequently the observation by Low (448) that the measured forward cross-sections correspond to much smaller values of ($\frac{d\bar{\mu}}{dc}$) than are consistent with bulk magnetization data is most probably a reflection of the inaccuracy of the data. In view of the importance attached to the interpretation of the neutron data particularly as regards the "special" nature of the Pd matrix it is surprising that apparently no other measurements have been made to check the original data.

Turning our attention to CuNi, PdNi, CrNi alloys, etc. in the critical concentration region we agree with the interpretation of the sharp forward peak in the neutron diffuse cross-section as arising from polarization clouds. Such neutron data where they exist provide, in our opinion, conclusive evidence of the inhomogeneous nature of the onset of ferromagnetism. However we need to re-examine certain aspects of the model which appear either to be physically unsatisfactory or incapable of explaining some of the other experimentally observed characteristics.

(i) Firstly the model requires that while the total moment within a cloud remains constant (or approximately so) the cloud concentration goes to zero with the spontaneous magnetization at the critical concentration. However a number of experimental observations notably low temperature resistance minima, heat capacity measurements and the

temperature dependence of the magnetic susceptibility all indicate that clusters persist well into the non-magnetic regime below the critical concentration. One way out of this dilemma would be to take the cloud concentration as the effective concentration of "magnetically coupled" clusters but again this is unsatisfactory because we shall then beg the question of what the cluster size and the cluster percolation concentration should be. Clearly such a consideration would imply that the total moment within a cloud cannot be approximately independent of the impurity concentration. It would be largest at the critical concentration where an "infinite cluster" exists and decrease rapidly to a nearly constant value in the ferromagnetic and non-magnetic regimes. In addition in the ferromagnetic regime we would need to consider the paramagnetic scattering from "uncoupled" clusters and it is not clear that this can be easily done if at all. We have already questioned the customary idea of attributing the apparently constant term in the low temperature heat capacity of such systems to the "thermally excitable" clusters i.e. the supposedly uncoupled clusters in low molecular fields (see section 2.5(xi) for the details).

(ii) In any real system there must be a distribution of cluster sizes and hence of cluster moments. Acker and Huguenin (220) have found that for quenched CuNi alloys about 90% of the clusters have small moments varying from 8 μ_B in Cu 40%Ni to 12 μ_B in Cu 50%Ni while the remaining 10% of the clusters have moments lying between 40 and 220 μ_B. Thus the assumption of identical clusters while being necessary to aid a simple analysis of the neutron data is

nevertheless only approximate. A proper analysis would have to consider the fluctuations in the cluster moments.
(iii) Thirdly there is the need to explain the observed concentration dependence of the polarization range (270).

Now in view of our suggestion that the onset of ferromagnetism in these giant moment alloys is a phase transition it would seem relevant to consider whether a critical scattering of neutrons is possible and in what form. Before doing this it is pertinent to describe the probable physical processes involved in the transition to ferromagnetism. In section 2.2 we described how and why magnetic clusters are formed. Well below the critical concentration the concentration of magnetic clusters is small so that the average distance between them is large. Consequently the RKKY coupling which must exist between them is so weak that no cluster-glass ordering is observed within the usual temperature range of observation ($\gtrsim$ 0.5K). However their presence can be readily inferred; being nearly independent of one another they can give rise to a resistance minimum at low temperatures through the spin-flip scattering of conduction electrons and also to a nearly constant term in the heat capacity. At sufficiently high temperatures the magnetic susceptibility obeys a Curie-Weiss law. The resulting paramagnetic Curie temperature is usually negative reflecting either some effective antiferromagnetic coupling or, according to Claus and Kouvel (456), to local anisotropy effects. As the impurity concentration increases so does the cluster concentration; the average distance between the clusters decreases and the RKKY coupling becomes stronger thereby increasing the probability of a cluster-glass forming at conveniently observable temperatures. The paramagnetic

Curie temperatures gradually become positive indicating an increasing tendency towards ferromagnetic interactions. In other words as the impurity concentration increases the cluster spins begin to experience exchange forces aligning them with their immediate neighbours and a correlation develops in which such near-neighbour spins tend on the average to be parallel to one another. Close to the critical concentration the correlation range becomes large and characteristics typical of mictomagnets may be observed. There is, of course, no spontaneous magnetization yet because the aligning tendency averages to zero over the whole alloy system but if a sufficiently large magnetic field is applied some net magnetization will be detected. At the critical concentration the correlation range tends to infinity marking the onset of the infinite range correlation of a truly ferromagnetic system. The essential viewpoint that ferromagnetism arises through the exchange interaction of the magnetic clusters had been previously suggested by Kouvel and Comly (202) and lately by Muellner and Kouvel (457).

At a ferromagnetic transition point one usually considers the thermally induced fluctuations in say the Z-component of the spins in the system; these fluctuations give rise to a critical scattering of neutrons. Following the analysis given by Marshall and Lowde (269) and Marshall and Lovesey (433) the partial differential cross-section for critical neutron scattering is given by equation (3.38). If we define

$$\delta S^{\alpha}_{\underline{K}} = \sum_{l} e^{i\underline{K}\cdot\underline{l}} \{S^{\alpha}_{l} - \langle S^{\alpha}_{l} \rangle\} \qquad 3.128$$

then for a ferromagnet

$$S^{\alpha\alpha}(\kappa,\omega) = N^2 \delta_{\kappa,0} \langle S^{\alpha} \rangle^2 \delta(\hbar\omega) + \frac{1}{2\pi\hbar} \int_{-\infty}^{\infty} dt\, e^{-i\omega t} \langle \delta S^{\alpha}_{-\kappa}(0)\, \delta S^{\alpha}_{\kappa}(t) \rangle \qquad 3.129$$

The first term of equation (3.129) gives the coherent magnetic scattering (cf equation (3.43)). It is small because near the critical concentration $\langle S^{\alpha} \rangle \to 0$. In a quasistatic approximation in which the spin fluctuations appear to be nearly static to the probing neutrons the inelasticity of the scattering is small (433). Thus if we choose the z-direction say the diffuse neutron cross-section is given by equation (3.45) with $T(\kappa)$ now defined as

$$T(\kappa) = \frac{1}{N} \langle \delta S^{z}_{-\kappa}(0)\, \delta S^{z}_{\kappa}(0) \rangle \qquad 3.130$$

which is essentially the same as equation (3.46). Recall that in section 2.5(vi) we related the isothermal static susceptibility to the magnetization fluctuations through the classical fluctuation theorem obtaining

$$\chi(\kappa) = \frac{1}{N K_B T} \langle (\delta M_{\kappa})^2 \rangle \qquad 3.131$$

(N.B. in equation (2.200) $\chi(\kappa)$ is defined per atom whereas in equation (3.131) M refers to the total magnetization). Thus the diffuse neutron cross-section is

$$\frac{d\sigma}{d\Omega} = \frac{N}{4} (\gamma r_0)^2 (1 - \hat{\kappa}_z^2) K_B T \chi(\kappa) \qquad 3.132$$

which shows that the neutron cross-section is proportional to the static wave-vector dependent susceptibility. In

particular in the forward direction

$$\left(\frac{d\sigma}{d\Omega}\right)_0 = \frac{N}{4}(\gamma r_0)^2 (1-\hat{K}_z^2) K_B T \chi(0) \qquad 3.133$$

where $\chi(0)$ is the initial static susceptibility. This quantity diverges at the transition point causing the critical scattering of neutrons.

For the phase transition that occurs at the critical concentration (at T=0) the only varying parameter is obviously the impurity concentration so that as in the case of strongly ferromagnetic dilute alloys the magnetization fluctuations are due to fluctuations of concentration. Therefore we can immediately carry over some of the expressions obtained in section 3.3; thus in the forward direction

$$T(0) = c(1-c) S(0) \left(\frac{d\bar{\mu}}{dc}\right)^2$$

(see equation (3.87)).

Now $\frac{d\bar{\mu}}{dc}$ may be related to the bulk initial susceptibility through equations (2.90) and (2.96).

$$T(0) = c(1-c) S(0) \frac{\alpha^2}{2b} \chi_f(0) \qquad 3.134$$

In general we can therefore write

$$T(K) = c(1-c) S(K) \frac{\alpha^2}{2b} \chi_f(K) \qquad 3.135$$

In retrospect we may have obtained the form of equation (3.135) by replacing the factor $k_B T$ representing the thermal fluctuation energy in equation (3.134) by the factor c(1-c) in the case of concentration fluctuations.

In order to deduce the form of $\chi_f(\kappa)$ we go back to equation (2.201) which gives the expansion of the thermodynamic potential in terms of the magnetization i.e.

$$G = G_0 + aM^2 + \delta(\nabla M)^2 + \cdots\cdots \quad \text{(equation (2.201))}$$

In this case, for small wave-vectors, $\chi(\kappa)$ assumes the familiar Ornstein - Zernicke form

$$\chi(\kappa) = A_0 \{\kappa_0^2 + \kappa^2\}^{-1} \quad \text{(equation (2.203))}$$

where $A_0 = \frac{1}{4\delta}$ and $\kappa_0^2 = a/\delta$ as mentioned in section 2.5(vi). Thus near the forward direction

$$\frac{d\sigma}{d\Omega} \propto \{\kappa_0^2 + \kappa^2\}^{-1} \qquad 3.136$$

By plotting $(\frac{d\sigma}{d\Omega})^{-1}$ against κ^2 both κ_0 and $(\frac{d\sigma}{d\Omega})_0$ may be obtained. This extrapolation procedure is slightly different from that mentioned earlier (equation (3.124)) which required plotting $(\frac{d\sigma}{d\Omega})^{-1/2}$ versus κ^2. Both plots for CuNi alloys exist in the literature (204,458) and apparently give equally good fits to the observed cross-sections in the forward region. That this is so is not surprising because for $\kappa \leq \kappa_0$ (and $\kappa_0 \leq 0.5$ Å^{-1}) terms of higher order than κ^2 may be neglected and equation (3.124) then reduces essentially to the same form as equation (3.136). However as would be expected the values of the forward cross-section and the correlation range deduced from the two fits are different. For example for Cu 50%Ni Hicks et al (204) deduced that $(\frac{d\sigma}{d\Omega})_0$ = 24 mb/sr.atom and $\kappa_0 = 0.41 A^{o-1}$ whereas the use of equation (3.136) leads to $(\frac{d\sigma}{d\Omega})_0$ = 30 mb/sr.atom and $\kappa_0 = 0.21 A^{o-1}$. Similarly for Cu 48%Ni the values are 17.5 mb/sr.atom and $0.37 A^{o-1}$ (204) and 26 mb/sr.atom and $0.17 A^{o-1}$ respectively.

The forward cross-section for the Cu 48% Ni alloy is much smaller than would be expected from the fact that this concentration is very close to the critical concentration. As shown in fig. 2.27 the bulk magnetization and Curie temperature of CuNi alloys in the critical concentration region may be represented by

$$M^2_{oo} = 15.34 \times 10^{-4} (c - 47.6) \quad (\mu_B/\text{atom})^2 \qquad 3.137a$$

$$T_c = 15.38 (c - 47.6)\text{K} \qquad 3.137b$$

Thus for Cu 48% Ni $\frac{d\bar{u}}{dc} \simeq 3.1\ \mu_B/\text{atom}^2$ and $T_c \simeq 6\text{K}$; the relatively large value of $\left(\frac{d\bar{u}}{dc}\right)$ and the fact that its true Curie temperature is close to the temperature at which measurements are made (4.2K) should lead one to expect a large forward cross-section. The fact that for Cu 48% Ni and Cu 50% Ni alloys the observed forward cross-sections are much less than would be expected from the concentration dependence of the spontaneous magnetization but instead are of the same order of magnitude as for the non-ferromagnetic alloys does suggest that the scattering from these weakly ferromagnetic alloys may be similar to the paramagnetic scattering from the non-ferromagnetic alloys (see immediately below).

The correlation range κ_o is both concentration and temperature dependent. This is because

$$\kappa_o^2 = \frac{a}{\delta} \simeq \frac{\alpha_t}{\delta}(c - c_f) \qquad 3.138$$

where α_t is a function of temperature only. Thus within the mean field approximation in which the Landau theory of phase transitions is valid $\kappa_o \sim (c - c_f)^{1/2}$.

However, as discussed in section 2.5(vi) the observed dependence of κ_0 on $(c-c_f)$ appears to suggest that a three-dimensional Ising model is more appropriate than mean field theory. Also we note that, in principle, one should distinguish between a polarization range and a correlation range the latter being of more general applicability.

Finally below the critical concentration some paramagnetic scattering can be observed since magnetic clusters are still present. An estimate of the magnitude of this term is readily obtained. We consider a "field-on - field-off" type of measurement usually used to determine the ferromagnetic diffuse scattering. In the absence of a magnetic field forward cross-section is from equation (3.25)

$$\left(\frac{d\sigma}{d\Omega}\right)_0^{B_0=0} = c^* \frac{N}{4} (\gamma r_0)^2 \, 2/3 \, S_{cl}(S_{cl}+1) \qquad 3.139$$

where S_{cl} is the spin of a cluster and c* is the cluster concentration. A field is then applied in a direction parallel to κ_z. According to equation (3.29) the forward cross-section now becomes

$$\left(\frac{d\sigma}{d\Omega}\right)_0^{B_0\neq 0} = c^* \frac{N}{4} (\gamma r_0)^2 \left\{ S_{cl}(S_{cl}+1) - \langle (S_{cl}^z)^2 \rangle \right\} \qquad 3.140$$

The difference cross-section is therefore

$$\Delta\left(\frac{d\sigma}{d\Omega}\right)_0 = \frac{c^* N}{4} (\gamma r_0)^2 \left\{ \langle (S_{cl}^z)^2 \rangle - \tfrac{1}{3} S_{cl}(S_{cl}+1) \right\} \qquad 3.141$$

For large uncoupled clusters the spins may be aligned in relatively low fields so that we can take $\langle S_{cl}^z \rangle \approx S_{cl}$.

Hence

$$\Delta\left(\frac{d\sigma}{d\Omega}\right)_o \simeq c^* \frac{N}{4} (\gamma r_o)^2 \left\{\frac{2}{3} S_{Cl}^2 - \frac{1}{3} S_{Cl}\right\} \qquad 3.142a$$

For $c^* \sim 0.5\%$ and $S_{Cl} \simeq 10\,\mu_B$

$\Delta\left(\frac{d\sigma}{d\Omega}\right) \sim$ 23 mb/sr. atom;

which is of the same order of magnitude as the forward cross-section for the ferromagnetic CuNi alloys. Observe that for the same experimental set-up equations (3.122) and (3.142) are almost equivalent. Note however that it is possible to check if the observed scattering cross-section is actually ferromagnetic or paramagnetic scattering by using a different field geometry. If a vertical field is used then the difference cross-section for paramagnetic scattering would be

$$\Delta\left(\frac{d\sigma}{d\Omega}\right)_o^{pm} \simeq c^* \frac{N}{4} (\gamma r_o)^2 \left\{\frac{2}{3} S_{Cl}^2 + \frac{1}{6} S_{Cl}\right\} \qquad 3.142b$$

which is nearly of the same magnitude as in equation (3.142a), but the ferromagnetic scattering becomes

$$\Delta\left(\frac{d\sigma}{d\Omega}\right)_o^{fm} = -\frac{1}{3} \frac{N}{4} (\gamma r_o)^2 \, c^*(1-c^*) \, M(0)^2$$

instead of as in equation (3.122).

3.5 Polarized Diffuse Neutron Diffraction From Binary Alloys

(i) Theory: Recently a number of diffuse scattering measurements have been carried out on a few alloy systems using polarized neutrons (370,462,463). While unpolarized neutron measurements determine all of the static moment fluctuations from the average, polarized neutron measurements select out only those fluctuations at one site, n, which are

correlated with the presence of an impurity at another site, $\underline{m}$. With the incident neutron polarization parallel or anti-parallel to the sample magnetization and perpendicular to the scattering plane the scattering amplitude at site $\underline{n}$ is $b_n \pm P_n$ where b_n and P_n are the nuclear and magnetic scattering amplitudes respectively.

$$P_n = \tfrac{1}{2}\gamma r_0 F_n(\kappa)\mu_n \qquad 3.143a$$

$$= 0.27 F_n(\kappa)\mu_n \qquad 3.143b$$

if the cross-section is measured in barns. The $\pm$ signs refer to the spin state (i.e. polarization) of the neutron.

As in the case of unpolarized neutrons the diffuse cross-section measures the fluctuations from the mean and is given by

$$\left(\frac{d\sigma}{d\Omega}\right)^{\pm} = \frac{1}{N}\left\{\sum_n e^{i\underline{\kappa}\cdot\underline{n}}\left[b_n - \langle b\rangle \pm 0.27\{\mu_n F_n(\kappa) - \langle \mu F(\kappa)\rangle\}\right]\right\}^2 \qquad 3.144$$

The difference cross-section for the two neutron spin states is therefore

$$\Delta\frac{d\sigma}{d\Omega} = \frac{1.08}{N}\sum_{n,m} e^{i\underline{\kappa}\cdot(\underline{n}-\underline{m})}\{b_n - \langle b\rangle\}\{\mu_m F_m(\kappa) - \langle \mu F(\kappa)\rangle\}$$

$$\equiv 1.08 \sum_{n,r} e^{i\underline{\kappa}\cdot\underline{r}}\langle\{b_{n+r} - \langle b\rangle\}\{\mu_n F_n(\kappa) - \langle \mu F(\kappa)\rangle\}\rangle \qquad 3.145$$

For a binary alloy one can then proceed as for unpolarized neutrons by introducing the site occupation operator (see section 3.3). One finally obtains (370) that

$$\Delta\frac{d\sigma}{d\Omega} = 1.08\, c(1-c)(b_i - b_h)\, M(\kappa) \qquad 3.146$$

where

$$M(K) = F_i\bar{\mu}_i - F_h\bar{\mu}_h + (1-c)F_h G(K) + c\,H(K) \quad . \qquad 3.147$$

In the forward direction

$$\left(\Delta \frac{d\sigma}{d\Omega}\right)_0 = 1.08\,c(1-c)(b_i - b_h)M(0) \qquad 3.148a$$

$$\equiv 1.08\,c(1-c)(b_i - b_h)\frac{d\bar{\mu}}{dc} \qquad 3.148b$$

Again the effect of short-range atomic order can be allowed for by including the order parameter $S(K)$ to give

$$\Delta \frac{d\sigma}{d\Omega} = 1.08\,c(1-c)(b_i - b_h)S(K)M(K) \qquad 3.149$$

We shall now discuss a number of points that have emerged from the results of polarized neutron diffuse measurements on some alloys.

(ii) Non-linear and Non-local Effects in (Cr,V) Ni Alloys

Cable and Medina (370) have carried out polarized neutron diffuse scattering measurements on three CrNi alloys containing 99, 95 and 90% Ni and one V 95%Ni. By comparing their results with earlier unpolarized neutron results (368, 446) the authors concluded that non-linear and non-local effects were important in these alloys and therefore that both polarized and unpolarized neutron data are required for a complete understanding of the variation of the magnetic moment of both impurity and host atoms with concentration. As is obvious from equations (3.65), (3.80) and (3.102)

the moment difference ($\bar{\mu}_i - \bar{\mu}_h$) cannot be accurately determined from unpolarized neutron cross-sections at large α because of the additional terms present in the scattering amplitude. These extra terms are absent in the scattering amplitude for polarized neutron diffuse cross-section (equation (3.147)).

The experimental results show that at low Cr concentrations ($\leq$ 1.5%Cr) both the polarized and unpolarized neutron cross-sections are identical but at higher Cr concentrations the two cross-sections are different particularly in the forward direction. The difference given by $\{\overline{T(\alpha)} - M^2(\alpha)\}$ was then analysed in terms of the parameter $a(\underline{r},\underline{R})$ introduced in section 3.3(f). However, we do not wish to comment in any great detail on the magnetization and neutron data for the CrNi system except to say that

(a) it is unusual for the value of $\frac{d\bar{\mu}}{dc}$ obtained from bulk magnetization measurements to remain nearly constant right up to the critical concentration. Chiffey and Hicks (444) found that $\frac{d\bar{\mu}}{dc}$ remains constant only to about 4% Cr and then increases; in fact a careful examination of all the available magnetization data on this system shows that the initial value of $\frac{d\bar{\mu}}{dc}$ is -5.8 μ_B/Cr atom, in good agreement with the value determined from neutron experiments (370,446). This rate of decrease of the magnetic moment extrapolates to a critical concentration of about 10.6% Cr as determined by other methods (see fig. 2.29). This latter observation also applies to CuNi. Now the fact that the magnetic moment of a given atom depends on its chemical and magnetic environment is of general applicability so that one has to look for some other reason, probably experimental, to explain why the value

of $\frac{d\bar{\mu}}{dc}$ as determined from the neutron forward cross-sections for both polarized and unpolarized neutrons are less than the corresponding bulk magnetization values.

(b) Some, if not all, of the non-linear terms should contribute to the "background" scattering at large κ. In particular one should expect a large contribution from the $(1-c)\langle(\delta\mu_{Ni})^2\rangle$ term for the Ni 5%Cr alloy at least, because at about this composition the root-mean-square of the Ni moment fluctuations should be equal to μ_{Ni}. Experimentally the unpolarized neutron scattering cross-section is practically zero for $\kappa \geq 1\,\text{Å}^{-1}$, which seems odd.

(c) It is important to bear in mind that "field-on - field-off" types of measurements using unpolarized neutrons are essentially zero field measurements. Some caution must therefore be exercised in comparing data obtained in zero fields with those obtained in very high magnetic fields as often used in polarized neutron measurements. In particular in the critical concentration region the unpolarized neutron measurements determine the initial susceptibility (which is the susceptibility specified in equation (3.132)) whereas polarized neutron measurements give the high field susceptibility. This latter quantity will, of course, be smaller than the initial susceptibility because the applied magnetic field will tend to suppress any fluctuations of magnetization, and correspondingly, the forward cross-section for polarized neutrons will be smaller. The polarized neutron measurements on the CrNi alloys were carried out in a field of 57.3KG at 4.2K. Such a field in the critical concentration region will give the maximum ferromagnetic cross-section for a given set-up for unpolarized neutrons and a minimum ferro-

magnetic cross-section for polarized neutrons.

(d) Just as in CuNi alloys some mictomagnetic behaviour is expected in the critical concentration region. Magnetic clusters in the system overlap to give local ferromagnetic regions spanning tens of lattice spacings. Such extended local ferromagnetic regions are responsible for the mictomagnetic behaviour which is expected to reduce the neutron magnetic cross-sections that may be observed.

(iii) Polarized Neutrons and Polarization Clouds

Recent polarized neutron diffuse scattering measurements (462,463) on CuNi alloys in the critical concentration region have been interpreted without any reference to the magnetic clusters which are known to be present. Both Medina and Cable (462) and Radhakrisha et al (463) discussed their results in terms of the formalism developed for dilute but strongly ferromagnetic binary alloys i.e. in terms of a linear superposition of moment defects around the Cu atoms (see section 3.3(b)). Thus in the forward direction the diffuse cross-sections per atom for unpolarized and polarized neutrons are respectively

$$\left(\frac{d\sigma}{d\Omega}\right)_0 = \frac{1}{4}(\gamma r_0)^2(1-\hat{K}_z^2)\,c(1-c)\,S(0)\left(\frac{d\bar{\mu}}{dc}\right)^2 \qquad 3.150$$

and

$$\left(\Delta\frac{d\sigma}{d\Omega}\right)_0 = 1.08(b_i-b_h)\,c(1-c)\,S(0)\,\frac{d\bar{\mu}}{dc} \qquad 3.151$$

In an experimental set-up in which the cross-section for unpolarized neutrons is obtained by taking the difference of measurements made without and with an applied field parallel to the scattering vector the factor $\frac{1}{4}(\gamma r_0)^2(1-\hat{K}_z^2) = 0.0486$

if the cross-section is given in barns/steradian atom. Thus equation (3.150) may be written as

$$\left(\frac{d\sigma}{d\Omega}\right)_o = 0.0486\, c(1-c)\, S(0) \left(\frac{d\bar{\mu}}{dc}\right)^2 \qquad 3.152$$

Whereas Medina and Cable confined their discussion of the polarized neutron data for Cu 47.5%Ni to merely showing that the forward cross-section $\left(\Delta \frac{d\sigma}{d\Omega}\right)_o$ was compatible with the bulk magnetization value of $\frac{d\bar{\mu}}{dc}$ Radhakrisha et al went a bit further to evaluate the assumed moment defect around a Cu atom.

Hicks (464) has however attempted to show that these polarized neutron diffuse scattering data are consistent with the model used by Hicks et al (204) in interpreting the unpolarized neutron measurements i.e. that the polarized neutron data can be similarly interpreted in terms of giant magnetization clouds of moment M(o) and concentration c*. Writing the moment on any atom as

$$\mu_{\underline{m}} = P_{\underline{m}} \sum_{\underline{r}} g(\underline{m}-\underline{r})\, P^*_{\underline{r}} \qquad 3.153$$

where $P_{\underline{m}}$ is zero if a Cu atom is at site $\underline{m}$ and unity otherwise and $P^*_{\underline{r}}$ is unity if a Ni atom is at site $\underline{r}$ and also belongs to a polarization cloud Hicks derived that

$$\Delta \frac{d\sigma}{d\Omega} = 1.08\left[c(1-c)\,(b_{Ni}-b_{Cu})\,c^* \sum_{r\neq 0} g(r) + (b_{Ni}-\langle b\rangle)\,c^*\left\{c\sum_{r\neq 0} g(r)\, e^{i\underline{K}\cdot\underline{r}} + g(0)\right\}\right] \qquad 3.154$$

In the above equation $\langle b\rangle$ is the average nuclear scattering length; and the first term is the product of the average deviations of nuclear and magnetic scattering lengths. The

parameter $M(\underline{K})$ used in the analysis of the unpolarized data was then identified as

$$M(\underline{K}) = c\sum_{\underline{r}\neq 0} g(\underline{r})\, e^{i\underline{K}\cdot\underline{r}} + g(0) \qquad 3.155$$

However since the Ni atoms within a polarization cloud are absolutely correlated equation (3.154) is modified to read, for a random alloy,

$$\left(\Delta\frac{d\sigma}{d\Omega}\right) \simeq 1.08\left[c(1-c)(b_{Ni}-b_{(u)})c^{*}\sum_{\underline{r}=0,\,\underline{r}_0} g(\underline{r}) + (b_{Ni}-\langle b\rangle)c^{*}M(\underline{K})\left\{1+\left(1-\frac{1}{11(1-c^2)}\right)\sum_{\underline{r}_0} e^{i\underline{K}\cdot\underline{r}_0}\right\}\right] \qquad 3.156$$

where $\underline{r}_0$ is the nearest-neighbour distance vector. In obtaining this expression Hicks used the experimental observation by Kouvel and Comly (202) that only clusters of about 12 or 13 Ni atoms are magnetic. Finally the effect of atomic short range order which is to partially correlate further Ni atoms with a given cluster is allowed for. If the short range order parameter for nearest-neighbours is α_1 then there is an extra probability of $(1-c)\alpha_1$ above the random probability that the nearest-neighbour sites of Ni atoms already in a magnetic cluster are occupied by other Ni atoms. Thus for a polycrystalline specimen

$$\Delta\frac{d\sigma}{d\Omega} \simeq 1.08\left[c(1-c)(b_{Ni}-b_{(u)})\left\{1+12\alpha_1\frac{\sin Kr_0}{Kr_0}\right\}c^{*}\sum_{\underline{r}\neq 0,\,\underline{r}_0} g(\underline{r}) + (b_{Ni}-\langle b\rangle)c^{*}M(\underline{K})\left\{1+12\left(1-\frac{1}{11(1-c^2)}\right)\frac{\sin Kr_0}{Kr_0}+84(1-c)\alpha_1\right\}\right] \qquad 3.157$$

Using values of c* and $M(\underline{K})$ obtained from unpolarized neutron measurements (204) and taking $\alpha_1 \simeq 0.13$ (as determined by Medina and Cable for 47.5%Ni alloy (462))

Hicks (464) was able to show that the polarized neutron data of Medina and Cable (462) and Radhakrishna et al (463) were indeed consistent with the model of polarization clouds.

Now in our discussion of diffuse neutron scattering in the critical concentration region (see section 3.4) we had agreed that fluctuations of magnetization did result from concentration fluctuations, and hence that equation (3.150) and (3.151) above are valid but with the proviso that $\frac{d\bar{\mu}}{dc}$ is related to the initial susceptibility of the ferromagnetic alloys (equations (3.134) and (3.135)). An important consequence of this observation is that the forward cross-section for unpolarized neutron diffuse scattering should be obtained by plotting $\left(\frac{d\sigma}{d\Omega}\right)^{-1}$ against κ^2 and extrapolating to zero i.e. the cross-section in the forward region is Lorentzian. As already mentioned (section 3.4) this procedure gives for Cu 50%Ni $\left(\frac{d\sigma}{d\Omega}\right)_o$ = 30 mb/sr. atom and $\kappa_o = 0.21 A^{o-1}$ using the data of Hicks et al (204). On the other hand for polarized neutron measurements the forward cross-section should be determined by plotting $\left(\Delta \frac{d\sigma}{d\Omega}\right)^{-\frac{1}{2}}$ against κ^2. This has been done (not shown here) for the data of Radhakrishna et al and gives $\left(\Delta \frac{d\sigma}{d\Omega}\right)_o$ = 140 mb/sr. atom and $\kappa_o = 0.66 A^{o-1}$ (only the data for $\kappa \leq 0.72 A^{o-1}$ were used). Using these values in equations (3.151) and (3.152) one obtains that

$$\frac{d\bar{\mu}}{dc} = \frac{1.08\,(b_{Cu} - b_{Ni})\left(\frac{d\sigma}{d\Omega}\right)_o}{\left(\Delta \frac{d\sigma}{d\Omega}\right)_o} = -1.14$$

since $b_{Cu} - b_{Ni} = -0.24 \times 10^{-14}$m. This value of $\frac{d\bar{\mu}}{dc}$ is slightly less than that quoted by Radhakrishna et al (462) but is higher than the value given by equation (3.137a); however, it does show that equations (3.151) and (3.152)

are generally valid, independent of the details of the microscopic behaviour. One way to reconcile equation (3.152) with the known existence of magnetic clusters is implicit in the observation made at the end of section 3.4 about the similarity of the expression deduced for the paramagnetic scattering from an assembly of uncoupled clusters of concentration c* (equation (3.142)) and the relation used by Hicks et al (204) for the analysis of their unpolarized neutron data (equation (3.122)). For the same experimental set-up equation (3.122) reduces to

$$\left(\frac{d\sigma}{d\Omega}\right)_0 = \frac{N}{4}(\gamma r_0)^2 \tfrac{2}{3} c^*(1-c^*) M^2(0)$$

$$\simeq \frac{N}{4}(\gamma r_0)^2 \tfrac{2}{3} c^* M^2(0) \qquad 3.153$$

since c* is very small ($\sim$ 0.005). This is clearly of the same form as equation (3.142) if we take $S_{cl} \simeq M(0)$ and neglect the $\frac{1}{3}S_{cl}$ term (justified since $S_{cl} \gg 1$). In other words we can regard the diffuse cross-section observed for the weakly ferromagnetic alloys as being essentially the same as the paramagnetic scattering from an assembly of clusters. This is a plausible assumption because the low Curie temperatures of these alloys show that the cluster are only very weakly coupled. Note however, that c* is then the <u>actual</u> concentration of the magnetic clusters and not the effective number of aligned clusters as used by Hicks et al (204). Thus we shall require that

$$c^* M(o) = Msat \qquad 3.159$$

where Msat is the saturation magnetic moment obtained by

applying a sufficiently large magnetic field. M_{sat} does not vanish at the critical concentration as is required for the spontaneous magnetization M_{oo}. The difference between M_{oo} and M_{sat} is clearly shown by the magnetization data of Muellner and Kouvel on RhNi (457). As discussed by these authors S_{cl} and c* may be simply obtained by using both the effective Curie-Weiss constant determined above T_c and M_{sat}.

Also on a microscopic model the diffuse cross-section for polarized neutrons is as given by equations (3.156) or equation (3.157) in the case where short range order occurs. But we shall make two comments. Firstly the number of Ni atoms needed to form a magnetic cluster is expected to decrease as the alloy gets more strongly ferromagnetic. The figure of 12 or 13 used in equation (3.156) was determined for concentrations well below the critical concentration for ferromagnetism. Just above the critical concentration the minimum number of Ni atoms needed to form a magnetic cluster in CuNi alloys is between 8 and 10. Secondly because of the factor of $84(1-c)\alpha_1$ (= 5.46 for c=0.5 and $\alpha_1 \simeq 0.13$) the correction for short range order is appreciable so that α_1 has to be accurately known. The quoted value of α_1 for CuNi was determined (462) for the critical alloy (Cu 47.5%Ni). It would be better if were determined for a more ferromagnetic alloy such as Cu 53%Ni, which is well away from the critical region so as to avoid critical scattering effects.

Finally inspite of the apparent consistency between the polarized and unpolarized neutron data for Cu 50%Ni we shall still caution that care should be exercised in comparing both sets of data particularly in the critical

concentration region (say (c-cf) $\lesssim$ 2%). The reason for this caution has already been stated (see section 3.5(i)).

(iv) Conduction Electron Polarization

In their neutron diffraction experiments on CuNi alloys containing 0-40% Cu Aldred et al (438) observed that while the Ni moment decreased by about 40% the quantity $\{\mu_{Cu} + \mu_{cond}\}$ remained approximately constant. μ_{cond} is the magnetic moment due to the conduction electrons. If $\{\mu_{Cu} + \mu_{cond}\}$ is regarded as a magnetic polarization induced by the Ni moments via exchange interactions then one would expect it to decrease as $\bar{\mu}_{Ni}$ decreases. Ito and Akimitsu (466) indeed not only found that μ_{cond} decreases almost linearly to zero near the critical concentration for ferromagnetism but also were able to confirm the absence of any magnetic moment on Cu atoms. In order to account for the difference in the composition dependence of both $\bar{\mu}_{Ni}$ and μ_{cond} between their results and those of Aldred et al (438) Ito and Akimitsu suggested that non-linear disturbance effects were important, an observation that was also made by Aldred et al (438) although in a slightly different context. The first attempt to explain the apparent constancy of $\{\mu_{Cu} + \mu_{cond}\}$ as a function of the Cu concentration was made by Felcher et al (436) who pointed out the importance of the contribution to the diffuse scattering cross-section of the second moment of the fluctuation of the Ni moment (see section 3.3(d), equation (3.80)). Using the experimental results of Aldred et al (438) and Ito and Akimitsu (466) Felcher et al (436) showed that $\bar{\mu}_{Ni}$ decreased steadily from its value for pure Ni ($\simeq$ 0.71 μ_B/atom) to zero at a concentration of about 52.5% Cu ($\simeq$ cf) while $\{\langle(\delta\mu_{Ni})^2\rangle\}^{1/2}$

rises from zero to a maximum at about 40% Cu.

Although the above explanation appears satisfactory some doubt has recently been expressed as to the exact cause of the conduction electron polarization. Moon (467) has suggested that the nearly constant negative polarization observed in all the ferromagnetic transition metals and in some of their alloys could be attributed to an overlap of the 3d-wavefunctions. Using a tight-binding formalism together with spin-polarized atomic wavefunctions he obtained good agreement with the experimental data on Fe. Moon's suggestion has been taken up by Medina and Cable (462) who argued that if the observed negative magnetization is truly uniform, thereby necessitating the use of a δ-function form factor, then the forward cross-section should agree with the derivative of the local moment rather than with the derivative of the bulk moment. Now in their polarized neutron experiments on CuNi alloys (462) these authors observed that the forward cross-sections gave rather good agreement with the derivatives of the bulk moment and therefore they concluded that some other kind of form factor (than a δ-function) should be associated with the negative polarization. Such a form factor should be large for the usual range of κ values characteristic of diffuse scattering experiments (i.e. small κ) but should be negligible for Bragg scattering. The proper form factor to be used in the analysis of diffuse scattering data has been derived by Felcher et al (465) as

$$F(\underline{\kappa}) = (1+\alpha) F_{lo}(\underline{\kappa}) - \alpha F_{ov}(\underline{\kappa}) \qquad 3.160$$

where $F_{lo}(\kappa)$ is the form factor for the local moment, $F_{ov}(\kappa)$

is the non-local or overlap form factor and α is a constant which measures the size of the overlap bonding or antibonding spin density. Thus in NiCu alloys the Ni form factor used by Medina and Cable (462) was

$$\langle F_{Ni}(K)\rangle = \{1+\alpha(1-c)F_{Lo}(K)\} - \alpha(1-c)F_{ov}(K) \qquad 3.161$$

where c here is the Cu concentration and α = 0.154.

Since the measurements to be reported here have been made with unpolarized neutrons only there is, as is obvious from the discussion given so far, a severe limitation on the amount and accuracy of the information that can be obtained. We shall therefore leave out further details of the overlap spin density. However, in concluding the discussion in this section we note that another possible source of error in analysing the unpolarized neutron diffraction cross-section at large K comes from the assumption that

$$\langle S(K)M(K)^2\rangle_{av} \equiv S(K)M(K)^2 \qquad 3.162$$

where the left hand side of the above relation denotes a spherical average. Medina and Cable (462) have stated that this assumption is only correct at small K values. They believe that the difference between their values of $\{\bar{\mu}_{Cu} - \bar{\mu}_{Ni}\}$ and those of Cable et al (437) and Aldred et al (438) can be attributed partly to the latter authors' use of the above equality (equation (3.162)) and partly to the neglect of the contribution to the cross-section from the second moment of the fluctuation of the localized

magnetic moments.

3.6 Hicks' Model for the Moment Disturbance in Ferromagnetic Alloys

The moment disturbance in ferromagnetic binary alloys has been discussed within the framework of a linear model according or to which the moment defect caused by the introduction of an impurity atom is independent of concentration (see section 3.3(b)). Such an approximation is probably satisfactory for magnetic hosts doped with small concentrations of impurities. In such cases the moment defects are similar and sufficiently well-separated to justify the linear superposition approximation. Also in the critical concentration region for the onset of ferromagnetism we have seen that there exists a dilute concentration of nearly identical magnetic clusters in an otherwise non-magnetic but highly-polarizable medium. These magnetic clusters are only very weakly interacting (as shown by the low Curie temperatures of alloys in this concentration region) and may, for practical purposes, be considered essentially independent of one another. Consequently, a linear model using the magnetic clusters as units may also be satisfactory. However, for concentrated alloys it is only logical to doubt the validity of a linear superposition of separate moment defects and, as discussed in section 3.3(f), Balcar and Marshall (443) have attempted to relax this linear approximation by considering second-order changes of magnetization arising from different local atomic configurations. The predicted change in the moment disturbance with concentration is proportional to c(1-c) (see equation (3.102)). On the other hand from the analysis of the neutron diffuse scattering data on CuNi alloys (438) Hicks (455)

has suggested that the parameters characterising the moment disturbance in these alloys cannot be described as constants modified by correction terms proportional to the impurity concentration. Therefore in order to avoid having to consider still higher order corrections to the linear model Hicks (455) has recently modified an earlier model of his (458) which was introduced specifically to explain the characteristics of the diffuse neutron scattering cross-sections observed in the critical concentration region of CuNi (204).

Hicks' model involves the physically very meaningful generalization of the local environment effect according to which the magnetic moment at a given Ni site not only depends on its local atomic environment through its initial susceptibility but also on the local magnetic environment through exchange interactions. Using a molecular field approach the moment, $m(\underline{r})$, at a Ni site is chosen to be a simple saturating function of the exchange field, $b(\underline{r})$, acting on the site so that

$$m(\underline{r}) = \frac{\chi(\underline{r})\, b(\underline{r})\, p(\underline{r})}{1 + \beta\, b(\underline{r})} \qquad 3.163$$

where $p(\underline{r})$ is zero or unity respectively for non-Ni and Ni sites; $\chi(\underline{r})$ is the initial susceptibility of a Ni site and $\frac{\chi(r)}{\beta}$ is the high-field moment which can be developed at $(\underline{r})$ and β is an arbitary constant. The fluctuations in the susceptibility are assumed to be a superposing function of the atomic environment, i.e.

$$\chi(\underline{r}) = \chi(0) + \sum_{\underline{r}' \neq \underline{r}} \alpha(\underline{r} - \underline{r}')\, p(\underline{r}') \qquad 3.164$$

so that with the addition of magnetic atoms at $\underline{r}'$ there is

an addition to the susceptibility, $\chi(0)$, of a completely isolated Ni atom at $\underline{r}$. The interaction between the Ni atoms is represented by an exchange field generated by the moments at all other sites acting through an exchange interaction $J(\underline{r}-\underline{r}'')$: thus

$$b(\underline{r}) = \sum_{\underline{r}''\neq\underline{r}} J(\underline{r}-\underline{r}'')\, m(\underline{r}'') \qquad 3.165$$

Using equations (3.164) and (3.165) in (3.163) one obtains an integral equation involving the Fourier transforms of $m(\underline{r})$, $p(\underline{r})$, $\alpha(\underline{r})$ and $J(\underline{r})$ denoted respectively by $m(\underline{k})$, $P(\underline{k})$, $A(\underline{k})$, and $g(\underline{k})$. The integral equation is then solved by separating $m(\underline{k})$ and $P(\underline{k})$ into their average and fluctuating components, thus:-

$$m(\underline{k}) = \bar{\mu} \sum_{\underline{r}} e^{i\underline{k}\cdot\underline{r}} + L(\underline{k}) \qquad 3.166$$

$$P(\underline{k}) = c \sum_{\underline{r}} e^{i\underline{k}\cdot\underline{r}} + D(\underline{k}) \qquad 3.167$$

where $$L(\underline{k}) = \sum_{\underline{r}} e^{i\underline{k}\cdot\underline{r}} \{ m(\underline{r}) - \bar{\mu} \} \qquad 3.168$$

and $$D(\underline{k}) = \sum_{\underline{r}} e^{i\underline{k}\cdot\underline{r}} \{ p(\underline{r}) - c \} \qquad 3.169$$

The resulting solutions are then

$$\bar{\mu} = \frac{g(0)c\{\chi(0) + cA(0)\} - 1}{\beta g(0)} \qquad 3.170$$

and

$$L(\underline{k}) = \frac{g(0)\bar{\mu}\{\chi(0) + cA(0) + cA(\underline{k})\} D(\underline{k})}{1 - g(\underline{k})[cA(0) + c^2A(0) - \beta\bar{\mu}] + g(0)\beta\bar{\mu}} \qquad 3.171$$

$$\equiv \frac{\left[\frac{d\bar{\mu}}{dc} - \frac{c}{\beta}\{A(0) - A(\underline{K})\}\right] D(\underline{K})}{1 + \frac{g(0) - g(K)}{\beta \bar{\mu}\, g(0)^2}} \qquad 3.172$$

For unpolarized neutrons the magnetic diffuse cross-section is given by

$$\frac{d\sigma}{d\Omega} = \frac{N}{4}(\gamma r_0)^2 (1 - \hat{K}_z^2)\, T(K) \qquad \text{(equation (3.45))}$$

where $$T(K) = F(K)^2 L(K) L(-K) \qquad 3.173$$

Writing equation (3.172) in the form

$$L(\underline{K}) = M(K)\, D(K) \qquad 3.174$$

equation (3.173) now becomes

$$T(K) = F(\underline{K})^2 c(1-c) S(K) M(\underline{K}) M(-\underline{K}) \qquad 3.175$$

where it has been used that

$$D(K)\, D(-K) = c(1-c) S(K) \qquad 3.176$$

$S(K)$ is of course the Fourier transform of the atomic short-range order parameter defined in section 3.3(d) above. In the forward direction

$$T(0) = c(1-c)\, S(0) \left\{\frac{d\bar{\mu}}{dc}\right\}^2 \qquad 3.177$$

in agreement with equation (3.87). For polarized neutrons the difference cross-section is

$$\Delta \frac{d\sigma}{d\Omega} = 1.08\, F(\underline{k})\,(b_i - b_h)\, L(k)\, D(-k)$$

$$= 1.08\, F(\underline{k})\,(b_i - b_h)\, c(1-c)\, S(k)\, M(k) \qquad 3.178$$

and hence

$$\left(\Delta \frac{d\sigma}{d\Omega}\right)_0 = 1.08\,(b_i - b_h)\, c(1-c)\, S(0)\, \frac{d\bar{\mu}}{dc}$$

as given by equation (3.151). Now from equations (3.172) and (3.174)

$$M(k) = \frac{\frac{d\bar{\mu}}{dc} - \frac{c}{\beta}\{A(0) - A(k)\}}{1 + \frac{g(0) - g(k)}{\beta \bar{\mu} g(0)^2}} \qquad 3.179$$

For small k it was assumed that

$$A(k) \simeq A(0)\{1 - a_0 k^2\} \qquad 3.180$$

and

$$g(k) \simeq g(0)\{1 - b_0 k^2\} \qquad 3.181$$

so that

$$M^{-1}(k) \simeq \left(\frac{d\bar{\mu}}{dc}\right)^{-1}\left\{1 + \frac{b_0}{\beta \bar{\mu} g(0)} k^2\right\}\left\{1 - \frac{c A(0) a_0}{\beta \frac{d\bar{\mu}}{dc}} k^2\right\}^{-1} \qquad 3.182$$

which becomes

$$M^{-1}(k) \simeq \left(\frac{d\bar{\mu}}{dc}\right)^{-1}\left\{1 + \left[\frac{b_0}{\beta \bar{\mu} g(0)} + \frac{c A(0) a_0}{\beta \frac{d\bar{\mu}}{dc}}\right] k^2\right\} \qquad 3.183$$

if

$$\frac{c A(0) a_0}{\beta \frac{d\bar{\mu}}{dc}} << 1 \qquad 3.184$$

By fitting the magnetization values of $\bar{\mu}$ against c the phenomenological parameters $\frac{\chi(0)}{\beta}$, $\frac{A(0)}{\beta}$, and $\frac{1}{\beta g(0)}$

may be determined and with the further assumption of nearest neighbour interactions giving $a_0 \simeq b_0 \simeq 1.05\,\text{Å}^2$, $M(K)$ may be completely determined and compared with the available neutron data. Such a comparison shows that reasonable fits to the neutron data are obtained only for highly rich Ni matrices in NiCr and NiCu alloys and in particular for NiCu alloys the fits are very unsatisfactory in the critical concentration region. Anticipating our conclustion stated below that Hick's model is in reality a more physically meaningful interpretation of Marshall's theory we shall leave out further details of the model but only mention some of its less acceptable points. These are that

(i) The concentration dependence of the average magnetic moment is rather <u>self-inconsistent</u>. According to equation (3.170)

$$\bar{\mu} = \frac{c}{\beta}\{\chi(0) + c\,A(0)\} - \frac{1}{\beta J(0)} \qquad 3.185$$

At least for a given alloy species the parameter $\frac{1}{\beta J(0)}$ is constant so that we can further rewrite equation (3.185) in the obvious form

$$\bar{\mu} = \frac{c}{\beta}\mu_{Ni}(c) - \frac{1}{\beta J(0)} \,. \qquad 3.186$$

For

$$c = 0 \,, \quad \bar{\mu} = -\frac{1}{\beta J(0)} \neq 0 \,. \qquad 3.187$$

Thus for say a Cu matrix there is a measurable negative magnetization polarization which apparently remains constant as the Ni concentration is varied!!

(ii) Again from equation (3.170)

$$\frac{d\bar{\mu}}{dc} = \frac{\chi(0)}{\beta} + 2c\,\frac{A(0)}{\beta} \qquad 3.188$$

Experimentally for CuNi $\frac{d\bar{\mu}}{dc}$ is approximately constant (with an absolute value just greater than unity) for a wide concentration range (0-40%Cu), whereas equation (3.188) with $\frac{\chi(0)}{\beta}$ = 0.276 and $\frac{A(0)}{\beta}$ = 0.687 shows that $\frac{d\bar{\mu}}{dc}$ decreases <u>steadily</u> from a value of 1.239 at c=1 to 1.018 at c=0.6.

(iii) Equation (3.177) is exact and therefore incorrect because it does not allow for the contribution of the second moment of the fluctuation of the Ni moments, as shown in equation (3.80). In addition equations (3.151) and (3.171) imply that for all concentrations $T(0) \equiv M(0)^2$. Such an identity is generally incorrect because T(0) is determined in an essentially zero-field measurement whereas M(0) is measured in a high-field. It is clear from equation (3.188) that $\frac{d\bar{\mu}}{dc}$ is related to the variation of the <u>initial</u> susceptibility and this quantity is only truly determined by T(0).

(iv) The model is clearly not applicable in the critical concentration region where fluctuations of magnetization are both large and <u>long-ranged</u>. In this concentration region $\bar{\mu} \propto (c-c_f)^{\frac{1}{2}}$ (see equation (2.90), a thermodynamic result which any plausible microscopic theory must reproduce. However, a useful aspect of Hick's model is that it enables us to give a more physically meaningful interpretation of the theory formulated by Marshall which has hitherto formed the basis of our discussion of the binary alloy problem in this chapter. We recall (section 3.3(b)) that the effect of introducing an impurity into a ferromagnetic host is to cause "moment defects" or disturbances which could be either positive or negative. A positive defect increases the moment

on a host site adjacent to an impurity and conversely. What has not been made clear is the actual physical meaning of a moment defect. Does it refer to a real change in the intrinsic magnetic moment of the host site? Surely not, because it is difficult to imagine that the mere physical process of alloying can alter the intrinsic moment on a magnetic transition metal atom. This moment, as has been stated, results from intra-atomic interactions which involve energies far in excess of the melting temperatures of the alloy constituents. It is now clear, with some hindsight! that what really happens is that the introduction of an impurity atom leads to changes in both the local exchange field and in the local atomic susceptibility thereby altering the observable moment on the adjoining host sites. Note that in principle this effect has an infinite range because of the implicit chain-reaction. In practice for dilute impurity concentrations the moment disturbance may be confined to just the nearest-neighbours except when there are accompanying large charge perturbations which are not properly screened. The above interpretation of a moment defect merges naturally with the idea of spin fluctuations in the limit of a single magnetic impurity atom in a non-magnetic host where the intrinsic moment of the impurity atom is not observable with any probe whose frequency is less than $\frac{K_B T_o^*}{h}$ (T_o^* is the spin fluctuation temperature - see section 2.2).

For a ferromagnetic host with a non-magnetic impurity we shall assume that equation (3.163) is valid and that

$$\chi(\underline{r},c) = \chi(\underline{r},0) + \sum_{\underline{r}'} \alpha(\underline{r}-\underline{r}')\, p(\underline{r}') \qquad 3.189$$

where $p(\underline{r}')$ is redefined as unity if an impurity is at site $\underline{r}'$ but zero otherwise. $b(\underline{r})$ remains as in equation (3.165) Carrying through the algebra as before we arrive at similar relations i.e.

$$\bar{\mu}_{N_i}(c) = \frac{c}{\beta}\{\chi_{oo} + c A(0)\} - \frac{1}{\beta J(0)} \qquad 3.190$$

and $$\frac{d\bar{\mu}_{N_i}}{dc} = \frac{\chi_{oo}}{\beta} + 2c\frac{A(0)}{\beta} \qquad 3.191$$

Note that equation (3.190) gives the variation of the average Ni <u>local</u> moment with the impurity concentration. At c=0

$$\mu_{N_i}(0) = -\frac{1}{\beta J(0)} = 0.71\ \mu_B/\text{atom} \qquad 3.192$$

Note that if b(o) is the exchange field in pure Ni then to be self-consistent $\beta \equiv -1/b_o$, from equation (3.165). The average magnetization is given by

$$\bar{\mu} = c\bar{\mu}_i + (1-c)\bar{\mu}_{N_i}(c) + \mu_{cond}$$

where μ_{cond} is either the conduction electron polarization or the overlap spin density or their sum. We shall assume that

$$\mu_{cond}(c) \simeq -\alpha\mu_{N_i}(c) \qquad 3.193$$

and since for pure Ni $\mu_{cond} = -0.105\ \mu_B$ /atom $\alpha \simeq 0.15$. If in addition $\bar{\mu}_i$ is zero, say for a non-transition metal impurity, then

$$\bar{\mu} = (1-c-\alpha)\bar{\mu}_{N_i}(c) \qquad 3.194$$

In Marshall's theory for the equivalent case

$$\frac{d\bar{\mu}_{N:}}{dc} = G(0) \qquad \text{(equation (3.60)).}$$

and $$\frac{d\bar{\mu}}{dc} = -\bar{\mu}_{N:}(c) + (1-c)G(0) \qquad \text{(equation (3.61)).}$$

Thus from equation (3.191),

$$G(0) \equiv \frac{\chi_{00}}{\beta} + 2c\frac{A(0)}{\beta} \qquad 3.195$$

and hence $$g(r) \sim \frac{\chi(r,c)}{\beta} . \qquad 3.196$$

We can thus relate the moment defect in Marshall's theory to the physically more meaningful variation of the local atomic susceptibility. In other words Hick's model is not really different from the theory already given by Marshall and therefore it does not relax the assumption of the linear superposition of moment defects which it set out to do. In fact it does not seem to us that the linear superposition approximation is invalid for CuNi alloys. The neutron measurements of Aldred et al (438) give that

$$G(0) = -0.36 - 1.68c \qquad 3.197$$

which is clearly of the form of equation (3.195) so that we may take

$$\frac{\chi_{00}}{\beta} = -0.36 \quad \text{and} \quad \frac{A(0)}{\beta} = -0.84$$

and so from equation (3.190)

$$\bar{\mu}_{N:}(c) = 0.71 - c\{0.36 + 0.84c\} \qquad 3.198$$

The observation by Hicks (455) that the parameters characterising the moment disturbance in CuNi alloys cannot be

described by constants modified by correction terms proportional to c is not quite correct. In the first place, as shown in figure 6 of ref. 438, the parameters $g(r_i)$ tend to vary linearly with c with the exception of the values for the 40% Cu alloy. Secondly Aldred et al (438) did emphasize that because of the large statistical errors involved in evaluating these parameters only the values of $g(r_1)$, corresponding to the first-neighbour shell, should be given some credibility.

It should be noted that instead of equation (3.177) the forward cross-section is now given by

$$T(0) = c(1-c)\,S(0)\left(\frac{d\bar{\mu}_{Ni}}{dc}\right)^2 \qquad 3.199$$

which involves the derivative of the <u>local</u> Ni moment rather than the derivative of the bulk moment. A similar modification applies to the forward cross-section for polarized neutrons. Also an apparently trivial but important point is that $\bar{\mu}$ given in equation (3.198) should be regarded as the saturation magnetization rather than the spontaneous magnetization. In the dilute impurity concentration region the exchange field acting on a magnetic site is sufficiently large that both the saturation and spontaneous magnetizations are identical. In the critical concentration region the two are very different. We should note that equation (3.163) could have important consequences for the ferromagnetic transition metals Fe, Co and Ni. As is implicit in equation (3.165) the moments observed for these atoms are those determined by the magnitude of the exchange fields in the pure metals rather than their saturation values.

Of the three metals Co which has the highest Curie temperature shows the least change between the maximum value of its magnetic moment in any matrix and the moment in the pure metal ($\sim$ 2.1 and 1.99 μ_B /atom respectively). For Fe the change is up to 30% whereas for Ni it is up to 70% (values of $\mu_{Ni} \sim 1.2\,\mu_B$ /atom have been reported for FeNi (468) and PdNi (469)). The maximum values of the moments observed for Fe, Co and Ni atoms in certain matrices correspond nearly to a spin value, S, of $^3/2$, 1 and $\frac{1}{2}$ respectively. To these spin moments should be added an orbital contribution of about 10%.

Finally we should also mention that Medina and Cable (472) have also proposed the generalized local environment model. Specifically for the CuNi system the moment on a Ni atom is assumed to be a function of the number of Cu neighbours and of an effective exchange field produced by its neighbours. Thus

$$\mu_{Ni}(\underline{r}) = \{1 - p(\underline{r})\} F\{b(\underline{r}), \nu(\underline{r}), c\} \qquad 3.200$$

where $b(\underline{r})$ is as defined in equation (3.165) and $\nu(\underline{r})$ is the number of Cu near neighbours i.e.

$$\nu(\underline{r}) = \sum_{f} P_{\underline{r}+f}$$

The main difference between the proposals of Hicks (455) and Medina and Cable (472) is the fact that Hicks used an explicit form for the response function $F\{b(\underline{r}), \nu(\underline{r}), c\}$.

CHAPTER 4

EXPERIMENTAL METHODS

4.1 Diffuse Magnetic Scattering Measurements

(a) Separation of the Magnetic Diffuse Scattering

The magnetic diffuse scattering which is primarily of interest to us appears in the neutron diffuse scattering along with other diffuse scattering components like phonon diffuse scattering and isotopic or nuclear spin disorder scattering. Usually the magnetic scattering is only about 5% of the total diffuse scattering so that great care must be taken to eliminate the effects of the other forms of diffuse scattering from the measurements. Fortunately the ferromagnetic diffuse scattering is sensitive to the application of an external magnetic field because of the factor $(1 - \hat{\kappa}_z^2)$ which occurs in equation (3.45) and can therefore be separated by magnetizing the sample in different directions with respect to the scattering vector. All the other diffuse components should not vary with the direction of the magnetization. If α is the angle between the direction of the scattering vector and the direction of magnetization then $(1 - \hat{\kappa}_z^2) \equiv \sin^2\alpha$. It therefore follows that if the sample is magnetized along the direction of $\underline{\kappa}$ (i.e. $\alpha = 0$) the magnetic diffuse scattering is extinguished; hence the difference between the measured intensities with and without a field should give only the magnetic scattering.

Although not nearly as large as the nuclear diffuse scattering a more troublesome form of diffuse background is that which is partly attributable to magnetic interactions. Such scattering varies with the direction of

magnetization and thus contributes to the difference counts described above. It may arise from

(i) magnetic inelastic scattering:

(ii) for polycrystalline samples, from multiple Bragg scattering in which at least one of the reflections is of magnetic origin:

(iii) the single transmission effect - a change in the transmission of the sample when magnetized.

The effects of multiple scattering and the single transmission effect are greatly reduced by using neutrons whose wavelengths lie beyond the Bragg cut-off for the alloy in question ($\lesssim 5\text{Å}$). The inelastic scattering is excluded by using some form of neutron time-of-flight analysis. Any long wavelength neutrons which are inelastically scattered gain relatively large energy increases so that even a crude velocity selection in sufficient.

(b) The Glopper Diffractometer

The diffuse scattering experiments were performed on the Glopper diffractometer which is positioned in the Pluto reactor hall, A.E.R.E., Harwell. A description of this apparatus has been given previously by Low and Collins (445) and Low (470, 471). The essential components of the apparatus are shown in figure 4.1 (see also plate 4a).

A neutron beam emerging from a tangential hole (7H3L) of the Pluto reactor is incident on a neutron source block near the reactor core. The thermal neutrons are collimated by a concrete and stainless steel flight tube, slightly over a metre long, giving a neutron beam of about 5 cm square with a horizontal and vertical collimation of 2^{o}.

Fig. 4.1 Schematic diagram of the Glopper diffractometer

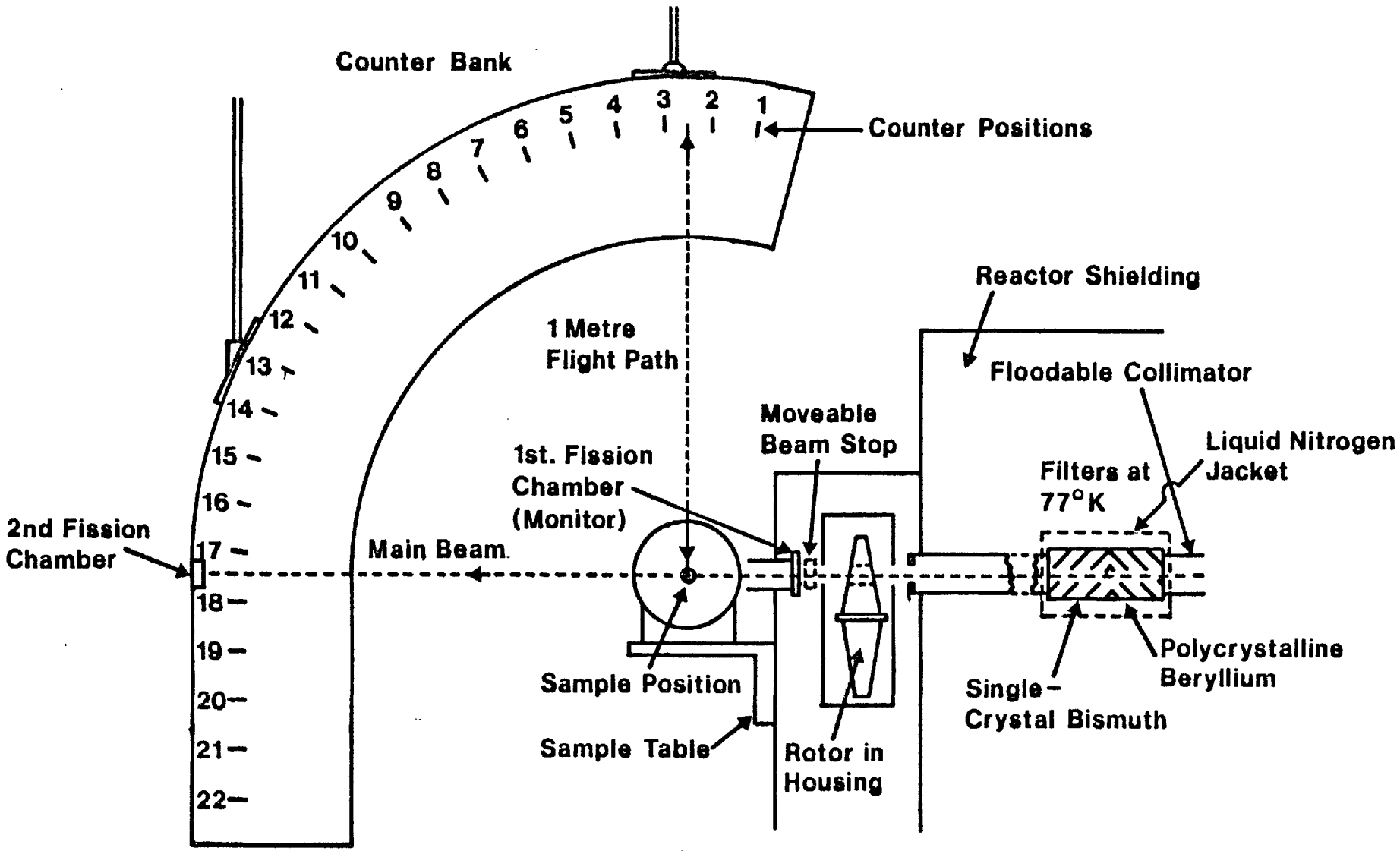

The neutron beam then passes through a filter consisting of polycrystalline beryllium and large single crystals of bismuth. The Be filter only lets through those neutrons whose wavelengths exceed the Bragg cut-off ($=2d_m$, where d_m is the maximum interplanar spacing of the Be crystal); for Be the Bragg cut-off is 3.95Å so that neutrons of a smaller wavelength are reflected by the polycrystalline sample in all directions and finally absorbed by the walls of the filter. The Bi crystal cuts down the amount of gamma-radiation in the neutron beam. The filter is maintained at 77K by a continuous flow of liquid nitrogen in order to reduce the intensity loss due to inelastic phonon scattering in the filter materials.

The filtered beam is then chopped into pulses by a rotor having six equi-spaced 2.5 cm square neutron ports or windows. The chopper is a 25 cm diameter Al-Cd-Al sandwich disc driven by a belt system at a speed of 94.5 r.p.s., with its axis parallel to the beam direction, producing pulses of about 200 μS duration at intervals of 1764 μS. The rotor speed is monitored by a magnetic pick-up mounted alongside the rotor; this produces one electrical pulse per neutron port and is used to trigger the delay electronics. At a speed of 94.5 r.p.s. the rotor can be used to produce neutron pulses of wavelength up to 7.5Å; beyond this wavelength overlapping of successive neutron pulses is likely to occur because the time of flight of the neutrons from the chopper to the counters becomes equal to the interval between the neutron pulses. If neutrons of wavelength greater than 7.5Å are required it will be therefore necessary to reduce the rotor speed

accordingly. However, all measurements to be reported here have been done at a wavelength of 5Å.

A steel collimator 2.5 cm square collimates the neutron beam before and after passing through the chopper. The intensity of the pulsed beam is monitored by a fission chamber mounted in the beam just after the rotor. The fission chamber is a low efficiency counter and is used as a counting base. At the start of this series of experiments the fission chamber used to give a count of about 1800 c/s for a neutron beam flux of $\sim 10^{10}$ neutrons $m^{-2}s^{-1}$ but this decreased to about 1300 c/s a year later when the steel collimator tube was relined with Cd. The counting period is determined by setting a limit to the counts registered by this fission chamber. To avoid the effects of any large fluctuations in the reactor power the counting period in a given mode is usually kept short; a limit count of 2×10^6 was used thus restricting the counting period to about 26 minutes.

The neutron beam may be shut-off by flooding the collimator. The stop-cocks are located on the reactor face to the left of the instrument and there are sight-glasses which indicate when the tube is flooded or empty. A movable Cd-faced beam stop which interrupts the beam between the rotor and the fission chamber is also provided. After the fission chamber the neutron beam finally emerges from a cadmium lined steel snout at a distance of about 20 cm from the sample position. Sometimes this steel snout is replaced by an all-Cd snout especially if it is thought that the magnetic field near the snout will be

appreciable. The snout is 2.5 cm square but appropriate Cd masks may be used to reduce the incident neutron beam to any size required.

The sample table which may be rotated through an angle of up to 45° with respect to the straight-through position is designed to support a number of specimen mountings. The mountings which are of interest to us are a cryostat with a superconducting magnet, a room temperature mounting with a water-cooled electromagnet (this will be referred to simply as the RT magnet), and a second room temperature device (called the Crilth) in which the sample forms an integral part of a low reluctance magnetic circuit of a light electromagnet. These devices will be described in a little more detail below [see section 4.1(c)].

The neutrons scattered by a specimen are counted by a bank of 22 BF_3 detectors mounted in an arc at the end of a 1.6 m flight path. The detectors cover a range of scattering angles, θ, from -11.5° to +49.5° [i.e. 2θ varies from -23° to +99°] with respect to the straight-through position. A second fission chamber is located in this straight-through position and its count may be used in the determination of the transmission coefficient of the sample when this parameter is required.

The counter assembly is gated in synchronism with the chopper so that it records for a short time interval (the gate width, usually $\sim$ 200 μs) after a delay which corresponds to the time of flight of neutrons of a wavelength of 5Å. The crude time-of-flight analysis not only excludes any inelastic scattering but also helps to improve

the wavelength resolution of the whole instrument above that obtainable with only the Be filtered spectrum. The open time of the chopper (i.e. the duration of the neutron pulse) together with the delay time and the open time of the electronic gate for the counters define a wavelength resolution of about 25% (full width at half-height) at 5Å. The counters have a common E.H.T. supply (3.3 KV for counters 1-8 and 2.5 KV for counters 9-22). Each counter has a filter unit attached to it to cut down on electronic noise. The output passes through screened cables to individual charge sensitive amplifiers which have a fixed gain (X1 for counters 1-8 and X20 for counters 9-22) and bias level (varying from 250-375 mV) selected for each counter. The counters are run on the E.H.T. and bias plateaus so that the counting rate remains unaffected by minor fluctuations in the E.H.T. and mains supplies. The amplified pulses are fed via the gating-delay unit to the scalers.

(c) Sample Mountings

The Glopper Cryostat

The cryostat used in the present measurements is shown in fig. 4.2. It is designed to accommodate plate specimens of about 3 cm square although some samples have had to be first mounted on a suitable Cd plate with a central hole of diameter about 2.2 cm. The cryostat has a superconducting magnet which provides a horizontal magnetic field of up to 5 KG. Measurements were carried out at 4.2 K although it is possible to go to lower temperatures ($\sim$ 2 K) by pumping on He. One major disadvantage

Fig. 4.2 The Glopper Cryostat

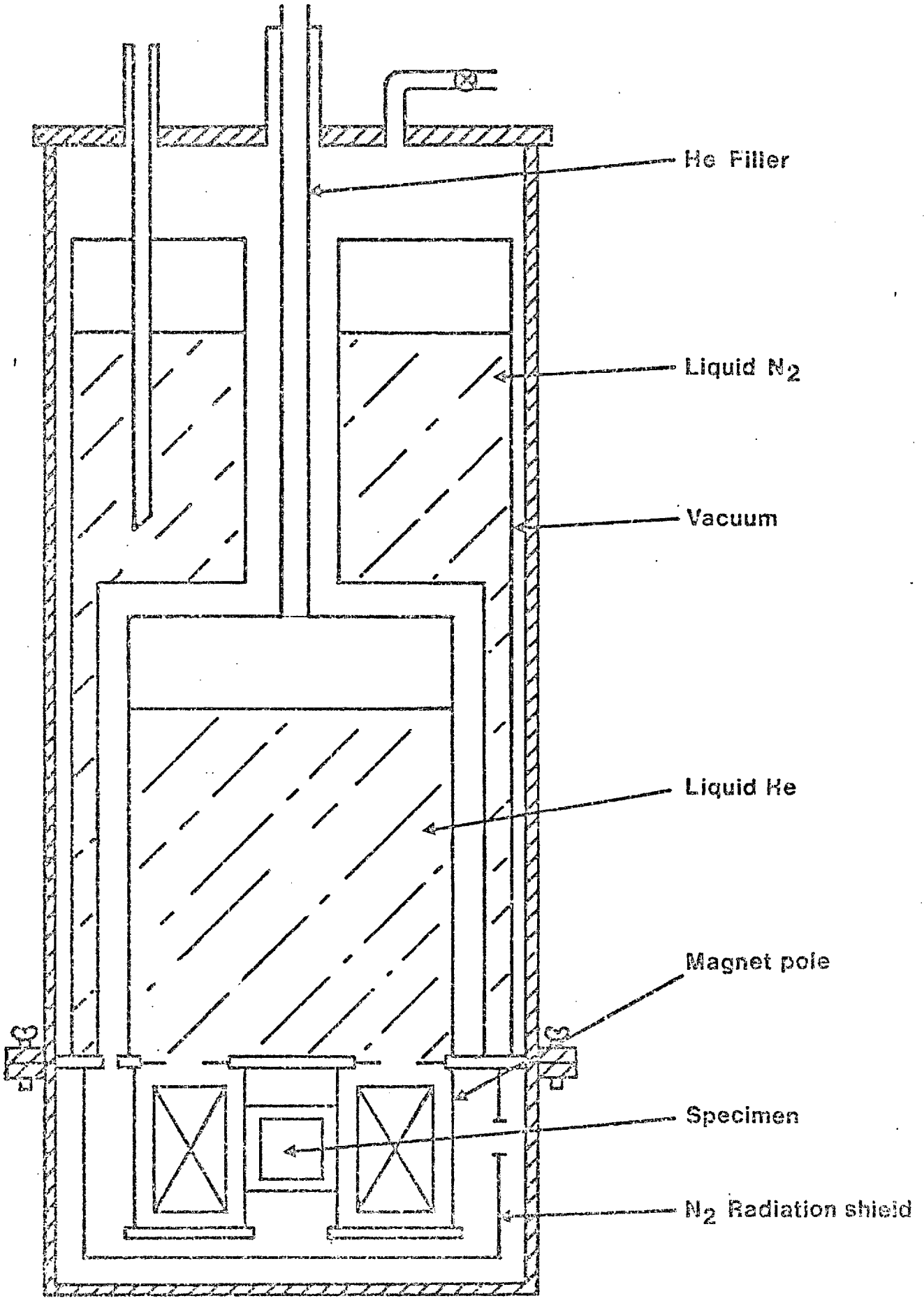

of the cryostat is that it is bottom-loading so that in order to change samples it is necessary to warm it up to room temperature. This means a considerable loss of valuable neutron beam time and a wastage of liquid helium. The magnet is used in the "field off" or "field on" mode. In the "field off" mode the factor

$$\langle 1 - \hat{\kappa}_z^2 \rangle \equiv \langle \sin^2\alpha \rangle = 2/3$$

whereas in the "field on" mode it is zero. Thus the magnetic cross-section is switched between $^2/3$ of its maximum value and zero. In the switching off process the field is cycled to zero in order to demagnetize the sample.

The RT Magnet

This magnet provides a vertical magnetic field of up to 12 KG so that the direction of the magnetization is perpendicular to the scattering vector. It is also used in the "off" or "on" mode and therefore switches the magnetic cross-section between $^2/3$ and unity. It has an adjustable Al or steel pole-piece with a flat end. When the steel pole-piece has had to be used that part of it which was likely to be in the neutron beam was covered with Cd. Since no sample holder was provided a Cd plate with a hole in the centre was attached to the flat end of the upper pole piece and the samples were then attached to this Cd plate with Kwikfill. A voltage cycling device is provided in the power supply unit in order to demagnetize the pole-pieces on switching off. The use of a Cd plate for mounting the samples implies that an air-gap is left between the pole-pieces to facilitate demagnetization. It takes about 10 minutes to go from the "on" to

the "off" condition so that it is necessary to count for fairly long times in each position to minimise loss of time on cycling. The magnet is water-cooled from the reactor cooling system.

The Crilth

This is a simple and light electromagnet which is alternately rotated by 90^{o} so that the magnetization vector which is in the plane of the specimen is alternately vertical and horizontal; the magnetic scattering is correspondingly switched on and off completely and the difference in the scattered intensities gives the maximum switchable magnetic cross-section. The electromagnet is not water-cooled so that a maximum current of 5A only can be used but this is sufficient to saturate the sample because the latter forms part of a low reluctance magnetic circuit. One disadvantage is that since counting is done continuously for up to 30 hours at each of two settings of the angle between the plane of the specimen and the direction of the neutron beam (0 and 30 degrees) the sample often gets quite hot (up to $\sim$ 50K above room temperature).

Plate 4a is a photograph of the Glopper with the crilth in position.

(d) Sample Preparation

The Invar Alloys

Three samples of wrought Fe-Ni binary alloys were prepared at the Research and Development Centre of International Nickel Limited (InCo). High purity iron and nickel pellets were vacuum-melted and cast as 5 cm square section ingots. They were then homogenised at 1373K for 2 hours,

Plate 49

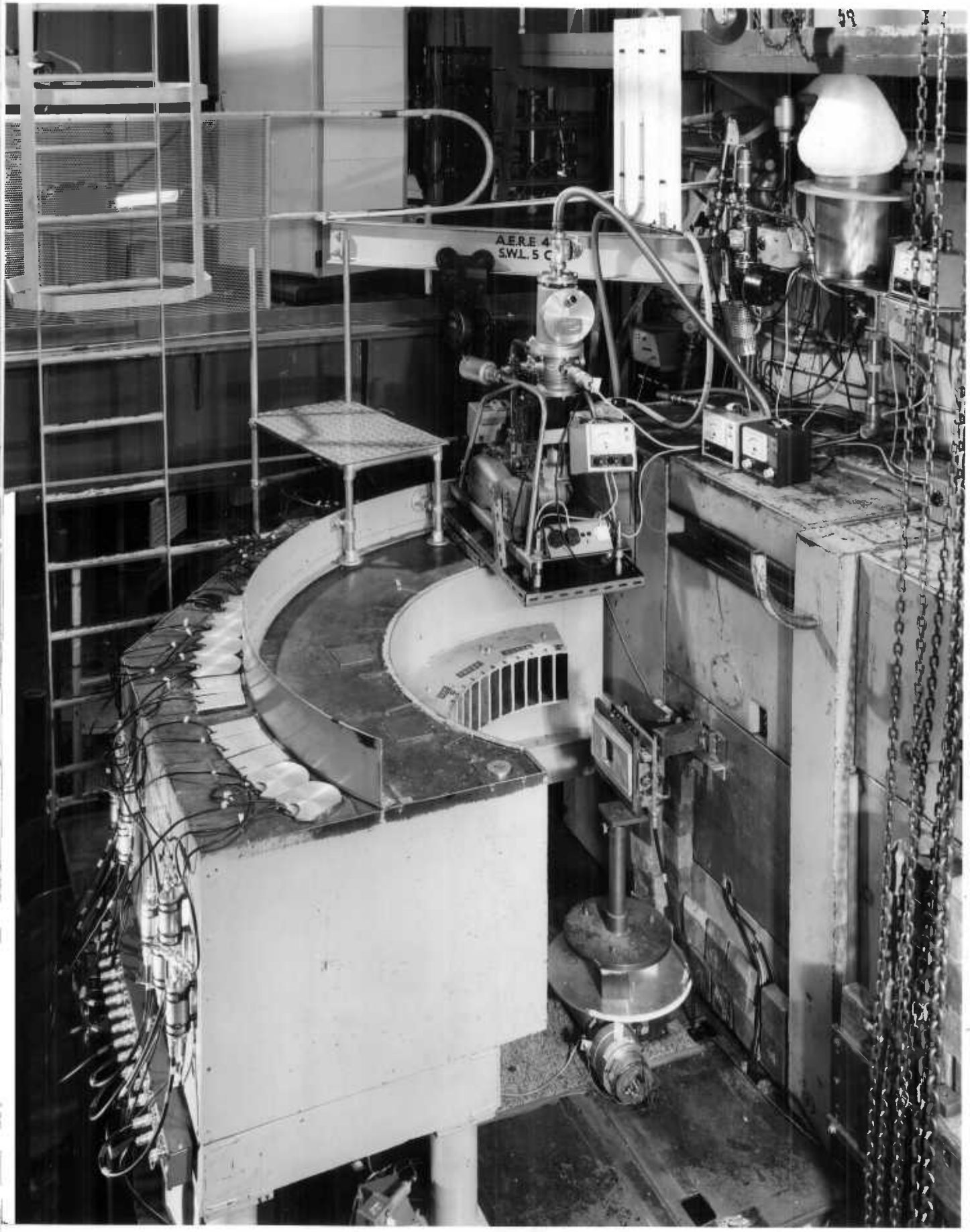

forged to a thickness of about 1.3 cm, hot-rolled to about 6 mm and finally annealed at 1073K for 1 hour in an atomsphere of argon containing 5% hydrogen. The analysed compositions of the samples are as follows:

Invar 1: 32.285% Ni; 67.597% Fe

Invar 2: 35.040% Ni; 64.84 % Fe

Invar 3: 38.00 % Ni; 61.88 % Fe

The main impurities are 0.052% Mn, 0.021% Al, 0.020% Si, 0.014% C, 0.008% S and 0.004% P.

As received the samples were in bars each about 5.6 cm wide, 6 mm thick and about 20 cm long. From these bars plates of about 3 cm square for the cryostat and RT magnet and discs of about 6 cm diameter for the crilth were cut and polished.

The Rh-doped invar specimen was accidentally prepared as Ni 5% Rh by Dr. H. E. N. Stone of the Metal Physics Group, Imperial College, London, by melting pure Rh (Eng.4N) and what was thought to be pure Ni (InCo). The specimen started to crack on very light hammering and so was spark machined to size ($\sim$ 4 mm thick). The anomalously large cross-section obtained for this alloy necessitated a check on possible Fe contamination. An initial microprobe analysis showed the Fe content in this alloy to be very high and it was therefore decided to measure the actual compositions of both the alloy and the original "Ni" rod. This was done by microprobe analysis in which measurements were made by scanning areas of about 100 μm square, using pure Ni, Fe and Rh as standards. The "Ni" rod in fact turned out to be a bar of invar 2 (65% Fe, 35% Ni) and

the "Ni 5% Rh" to be 63% Fe, 33% Ni and 4% Rh with a trace of Mn.

Ni-Rh Alloys

Eight Ni-Rh samples were measured. With the exception of Ni 2% Rh and Ni 36% Rh all the alloys were prepared by Dr. H. E. Stone. Details are as follows:

Ni 2% Rh

This was a Harwell sample which had been used in a previous measurement reported by Comly et al.(473). This earlier measurement was carried out on the Crilth so that the sample was in the form of a disc about 6 cm in diameter and about 6.5 mm thick. From this disc a plate of dimensions 3.05 x 3.17 x 0.65 cm was cut out for use with the cryostat and the RT magnet. A later microprobe analysis of this Ni 2% Rh plate showed it to be very inhomogeneous with regions of high Rh content. Off-cuts from the original sample were also remelted to form another Ni 2% Rh sample in the shape of a thin disc ($\sim$1.2 mm thick) but a microprobe check of this sample after the neutron diffraction measurements have been carried out showed, that this sample was only fairly homogeneous. Unfortunately in all cases the microprobe checks were carried out after the neutron measurements have been completed so that we are not sure whether neutron irradiation at low temperatures contributed to the observed inhomogeneity.

Ni 4% Rh

This sample was prepared by melting a portion of the Ni 15% Rh sample with pure Ni (KL 3N). It was coldforged and rolled down to

a thickness of 1.64 mm. The almost exact correspondence of the magnetic cross-section of this alloy with that of Pt 3% Co forced us to request an analysis of the alloy. The analysis showed that the alloy was fairly homogeneous with a composition of Ni 3.4% Rh which is very close to the nominal concentration.

Ni 10, 15, 20, 24 and 30% Rh

These alloys were prepared by melting appropriate amounts of the pure metals - Rh(ENG. 4N or JM 3N) and Ni (KL-4N). The weight loss on melting was generally about 1% so that we have assumed that the nominal concentrations are correct. As a further check on the composition the lattice spacings of some of these alloys were measured as described below. The 10% Rh alloy was cold-forged to a button 2.5 cm in diameter and $3\frac{1}{2}$ mm thick. It was then annealed at 1073 K for about 5 minutes only and spark machined to a final thickness of 2.06 mm.

The 15% Rh ingot was hammered down to a thickness of about 2.5 mm, annealed in air at 1073 K for a few minutes, forged and cold-rolled to a thickness of 2 mm when it started cracking.

The 20, 24 and 30% Rh were cold-forged and rolled down to buttons of thickness 1.88 , 1.0 and 1.24 mm respectively. Another sample of Ni 30% Rh had been made much earlier (in June 1973, whereas the other sample was made in April 1975) by melting suitable amounts of pure Rh (ENG 4N) and Ni (InCo). The ingot, which had a dull surface, was then hot-worked with numerous heatings at 1073 K and the button given a final anneal at the same temperature for a few minutes. The resulting specimen was rather poor - it had a non-uniform thickness (in fact it resembled a thin

wedge), and the surface was very uneven because of numerous cracks. On examination this alloy appeared to be inhomogeneous, with slightly Ni-rich regions.

Finally the Ni 36% Rh alloy was another Harwell sample. It was a thin metal plate of dimensions 3.073 x 3.180 x 0.1 cm and had also been used in an earlier measurement which was reported briefly by Hicks et al (204).

A microscopic examination of many of these alloys did not show any sign of a second phase. The Fe impurity content of the alloys as estimated by emission spectrography was less than 10 p.p.m.

PtCo and PtFe Alloys

Three slabs of Pt 1½% Co, Pt 1½% Fe and Pt 2% Fe originally prepared for Dr. G. G. Low of A.E.R.E. Harwell were handed over to us. Each slab was about 3 cm square and nearly 6 mm thick!! After the initial runs on these samples it was decided to remelt them and prepare smaller buttons. Portions of these alloys were also diluted with either Pt, Co or Fe as necessary to prepare other samples - Pt 1% Co, Pt 3% Co, Pt 6% Co and Pt 5% Fe and Pt 10% Fe.

(e) Experimental Procedure

Cryostat Runs

The specimen holder is placed in position and the specimen table adjusted vertically and/or laterally until the sample position is in the centre of the neutron beam. This is checked by taking a photograph with a Polaroid camera with a small Cd cross placed across the snout through which the neutron beam emerges.

The sample is then attached to the holder using durofix or kwikfill, making sure none of the material is on the exposed surface of the sample. The radiation shields are replaced, as is also the helium bin, and finally the base is screwed on. The cryostat is pumped down, first with a backing-up pump and later with a diffusion pump until a pressure of $\sim 10^{-4}$ torr is obtained. The cryostat is then filled with liquid nitrogen and left to cool down for nearly 14 hours while the pump-down continues. It is filled with helium and attention is now turned to the controls. First the delay setting and the gate width are checked; the movable beam stop is removed and the reading of the first fission chamber checked to make sure it is steady. This reading is called the "flux" and is typically 1.3 kc/s when the reactor is at full power ($\sim$ 22 MW). The limit count (usually 2×10^6), the automatics setting (mode 2, magnet off/on), the number of repeat counts per cycle and the total number of cycles required are also set. By a cycle we mean one set of counts with the field off and with the field on; this would usually imply 4 repeat counts, each lasting about 26 minutes, with the field off and another 4 such counts with the field on. Thus one cycle would last for nearly $3\frac{1}{2}$ hours. When the set number of cycles is reached the counting would automatically stop but in practice this number is set high enough that the observer can stop the run himself.

The counter readings are punched on an 8-hole tape so that the paper tape punch is also checked. It is switched on and the run number, sample, wavelength, angle and date are punched on it using an attached teletype.

It is then switched off (i.e. to remote automatic control).

When the observer is satisfied that all the necessary controls have been checked and found to be in order the programme reset button is pressed followed by the start button to start the counting. Plate 4b shows the control system for the Glopper electronics.

After the first filling of the cryostat with helium it is necessary to top it up about 10 hours later. Thereafter it may only be necessary to fill up again at intervals of about 30-36 hours until the run is stopped.

Owing to the long wavelength of the neutrons used it is necessary to carry out the measurements at two settings of the angle between the plane of the specimen and the direction of the neutron beam in order to cover a reasonable range of values of the scattering vector (up to $\sim 1.7 \text{Å}^{-1}$). The two angles are usually 0° (incident neutron beam perpendicular to the plane of the specimen) and either 30° or 45°. The duration of each run is determined by the magnitude of the difference counts. For the invar and Pt alloys where the difference counts were reasonably large counting was carried on continuously for only about 48 hours at each angle but for NiRh alloys the counting time was increased to over 72 hours. Thus measurements on each NiRh alloy took about a week to complete.

When measurements have been completed at both angles for a given sample the collimator is flooded, excess liquid nitrogen and helium are blown off and the cryostat allowed to warm up. The sample is then changed and the

Plate 4b

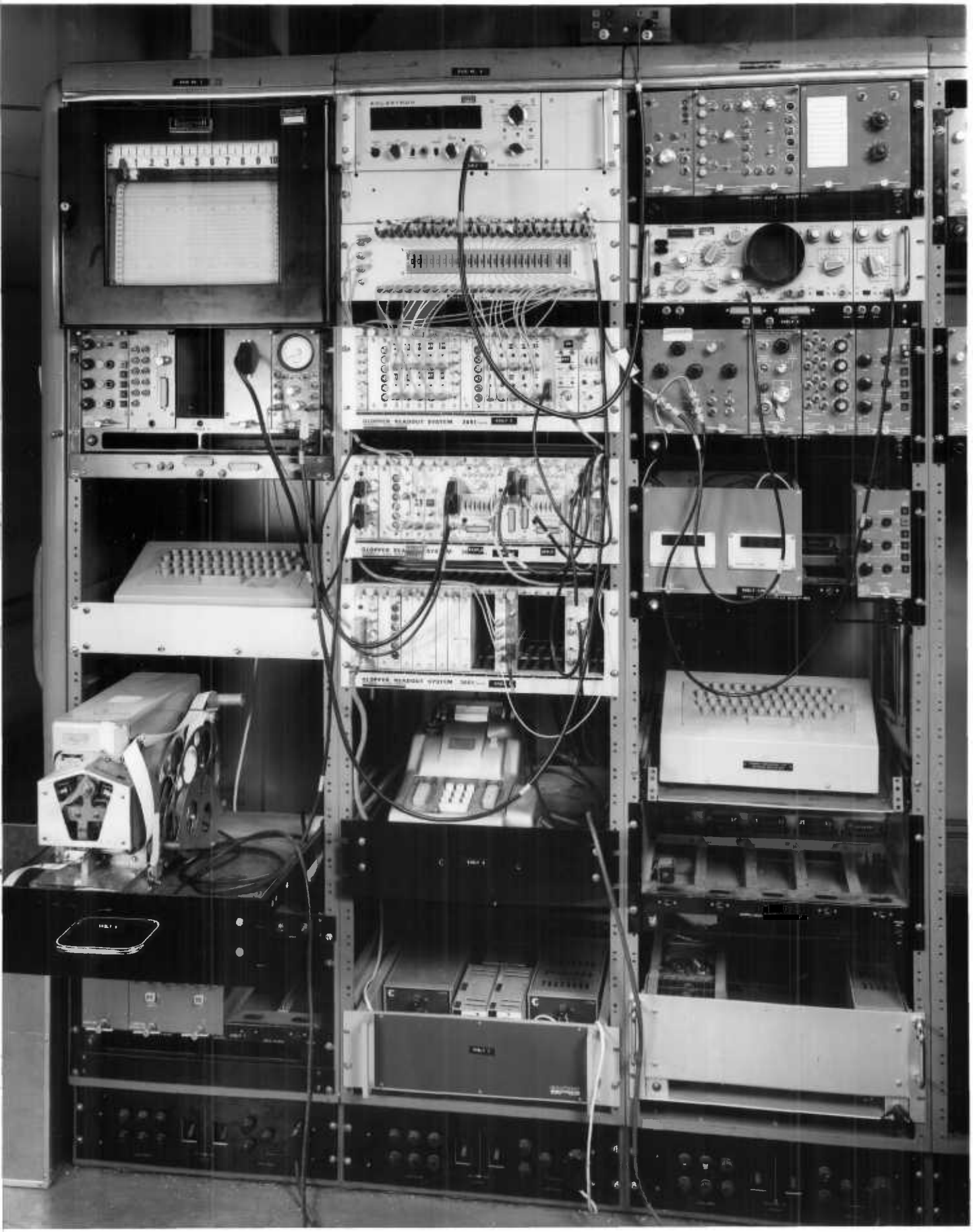

whole process repeated with the new sample.

In order to eliminate various unknown instrumental factors such as the efficiency of the counters, counter acceptance angles, air absorption during flight etc, the scattering from a standard specimen is used to calibrate the apparatus. The standard chosen is Vanadium because (a) it has negligible coherent scattering (b) it has a large diffuse scattering cross-section - 5.13 barns/atom and (c) it can be obtained in a pure stable form. The neutron absorption cross-section for vanadium is very large (13.9 barns/atom at 5Å) but then only a thin specimen is required because of the high incoherent cross-section.

The intensity calibration is very important because it is used to obtain the absolute value of the cross-sections given by the difference counts in the magnetic scattering. It was therefore carefully carried out at the beginning of each set of experimental runs (i.e. for each reactor cycle lasting about 24 days). For the intensity calibration three separate runs are required:-

(a) Vanadium run:- this was carried out at the temperature of liquid nitrogen. The vanadium specimen used was a rolled vanadium plate, about 3 cm square and about 1.5 mm thick and was attached to the specimen holder so that it was not only in the same position as the sample but also had the same surface area exposed to the beam. Counting was carried on continuously for about 12 hours and the average of the "on" and "off" counts taken since the cryostat magnet could not function at 77K.

(b) Air run:- the vanadium specimen is removed and a run

carried out with only the specimen holder in position. This run is used to determine the amount of air scattering in the vicinity of the sample.

(c) Cadmium run:- a Cd plate is attached to the sample holder. This run determines both the background count and the electronic noise recorded by the counters. However the electronic noise is usually small since the counters are run on the plateaus of the E.H.T. and bias voltage.

The air and Cd runs were carried out at room temperature and lasted about 5 and $1\frac{1}{2}$ hours respectively. The intensity calibration is, of course, done at both angles (i.e. at 0^{o} and 30^{o} or 45^{o}).

RT Magnet and Crilth Runs

The procedure for these is almost as outlined above except that all measurements are carried out at room temperature and a few other minor differences e.g. in the case of the crilth, the magnet is always on and instead of "off" and "on" counts we have counts alternately with field horizontal and vertical. For obvious reasons the difference counts in the RT magnet and crilth runs are negative.

(f) Reduction of Data

The data from the Glopper are punched on an 8-hole paper tape and include the 22 counter readings, the limit count, the control digit (i.e. magnet off or on) etc. The paper tape is transferred to magnetic tape by a PDP-8 and later processed using programmes already existing. For each counter the counts are added, the mean found and counts falling outside the standard deviation are rejected. The counts are reaveraged and the mean count and error printed

out in a standard format. This consists of a title - the run number, sample, angle, wavelength, temperature, date and any other relevant information as originally punched on the tape before the start of the particular run - followed by seven columns giving the counter number, total on counts, total off counts, the means of the "on" and "off" counts, the difference count and the error in this difference count.

The errors given with the processed data, and with any computed results, are due to statistical errors only in the counts. Counting statistics are assumed to follow a Poisson distribution which approximates to a Gaussian for very large counts. Consequently the standard error on a single count x_i is given by $\sqrt{x_i}$. If the average, $\bar{x}$, of such counts is determined then the standard deviation on this is $\pm\sqrt{\bar{x}}$. Therefore counts falling outside the limits $\bar{x} \pm 2.8\sqrt{\bar{x}}$ are rejected. The standard error quoted on the means is $\sqrt{\frac{\bar{x}}{n}}$ and is the value printed out. If s_1 and s_2 are the standard errors for the mean "on" and mean "off" counts then the standard error of the difference count is $\pm (s_1 + s_2)^{\frac{1}{2}}$. It is clear from the foregoing that the accuracy of any measurement depends on both the magnitude of the count and the number of counts determined. Cadmium and air counts become important when their standard errors approach that on the vanadium count.

For the intensity calibration runs the difference count is ignored (in any case it should not be significant); the average of the mean "on" and mean "off" counts is taken and the standard error on this average is taken as

$\frac{1}{\sqrt{a}}$ times the standard error on the corresponding difference count.

If C_V, C_{Air} and C_{Cd} are respectively the observed Vanadium, air and Cadmium counts in a given calibration run then the true Vanadium count, correcting for the air and background scattering, is given by

$$C_V^c = C_V - (C_{Air} - C_{Cd})e^{-\tau/\cos\phi} - C_{Cd} \qquad 4.1$$

where $\tau = n\sigma t$. 4.2

n is the number of atoms per unit volume, t is the thickness of the specimen (assumed to be uniformly thick) and σ is the total cross-section i.e.

$$\sigma = \sigma_s + \sigma_a \qquad 4.3$$

where σ_s is the mean incoherent scattering cross-section and σ_a is the corresponding absorption cross-section at the appropriate neutron wavelength. ϕ is the angle between the neutron beam and the normal to the (planar) sample face. The corrected observed vanadium count, of course, depends on a number of factors such as the efficiency, η of the counter, the incident neutron flux, Io, the area, A, of the pupil on the Cd sample holder, the solid angle, $d\Omega$, subtended at the sample by the counter, the absorption of the sample, and finally the amount of multiple scattering. The absorption correction is given in terms of the transmission, T, of the sample which in the case of a sample of plane geometry is given by

$$T = \frac{e^{-\frac{\tau}{\cos(\phi-2\theta)}} - e^{-\frac{\tau}{\cos\phi}}}{\tau/\cos\phi - \frac{\tau}{\cos(\phi-2\theta)}} \qquad 4.4$$

The multiple scattering correction is taken to be isotropic with the same absorption correction as the primary scattering. Consequently it is only necessary to introduce a multiplicative factor, F_M, into the expression for the observed counts. The factor F_M is defined as

$$F_M = 1 + \frac{S_{mo}(\tau, \omega)\, e^{\tau}}{\omega\tau} \qquad 4.5$$

where

$$\omega = \frac{\sigma_s}{\sigma} \qquad 4.6$$

and Smo is a function which has been tabulated by Brockhouse et al (474). In terms of the above parameters the corrected observed vanadium count is given by

$$C_V^c = \eta I_0 A\, d\Omega \cdot nt \cdot \frac{\sigma_s}{4\pi}\, T F_M \qquad 4.7$$

Equation (4.7) enables us to obtain a calibration constant or factor (calfac) which is defined as

$$\text{Calfac} \equiv \eta I_0 A\, d\Omega = \frac{4\pi C_V^c}{nt\sigma_s T F_M} \qquad 4.8$$

$$\equiv \frac{4\pi C_V^c}{\omega\tau T F_M} \qquad 4.9$$

In deriving an expression for the difference count obtained by using the appropriate use of a magnetic field it is assumed that (a) the multiple scattering is unchanged (b) the total scattering cross-section is nearly unchanged on switching, i.e. the switched cross-section is small compared with the remaining cross-section and the absorption cross-section; thus (c) the absorption cross-section is unchanged. It is also assumed that the sample geometry

is unchanged on switching, i.e. there is no bulk movement of the sample when the magnetic field is switched on. If the difference count is represented by C_{diff} then from equation (4.7) we have that

$$C_{diff} = \eta I_o A d\Omega (nt)_s \frac{d\sigma}{d\Omega} T_s \qquad 4.10$$

where the subscript s refers to the sample as distinct from vanadium. Thus the magnetic differential cross-section is

$$\frac{d\sigma}{d\Omega} = \frac{C_{diff}}{T_s} \times \frac{1}{(nt)_s} \times \frac{1}{Calfac} \qquad 4.11$$

The above cross-section is dependent on the particular set-up used i.e. whether the cryostat, RT magnet or the crilth is used. To obviate this problem the switching fraction, S.F., for a given set-up is introduced into the denominator of equation (4.11) so that the resulting differential magnetic cross-section is the maximum switchable. Thus

$$\frac{d\sigma}{d\Omega} = \frac{C_{diff}}{T_s} \times \frac{1}{(nt)_s} \times \frac{1}{Calfac} \times \frac{1}{S.F.} \qquad 4.12$$

As explained in section 4.1(c) the switching fraction is $\frac{1}{3}$ for the RT magnet, $^2/3$ for the cryostat and unity for the crilth. However, for both the cryostat and the crilth when the magnetic field is horizontal one has to make a correction for the fact that in a given set of measurements the magnetization vector is only parallel to the scattering vector at one scattering angle only. Thus the switching fraction is angle dependent and is given by

$$S.F.(\theta) = 0.666667 - \sin^2(\phi - \theta) \qquad 4.13$$

for the cryostat and

$$S.F.(\theta) = 1 - \sin^2(\phi - \theta) \qquad 4.14$$

for the crilth.

4.2 Magnetization Measurements

(a) A Brief Account of the Apparatus and Experimental Method

Magnetization measurements were carried out on a few NiRh samples using the vibrating sample magnetometer (VSM) originally built by Murani (475) and extensively described by him and also by Tari (214a). Accordingly it will be sufficient here to only give a brief outline of the principles involved in the measurements.

The VSM is based on the well-known principle of electromagnetic induction namely a magnetic sample is made to vibrate inside a pick-up coil and the voltage induced in the coil is amplified and detected. The vibration frequencies utilized are usually in the audio frequency range so that an extremely high sensitivity can be obtained by using suitable narrow-band amplifiers and detectors. The sample vibration is produced by a piezo-electric transducer, called a bimorph, used in a tuning-fork arrangement designed to reduce the direct transmission of the sample vibrations to the arrangement housing the pick-up coil. Such a transmission of the sample vibrations to coil-housing will lead to a "synchronous voltage" being induced in the pick-up coil and which can only add to the general noise level of the instrument. Null measurements of the magnetic moment of the sample are made by passing a current through a pure Cu coil (SWG 49) wound round a

cylindrical glass-former in which sample is placed. The nulling current is directly proportional to the magnetic moment and the latter can be obtained in absolute units by calibrating the instrument using pure Pd.

The elastic constants of the bimorph change with temperature. Specifically the stiffness of the bimorph increases on cooling so that the resonance frequency also increases. Typically at room temperature the resonance frequency is about 42 Hz while at helium temperature it is about 56 Hz, showing a 33% increase. Consequently when measurements are made as a function of temperature the frequency of the driving signal to the bimorph is altered to keep pace with the increasing resonant frequency. Simultaneously the phase shifter is adjusted also to keep the input and output signals in phase.

Two advantages of the VSM over the conventional force methods of measuring both magnetization and susceptibility are that the VSM is suitable for measurements in zero and/or uniform magnetic fields, and also is much simpler and hence easier to use. The limiting factors to the accuracy of measurement include the thermal noise (i.e. Johnson noise) of the pick-up coil, the noise figure of the amplifier, the paramagnetism of the glass-former on which the coil is wound and, most importantly, the synchrono voltage induced in the pick-up coil through vibrations transmitted to the pick-up coil. After many interrupted runs it was found necessary to take the apparatus to bits and reassemble it again, completely rewiring it in the process and re-introducing the compensating pick-up coils which were present in the original VSM but somehow were

absent in the apparatus as found. Afterwards a signal to noise ratio of about 50 was obtained in applied fields as large as 6 KG. For example for an input signal of 8.5v (rms) at a frequency of 50 Hz a current of 10 mA in an empty nulling coil gave an output of 1.52v for an amplifier gain of 80 dB ,whereas the total noise from the empty coil at a field of 6 KG has a maximum value of about 30 mV.

The nulling current method of measurement is impracticable for strongly magnetic materials because the large nulling current that would be required would lead to an excessive heating of the sample. A direct measurement of the induced signal is made and this is then converted to the equivalent nulling current by measuring the corresponding output signal in zero applied field for a known current in the nulling coil. For ferromagnetic samples even the above procedure is unsuitable for obvious reasons, and had to be modified. The samples were found to saturate in fairly low fields (about 100 oe) so that in applied fields greater than about 3KG only the high field susceptibility (which turned out to be constant) was observed. Calibration was therefore carried out by first saturating the sample by applying a sufficiently high field and then measuring the change in the output signal when a known current is passed through the nulling coil and its direction reversed. For example one NiRh sample gave a direct output voltage of 8.96v in a field of 6KG (amplifier gain = 60 dB). When a current of 10 mA was passed through the nulling coil and then its direction reversed the output voltage changed to 10.10v and 9.82v respectively. Thus

an output voltage of 0.28v is equivalent to a nulling current of 10 mA. Such a procedure may be subject to a large error so that the absolute values of the magnetization quoted here may be inaccurate but the relative values are precise and accurate.

The samples used in the magnetization measurements were also prepared by Dr. H. E. N. Stone and were in the form of small cylinders of diameter about 1 mm and length about 14 mm. The samples were not made from those used in the neutron diffraction measurements, although such a procedure would have been ideal.

Measurements of the magnetization, M, as either a function of temperature ($1.65 \leq T \leq 300K$) for a given field or as a function of field ($0 \leq H \leq 8KG$) for a given temperature were carried out. From these measurements it was possible to deduce the spontaneous magnetization, $M_o(T)$, the ferromagnetic Curie temperature, T_c, and the paramagnetic Curie temperature (or the Curie-Weiss constant), θ_p, as discussed below.

(b) Analysis of Magnetization Data

(i) Determination of the spontaneous magnetization, M_o

In determining the spontaneous magnetization of a ferromagnet several processes must be taken into account. These are the "approach to saturation", the "paraprocess effect" (i.e. high-field susceptibility) and the demagnetizing field. A typical magnetization curve for a polycrystalline ferromagnet has been sketched in fig. 2.16, in which the magnetization is plotted as a function of the external magnetic induction, Ba. The initial slope, OA,

is determined by the demagnetizing field. When the point A is reached ferromagnetic domains will have aligned themselves along easy directions of magnetization closest to the field direction. From A to C the applied field rotates the moments towards the field direction. For $T \lesssim \frac{1}{2}T_c$ a semi-empirical approximation for the approach to saturation along AC has been given (476, 477) as

$$M_{Ba}(T) = M_0(T)\left\{1 - \frac{a}{B} - \frac{b}{B^2}\right\} + \chi_V B \qquad 4.15$$

In equation (4.15) the term $^a/B$ is said to account for the "magnetic hardness" of the specimen, an effect due to the presence of cavities and non-magnetic inclusions. The term $^b/B^2$ arises from magnetoelastic, anisotropic and crystallite effects. χ_V is clearly the high-field (or paraprocess) susceptibility. For χ_V sufficiently small a plot of M versus $^1/B$ for fields above point A should give a nearly straight line from which M_0 may be extrapolated as the intercept on the ordinate. Note that M should strictly be plotted against the internal magnetic induction, Bi, given by

$$Bi = B_a - NM \qquad 4.16$$

where N is the demagnetizing factor. In the measurements reported here no corrections have been made for the demagnetizing field because we have assumed with Murani (475) that this field is negligible for a thin cylinder. However, it appears that this is only so if the applied magnetic field is parallel to the axis of the cylinder. In the VSM used here the magnetic field is perpendicular to the axis

of the cylinder and for an infinitely thin cylinder the demagnetizing factor $N = 2\pi$. If required an estimate of the effective demagnetization factor can be obtained from the initial slope of the M vs B_a curve by assuming that the magnetization distribution is such as to make the internal field zero. Thus

$$B_i = B_a - NM = 0$$

giving

$$N = B_{a/M} \qquad 4.17$$

(see also the discussion given by Claus (388)). The portion, OA, of fig. 4.3 may be used to determine this effective N.

For temperatures $T > \frac{1}{2}T_c$, χ_v may not be regarded as being small and, more importantly, it can no longer be determined by anisotropy since the latter decreases rather rapidly with increasing temperature. M_o is now determined by plotting M against B_i and projecting back to $B_i = 0$ from high-field values.

Having obtained the values of $M_o(T)$ the next problem is to determine M_{oo}. In view of our earlier comment on the temperature dependence of the spontaneous magnetization of the ferromagnetic transition metals and their alloys (see section 2.7, equation (2.307) et seq.) perhaps it may be more correct to plot $M_o(T)$ against T^2 instead of against $T^{3/2}$. However, it is probably best to obtain $M_o(T)$ for as low temperatures as possible (down to say 1.6K) and then to simply extrapolate to absolute zero.

(ii) Determination of the Curie Temperatures T_c and θ_p

Various methods of determining T_c from magnetization measurements have been recently summarized by Mcguire and

Flanders (478). One method which has been used is based on the equation

$$\alpha(T - T_c)\, M + bM^3 = Bi \qquad 4.18$$

which may be obtained either by expanding the Brillouin function (479) or the free energy (232) in a power series in M. (cf equation (2.92)). A plot of M^2 against Bi/M (the Belov-Arrott plot) should therefore give a straight line with an intercept of $\alpha(T_c - T)$ on the M^2 axis. When this has been done for a number of temperatures around T_c (above and below) the M^2 intercepts are then plotted against T to obtain T_c. This procedure is more precise than attempting to directly obtain T_c as that temperature for which the Belov-Arrott straightline passes through the origin.

A second method of obtaining T_c which is less demanding both in time and effort but correspondingly less precise and semi-empirical is to plot the M_o versus T curve for very small fields and to estimate T_c from the projection of the points of inflection on these curves onto the temperature axis. The justification of this procedure follows from the fact that the Brillouin function has a discontinuity in slope at T_c and in very small fields this point will appear as an inflection in the M vs T curve.

The paramagnetic Curie temperature was determined by measuring the magnetization as a function of temperature for a given low field, and then plotting the inverse magnetization against T. θ_p is given by the intercept on the T-axis. In concluding the discussion in this section we

note that recently Praddaude and Foner (480) have argued that the method of using Belov-Arrott plots to determine T_C for dilute ferromagnetic alloys is unsatisfactory and have instead suggested the use of low-field methods which depend mainly on the demagnetization factor of the specimen e.g. low-field ac susceptibility measurements or the "kink effect" measurements (482) using low dc fields. (NB the "kink effect" refers to the fact that in low dc fields the magnetization in the ferromagnetic state is limited to a maximum value by the demagnetization factor.) However, as regards the ac measurements Maartense and Williams (392, 481) now propose that it is the point of inflection, rather the position of the maximum, of the zero-field ac susceptibility versus temperature curve which gives the Curie temperature in the "giant moment" systems. It thus appears that the most convenient method of measuring T_C for the alloys in question is the second method discussed above.

4.3 Determination of Lattice Constants

The lattice constants of some of the NiRh samples used in the neutron diffraction measurements have been determined primarily as a check on their nominal concentrations. X-ray reflections from the same NiRh buttons or plates used for the neutron experiments were measured at room temperature using Cu K_α radiation. The lattice spacing were computed using $\lambda_{K_{\alpha_1}} = 1.54051\,\text{Å}$ and $\lambda_{K_{\alpha_2}} = 1.54433\,\text{Å}$ in the few cases where the doublet was clearly resolved and $\lambda_{K_\alpha} = 1.541783\,\text{Å}$ otherwise. The calculated lattice-parameter values were then plotted

against the standard Nelson-Riley function

$$f(\theta) = \frac{1}{2}\cos^2\theta\left(\frac{1}{\theta} + \frac{1}{\sin\theta}\right) \qquad 4.19$$

to obtain an extrapolated value for each sample.

CHAPTER 5

WEAKLY FERROMAGNETIC PtCo AND PtFe ALLOYS

5.1 Introduction: Review of existing magnetization, electrical resistivity and other data for dilute PtCo and PtFe alloys.

Pt is generally expected to have similar properties with Pd which lies immediately above it in the periodic table. It is therefore accepted to be exchange enhanced but with a much smaller exchange enhancement factor, ~ 1.8 (483) as compared with a value of 7-10 for Pd (127,484). Consequently, the onset of ferromagnetism and the concomitant occurrence of "giant" moments when small amounts of Fe and Co are added to Pt are not surprising. The smaller values of the "giant" moments $\sim 5\,\mu_B$/Fe atom and $\sim 3.4\,\mu_B$/Co atom (373, 485) as compared with about 10-12 μ_B/impurity atom in a Pd host (373, 374, 485, 486) as well as the fact that the critical concentration for the onset of ferromagnetism is about an order of magnitude larger for a Pt host (see below) are thought to reflect the smaller exchange enhancement factor of the Pt matrix.

However, while the experimental evidence for the existence of localised spin fluctuations for dilute, i.e. $c \ll c_f$, Co and Fe impurities in a Pd matrix is still scanty (460, 487) there is a considerable amount of evidence for the existence of spin fluctuations in dilute PtFe and PtCo alloys. For PtCo NMR measurements (488, 489) not only showed that for $c \lesssim 0.1\%$ Co no long range magnetic order existed but also that impurity moments were coupled by RKKY interactions because the Pt line width was proportional to the impurity concentration and was also a function of B_o/T where B_o is the magnetic induction. More significantly below

$\sim$5K the linewidth was no longer a function of $^{8}o/T$ thereby suggesting the existence of a "Kondo state". This suggestion was confirmed by nuclear orientation measurements (490) of the hyperfine field acting on ^{60}Co nuclei in an alloy containing 1 ppm Co. The hyperfine field was found to be proportional to the external field up to 4KG and from the value of this susceptibility the "Kondo temperature", T_k, was determined as 1.6 $\pm$ 0.3K. A similar but more extensive investigation has been carried out by Ali et al (521) who conclude that the observed behaviour can best be fit with a localized spin-fluctuation model with $T_k \sim 1K$. Resistivity measurements (491-6) also show that the impurity resistivity closely resembled that of a localized spin fluctuating system (see section 2.5(vii)) and, in fact, Williams et al (496) deduced a value of 0.7K for the spin fluctuation temperature in a 0.061% Co alloy. The detailed magnetic susceptibility measurements of Tissier and Tournier (497) support the existence of localized spin fluctuations with a spin fluctuation temperature of 1.65K in the single impurity limit, a value close to that obtained from nuclear orientation studies (490). Also the magnetization measurements revealed the occurrence of "residual magnetism" below $\sim$ 1.65K. Co atoms which have no Co neighbour within a critical distance of $\sim$ 8A are "non-magnetic" whereas Co pairs within this distance are magnetic and interact to give rise to some form of magnetic ordering with an ordering temperature which, for c $\lesssim$ 0.31% Co, is proportional to c^2. The more recent susceptibility measurements of Swallow et al (498) on a Pt 0.061% Co alloy indicate a reduction in the value of the effective moment ($\simeq 5.6\,\mu_B$) and an inter-

action range of $\sim$ 8A within which two interacting dilute Co moments stabilize each other (cf 497).

For PtFe Mossbauer effect (500) and NMR (489) measurements indicate that above $\sim$ 1.5K the impurity magnetization exhibits free spin behaviour (both the Mossbauer splitting and the NMR linewidth are simple functions of $^{B_o}/_T$) with a magnetic moment of $\sim 6.5\,\mu_B$. For temperatures $\lesssim$ 1K significant deviations from free spin behaviour are observed. Resistivity measurements (493, 501-2) show that a spin fluctuation model is applicable to PtFe with a spin fluctuation temperature of $\simeq$ 0.4K in close agreement with a Kondo temperature of 0.5K estimated from Mossbauer effect studies (500). It is also significant that the thermoelectric power of very dilute PtFe alloys ($\lesssim$ 0.2% Fe) is large and negative and becomes temperature independent after an initial rapid increase in magnitude (503). The behaviour is similar to that of dilute AuFe alloys ($\sim$ 22 ppm Fe) although the thermoelectric power is about an order of magnitude larger (503). In the single impurity limit an Fe atom is non-magnetic in a Au matrix so that we may expect a similar behaviour for Fe in Pt.

Thus the PtCo and PtFe alloy systems appear to follow the general description of the onset of magnetism in transition metal alloys already outlined in section 2.3. In the dilute limit there exists a non-magnetic state with localized spin fluctuations. The spin fluctuation temperature in the single impurity limit, T*(o), $\sim$ 1.6K for Co (490, 497) and $\sim$ 0.5K for Fe (500, 501). Even in this non-magnetic state two neighbouring Co atoms within a critical distance of $\sim$ 8A can mutually stabilize the moments

on each other and polarise their environment thereby leading to giant moments. The RKKY coupling between the giant moments leads to some magnetic ordering, necessarily of the spin-glass type, with a spin-glass temperature Tsg that should vary as c^2. A similar behaviour is expected for PtFe. As the impurity concentration increases the coupling between the giant moments gradually becomes dominantly ferromagnetic, as reflected in the change from negative to positive values of the paramagnetic Curie temperature (497). Finally, at the critical concentration long range ferromagnetic order sets in without all the impurity atoms being necessarily magnetic; for example, isolated impurity atoms may still have a finite spin fluctuation temperature in the weakly ferromagnetic regime.

Figure 5.1 shows the concentration dependence of M_{oo} and T_c for PtCo alloys. Both T_c and M_{oo} appear to vary linearly with c with

$$T_c \triangleq 2240(c - 0.0075)K \qquad 5.1$$

and

$$M_{oo} \triangleq 3.4\ c\ \mu_B\ /atom \qquad 5.2$$

Since by definition $T_c = 0$ at $c = c_f$ we deduce that for PtCo $c_f \triangleq 0.75 \pm 0.05\%$ Co. It would appear that eq.(2.90) i.e. $M^2_{oo} \propto (c - c_f)$ which has been shown to be valid for many transition metal alloy systems (see section 2.6) does not hold for the PtCo system. We must note that the fact that eq.(5.2) passes through the origin is apparently incompatible with the existence of spin fluctuations for very dilute solute concentrations. However, since $T^*(o) \sim 1.6K$ and it is expected that for this system $T^*(c)$ should decrease as c increases it is very probable that for

Fig. 5.1

Pt Co: Concentration Dependence of T_c and M_{sat}. The Inset is an enlargement of the left hand corner of the diagram with additional data points.

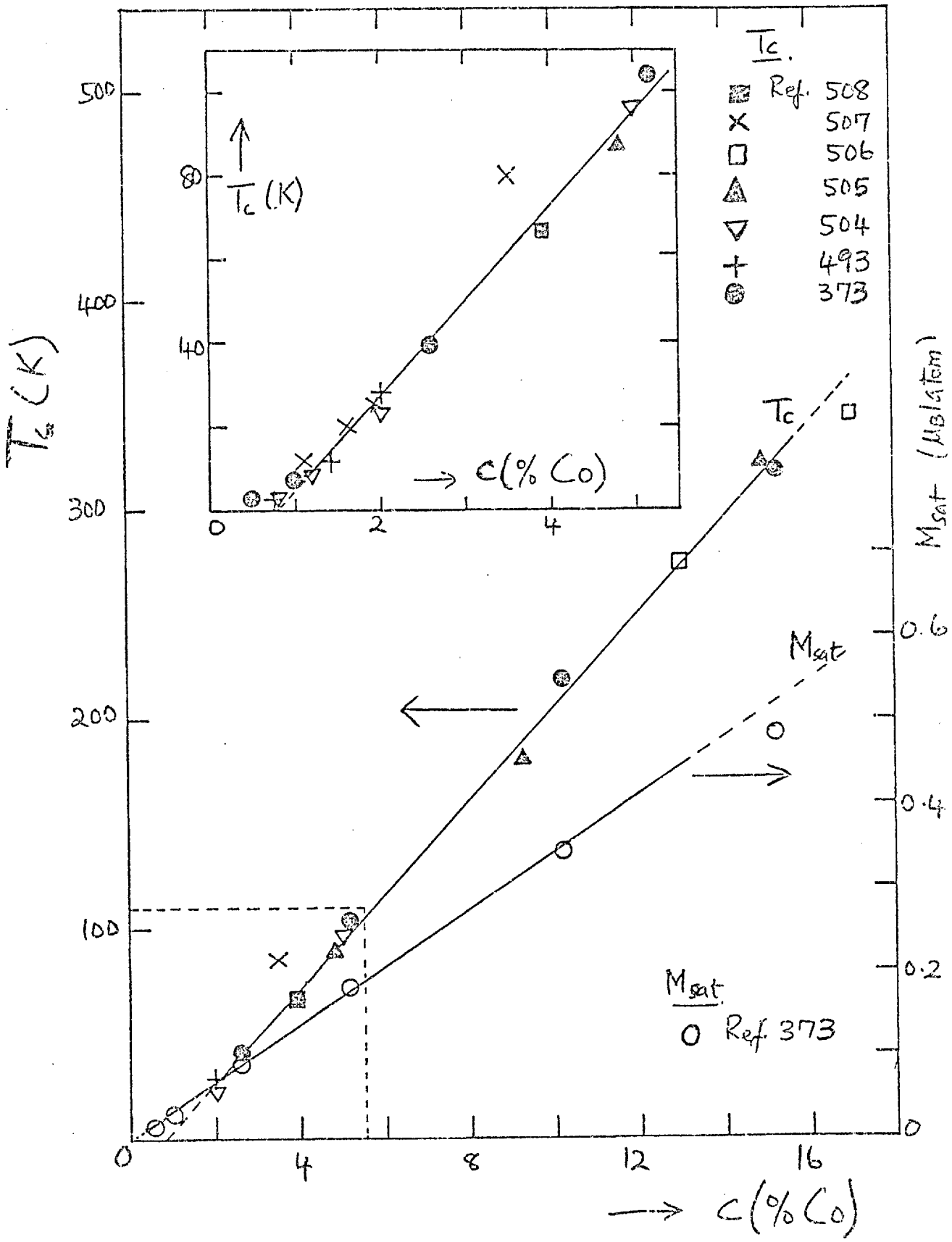

the temperatures ($T \gtrsim 1.5K$) and magnetic fields (up to 20KG) at which the magnetization measurements (373) were made all the Co atoms are magnetic and contribute to the measured magnetization. Thus for $c \lesssim c_f$ the observed M_{oo} values should be regarded as measures of the saturation rather than the spontaneous magnetization. For $c < c_f$ (=0.75% Co) spin-glass ordering is expected. Since NMR measurements (488,489) have shown the existence of RKKY interactions it maybe assumed that the magnetic ordering reported by Tissler and Tournier (497) is of the spin-glass type and the spin-glass "freezing" temperatures maybe identified with the temperatures at which a maximum in the initial susceptibility was observed.

In fig.5.2 we similarly show the concentration dependence of T_c and M_{oo} for PtFe. Again, M_{oo} is linear in c with a slope of $\simeq 4.9\ \mu_B$/atom. The comment made above about the linear dependence of M_{oo} on c in the case of PtCo will also apply to PtFe. Between ~2-10% Fe T_c is linear in c $\left(T_c \triangleq 2000(c-0.013)K\right)$ and extrapolates to zero at a critical concentration of 1.3 ± 0.1% Fe. It is surprising that although T*(o) for PtFe is only ~0.5K as compared with ~1.6K for PtCo the critical concentration for the onset of ferromagnetism in PtFe is significantly higher than in PtCo. Below c_f spin-glass behaviour is again expected. Loram et al (493, 501) report that the resistivity of a 1% Fe alloy decreases sharply below ~4K indicating some magnetic ordering but the resistivity "step-height" defined as $\{\Delta\rho(T_c) - \Delta\rho(0)\}$, where $\Delta\rho(T)$ is the impurity resistivity at a temperature T, shows both ferromagnetic and antiferromagnetic coupling (but see ref.511). Koon

Fig. 5.2

Pt Fe: Concentration Dependence of T_c and M_{sat}.

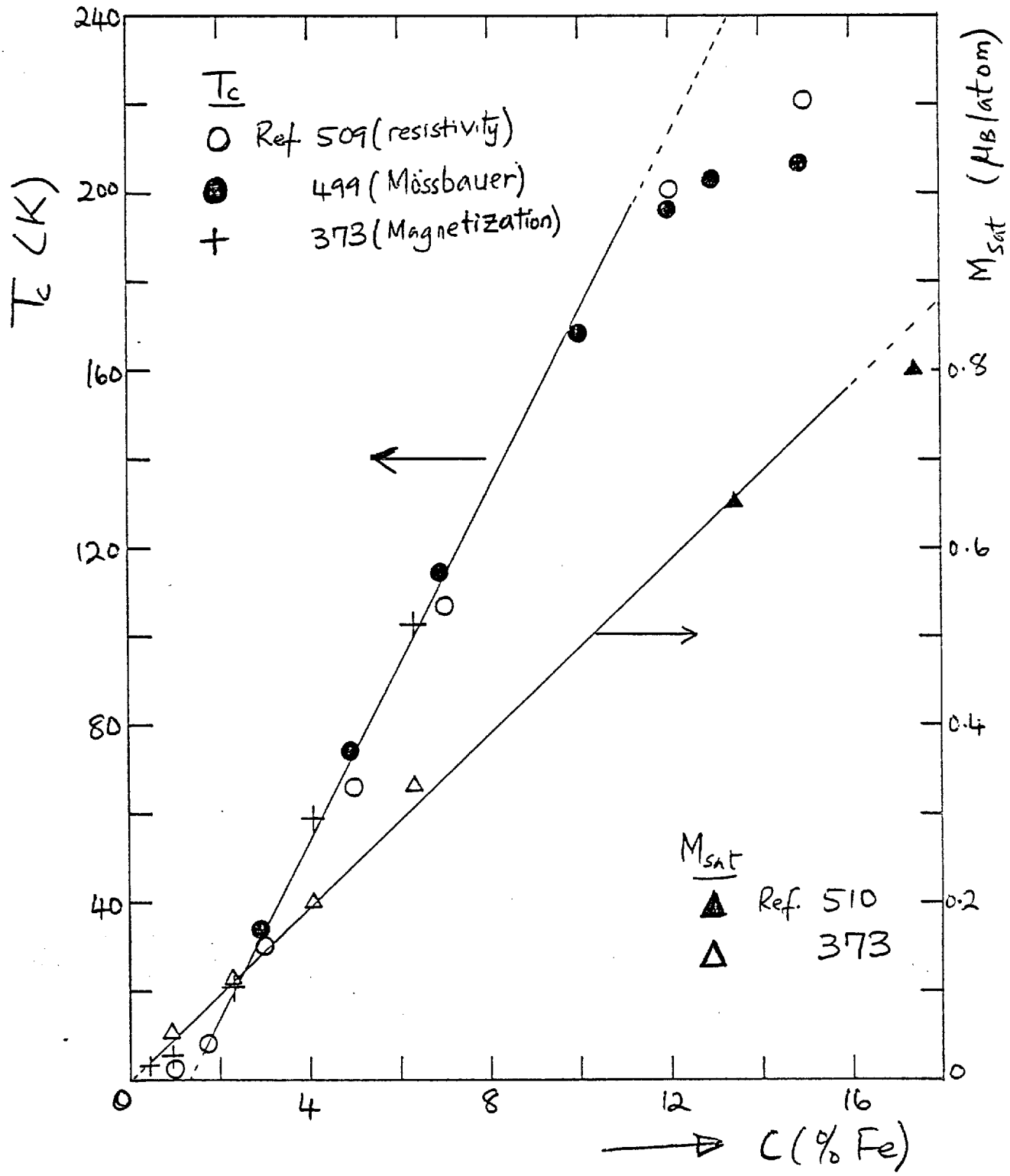

and Gubser (512) also report that the magnetic behaviour of Pt 1% Fe is anomalous. Although a well-defined magnetic ordering is observed near 4K no hysteresis occurs until well below 1K. Also the square shape of the hysteresis loop and the temperature dependence of the coercive force were attributed to random uniaxial anisotropy caused by dipolar forces rather than to magnetocrystalline anisotropy. Random uniaxial anisotropy is, of course, characteristic of spin-glasses.

We also notice in fig.5.2 that for $c \gtrsim$ 10% Fe the Curie temperatures appear to flatten off. This effect has been attributed (499, 509) to the formation of a Pt_3Fe superlattice which is known to exhibit antiferromagnetic ordering (510, 513-4). In the disordered state Pt_3Fe is ferromagnetic (510) so that as pointed out by Kawatra et al (509) sample preparation could be important for high Fe concentrations.

It is pertinent to briefly discuss the heat capacity measurements that have been made on PtCo alloys (515-520). Of these the most extensive are those of Wheeler (516) and Ribeiro (520). For the 0.08, 0.16, 0.27 and 0.31% Co samples Ribeiro found that the excess specific heat curve exhibited a flat maximum as a function of temperature. The amplitude of this maximum was proportional to the impurity concentration and this result was taken as evidence for the single impurity effect (i.e. existence of localized spin fluctuations or a Kondo state). The maximum in the excess heat capacity occurred at $\sim$ 1.2K, close to the spin fluctuation temperature ($\simeq$ 1.6K) determined from nuclear orientation and magnetic susceptibility measurements.

In addition by measuring the nuclear specific heat for $T \leq 200$ mK Ribeiro was able to confirm the existence of "residual magnetism" below the spin fluctuation temperature T^*, i.e. a fraction of the solute atoms remains magnetic even below T^*. The concentration of such magnetic solute atoms was found to vary as c^2 for $c \lesssim 1\%$ Co and in this limit it was again shown that only those Co atoms which had no other Co atom within a critical distance of ~ 8A were non-magnetic. For $c \gtrsim 0.6\%$ Co both Wheeler (516) and Ribeiro (520) found that the excess heat capacity was linear in temperature at low temperatures. In fact, Ribeiro showed that allowing for the contribution of isolated (and hence non-magnetic) Co atoms the excess specific heat, ΔC_m, is given by

$$\Delta C_m \simeq \gamma_m T \qquad 5.3$$

where $\gamma_m \simeq 7 m J\, mole^{-1} K^{-2}$, approximately <u>independent</u> of the solute concentration. Although such a result is expected for spin-glasses (see section 2.8) the fact that it is also valid for the ferromagnetic alloys (0.8, 0.88, 1.6, 1.9, 2.6, and 3.5% Co) is interesting. However, we doubt the validity of the procedure used in correcting for the specific heat of non-magnetic Co atoms so that eq.(5.3) should be treated with some caution.

In section 2.6 we saw that for a number of alloy systems the coefficient, γ, of the term linear in temperature in the specific heat of alloys, obtained by extrapolatin the high temperature linear portion of a C/T versus T^2 plot to the ordinate, exhibited an asymmetric peak at the critical concentration for the onset of long-range ferromagnetic order. No such values of γ in the region spanning the

critical concentration for PtCo have been published. For PtFe a remark by Sacli et al (522) would appear to suggest that some specific heat measurements have been carried out but apparently the results have not been published.

Two observations about the PtCo system merit a brief discussion. The first is the occurrence of resistance minima in relatively concentrated PtCo alloys at temperatures well below the corresponding magnetic ordering temperatures, whereas no resistance minima occur in the dilute impurity limit. Laborde et al (495) report observing a weak resistance minimum in a Pt 0.6% Co alloy at $\sim$0.07K whereas the susceptibility measurements of Tissier and Tournier (497) show that this alloy has a spin glass "freezing" temperature of $\simeq$ 1K. Also Rao et al (504) observed a clear resistance minimum in a Pt 5% Co alloy at $\sim$7K, a temperature which is well below the ferromagnetic Curie temperature of this alloy ($\simeq$96K). In this case such a resistance minimum is no longer surprising having been previously observed in ferromagnetic PtNi alloys (298, 386) and in amorphous ferromagnetic $Pd_{71}Si_{20}Co_9$ (523) and in amorphous Fe-Pd-P alloys (524). The resistance minimum in such ferromagnetic alloys can be explained by assuming that some (or even all!) of the magnetic solute atoms are in low effective internal fields (particularly true for alloys with low Curie temperatures) so that the moments are "quasi-free" and may participate in the spin-flip scattering of conduction electrons (524). An attempt by Beal-Monod (428) to account for the resistivity minimum in disordered ferromagnetic PtNi alloys is unacceptable because the minima are predicted to occur just below the ferromagnetic ordering

temperatures. The resistance minimum in the Pt 0.6% Co alloy is more puzzling. If this minimum had occurred above the spin glass "freezing" temperature it would have been readily understood as a "normal" Kondo resistance minimum. However, as explained previously (see section 2.8) below the spin glass "freezing temperature the resistivity should vary as T^2 at the lowest temperatures and as T up to the ordering temperature. It should be noted that resistivity minima observed in the PtMn system (95), which is a spin-glass alloy system (529), had been explained (530) in terms of the relative magnitude of the electrostatic potential, V, due to the charge difference between the host and solute atoms and the bandwidth, 2W, of the host matrix. We recall (see section 2.8) that Rivier and Adkins (94) had proposed that at low temperatures the resistivity of a spin-glass should vary as $T^{3/2}$. Rivier (530) then suggested that the coefficient of the $T^3/2$ term will be negative if $\frac{|V|}{2W} > 1$ in which case a resistance minimum will obviously arise. The inequality is expected to be satisfied for transition metal hosts with solute atoms from a fairly distant column so that the explanation advanced by Rivier is certainly plausible for PtMn but not for PtCo. A possible explanation for the resistivity minimum in PtCo alloys, particularly the spin-glass alloy (0.6% Co), is in terms of the reduction of the phonon-assisted interband s-d scattering (see section 2.5(vii)). This "band resistivity", varying as $(1-AT^2)$, may combine with the spin-glass resistivity (and the phonon resistivity) to give a resistance minimum. In passing, we remark that the inference made by Rao et al (504) about observing spin

fluctuation effects in Pt 0.6 and 0.8% Co alloys is incorrect. These solute concentrations are not dilute enough for spin fluctuation effects to be dominant especially as the observation of magnetic ordering in these alloys (497, 504) would confirm the importance of inter-impurity interactions. We believe that the observed resistivity behaviour is not inconsistent with spin-glass (or mictomagnetic) behaviour.

The second observation refers to the "mictomagnetic" behaviour of some ferromagnetic PtCo alloys as reflected in the temperature dependence of the magnetic a.c. susceptibility (504). Normally for a ferromagnet the initial susceptibility attains a limiting value below the ferromagnetic Curie temperature. As already explained by a number of authors (see for instance 388 and 526) the true initial susceptibility, χ_t° , is related to the observed initial susceptibility, χ_{ob}° , according to

$$\chi_t^\circ = \frac{\chi_{ob}^\circ}{1 - N\chi_{ob}^\circ} \qquad 5.4$$

where N is the demagnetization factor. The above relation follows trivially from eq.(4.16). At T_c χ_t° should diverge so that

$$\lim_{T \to T_c} \chi_{ob}^\circ = 1/N \qquad 5.5$$

Thus the observed initial susceptibility should vary with temperature as sketched in fig.5.3(a).

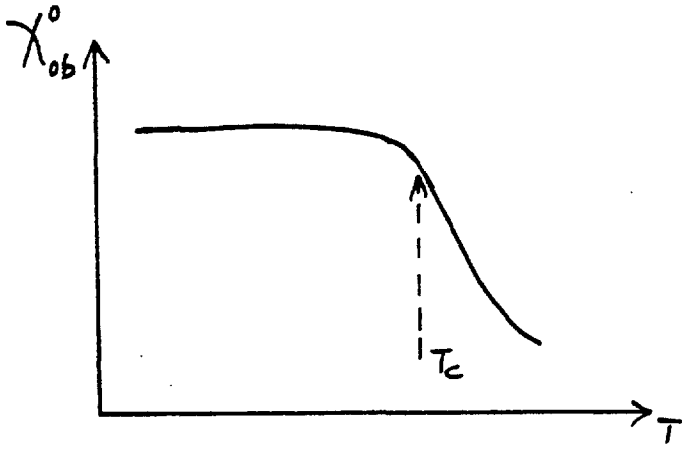

Fig 5.3(a): Normal form of $\chi^o_{ob}(T)$ for a ferromagnet.

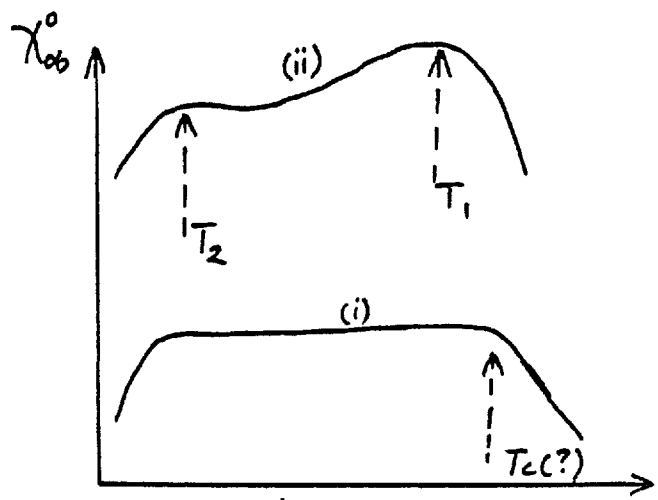

Fig 5.3(b): Observed $\chi^o_{ob}(T)$ for weakly ferromagnetic transition metal alloys.

However, experimentally χ^o_{ob} is found to vary with temperature as sketched in fig.5.3(b), in which either the initial susceptibility decreases again after appearing to attain a limiting value at some higher temperature (curve (i)) or the susceptibility decreases steadily below some ordering temperature (T_1) but still shows a knee at a lower temperature (T_2) (curve (ii)). Below T_2 effects commonly associated with spin-glass behaviour are often observed. Besides PtCo alloys (504) a marked reduction in the initial susceptibility below the ferromagnetic Curie temperature has been observed in AuFe (407, also 195, 290), $(Pd_{75}Ag_{25})_{99}Fe_1$ (527), FeCr (528), FeAl (526), VFe (299), PdCo and $(Pd_{95}Rh_5)$ Co alloys (392, 481). A.C. susceptibility measurements on a Pd 3% Fe alloy (525) also appear to indicate a similar behaviour. Thus it would appear that the observed decrease of the initial susceptibility below the ferromagnetic Curie temperature is characteristic of weakly ferromagnetic transition metal alloys. However, we shall not attempt here to explore the possible causes of the observed behaviour. As a sort of historical footnote

we may add that it is, in fact, possible that Constant (505) may have been the first to observe the decrease of the susceptibility below T_c in PtCo alloys because he did report that not only was there no hysteresis in a Pt 4.8%Co alloy but also that the magnetization increased initially with increasing temperature but later decreased to zero near T_c. Since the measurements were performed in relatively low fields ($\sim$ 600-1000 oe) he incorrectly attributed the anomalous behaviour of the magnetization to the fact that saturation was not reached.

From the above discussion, it is clear that existing magnetization, resistivity and other data (NMR, Mossbauer effect and nuclear orientation studies) allow a fairly comprehensive picture of the onset of magnetism in PtCo and PtFe alloys to be built up. Neutron diffraction work on dilute alloys is, however, necessary not only to confirm the existence of giant polarization clouds but also to determine the extent or spread of these clouds and the actual magnetic moment localized on the solute atoms themselves.

5.2. Neutron Diffraction Results for PtCo Alloys

The diffuse elastic magnetic scattering cross-sections of four dilute PtCo alloys (1, 1.5, 3 and 6% Co) have been measured at 4.2K using the Glopper cryostat (see section 4.1(b,c)). As already discussed in section 3.3 the maximum switchable magnetic cross-section in mb/sr.atom is given by

$$\frac{d\sigma}{d\Omega} = 73c(1-c)\Gamma^2(K) + 73c\,F_i(K)^2\langle(\delta\mu_i)^2\rangle + 73(1-c)F_h(K)^2\langle(\delta\mu_h)^2\rangle \qquad 5.6$$

where

$$\Gamma(K) = F_i(K)\bar{\mu}_i - F_h(K)\bar{\mu}_h + c F_i(K) H(K) + (1-c) F_h(K) G(K) \qquad 5.7$$

i.e. the factor $c(1-c)\Gamma^2(K) \equiv T(K)$ defined in Chapter 3. In writing eq.(5.6) and (5.7) we have neglected the effect of chemical short-range order (section 3.3(d)) and any non-linear effects (section 3.3(f)). As mentioned in the preceding section the spin fluctuation temperature, T*(o), of Co in Pt in the single impurity limit is $\sim$1.6K. For the PtCo system the spin fluctuation temperature is expected to decrease as the solute concentration increases so that since the neutron scattering experiments were carried out at 4.2K <u>all</u> the Co atoms should have well-defined moments. Also for dilute solute concentrations the immediate environment of each impurity should be the same and it is certainly plausible to assume that all the impurity atoms have the same moment μ_i which is almost independent of composition. Thus

$$\langle (\delta\mu_i)^2 \rangle \sim 0$$

and

$$\frac{d\bar{\mu}_i}{dc} \equiv H(0) \sim 0$$

In addition $\bar{\mu}_h$ is not expected to be large (because of the low average molecular field in these dilute alloys) and hence we may also neglect $\langle (\delta\mu_h)^2 \rangle$. Consequently

$$\frac{d\sigma}{d\Omega} \simeq 73 c(1-c)\Gamma^2(K) \qquad (5.8)$$

with

$$\Gamma(K) \simeq F_i\bar{\mu}_i - F_h\bar{\mu}_h + (1-c)F_h G(K) \qquad (5.9)$$

Fig.5.4 shows the k-dependence of $\Gamma(k)$ for the four PtCo alloys. There is a forward peak in each case which can be taken to imply that both $(\bar{\mu}_i - \bar{\mu}_h)$ and G(o) have the same sign (which must be positive as $\frac{d\bar{\mu}}{dc}$ is). We shall make the usual assumption that $G(k)$ is Lorentzian i.e.

$$G(k) = \frac{G(0)k_0^2}{k_0^2 + k^2} \qquad (5.10)$$

where k_0 measures the range of the moment disturbance, g(r). At large values of k $G(k)$ becomes relatively unimportant and we obtain that

$$\Gamma(k \text{ large}) \simeq F_i\bar{\mu}_i - F_h\bar{\mu}_h \qquad (5.11)$$

Thus from the cross-section at large k we can determine $(F_i\bar{\mu}_i - F_h\bar{\mu}_h)$. By combining this with the average saturation moment for PtCo alloys as determined by Crangle and Scott (373) i.e.

$$\bar{\mu} = c\bar{\mu}_i + (1-c)\bar{\mu}_h \qquad \text{(cf eq.(3.78))},$$

values of $\bar{\mu}_{Co}$ and $\bar{\mu}_{Pt}$ may be found. Using these values the cross-section was then fitted to eq.(5.4) by a least squares method to determine G(o) and k_0. In the fitting process it was assumed that

$$F_{Pt} \simeq e^{-0.1k^2} \quad ; \quad F_{Co} \simeq e^{-0.05k^2} \qquad (5.12)$$

The solid lines drawn through the experimental points in fig.5.4 represent the fit of eq.(5.9) to the data and the resulting values of $\bar{\mu}_{Co}$, $\bar{\mu}_{Pt}$, k_0 and G(o) are given in table 5.1. Also tabulated are the values of $\frac{d\bar{\mu}}{dc}$ deduced from the forward cross-section.

$$\frac{d\bar{\mu}}{dc} = \bar{\mu}_{Co} - \bar{\mu}_{Pt} + (1-c)\,G(0) \qquad (5.13)$$

Fig. 5.4 : $\Gamma(K)$ vs K for Weakly Ferromagnetic PtCo Alloys.

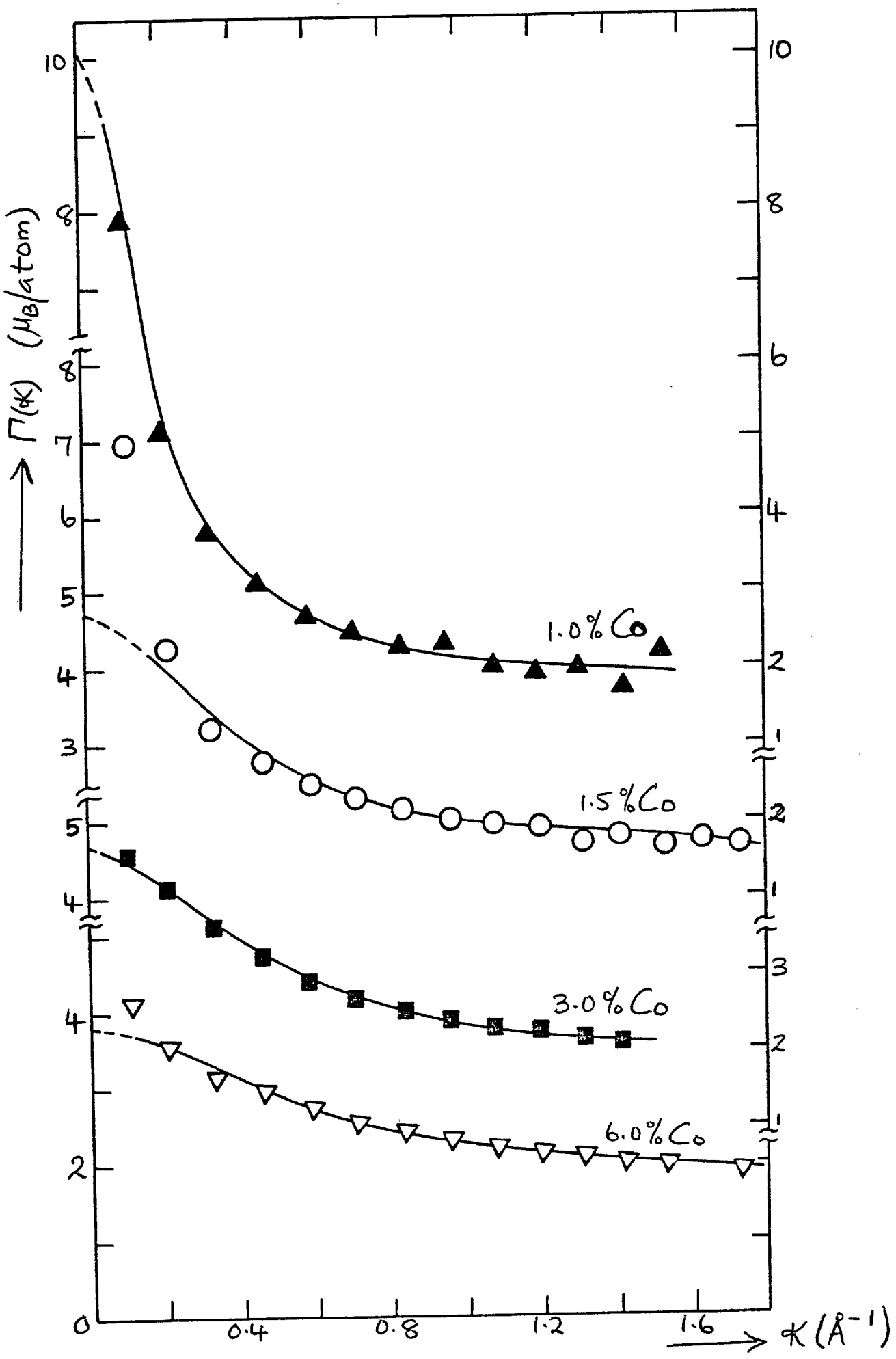

Table 5.1: Individual moments and moment disturbance parameters for dilute PtCo alloys.

Co conc c %	$\bar{\mu}_{Co}$ μ_B	$\bar{\mu}_{Pt}$ μ_B	K_0 $Å^{-1}$	$G(0)$ μ_B/atom	$\frac{d\bar{\mu}}{dc}$ μ_B/atom
1.	2.09±0.07	0.0092±0.0007	0.17±0.06	8.0±0.6	10.1±0.6
1.5	1.86±0.08	0.020±0.001	0.34±0.06	2.9±0.4	4.7±0.4
3	2.20±0.03	0.038±0.001	0.41±0.02	2.50±0.07	4.66±0.08
6	2.15±0.03	0.076±0.002	0.48±0.04	1.8±0.1	3.8±0.1

The errors quoted represent the statistical and fitting errors only.

We have also considered the possibility of the observed magnetic cross-section being the "paramagnetic" scattering from an assembly of magnetic clusters (see section 3.4). In this case

$$\frac{d\sigma}{d\Omega} = \left(\Delta \frac{d\sigma}{d\Omega}\right)_{cl} + 73c(1-c)\{F_i\bar{\mu}_i - F_h\bar{\mu}_h\}^2 + 73\{c\langle(\delta\mu_i)^2\rangle + (1-c)\langle(\delta\mu_h)^2\rangle\} \qquad (5.14)$$

where $\left(\Delta \frac{d\sigma}{d\Omega}\right)_{cl}$ is the paramagnetic scattering given by eq.(3.142). However, since $\frac{d\sigma}{d\Omega}$ has been obtained as the maximum switchable cross-section eq.(3.142) has to be multiplied by a factor of $^3/_2$ in the case of the Glopper cryostat (see section 4.1(f)). Thus

$$\frac{d\sigma}{d\Omega} = 109.5c^* F_{cl}^2\left\{\tfrac{2}{3}M_{cl}^2 - \tfrac{1}{3}M_{cl}\right\} + 73c(1-c)\{F_i\bar{\mu}_i - F_h\bar{\mu}_h\}^2 + 73\{c\langle(\delta\mu_i)^2\rangle + (1-c)\langle(\delta\mu_h)^2\rangle\} \qquad (5.15)$$

where c* is the concentration of the magnetic clusters and F_{cl} is the cluster form factor. Since all the Co

atoms are "magnetic" at 4.2K c* is taken to be equal to the nominal Co concentration. F_{cl} is assumed to be Lorentzian i.e.

$$F_{cl}(\kappa) \simeq \frac{\kappa_1^2}{\kappa_1^2 + \kappa^2} \qquad (5.16)$$

where κ_1^{-1}, now measures the radius of a magnetic cluster. Again we neglect the contribution to the cross-section from the second moment of the spatial fluctuations of the local Pt and Co moments so that

$$\frac{d\sigma}{d\Omega} = 109.5 c F_{cl}^2 \left\{\frac{2}{3} M_{cl}^2 - \frac{1}{3} M_{cl}\right\} + 73 c(1-c)\left\{F_i \bar{\mu}_i - F_h \bar{\mu}_h\right\}^2 \qquad (5.17)$$

At large κ the cluster contribution is small and $(F_i \bar{\mu}_i - F_h \bar{\mu}_h)$ can be determined as in the preceding analysis i.e. $\bar{\mu}_{Pt}$ and $\bar{\mu}_{Co}$ are the same as in table 5.1. Fig. 5.5 shows the experimental values of $\frac{d\sigma}{d\Omega}$ together with the fit of eq.(5.17) to the data (solid lines). The values of M_{cl} and κ_1 obtained in the fits are given in table 5.2. The table also shows values of $\bar{\mu}_{sat} = c M_{cl}$ and $\bar{\mu}_{expt}$ determined from magnetization measurements (373).

Table 5.2: Cluster moments and inverse radii for PtCo alloys.

c% Co	M_{cl}, μ_B	$\kappa_1, \text{Å}^{-1}$	$\frac{\mu_{sat}}{\mu_B/\text{atom}}$	$\frac{\bar{\mu}_{expt}}{\mu_B/\text{atom}}$
1	6.96	0.34	0.07	0.03
1.5	4.52	0.43	0.07	0.048
3	4.11	0.55	0.12	0.103
6	3.31	0.61	0.20	0.20

Discussion

A number of points of interest arises from the analyses outlined above.

Fig. 5.5: Cluster Model Fit to $\frac{d\sigma}{d\Omega}$ for PtCO Alloys.

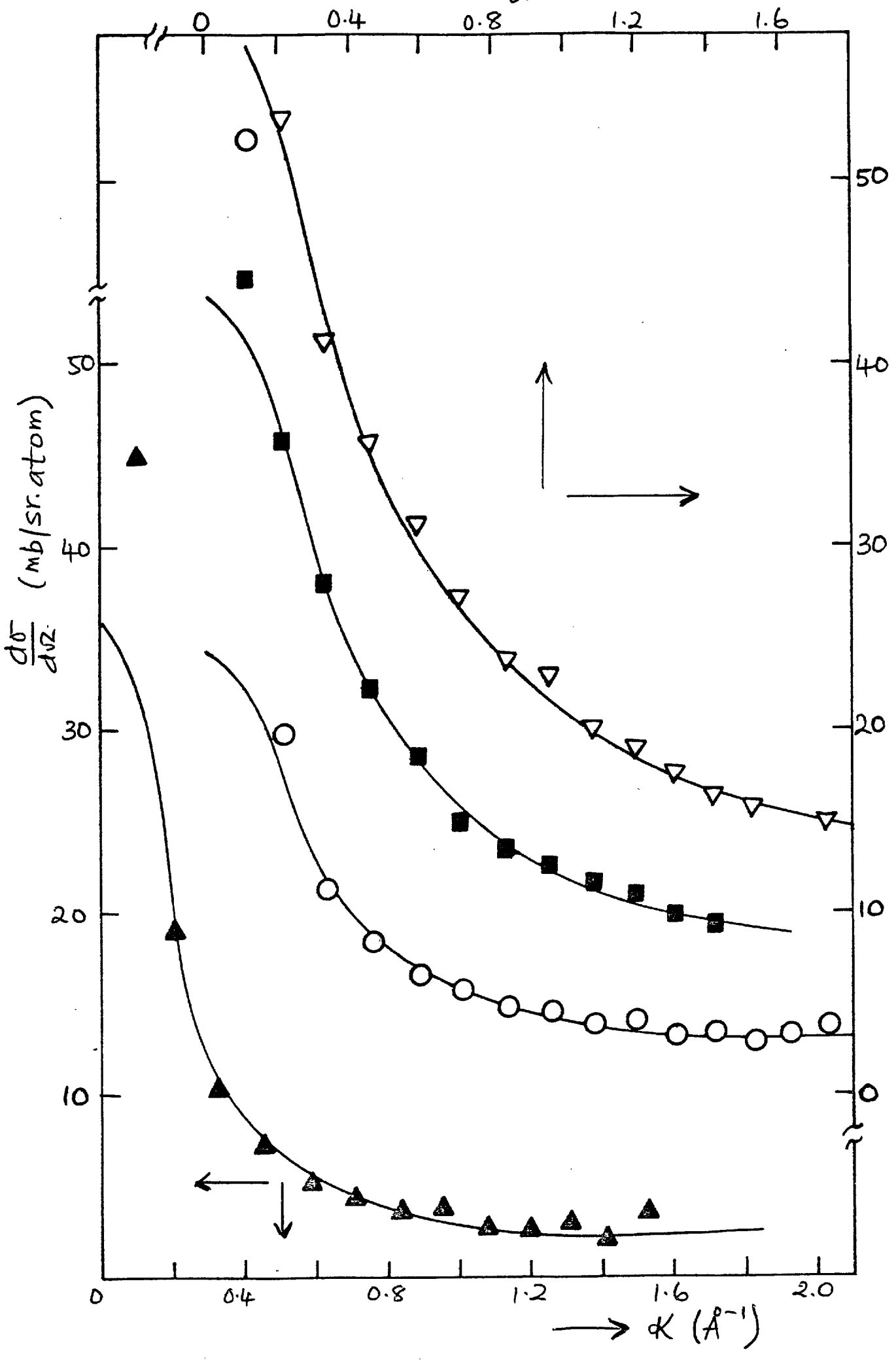

(1) From table 5.1 the average localized magnetic moment on a Co atom is $2.08 \pm 0.06\,\mu_B$. This value is about the same as for Co in dilute PdCo alloys i.e. $2.1 \pm 0.3\,\mu_B$ (197) and also in a number of other Co alloys (446, 531-3). We had earlier remarked (see end of section 3.6) that the <u>local</u> magnetic moment on a Co atom in nearly all its alloys in which it is magnetic is almost the same ($\sim 2\mu_B$) as in pure Co (hcp) apparently irrespective of the crystal structure of the alloys (fcc or bcc).

On the other hand the average moment on a Pt atom is small and concentration dependent as should be expected. A number of polarized neutron diffraction measurements on more concentrated PtCo alloys - mostly Pt_3Co (534-5) and equiatomic PtCo (536-7) - give a value of $\bar{\mu}_{Pt} \simeq 0.25\,\mu_B$ although Antonini et al (537) obtained $\bar{\mu}_{Pt} \simeq 0.5\mu_B$ for disordered PtCo. Following the discussion given in section (3.6) it is expected that the measured value of $\bar{\mu}_{Pt}$ should increase as the average internal molecular field increases i.e. as the Co concentration (and hence the Curie temperature, T_C) increases. The Curie-Weiss constant for pure Pt (eq.(2.49)) gives a limiting value of $\sim 0.46\,\mu_B$ for $\bar{\mu}_{Pt}$ if a g-factor of 2 is assumed. Fig.5.6 shows that in dilute PtCo alloys $\bar{\mu}_{Pt}$ varies linearly with the Co concentration with $\frac{d\bar{\mu}_{Pt}}{dc} \simeq 1.3\,\mu_B$ /atom. By definition $G(0) \equiv \frac{d\bar{\mu}_{Pt}}{dc}$ and therefore G(o) should have this constant value, in clear disagreement with the values tabulated in table 5.1.

(2) The values of $\frac{d\bar{\mu}}{dc}$ shown in table 5.1 are clearly significantly greater than the constant value of $\simeq 3.4\,\mu_B$ /atom suggested by the magnetization data

Fig. 5.6: Concentration Dependence of $\bar{\mu}_{Pt}$ in Dilute (a) PtCo and (b) PtFe Alloys.

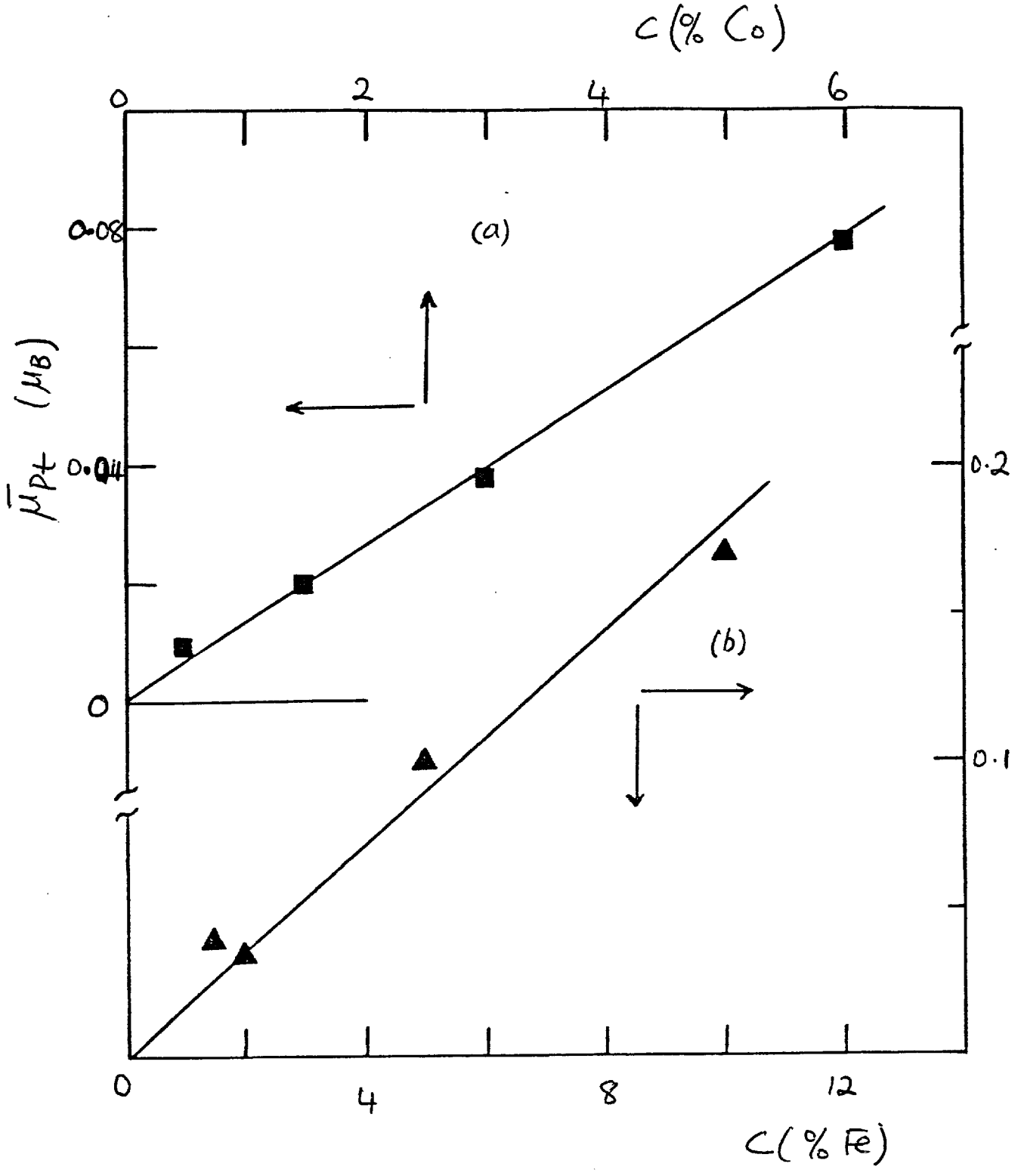

(see fig. 5.1). In particular $\frac{d\bar{\mu}}{dc}$ for the 1% Co alloy is nearly three times greater than the magnetization value. However, the value of $\frac{d\bar{\mu}}{dc}$ obtained from the neutron measurements is not implausibly large. Although apparently not valid for the PtCo and PtFe systems, we showed in section 2.6 that for other giant moment alloy systems, the spontaneous magnetization $M_{oo} \propto (c-c_f)^{\frac{1}{2}}$. Consequently $\frac{dM_{oo}}{dc} \propto (c-c_f)^{-1/2}$ and for $c \sim c_f$ a large value of $\frac{dM_{oo}}{dc}$ is expected. As already mentioned above the magnetization data (373) give the saturation magnetization, μ_{sat}, and there is no a priori reason why $\frac{d\bar{\mu}_{sat}}{dc}$ should always be equal to $\frac{dM_{oo}}{dc}$. We should also mention that the values of the effective moment per Co atom obtained by Tissier and Tournier (497) from the Curie-Weiss constants of the PtCo alloys would lead one to expect significantly higher saturation moments than those obtained by Crangle and Scott (373). For example for a 0.88% Co alloy the effective cluster spin of 2.43 would lead to a saturation moment of $\simeq 4.86\,\mu_B$ if the g-factor $\simeq 2$. An interesting observation is that if we consider

$$\frac{d\bar{\mu}}{dc} \simeq \bar{\mu}_{Co} - \bar{\mu}_{Pt} + (1-c)\frac{d\bar{\mu}_{Pt}}{dc}$$

(cf eq.(5.13)) and use the observed value of $\frac{d\bar{\mu}_{Pt}}{dc} \simeq 1.3\mu_B$/atom (fig. 5.6(a)) and $\bar{\mu}_{Co} - \bar{\mu}_{Pt} \simeq 2\mu_B$ then one obtains $\frac{d\bar{\mu}}{dc} \simeq 3.3\,\mu_B$ /atom in good agreement with the magnetization value. The implication of this result is that the model used to analyse the forward cross-section may not be correct even though it gives a good fit to the data.

(3) The range parameter, κ_0 , is concentration-dependent increasing from $0.17A^{o-1}$ for the 1% Co alloy to $0.48A^{o-1}$ for the 6% Co alloy. The value of $0.17A^{o-1}$ obtained for the 1% Co alloy is in agreement with estimates for the range parameter obtained from neutron diffraction measurements on alloys within the critical concentration region for the onset of ferromagnetism e.g. $\sim$0.3% Fe or Co in Pd (448, 473), 3-4.7% Ni in Pd (128), $\sim$ 0.1% Fe in Ni_3Al (538) or Ni_3Ga (539, 540). The range parameters in CrNi (368) and CuNi (204) alloys are, however, much larger. The concentration-dependence of the range parameter can, of course, be interpreted as indicating a non-linear superposition of overlapping moment distributions as has been assumed for PdCo and PdFe (197, 448, 473) and PdNi (128).

However, an alternative explanation of the concentration-dependence of the range parameter can also be given in terms of the critical fluctuations of magnetization (see sections 2.5(vi) and 3.4(b)). In this case the cross-section in the forward region is given by

$$\frac{d\sigma}{d\Omega} \simeq 73 \sin^2\alpha \; c(1-c) \; \frac{\alpha^2}{2b} \; \chi_f(K) \qquad (5.18)$$

(cf eq. (3.135) with $S(o) \simeq 1$), where

$$\chi_f(K) \simeq \frac{A_o}{\kappa_c^2 + K^2} \quad ; \quad (\text{eq. } (2.203))$$

and

$$\kappa_c^2 \propto (c - c_f) \qquad (\text{eq. } (3.138)) \; .$$

K_c is an inverse correlation length as compared with κ_0 which is the inverse polarization range. In order to use eq. (5.18) to analyse the diffuse neutron data, we must include the scattering due to variations in the local moments at the lattice sites. Thus the maximum switchable

cross-section is given by

$$\frac{d\sigma}{d\Omega} = 73c(1-c)\left[\frac{\alpha^2}{2b}\chi_f(K) + \{F_i\bar{\mu}_i - F_h\bar{\mu}_h\}^2\right] + 73c\langle(\delta\mu_i)^2\rangle + 73(1-c)\langle(\delta\mu_h)^2\rangle \qquad (5.19)$$

As in the previous analyses we shall neglect the last two terms in eq.(5.19) so that

$$\frac{d\sigma}{d\Omega} \simeq 73c(1-c)\left\{\frac{\alpha^2}{2b}\chi_f(K) + (F_i\bar{\mu}_i - F_h\bar{\mu}_h)^2\right\}. \qquad (5.20)$$

$\chi_f(0)$ is the initial static susceptibility and

$$\frac{\alpha^2}{2b}\chi_f(0) \equiv \left(\frac{dM_{oo}}{dc}\right)^2 \propto (c-c_f)^{-1}.$$

The neutron data have been analysed using eq.(5.20) and the parameters obtained from the fitting are shown in table 5.3 while fig.5.7 shows the resulting fit for the alloys. In table 5.3 the parameter $d\sigma_o \equiv 73c(1-c)\frac{\alpha^2}{2b}\chi_f(0)$

Table 5.3: Initial susceptibility and inverse correlation range for PtCo alloys.

Co. conc. c at.%	$d\sigma_o$ mb/sr.atom	$\frac{\alpha^2}{2b}\chi_f(0)$ mb/sr.atom	K_c Å^{-1}
1	294	407	0.052
1.5	92.4	85.7	0.096
3	73.3	34.5	0.18
6	58.5	14.2	0.26

It is obvious from fig.5.7 that eq.(5.20) also gives an excellent fit to the neutron data, particularly at small angles for the two most dilute alloys. As a further test of this method of analysis we plot $\left\{\frac{\alpha^2}{2b}\chi_f(0)\right\}^{-1}$ and K_c^2 against c in fig.5.8. It is seen that straight lines are obtained extrapolating to a critical concentration $c_f \simeq 0.75\%$ in agreement with the value estimated from

Fig. 5.7: Fit of the Critical Scattering Model to $\frac{d\sigma}{d\Omega}$ for PtCo Alloys.

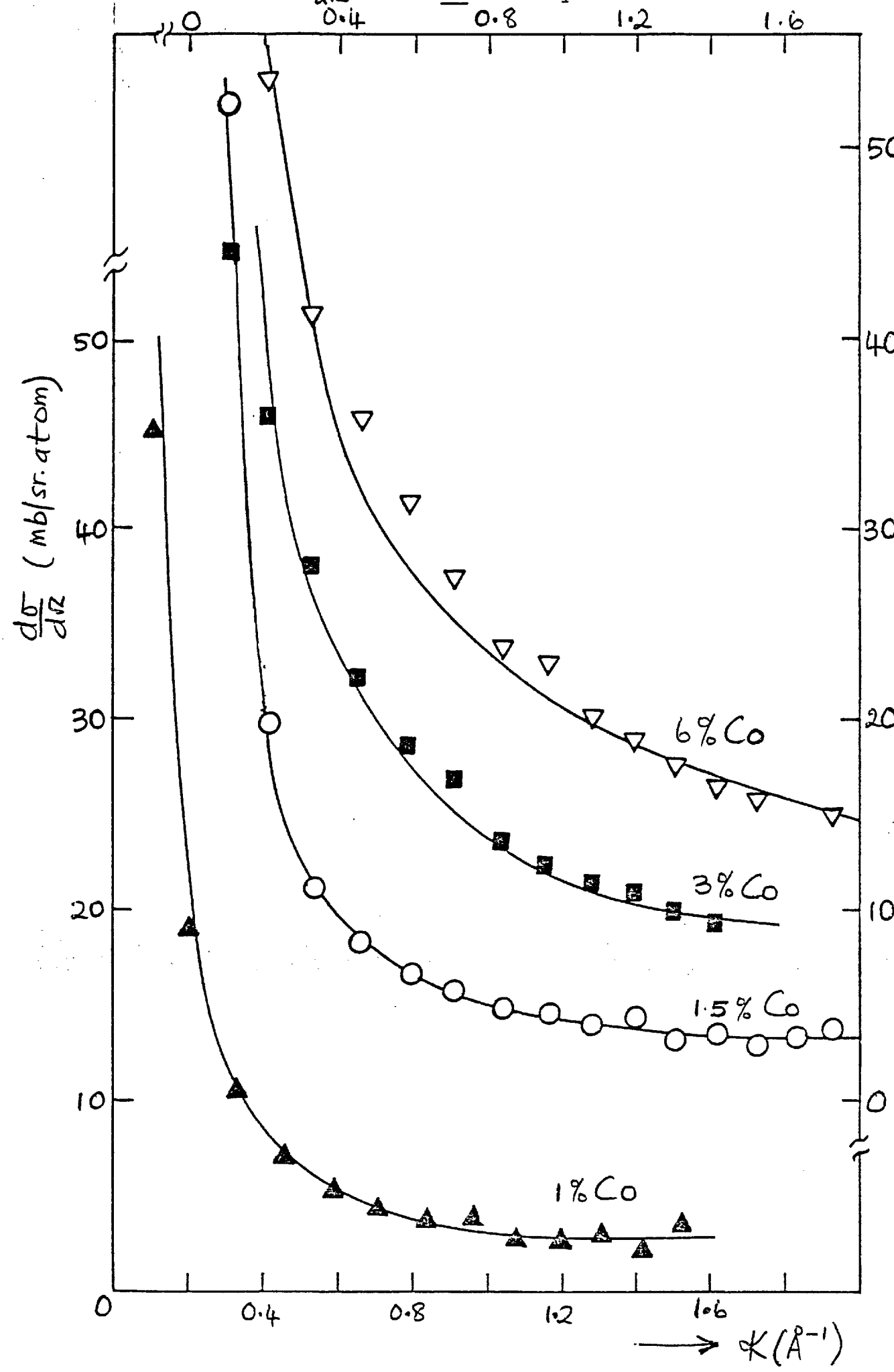

Fig. 5.8: Concentration Dependence of $\{\chi_f(0)\}^{-1}$ and $\frac{d\sigma}{d\Omega}$ for Weakly Ferromagnetic PtCo Alloys.

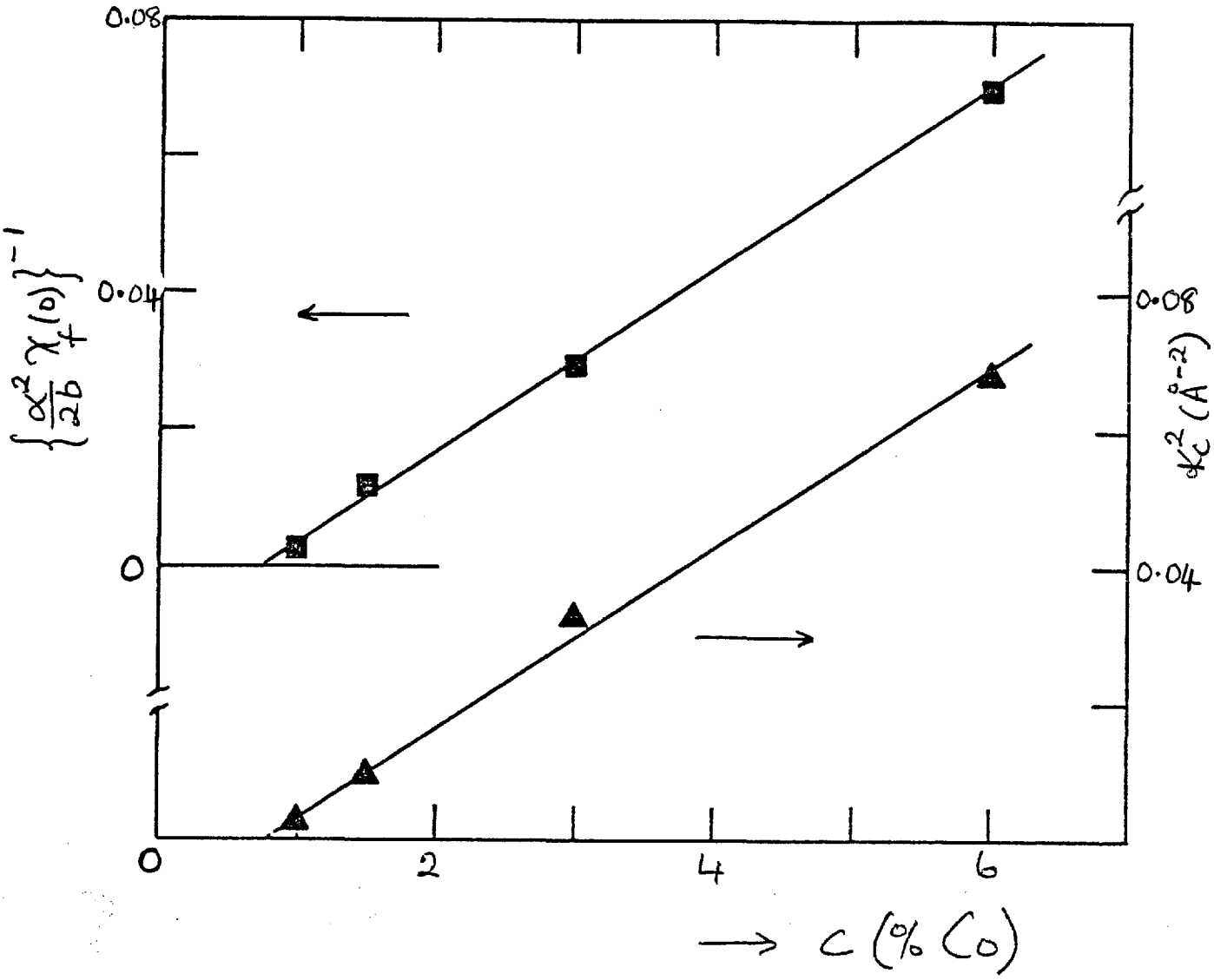

the concentration dependence of T_c (fig.5.1).

(4) Although the cluster model (eq.(5.15)) gives a fairly good fit to the cross-sections the cluster moments and hence the saturation magnetization are much larger than the experimental values (see table 5.2) for the two most dilute alloys. However, it appears that as the Co concentration increases and the cluster radius (or polarization range) decreases the cluster model becomes gradually more applicable e.g. for Pt 6% Co the cluster moment of 3.3 μ_B is exactly the same as the magnetization value (373).

(5) Of the three methods of analysis outlined above it appears that the model which treats the diffuse scattering as a type of critical scattering (eq.(5.20)) gives the most consistent set of parameters. As discussed below an alternative interpretation of the parameter $G(\kappa)$ in eq.(5.9) would be in terms of the Fourier transform of the polarization of the host matrix, as supposed by Low and Holden (197) i.e. the factor $(1-c)F_h G(\kappa)$ in eq.(5.9) is equivalent to $M_h F_h(\kappa)$ defined in eq.(3.105). However, we would now have to explain why the matrix polarization is much greater than the value given by magnetization measurements. A brief comparison of the analysis of the neutron data for PdCo and PdFe (197, 198, 448) with that given above for PtCo alloys and below for PtFe alloys will be made later.

5.3 Neutron Diffraction Data for PtFe alloys

Diffuse scattering measurements have also been made on Pt containing $1\frac{1}{2}$, 2, 5 and 10% Fe. The results are

shown in fig.5.9 in which the cross-section has been expressed as $\Gamma(\kappa)$ (see eq.(5.8)). The cross-sections for the 5 and 10% Fe alloys appear to show a dip at small angles before rising steeply at even smaller κ-values although if the single point at $\kappa = 0.066 A^{o-1}$ is neglected then the cross-section for the 10% Fe alloy merely dips in the forward direction. On the basis of the Marshall model (see end of section 3.3(b)) a dip in the forward direction would imply that $(\bar{\mu}_{Fe} - \bar{\mu}_{Pt})$ and G(o) have opposite signs with $|\bar{\mu}_{Fe} - \bar{\mu}_{Pt}|$ being greater than $|G(0)|$. However, in view of the preceding discussion of the PtCo data we are not certain that the Marshall model really applies to <u>unpolarized</u> neutron cross-sections for <u>weakly ferromagnetic alloys</u>. We shall therefore note that the κ-dependence of the cross-sections for the 5 and 10% Fe alloys is similar to that of <u>concentrated</u> fcc FeNi alloys (435, 542-4) which has been attributed to the presence of short range magnetic order even in the quenched alloys. We believe that the observed κ-dependence of the neutron cross-sections for the two more concentrated PtFe alloys is due to the presence of short range magnetic order. We recall that fig.5.2 shows that T_c for PtFe alloys tends to flatten off for c $\gtrsim$ 10% Fe, an effect that was attributed to the occurrence of a Pt_3Fe superlattice. The samples used for these neutron measurements were not annealed after they had been forged down to buttons. As observed in PdFe (377) it would appear that annealing is also very necessary for PtFe alloys. Since the magnetic moments are essentially localized magnetic short range order would also imply nuclear short range order. However, since Pt

Fig. 5.9: $\Gamma(K)$ vs K for Weakly Ferromagnetic PtFe Alloys.

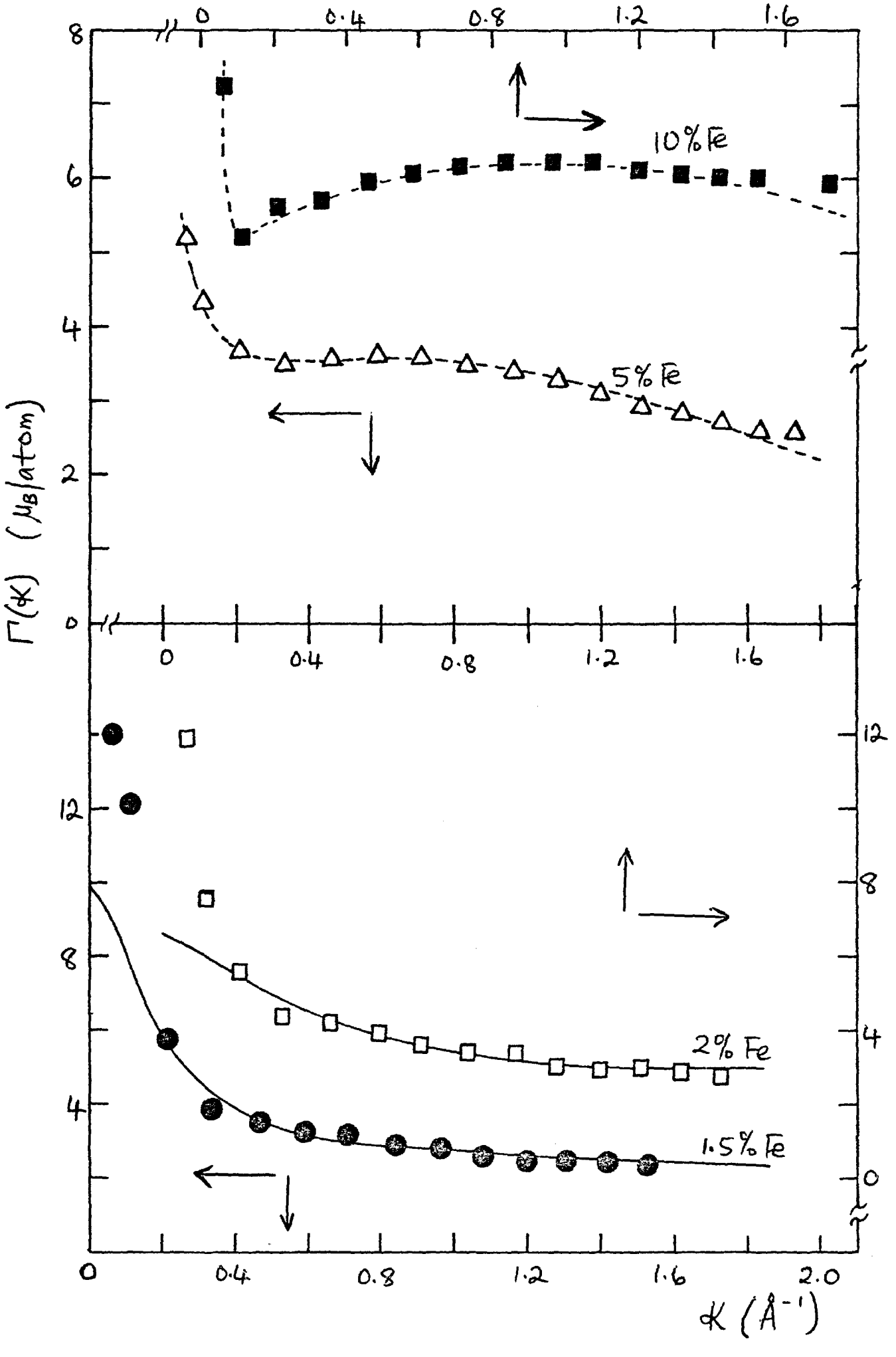

and Fe have the same nuclear scattering lengths it was impossible to estimate the nuclear short range order from the observed nuclear scattering. No attempts have been made to analyse the forward cross-sections of the 5 and 10% Fe alloys in terms of any model but the cross-sections at large κ have been used, together with the saturation magnetization, to obtain values of $\bar{\mu}_{Fe}$ and $\bar{\mu}_{Pt}$ which have been included in table 5.4.

The cross-sections for the 1½ and 2% Fe alloys resemble those of PtCo alloys (see fig.5.4) and have been similarly analysed making the same assumptions i.e. (a) (a) all the Fe atoms have well-defined magnetic moments at least at the temperature at which the experiments were performed (note that the spin fluctuation temperature of Fe in Pt in the single impurity limit is $\simeq$ 0.5K, much smaller than the corresponding value for Co, $\simeq$ 1.6K); (b) $H(0) \equiv \frac{d\bar{\mu}_{Fe}}{dc} \sim 0$ i.e. $\bar{\mu}_{Fe}$ is concentration independent and (c) that $\langle(\delta\mu_{Fe})^2\rangle$ and $\langle(\delta\mu_{Pt})^2\rangle$ are negligible.

The parameters obtained by using the Marshall model i.e. fitting eq.(5.8) to the neutron cross-sections, are listed in table 5.4. The resulting fits are the solid lines in fig. 5.9.

Table 5.4: Individual moments and moment disturbance parameters for dilute PtFe alloys.

Fe conc. c at.%	$\bar{\mu}_{Fe}$ μ_B	$\bar{\mu}_{Pt}$ μ_B	K_0 $Å^{-1}$	$G(0)$ μ_B/atom	$\frac{d\bar{\mu}}{dc}$ μ_B/atom
1.5	2.72	0.04	0.17	7.2	9.8
2	3.13	0.035	0.33	3.5	6.5
5	3.12	0.10	=	=	=
10	3.49	0.17	=	=	=

It is seen in fig. 5.9 that except for very small κ ($\lesssim 0.15 \text{Å}^{-1}$) eq. (5.8) gives a good fit to the data. The average value of $\bar{\mu}_{Fe}$ (=3.1 ± 0.2 μ_B) is in good agreement with the values obtained by Bacon and Crangle (513) for all alloys in the composition range Pt_3Fe and by Kren and Szabo for ordered Fe_3Pt (541). A similar value of $\bar{\mu}_{Fe}$ has also been obtained for Fe in Pd over a very wide range of composition (197, 545-9). It is interesting to note that $\bar{\mu}_{Fe} \simeq 3\mu_B$ in a wide variety of <u>alloys</u> such as PdFe (197, 531, 545-9), PtFe (513, 541, this work), fcc NiFe (435, 445, 542), Au(FeNi) with less than 60 at.% Au (550), Ni_3Al (538), Ni_3Ga (539, 540), FeCo, both ordered (CsCl structure) and disordered (bcc) alloys (551), and for Fe atoms in body-corner positions in ordered (CsCl structure) ferromagnetic and antiferromagnetic FeRh alloys (552-3). The above list does not include references where $\bar{\mu}_{Fe}$ has been estimated from susceptibility and/or saturation magnetization measurements only.

$\bar{\mu}_{Pt}$ is small and as for PtCo alloys it varies linearly with concentration with $\frac{d\bar{\mu}_{Pt}}{dc} \simeq 1.8\,\mu_B$ /atom (see fig 5.6(b)). Again we find that

$$\frac{d\bar{\mu}}{dc} \equiv \bar{\mu}_{Fe} - \bar{\mu}_{Pt} + (1-c)\frac{d\bar{\mu}_{Pt}}{dc}$$

$$\simeq 4.8\,\mu_B \text{ /atom}$$

which agrees with the magnetization value (fig. 5.2). It is, however, clear that the values of G(o) and hence $\frac{d\bar{\mu}}{dc}$ obtained in the fitting process (refer to table 5.4) do not agree with the magnetization values. We shall also ascribe this discrepancy to the fact that the magnetization experiments give $\frac{d\bar{\mu}_{sat}}{dc}$ whereas these unpolarized neutron diffraction measurements, which are truly zero

field measurements, give $\frac{dM_{oo}}{dc}$, where M_{oo} is the spontaneous magnetization.

The range parameter, κ_o , also varies with concentration and its values for 1½ and 2% Fe alloys are similar to those obtained for the 1 and 1½% Co alloys.

The cluster model (eq. (5.17) also gives a good fit to the data (shown as the dotted lines in fig.5.10). In table 5.5 we list the cluster moments, M_{cl}, and inverse cluster radii, κ_1 , for the 1½ and 2% Fe alloys.

Table 5.5: Cluster moments and inverse cluster radii for PtFe alloys

Fe conc. c at.%	M_{cl}, μ_B	κ_1, $\AA^{-1}$	$\bar{\mu}_{sat}$ μ_B	$\bar{\mu}_{expt}$ μ_B
1.5	4.9	0.48	0.074	0.08
2	4.9	0.61	0.098	0.097

The cluster moments, and hence $\bar{\mu}_{sat} (\equiv c M_{cl})$, are in good agreement with experimental values. Also the cluster radii are similar to corresponding values for the 3 and 6% Co alloys for which M_{cl} was closest to the magnetization values (table 5.2). These cluster radii suggest that a Co or Fe atom polarizes its nearest-neighbour host atoms only.

Finally the data have also been analysed on the critical scattering model, i.e. using eq.(5.20). This model gives the best overall fit at both small and large κ (see solid lines in fig 5.10) and the parameters obtained are listed in table 5.6 •

Table 5.6: Initial susceptibility andiinverse correlation range for PtFe alloys.

Fe conc. c at.%	$d\bar{\sigma}_o$ mb/sr.atom	$\frac{\alpha^2}{2b}\chi_f(0)$	K_c, $\AA^{-1}$
1.5	385	357	0.05(3)
2	121	84.6	0.11

Fig. 5.10: Fits of the Cluster (dotted line) and Critical Scattering (solid line) Models to $\frac{d\sigma}{d\Omega}$ for PtFe Alloys.

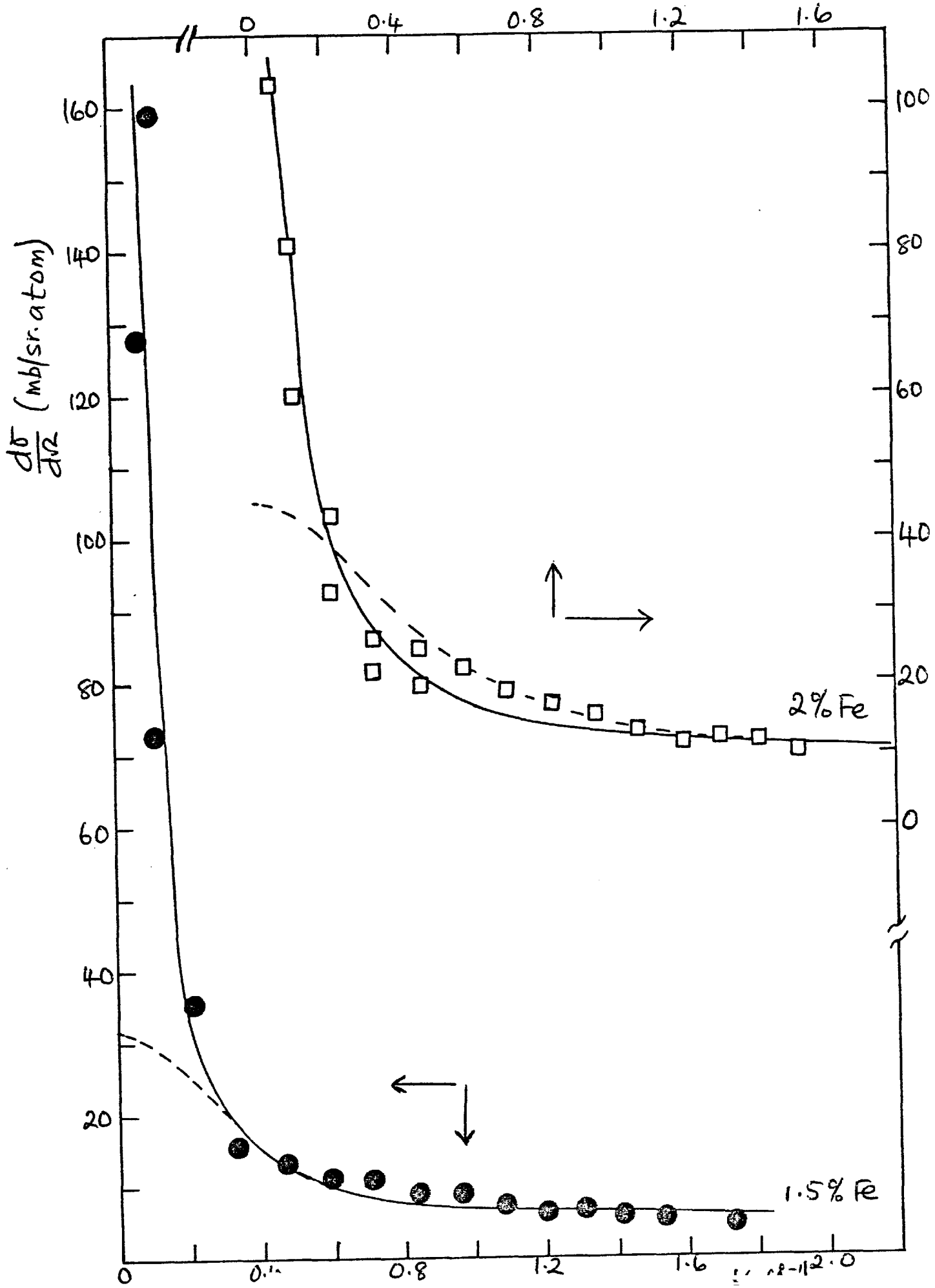

Again we find that near c_f ($\simeq$ 1.3% Fe) the correlation range is large ($\gtrsim 20\text{Å}^{-1}$). Since the data for only two alloys have been so analysed it is not possible to check if $\chi_f(0)^{-1}$ and κ_c^2 vary as $(c-c_f)$ as was done for PtCo alloys but it is significant that for both alloy systems $\left\{\frac{\alpha^2}{2b}\chi_f(0)\right\}^{-1} \simeq \kappa_c^2$. It would be necessary to obtain data for say 2.5 and 3% Fe alloys in order to confirm the applicability of this model to PtFe alloys.

It is pertinent to point out that an important criterion for accepting a set of neutron cross-section data for a given sample as being satisfactory is that data obtained at the two sample angles (ϕ = 0 and ϕ = 30 or 45°, see chapter 4) should be consistent in the region of κ -values where they overlap. Thus, for example, the first set of measurements made on the original Harwell Pt 2% Fe sample was rejected because the discrepancy between the data at ϕ=0 and those at ϕ=45° was much too large to be ascribed to statistical counting errors - see fig. 5.11(a). When a portion of the original slab was remelted to make a new 2% Fe sample and the measurements were repeated excellent agreement between the ϕ=0 and ϕ=30° data was achieved. Similarly, agreement between the ϕ=0 and ϕ=45° data for both Pt 1.5% Fe and Pt 1.5% Co alloys was obtained for samples made by remelting portions of the original samples. This observation perhaps emphasizes the fact that these Pt alloys should be well annealed, although the possibility of a systematic error occurring in the previous measurements cannot be discounted.

Fig. 5.11: $\frac{d\sigma}{d\Omega}$ vs κ for two samples of Pt 2% Fe
(a) Original Harwell Slab
(b) Remelted Portion of same
(Ø is the specimen angle)

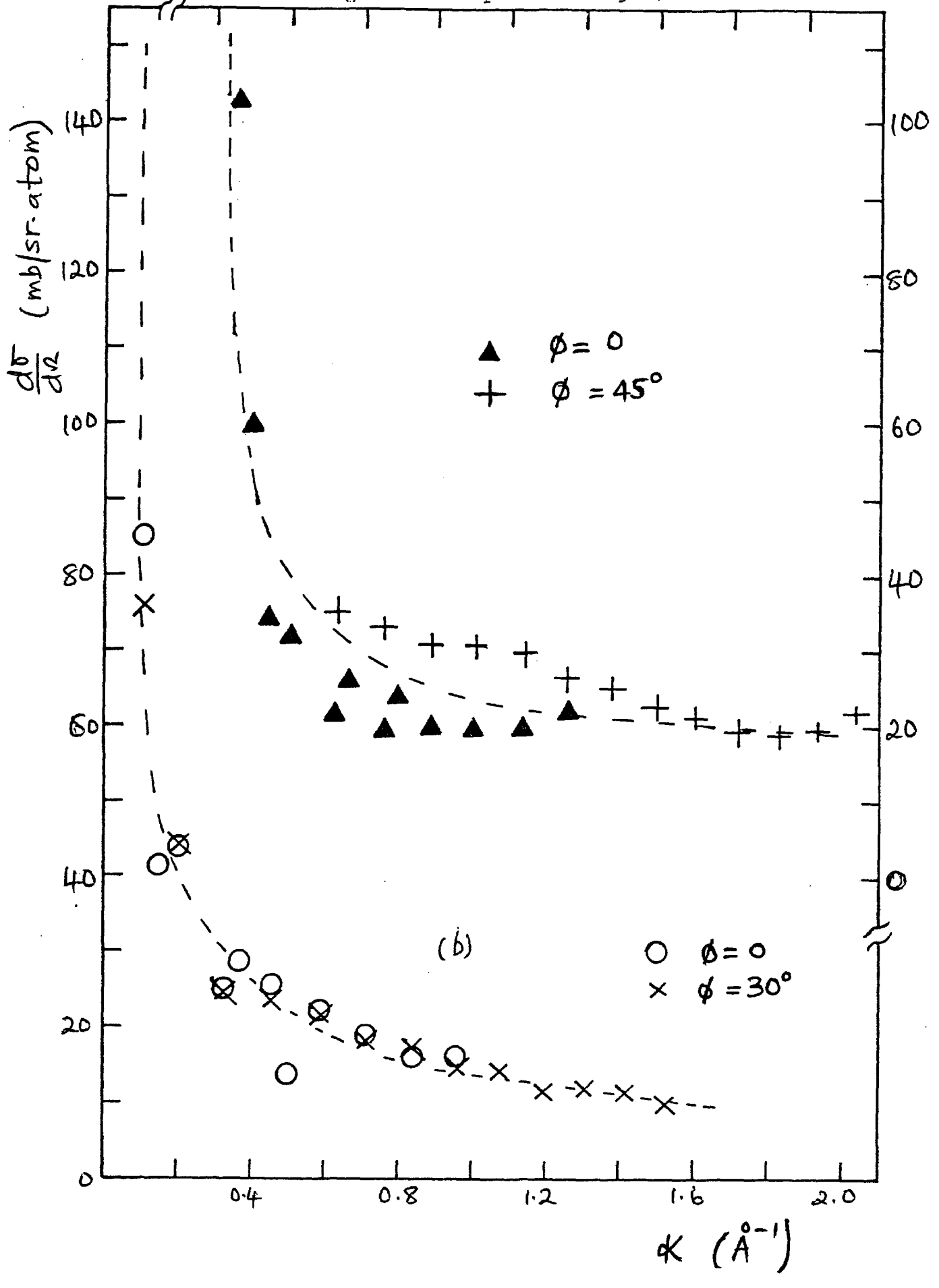

5.4 Summary of Results for Pt Alloys

Our unpolarized neutron diffraction measurements on weakly ferromagnetic PtCo and PtFe alloys lead to the following conclusions:-

(1) The diffuse cross-sections show a marked forward peak which for weakly ferromagnetic transition metal alloys is usually taken to indicate an inhomogeneous distribution of magnetization. Although we cannot question the fact that a solute atom may polarize the host matrix we are no longer certain that a forward peak in the neutron cross-section necessarily implies an inhomogeneous distribution of magnetization.

(2) The scattering at large angles together with the saturation magnetization gives

$$\bar{\mu}_{Co} = 2.08 \pm 0.06\,\mu_B \quad \text{and} \quad \bar{\mu}_{Fe} = 3.1 \pm 0.2\,\mu_B$$

approximately independent of solute concentration. The average local Pt moment is small and concentration-dependent. For each alloy system $\frac{d\bar{\mu}_{Pt}}{dc}$ is approximately constant and together with $(\bar{\mu}_i - \bar{\mu}_{Pt})$ gives a value of $\frac{d\bar{\mu}_{sat}}{dc}$ in very good agreement with the corresponding magnetization value.

(3) It is not possible to assign a characteristic polarization range to the Pt matrix as a result of the analysis of the neutron data using the Marshall model. On this model we have seen that κ_0 increases steadily with solute concentration. However, if, following Low and Holden (197), we take κ_0 $(= 0.17 \text{Å}^{-1})$ for the most dilute alloy we have studied in each system (Pt 1% Co and Pt 1.5% Fe) as being characteristic of the host matrix then we obtain that the polarization range in Pt is larger than

in Pd inspite of the much smaller exchange enhancement of the former. On the contrary Moriya (60) has stated that a spin-polarization parallel to the impurity is not expected to extend much beyond the nearest-neighbour distance in Pt alloys and Swallow and White (511), after a detailed analysis of the resistivity step-height, suggest that only impurities which are nearest-neighbours of one another order ferromagnetically with no other ordering taking place. In fact it is possible that a good estimate of the range of the matrix polarization can only be obtained on the cluster model and from tables 5.2 and 5.5 the inverse cluster radius $\simeq 0.55\text{Å}^{-1}$ indicating a range of about the nearest-neighbour distance.

(4) Three different models have been used to analyse the neutron data namely (a) the Marshall model (eq.(5.8)) which is strictly valid for impurities introduced dilutely into a ferromagnetic host (b) the cluster model, which considers the scattering as being the paramagnetic scattering from an assembly of very weakly coupled magnetic clusters and (c) the critical scattering model which follows naturally from the fact that the onset of ferromagnetism as a function of concentration is a critical phenomenon. It has been shown that if we do not consider the scattering at small wavevectors ($\kappa \lesssim 0.15\text{Å}^{-1}$) all three models give reasonably good fits to the data so that a choice between the models can only be made on the basis of the self-consistency of the parameters determined in the fitting processes. On such a basis it seems that the critical scattering model is the most suitable and in addition it is the only model that gives a good fit to the small angle scattering

particularly for the alloys closest to the critical concentration. As already explained in section 3.4(b) the usual critical scattering at a ferromagnetic Curie point results from magnetization fluctuations which are thermally induced and is given by eq. (3.132). In the critical concentration region magnetization fluctuations also exist but these are caused by concentration fluctuations so that in the forward direction the diffuse scattering cross-section is given by

$$\frac{d\sigma}{d\Omega} = 73 \sin^2\alpha \; c(1-c)\left(\frac{d\bar{\mu}}{dc}\right)^2$$

which is, of course, identical with the Marshall formula (eq.(5.8)); note that $\Gamma(0) \equiv \frac{d\bar{\mu}}{dc}$). We shall, however, make the necessary distinction that in the above equation $\bar{\mu}$ refers to the <u>spontaneous</u> magnetization M_{oo} (or μ_{sp}) rather than the <u>saturation</u> magnetization $\bar{\mu}_{sat}$. For strongly ferromagnetic matrices with dilute solute concentrations there is essentially no distinction between $\bar{\mu}_{sat}$ and M_{oo} and the Marshall formula is valid but in the critical concentration region $\bar{\mu}_{sat}$ is different from M_{oo} since it is well known that magnetic clusters persist well below the critical concentration i.e. at $c=c_f$, $M_{oo} = 0$ by definition but $\bar{\mu}_{sat}$ is still finite. Thus we strictly should write that

$$\frac{d\sigma}{d\Omega} = 73 \sin^2\alpha \; c(1-c)\left(\frac{dM_{oo}}{dc}\right)^2 \qquad 5.21(a)$$

$$\propto 73 \sin^2\alpha \; c(1-c)\,\chi_f(0) \qquad 5.21(b)$$

since $\left(\frac{dM_{oo}}{dc}\right)^2 \propto \chi_f$, where χ_f is the initial susceptibility (see eq.(2.90) and (2.96)). This latter quantity can only be determined by using <u>unpolarized</u> neutrons in

"field-on, field-off" experiments which are truly zero-field measurements since the magnetic field is only used to suppress the magnetic scattering (for a horizontal magnetic field). If a magnetic field is permanently applied as in polarized neutron diffraction measurements it will tend to suppress the fluctuations of magnetization and we should then expect $\left(\frac{d\sigma}{d\Omega}\right)_0 \propto \left(\frac{d\bar{\mu}_{sat}}{dc}\right)^2$.

Thus we shall stress the point which has been previously made in Chapter 3 that in the critical concentration region it should not be expected that polarized and unpolarized neutron deffraction measurements will give the same forward cross-section. It also implies that the same extrapolation procedure cannot be used for both types of measurements in this region.

Support for the critical scattering model comes from a detailed investigation of the small angle scattering near the Curie temperature and well below it in some FeNi invars (554). The study showed that whereas in say pure Ni critical scattering is restricted to a relatively narrow temperature range $\left\{\left|1-\frac{T}{T_c}\right| \sim 0.2\right\}$, in the FeNi invars critical scattering appears to extend down to the lowest temperatures investigated - see fig. 5.12.

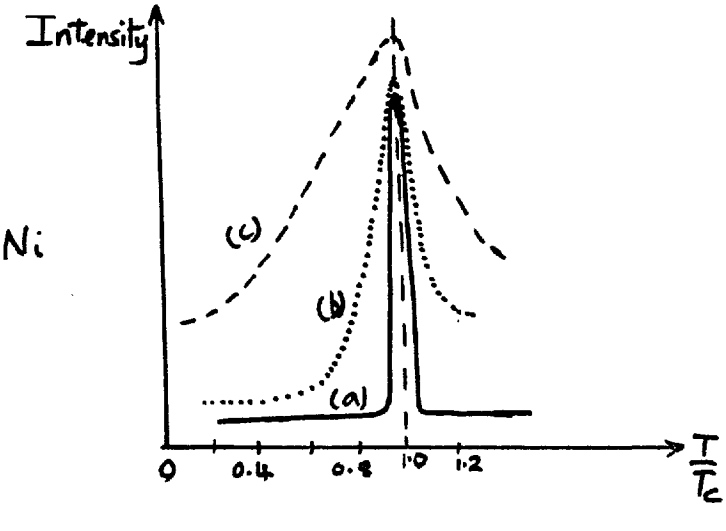

Fig. 5.12 : Sketch of the temperature dependence of the small angle scattering for (a) pure Ni (b) Fe 50% Ni and (c) Fe 35% Ni invar. (after ref. 554).

As pointed our by Men'shikov et al (554) one would normally expect some smearing out of the phase transition at the ferromagnetic Curie point of an alloy owing to random concentration fluctuations. This explains why for Fe 50% Ni critical scattering begins from about 0.7 T_c. However for the invar alloys the magnetization fluctuations apparently persist to very low temperatures, an effect that was attributed to the existence of both ferromagnetic and antiferromagnetic exchange interactions in these alloys (554). Our neutron data for some FeNi invar alloys will be discussed in Chapter 7.

(5) Although not directly deducible from the neutron results we shall suggest that the magnetic phase diagram of PtFe is similar to that of AuFe (see fig. 2.9) so that under our classification scheme (see section 2.3) PtFe should be labelled a spin-glass alloy system inspite of the fact each solute atom polarizes the surrounding Pt matrix. This is because it appears that all Fe atoms have well-established moments long before long-range ferromagnetic order sets in, in contrast with the usual situation in "giant-moment" alloys where not all the impurity atoms are magnetic just above the critical concentration e.g. PtCo. Thus we support the conclusion by MacDonald et al (503), drawn from the similar behaviour of the thermoelectric power of their respective dilute alloys, that the PtFe and AuFe systems are similar in their magnetic properties.

5.5. Comparison with the Neutron Data for PdFe and PdCo Alloys

A resume of the neutron diffraction studies of

ferromagnetic PdFe and PdCo alloys has already been given in section 3.4. It has been shown that for a strongly ferromagnetic host with a concentration c of magnetic or non-magnetic impurities

$$\frac{d\sigma}{d\Omega} = 73 \sin^2\alpha \, c(1-c) \, \Gamma(K)^2 \qquad 5.22$$

where $\Gamma(K) \simeq \left| \int_{V_s} dr \, \Delta\rho(r) e^{iK.r} \right|^2$

(see eq.(3.46) and 3.104)). In the above equation $\Delta\rho(r)$ is the <u>disturbance</u> in the magnetic moment density due to the presence of a single solute atom. In terms of the moment disturbance parameters $G(K)$ and $H(K)$ of the Marshall model

$$\Gamma(K) = F_i \bar{\mu}_i - F_h \bar{\mu}_h + (1-c) F_h G(K) + c F_i H(K)$$

(eq.(5.7)). However, for the strongly paramagnetic Pd host with a sufficient concentration of Fe or Co impurities to make the whole ferromagnetic Low and Holden (197) found it necessary to assume that $\Delta\rho(r)$ is the ferromagnetic <u>polarization density</u> associated with a single solute atom so that

$$\Gamma(K) \simeq F_i \bar{\mu}_i + M_h F_h(K) \qquad 5.23$$

(see eq.(3.105)), where $M_h F_h(K)$ is the matrix polarization which is proportional to the uniform strongly exchange-enhanced susceptibility of the Pd matrix (eq. (3.113)). Clearly the model is equivalent to Marshall's for the case where $H(0) \equiv \frac{d\bar{\mu}_i}{dc} \sim 0$ provided we identify $M_h F_h(K)$ with $(1-c)F_h G(K)$ and neglect $\bar{\mu}_h$. Thus we may regard eq.(5.9) which has been used in the analysis of the neutron data for Pt alloys as a more theoretically valid form of the model introduced by Low and Holden.

Furthermore it appears that in the analysis of the neutron data for the most dilute Pd alloys studied

(Pd 0.26% Fe and Pd 0.3% Co) a smooth curve was handdrawn through the observed points and the point at $\kappa = 0$ which was fixed by the magnetization value of $\frac{d\bar{\mu}}{dc}$. The smooth curve was then Fourier-inverted to obtain a polarization distribution in real space. In other words the data were not quantitatively fitted to eq. (3.105) and hence in our view the validity of the assumed model is questionable. A quantitative fit of eq.(3.105) to the data is necessary to show that $\left(\frac{d\sigma}{d\nu}\right)_{\kappa=0}$ is indeed determined by $\frac{d\bar{\mu}}{dc}$ and hence confirm the applicability of the Marshall model to weakly ferromagnetic alloys. A fit of eq.(5.9) to the Pd 0.26% Fe data gives $G(o) = 4.5\ \mu_B$/atom, $\kappa_0 = 0.26 \text{Å}^{-1}$ $\bar{\mu}_{Fe} = 3.62\ \mu_B$ and $\bar{\mu}_{Pd} = 0.024\ \mu_B$ so that $\frac{d\bar{\mu}}{dc}$ $\simeq$ 8.1 μ_B/atom as compared with the magnetization value of $\sim$11.8 μ_B/atom. The observed points and the fitted line are shown in fig. 5.13. The dotted line in approximately the curve drawn through the points by Low and Holden (197). The above fitting clearly shows that either the assumed model is incorrect or that the data are inaccurate. Several other points concerning the analysis of the neutron data of the Pd alloys are worth noting. (a) It was stated (197) that the neutron cross-sections suggested that below about ½% solute content the scattering per impurity became largely independent of concentration. Consequently, the results for Pd 0.26% Fe and Pd 0.3% Co were taken to approximate the scattering for infinite dilution (197) in which limit the interactions between the polarization clouds is minimal! (448). This observation is in error. In the first place the critical concentration

Fig. 5.13: $\frac{d\sigma}{d\Omega}$ vs κ for two PdFe Alloys (Data from Ref. 197).

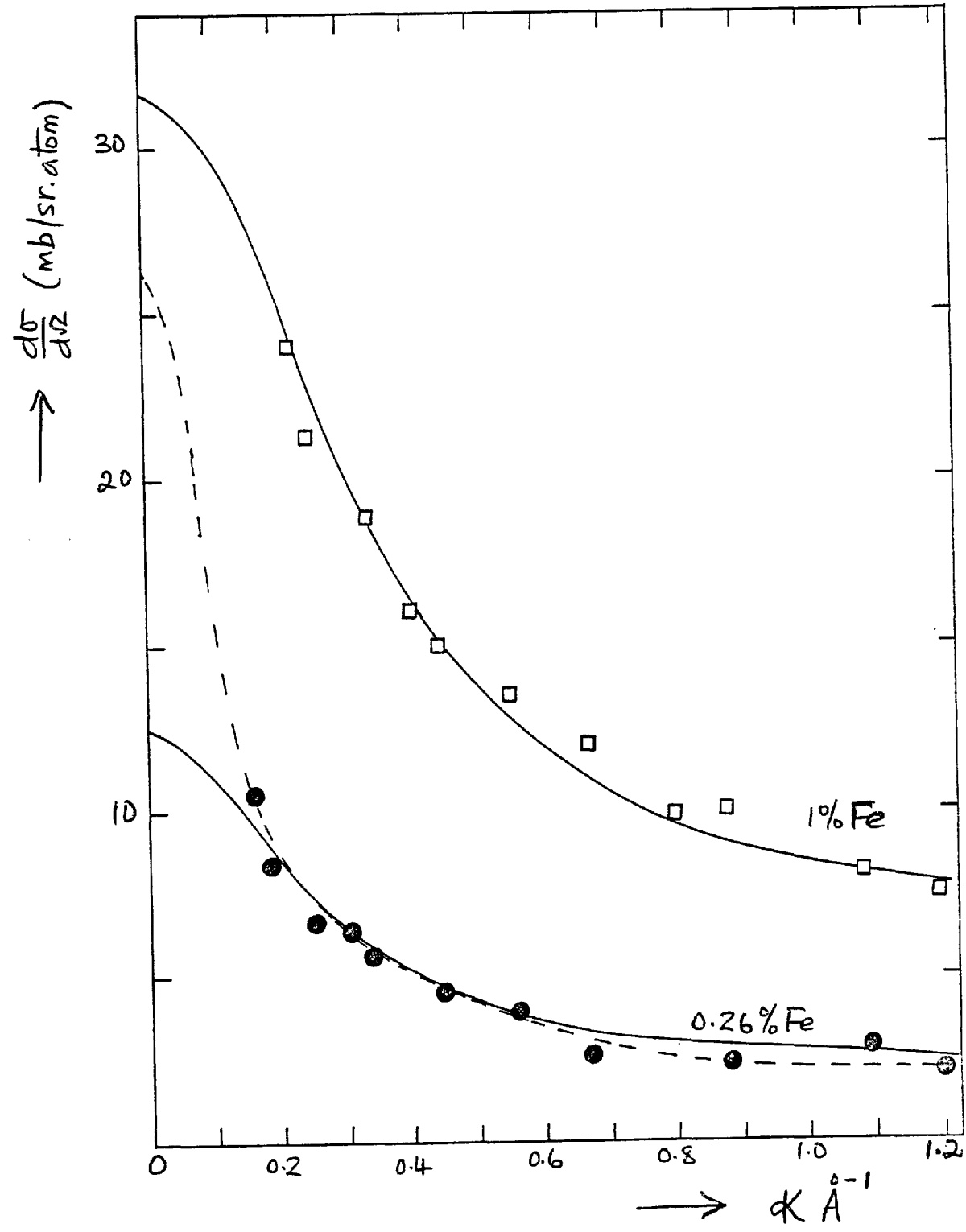

c_f, for the onset of ferromagnetism in PdFe is 0.12% Fe (section 2.6) so that a concentration of $\sim$ 0.26% Fe which is more than twice c_f cannot conceivably be taken as representing infinite dilution. Secondly one surely cannot "minimize" the interactions between the giant moments because it is the coupling between these moments that ultimately leads to the onset of long range ferromagnetic order as was first pointed out by Crangle and Scott (373).

(b) An inverse polarization range, κ_0, of $\sim 0.3 \text{Å}^{-1}$ (197) or $\sim 0.2 \text{Å}^{-1}$ (198, 448) was obtained as being characteristic of the Pd matrix. Again we cannot agree with this conclusion because any such estimate of the polarization range should strictly be made at c_f. An even more fundamental objection is that since that giant moments persist as magnetic units well above the ferromagnetic Curie temperatures (485, 486) a proper estimate of the size of the cloud can only be made on the cluster model (eq. (5.17)). An analysis of the Pd 0.26% Fe data on this model gives $\kappa_1 \simeq 0.4 \text{Å}^{-1}$ which would imply that a polarization cloud does not extend much beyond the nearest neighbour distance. The cluster moment $M_{cl} \sim 7.5 \mu_B$ compared with a magnetic moment per impurity atom of $\simeq 12.7 \mu_B$ (but see below). It may be recalled that from an analysis of the nuclear specific heat of two PdFe alloys Dreyfus et al (555) suggested that the number of Pd atoms affected by a single solute atom is $\sim$ 50, much less than the 200 or so atoms quoted by Low and Holden (197).

We should also note that in obtaining $\kappa_0 = 0.2 \text{Å}^{-1}$ Hicks et al (198) had to scale up their neutron cross-sections for a single crystal of Pd 0.25% Fe in such a

way that the large angle data agreed with those obtained by Low and Holden (197). According to Hicks et al (198) the scaling up was justified because the low Curie temperature of this alloy ($\sim$ 6.4K) made it necessary to correct the cross-sections for the temperature dependence of the magnetization. We do not understand why this correction was necessary for the single crystal but not for the polycrystalline specimen used by Low and Holden. Moreover our data for Pt 1% Co ($T_c \simeq 5.6$K) and Pt 1.5% Fe ($T_c \simeq 4$K), alloys which have even lower Curie temperatures than the Pd 0•25% Fe alloy, do not indicate that any significant corrections for the temperature dependence of the magnetization are necessary. In fact, a detailed study of some PdMn alloys (454, 556) has shown that the closeness to T_c of the temperature at which neutron diffraction measurements are carried out has no appreciable effect on the observed cross-sections. However, assuming that a correction for the temperature dependence of the magnetization was necessary the use of a constant scaling factor for all wave-vectors is surely incorrect. One would expect the high angle scattering data to be scaled up while the small angle data are scaled down (see section 3.3(e)). For example in a mean field approximation $\Gamma(0) \sim (T_c - T)^{-1/2}$ (eq.(3.93)) while at large κ $\Gamma(\kappa) \sim (T_c - T)^{1/2}$. Thus κ_0 is also temperature dependent and $\kappa_0(T)$ can either vary as $(T_c - T)^{\frac{1}{2}}$ or $(T_c - T)^{2/3}$ depending on the model used (again see section 3.3(e)). Therefore if $\kappa_0(4.2K) \sim 0.2 \text{Å}^{-1}$ then $\kappa_0(0) \sim 0.28 \text{Å}^{-1}$ or 0.31Å^{-1}. These values lead to shorter polarization ranges than indicated by the rough Fourier-inversion of the neutron cross-section (197).

(c) Is $\left(\frac{d\sigma}{d\Omega}\right)_{\kappa=0} \propto \left(\frac{d\bar{\mu}}{dc}\right)^2$? The observed data for PdFe alloys are apparently not in agreement with this relation. According to Low (448) the macroscopic magnetization measurements would give values of $\left(\frac{d\sigma}{d\Omega}\right)_0$ which are <u>far too large</u> to be consistent with simple extrapolations of the scattering data for solute concentrations $\gtrsim \frac{1}{2}\%$ Fe. To explain this observation Low noted that (i) the magnetization is highly non-linear so that there could be contributions to $\left(\frac{d\sigma}{d\Omega}\right)_0$ from higher order derivatives of $\bar{\mu}$. However, such contributions to $\left(\frac{d\sigma}{d\Omega}\right)_0$ are positive (eq.(3.103)) and usually small and therefore cannot account for the stated discrepancy; (ii) the measured scattering data do not extend to sufficiently low κ to enable an accurate extrapolation to $\kappa = 0$ to be made. It is possible that the cross-sections from the concentrated alloys could increase sharply at very low κ but this may lead to very small values of κ_0 ; (iii) some short range order could exist in the PdFe alloys. This is very plausible (for instance see ref.377) but it could be easily checked by using well-annealed specimens .

However, we do not find that for solute concentrations $\gtrsim \frac{1}{2}\%$ Fe the magnetization data give much larger forward cross-sections than observed. In fact, the converse appears to be true. For $c \lesssim 1.3\%$ Fe

$M_{oo} \simeq 0.88\ (c - c_f)^{\frac{1}{2}}$ (eq.3.126(a) and section 2.6); thus

$$\frac{dM_{oo}}{dc} \simeq 0.44\ (c - c_f)^{-\frac{1}{2}} \quad \mu_B/\text{atom} \qquad 5.24$$

and the variation of this quantity with solute content is plotted in fig.5.14. For $c = 0.01$, $\frac{dM_{oo}}{dc} \simeq 4.7\ \mu_B$/atom

Fig. 5.14: Concentration Dependence of $\frac{dM_{oo}}{dc}$ and $\frac{\bar{\mu}}{c}$ for PdFe Alloys

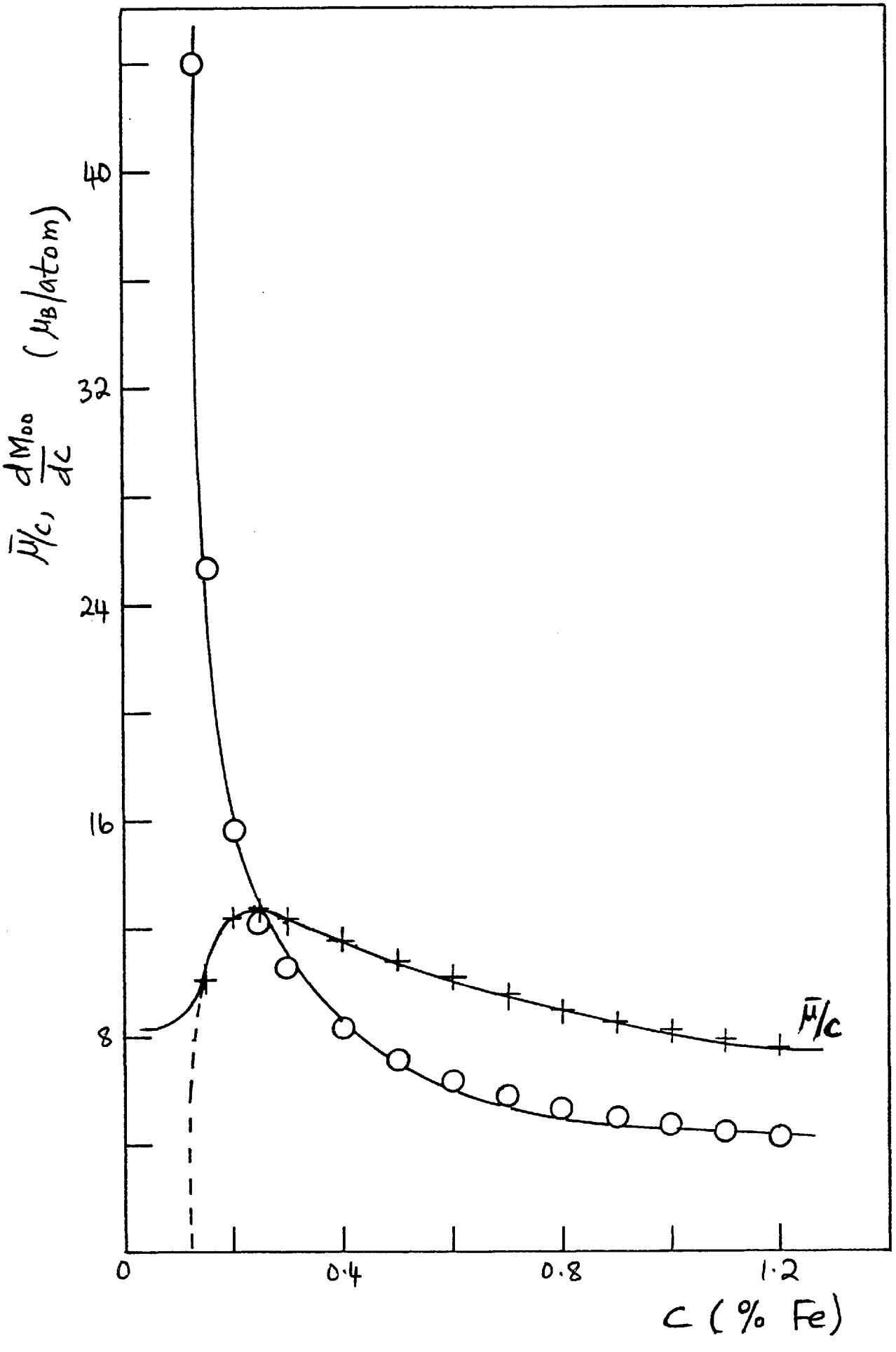

giving $\left(\frac{d\sigma}{d\Omega}\right)_0 \simeq 1.6$ bsr^{-1}/Fe atom ($\simeq$ 16 mb/sr.atom). The observed data for Pd 1% Fe have been replotted in fig.5.13 and a reasonable extrapolation (actually using the cluster model) gives $\left(\frac{d\sigma}{d\Omega}\right)_0 = 31.6$ mb/sr.atom (or 3.16 bsr^{-1}/Fe atom) which is apparently twice the expected value. On the other hand, one could also observe that for $0.5 \lesssim c \lesssim 5\%$ the magnetization varies approximately linearly with c and $\frac{d\bar{\mu}}{dc} \simeq 6.5\ \mu_B$ /atom. This gives a forward cross-section of 30.5 mb/sr.atom in good agreement with the extrapolated value. Similarly it is easy to check that the magnetization value of $\frac{dM_{oo}}{dc}$ for Pd 0.6% Fe gives a <u>smaller</u> value of $\left(\frac{d\sigma}{d\Omega}\right)_0$ than is observed.

It may be pertinent at this point to comment on the usefulness of expressing the average magnetization as so much <u>per solute atom</u>. For example, for Pd 0.53% Fe the magnetization is commonly given as $\sim 11.2\ \mu_B$/Fe atom. One automatically assumes therefore that all of this moment necessarily resides <u>within</u> the polarization cloud of each Fe atom. We do not think that such an interpretation is quite correct, i.e. the actual total moment associated with each cloud could be less than $11.2\ \mu_B$. Fig. 5.14 also shows the concentration dependence of $\bar{\mu}/c$ for PdFe alloys for $c \lesssim 1.2\%$. It is seen that $\bar{\mu}/c$ is fairly constant (at $\sim 8\ \mu_B$) below $\sim 0.15\%$ Fe and attains a maximum near $c \simeq 0.25\%$ Fe before falling off gradually. Note that $\frac{M_{oo}}{c}$ will decrease steeply to zero at c_f (dotted line on the figure). The decrease of the magnetic moment per impurity atom for $c \gtrsim 0.3\%$ Fe has been attributed to the overlap of the magnetization

clouds (197). However, the fact that the decrease is fairly sluggish must mean that the true polarization range decreases equally slowly with solute content. The magnitude of the polarization cloud round a solute atom can best be determined from measurements below c_f where no long-range ferromagnetic order exists. This will ensure that any Pd atoms not specifically falling within a polarization cloud would bear no moments since there is no longer an average molecular field acting on them. Also in this limit there can clearly be no overlapping of polarization clouds. Susceptibility measurements (461) show that the total moment in each polarization cloud is $\sim 8\mu_B$ which means that only $\sim 5\mu_B$ reside in the Pd matrix. The apparent maximum in $\bar{\mu}/c$ around 0.25% Fe is an algebraic artefact because if we write

$$\frac{\bar{\mu}}{c} = \bar{\mu}_{Fe} + \frac{1-c}{c}\bar{\mu}_{Pd}$$

then since $\bar{\mu}_{Fe}$ is approximately constant the concentration dependence of $\bar{\mu}/c$ is determined by that of the second term. This term is a product of two factors one of which $\left(\frac{1-c}{c}\right)$ is a rapidly decreasing function of c while $\bar{\mu}_{Pd}(c)$ increases from zero at c=0 and tends to a limiting value of $\sim 0.4\,\mu_B$ for sufficiently high solute concentrations. Therefore the second term must exhibit a maximum at some concentration.

In conclusion we feel that it is necessary to repeat the <u>unpolarized</u> neutron diffraction measurements on PdFe and PdCo alloys in order to obtain more accurate data especially at small scattering angles and to carefully

study the concentration dependence of the scattering in the critical concentration region ($0.1 \lesssim c \lesssim 1\%$). Only such a detailed study can help in deciding which of the models so far discussed is really applicable although from our analysis of corresponding Pt alloys we would opt for the critical scattering model i.e. eq.(5.20). Failing this the cluster model is probably the next best choice. It is possible that the critical scattering model can explain the large forward cross-sections observed in PdMn alloys (454, 556). As in the case of Pt alloys the neutron forward cross-sections are much larger than would be compatible with the magnetization data. Verbeek et al. (556) suggest that the large forward peaks may result from dynamical fluctuations (in the polarization clouds) of low energy ($\lesssim 1K$) and large amplitudes. These are, of course, the conditions required for the validity of the quasistatic approximation made in the critical scattering model. This model should also be tested on the small angle scattering observed by Murani et al. (188) in AuFe alloys.

-----oOo-----

CHAPTER 6

THE NiRh ALLOY SYSTEM

6.1 Introduction

The NiRh alloy system appears to be an interesting one to study because of the "anomalous" concentration-dependence of the spontaneous magnetization (379, 561). The magnetization increases initially with the addition of Rh, reaches a maximum around 3% Rh and then falls steadily to zero at $\sim$ 37% Rh. The variation is shown in fig.6.1 in which the published values of the spontaneous magnetization have been normalized to a value of 0.616 μ_B/atom for pure Ni (562) instead of the previously accepted value of 0.606 μ_B /atom. Since

$$\bar{\mu} = c\bar{\mu}_{Rh} + (1-c)\bar{\mu}_{Ni} \qquad \text{(eq. (3.78))}$$

$$\frac{d\bar{\mu}}{dc} = \bar{\mu}_{Rh} - \bar{\mu}_{Ni} + c\frac{d\bar{\mu}_{Rh}}{dc} + (1-c)\frac{d\bar{\mu}_{Ni}}{dc} \; ;$$

for small c($\lesssim$ ½% Rh) we may neglect $c\frac{d\bar{\mu}_{Rh}}{dc}$ and if we disregard $\frac{d\bar{\mu}_{Ni}}{dc}$ for now then $\frac{d\bar{\mu}}{dc} \simeq \bar{\mu}_{Rh} - \bar{\mu}_{Ni}$. According to Crangle and Parsons (561) the initial value of $\frac{d\bar{\mu}}{dc}$ is approximately 2 μ_B /atom which implies that $\bar{\mu}_{Rh} \simeq 2.7\,\mu_B$. However, if we draw a smooth curve through their data points then an initial value of $\frac{d\bar{\mu}}{dc} \simeq 3.5\,\mu_B$ /atom is possible (see fig 6.1(b)) giving $\bar{\mu}_{Rh} \simeq 4.1\,\mu_B$/atom. On the other hand the data obtained by Bölling (379), which differ significantly from those of Crangle and Parsons for c $\lesssim$ 5% Rh (see fig 6.1(b)), suggest that $\frac{d\bar{\mu}}{dc} \sim 1\,\mu_B$ /atom and hence that $\bar{\mu}_{Rh} \sim 1.7\,\mu_B$ /atom. What is clear from

Fig. 6.1: (a) Concentration dependence of the bulk magnetization, $\bar{\mu}$, of RhNi alloys.
(b) Enlargement of (a) for c ≦ 10% Rh showing why $\lim_{c \to 0} \frac{d\bar{\mu}}{dc}$ cannot be uniquely determined from the data.

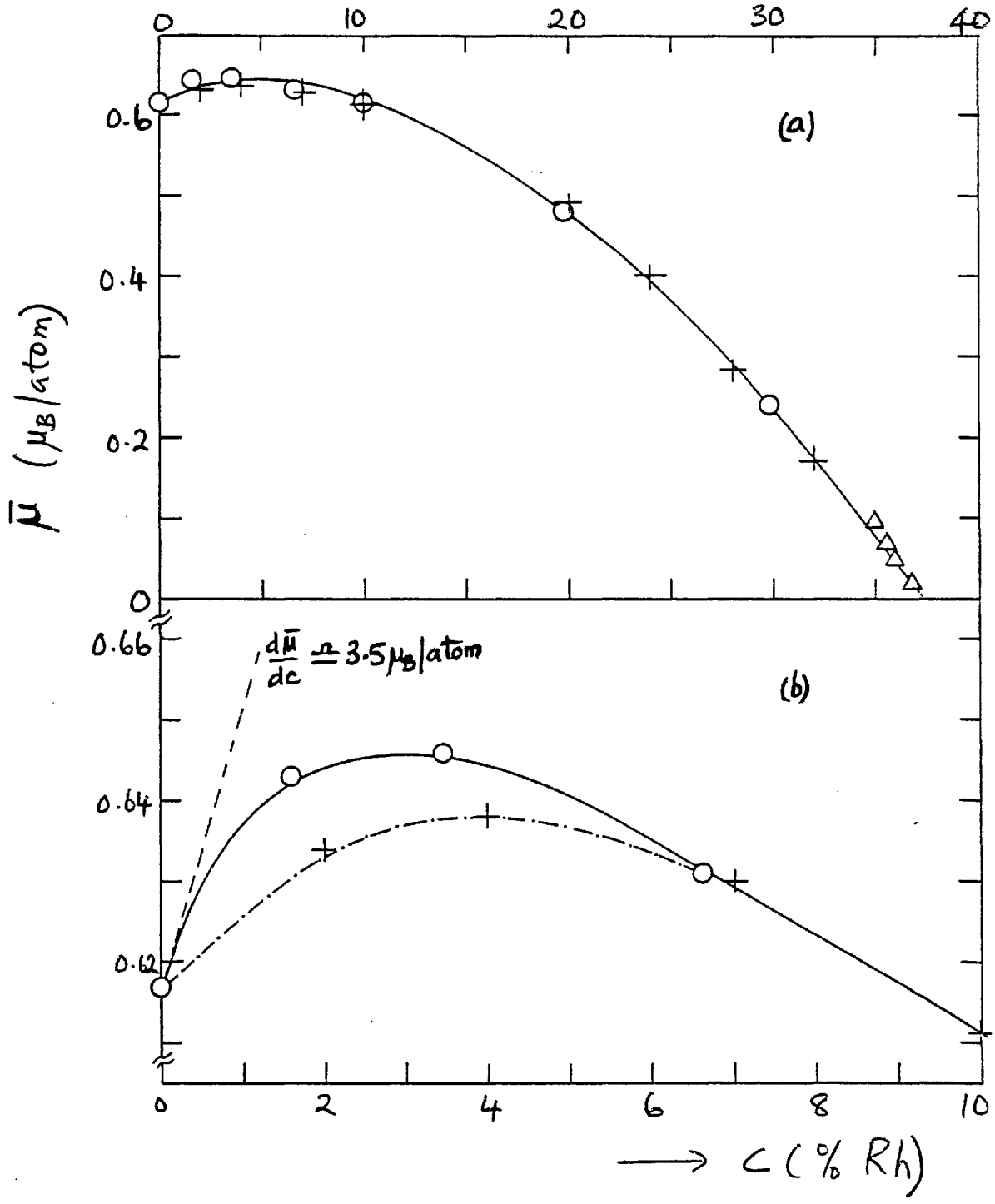

the magnetization data is that for dilute solute concentrations a Rh atom has a fairly large moment. Magnetization measurements for $c \lesssim 1\%$ Rh would be required to determine the true initial value of $\frac{d\bar{\mu}}{dc}$.

Unpolarized neutron diffraction measurements on a Ni 2% Rh alloy (473) gave an almost κ-independent cross-section with $(F_{Rh}\bar{\mu}_{Rh} - F_{Ni}\bar{\mu}_{Ni}) \simeq 1.7\,\mu_B$ at $\kappa = 1.2\ \text{Å}^{-1}$. Using $F_{Rh} = e^{-0.14\kappa^2}$ and $F_{Ni} = e^{-0.05\kappa^2}$ one obtains that $\bar{\mu}_{Rh} \simeq 2.6\,\mu_B$ for c = 2% Rh in fair agreement with the magnetization values.

From magnetic susceptibility and specific heat measurements on nearly ferromagnetic NiRh alloys Bucher et al. (337, 563) inferred that these alloys showed critical exchange enhancement accompanied by large spin fluctuations. This interpretation followed largely from the fact that an upturn at low temperatures was observed in the plot of $\frac{C_v}{T}$ versus T^2 for the specific heat data. For Ni 37% Rh the specific heat data at low temperatures were therefore fitted to the curve

$$\frac{C_v}{T} = \gamma^* + aT^2 + bT^2 \ln T$$

(cf eq.(1.51)) with γ^* determined as the intercept of the curve at T=0 instead of an extrapolated intercept from the high temperature data (see fig.2.6). Plots of γ^* and the magnetic susceptibility, χ, against concentration showed a sharp peak at $\sim 63\%$ Ni, the peak in γ^* being clearly asymmetric. The authors claimed that $\chi \propto |c - c_f|^{-1}$ and qualitatively $\gamma^* \sim -\ln|c - c_f|$ so that $\gamma^* \sim \ln\chi$ in apparent agreement with the uniform exchange enhancement model of paramagnons (see section 1.10). However, a subsequent analysis of the same specific heat data by Hahn Wohlfarth (321) showed that the low temperature anomaly

was equally consistent with the existence of magnetic clusters. Additional but qualitative support for this conclusion was thought to be provided by the temperature dependence of the inverse susceptibility of Rh 62 and 63% Ni alloys (564, 580). Below $\sim$ 100 K the plot of χ^{-1} vs T is no longer linear but curves downwards. This effect was taken to indicate the increasing contribution of ferromagnetic clusters to the bulk magnetic susceptibility. Using these susceptibility data and the magnetic isotherms for Rh 63% Ni Hahn and Wohlfarth (321) estimated the cluster moment to be $\sim$ 200 μ_B . Cottet et al. (564) also carried out E.P.R. of Gd and velocity of sound measurements on several NiRh alloys including some doped with Fe. For alloys outside the critical composition region the authors believed that their measurements showed that the magnetic properties of NiRh alloys were in general agreement with a band model. The Fe-doped alloys exhibited localized giant moments "in competition with the Kondo effect in Rh-rich specimens". Stronger support for the existence of magnetic clusters in the critical concentration region of the NiRh system came from the effect of an applied magnetic field on the specific heat. Triplett and Phillips (341) found that applying a field of 38KG was sufficient to suppress the upturn in the Cv/T vs T^2 plot for a Rh 62% Ni alloy. They therefore concluded that this observation was in agreement with the behaviour expected of magnetic clusters since a much larger magnetic field would have been required if, as suggested by Bucher et al. (337, 563), the heat capacity anomaly were due to spin fluctuations. Decisive evidence for the existence of

magnetic clusters in RhNi alloys in the critical concentration region has been provided by the detailed magnetization measurements of Muellner and Kouvel (457, 565). These measurements show that the magnetic clusters have relatively large moments, $\sim$ 20-24 μ_B per cluster, that are approximately constant for the concentration range studied but their concentration decreases smoothly, with decreasing Ni content, across the critical concentration. The cluster concentration was shown to qualitatively follow the statistical concentration of Ni atoms that have 12 other Ni atoms as nearest-neighbours. Confirmatory evidence for the presence of magnetic clusters in a weakly ferromagnetic Rh 65% Ni alloy was obtained from a detailed study of the critical behaviour of this alloy at its apparent ferromagnetic Curie point $T_c \simeq$ 44 K (566).

On the theoretical side Levin et al. (567) have attempted to calculate the spin susceptibility of disordered Pt-Pd, RhPd, RhNi and PdNi alloys using the coherent-potential approximation (CPA) and including potential-scattering effects. For RhNi in particular, these authors found that for $c \lesssim$ 50% Ni the spin susceptibility of RhNi can be calculated to within a 10% accuracy on a uniform exchange enhancement model, provided the density of states at the Fermi level is calculated self-consistently at each concentration using the CPA. Therefore both Rh and Ni atoms were considered to participate equally in the ferromagnetic phase transition in RhNi. However, the more recent work of Brouers et al. (557, 568) and van der Rest (569) have extended both the CPA and spin fluctuation

theories to take into account the experimentally observed local environment effects. Their theory shows that local susceptibilities depend on environment and concentration through the shape of the density of states, the charge transfers and shifts of energy levels, the Hartree-Fock (non-interacting) susceptibilities and the electron-electron interactions within and between clusters. For RhNi it was found that local moments should first appear on Ni atoms surrounded by twelve other Ni atoms but that at higher Ni concentrations Rh atoms surrounded by 12 Ni atoms may also bear a local moment. Electrical resistivity measurements have also been made on a number of RhNi alloys in the critical concentration region (570). Since magnetization measurements indicated the existence of magnetic clusters it was expected that their resistivity behaviour would be similar to that of corresponding CuNi alloys. In the latter the scattering of conduction electrons by giant moment clusters gives rise to an apparently complex concentration-dependent behaviour (207, 209, 293, 364). The resistivity behaviour of the RhNi alloys is apparently very simple (570), there being no visible significant differences in the temperature variation of the resistivity of alloys straddling the critical composition. A particularly obvious difference between the resistivity behaviour of RhNi and CuNi alloys is the absence of any low temperature resistance minima for the former alloys. Instead the resistivity of all the RhNi alloys studied varied as T^2 at the lowest temperatures and as T at higher temperatures; however, the temperature range of validity of the T^2 regime is

concentration- dependent being smallest for the 62% Ni alloy and increasing for compositions on either side of this. The observed temperature dependence of the resistivity is characteristic of localized spin fluctuations (106, 129, 130) and hence from the concentration-dependence of the range of validity of the T^2 law Houghton et al. (570) stated that the spin fluctuation temperature attains its minimum value at the critical concentration. The spin fluctuations are those of nearly magnetic Ni atoms and/or Ni clusters. The absence of any resistance minimum in RhNi alloys was therefore taken (570) to imply that the spin fluctuation resistivity outweighs the resistivity due to the spin-flip scattering of conduction electrons by magnetic clusters. This interpretation has been supported in subsequent analyses by Tournier (91) and Amamou et al. (301, 302, 571-2). However, we must point out that the latter authors analysed the resistivity using the phenomenological expressions

$$\rho(T) = \rho(0) + a(c)T^n \qquad \text{(cf eq. (2.218) and (2.230)),}$$

where n is a continuously varying exponent, or

$$\rho(T) = \rho(0) + BT + CT^2$$

where the coefficients B and C are concentration-dependent (573). We have already criticized the use of the first of these expressions (see section 2.5(viii)). A distribution of the spin fluctuation temperatures of the nearly magnetic clusters is supposed to justify the use of the second expression. This supposition is certainly plausible but there are other contributions to the low

temperature resistivity that must be considered. Firstly below the critical composition for the onset of ferromagnetism it is expected that the magnetic clusters will "freeze-in" at some temperature to form a cluster-glass. As explained in section 2.8 the resistivity of a cluster-glass (or a spin-glass in general) is similar to a spin fluctuation resistivity so that there could be contributions to either the T- or T^2- term depending on the relative magnitude of the cluster-glass freezing temperature to the observation temperature. Secondly near c_f there are fluctuations of the order parameter (the spontaneous magnetization) from which conduction electrons can be scattered to give a contribution to the T^2-term in the low temperature resistivity. This contribution is proportional to the initial susceptibility and since this quantity diverges at c_f it may be expected that the scattering from the critical fluctuations of magnetization should dominate the coefficient of the T^2-term in the resistivity. Hence it is the concentration-dependence of this term that should be physically significant because it should peak at c_f. What we want to emphasize is that care should be exercised in the analysis of the low temperature resistivity of "giant moment" alloy systems because of the number of possible contributions. It is not always certain that the coefficients of the terms obtained by fitting the resistivity to some plausible but simple phenomenological expression are physically meaningful. We certainly support the suggestion made by Houghton et al. (570) that the absence of resistance minima in RhNi alloys is due to the large spin fluctuation resistivity of nearly magnetic Ni atoms

or clusters. We, however, disagree with the statement by these authors that the spin fluctuation temperature attains its minimum value at c_f because in our view this assertion is not physically meaningful simply because such a minimum does not exist. Also we should remember that pure Rh itself is exchange-enhanced and has a spin fluctuation temperature which should steadily decrease as the magnetic solute concentration increases (see section 2.2). Therefore the contribution to the resistivity of nearly magnetic Rh atoms, especially those having a large number ($\gtrsim 10$) of Ni nearest-neighbours, is important. The concentration-dependence of the range of validity of the T^2 term in the resistivity can be understood in terms of the shifting importance of the spin fluctuation resistivity (well below c_f), the cluster-glass resistivity ($c \lesssim c_f$), and the resistivity due to critical magnetization fluctuations ($c \triangleq c_f$).

Two other systems in which the average magnetic moment exhibits a maximum as a function of the solute content are the NiMn (574) and FeRh (183, 576) alloy systems. In the NiMn system the saturation magnetization increases with Mn concentration up to about 8% Mn before it decreases again. The decrease has been attributed to competing antiferromagnetic Mn- Mn and ferromagnetic Ni-Mn and Ni - Ni exchange interactions and the concomitant decrease of the average Ni moment in the alloys (575).

In the FeRh system the average magnetic moment again increases with the addition of Rh but attains a maximum at $\sim$25% Rh. No explanation of the concentration-dependence of the magnetization of this system appears to have been given since most of the experimental study has been confined

to the ferromagnetic $\longrightarrow$ antiferromagnetic transition which, at room temperature, occurs near the equiatomic composition (576). However, a recent determination the magnon dispersion curves for equiatomic FeRh (577) has shown that in the ferromagnetic phase the exchange interaction between neighbouring Rh atoms is antiferromagnetic ($\sim$ -7.73 meV) while the Rh-Fe and Fe-Fe exchange interactions are ferromagnetic and smaller (4.46 and 5.12 meV respectively). It is thus significant that for NiMn and FeRh alloy systems whose concentration-dependence of the saturation magnetization is similar to that of NiRh the exchange interaction between the solute atoms is antiferromagnetic. We shall attempt to establish whether the available data rule out an antiferromagnetic Rh-Rh exchange interaction in NiRh.

Unpolarized neutron scattering measurements on the NiRh system were undertaken to determine the variation of $\bar{\mu}_{Ni}$ and $\bar{\mu}_{Rh}$ with concentration as has been done for CuNi (204, 438) but as it turned out a similar study was simultaneously carried out by Cable whose report has been published (583).

6.2 Determination of Lattice Constants

The lattice constants of Rh 64, 70 and 80% Ni were determined as described in section 4.3. The samples were the buttons and plate used for the neutron measurements but these were not annealed to remove any strains in the samples. Not surprisingly the peaks in the X-ray reflections were rather broad, as shown in fig 6.2, and it was not possible to resolve the doublet except for some of the reflections for Rh 64% Ni. The lattice constants calculated

Fig. 6.2: X-ray reflections for some RhNi alloys.

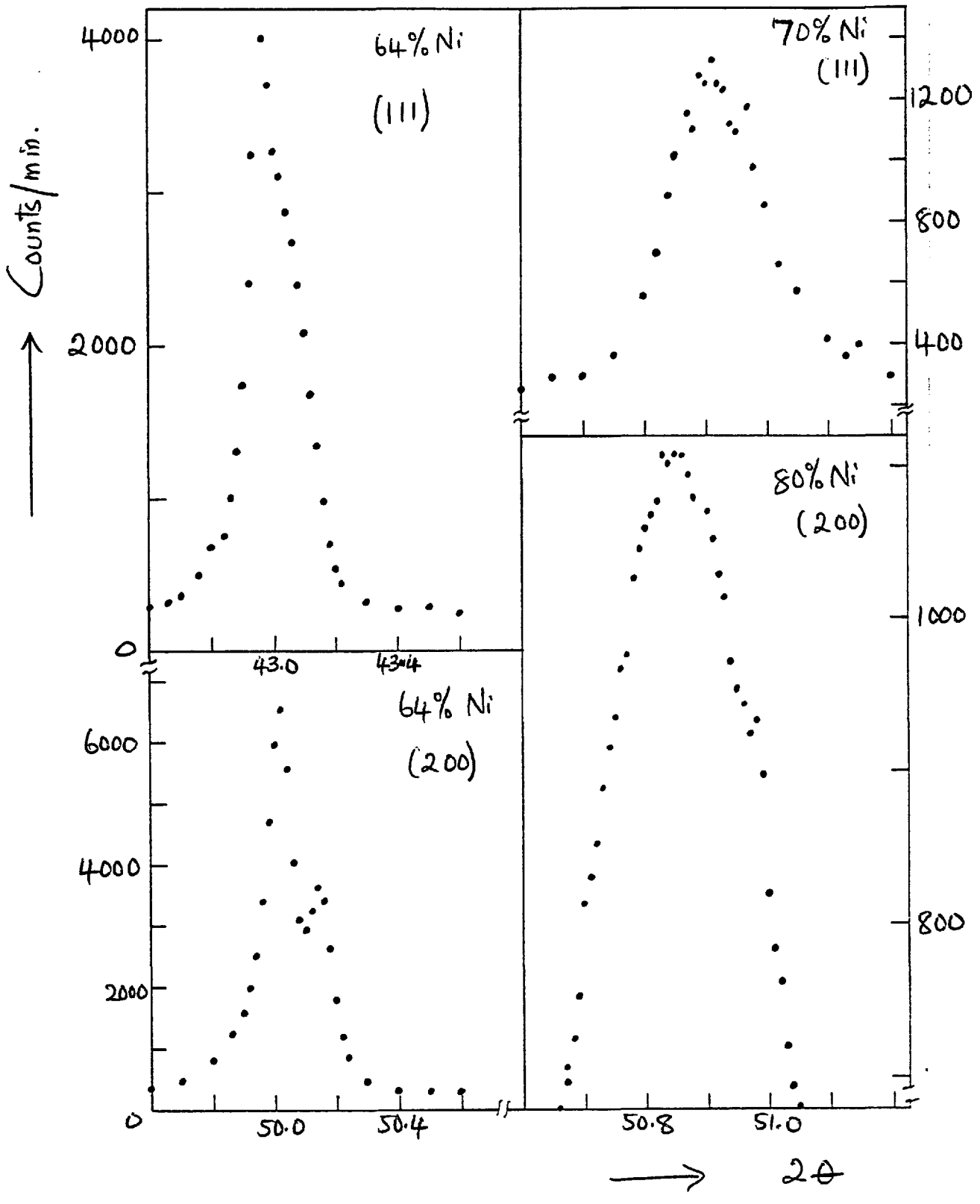

Fig. 6.3 Lattice constants determined from x-ray reflections plotted against the Nelson-Riley function

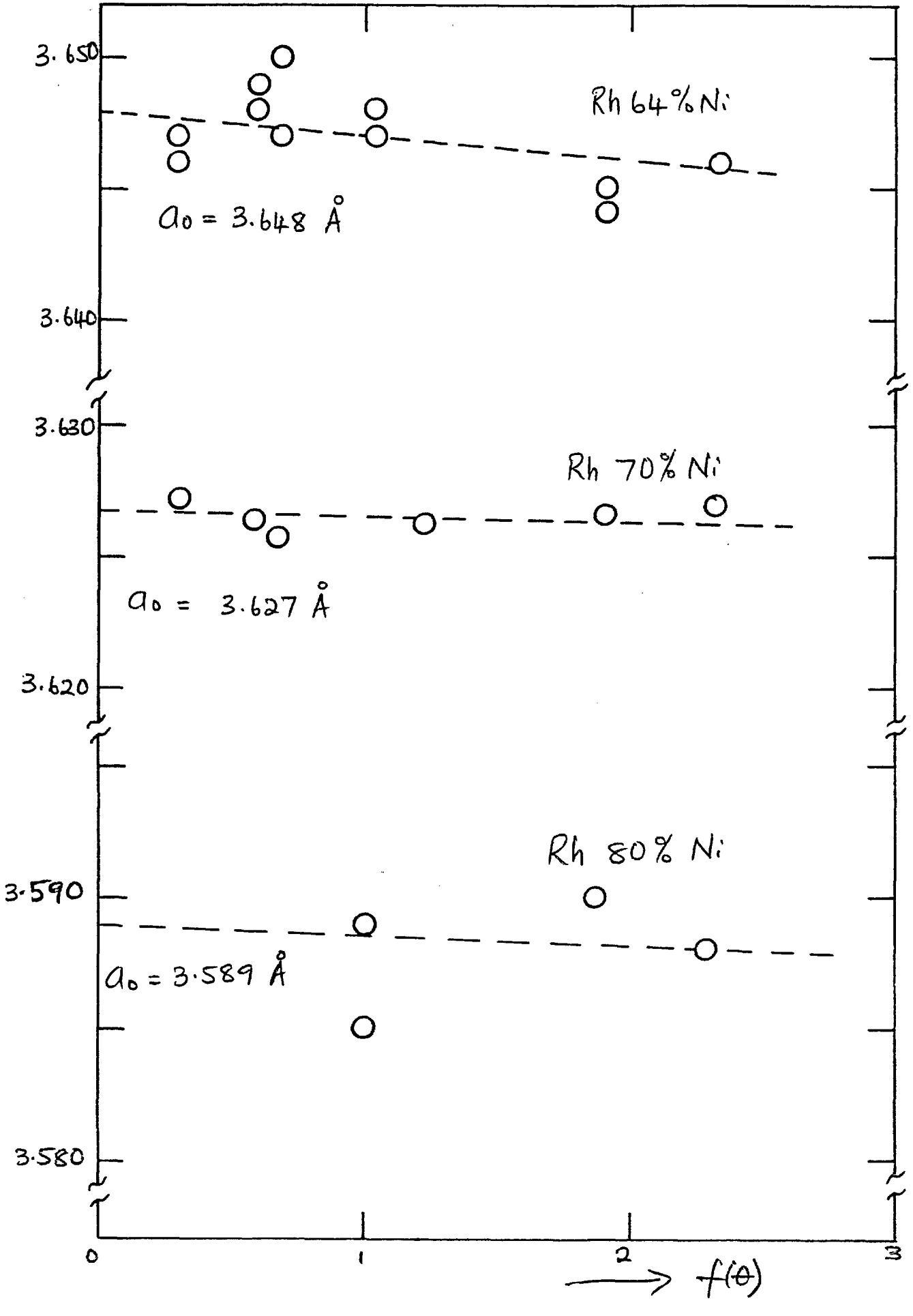

from the positions of the X-ray peaks have been plotted as a function of $f(\theta)$, the Nelson-Riley function (eq.(4.19)), in fig 6.3 to obtain a value of the true lattice constant for each sample.

In fig 6.4 we show the concentration-dependence of the lattice constant of NiRh alloys. From the general variation of $a_0(c)$ it would appear that the true concentrations of our alloys are very close to the nominal concentrations although there is some discrepancy between our value for the lattice constant of the 20% Rh alloy and that obtained by Luo and Duwez (578). However, this discrepancy may not be significant because as seen in fig 6.3 of the three lattice constants determined the value for the 20% Rh alloy is probably the least precise. The observed lattice constants for the NiRh system show a positive deviation from Vegard's law; in fact, between $\sim$ 22-80% Rh $a_0(c)$ is displaced nearly parallel to the line representing Vegard's law by $\sim$ 0.024Å. Fig 6.4 also shows the concentration-dependence of the lattice constant of CuNi and CoNi alloys. For CuNi there is a negative deviation from Vegard's law whereas for CoNi which is magnetic at all compositions there is no deviation at all. Just as in CuNi (579) there is a change of slope at $\simeq$ 22% Rh where the Curie temperatures of the alloys reach room temperature.

An interesting observation in fig 6.4 is that the broken line extrapolates to $a_0 = 3.542$Å for pure (but presumably non-ferromagnetic) Ni. This value compares very favourably with the lattice parameter ($\simeq$ 3.54Å) of Ni at at 673 K (593), a temperature that is slightly above the Curie temperature. An extrapolation to pure Rh would

Fig. 6.4: Room temperature lattice parameters for three fcc Ni-based alloys. Solid lines represent Vegard's law.

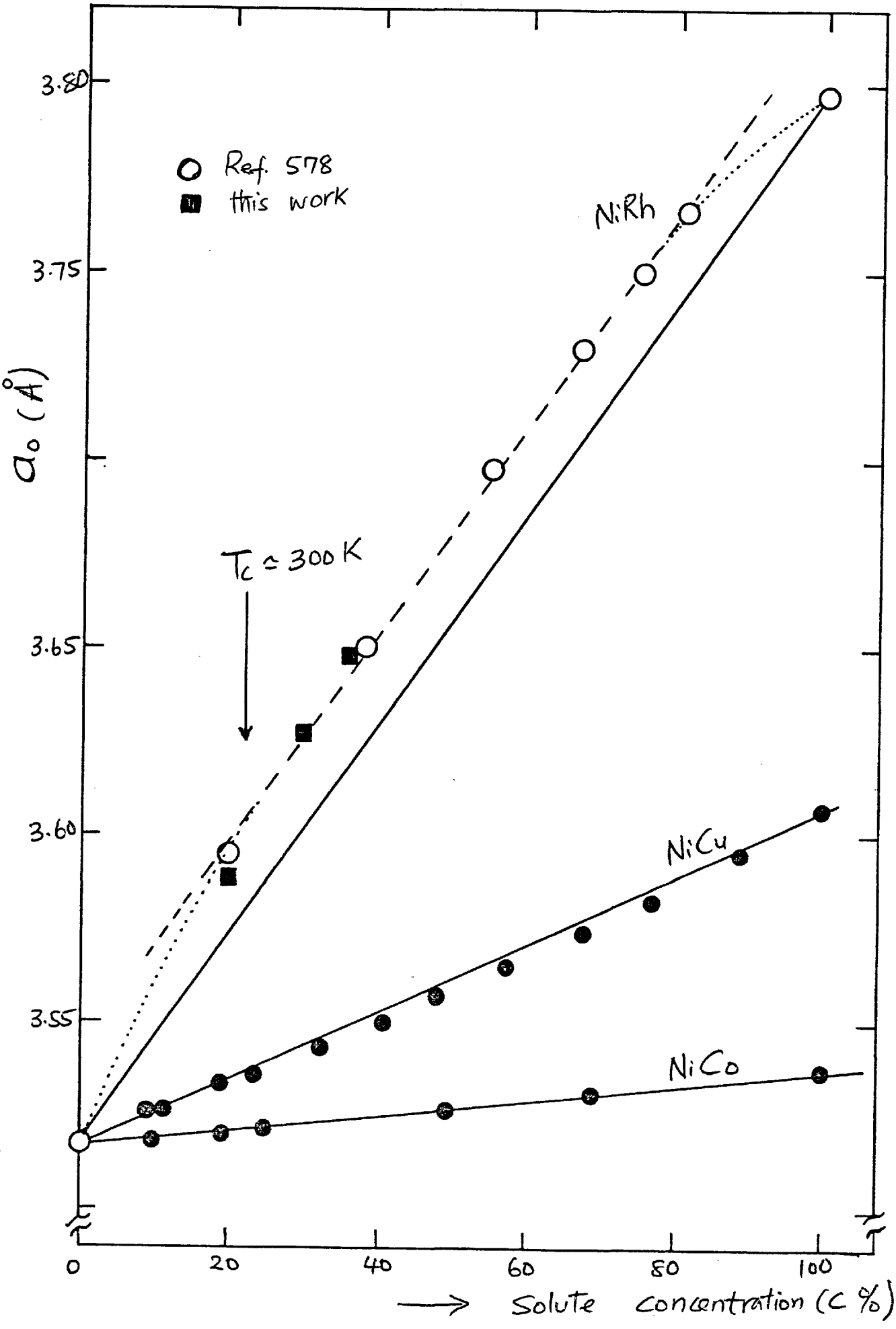

similarly imply the existence of a negative volume striction for this element but it is not presently known whether this has any physical significance.

6.3 Magnetization Measurements

Magnetization measurements, as described in section 4.2, have been made on Ni 26, 30 and 36% Rh alloys. Fig 6.5 shows the temperature-dependence of the magnetization of the 26% Rh alloy measured in a constant field of 20 Oe. From the figure a Curie temperature of $\simeq$ 230 K is deduced for this alloy. The magnetic field used in this measurement was, in retrospect, definitely too large because the magnetization was still increasing well below the Curie temperature instead of attaining a limiting value determined by the demagnetization factor of the specimen.

Fig 6.6 shows some magnetic isotherms for the 30% Rh alloy while in fig 6.7(a) graphs of M^2 versus H/M (i.e. Belov-Arrott plots) in the ferromagnetic transition region are plotted. By plotting the intercepts on the M^2 axis against temperature (see eq.(4.18)) a Curie temperature of 122.5 K for this alloy is obtained (fig 6.7 (b)). In order to determine the paramagnetic Curie temperature, θ_p, the magnetization in a field of 500 Oe was measured as a function of temperature and the inverse susceptibility ($\equiv H/M$) plotted against temperature to obtain θ_p =204 K (fig 6.8(a)). However, an interesting observation is that when these measurements were repeated using a constant field which was an order of magnitude smaller (specifically 52 Oe) it was no longer possible to uniquely determine θ_p because we could either obtain $\theta_p \simeq$ 150 K if we use measurements for T $\gtrsim$ 240 K only or $\theta_p \simeq$ 127K (which is

Fig. 6.5: Rh 74% Ni: Magnetization (at H=20 Oe) vs temperature.

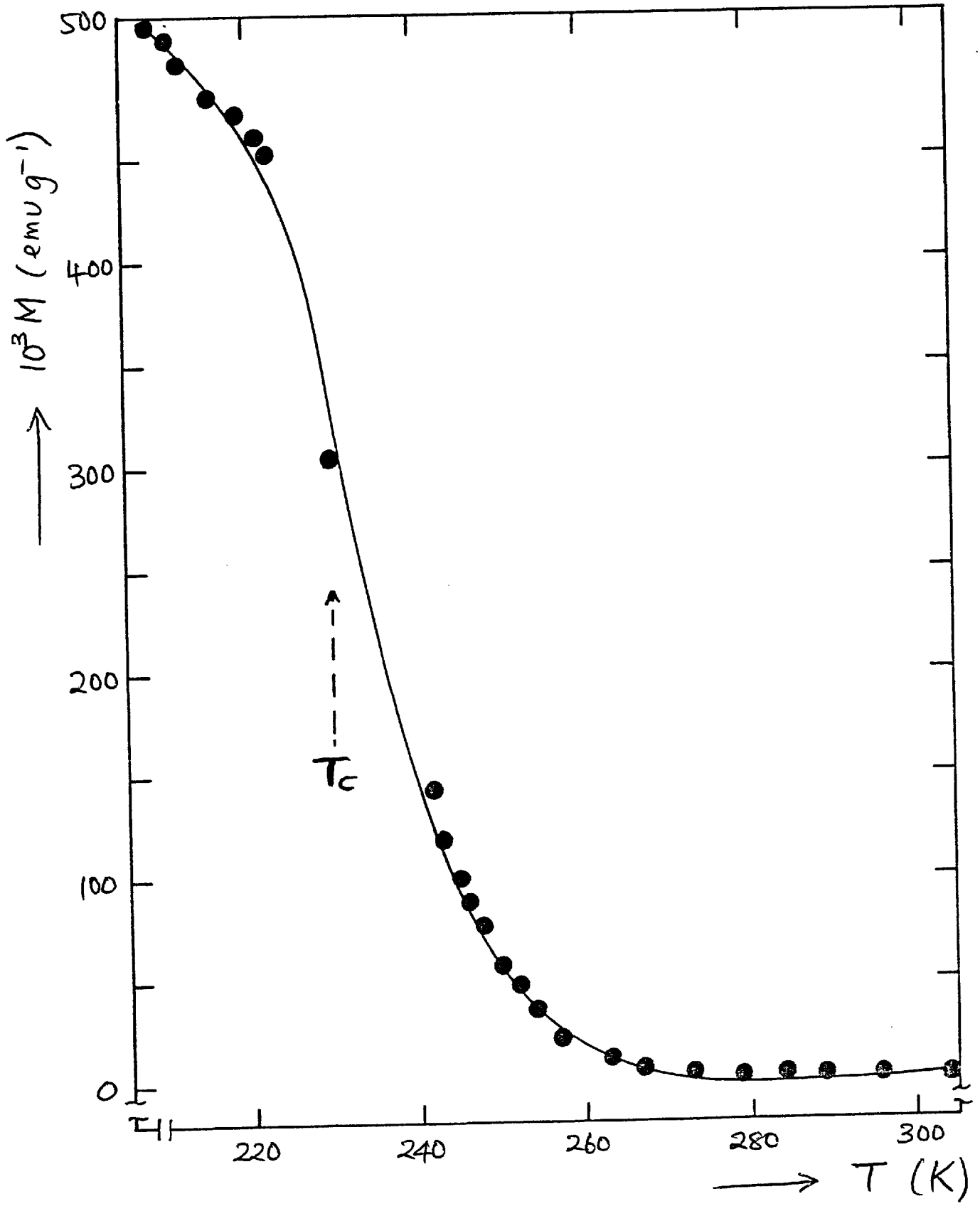

Fig. 6.6: Some magnetic isotherms for Rh 70% Ni

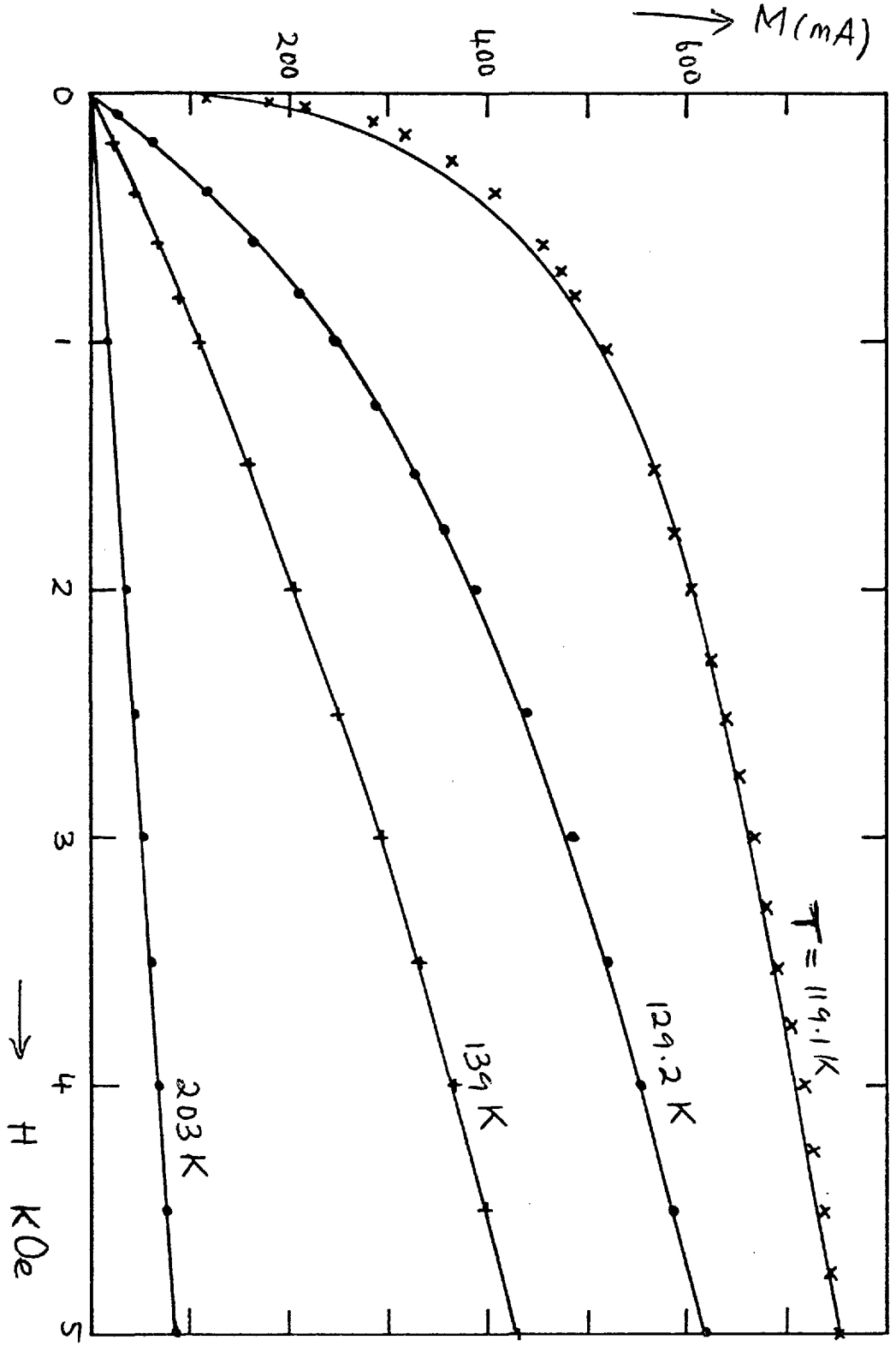

Fig. 6.7: Belov-Arrott plots for Rh 70% Ni
(a) M^2 vs H/M
(b) Intercepts on M^2 axis vs T

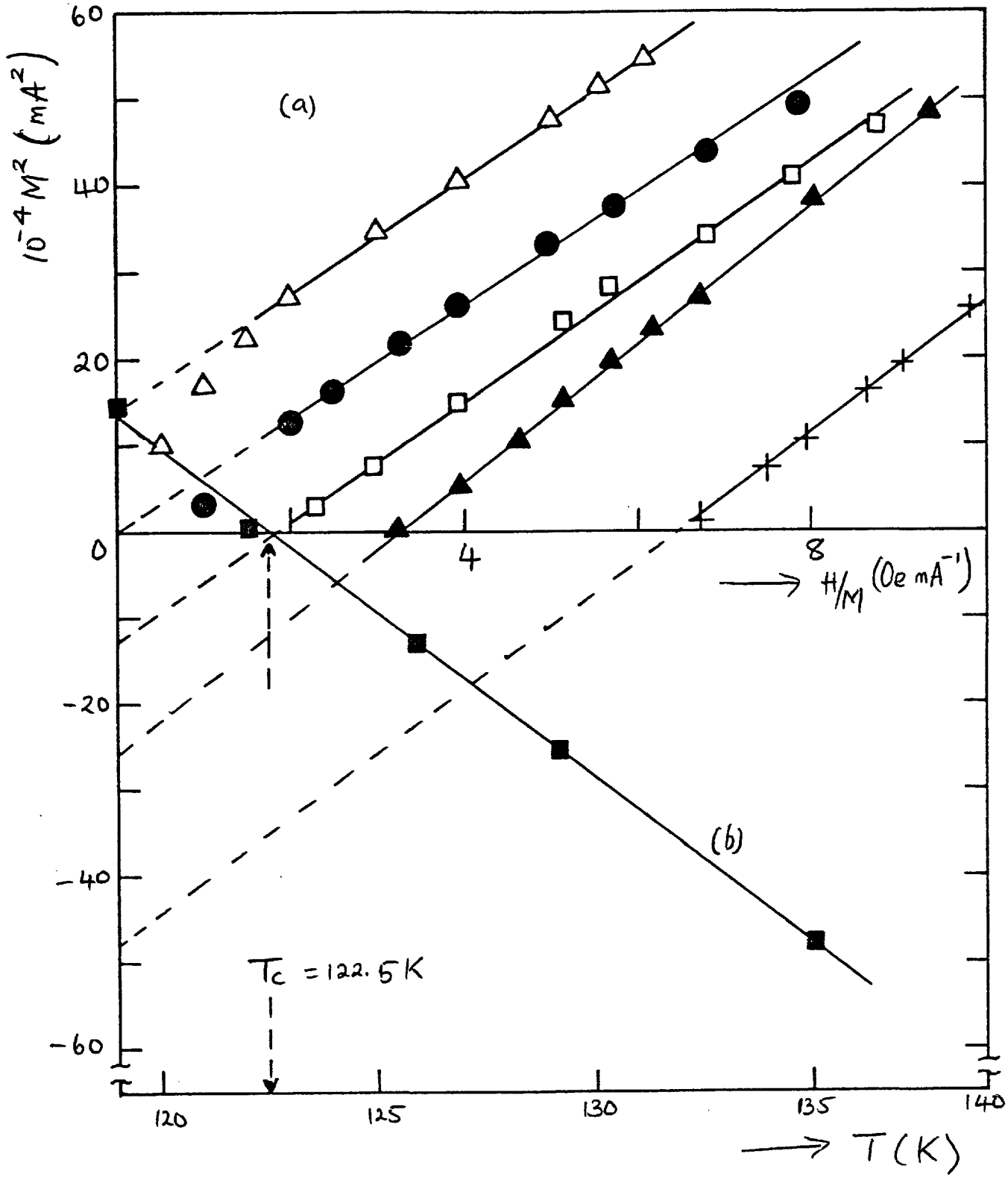

Fig. 6.8: Determination of Θ_p for Rh 70% Ni (in (b) the circles, crosses and triangles refer to different sets of measurements).

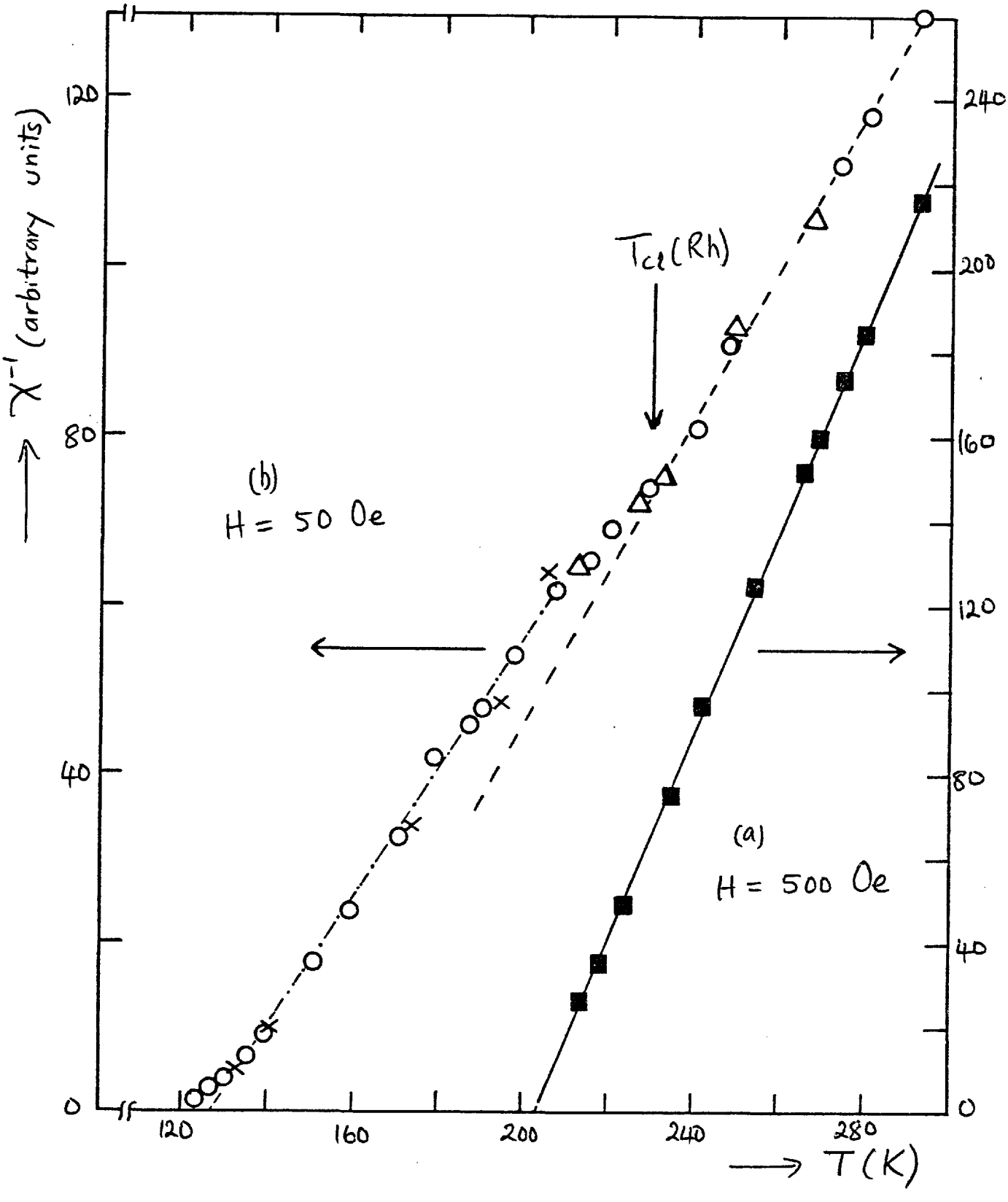

close to the Curie temperature of 122.5 K) for $135 \lesssim T \lesssim 200$ K (fig 6.8(b)). It would appear that this discrepancy is related to the change of slope that occurs near 230 K, a feature that did not seem to be due to some experimental error (because the measurement was repeated). According to the Curie-Weiss law the slope of the inverse susceptibility (per mole) versus T plot is given by $\frac{3K_B}{N_o c^* \langle M_{cl}^2 \rangle}$ where N_o is Avogadro's number, c* the concentration of magnetic clusters and $\langle M_{cl}^2 \rangle$ is the mean square value of the cluster moment. The increase of slope above $\sim$ 230K in fig 6.8(b) must therefore be due to a decrease in either the cluster concentration or $\langle M_{cl}^2 \rangle$ or both. From the discussion in section 6.1 it appears that a Rh atom has a fairly large moment ($\gtrsim$ 2.6 μ_B /atom) when introduced dilutely into a Ni matrix, but recent neutron diffraction measurements by Cable (583) show that the Rh moment is "destroyed" if the Rh atom has a Rh nearest-neighbour. It is therefore reasonable to expect that a Rh atom surrounded by 12 Ni nearest-neighbours would bear a moment even in the critical concentration region so that <u>in this region the magnetic clusters probably consist of both Rh and Ni atoms with twelve Ni nearest-neighbours</u>. While resistivity measurements (207) indicate that the <u>intra</u>-cluster interaction energy in Ni-centred Ni clusters is of the same magnitude as in pure Ni (i.e. $\sim$ 630 K) it may be expected that the intra-cluster exchange interaction in <u>Rh-centred</u> Ni clusters will be much less especially as the Curie temperature of NiRh alloys decreases monotonically with the increase in the Rh concentration. Consequently we suggest that the decrease in the concention of c* and/or

$\langle M_d^2 \rangle$ above $\sim$ 230 K is due to the break-up of the Rh-centred magnetic clusters i.e. the cluster temperature, T_{cl}, of these clusters is about 230 K. Thus the exchange integral, J_{Rh-Ni}, between Ni and Rh is about $0.37 J_{Ni-Ni}$ which compares favourably with an estimated value of $(0.6 \pm 0.2)\ J_{Ni-Ni}$ (583).

We have also attempted to determine T_c and θ_p for Ni 36% Rh as shown in fig 6.9. The susceptibility was measured in a constant field of 1.5 KG (a large field was used to obtain a measurable response especially at high temperatures, $T \gtrsim 150$ K) and the plot of χ^{-1} against T (fig 6.9(a)) gives $\theta_p \simeq 44$ K. Observe again the anomalous behaviour of the susceptibility near 230K. In order to determine T_c we measured the magnetization in what, at the time, was thought to be a small field ($\simeq$ 53 Oe). The result is shown in fig 6.9(b). It is seen that the magnetization remains constant up to about 20 K before it decreases. The rather broad transition may be due to the fact that the applied field is relatively large since such a field at 4.2 K is sufficient to give a magnetization that is more than 90% of the apparent saturation value in small fields (see fig 6.11(b)). We have therefore taken the transition temperature to be 21 K in agreement with a value of 19 K obtained by Muellner and Kouvel (457).

Fig 6.10 shows the concentration-dependence of θ_p. A change of slope occurs near $T \simeq$ 230 K which temperature we have suggested is that at which the Rh-centred clusters break up. Also shown in fig 6.10 is the concentration-dependence of T_c. A deviation from a linear dependence on c begins at about $\sim$ 230 K. For higher values $T_c^2 \propto c$ (also shown

Fig. 6.9: Determination of Θ_p and (T_c (?) for Rh 64% Ni
(a) M vs T (H = 1.5 kOe)
(b) χ^{-1} vs T (H = 53 Oe)

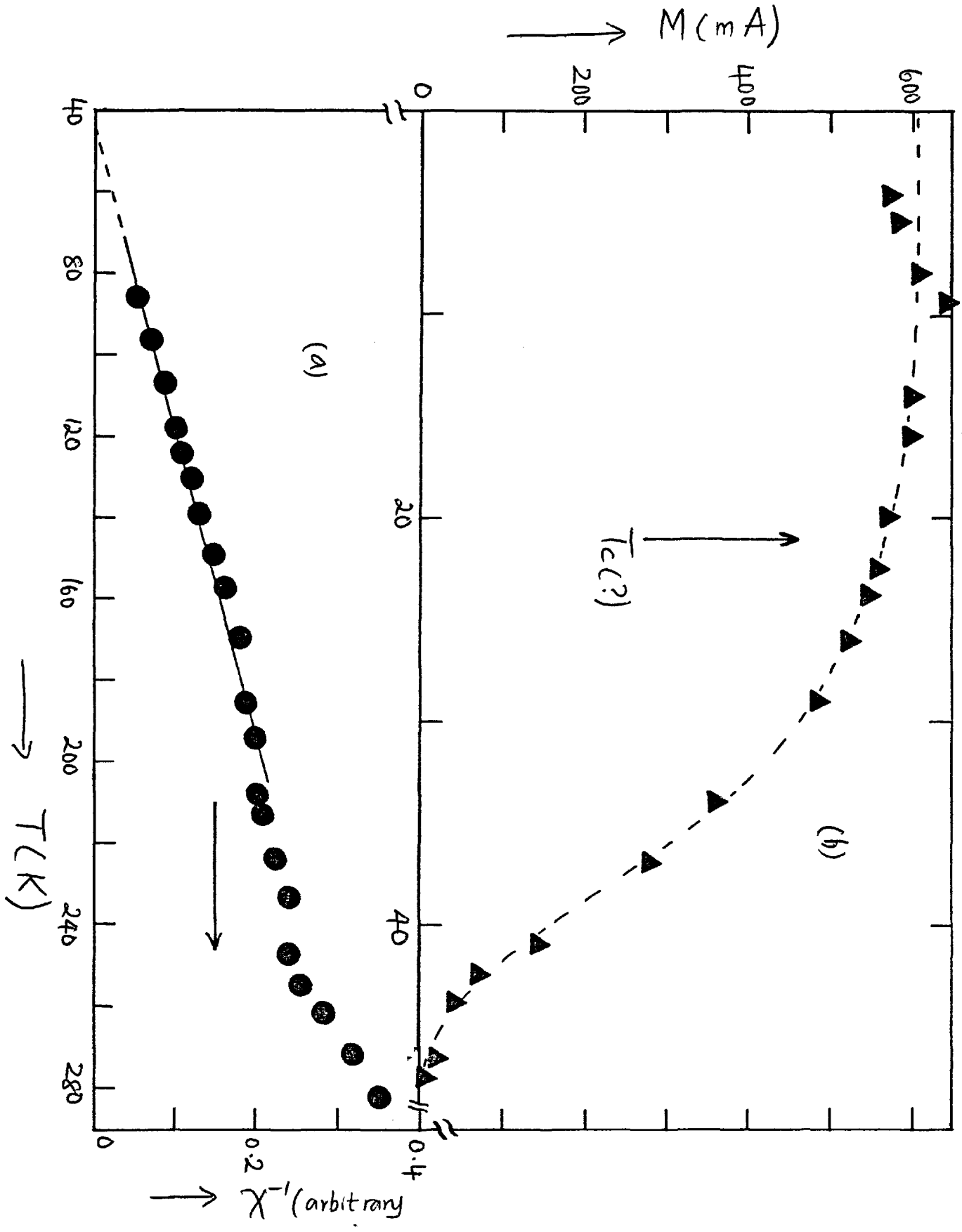

Fig. 6.10: Rh Ni: Concentration dependence of Θ_p, T_c and T_c^2.

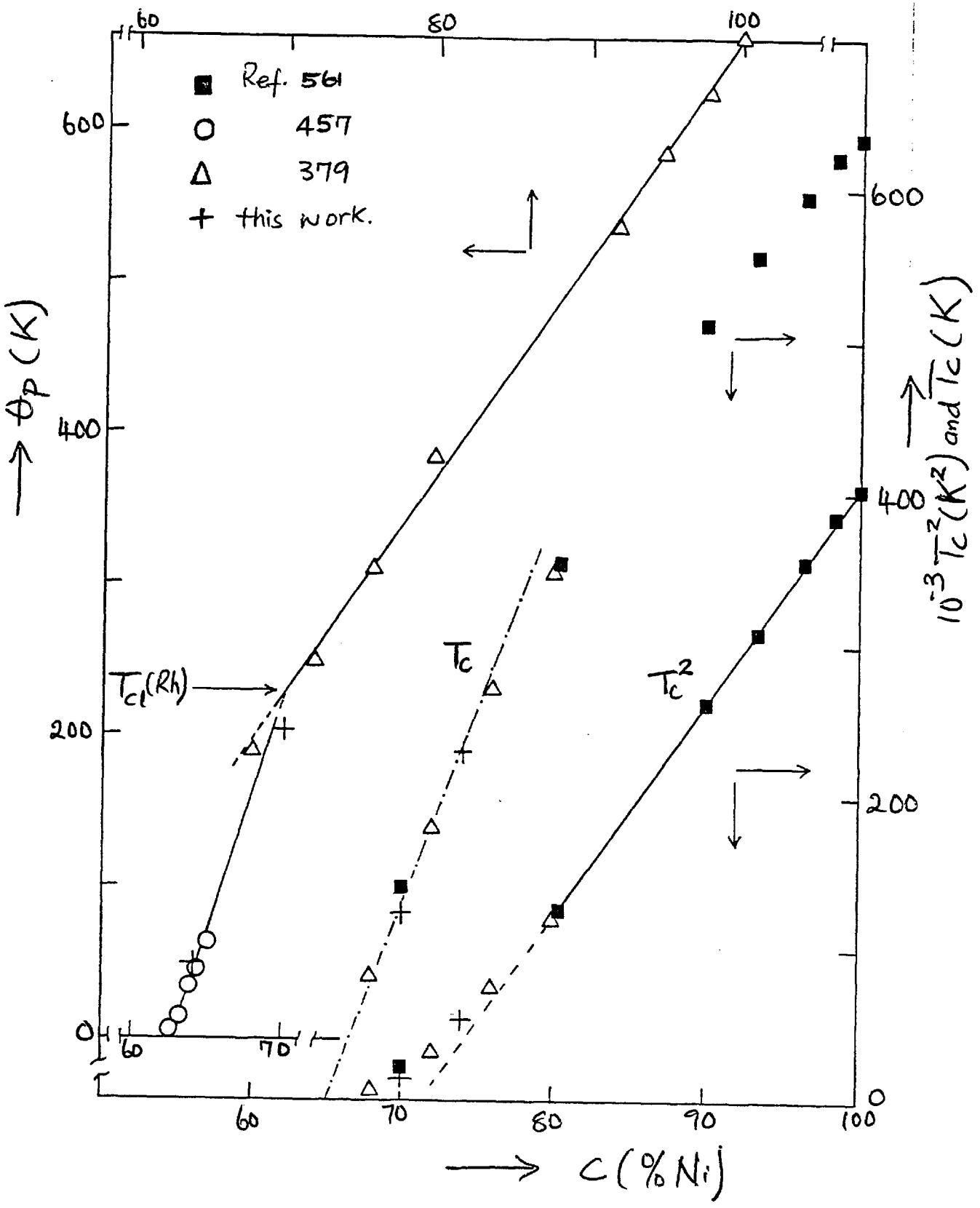

in the figure). This latter observation is interesting because such a concentration-dependence of T_c appears to hold only for alloy systems in which structural changes occur as a function of composition, e.g. AlNi (near the stoichiometric composition Ni_3Al - see section 2.6(g)) and FeNi in the invar composition range (396). It may also be easily checked that the Curie temperatures determined by Crangle and Parsons (561) for fcc CoRh alloys satisfy the same relation (i.e. $T_c^2 \propto C$). In this system a martensitic fcc $\longrightarrow$ hcp transformation is known to occur. It will be recalled that a number of authors had previously suspected the existence of an ordered structure (of the Cu_3Au type) in the NiRh system (586) although Luo and Duwez (578) subsequently did not observe any such ordering. If the ordering occurs in small regions then it may not be observable in lattice parameter measurements.

We must mention that while we have determined θ_p by a straight-forward plot of the reciprocal of the measured susceptibility against T Muellner and Kouvel (457) separated the susceptibility into a Curie-Weiss-like term and a very weakly temperature-dependent term i.e.

$$\chi = \frac{Nc^* \langle M_{cl}^2 \rangle}{3k_B(T-\theta)} + \chi_b(T) \quad . \tag{6.1}$$

$\chi_b(T)$ is normally associated with an exchange-enhanced band susceptibility which is fairly constant with composition (457) but it may contain a contribution from nearly magnetic clusters (301).

The vibrating sample magnetometer used for the magnetization measurements was not strictly designed for ferromagnetic substances because of the very high nulling currents that would be required. Although a way of using

the magnetometer for ferromagnets was devised, we feel that the method is most useful for measurements requiring relative (and not absolute) values e.g. the temperature-dependence of the magnetization in a given field. Consequently even though extensive measurements were made to determine the spontaneous magnetization of the 30 and 36% Rh alloys over a range of temperatures below their respective Curie temperatures we have chosen not to report these because of their possible inaccuracy. Instead we have shown the M-H curves at 4.2K for the two alloys in fig.6.11. These curves show that the spontaneous magnetization reaches its maximum value in very low fields ($\sim$ 300 Oe for Ni 30% Rh and $\sim$ 100 Oe for Ni 36% Rh) and that within the accuracy of our measurements there is very little remanence. The usefulness of the M-H plots lies in the fact that they clearly show that extremely low fields ($\lesssim$ 5 Oe) should be used for any accurate determination of Tc. Unfortunately we have used fields that were an order of magnitude larger ($\gtrsim$ 50 Oe) and to this extent we should treat our T_c values, particularly for the 36% Rh alloy, with caution. Also we should mention that because of the distinction between the spontaneous and saturation magnetizations for weakly ferromagnetic alloys the spontaneous magnetization should not be obtained by plotting M against H^{-1} (see eq.(4.15) in section 4.2). Instead it should be taken as the limiting value of M in the M-H plot at appropriately low fields (see fig.6.11).

An observation made in the course of the magnetization measurements is of interest. For the 36% Rh alloy it was found that at very low fields ($\lesssim$ 5 Oe) the apparent

Fig.6.11: M-H curves for (a) Rh 70% Ni and (b) Rh 64% Ni at T=4.2K

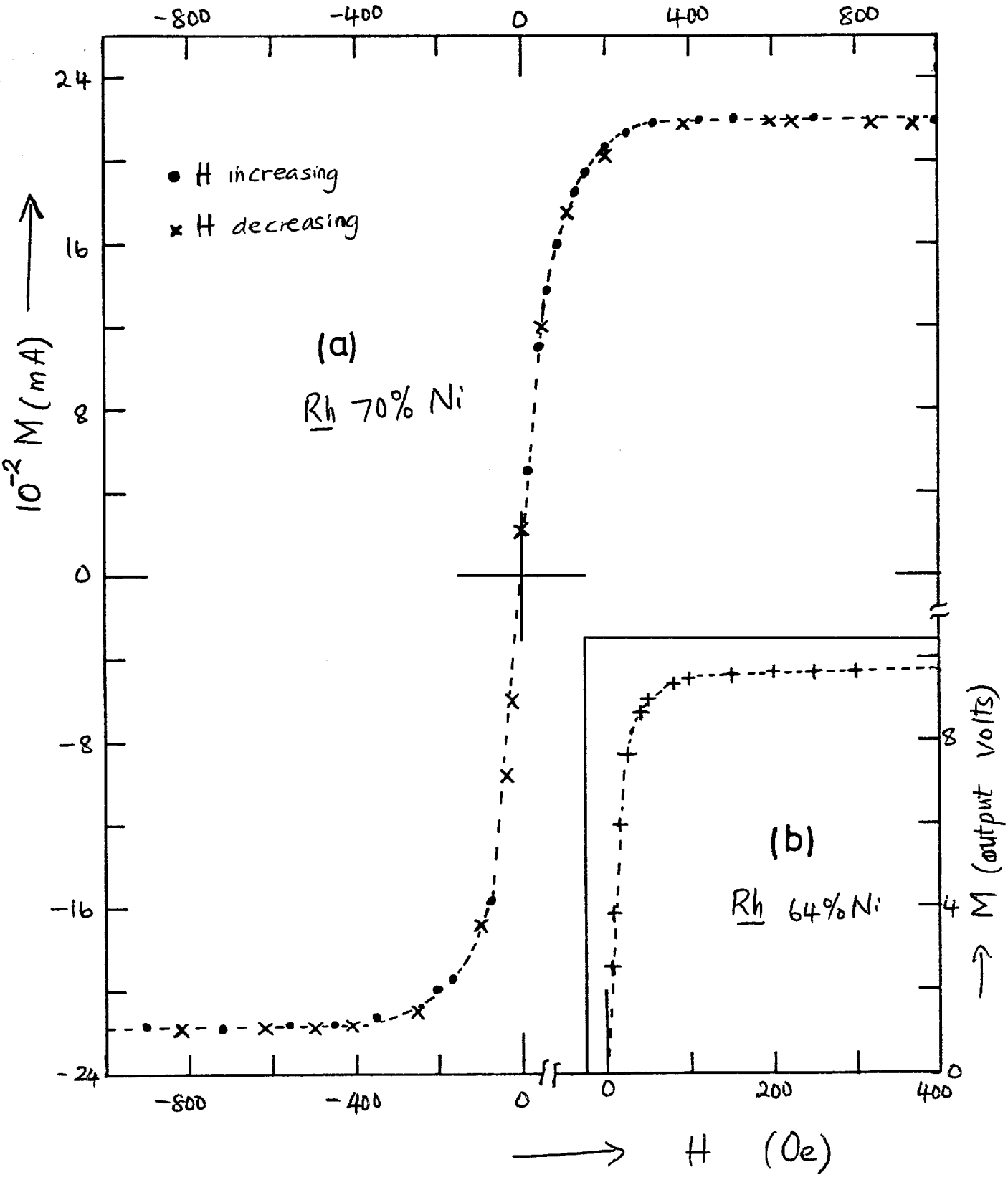

magnetization decays very rapidly. For example, at T=4.2K and for a field of 2 Oe the magnetization decreased from 32 mA (i.e. in terms of the equivalent nulling current) to less than 3mA in about 2s. The behaviour is apparently not characteristic of a true ferromagnet and it could be that the initial value of the magnetization is merely the response to the sudden application of a field rather than a real increase in the magnetization of the specimen.

6.4 The Critical Concentration for the Onset of Ferromagnetism and possible Invar Behaviour of Nearly and Weakly Ferromagnetic RhNi Alloys

The critical concentration for the onset of ferromagnetism in RhNi is now obtained by considering the concentration-dependence of the inverse initial susceptibility, the electronic specific heat, the square of the spontaneous magnetization and the Curie temperature as done for a number of "giant-moment" alloy systems in section 2.6. Fig.6.12 shows the variation of $\{\chi^{o}_{nf}\}^{-1}$, M^2_{oo}, and T_c with Ni concentration; these quantities extrapolate to zero at 62.4, 63.8 and 63.2% Ni respectively. If we take the average of these values as the critical concentration then we obtain c_f = 63.1% Ni for RhNi. Also shown in fig.6.12 is $\gamma(c)$; the values of $\gamma(c)$ have been obtained by extrapolating the linear portion of the $\frac{C_v}{T}$ versus T^2 curves published in reference 563 to the ordinate i.e. $\gamma(c)$ is not necessarily equal to $\gamma^*(c)$. Thus for Rh 63% Ni we obtain $\gamma = 12.4\ mJ\ mole^{-1}\ K^{-2}$, in agreement with Hahn and Wohlfarth (321), while $\gamma^* = 14.6\ mJ\ mole^{-1}\ K^{-2}$ (337). This value of γ for Rh 63% Ni appears to be too small because for Rh 62% Ni the measurements of Triplett and Phillips (341) show that

Fig. 6.12: Determination of c_f for Rh Ni:- Concentration dependence of T_c, M_{oo}^2, γ^s and χ_{nm}^{-1} .

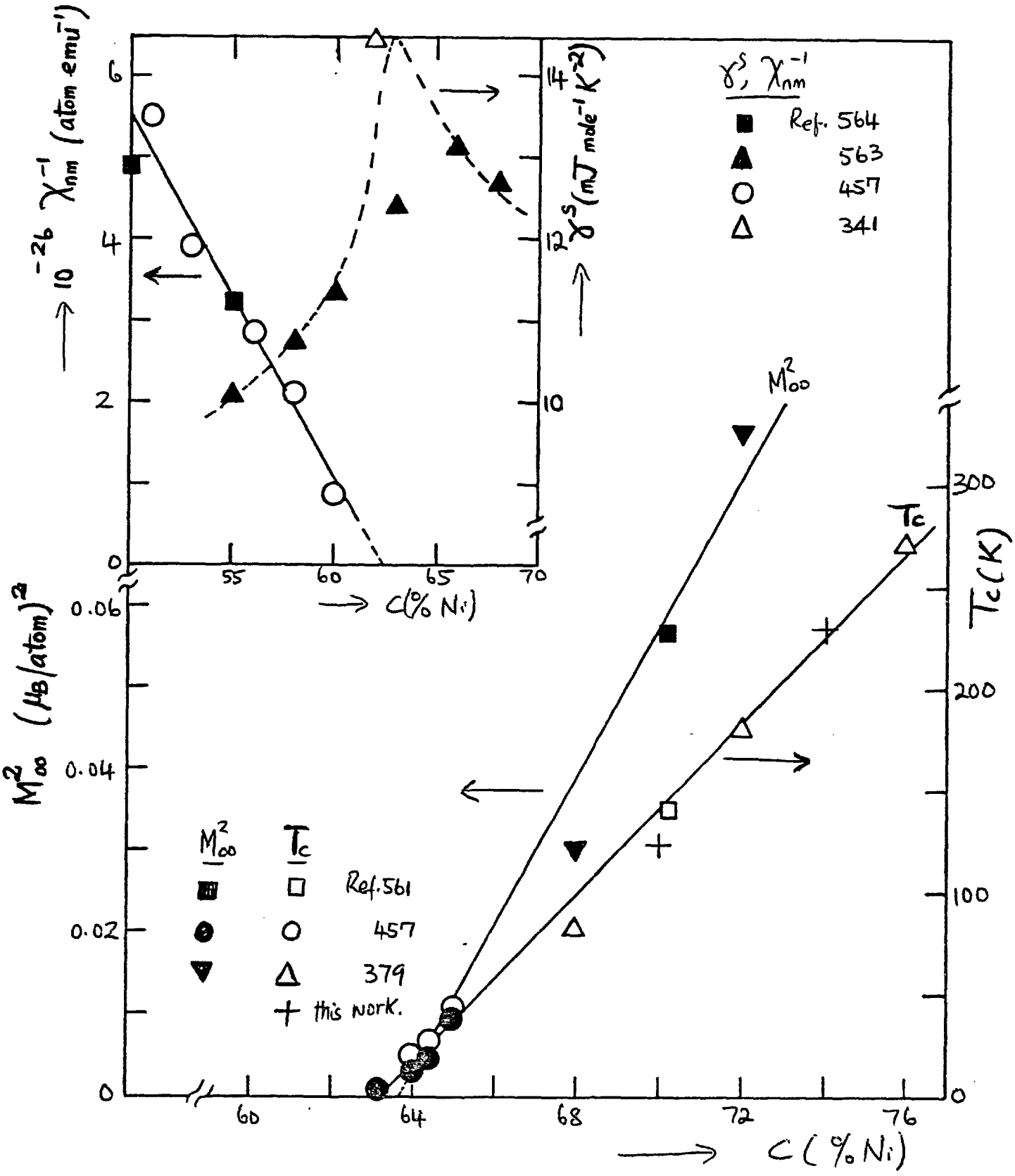

$\gamma \simeq 14.5\ mJ\ mole^{-1}K^{-2}$ in a field of 9 K Oe (the zero-field value would even be larger!). Thus $\gamma(c)$ also shows a peak around the critical concentration. However, it will be useful to determine the Curie temperatures of a few alloys near the suggested critical concentration by doing low field ($\lesssim$ 2 Oe) DC measurements. It will be recalled that Muellner and Kouvel (457) determined the Curie temperatures of some alloys in the critical region by using Belov-Arrott plots. This procedure is strictly inadmissible close to c_f because it certainly involves using fields greater than a few oersteds.

Sound velocity measurements (564) show that the quantity $\Delta V = \{V(77) - V(300)\}$, where V(T) is the velocity at a temperature T, has a minimum at about 61% Ni which is close to c_f. Although such a minimum may be understood in terms of the proposed reduction in the velocity of sound near c_f (see section 2.5(x)) what is really required is the concentration-dependence of v at a very low temperature ($T \lesssim 4.2K$) and in this connection we would have preferred to see the variation of v(77), rather than ΔV , with concentration.

Touger and Sarachik (581) have recently measured the temperature-dependence of the thermoelectric power of CuNi and RhNi alloys in their respective critical concentration regions. For CuNi a small peak was observed between 50-60 K for the 30-46% Ni alloys which are below c_f ($\simeq$ 47.6% Ni) but not in the ferromagnetic 50% Ni alloy. The fact that the peak occurred at a temperature which was independent of the solute concentration allowed it to be attributed to the spin-flip scattering of conduction

electrons by magnetic clusters. For RhNi alloys no such peak was found for the 56-64% Ni alloys studied but the authors reported an apparent change of slope at $\sim$ 25 K. Since the measurements did not extend well into the ferromagnetic regime ($>$ 65% Ni) it is not clear whether this change of slope can be attributed to the presence of magnetic clusters. It is, of course, much easier to see a small peak in the case of CuNi alloys where the thermopower is a decreasing function of temperature than in RhNi where it is an increasing function of temperature.

In section 2.5(iv) we proposed that large values of the spontaneous volume magnetostriction (and the forced volume magnetostriction) and a small or even negative thermal expansivity are intrinsic properties of metal alloys in the critical concentration region for the onset of ferromagnetism. Since these properties are usually associated with the canonical invars it follows that invar behaviour is generally characteristic of the onset of ferromagnetism in transition metal alloys. Fawcett et al. (249) have measured the forced magnetostriction, h'_o, and thermal expansivity of RhNi alloys near the critical concentration. They observed that the forced magnetostriction increases very rapidly, in fact, more rapidly than the initial susceptibility, χ_f^o. This is to be expected because $h'_o \propto (c-c_f)^{-1/2}$ (eq.(2.137)) whereas $\chi_f^o \propto (c-c_f)^{-1}$ (eq.(2.96)). Since the magnetic contribution to the thermal expansivity is given by

$$\beta_m \equiv -\left(\frac{\partial w}{\partial T}\right) = -h'_o\left(\frac{\partial B_o}{\partial T}\right)_M$$

(see eq.(2.150))

and $\left(\frac{\partial B_o}{\partial T}\right)_M > 0$ a large and positive forced

magnetostriction implies a large negative magnetic contribution to the expansivity. Fawcett et al. (249) observed that the temperature dependence of the thermal expansion of RhNi alloys was unusual in that the quantity $\frac{\Delta l}{l_0 T^2}$ (where $\frac{\Delta l}{l_0}$ is the linear magnetostriction) diminishes up to $T \sim 10K$ and then remains approximately constant up to $T \sim 20K$. Although the authors attributed this behaviour to a negative contribution to the entropy (from spin fluctuations) which tends to cancel the positive lattice contribution we feel that the observation shows the invar character of these alloys.

Recent pressure experiments (383, 582) have shown that $\frac{dT_c}{dP}$ is large and negative for RhNi alloys ($c < 90\%$ Ni). It may be shown (584) that if M(T) obeys the law of corresponding states, i.e. $\frac{M(T)}{M(0)} = f\left(\frac{T}{T_c}\right)$ then

$$\left(\frac{\partial w}{\partial B_0}\right)_P \equiv -\left(\frac{\partial M}{\partial P}\right)_{B_0} \simeq \frac{T}{T_c}\left(\frac{\partial M}{\partial T}\right)_P \left(\frac{\partial T_c}{\partial P}\right)_{B_0} \qquad (6.2)$$

and since $\left(\frac{\partial M}{\partial T}\right)_P < 0$ it follows that $\left(\frac{\partial w}{\partial B_0}\right)_{P,\, T \sim T_c}$ is large and positive. This result clearly implies that an invar behaviour should be expected but only <u>near the ferromagnetic transition point</u> i.e. it does not necessarily imply that an invar behaviour will be also observed at low temperatures ($T \ll T_c$) especially if the alloy concentration lies outside the critical region. The distinction is rather subtle but important.

A calculation of the volume paramagnetostriction of NiRh, PdRh and PtNi alloys on the itinerant election model has been recently reported (587). It was suggested that the main contributions to the magnetostriction come from the transfer of electrons from the s- to the d-band and

from the volume dependence of the d-band width.

6.5 Neutron Scattering Measurements

(a) Results

The observed κ -dependent neutron scattering cross-sections of eight NiRh alloys (2,4,10,15,20,24,30 and 36% Rh) are shown in figs. 6.13, 6.14 and 6.15 in which, as in the case of PtCo and PtFe alloys (Chapter 5), $\frac{d\sigma}{d\Omega}$ is the maximum switchable cross-section. For 4,15,30 and 36% Rh the plotted points are in each case the results of a single set of measurements (i.e. $\phi = 0^{o}$ and $\phi = 30^{o}$ or 45^{o}) whereas for the other alloys they represent the averages of two or more "acceptable" sets of measurements. By acceptable we mean that the cross-sections at the two specimen angles should be consistent (see section 5.3 and fig.5.11). For Ni 2% Rh the cross-sections for a slab of the original specimen used by Comly et al.(473) and for a button prepared by remetting off-cuts of the original specimen (see Chapter 4) agreed within the limits of the statistical errors. For the 10% Rh alloy four sets of measurements were averaged and almost an equal number rejected. A great deal of difficulty was encountered in measuring the cross-section of this alloy (as well as for 2% Rh) because of the relatively large statistical errors associated with each single set of measurements and because as we were finally forced to accept, the cross-section was essentially flat in contrast to the marked κ - dependence of the cross-sections of all the other alloys. Finally owing to what was considered to be an abnormally large cross-section at large κ for Ni 24% Rh the experiment was repeated to check for any systematic error. When the same cross-section (within the statistical error limits)

Fig. 6.13: K -dependent moment defects for dilute Ni Rh alloys. The arrows show the magnetization values of $\left|\frac{d\Pi}{dc}\right|$.

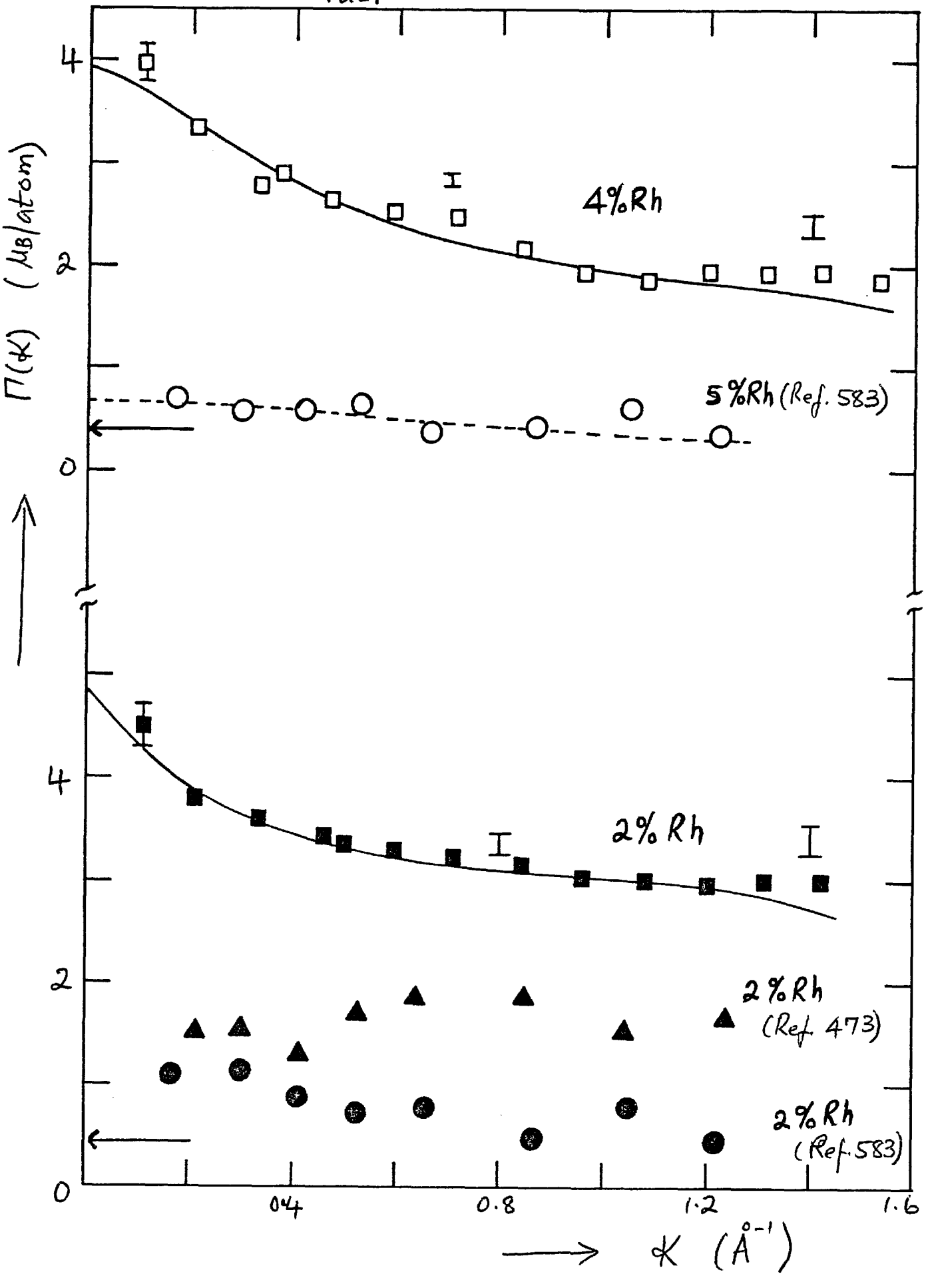

Fig. 6.14: $\frac{d\sigma}{d\Omega}$ vs K for Ni 10, 15 and 20% Rh alloys.

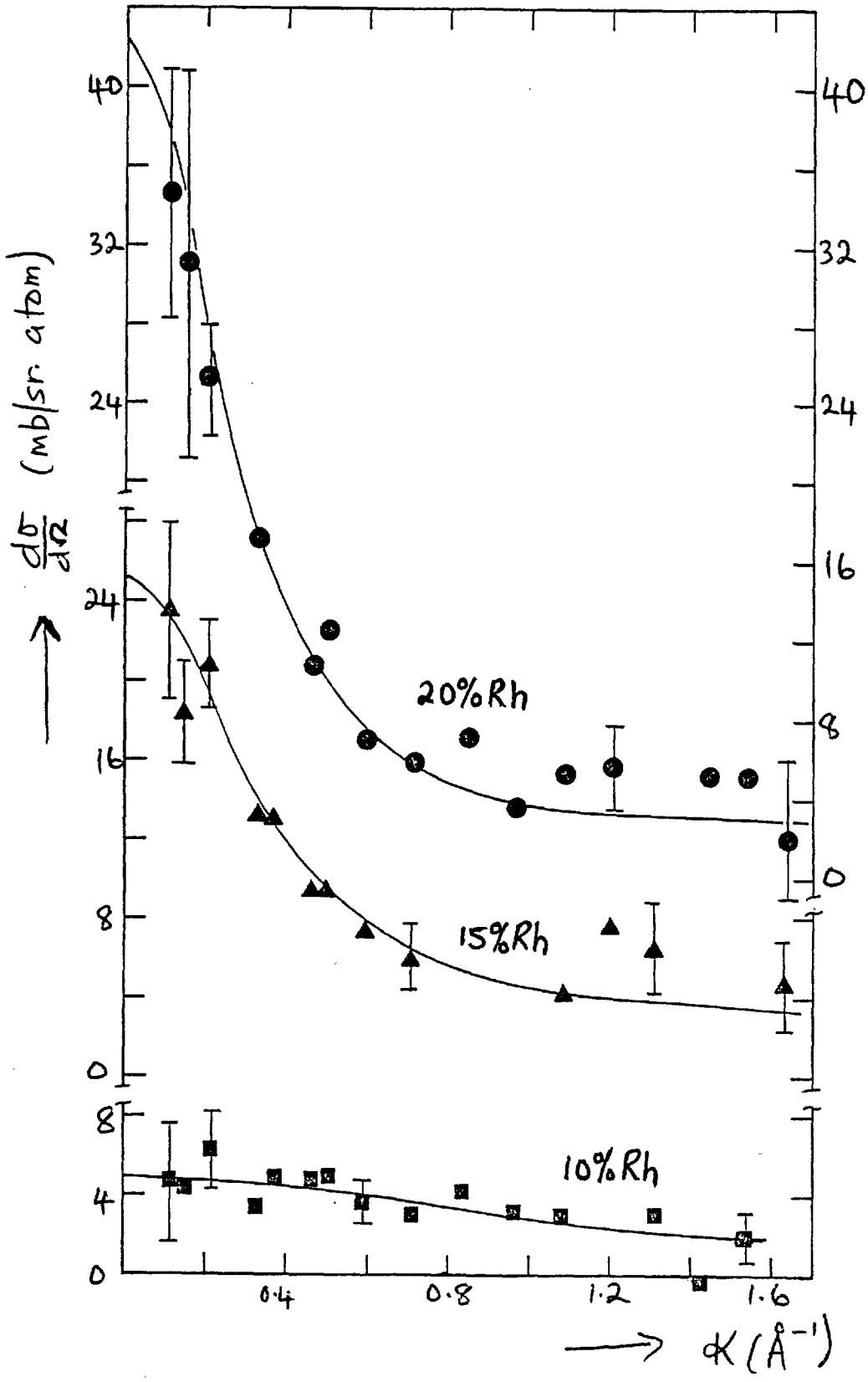

Fig. 6.15: $\frac{d\sigma}{d\Omega}$ vs K for Ni 24, 30 and 36% Rh alloys.

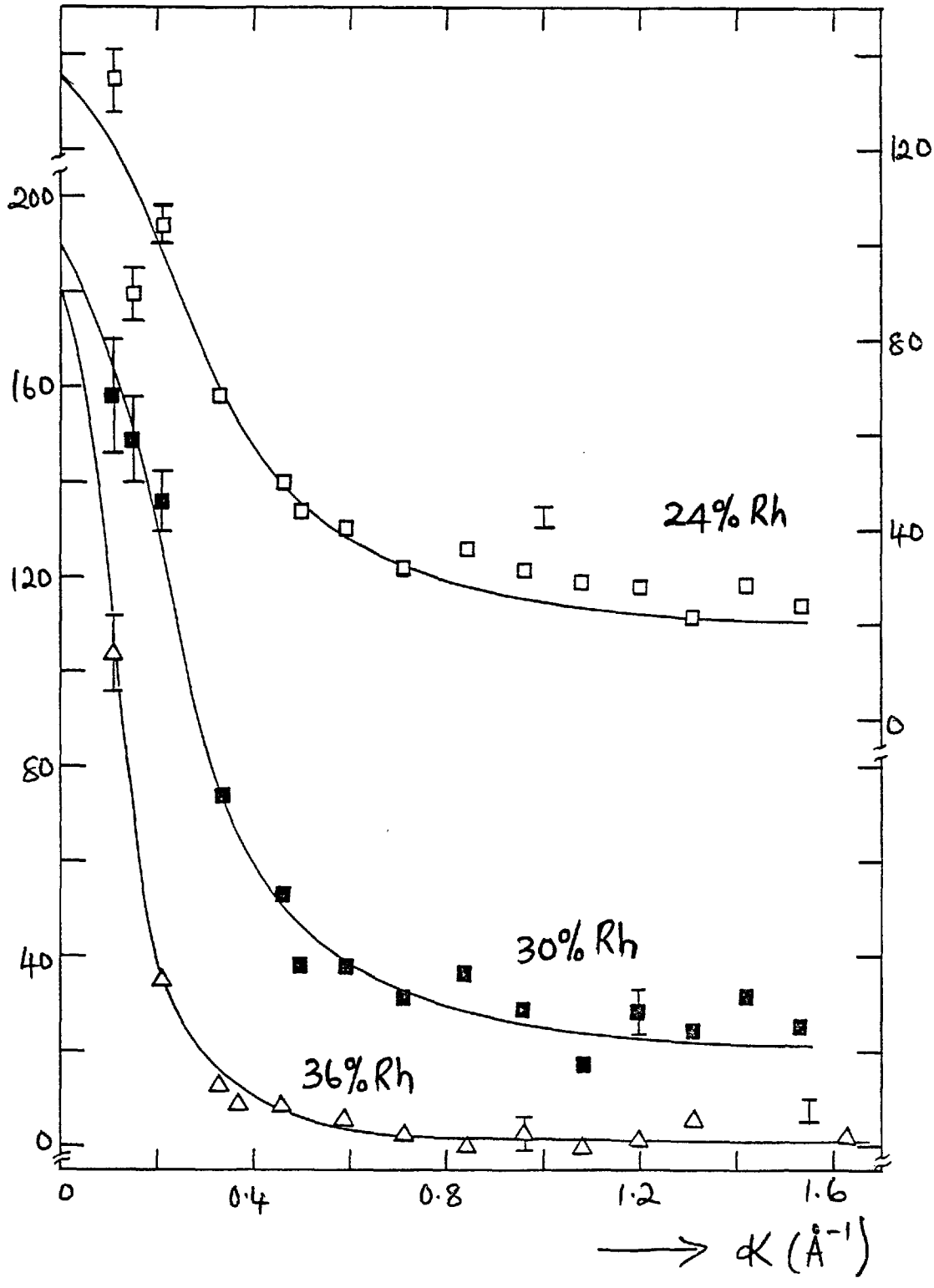

was obtained the alloy was annealed at 1273K for three days and water-quenched. Even after this treatment the measured cross-section was unchanged so that it does not appear that the rather large cross-section at large K is as a result of any metallurgical inhomogeneity of the samples.

With the exception of Ni 10% Rh it is seen from the figures (6.13, 6.15 and 6.16) that the cross-sections exhibit a forward peak which becomes sharper as the critical concentration is approached. However, as discussed below, the large forward cross-sections of the 2 and 4% Rh alloys are surprising because the magnetization measurements (fig.6.1) show that $\frac{d\bar{\mu}}{dc}$ is small for these two alloys.

(b) Analysis of the Neutron Scattering Data

Since (i) both Rh and Ni may carry local moments in this alloy system and

(ii) the bulk magnetization clearly exhibits a non-linear behaviour, the unpolarized neutron diffuse scattering cross-section should be given by

$$\frac{d\sigma}{d\Omega} = 73c(1-c)\Gamma^2(K) + 73c F_{Rh}^2 \langle(\delta\mu_{Rh})^2\rangle + 73(1-c)F_{Ni}^2\langle(\delta\mu_{Ni})^2\rangle + 73c^2(1-c)^2 Y(K) + \cdots \qquad 6.3$$

where, as usual,

$$\Gamma(K) = F_{Rh}\bar{\mu}_{Rh} - F_{Ni}\bar{\mu}_{Ni} + c\bar{F}_{Rh}H(K) + (1-c)F_{Ni}G(K) \qquad 6.4$$

and the last term in eq.(6.3) is a first-order correction term for the non-linear behaviour of the bulk magnetization (see section 3.3(f)).

$$Y(0) = \frac{1}{2Z_0}\left(\frac{d^2\bar{\mu}}{dc^2}\right)^2 \qquad 6.5$$

where Z_0 is the coordination number (which is twelve for

the fcc NiRh system). It is clear from eq.(6.3) that it is difficult to determine ($\bar{\mu}_{Rh} - \bar{\mu}_{Ni}$) accurately from unpolarized neutron scattering measurements. Although Cable (583) has recently reported both polarized and unpolarized neutron cross-sections for NiRh alloys spanning the same concentration range as in our present study no polarized neutron measurements were made for the dilute alloys so that no accurate values of $\bar{\mu}_{Rh}$ and $\bar{\mu}_{Ni}$ for this concentration range exist. Therefore in order to obtain estimates of $\bar{\mu}_{Rh}$ and $\bar{\mu}_{Ni}$ from our data we have, as a first approximation, assumed that only the first term in eq.(6.3) contributes to the observed cross-section. It is plausible to neglect $\langle(\delta\mu_{Ni})^2\rangle$ for the most dilute alloys but $Y(K)$ and probably $\langle(\delta\mu_{Rh})^2\rangle$ are not negligible. Also following Cable (583) we have put

$$c F_{Rh} H(K) + (1-c) F_{Ni} G(K) \equiv \phi(K) \simeq \phi(0)\left\{1 + \frac{K^2}{K_0^2}\right\}^{-1} \qquad 6.6$$

since both $\bar{\mu}_{Rh}$ and $\bar{\mu}_{Ni}$ are concentration-dependent and $H(K)$ and $G(K)$ cannot be independently determined from the limited amount of data available. Thus for 2 and 4% Rh the cross-sections have been fitted to the relation

$$\frac{d\sigma}{d\Omega} \propto 73 c(1-c)\Gamma^2(K) \equiv 73 c(1-c)\left\{F_{Rh}\bar{\mu}_{Rh} - F_{Ni}\bar{\mu}_{Ni} + \phi(K)\right\}^2 \qquad 6.7$$

with $F_{Rh} = e^{-0.1K^2}$ and $F_{Ni} = e^{-0.05K^2}$.

The fits are the solid lines in fig.6.13 which shows the K-dependence of $\Gamma(K)$ for the two dilute alloys. Also shown in this figure is the result of the room temperature measurement on Ni 2% Rh by Comly et al.(473) and the recent data of Cable (583) for 2 and 5% Rh at 10K. By combining the values of $\Gamma(K)$ at sufficiently large K ($\simeq 1.2$ Å^{-1}) with the bulk magnetization data values of $\bar{\mu}_{Rh}$ and $\bar{\mu}_{Ni}$

were estimated. These and the parameters obtained in the fitting are shown in table 6.1.

For 10–30% Rh we have used the values of $\bar{\mu}_{Rh}$ and $\bar{\mu}_{Ni}$ obtained by Cable (583) from polarised neutron data and fitted our unpolarized neutron cross-sections to the equation

$$\frac{d\sigma}{d\Omega} \simeq 73c(1-c)\,F^2(K) + A\,F^2_{av}(K) \qquad 6.8$$

where the second term in eq.(6.8) allows for the contributions to be cross-sections arising from the fluctuations in the Rh and Ni moments and $F_{av}(K)$ is an average form factor. For 10, 15 and 20% Rh where both $\bar{\mu}_{Rh}$ and $\bar{\mu}_{Ni}$ are significant $F_{av} \simeq e^{-0.075K^2}$ while for $c \gtrsim 24\%$ Rh $\bar{\mu}^2_{Rh} \ll \bar{\mu}^2_{Ni}$ so that $AF^2_{av}(K) \simeq \langle(\delta\mu_{Ni})^2\rangle e^{-0.1K^2}$. In fitting the relevant cross-sections to eq.(6.8) the $AF^2_{av}(K)$ term was adjusted to give the best fit to the data at <u>large</u> K. The fits are the solid lines in figs. 6.14 and 6.15 and the resulting parameters are also listed in table 6.1.

The cross-section for the Ni 36% Rh alloy has been analysed on three different models:-

(i) the Marshall model i.e. the same model as used for the 10-30% Rh alloys but with $\bar{\mu}_{Rh} \sim 0 \sim \bar{\mu}_{Ni}$. Thus

$$\frac{d\sigma}{d\Omega} \simeq 73c(1-c)\phi^2(K) + 73(1-c)F^2_{Ni}\langle(\delta\mu_{Ni})^2\rangle \qquad 6.9$$

This fit is the solid line in fig 6.15 and $\phi(0)$ and K_0 are shown in table 6.1.

(ii) the cluster model (see sections 3.4(b), 3.5(iii) and 5.2). According to this model the observed cross-sections for alloys in the critical concentration region can be

Tabel 6.1: Individual Moments and Moment Defect Parameters for NiRh Alloys

c% Rh	$\bar{\mu}$	$\bar{\mu}_{Rh}$*	$\bar{\mu}_{Ni}$*	A (mb/sr·atom)	K_0	$\phi(0)$	$\Gamma(0)$	$\frac{d\bar{\mu}}{dc}$
2	0.639	{ 3.90 { -2.56	0.57 0.70	-	0.16	±1.49	±4.82	0.43
4	0.642	{ 2.56 { -1.28	0.56 0.72	-	0.34	±1.86	±3.86	-0.40
10	0.615	0.5±0.1	0.63	-	1.54	-0.75	-0.88	-0.85
15	0.565	0.38	0.59	3	0.45	-1.33	-1.54	-1.38
20	0.483	0.32	0.50	2.5	0.38	-1.67	-1.85	-1.90
24	0.40	0.25	0.44	22	0.42	-2.72	-2.91	-2.50
30	0.225	0.17	0.28	22	0.38	-3.19	-3.30	-2.90
36	-	~ 0	~ 0	2.3	0.19	-3.24	-3.24	-

* Values for 10-30% Rh taken from Cable (583)

considered to be the "paramagnetic" scattering from an array of weakly coupled magnetic clusters. Hence for 36% Rh

$$\frac{d\sigma}{d\Omega} \simeq 109.5c^*\left\{1+\frac{\kappa^2}{\kappa_1^2}\right\}^{-2}\left\{\frac{2}{3}M_{cl}^2 - \frac{1}{3}M_{cl}\right\} + 73c(1-c)F_{Ni}^2\langle(\delta\mu_{Ni})^2\rangle \qquad 6.10a$$

$$\equiv \left(\Delta\frac{d\sigma}{d\Omega}\right)_{cl} + 73c(1-c)F_{Ni}^2\langle(\delta\mu_{Ni})^2\rangle \qquad 6.10b$$

(cf eq.(5.14)), where κ_1 is the inverse cluster radius and c* is the concentration of the magnetic clusters. The extrapolation procedure for $\left(\frac{d\sigma}{d\Omega}\right)_0$ and κ_1 is clearly the same as for Marshall model above and we obtain

$$\left(\Delta\frac{d\sigma}{d\Omega}\right)_{cl}(\kappa=0) \equiv \left(\Delta\frac{d\sigma}{d\Omega}\right)_{cl}^0 = 177 \text{ mb/sr.atom}$$

$$\kappa_1 = 0.19 \text{ Å}^{-1}.$$

(iii) the critical scattering model (sections 2.5(vi) and 3.4(b) in this case

$$\frac{d\sigma}{d\Omega} \simeq 73c(1-c)\chi(0)\left\{1+\frac{\kappa^2}{\kappa_c^2}\right\}^{-1} + 73c(1-c)F_{Ni}^2\langle(\delta\mu_{Ni})^2\rangle \qquad 6.11$$

(cf eq.(5.19)) where $\chi(0)$ is related to the initial susceptibility and κ_c is an inverse correlation range. This model also fits the data for this alloy giving

$$73c(1-c)\chi(0) = 170 \text{ mb/sr.atom}$$

and

$$\kappa_c = 0.092 \text{ Å}^{-1}.$$

6.6 Discussion of Results

For this purpose the NiRh alloys have been grouped into three categories as follows:-

(i) dilute alloys i.e. the 2 and 4% Rh alloys;

(ii) "intermediate" concentration alloys which include the 10, 15, 20, 24 and 30% Rh alloys;

(iii) nearly critical alloys: only the 36% Rh alloy belongs to this category.

Before proceeding we note a few points of general interest. Firstly, fig.6.16(a) shows the concentration-dependence of $\frac{d\bar{\mu}}{dc}$ for the NiRh system. It is clear from this figure that for $0.04 < c_{Rh} < 0.30$

$$\frac{d\bar{\mu}}{dc} \simeq -10c \qquad 6.12$$

hence $$\bar{\mu}(c) = 0.65 - 5\,c^2 \qquad 6.13$$

Although the above relation for $\bar{\mu}(c)$ leads to a critical concentration of 64% Ni which is in fair agreement with the value (63.1% Ni) obtained in section 6.4 we do not expect that eq.(6.13) will be valid in the critical concentration region. Note that as defined $\bar{\mu}(c)$ is the <u>saturation</u> magnetization whereas in the critical region we are more interested in the spontaneous magnetization (denoted by M_{oo} or μ_{sp}) which, in a mean-field approximation, has been shown to vary as $M_{oo} \propto (c-c_f)^{1/2}$ (cf eq.(2.90)).

For the dilute alloys ($c < 0.04$ Rh) it appears that $\frac{d\bar{\mu}}{dc}$ is again linear in c although its value as $c \longrightarrow 0$ is presently very uncertain (see fig.6.1(b)). If we take the average of the minimum ($\simeq 1\,\mu_B$/atom) and maximum ($\simeq 3.5\,\mu_B$/atom) values of the initial slope of the $\bar{\mu}(c)$ versus c curves in fig.6.1(b) then in the dilute Rh-concentration region

$$\frac{d\bar{\mu}}{dc} \simeq 2.25 - 70\,c \qquad 6.14$$

and thus $\frac{d^2\bar{\mu}}{dc^2} \simeq -70$. Such a large value of $\frac{d^2\bar{\mu}}{dc^2}$ would ensure that the non-linear contribution (see eq.(6.3) and (6.5)) to the unpolarized neutron cross-section is not negligible for the dilute alloys even though the factor $\frac{c^2(1-c)^2}{2z_o}$ is very small. Note, however, that if the true initial value of $\frac{d\bar{\mu}}{dc}$ turns out to be

Fig. 6.16: Concentration dependence of (a) $\frac{d\bar{\mu}}{dc}$ (b) $\bar{\mu}^2_{Ni}$ and $\bar{\mu}_{Rh}$.

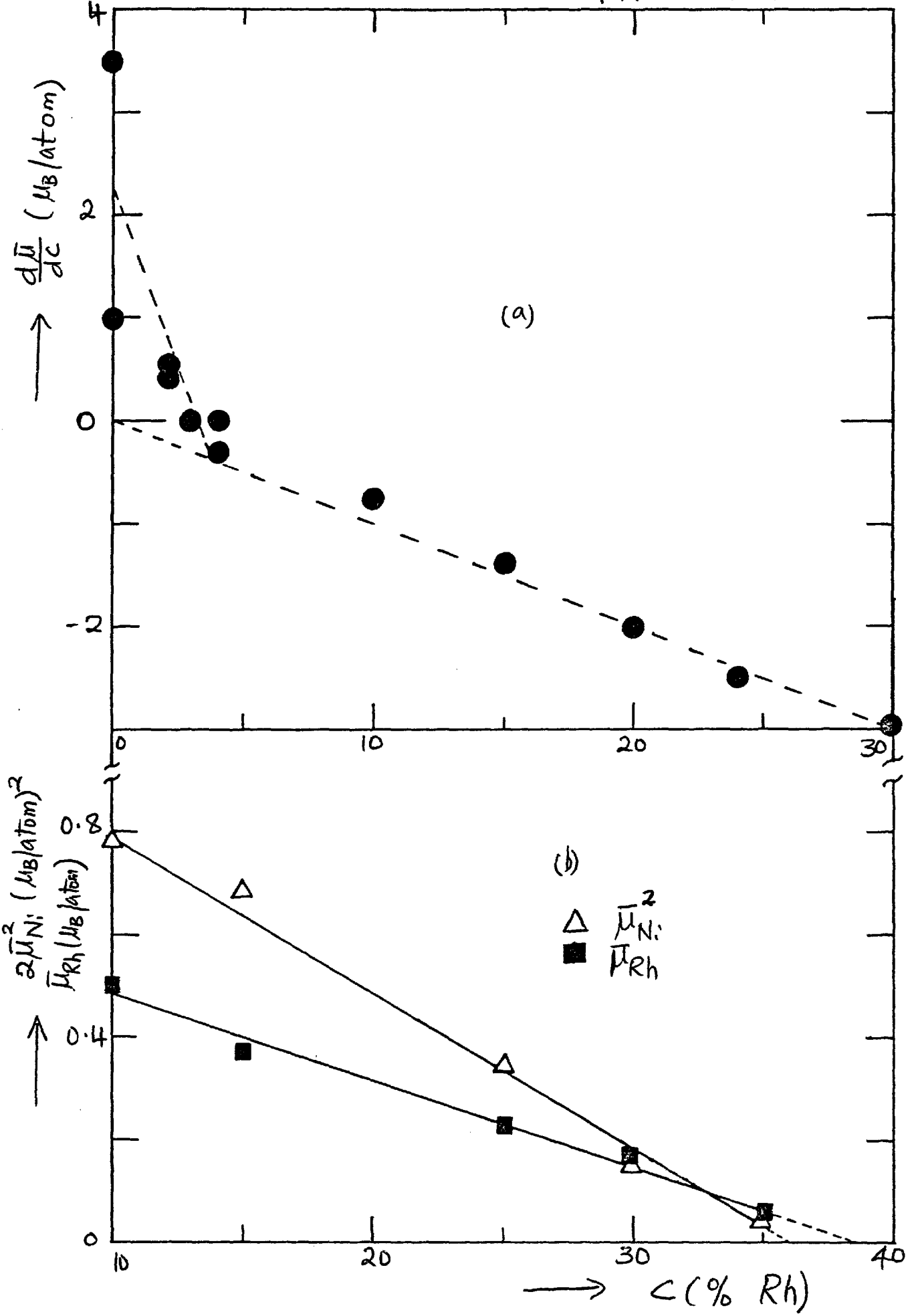

$\sim 1\mu_B$/atom, a value that may be expected from a simple (but incorrect) application of the rigid-band model (according to which the screening of the change in the core charge, $\Delta Z = -1$, at a Rh site by the minority spin-down carrier d-band of Ni should lead to an increase of moment at the solute site of $\sim 1\mu_B$/atom), then $\frac{d^2\bar{\mu}}{dc^2} \sim 30\mu_B/\text{atom}^2$ and hence the non-linear term will become unimportant for the dilute alloys.

Secondly, the values of $\bar{\mu}_{Rh}(c)$ and $\bar{\mu}_{Ni}(c)$ obtained by Cable (583) from an analysis of the polarised neutron cross-sections for concentrations greater than 10% Rh obey simple relations namely:

$$\bar{\mu}^2_{Ni}(c) \simeq 0.56 - 1.56c \qquad 6.15$$

and

$$\bar{\mu}_{Rh}(c) \simeq 0.66 - 1.7c \qquad 6.16$$

as shown in fig 6.16(b). The concentration-dependence of $\bar{\mu}_{Ni}$ is, surprisingly, of the form predicted for the spontaneous magnetization in the critical concentration region whereas $\bar{\mu}_{Rh}(c)$ is linear in c. Both $\bar{\mu}_{Ni}$ and $\bar{\mu}_{Rh}$ apparently "vanish" near the critical concentration - at 64.1 (cf eq.(6.13)) and 61.4% Ni respectively - although it must be remembered that the polarized neutron measurements were carried out in a magnetic field of 20 K Oe. We have used eq.(6.15) and (6.16) to obtain $\bar{\mu}_{Ni}$ and $\bar{\mu}_{Rh}$ for 20 and 24% Rh (values are those shown in table 6.1). What is of greater interest in fig.6.16(b) is whether we can justifiably extrapolate to zero Rh-concentration to obtain $\bar{\mu}_{Ni}$ and $\bar{\mu}_{Rh}$ in this limit. For Ni we obtain $\bar{\mu}_{Ni}(0) \simeq 0.75\,\mu_B$ which is sufficiently close to the value in pure Ni ($\simeq 0.71\,\mu_B$) to justify the extrapolation.

There is, of course, no a priori reason why $\bar{\mu}_{Ni}(c)$ may not have a maximum between 0 and $\sim$ 5% Rh (we show later that for Ni 5% Rh the values of $\bar{\mu}_{Ni}$ (and $\bar{\mu}_{Rh}$) obtained from eq.(6.15) and (6.16) give a reasonable fit to Cable's unpolarized neutron data for this alloy) so that any deductions from eq.(6.15) for $c < 5\%$ Rh should be treated with caution. Bearing this in mind, then from eq. (6.15)

$$\frac{d\bar{\mu}_{Ni}}{dc} \simeq -0.624\{0.36 - c\}^{-1/2} \qquad 6.17$$

so that for small c $\frac{d\bar{\mu}_{Ni}}{dc} \simeq -1\,\mu_B/\text{atom}$.

For Rh eq.(6.14) leads to $\bar{\mu}_{Rh}(0) = 0.66\mu_B$ a value which is much smaller than those suggested by both the saturation magnetization and unpolarized neutron scattering data. However, Stearns (585) has obtained a value of $0.8\,\mu_B$ for $\bar{\mu}_{Rh}(0)$ from an analysis of some hyperfine field data for NiRh. We do not think that in this case the extrapolation to $\bar{\mu}_{Rh}(0)$ is justified particularly in view of the marked non-linear behaviour of the bulk magnetization and the change in the concentration-dependence of $\frac{d\bar{\mu}}{dc}$ in the dilute region, effects that must surely be associated with $\bar{\mu}_{Rh}(c)$. This point will be further discussed shortly below.

(i) Dilute NiRh Alloys

An immediate observation about the cross-sections for 2 and 4% Rh shown in fig.6.13 is that these cross-sections (measured at 4.2K) are much larger than those obtained by Cable (583) for 2 and 5% Rh (at T=10K) and by Comly et al. (473) for 2% Rh (at room temperature). There is no agreement between the three sets of data for 2% Rh particularly at large k.

In analysing his unpolarized neutron data for 2 and

5% Rh Cable assumed that the cross-sections were almost α -independent so that $\phi(\alpha) \simeq 0$ and therefore determined $\{\bar{\mu}_{Rh} - \bar{\mu}_{Ni}\}$ as some undefined "weighted average" of the cross-sections. These cross-sections are shown in fig.6.13 and it is clear that for 5% Rh the cross-section is almost flat while, in spite of the large statistical errors associated with the 2% Rh data, we feel that these exhibit a definite α -dependence (note that $\Gamma(\alpha)$ doubles its value within the range of α -values investigated). Also for 5% Rh $\Gamma(0)$ has a value that is nearly equal to $\frac{d\bar{\mu}}{dc}$ for this alloy ($\simeq$ -0.5 μ_B /atom) whereas for 2% Rh $\Gamma(0)$ is much larger than $\frac{d\bar{\mu}}{dc}$ (=0.43 μ_B /atom).

[N.B. The quoted values do not apparently greatly depend on the rather uncertain value of the initial $\frac{d\bar{\mu}}{dc}$].

Consequently, we do not agree that the cross-sections for these two alloys should have been analysed in the same way. The behaviour of the 5% Rh alloy closely resembles that of our 10% Rh sample - a flat cross-section with $\Gamma(0)$ approximately equal to $\frac{d\bar{\mu}}{dc}$. A similar analysis is therefore appropriate. From eq.(6.15) and (6.16), which appear to be valid down to this concentration, we obtain that for 5% Rh $\bar{\mu}_{Rh} = 0.58\mu_B$ and $\bar{\mu}_{Ni} = 0.69\mu_B$. Using these values we have fitted Cable's data to eq.(6.7) to get $\phi(0) = -0.57\mu_B/\text{atom}$, $\alpha_0 = 0.85\ \text{Å}^{-1}$ and $\Gamma(0) = -0.68\mu_B/\text{atom}$. The fit is shown as the dotted line in fig.6.13. The forward cross-section is close to that expected from the magnitude of $\frac{d\bar{\mu}}{dc}$ for this alloy and from the non-linear contribution. Both contribution are of the same order of magnitude (0.87 and 0.59 mb/sr.atom respectively) so that although the non-linear contribution is

small it is certainly not negligible. Thus Cable's unpolarized neutron data for 5% Rh are consistent with the polarized neutron data for alloys of higher Rh-concentrations and therefore his values of $\bar{\mu}_{Rh}$ and $\bar{\mu}_{Ni}$ quoted for this alloy are incorrect.

We shall also argue that Cable's values of $\bar{\mu}_{Rh}$ and $\bar{\mu}_{Ni}$ for 2% Rh are inaccurate because the observed cross-sections are smaller than would be expected. The observed cross-sections (now expressed as the maximum switchable) are $\sim$1.7 mb/sr.atom in the forward direction and $\sim$ 0.36 mb/sr.atom at large α . However, from eq.(6.14) the non-linear contribution to the forward cross-section alone could be as large as $\sim$ 5.7 mb/sr.atom. Also since there is little doubt that $\bar{\mu}_{Rh}$ is greatly affected by local environment effects there should be some contribution to the cross-section from $\langle(\delta\mu_{Rh})^2\rangle$. If $\bar{\mu}_{Rh}$ is governed by the probability that a Rh atom has twelve Ni nearest-neighbours, then it may be easily seen that $\langle(\delta\mu_{Rh})^2\rangle \simeq 0.21\,\bar{\mu}^2_{Rh}$, leading to a "background" of $\sim$ 0.76 mb/sr.atom. A contribution of a similar magnitude is also expected at large α from $(F_{Rh}\bar{\mu}_{Rh} - F_{Ni}\bar{\mu}_{Ni})$. Finally Cable did not explain why the forward cross-section for this alloy is not consistent with corresponding $\frac{d\bar{\mu}}{dc}$; since $\frac{d\bar{\mu}}{dc} < (\bar{\mu}_{Rh} - \bar{\mu}_{Ni})$ it follows that $\phi(\alpha) < 0$ so that $\frac{d\sigma}{d\Omega}$ should show a pronounced dip in the forward direction. None of the available data for 2% Rh shows this dip.

On the other hand, there is at the moment no reason to believe that our data for 2 and 4% Rh are not sufficiently accurate in spite of the surprisingly large cross-sections observed. The resulting values of $\bar{\mu}_{Rh}$ are reasonable

(even though the cross-sections at large κ have not been corrected for any contribution due to $\langle(\delta\mu_{Rh})^2\rangle$ because strictly

$$\bar{\mu}(c) = c\bar{\mu}_{Rh} + (1-c)\bar{\mu}_{Ni} + \mu_{cond} \qquad 6.18$$

where μ_{cond} is the uniform negative magnetization associated with either the conduction electron polarization or, according to Moon (467), with the overlap of the 3d-wavefunctions (see section 3.5(iv)). From eq.(6.18)

$$\frac{d\bar{\mu}}{dc} = \bar{\mu}_{Rh} - \bar{\mu}_{Ni} + c\frac{d\bar{\mu}_{Rh}}{dc} + (1-c)\frac{d\bar{\mu}_{Ni}}{dc} + \frac{d\mu_{cond}}{dc} \qquad 6.19$$

whence $$\lim_{c\to 0}\frac{d\bar{\mu}}{dc} = \bar{\mu}_{Rh} - \bar{\mu}_{Ni} + \frac{d\bar{\mu}_{Ni}}{dc} + \frac{d\mu_{cond}}{dc}\,.$$

In the absence of any information about $\frac{d\mu_{cond}}{dc}$ we may neglect this quantity; also for very small c $\bar{\mu}_{Ni} \simeq 0.71\,\mu_B$, $\frac{d\bar{\mu}}{dc} \sim 2.25\,\mu_B/\text{atom}$ and if we assume that eq.(6.15) is valid in this concentration limit then $\frac{d\bar{\mu}_{Ni}}{dc} \simeq -1\,\mu_B/\text{atom}$ (eq.(6.17)) and so $\bar{\mu}_{Rh}(0) \simeq 3.96\,\mu_B$ in good agreement with the value of $3.90\,\mu_B$ obtained for Ni 2% Rh (see table 6.1). Alternatively, the large value of $\bar{\mu}_{Rh}(0)$ determined from our neutron data may be regarded as providing some further justification for the validity of eq.(6.17). The rather smaller values of $\bar{\mu}_{Ni}$ (relative to $\bar{\mu}_{Ni}(0)$) are probably due to the neglect of μ_{cond}. It should be more correct to combine the neutron data with

$$\bar{\mu}_{local} \equiv \bar{\mu}(c) - \mu_{cond} = c\bar{\mu}_{Rh} + (1-c)\bar{\mu}_{Ni} \qquad 6.20$$

in order to determine the true values of $\bar{\mu}_{Rh}$ and $\bar{\mu}_{Ni}$. Since this correction was not made the tabulated values of $\bar{\mu}_{Rh}$ and $\bar{\mu}_{Ni}$ must be regarded as the <u>total</u> moment per site (439) i.e. the true local moment plus the conduction

electron polarization. Although we have argued above that the large cross-sections observed at high scattering angles for these dilute alloys are reasonable there is still the problem of explaining why the forward cross-sections do not agree with the magnetization values of $\frac{d\bar{\mu}}{dc}$. From the values of the latter it is expected that $\left(\frac{d\sigma}{d\Omega}\right)_0 \sim 0$. Part of the observed forward cross-sections of these alloys is certainly due to the non-linear contribution but even the most optimistic estimates of this contribution (taking into account the uncertainty in the initial value of $\frac{d\bar{\mu}}{dc}$) cannot account for the forward cross-sections. However, we will recall that Comly et al. (473) observed that both dilute transition metal and non-transition metal solutes in Ni gave essentially similar widespread magnetic disturbances irrespective of both the core charge difference and any solute moment. For example, although Ru has a local moment (of $\sim 0.8 \mu_B$) in a Ni matrix and has been reported (591,592) to suffer the same type of severe local environment effects as recently proposed by Cable (583) for Rh the magnetic disturbance in Ni has the same shape as for other solute atoms and the forward cross-section is larger than the value given by $\frac{d\bar{\mu}}{dc}$. It was therefore concluded that the observed behaviour was more characteristic of the host-matrix than of the solute. However, we shall not attempt a similar analysis of our neutron data for the dilute NiRh alloys until we have a clearer idea of what unpolarized neutron scattering from strongly ferromagnetic hosts containing a dilute concentration of solute atoms really measures.

Finally, the smaller Rh moment ($\simeq 2.6 \mu_B$) obtained from the room-temperature data of Comly et al. (473) for

the same 2% Rh sample would suggest that $\bar{\mu}_{Rh}$ is temperature-dependent as is the case for $\bar{\mu}_{Mn}$ in FeMn (588, 589). However, Cable's data for an alloy of the same composition would appear to rule out such a supposition although it must be noted that his large angle data (see fig.6.13) give a value of $\bar{\mu}_{Rh}$ which is $\sim$ 50% smaller than that deduced from Comly et al's data and $\sim$ 67% smaller than our value.

In conclusion our unpolarized neutron scattering measurements for dilute NiRh alloys show that $\bar{\mu}_{Rh}$ is large but decreases rapidly with increasing Rh concentration and that the forward cross-sections are much larger than are consistent with $\frac{d\bar{\mu}}{dc}$.

(ii) Intermediate Concentrations; Ni 10-30% Rh

There is agreement between the observed forward cross-sections and the magnetization values of $\frac{d\bar{\mu}}{dc}$ for these alloys although it is a little less satisfactory for 24 and 30% Rh. The parameter κ_0 which characterizes the range of the moment disturbance decreases (from its maximum value at 10% Rh) up to 20% Rh and then remains fairly constant up to 30% Rh. For the 10-20% Rh alloys both $\langle(\delta\mu_{Ni})^2\rangle$ and $\langle(\delta\mu_{Rh})^2\rangle$ appear to be small (as shown by the small "background" correction) and consequently the discussion already given by Cable (583) in terms of a magnetic-environment model is adequate.

For 24 and 30% Rh the discrepancy between $\Gamma(0)$ and $\frac{d\bar{\mu}}{dc}$ is partly due to the increasing importance of the non-linear term and partly to the fact that the critical concentration region is being rapidly approached. Large fluctuations of the Ni moment occur (giving rise to a large cross-section at large κ) and it is therefore not

surprising that Cable's theory, which is valid for small Ni moment fluctuations, breaks down for concentrations greater than $\sim$ 25% Rh. It should be expected that as the Rh concentration increases and local environment effects become more severe only those Ni atoms which have a critical number of Ni nearest-neighbours may remain magnetic. In other words, it is useful to begin to think of these high Rh-concentration alloys in terms of an assembly of coupled magnetic clusters. The critical number of Ni nearest-neighbours increases as the critical composition is approached and in this limit only clusters of thirteen or more Ni atoms are known to be magnetic (457) although we have suggested above (section 6.3) that Rh atoms surrounded by twelve Ni nearest-neighbours are also magnetic. A moot question is then whether such magnetic clusters play an <u>explicit</u> role in the observed neutron scattering. To test this supposition we have fitted the neutron cross-sections for 24 and 30% Rh to the cluster model, i.e.

$$\frac{d\sigma}{d\Omega} = \left(\Delta \frac{d\sigma}{d\Omega}\right)_{cl} + 773c(1-c)\left\{F_{Rh}\bar{\mu}_{Rh} - F_{Ni}\bar{\mu}_{Ni}\right\}^2 + 773(1-c)F_{Ni}^2\langle(\delta\mu_{Ni})^2\rangle \qquad 6.21$$

(cf eq.(5.14 and (6.10)). The fits are as good as obtained with the Marshall model as may be seen in fig.6.17 in which $\left(\Delta \frac{d\sigma}{d\Omega}\right)_{cl}^{-\frac{1}{2}}$ is plotted against K^2. The following parameters are obtained:

	c^*(%)	M_{cl} (μ_B)	K_1 (Å^{-1})
Ni 24% Rh	10.6	3.8	0.47
Ni 30% Rh	2.4	9.3	0.42

Although c^* and M_{cl} vary in the expected way a great deal of

Fig. 6.17: Plot of $\left(\Delta \frac{d\sigma}{d\Omega}\right)^{-1/2}_{cl}$ vs K^2 for Ni 24, 30% Rh.

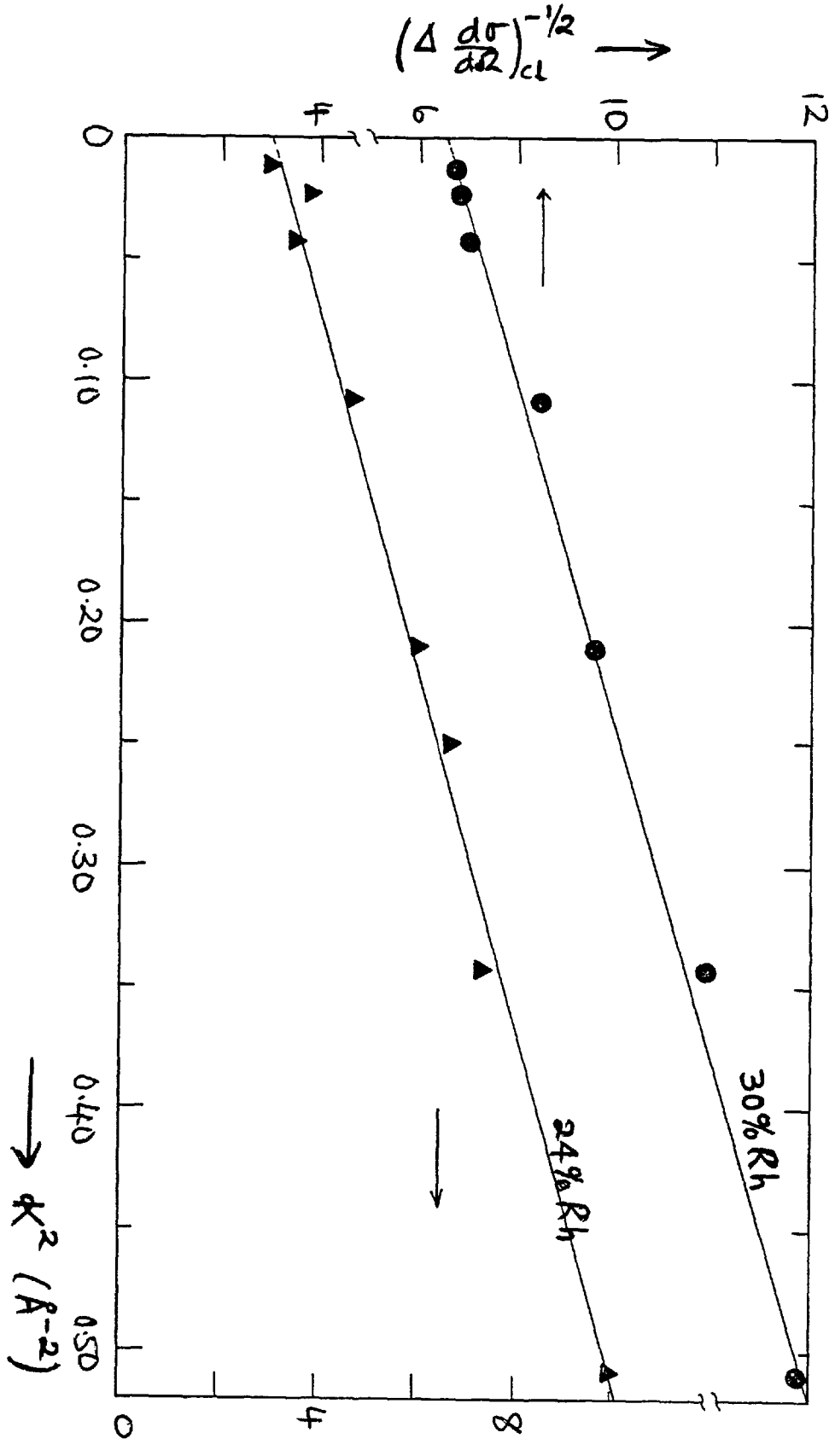

significance should not be attached to this fitting because as long as $\bar{\mu}_{Rh}$ and $\bar{\mu}_{Ni}$ are small (as at these alloy concentrations) eq(6.8) and (6.20) are very similar in form.

An important problem is again the concentration-dependence of $\bar{\mu}_{Rh}$. We have seen above that for small Rh concentrations $\bar{\mu}_{Rh}$ is large and rapidly decreases with increasing Rh-concentration. However, for c $\gtrsim$ 10% Rh $\bar{\mu}_{Rh}$ is small and varies linearly with c (eq.(6.16)). Since these latter values were determined by polarized neutron scattering measurements it may be assumed that they are more precise and accurate than the values obtained from unpolarized neutron data. It has been previously mentioned that eq.(6.16) extrapolates to a value of $\bar{\mu}_{Rh}(0)$ (=0.66 μ_B) which is rather small compared with values of $\gtrsim$2.6 μ_B suggested by the magnetization and unpolarized neutron scattering data.

It is possible that the rapid decrease of $\bar{\mu}_{Rh}$ for c $\lesssim$ 4% Rh may be governed by the probability that a Rh atom has twelve Ni nearest-neighbours, as suggested by Cable (583). For higher Rh concentrations the decrease of $\bar{\mu}_{Rh}(c)$ is linear and less rapid than the suggested probability function. According to Low and Collins (445) for solute concentrations greater than about 10% the environment of all atoms, both solvent and solute, departs very little from the average environment appropriate to the constituent concerned. Thus for c $\gtrsim$ 10% Rh the P_{12}-dependence for $\bar{\mu}_{Rh}(c)$ should not be expected to be valid. Now within the framework of the magnetic environment model the magnitude of the <u>observed</u> moment on an atom at a given site is partly determined by the effective molecular

field acting on that site. Thus the concentration-dependence of $\bar{\mu}_{Rh}$ may be taken to reflect that of the average effective field on a Rh atom. Following the procedure adopted by Dubinin et al.(594) for FeNi alloys the effective field acting on a Rh atom a Ni c% Rh alloy is given by

$$B_{eff}(Rh) = \frac{2z_0}{g^2\mu_B^2}\left\{(1-c)\bar{M}_{Ni}J_{Ni-Rh} + c\bar{M}_{Rh}J_{Rh-Rh}\right\} \qquad 6.22$$

where z_0 is the coordination number of the lattice and $\bar{M}_{Ni}$ and $\bar{M}_{Rh}$ are respectively the average magnetic moments created by Ni and Rh atoms. The fact that a Rh atom which has a Rh nearest-neighbour has a very small moment can be interpreted to mean that J_{Rh-Rh} is large and negative. It therefore follows that $B_{eff}(Rh)$ will rapidly decrease as the Rh concentration increases and possibly for $c \gtrsim 10\%$ Rh it will be dominated by the term involving J_{Rh-Rh}. Such an assumption can explain the small values of $\bar{\mu}_{Rh}$ observed for $c \gtrsim 10\%$ Rh and their linear dependence on the Rh concentration. Contrary to Cable's assertion (583) we do not think that existing neutron scattering data can justifiably rule out the existence of antiferromagnetic interactions between Rh atoms for an obvious reason - $J_{rh-Rh} < 0$ does not imply that the Rh moments are necessarily antiferromagnetically aligned (cf FeRh, FeNi and NiMn in which J_{Rh-Rh} J_{Fe-Fe} and J_{Mn-Mn} respectively are negative) especially as the alloys have a fcc structure and are completely disordered. We shall, however, suggest that because $J_{Rh-Rh} < 0$ there could be a tendency towards the formation of a magnetic superlattice (based on either Ni_3Rh or Rh_3Ni) in very small volume elements in an otherwise completely disordered lattice. We had implicitly made such a suggestion earlier on by remarking that the observed concentration-dependence of the Curie temperature (i.e.

$T_c^2 \propto c$, see fig.6.10) of NiRh alloys for c $\lesssim$ 24% Rh (in which concentration range magnetic clusters are not important) is typical of alloy systems (fcc CoRh, Ni_3Al, FeNi in invar region) in which structural changes are known to occur.

The "background" correction term, $A\langle(\delta\mu)^2\rangle$, is particularly large for 24 and 30% Rh and small for other alloy concentrations. For c $\gtrsim$ 15% Rh we may associate this term mainly with fluctuations in the Ni moments and thus obtain the concentration-dependence of the root-mean-square fluctuation of the Ni moments. Fig.6.18 shows that this rms value has its maximum value of $\sim\bar{\mu}_{Ni}(0)$ near 27%Rh. A similar behaviour was observed for CuNi (436).

(iii) Nearly Critical Alloys

Unfortunately only one alloy - Ni 36%Rh - was studied in this concentration range. We have shown that both the cluster and critical scattering models give equally good fits to the observed data (vide section 6.5). In the cluster model $\left(\Delta\frac{d\sigma}{d\Omega}\right)^0_{cl}$ = 177 mb/sr.atom and $\kappa_1 = 0.19\,\text{Å}^{-1}$. For this alloy $\bar{\mu}_{sat}$ = 0.122 μ_B/atom (457) so that c* = 0.61% and $M_{cl} \approx 20\,\mu_B$ which values are in good agreement with the corresponding magnetization values (457). The lattice parameter for this alloy is 3.648Å (fig.6.3) so that the average distance between the clusters is nearly 11Å. Since κ_1 = 0.19Å^{-1} it follows that each cluster has a diameter of the order of 10.6Å showing that neighbouring magnetic clusters are just about to overlap. In the critical scattering model $\left(\frac{d\sigma}{d\Omega}\right)_0$ = 170 mb/sr.atom and κ_c = 0.092Å^{-1}. This forward cross-section appears reasonable since the alloy concentration is above that for

Fig. 6.18: Concentration dependence of $\langle (\delta\mu_{Ni})^2 \rangle$ and $\bar{\mu}_{Ni}$ (c).

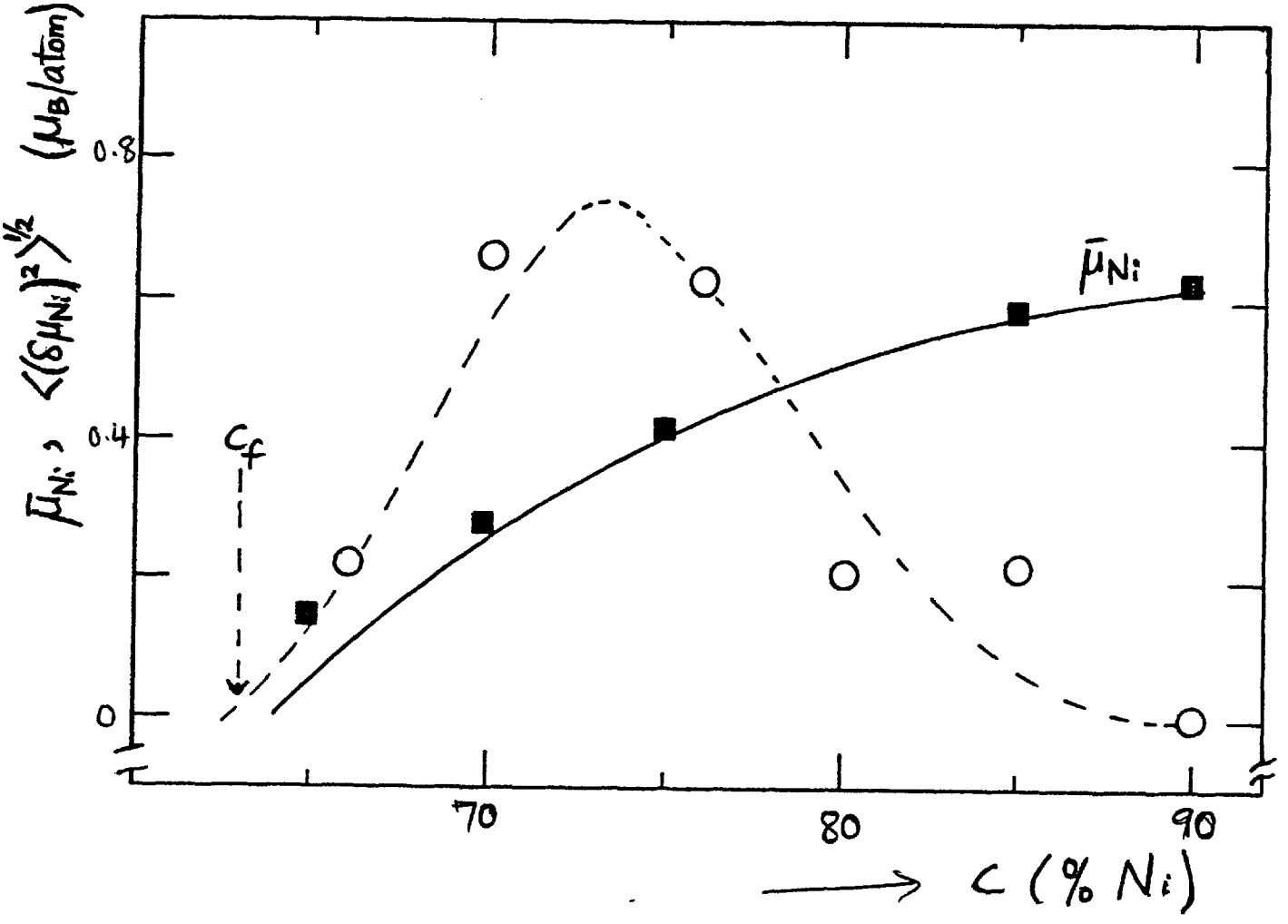

criticality ($\triangleq$ 63% Ni) whilst the correlation length (κ_c^{-1}) is, like the cluster diameter, just slightly less than the average cluster separation. A much larger forward cross-section and correlation length should be observed for Ni 37% Rh which is much closer to criticality. There is nothing to choose between the cluster and critical scattering models for the 36% Rh alloy. Both models are physically satisfactory and give reasonable values of the appropriate model parameters. In our view the two models are not necessarily mutually exclusive but it may be expected that critical scattering will dominate at very small scattering angles ($\kappa \leq 0.1 \text{Å}^{-1}$). If the critical scattering is suppressed by applying a sufficiently large magnetic field the resulting cross-section should be given by the cluster model.

6.7 Conclusions

Magnetization and neutron scattering studies of the NiRh system enable us to draw the following conclusions:-

(1) For small additions of Rh the response of the system appears to be similar to that reported for other transition and non-transition metal solutes in Ni. This similarity strongly suggests that the response may be largely determined by the Ni matrix but a further study is required to confirm this.

(2) In this concentration limit (i.e. $\lesssim$ 4% Rh) the Rh atom has a large moment ($\gtrsim 3\ \mu_B$) which is rapidly "destroyed" as the Rh-concentration is increased. Unfortunately the existing unpolarized neutron data (including this work) do not agree with one another and cannot be used to determine μ_{Rh} accurately. Consequently, there is no confirmation of the plausible suggestion made by Cable (583)

that the concentration-dependence of $\bar{\mu}_{Rh}$ is essentially determined by the probability that a Rh atom has twelve Ni nearest-neighbours. For higher Rh concentrations ($\gtrsim$ 10% Rh) $\bar{\mu}_{Rh}$ decreases rather more slowly and linearly with c. Extrapolating this linear dependence to the single impurity limit leads to a smaller Rh moment ($\simeq 0.66\mu_B$) than $\sim 3\mu_B$ suggested by the initial value of $\frac{d\bar{\mu}}{dc}$ and unpolarized neutron scattering data. It has therefore been suggested that the exchange interaction between Rh atoms is negative and large thus ensuring that the effective molecular field at a Rh site becomes small at relatively low Rh concentrations.

(3) The local Ni moment, $\bar{\mu}_{Ni}(c)$, also exhibits a simple concentration-dependence which extrapolates to $\bar{\mu}_{Ni}(0) \simeq 0.75\mu_B$. This value is sufficiently close to the value in pure Ni to justify the extrapolation. Thus $\bar{\mu}_{Ni}(c)$ appears to decrease steadily from its value in a pure Ni matrix to zero near c_f. We do not see any evidence to justify Cable's contention that $\bar{\mu}_{Ni}(c)$ slightly increases initially attaining a maximum near 10% Rh. It is clear that the tabulated values of $\bar{\mu}_{Ni}(c)$ obtained by Cable are always less than the value of $\bar{\mu}_{Ni}$ in pure Ni and this is mainly because these values represent the total moment per site since no correction was made for the negative uniform magnetization. By analogy with the CuNi system (446) the uniform magnetization should be proportional to the bulk magnetization so that any correction for its effect will be more important for the dilute alloys.

(4) For $10 \leq c \leq 20$%Rh the forward neutron scattering cross-sections are in good agreement with the

bulk magnetization values of $\frac{d\bar{\mu}}{dc}$; hence the discussion (583) of the properties of these alloys within the framework of the magnetic-environment model is adequate.

(5) For c $\geq$ 24% Rh the forward cross-sections in our unpolarized neutron data are significantly larger than expected from the corresponding values of $\frac{d\bar{\mu}}{dc}$. This discrepancy is partly due to the increasing importance of the non-linear terms in the cross-section and partly to the fact that it may become necessary to consider the explicit role of magnetic clusters in the neutron scattering. After all these magnetic clusters are the ultimate consequence of local magnetic-environment effects. It is also significant that in this concentration region (24-30% Rh) $\langle(\delta\mu_{Ni})^2\rangle$ attains its maximum value, decreasing rapidly for other concentrations.

(6) The critical concentration for the disappearance of ferromagnetism is $\simeq$ 63% Ni but the exact location of the peak in $\gamma(c)$ is slightly ambiguous. Further measurements are necessary in order to check the above value of the critical concentration.

(7) For Ni 36% Rh which is in the critical concentration region both the critical scattering and cluster models give equally good fits to the unpolarized neutron data with reasonable parameters. It is likely that the two models are complimentary with critical scattering being more important (and hence dominant) for small scattering angles.

We have already argued that polarized neutron measurements are not suitable for studying the phenomenology of the onset of ferromagnetism (see chapter 3) and as such there should be a significant difference between polarized and

unpolarized neutron cross-sections in this region. Any polarized neutron data for alloys in this critical region should be interpreted in terms of scattering from magnetic clusters (464).

(8) The existence of magnetic clusters has, of course, been unequivocally demonstrated by the magnetization measurements of Muellner and Kouvel (457). We have suggested that near c_f these clusters consist of those Rh and Ni atoms which have 12 Ni nearest-neighbours. The Ni-centred clusters are probably stable up to a temperature corresponding to the Curie temperature of pure Ni (cf CuNi) while the Rh-centred clusters break up at $\sim$ 230K. Thus $J_{Rh-Ni} \simeq 0.37\ J_{Ni-Ni}$.

(9) Finally we have suggested that invar characteristics are intrisincally associated with a concentration-dependent magnetic phase transition which in this case is the onset of ferromagnetism. We believe that there is evidence (249) to confirm such invar behaviour in NiRh but more detailed experiments on this aspect of the behaviour of this alloy system are required.

Overall the NiRh system appears to be a challenging (and therefore interesting) system to study. A lot has been learnt about its gross behaviour but further careful work is needed particularly for dilute solute concentrations ($c \lesssim 5\%$ Rh) for a fuller understanding of its detailed magnetic behaviour.

CHAPTER 7

THE INVAR PROBLEM

7.1 Introduction

Invar was originally the name given to a Fe 35% Ni alloy by Guillaume (595) who found that it had a very small thermal expansivity at room temperature, i.e. its length was invariant to temperature. Since this discovery a number of other alloys with equally small (or even smaller) expansivities has been found including super Invar ($Fe_{64}Ni_{32}Co_4$), stainless Invar ($Fe_{37}Co_{52}Cr_{11}$), Fe-Pt Invar (Fe 25% Pt), Fe-Pd Invar (Fe 31% PD), etc. However, a low thermal expansivity can also be obtained over a small temperature range near the Neel temperature of an antiferromagnet since this ordering is usually accompanied by a volume expansion. Therefore, in order to exclude the latter group of alloys, Invar is now taken as the "generic" name for these alloys which have a large spontaneous volume magnetostriction at 0 K.

In addition to a low thermal expansivity, Invar materials also exhibit some apparently unusual magnetovolume effects, namely, a large forced volume magnetostriction and a large pressure dependence of both the spontaneous magnetization and the Curie temperature. These effects follow directly or indirectly from the existence of a large positive spontaneous volume magnetostriction at 0 K so that an explanation of the cause of the latter is essential to the understanding of the Invar problem.

In section 2.5 we considered the effects associated with the onset of ferromagnetism in some transition metal alloys, specifically the "giant-moment" alloys and it was

suggested that such alloys in the critical concentration region should exhibit some of the above Invar characteristics; indeed such behaviour has been reported for Ni_3Al and PtNi alloys (246, 256, 596). Some existing measurements for RhNi (249) also indicate similar behaviour. What, perhaps, makes the binary Fe Invars peculiar is the fact that the Invar characteristics occur in a relatively narrow concentration region close to the boundary between the α- and γ -phases in these alloys. This is illustrated in fig.7.1 which also shows the variation of the spontaneous magnetization, M_{oo}, Curie temperature, T_c, and the room temperature thermal expansivity, β.

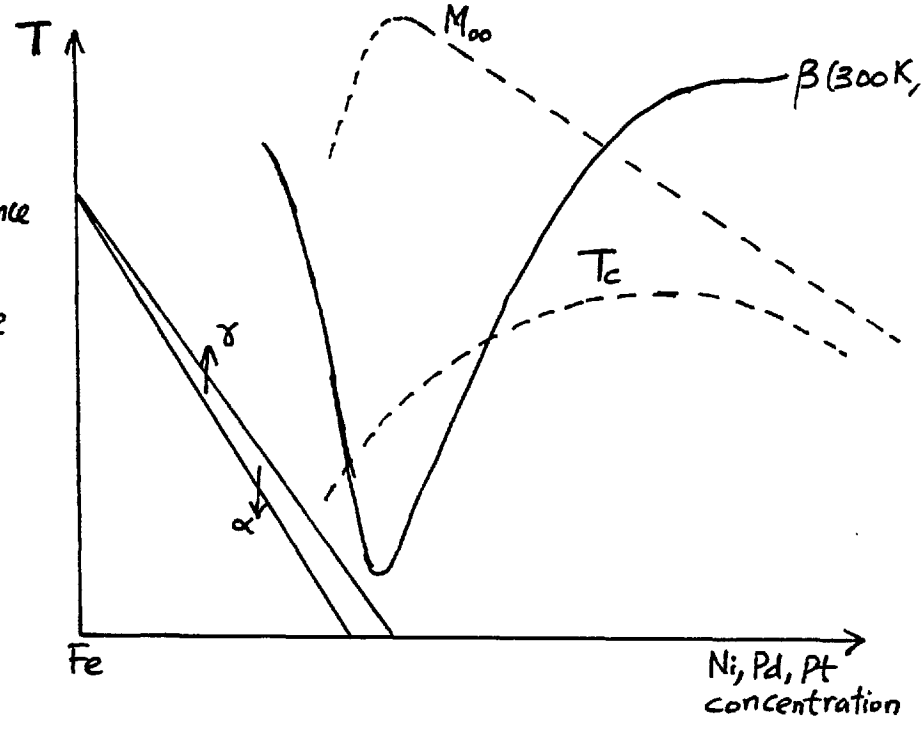

Fig. 7.1: Schematic representation of the concentration dependence of M_{oo}, T_c, β and the martensite temperature for Fe Invars. (After Chikazumi et al. (597)).

The theme which will be developed later in this chapter is that the prominent Invar characteristics, i.e. the magnetovolume effects, follow essentially from the existence of a concentration-dependent magnetic phase transition. In giant moment alloys the phase transition is from a non-ferromagnetic to ferromagnetic state at the critical concentration c_f and we have already argued (section 2.5(x)) that no abnormally large changes in the elastic moduli should

accompany this phase transition.

In the canonical Fe Invars, we believe that such a phase transition occurs owing to competing ferromagnetic (Fe-solvent) and antiferromagnetic (Fe-Fe) exchange interactions. It could well be that some of the peculiar properties of Fe Invars result from the tendency towards antiferromagnetic order. For example Kim (598) has recently proposed, from theoretical considerations, that in metals and alloys structural instabilities are closely related to magnetic instabilities and that a structural change may be regarded as taking place by interrupting a possible magnetic instability. Thus in FeNi the martensitic fcc $\longrightarrow$ bcc transformation probably interrupts a ferromagnetic $\longrightarrow$ antiferromagnetic transition at sufficiently low Ni concentrations.

Previous experimental studies of Invar materials are reviewed at some length in section 7.2, appropriate inferences from these are made (section 7.3) and previous theories of the Invar effect are described in section 7.4. We then present and analyse our neutron scattering data for a number of FeNi alloys in section 7.5 and discuss any new useful information provided by these data (section 7.6). Finally a brief account of our explanation of the Invar effect in Fe alloys is given (section 7.7).

7.2 Review of Existing Data on FeNi Invars

Although the properties of Invar materials have been recently reviewed (240,599,600) yet an account will still be given here in order to highlight those properties which we consider to be essential to an understanding of Invar behaviour.

(a) Magnetic Properties

(i) The Spontaneous Magnetization M_{oo} (or μ_{sp})

The concentration dependence of the spontaneous magnetization of FeNi alloys has been investigated both for bulk samples (601-4) and for fine particles (605-6). On adding Fe to Ni the spontaneous magnetization, M_{oo} (or $\bar{\mu}_{sp}$), follows the Slater-Pauling curve with M_{oo} increasing at a rate of $\simeq$ 2.2 μ_B /atom. However, for concentrations greater than $\sim$ 60% Fe the magnetization starts to deviate from the Slater-Pauling curve and above 64% Fe M_{oo} decreases quite rapidly. In this region (i.e. c $\leq$ 36% Ni) the concentration dependence of the spontaneous magnetization is well represented by

$$M^2_{oo(c)} \simeq 32.67\,(c - 0.258) \qquad 7.1$$

as shown in fig. 7.2(a). Only the values of M_{oo} for bulk samples have been used in the fitting in order to avoid any uncertainty as to whether the spontaneous magnetization of fine FeNi particles should be identical with that of a bulk sample of the same composition. Eq.(7.1) shows that the critical concentration for ferromagnetism in fcc FeNi alloys is 25.8% Ni. This concentration is consistent with the finding that alloys containing less than 24% Ni become antiferromagnetic at low temperatures (606) and with the value of 25.6% Ni obtained by Sidorov and Doroshenko (614) in a mean field theory in which it is assumed that $J_{Fe-Fe} < 0$ but J_{FE-Ni}, $J_{Ni-Ni} > 0$ in an obvious notation. In the past a lot of importance has been attached to the fact that for Fe Invars the spontaneous magnetization appears to vanish when the average electron concentration is $\sim$ 8.3 - 8.5 (597),

Fig. 7.2: Concentration dependence of (a) M_{oo}^2 and (b) T_c^2.

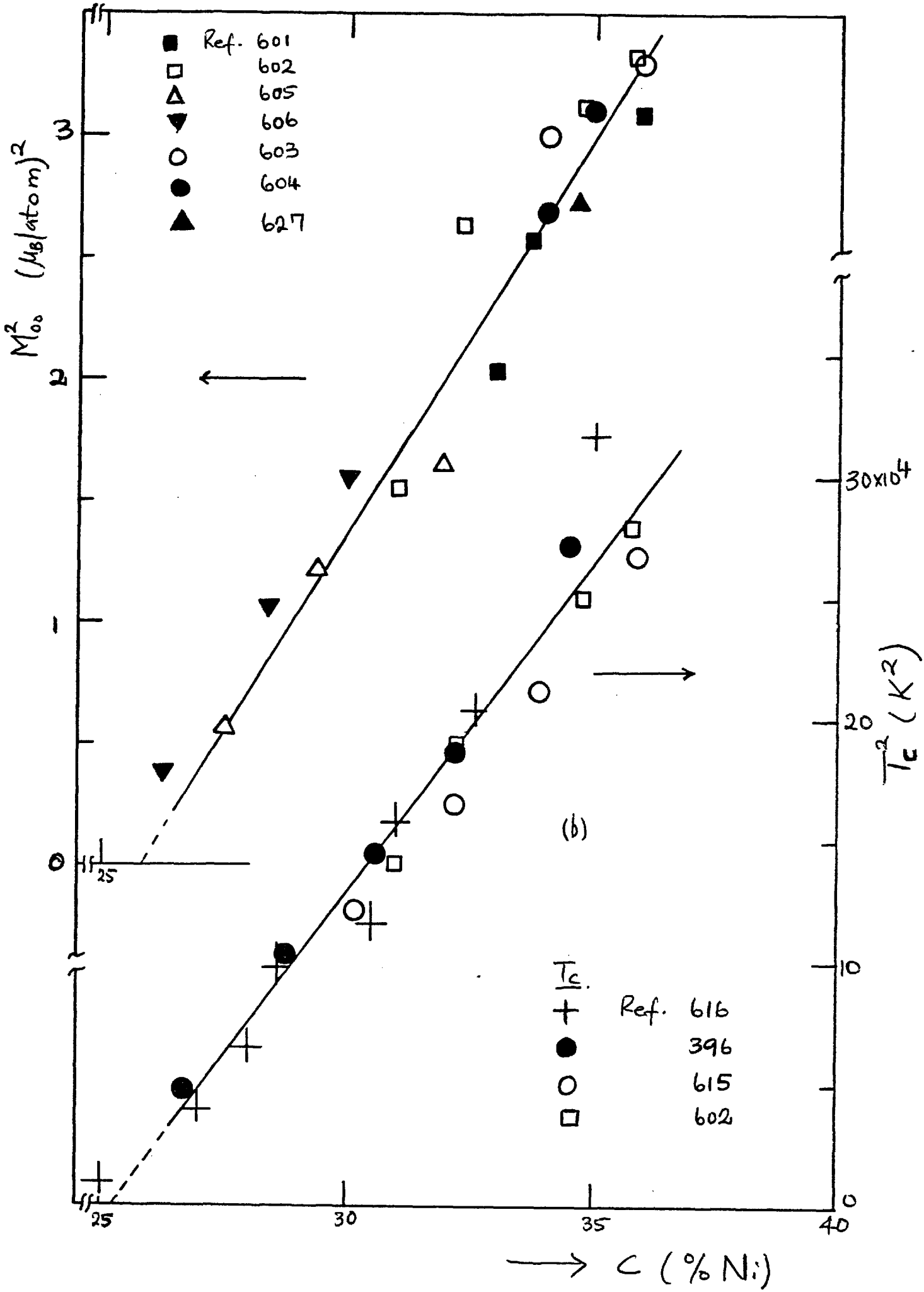

independent of the particular Invar alloys. However, it is not presently clear (to us) exactly in what context the Slater-Pauling curve should be meaningful since it is now generally accepted that a rigid band approach to the ferromagnetism of the transition metals is incorrect. In any case, there are two observations that can be made from an examination of the Slater-Pauling curve. Firstly, the alloys whose $\bar{\mu}_{sp}$ deviate from the curve have close-packed structures (hcp or fcc). Secondly, the solutes are such that the solute-solute interactions are either intrinsically antiferromagnetic or eventually become so. We recall that for the 3d transition metals a change of lattice structure occurs when the electron/atom ratio changes from 8 (bcc Fe) to 9 (hcp Co) and that in many cases the spontaneous magnetization of Fe-rich fcc alloys cannot be determined because such alloys usually transform to a bcc structure below a certain temperature. As shown in fig.7.1 in the Fe Invars, this change of lattice structure occurs in the same region where the spontaneous moment vanishes (i,e for an electron/atom ratio of $\sim$ 8.3 - 8.5). It seems that a fcc lattice cannot support a significant concentration of large magnetic moments which interact antiferromagnetically and as pointed out above (section 7.1) there is a close correlation between the increasing importance of antiferromagnetic interactions in a fcc lattice and the subsequent transformation to a bcc structure.

The temperature dependence of the spontaneous magnetization of Invar Alloys (602, 604) is regarded as unusual in the sense that M_o exhibits a "flat" variation with temperature in contrast with that of pure Fe or Ni which follows approxi-

mately the Brillouin function. The lower the Ni content the "flatter" is the M_o vs T curve. In addition, the law of corresponding states is not obeyed but this is not of much significance because such a law is not strictly valid even for the pure ferromagnetic materials. Schlosser (398, 607) has shown that a useful representation of the experimental data for Fe, Ni and Fe 34.8% and 35.8% Ni for $T \lesssim 0.5\ T_c$ is

$$M_o^2 = M_\infty^2 \left\{ 1 - bT^2 \right\} \qquad 7.2$$

where the constant, b , can be taken as a "normalising factor" i.e. $b \sim T_c^{-2}$. That eq.(7.2) appears to be valid for all three materials despite the failure of the law of corresponding states and the differences in their detailed magnetic behaviour is surprising. Yamada et al. (608-9) have also recently shown that a similar expression holds for Fe 32.3, 34.7, 35.4 37 and 38.6% Ni up to room temperature and with b exactly equal to T_c^{-2} (cf eq. (2.161)). This latter form, which is usually ascribed to single particle excitations (235, 252), would clearly imply the absence of any spin-wave contributions to M_o at low temperatures in these FeNi alloys. However, inelastic neutron diffraction measurements (610-1) have demonstrated not only the existence of spin-waves in these FeNi alloys but also that these spin-waves are easily excited (because of the small spin-wave stiffness constants) so that eq. (7.2) is either totally incorrect or is an approximation to the true expression.

It may be significant that the temperature dependence of the spontaneous magnetization of Invar alloys is similar to that of CuNi (363), PdFe (374, 612) and some amorphous alloys (613). In the latter alloys the flat variation of

M_o with temperature has been attributed to a distribution of exchange fields (612-3) and, in fact, Dubinin et al.(594) had earlier used the same idea to obtain an $\frac{M_o}{M_{oo}}$ vs T/T_c curve that was in good agreement with experimental observation.

(ii) Concentration Dependence of the Curie Temperature

With the addition of Fe to Ni the Curie temperature, T_c, increases reaching a maximum value of $\sim$885 K near 66% Ni before decreasing gradually again. In the Invar region it is found that

$$T_c^2 \simeq 2.7\times10^6\{c - 0.253\}\,, \qquad 7.3a$$

a relation that was first found by Bolling et al.(396). However, if we consider only the Curie temperature of those alloys whose martensite-start temperatures (617-8) are up to $\sim$30 K above room temperature i.e. $c \gtrsim$ 30% Ni then

$$T_c^2 \simeq 2.7\times10^6\{c - 0.262\}\,. \qquad 7.3b$$

Such a procedure would eliminate any uncertainties arising from the use of additives (such as carbon) to stabilize the fcc matrix. Thus both M_{oo}^2 and T_c^2 have been fitted essentially over the same concentration range and the resulting relations extrapolate to a critical concentration $c_f \simeq$ 25.6% Ni. Both Kouvel (619) and Dubinin et al.(594) have made good attempts at explaining the variation of T_c with concentration within the framework of molecular field theory (suitably modified to accommodate local environment effects).

(iii) Field Dependence of the Magnetization

Yamada et al.(608-9, 620) have shown that plots of M^2 against $\frac{B_o}{M}$ at various temperatures are straight lines for FeNi alloys with $c \lesssim$ 39% Ni but not for alloys of higher

Ni content. This behaviour was taken as indicating the weak itinerant character of Invar alloys. However, as fully discussed in section 2.5(ii), the observed relation is essentially a thermodynamic consequence of the existence of a magnetic phase transition.

Values purported to represent the high-field susceptibility of FeNi invars have been published in the literature (608-9, 620-3). Such values are about an order of magnitude larger and increase more rapidly with increasing temperature than those of either pure Fe or Ni or even other FeNi alloys containing more than $\sim$ 50% Ni. We shall, however, note that since $M^2 \propto \frac{B_o}{M}$ a high-field susceptibility cannot obviously be uniquely, and hence meaningfully, defined but the initial susceptibility is, of course, uniquely defined at all temperatures. In view of this we do not think that it is useful to consider either any single-particle and spin-wave contributions to an ill-defined high-field susceptibility or any relationship between such a spin-wave contribution and the spin-wave stiffness constant.

An interesting observation is that at very high fields ($\gtrsim$ 100 K Oe) the M^2 vs $\frac{B_o}{M}$ plots deviate upwards from a straight line suggesting that there exists an additional induced magnetization probably due to the polarization of "low spin states" of Fe (624-5). The behaviour of the magnetoresistivity at high fields supports the above interpretation (625). We will recall that Kouvel and Wilson (584) had shown that the inverse susceptibility vs $T(> T_c)$ curves for Fe 39, 32.8, 35.9, 39.8 and 43.3% Ni were all parallel. They therefore concluded that the paramagnetic moment which represents an average that is independent of the

mutual alignments of the individual atomic moments is almost constant over the investigated composition range. On the other hand M_{oo}, which is sensitive to the alignment of the moments, decreases rapidly with decreasing Ni concentration so that some of the moments must be antiferromagnetically coupled. To account for the increase of the magnetization with applied fields Kouvel and Wilson noted that in disordered alloys atoms have a variety of local environments so that the net exchange field acting on some atoms will be fairly small and comparable to an applied field. Consequently, an increase in the applied magnetic field may lead to a reversal of some atomic moments and thus the bulk magnetization will continue to increase up to very high fields.

(b) Magnetovolume Effects

(i) Thermal Expansivity and Spontaneous Volume Magnetostriction (607,615, 626-31)

As mentioned in the introduction Fe 35% Ni has a very low thermal expansivity near room temperature. Fig.7.3a shows the temperature dependence of the thermal expansivity, $\beta(T)$, for Fe 36% Ni as measured by White (626). $\beta(T)$ is negative at the lowest temperatures ($\lesssim$ 50 K), fairly constant between $\sim$ 150-350 K and thereafter increases with temperature. In the figure β_{ph} shows the expected variation of the lattice contribution; subtraction of this from the observed expansivity gives the sum of the electronic and magnetic contributions (lower broken curve in fig.7.3a). Since the electronic term is small and positive the latter curve essentially represents the magnetic contribution, β_m. Such a magnetic contribution would arise from a positive spontaneous volume magnetostriction which is large at 0 K and

Fig. 7.3(a): β (T) vs T for Fe 36% Ni (after White (626)).

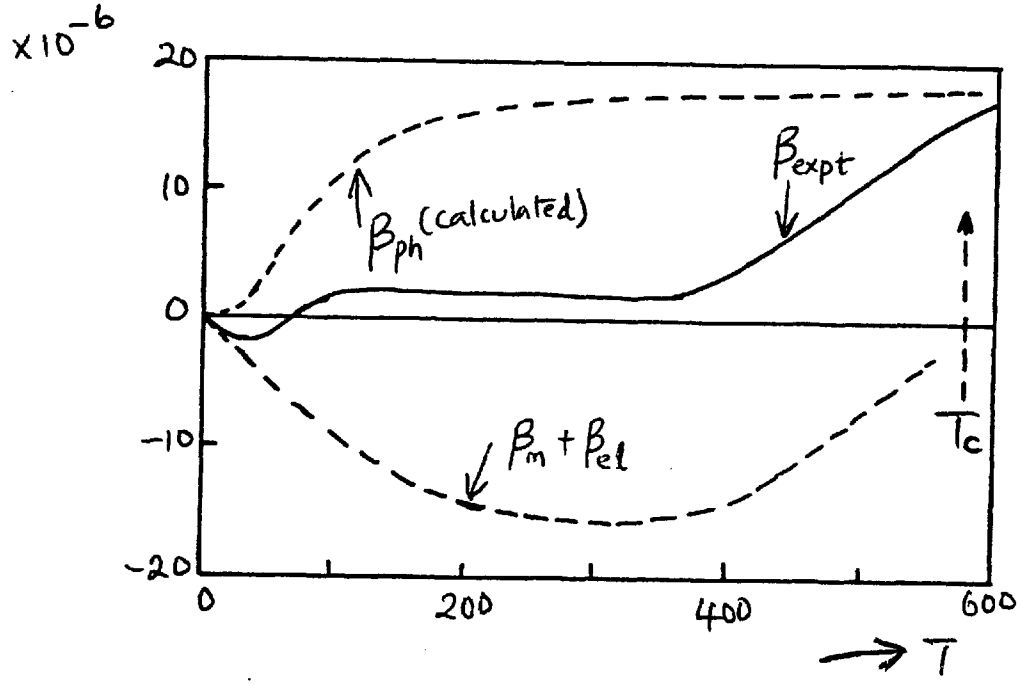

Fig. 7.3(b): Sketch of the spontaneous volume magnetostriction that would give rise to β_m .

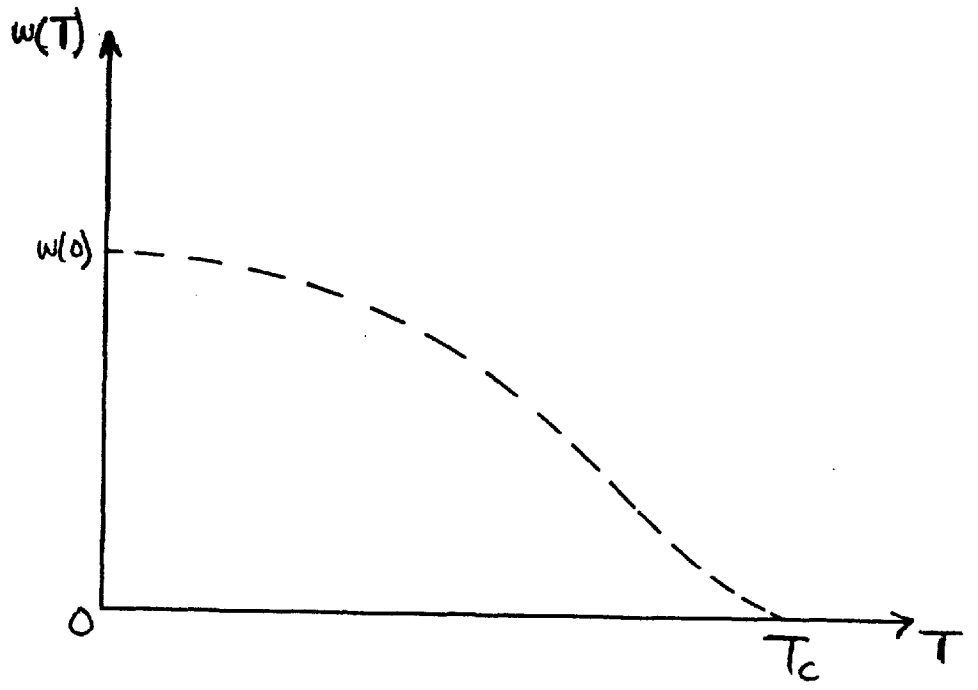

decreases as the Curie temperature is approached, as sketched in fig.7.3b.

Fig. 7.4 shows the concentration-dependence of the spontaneous magnetostriction of FeNi alloys at OK. The values obtained by Tanji (672) are systematically lower than those of Hayase et al.(630, 642) but the difference is probably due to the fact that the measurements made by Tanji did not extend to sufficiently low temperatures ($\sim$ OK). For c $\lesssim$ 36% Ni we obtain that

$$w(c) \simeq 0.187\{c - 0.252\} \qquad 7.4$$

and by comparison with eq.(7.1) it is clear that $w(c) \simeq M_{oo}^2$ as required by the thermodynamic theory of a cooperative magnetic phase transition (section 2.5(iv)). For c > 36% Ni w(c) decreases showing that this concentration closely defines the upper limit of the critical region for the magnetic phase transition which occurs in fcc FeNi alloys.

(ii) Lattice Constant (593, 630, 632)

The low thermal expansivity of Invar alloys is, of course, reflected in the lattice constant because the lattice parameters at OK and at room temperature coincide. At 1000K (which is above the Curie temperatures of all fcc FeNi alloys) the lattice constants of alloys containing less than 60% Ni deviate downwards from the straight line predicted by Vegard's law (630). This implies that a contraction still exists above T_c over a wide concentration range. It is also worth noting that in the Invar region the concentration dependence of the lattice constant at OK is almost identical with that of the spontaneous magnetization.

(iii) Forced Magnetostriction Coefficient (603, 615, 628, 633)

The forced magnetostriction coefficient, h', (see section 2.5(iv)) of disordered fcc FeNi alloys at room temperature has a small

Fig. 7.4: Concentration dependence of the spontaneous volume magnetostriction.

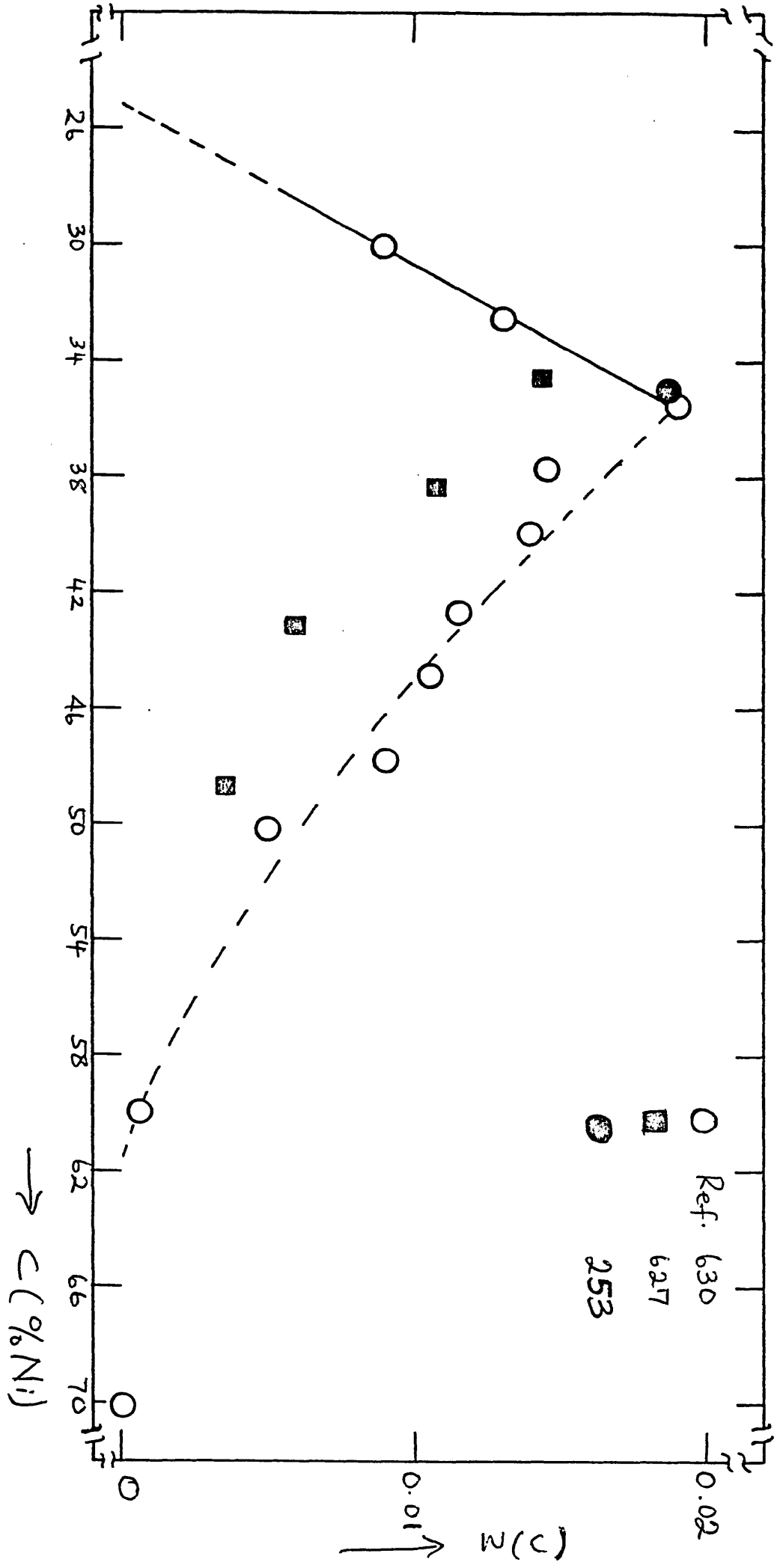

maximum near 75% Ni (633) and large values (about two orders of magnitude larger than h_o' for either Fe or Ni) in the Invar region. If, as we believe, a magnetic phase transition occurs in fcc FeNi alloys in the Invar composition range then, $h_o' = 2\gamma M_o \chi_f^o$ (eq. (2.136)), and large values of h_o' may be expected because of the large susceptibilities of the Invar alloys. It was also suggested in section 2.5(iv) that h_o' should attain a maximum at the critical concentration for the onset of ferromagnetism in "giant-moment" and similar alloys. Now for FeNi alloys the forced magnetostriction coefficient at room temperature has been found (615) to have a maximum near 30% Ni. We do not think that this maximum defines a critical composition for the magnetic phase transition in FeNi because no data for fcc alloys with $c \lesssim 29\%$ Ni were available and moreover it is the concentration dependence of the forced magnetostriction coefficient at low temperatures ($T \sim 0K$) that is required.

(iv) Pressure Dependence of the Spontaneous Magnetization and the Curie Temperature (584, 603, 634-41)

Since $\left(\frac{\partial \omega}{\partial B_o}\right)_P = -\left(\frac{\partial M}{\partial P}\right)_{B_o}$ large positive values of the forced magnetostriction coefficient imply that the spontaneous magnetization will greatly decrease under pressure as experimentally observed (584, 603, 634-5).

Also if M_o obeys the law of corresponding states then the forced magnetostriction coefficient may be related to $\frac{dT_c}{dP}$ (see eq.(6.2)). In the Invar region ($\lesssim 36\%$ Ni) $\frac{dT_c}{dP}$ is large and negative with values of -3.5K/kbar for Fe 35, 36% Ni and down to -5.58K/kbar for Fe 29% Ni (639-41).

However, Belov (232) has pointed out that the direct determination of $\frac{dT_c}{dP}$ especially in experiments involving hydrostatic pressure is difficult and suggested that it is probably best to calculate $\frac{dT_c}{dP}$ from magnetostriction data using thermodynamic theory. For the phase transition that occurs at T_c it may be easily shown that

$$\frac{dT_c}{dP} = -\frac{\gamma}{\alpha_c} \qquad \text{(cf eq.(2.114))}$$

where near T_c $a \simeq \alpha_c (T' - T_c)$. Experimental values of γ and α_c lead to $\frac{dT_c}{dP} \simeq -5.5\,K/Kbar$ for Fe 29, 32% Ni and $\simeq -4\,K/Kbar$ for Fe 36% Ni in good agreement with the values determined directly.

Leger et al.(641) also found that for Fe 34% Ni

$$\frac{T_c^2(P)}{T_c^2(0)} \simeq 1 - \frac{P}{P_c} \qquad 7.5a$$

where P_c is the pressure at which T_c vanishes. Eq.(7.5a) holds if $\frac{dT_c}{dP} = -\frac{A}{T_c}$ (with $P_c = \frac{T_c^2(0)}{2A}$) where A is a constant. Although such a relation is supposed to be valid for weak itinerant ferromagnets (see section 2.5(iii)) Schlosser (745) has shown that it could be an approximation to the more valid expression

$$\frac{T_c(P)}{T_c(0)} = 1 + \ln\left\{1 + P\left(\frac{\partial w}{\partial P}\right)_{T,P=0}\right\}. \qquad 7.5b$$

Eq.(7.5a) also appears to be valid for MnSb (638) but it is significant that it is not valid for both Fe 29% Ni (641) and $Fe_{65}(Ni_{1-x}Mn_x)_{35}$ alloys for $0 < x \leq 0.19$ (638) which should be even better "weak itinerant ferromagnets" than Fe 34.9% Ni. For these latter alloys $T_c \propto P$.

(c) Mossbauer Effect Measurements

Mossbauer effect measurements are useful for obtaining information about local environment effects in alloys. The

hyperfine field at both Fe and Ni sites in the FeNi system have been investigated (606,615,643-68). The results of such experiments may be summarized as follows:-

(i) Magnitude of the Internal Fields

At room temperature the hyperfine field at an Fe site is given approximately by

$$B_{hf}(Fe) \simeq -\{90\bar{\mu}_{Fe} + 60 M_{oo}\} \quad (\text{in KOe})$$

and thus is $\sim$ -330K Oe; near c=30% Ni there is a sudden decrease in the magnitude of this field to about 30KOe. This decrease is mainly due to the fact that for c $\lesssim$ 30% Ni the alloys are paramagnetic at room temperature. Erich et al.(648) have also determined the field at a Ni site; again at room temperature

$$B_{hf}(Ni) \simeq -\{20\bar{\mu}_{Ni} + 100 M_{oo}\} \quad (\text{in KOe})$$

but there was a slight irregularity in the variation of $B_{hf}(Ni)$ near the phase boundary between the bcc and fcc alloys (i.e. in the Invar region).

(ii) Characteristics of the Mossbauer Spectra for fcc Alloys

Since the martensite-start temperature is $\sim$300K for Fe 30% Ni measurements on alloys of lower Ni content have to be made either on fine particles for which the martensitic transformation is suppressed (642) or on bulk samples with carbon added to stabilize the fcc structure (396).

For c $\lesssim$ 24% Ni the spectra at room temperature and 77K consist of a single paramagnetic absorption line which is broadened at 4.2K; such alloys are therefore antiferromagnetic with Neel temperatures, T_N, lying between 4.2 and

77K (606, 646). This observation is consistent with the suggestion made above that the critical concentration for ferromagnetism in this system is about 25-26% Ni.

For $26 < c \lesssim 30$% Ni the spectra consist of a superposition of the six absorption lines characteristic of ferromagnetic Fe together with a single line characteristic of paramagnetic Fe. This single line becomes broadened at low temperatures indicating antiferromagnetic ordering. For these alloys ferromagnetism and antiferromagnetism appear to coexist (644-7, 662-3).

For $30 < c \lesssim 50$% Ni the Mossbauer spectrum of a properly homogenised sample consists of six ferromagnetic lines but these are unusually broad and also asymmetric. Earlier investigations (644 -5,647) of fine particle samples in this concentration range (specifically 30-32% Ni) appeared to show the coexistence of ferromagnetic and antiferromagnetic regions as in the preceding group of alloys (i.e. $26 < c \lesssim 30$% Ni) but Ok and Han (653) have since shown that the nature of the spectrum depends on the size of the particles. For particle sizes $\lesssim 100$Å the spectrum is indeed as in the preceding case but after suitable heat treatment to increase the average size of the particles to more than 1000Å the paramagnetic central peak disappears so that the spectrum now resembled that for a homogenised bulk sample. The dependence of the central absorption line on particle size led Ok and Han to conclude that it originated from the superparamagnetic relaxation of ferromagnetic or antiferromagnetic fine particles. This conclusion must, however, be viewed against the fact that it is not certain that the heat treatment which was designed simply to increase the size of

the particles did not effectively homogenise the bulk sample.

The broadening and asymmetry indicate a distribution of hyperfine fields and the existence of appreciable dipolar magnetic fields and electric field gradients, the latter arising from site deviations from cubic symmetry. Using a simple model Window (659) demonstrated that the dipolar field could be an order of magnitude larger than expected on classical grounds.

(d) Structural inhomogeneity of FeNi Alloys

Atomic short range order is known to persist up to the melting point of $FeNi_3$ (669) and occurs in alloys containing up to 60-70% Fe even after quenching from $\sim$ 800-1273 K (542,671). The atomic ordering extends only to the next nearest-neighbour distance.

Atomic ordering of the tetragonal CuAu-type has also been found especially for compositions close to Fe 50% Ni (619,656,672-3). It is enhanced by electron or neutron irradiation at room temperature and/or in an applied magnetic field.

In the Invar region existence of the Fe_3Ni superstructure has also been reported either from specific heat measurements (642), electron diffraction from very thin single crystal FeNi foils (674) or from the examination of the Mossbauer spectra of electron-irradiated alloys (673-3). Long term annealing or irradiation at 873K enhances the Fe_3Ni ordering while this superstructure, in turn, tends to stabilize the fcc matrix (672-3). Ordering is again short-range and does not occur for bulk samples (642,674-5).

It is clear from the foregoing that fcc FeNi alloys are structurally (i.e. metallurgically) inhomogeneous and

that in the Invar region all three superstructures ($FeNi_3$, FeNi and Fe_3Ni) can exist, at least in very small regions, the dominance of any particular type being determined by both the composition and history of the sample.

(e) Electrical Resistivity

The residual electrical resistivity of FeNi alloys increases rapidly with Fe content starting at the composition at which the spontaneous magnetization deviates from the Slater-Pauling curve (634-5, 676-7). On a model of "latent antiferromagnetism" (676, 678) the rapid rise of the residual resistivity in the Invar region is due to conduction electron scattering by magnetic heterogeneities (635,676). Evidence in support of this explanation is the increase of the residual resistivity (and a decrease of the spontaneous magnetization) as an external pressure is applied (634-5). On the other hand, Armstrong and Fletcher (677), using a rigid-band approach, suggest that for c $\gtrsim$ 50% Ni the alloys are "strong" ferromagnets with only down-spin d-states at the Fermi level whereas for lower Ni concentrations the alloys are "weak" ferromagnets in which both up-spin and down-spin d-states exist at the Fermi level. Cadeville and Loegel (679) and Cadeville et al.(680) also conclude that a transition from "strong" to "weak" ferromagnetism occurs at $\sim$ 50% Ni from an analysis of low temperature measurements of the electrical resistivity, thermoelectric power and specific heat of both FeNi and (FeNi)C alloys containing more than 34% Ni. These authors did not use the incorrect (681) rigid-band model but instead assumed that the occurrence of both down-spin and high-density up-spin d-states at the Fermi level is determined

by the local environment of a given atom (thus allowing for magnetic inhomogeneity). However, from resistance anisotropy measurements Campbell (682) has argued that the transition from "strong" to "weak" ferromagnetism, in fact, occurs near $FeNi_3$ and cited various other experimental data to support his contention. This uncertainty about the exact concentration for strong $\longrightarrow$ weak ferromagnetism questions the validity of the explanation that the high residual resistivity of alloys in the Invar region is due to the occurrence of both majority (i.e. up-spin) and minority d-holes at the Fermi level. On balance we favour the interpretation based on the existence of magnetic heterogeneities in the Invar region especially in view of the fact that at 1123 K ($> T_C$ for all the fcc alloys) the resistivity varies in a manner that is compatible with Nordheim's rule (683).

(f) Galvomagnetic and Magnetocaloric Effects

With the exception of some magnetoresistance data on Fe 38, 45% Ni (634) these effects have only been recently investigated so that only a few results are available.

(i) Magnetoresistance

Rode et al.(684) have shown that the concentration dependence of the magnetoresistance of FeNi (20-36% Ni) and $Fe_{65}(Ni_{1-x}Cr_x)_{35}$ alloys are similar and can be explained by assuming that the volume fraction of the antiferromagnetic regions in these alloys is small so that they act as magnetic inhomogeneities which contribute strongly to the magnetic part of the electrical resistivity. Since $Fe_{65}(Ni_{1-x}Cr_x)_{35}$ becomes antiferromagnetic at some Cr content the similarity in the electrical (and magnetic) behaviour between these

alloy systems was assumed to demonstrate the "latent antiferromagnetism" of the FeNi system. It must be stated that the alloys were slowly cooled after annealing so that those alloys containing less than ~29% Ni consisted of both γ- and α-phases at low temperatures. For the same FeNi alloys Rode and Deryabin (685) later showed that the quantity $\frac{1}{\rho_{4.2}} \frac{\Delta\rho}{\Delta B_0}$ (where $\rho_{4.2}$ is the resistivity at 4.2K) not only decreased rapidly below about 15K, as first observed by Kondorskii and Sedov (634,688), but also exhibited maxima in the temperature range 25-40K. In this connection it is of interest to note that the "high-field susceptibility" at 8.2 KOe has also been reported to decrease rapidly below ~15K (634,688), an effect that was attributed to the antiferromagnetic ordering of those regions of the alloys containing "excess" Fe (688).

For Fe 29.9% Ni Hatta et al.(625) observed that the magnetoresistance at 543K at high fields (up to 290 KOe) decreases more rapidly than linearly and interpreted this to be due to an additional magnetization resulting from the polarization of low spin Fe states. Finally, the existence of a magnetovolume contribution to the magnetoresistance of some FeNi invars has been reported (686).

(ii) The Magnetocaloric Effect

According to Rode and Deryabin (685) the heat capacity of the FeNi alloys they investigated had "local maxima" in the temperature range 30-50K. In addition the magnitude of the magnetocaloric effect was less than expected from the temperature dependence of the magnetization (see eq.(2.176)), particularly for $4.2 \leq T \leq 40$K. The difference was attributed to a negative contribution from the paraprocess in anti-

ferromagnetic regions of the alloys.

(iii) The Spontaneous Hall Coefficient

The spontaneous Hall coefficient, R_s (see eq.(2.193)), of FeNi alloys containing 34.5-42% Ni has been measured in the temperature range from 77K to the corresponding Curie temperature (687). R_s is very large in the Invar region and increases as the Ni concentration decreases, a variation that correlates with the low temperature resistivity of these alloys. For the 34.5-40% Ni alloys $R_s \sim T^2$ at low temperatures and $\sim T$ at high temperatures while for Fe 42% Ni $R_s \propto T^4$ at low temperatures and $\propto T^2$ for $T \gtrsim 400K$. It was concluded that the behaviour of R_s can be understood on the basis of a spin-orbit coupling between conduction electrons and localized magnetic electrons for 34.5-40% Ni alloys while an itinerant picture appears to be valid for the 42% Ni alloy.

(g) The Electronic Specific Heat

Measurements (361,626,689-92) of the low temperature heat capacity of some fcc FeNi alloys have shown that the electronic heat coefficient, γ_s, has large values in the Invar region, as shown in fig.7.5. Also shown in the figure are values of γ_s for two carbon-doped FeNi samples. Since addition of carbon is known to decrease γ_s in the Invar region (680,689) it follows that the electronic heat coefficients of the undoped samples will be larger than the values shown. Even larger values of γ_s have been observed for $Fe_{65}(Ni_{1-x}Mn_x)_{35}$ alloys near the critical composition, $x \simeq 0.2$ (691) and for some austenitic stainless steels (694).

Since the observed values of γ_s depend on such factors as the carbon content (680,689) and applied magnetic

Fig. 7.5: Concentration dependence of the electronic heat coefficient of fcc FeNi alloys.

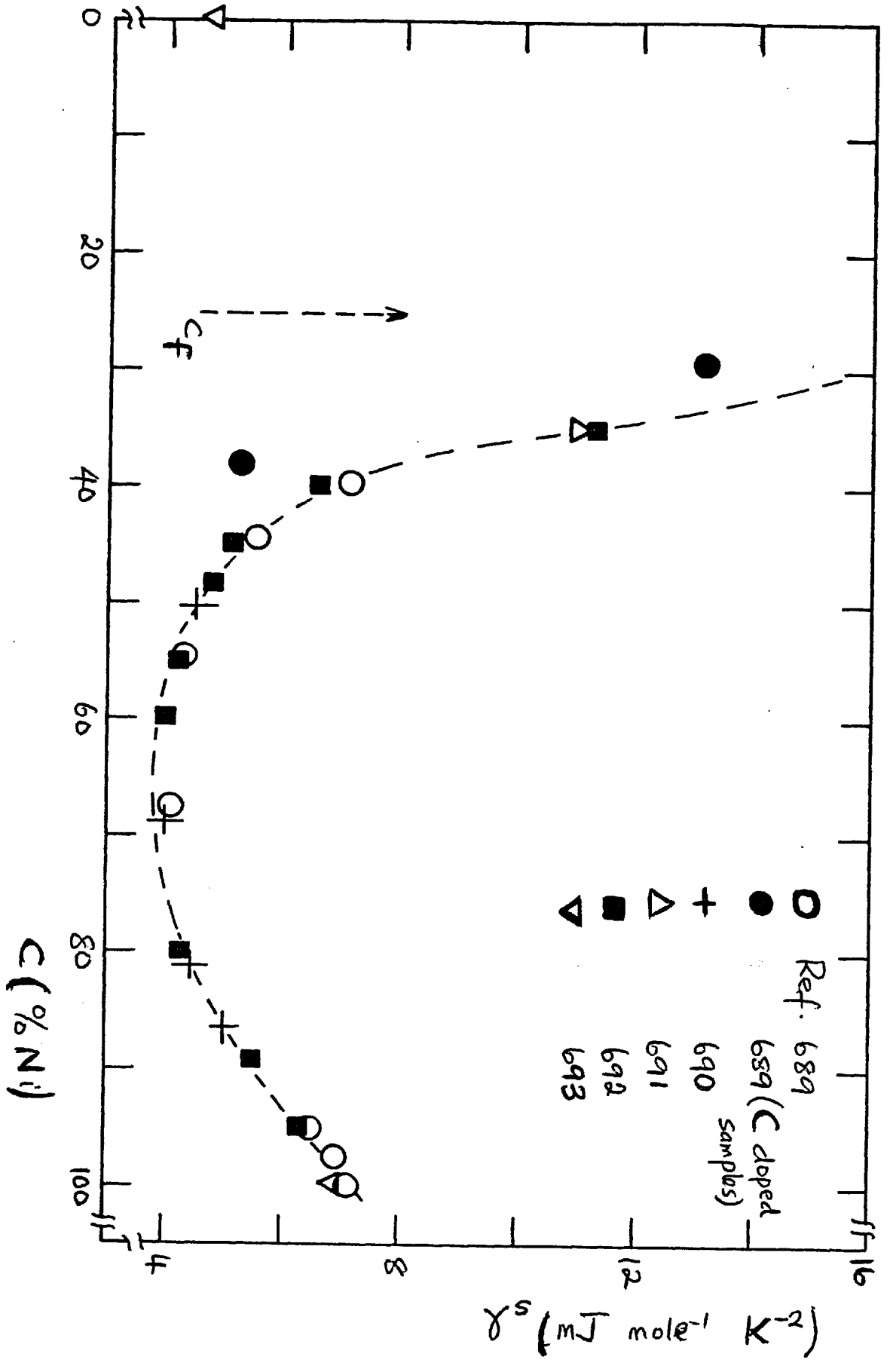

fields (689) there clearly exists a magnetic contribution to this coefficient so that we shall rule out any explanation of the large γ_s values purely in terms of the simultaneous occurrence of high up-spin and down-spin densities of state at the Fermi level. Gupta et al.(689) have attributed the large values of γ_s to a contribution from thermally excitable magnetic clusters. These are clusters which are located in effective molecular fields $B_{eff} \leq \frac{K_B T}{M_{cl}}$ where M_{cl} is the cluster moment. According to Zoller et al.(694) only a small number of magnetic clusters in low effective fields is needed to give large γ_s values. This explanation is, of course, similar to that proposed for dilute magnetic alloys by Marshall (348) although we shall argue elsewhere that Marshall's suggestion is more applicable in the present context than to spin-glasses. As mentioned above (section 7.2(c)) Mossbauer effect data have confirmed the existence of a distribution of hyperfine fields in FeNi alloys containing less than 50% Ni. The distribution of hyperfine fields arises from the presence of competing ferromagnetic and antiferromagnetic interactions in the system.

Another contribution to γ_s could come from critical fluctuations of the spontaneous magnetization. For "giant moment" alloy systems we have shown that such critical fluctuations give rise to a contribution to γ_s which is proportional to the initial susceptibility (see section 2.5(ix)) and which is therefore largest at the critical concentration for the onset of ferromagnetism. In the FeNi Invar system ferromagnetism disappears at $\sim$ 25% Ni and a large contribution to γ_s is therefore to be expected. A

similar suggestion has been made by Caudron et al.(692) and Sumiyama (599) although these authors incorrectly referred to it as some sort of effective mass enhancement by paramagnons.

Also in the Invar region the phonon specific heat coefficient increases with decreasing Ni concentration. This contrasts the situation in giant-moment alloys where the lattice specific heat attains a minimum at the critical concentration (see section 2.5(xi)). Measurements of the elastic constants FeNi alloys at low temperatures also show that the Debye temperature decreases with decreasing Ni content. It thus seems reasonable to associate the increasing phonon specific heat with the increasing tendency towards a martensitic transformation which gives rise to softer phonon modes (also see the following discussion).

(ii) Elastic Constants

The elastic properties of fcc FeNi alloys have also been widely investigated (397,690,695-700). In particular the temperature dependence of the elastic moduli of these alloys, which is sketched in fig.7.6, is interesting because of the technological importance of the "Elinvar" alloys - those alloys which have a small temperature coefficient of elastic moduli.

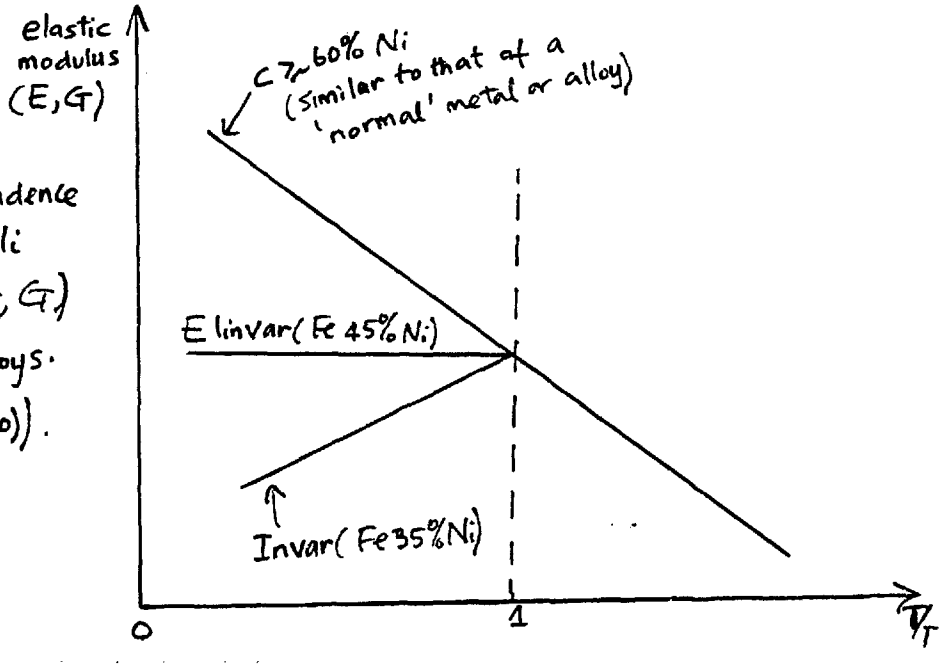

Fig 7.6: Sketch of the temperature dependence of the elastic moduli (Young's, E, and shear, G) of fcc FeNi alloys. (After Nakamura (600)).

Usually the elastic constants of a non-magnetic metal (or alloy) should increase with decreasing temperature because of the decrease in lattice spacing. For a ferromagnetic material some magnetic contribution to the elastic constants must be expected if only because the magnetic interactions contribute to the total energy of the material and the elastic constants represent the second derivatives of this total energy with respect to the appropriate strains (701). For pure Ni and fcc FeNi alloys containing more than 60% Ni the magnetic contribution to the elastic moduli is relatively small so that the temperature dependence of the moduli is similar to that of a non-magnetic metal. With decreasing Ni concentration the temperature coefficient of the elastic moduli below T_C gradually increases becoming zero for Fe 45% Ni (Elinvar) and positive for still lower Ni contents (see fig.7.6). The temperature coefficient has its largest value for a composition close to Fe 35% Ni where also the spontaneous volume magnetostriction is largest (fig.7.4).

It is now known that both the " ΔE_λ effect" due to domain reorientation and magnetization rotation effects and the " ΔE_ω effect" due to the forced volume magnetostriction are too small to account for the observed temperature dependence of the elastic moduli. Therefore the observed effect is attributed to the spontaneous volume magnetostriction of the alloys; this is understandable because the net increase in volume as the temperature decreases implies that the elastic constants will decrease with decreasing temperature. Just as the Invar effect is the result of negative magnetic and positive lattice (and electronic) contributions to the thermal expansivity the Elinvar effect results from the

associated positive magnetic and negative lattice contributions to the temperature coefficient of the elastic moduli. Thus an explanation of the Elinvar effect is closely linked to that of the Invar effect.

(i) Effect of Cold Work

In the Invar region cold rolling reduces the thermal expansivity and makes it anisotropic (702), decreases the saturation magnetization (597,703-4) but increases the high field susceptibility (597). It has also been reported to reduce the forced magnetostriction coefficient near the Curie temperature (615), the average hyperfine field and hence also the Curie temperature (651) and also to induce partial martensitic transformation particularly for those alloys close to the $\gamma \rightarrow \alpha$ phase boundary.

The effects of cold work have been explained by assuming that it produces dislocations, stacking faults and internal stresses (597,703-4). For example, since $\frac{\partial M_{oo}}{\partial P} < 0$ the decrease of the saturation magnetization on cold rolling can be understood by assuming that the hydrostatic pressure round an edge dislocation is increased. On the other hand, it may be assumed that cold work increases the magnetic inhomogeneity of a sample and therefore enhances the distribution of internal fields. Such a distribution of internal fields would give rise to non-uniform deformations or local strains and hence to smaller thermal expansivity (664-5).

(j) Ultrasonic Experiments

Measurements of the velocity and attenuation of sound in a polycrystalline Fe 34% Ni bulk sample showed an increase of $\sim$ 4% in the longitudinal velocity below 35K and a peak

in the attenuation for longitudinal waves at ~ 22K (705). The transverse velocity showed a small minimum at this latter temperature. The results were completely reversible and consequently could not have been due to a martensitic transformation which is known to exhibit a large temperature hysteresis. A magnetic field of up to 15 KOe applied to remove domain wall effects caused a change of ~ ½% in the magnitude of the sound velocity but it did not change its temperature dependence. The authors therefore concluded that their results were consistent with an antiferromagnetic ordering (at T ≃ 22K) of paramagnetic regions of high Fe content in a bulk sample. The authors contended that the Mossbauer effect was not sufficiently sensitive to detect the much smaller amount of antiferromagnetic material at this concentration.

Similar measurements on Fe 35, 38, 40 and 47% Ni samples were carried out by Fletcher (706) who also studied the frequency dependence of the observed effects. Although the results for the 35-40% Ni alloys were consistent with those of Meincke and Litva (705) the author interpreted these by assuming the existence of a relaxation mechanism which was magnetic in origin. The effects disappear rapidly with increasing Ni concentration and are negligible for 47% Ni. In order to check if the observed relaxation effects were an intrinsic property of Invar, Hausch (397) measured the sound velocities and attenuation of single crystals of Fe 36.6% Ni and ordered Fe 28.2% Pt alloys. While the relaxation effects found by previous authors (705-6) were confirmed for the FeNi alloy the ordered FePt alloy exhibited a vanishingly small low temperature anomaly. Hausch therefore concluded that the

observed relaxation effects were peculiar to FeNi alloys which are magnetically inhomogeneous. Owing to varying local environments the Fe atoms may either have large or small moments. It was proposed that the relaxation process results from a stress-induced interchange of Fe atoms with large and small moments i.e. the observed effects are induced by the measurement process.

However, we agree with the point of view expressed by Meincke and Litva (705) that the observed effects are due to a paramagnetic-antiferromagnetic transition in small Fe-rich regions in otherwise ferromagnetic samples. The fact that the effects are both frequency and field dependent support this interpretation (see section 2.5(x)). The Neel temperature for the phase transition is the temperature at which the peak in the attenuation occurs, $\sim$ 22-25K. Further evidence for such a paramagnetic-antiferromagnetic transition is provided by the observation of exchange anisotropy in Fe-rich FeNi alloys by Nakamura et al.(647). These authors suggested that the temperatures at which rotational hysteresis loss vanishes in these alloys may be taken as the lower limits of the Neel temperatures of the antiferromagnetic regions. These temperatures together with the temperatures of maximum attenuation in the ultrasonic experiments are plotted in fig.7.7. The Neel point ($\simeq$ 67K) for pure γ-Fe (707) is also shown. From the figure it would appear that the antiferromagnetic ordering temperature decreases as the Ni concentration increases attaining a limiting value of $\simeq$ 22K for c $\geq$ 34% Ni. It is known that the ordering temperature of γ-Fe particles is a function of the size of the particles (708), the maximum value of 67K being observed only for

Fig. 7.7: Concentration dependence of T_N for γ-FeNi alloys. The inset shows the variation of T_N with average size for γ-Fe particles (after Ref. 708).

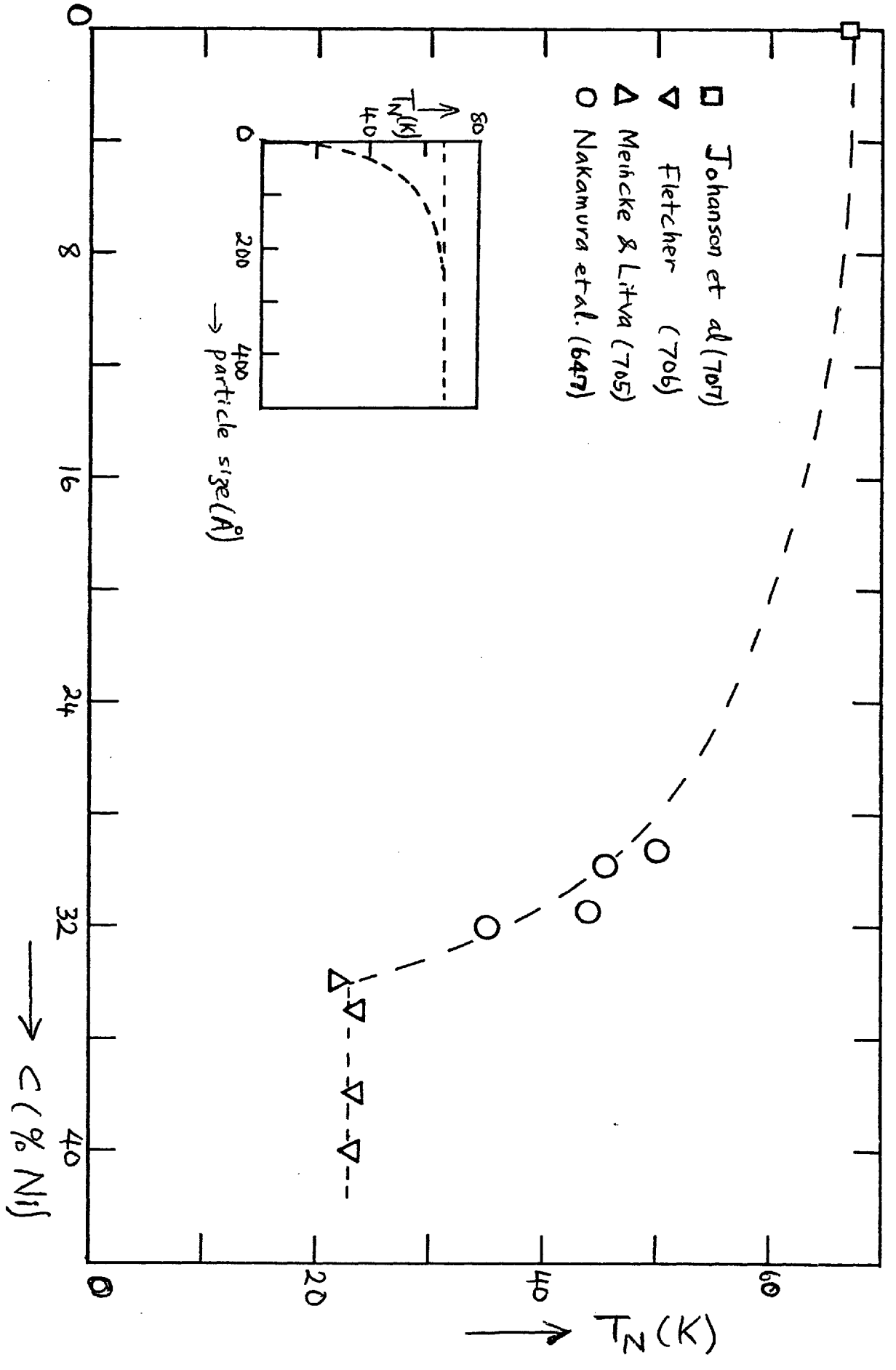

particles whose size is greater than about 200Å. We shall suggest that the limiting value of $\sim$ 22K observed in FeNi invars with $c \gtrsim$ 34% Ni applies to the smallest Fe-rich region that can be antiferromagnetically ordered. From the variation of T_N with particle size for pure γ-Fe (708) we estimate that such Fe-rich regions have a diameter of $\simeq$ 10Å. The concentration of such Fe-rich regions will clearly decrease as the Ni concentration increases eventually becoming negligible.

(k) Neutron Diffraction Experiments

The concentration dependence of the Fe and Ni moments in fcc FeNi alloys has been determined by unpolarized diffuse diffraction measurements (435,542,544). For alloys containing more than 40% Ni the cross-section dips in the forward direction, an effect Shull and Wilkinson (435) attributed to short range magnetic order. The more detailed measurements of Collins et al.(542) not only confirmed the presence of both nuclear and magnetic short range order but also, because of the similar angular dependence of the nuclear and magnetic scattering, it was possible to conclude that the Fe and Ni atoms had characteristic local moments. For $c \lesssim$ 50% Ni $\bar{\mu}_{Fe}$ and $\bar{\mu}_{Ni}$ appear to remain constant at $\simeq 2.8$ and $0.6\,\mu_B$ respectively but it must be remembered that (i) no correction was made for the uniform negative magnetization in the alloys so that the observed values represent the total moment per site (i.e. local moment + the uniform magnetization); (ii) although the measurements were made at room temperature it does not appear that any corrections were made for the temperature dependence of the magnetization.

For c $\lesssim$ 40% Ni some magnetic small-angle scattering appears the magnitude of which increases rapidly with decreasing Ni concentration (543-4, 671, 709). It is generally agreed that this small angle diffuse scattering is due to magnetic inhomogeneity and that this inhomogeneity is essentially a local environment effect but there is no such consensus on exactly how the local environment effect gives rise to the forward angle scattering. According to Arkhipov et al.(543) and Men'shikov et al.(544) the existence of mixed exchange interactions ($J_{Fe-Fe} < 0$, J_{Fe-Ni}, $J_{Ni-Ni} > 0$) and the statistical distribution of atoms imply that the z-projection, say, of the atomic moments assumes different values from site to site thereby giving rise to spatial magnetic inhomogeneity. On this model the forward cross-section can be calculated by using Marshall's formula allowing also for the occurrence of short range order (eq.(3.68)). On the other hand, Komura et al.(709) contend that the small angle scattering is due to paramagnetic voids defined as local Fe-rich regions (c$\lesssim$29% Ni) which have no net magnetic moment because of the antiferromagnetic coupling between neighbouring Fe atoms. The forward cross-section is then given by the relation

$$\frac{d\sigma}{d\Omega} = \frac{n^2}{NV_c} v(1-v)\left\{\bar{P}_{cl} - \bar{P}_h\right\}^2 e^{-\frac{K^2}{3}R_g^2} \qquad 7.6$$

where n is the number of atoms per cluster, v the volume fraction occupied by the clusters, Vc the volume of a cluster and N is the number of atoms per unit volume. $\bar{P}_{cl}$, $\bar{P}_h$ are respectively the average magnetic coherent scattering amplitudes of the void and host and Rg is the radius of gyration of a cluster (for a spherical cluster $R_g = \sqrt{\frac{3}{5}}\,R$, where R is the radius of the cluster).

The volume fraction occupied by the clusters was estimated as 15.4% for Fe 35% Ni using a model of concentration fluctuations proposed by Kachi and Asano (710). The calculated scattering cross-section gave only a qualitative agreement with the observed cross-section from a single crystal of Fe 35% Ni. Moreover, the above estimate of the volume fraction occupied by the paramagnetic voids has been questioned by Kohgi et al.(611) who in addition to determining the spin wave stiffness constant for Fe 35% Ni at 4.2K also unsuccessfully tried to detect the antiferromagnetic regions that would result from the ordering of the paramagnetic voids at a sufficiently low temperature. From the sensitivity of their measurements Kohgi et al. concluded that the volume fraction occupied by the paramagnetic voids must be less than 0.01%. In their measurements Komura et al.(709) observed that the forward cross-sections in the (100), (110) and (111) directions were different but only later and more detailed measurements (711) confirmed that the differences were significant and were probably due to magnetocrystalline anisotropy.

An important observation made by Dubinin et al.(712) and Teploukhov et al.(713) is that at 4.2K neutron diffraction from disordered Fe 37% Ni exhibits magnetic reflections of type ($\frac{1}{2}$ $\frac{1}{2}$ o) and ($\frac{1}{2}$ $\frac{1}{2}$ 1) which the authors attribute to a fourth-order antiferromagnetic ordering in a fcc lattice (i.e. in the x, y directions the magnetic unit cell is twice the chemical unit cell). The intensity of the ($\frac{1}{2}$ $\frac{1}{2}$ 0) reflection falls rapidly between 15-20K and more slowly thereafter. Also the (111) structure reflection has a smaller intensity and a greater width at 4.2K than at 78K showing that the antiferromagnetic ordering distorts the

fcc lattice with a change of volume.

The temperature dependence of the neutron scattering from these alloys has also been studied (554,670,714-6). Collins (670) measured the paramagnetic scattering from Fe 35% Ni up to $\sim 2T_C$ ($\cong$ 1000K) and showed that there was an apparent average Fe moment of about 1.4 μ_B which was almost temperature independent. The observed value of $\bar{\mu}_{Fe}$ was significantly less than the average value of low temperatures (estimated as $\gtrsim$ 2.3 μ_B). Arkhipov et al. (714) investigated the diffuse magnetic scattering from Fe 33, 35, 37 and 40% Ni alloys at 100, 293 and 373K and compared their experimental results with theoretical values calculated on a molecular field model. A temperature dependence of the small angle scattering is also expected on the model that attributes this scattering explicitly to paramagnetic voids (709). With increasing temperature these paramagnetic voids should grow at the expense of the ferromagnetic matrix. Thus the forward cross-section should steadily increase with temperature and diverge at the Curie temperature. Komura et al. (715) measured the neutron diffuse scattering around the (111) reciprocal lattice point of a single crystal of Fe 35% Ni from room temperature up to 723K. It was observed that the magnitude of the magnetic scattering, which was essentially elastic for small κ , was nearly constant for $T \leq T_C$ but gradually decreased for $T > T_C$. The cross-section in the forward direction was better fitted by a Gaussian rather than a Lorentzian and this was interpreted as showing the predominant inhomogeneity of the sample. The magnetic inhomogeneities have an average correlation range of about 9Å which is approximately constant for $T \leq T_C$ and

decreases slowly above T_c. More detailed measurements of the temperature dependence of the diffuse magnetic scattering from fcc FeNi alloys have been made by Men'shikov et al.(554). Their main observation is that for Fe 50% Ni, which is in the concentration region where $M_{oo}(c) \propto c$, critical scattering begins from $\sim 0.7T_c$ while in the invar region ($c \lesssim 40\%$ Ni) this scattering appears to exist through out the investigated temperature region (from 80-1000K) - see fig.5.12. Now according to Krivoglaz (717) the differential cross-section for the critical diffuse scattering of unpolarized neutrons in cubic crystals in an arbitrary magnetic field is (in mb/sr.atom)

$$\frac{d\sigma}{d\Omega} = 73 F^2(\vec{K}) K_B T \left\{ \frac{1 + \hat{K}_z^2}{\chi_\perp^{-1} + \Lambda K^2} + \frac{1 - \hat{K}_z^2}{\chi_{||}^{-1} + \Lambda K^2} \right\} \qquad 7.7$$

where $\chi_\perp$ and $\chi_{||}$ are the transverse and longitudinal components of the initial magnetic susceptibility and Λ is a constant factor. In general

$$\chi_{||} = (K_{||} r_1)^{-2} \qquad 7.8a$$

$$\chi_\perp = (K_\perp r_1)^{-2} \qquad 7.8b$$

$$r_1 = \frac{a_o^2 T_c}{z_o T} \qquad 7.8c$$

where $K_{||}$ and $K_\perp$ are the longitudinal and transverse inverse correlation lengths, a_o is the lattice constant and z_o is the lattice coordination number. However, in a mean field approximation it has been shown (269,433) that for $T > T_c$

$$\chi_{||} = \chi_\perp = \frac{\chi_c}{(K_c r_1)^2} \qquad 7.9a$$

where

$$K_{||} = K_\perp = K_c \; ;$$

$$\Lambda = \frac{r_1^2}{\chi_c} \qquad 7.9b$$

$$\chi_c = \frac{g^2\mu_B^2 S(S+1)}{3K_B T_c} \quad ; \quad r_1^2 = \frac{J^{(2)}}{6J^{(0)}} \quad ; \qquad 7.9c$$

$$K_c^2 = \frac{6J^{(0)}}{J^{(2)}} \frac{T-T_c}{T_c} \qquad 7.9d$$

and $J^{(n)} \equiv \sum_r r^n J(r)$.

Men'shikov et al.(554) suggest that although eq.(7.7) applies to an ideal ferromagnet it may also be valid well below T_c if magnetization fluctuations happen to exist in the magnetic system. Owing to concentration fluctuations magnetization fluctuations occur in alloys and in such cases the longitudinal susceptibility becomes dependent on the longitudinal magnetization and in the low temperature limit one obtains the Marshall formula (eq.(5.6)). If $\left(\frac{d\sigma}{d\Omega}\right)_0$, $\left(\frac{d\sigma}{d\Omega}\right)_{\parallel}$ and $\left(\frac{d\sigma}{d\Omega}\right)_{\perp}$ are respectively the forward cross-sections in the absence of a magnetic field and with a field applied parallel and perpendicular to the scattering vector then from eq.(717) it may be shown (554) that for $T < T_c$

$$\left(\frac{d\sigma}{d\Omega}\right)_0 - \left(\frac{d\sigma}{d\Omega}\right)_{\parallel} = \frac{146}{3} K_B T \left\{\chi_{\parallel} - \chi_{\perp}\right\} \; ; \qquad 7.10a$$

$$\left(\frac{d\sigma}{d\Omega}\right)_0 - \left(\frac{d\sigma}{d\Omega}\right)_{\perp} = -\frac{73}{3} K_B T \left\{\chi_{\parallel} - \chi_{\perp}\right\} \qquad 7.10b$$

$$\left(\frac{d\sigma}{d\Omega}\right)_{\perp} - \left(\frac{d\sigma}{d\Omega}\right)_{\parallel} = 73 K_B T \left\{\chi_{\parallel} - \chi_{\perp}\right\} . \qquad 7.10c$$

From eq.(7.8) and the observed difference cross-sections the longitudinal and transverse correlation lengths were calculated. At a given temperature these lengths were found to increase with decreasing Ni concentration but for Fe 35% Ni the correlation lengths were almost constant at $\sim$ 9Å until close to T_c where $K_{\parallel}^{-1}$ increased (to $\sim$11Å) while $K_{\perp}^{-1}$ decreased. The

observed behaviour of $K_{\parallel}^{-1}$ appears to corroborate the earlier finding of Komura et al.(715).

Finally Komura et al.(716) have recently remeasured the small angle scattering from a single crystal of Fe 35% Ni in the temperature range from 298K to 695K with a magnetic field of 6.2KOe applied both parallel and perpendicular to the scattering vector. Both $\left(\frac{d\sigma}{d\Omega}\right)_{\perp}$ and $\left(\frac{d\sigma}{d\Omega}\right)_{\parallel}$ exhibited a maximum for very small κ at 453K which is significantly below T_c ($\simeq$ 500K). Above T_c the scattering intensity was better fitted by a Lorentzian rather than by a Gaussian (eq.(7.6)) in contrast to a previous observation (715). Surprisingly the inverse correlation length obtained from the Lorentzian fit was large ($\sim$ 11Å) and appeared to be independent of temperature for $T > T_c$. However, since it was not possible to isolate the elastic magnetic diffuse scattering the analysis given by these authors may be questionable.

7.3 Inferences that can be made from Existing Experimental Results

From the experimental data summarized above, we can draw the following conclusions.

(i) As Fe is gradually added to Ni there is a change in magnetic character from the "strong" ferromagnetism of pure Ni to "weak" ferromagnetism at $\sim$ 75% Ni (682) and ultimately to a non-ferromagnetic regime at $\sim$ 25% Ni. Thus we believe that a magnetic phase transition occurs near the latter concentration. The phase transition occurs mainly because J_{Fe-Fe} is antiferromagnetic in this alloy system as deduced from measurements of the spin wave energies of FeNi alloys (718) and from high pressure studies of Fe 30% Ni

(719). Mossbauer effect (606,644-7,662-3), thermal neutron diffraction (712-3), magnetization - exchange anisotropy and displaced hysteresis loops (647,684-5) - and ultrasonic (397, 705-6) studies all show the existence of some antiferromagnetic order but this probably occurs in isolated small volume elements and we do not think that there is a direct transition from ferromagnetic to antiferromagnetic order at $c \simeq 25\%$ Ni. Instead we suspect that if it were possible to stabilize the fcc phase in bulk samples near the critical composition a spin-glass regime would separate the ferromagnetic and antiferromagnetic regions. Such a spin-glass region exists in $Y_6(Fe_{1-c}Mn_c)_{23}$ for $0.4 \lesssim c \lesssim 0.7$ (720), in CrFe for $14 < c < 19\%$ Fe (Rainford, private communication) and probably in $Fe_{65}(Ni_{1-c}Mn_c)_{35}$ for $0.243 \lesssim c \lesssim 0.295$.

It may be necessary to emphasize here that although $J_{Fe-Fe} < 0$ in fcc FeNi alloys it is clearly not necessarily true for all fcc alloys of Fe as otherwise there would be no ferromagnetism in say AuFe. It is better to assume that J_{Fe-Fe} is a function of the Fe-Fe separation and can therefore be ferromagnetic or antiferromagnetic depending on the lattice constant of the alloy. In section 2.3 we used the FeRh system near the equiatomic composition to fully illustrate this point; we also referred to the AuFe system and suggested that at some Fe concentration (well into the ferromagnetic regime) the lattice constant will decrease below a critical value so that J_{Fe-Fe} becomes antiferromagnetic. Colling and Carr (721) have given a physical argument, based on Zener's theory of ferromagnetism, to support the contention that J_{Fe-Fe} is a function of distance and more recently Kummerle and Gradmann (590) have reported some direct experimental confirmation of this. These authors observed that ferromagnetic

order occurs in γ-Fe films where the lattice constant, a_o, is 3.615Å whereas in γ-Fe precipitates with $a_o = 3.58$Å antiferromagnetism occurs.

(ii) The fcc FeNi system is magnetically inhomogeneous reflecting the existence of local environment effects caused essentially by statistical concentration fluctuations. These local environment effects are responsible for the distribution of hyperfine fields observed in Mossbauer effect spectra and for the large magnetic small-angle diffuse cross-sections in neutron scattering experiments.

(iii) The alloy system is also structurally (i.e. metallurgically) inhomogeneous since even after annealing at sufficiently high temperatures and quenching atomic short range order based on either $FeNi_3$, FeNi or Fe_3Ni may occur in the appropriate composition regions. The atomic ordering may, of course, be enhanced by suitable heat treatment and/or election irradiation but Fe_3Ni ordering does not occur for bulk samples. In particular in the Invar region ($\lesssim$ 40% Ni) we believe that atomic short range order of both the $FeNi_3$ and Fe_3Ni types may occur.

(iv) As mentioned already, antiferromagnetism occurs in small volume regions below $\sim$ 25K, while the bulk of the sample is still ferromagnetic. We shall suggest that it is only the ordered Fe_3Ni regions which undergo this transition from paramagnetism to antiferromagnetism at low temperatures while other Fe-rich regions remain paramagnetic down to the lowest temperatures.

7.4 Resume of Previous Theories of The Invar Effect

Some of the models or theories hitherto used to describe the Invar effect will now be discussed. An account of these theories has been given by Nakamura (600).

A qualitative explanation of the magnetovolume effects in Invar can be given in terms of the Bethe-Slater curve which is a semi-empirical curve showing the volume dependence of the exchange integral in transition metals and alloys. Now if $\frac{\partial J}{\partial r}$ is positive then a volume expansion may be expected upon the onset of ferromagnetism (see for example, Ref.627). The Invar alloy is located on the Bethe-Slater curve at a point where $\frac{\partial J}{\partial r}$ has its maximum value so that a large positive spontaneous magnetostriction and a large negative value of $\frac{dT_c}{dP}$ can be assumed to follow. Both pure Ni and γ-Fe have smaller and negative values of $\frac{\partial J}{\partial r}$. However, the Bethe-Slater curve itself is crudely qualitative and has not yet been rigorously justified theoretically although this does not mean that it is not physically reasonable. A more serious objection is the fact that it cannot explain the large positive volume magnetostriction observed for some antiferromagnetic alloys such as $Fe_{65}(Ni_{1-c}Mn_c)_{35}$, $c \gtrsim 0.3$ (253) but we can interpret this to mean that there is some other contribution to the spontaneous volume magnetostriction apart from the volume dependence of the exchange integral.

Kondorskii and Sedov's model of "latent antiferromagnetism" (676) is based on the fact that $J_{Fe-Fe} < 0$ while J_{Fe-Ni} and J_{Ni-Ni} are both positive in fcc F-Ni alloys. Since $\bar{\mu}_{Fe} > \bar{\mu}_{Ni}$ addition of Fe to Ni will lead to an initial increase of the average magnetic moment. With increasing Fe content the

concentration of near-neighbour Fe atoms increases and local antiferromagnetic alignment of the Fe spins may occur eventually leading to a decrease of both the spontaneous magnetic moment and the Curie temperature. If the antiferromagnetic regions have a smaller volume than the ferromagnetic regions then the magnetic contribution to the volume of the alloy will decrease with increasing temperature as more spins become antiferromagnetically aligned. The negative values of $\frac{\partial M_{oo}}{\partial P}$ and $\frac{dT_c}{dP}$ can also be similarly explained. Sidorov and Doroshenko (614) and Dubinin et al. (594) have incorporated the above ideas into a molecular field theory that also takes into account the statistical distribution of the atoms and obtained the concentration dependence of both the spontaneous magnetic moment and the Curie temperature and also the temperature dependence of the magnetization all of which are in good quantitative agreement with experiment.

Based on the study of the $\alpha \longleftrightarrow \gamma$ transformation in pure Fe Kaufmann et al.(722) suggested the existence of two electronic states of γ-Fe , γ_1 and γ_2 . γ_1-Fe is intrinsically antiferromagnetic and has a small moment ($\sim 0.5 \mu_B$) and a lattice constant of $\sim$ 3.54Å; γ_2-Fe is ferromagnetic with a large moment ($\simeq 2.8 \mu_B$) and a larger lattice parameter ($\simeq$ 3.64Å). Weiss (723) extended this suggestion to Invar alloys and assumed that for c $\leq$ 30% Ni γ_1-Fe is the ground state whereas for alloys with more Ni γ_2-Fe is the ground state. In the latter alloys γ_1-Fe is excited as the temperature is increased and as these states have a smaller volume the spontaneous volume magnetostriction is explained. Also the thermal excitation of γ_1-Fe states

explains the rapid decrease of the magnetization with temperature while the increase of these states under pressure accounts for the large negative pressure dependence of M_{oo} and T_c.

According to Zener's theory of ferromagnetism two competing exchange interactions exist in a metal, namely, an indirect ferromagnetic coupling of localized spins through the conduction electrons in the metal and a direct antiferromagnetic coupling due to the overlap of neighbouring d-wavefunctions. The ferromagnetic coupling is only weakly dependent on strain because it is relatively long ranged while the indirect coupling is strongly dependent on strain. Among the 3d transition metals the size of the d-shell decreases along a period (i.e. left to right) so that for a given interatomic distance the antiferromagnetic exchange interaction between Fe atoms is greater than for Ni atoms. Thus in fcc FeNi alloys the overlap of Ni atoms is negligible whereas that of Fe atoms is large enough to give a net antiferromagnetic coupling at a sufficiently high Fe concentration. However, the important point in the above argument is that the magnitude and sign of the exchange interaction between similar (transition metal) atoms is a critical function of their separation. From the foregoing Colling and Carr (721) argue that parallel spins on neighbouring Fe atoms are unfavourable with respect to the highly strain dependent direct coupling and therefore repel one another but antiparallel spins will attract. Thus ferromagnetic ordering causes the lattice to expand at low temperatures and consequently up to $\sim T_c$ a contraction is produced with increasing temperature. The spontaneous volume magneto-

striction will increase with increasing amounts of Fe until the concentration is reached where antiferromagnetic coupling of near-neighbour Fe atoms becomes dominant.

One unacceptable point about all the models so far outlined is that they always predict a lattice contraction for antiferromagnetic ordering whereas a lattice expansion has been observed for some antiferromagnetic alloys (253). However, as already noted, it could well be that some other causes of volume magnetostriction may be equally or even more important than the exchange contribution.

There have also been attempts to explain the origin of the Invar effect on the itinerant electron model of ferromagnetism. In this connection we do not think that it is useful to discuss any models that are based on the rigid band concept such as those of Shimizu and Hirooka (724-6), Katsuki (727) and Mizoguchi (728) because it is now obvious that such a concept is neither a meaningful approximation even for alloys of neighbouring elements in the periodic table nor is it consistent with current theories of the single impurity limit of the dilute alloy problem (681). The coherent potential approximation (CPA) is an attempt to introduce a more realistic band model and has been applied to the fcc FeNi system (681). The calculated values of the individual moments at Fe and Ni sites are in fair agreement with existing data and it is also shown that ferromagnetism becomes unstable at $\simeq$ 35% Ni (i.e. in the Invar region).

Following the observation by Bolling et al.(396) that eq.(7.3) appears to be valid Mathon and Wohlfarth (395) suggested that fcc FeNi alloys were weak itinerant ferromagnets (WIF) and have since proceeded to show how the various

properties of these alloys, particularly the magnetovolume effects, can be understood on the basis of the proposed model (240, 254, 332, 729, 730). However, we have already criticized the theory of weak itinerant ferromagnetism (section 2.7) pointing out in the process that many of the characteristics which are supposed to be peculiar to WIF are just the thermodynamic consequences of a ferromagnetic → non-ferromagnetic phase transition which occurs as a function of composition. Moreover, the experimental data reviewed above in section 7.2) clearly indicate that FeNi alloys in the Invar region are both magnetically and metallurgically inhomogeneous and therefore cannot, by definition, be weak itinerant ferromagnets. It should also be noted that the WIF model is partly based on the incorrect rigid band approach to the magnetism of transition metals.

Since the experimental results, particularly of Mossbauer effect and neutron diffraction studies, have shown the inhomogeneity of FeNi Invars it is not surprising that a number of explanations of the Invar effect has been based on such inhomogeneity. One such model is that of concentration fluctuations first proposed by Kachi et al. (731) and subsequently used to discuss some properties of Invar alloys (606,632,709-10). This model assumes that if fcc FeNi alloys were ideally homogeneous then a <u>first order</u> phase transition from a ferromagnetic to a non-ferromagnetic (paramagnetic or antiferromagnetic) state would occur at $c \leq 29\%$ Ni. For $c > 29\%$ Ni $\bar{\mu}_{Fe} = 2.8\,\mu_B$ and $\bar{\mu}_{Ni} = 0.6\,\mu_B$ independent of composition while below this composition $\bar{\mu}_{Fe} = 0 = \bar{\mu}_{Ni}$. However, owing to statistical composition fluctuations, the predicted discontinuous transition is smoothed out into a gradual one. In order to quantify these statistical

fluctuations the authors then assumed that an alloy can be divided into cells containing n atoms each and that in each cell the concentration fluctuations follow either the Gaussian error function i.e.

$$P_G(x) = \frac{h}{\sqrt{\pi}} e^{-h^2x^2} \qquad 7.11$$

where $x \{= c_{Ni} - \langle c_{Ni} \rangle\}$ is the deviation from the average Ni concentration of the alloy and h is a "precision" parameter, or the binomial distribution function

$$P_B(r) = {}^{n}C_r \langle c_{Ni} \rangle^r \{1 - \langle c_{Ni} \rangle\}^{n-r} \qquad 7.12$$

where r is the local number of Ni atoms. h is obtained from the best fit to the experimental values of M_{oo} and then n is determined as that value (=60) for which eq.(7.11) and (7.12) give almost identical distribution functions. For an average alloy composition of 35% Ni this approach gives that the non-ferromagnetic regions constitute about 15.4% of the total volume of the alloy (606) which fraction now appears to be too high (611).

A particular type of inhomogeneity forms the basis of Schlosser's model for Invar alloys (732). It assumes that such an alloy consists of a Ni-rich region which is fully ordered (Ni_3Fe type) and in which the Fe atoms have large moments ($\sim 2.8 \mu_B$) and large atomic volumes and an Fe-rich region with low moments ($\lesssim 1 \mu_B$) and small atomic volumes with a well-defined interface (or transition region) between the Ni-rich and Fe-rich regions. It also assumes that the Fe moment is dependent on its local environment, assuming its maximum value when the Fe atom is surrounded by a minimum number of Ni nearest neighbours, while the Ni moment is

independent of the environment. Thus Fe atoms in the transition region between the Fe-rich and Ni-rich regions have variable moments and volumes whose values are also dependent on external variables. With these assumptions Schlosser was able to give a detailed but qualitative explanation of many Invar properties.

Tomiyoshi et al.(650), Window(654) and Shiga et al.(662) have all suggested models for Invar behaviour based on local environment effects. According to Tomiyoshi et al.(650) an Fe atom has zero moment if it has nine or more nearest neighbour Fe atoms but the Ni moment is again assumed to be independent of local environment effects. Shiga et al.(662) improved this model by taking into account the effect of second or further near neighbours and the possibility of antiferromagnetic coupling between some Fe spins. They therefore suggested that (i) an Fe atom is magnetic when it has more than N nearest neighbour Ni atoms; (ii) when it has N Ni nearest neighbour atoms it is magnetic if and only if it has more than M magnetic Fe atoms in its immediate neighbourhood; such Fe atoms are said to be "critical". Using a molecular field approach the authors obtained the best fit to $M_{OO}(c)$ with N=M=3. Furthermore, the "critical" Fe atoms are assumed to lose their magnetic moments above T_C which event, according to Shiga (733-5), should lead to a decrease of atomic volume and hence account for the spontaneous volume magnetostriction of these alloys. In support of this latter idea Shiga et al.(662) showed that the concentration dependence of the spontaneous volume magnetostriction is proportional to the concentration of the critical Fe atoms.

The model proposed by Window (650) is essentially similar to the preceding ones since it also allows for both

magnetic and non-magnetic (but polarizable) Fe atoms but the minimum number of Ni nearest neighbour atoms required for an Fe atom to be magnetic is only five. Owing to the possibility of giant moments occurring through the polarization of nearly magnetic Fe atoms the author compared Invar alloys to PdFe and CuNi giant moment alloys and attempted a quantitative explanation of some prominent Invar characteristics; however, his subsequent Mossbauer work (659) failed to confirm the simple expectations of his model for FeNi samples containing more than 32% Ni.

Finally Billard and Natta (736) and Natta (737) have also proposed a semi-microscopic theory of Invar behaviour which incorporates some features of Weiss's two γ-Fe states model and Kachi and Asano's model of conentration fluctuations in a generalized Landau theory. The authors reported some theoretical and experimental evidence which may be interpreted as showing tunnelling between paramagnetic and ferromagnetic states.

7.5 Neutron Scattering Results and Analysis of Data

(a) Results

The elastic diffuse magnetic scattering of neutrons from Fe 32.3, 35 and 38% Ni, $Fe_{63}Ni_{33}Rh_4$ and Fe 50% Ni alloys have been measured. For Fe 35, 38% Ni measurements were made at room temperature using both the Crilth and the room temperature magnet (RTMAG) and at helium temperature, using the Glopper cryostat (see chapter 4). For the 32.3% Ni alloy no measurements were made at 4.2K because of the possibility of a martensitic transformation occurring before this temperature is reached (the martensite-start temperature

for this alloy is about 125K (617)). For the Rh-doped Invar the neutron scattering was measured at room temperature with the RTMAG only and at 4.2K with the cryostat while for Fe 50% Ni it was only possible (owing to neutron beam time limitations) to carry out a single measurement at a specimen angle of 30° with the RTMAG.

We briefly recall that the crilth is a light electromagnet which is alternately rotated through 90° so that the magnetization vector (which is in the plane of the specimen) is alternately parallel and perpendicular to the scattering vector. The difference cross-section obtained is thus the maximum switchable. Both the RTMAG and cryostat employ the "field-off-field-on" method with vertical and horizontal fields respectively. The difference counts are then normalised to give the maximum switchable cross-sections.

The magnetic cross-sections, which in all cases are the maximum switchable, are shown in figs. 7.8-7.11. A number of observations about the data can be made immediately.

(i) With the exception of the Fe 50% Ni alloy both the crilth and cryostat data exhibit sharp forward peaks which are similar to those observed for PtCo, PtFe and NiRh alloys in the critical concentration region for the onset of ferromagnetism. Such peaks are characteristic of an inhomogeneous distribution of magnetization.

(ii) For $\kappa \gtrsim 0.4\text{Å}^{-1}$ the RTMAG data agree with the crilth data (both having been determined at room temperature). However, at small angles the RTMAG data fall off very rapidly and, in fact, become negative at the smallest angles (not shown on the diagrams). This fall-off indicates that there is an additional contribution to the RTMAG cross-

Fig. 7.8: $\frac{d\sigma}{d\Omega}$ vs κ for Fe 32.3% Ni
Inset shows the cross-section at the largest κ .

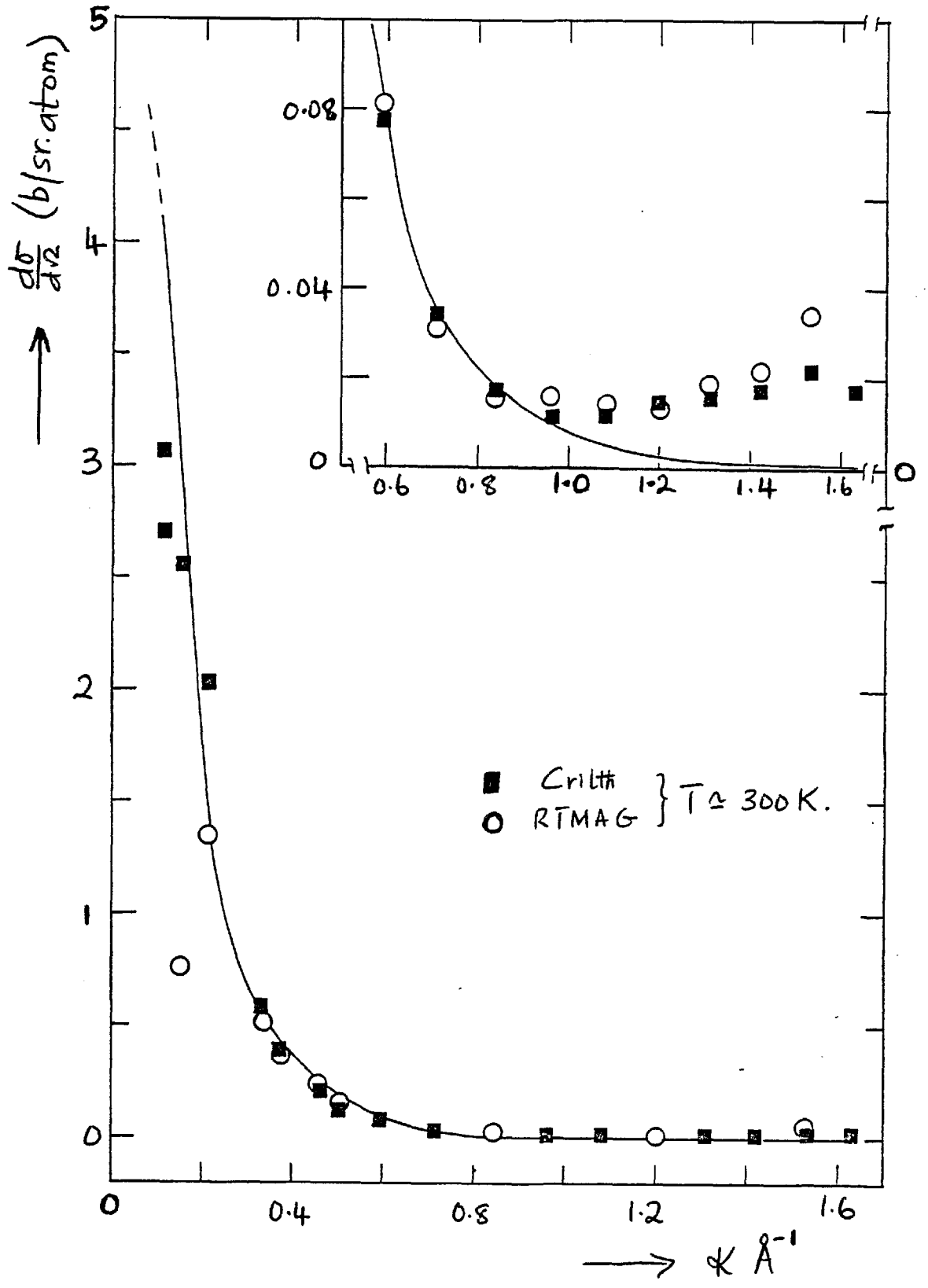

Fig. 7.9: $\frac{d\sigma}{d\Omega}$ vs $\mathcal{K}$ for Fe 35% Ni.

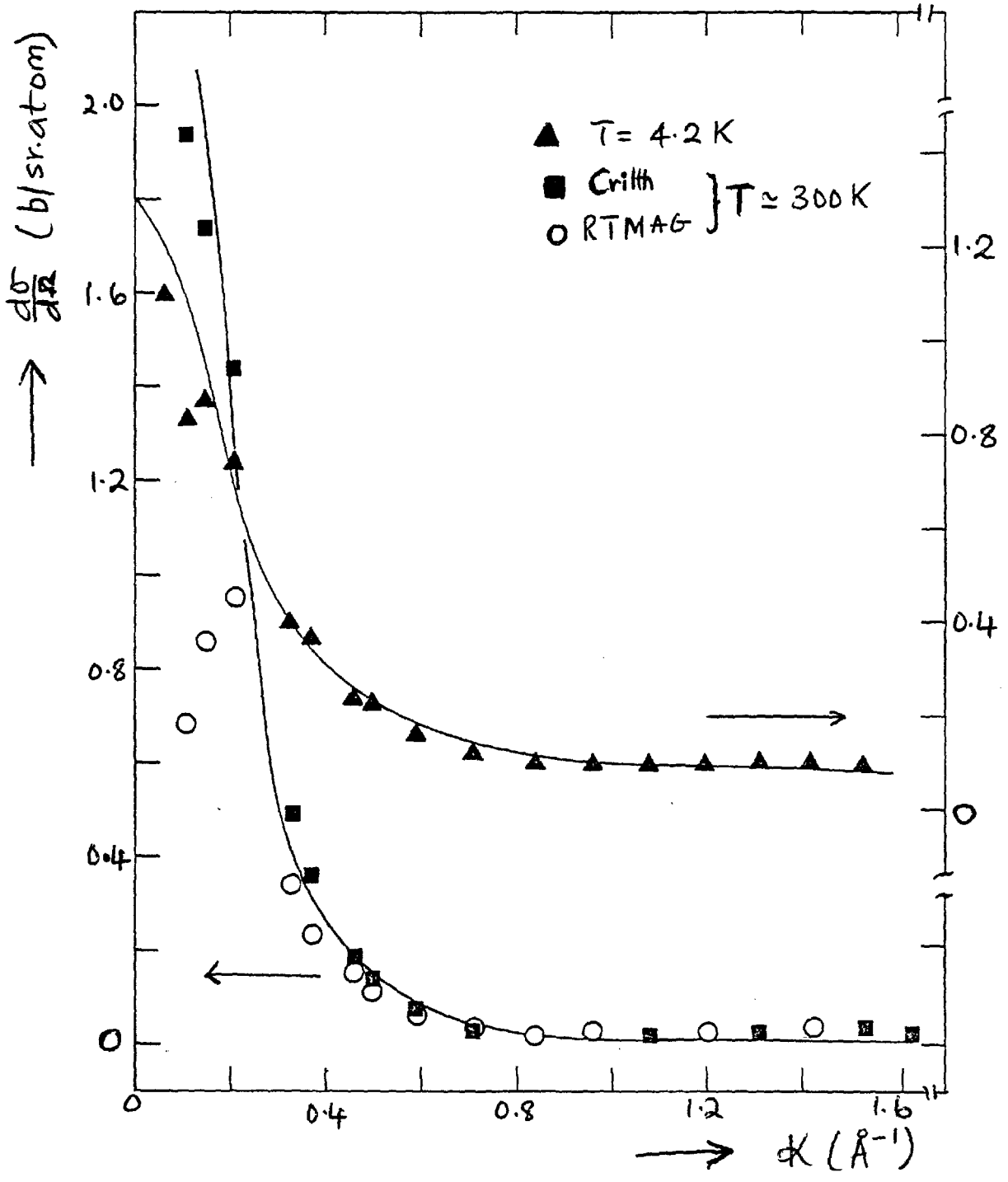

Fig. 7.10: $\frac{d\sigma}{d\Omega}$ vs K for Fe 38% Ni

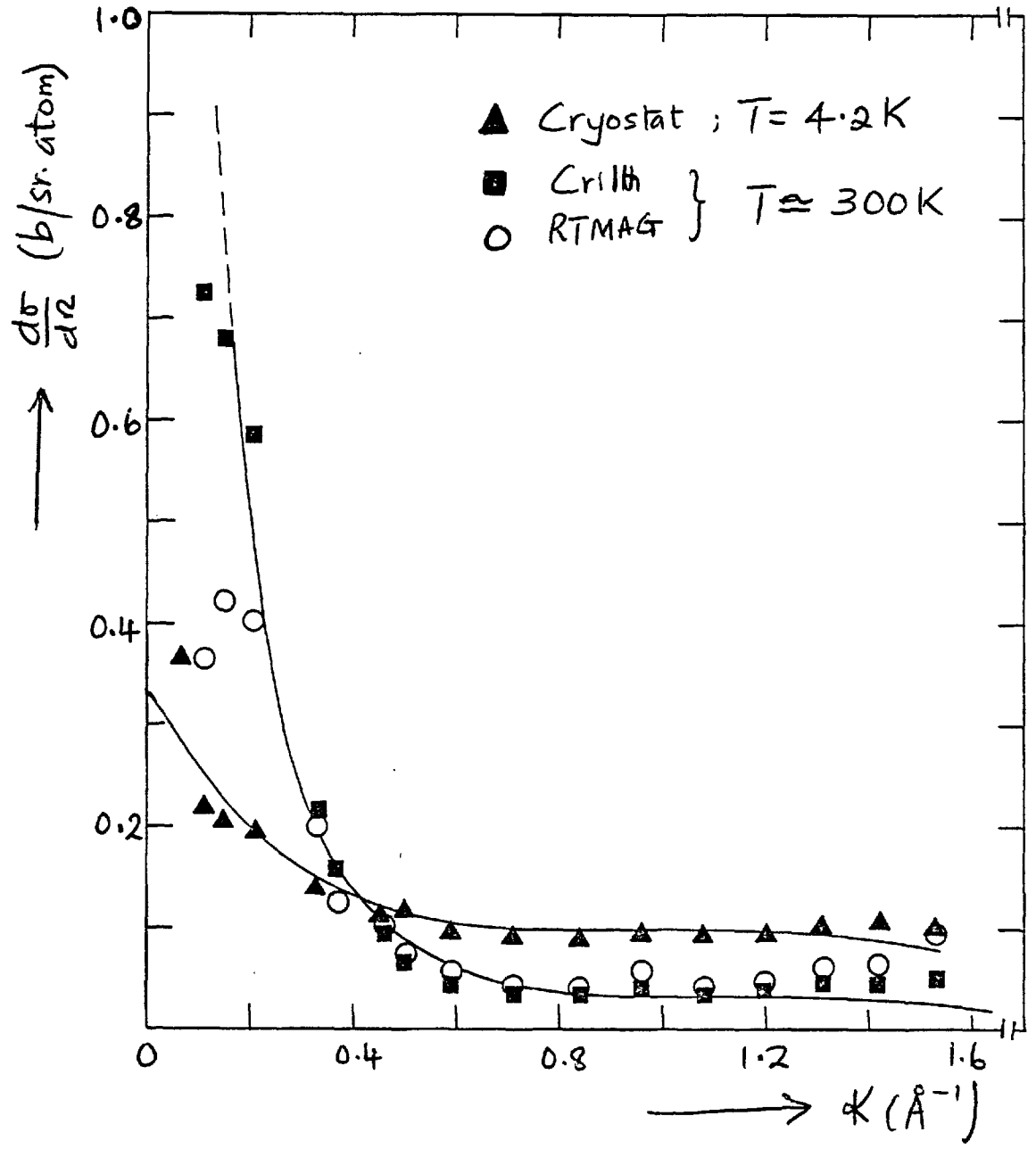

Fig. 7.11: $\frac{d\sigma}{d\Omega}$ vs κ for Fe 50% Ni and $Fe_{36}Ni_{33}Rh_4$ The solid line through the data points for 50% is merely a guide to the eye while the dotted line through the crilth data points for the Rh-doped invar is the fit to the corresponding data for Fe 35% Ni.

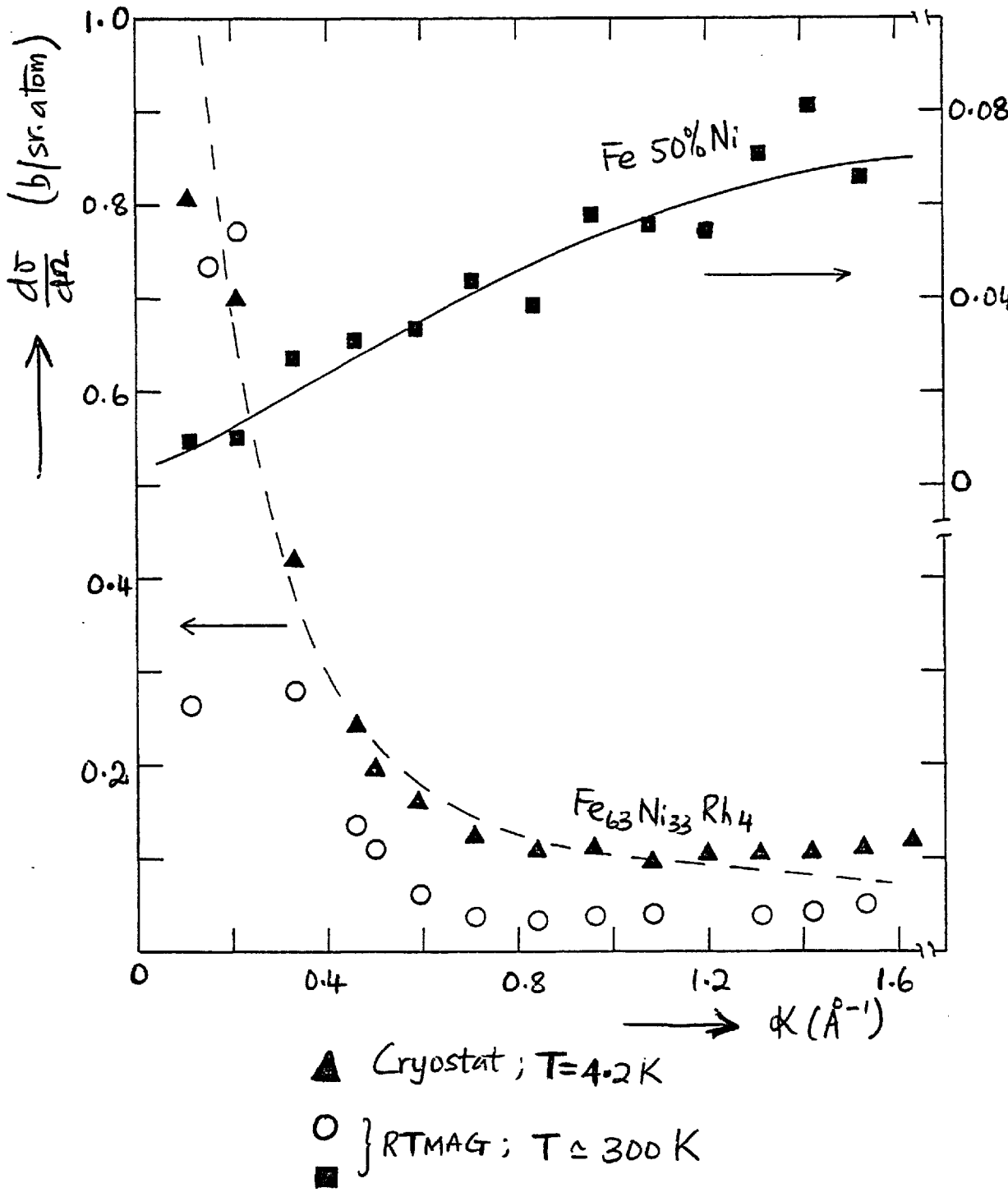

sections at small angles which has the opposite sign to the large angle cross-section.

(iii) The cross-sections exhibit a marked dependence on temperature in those cases where measurements have been made at two temperatures. The forward cross-sections at 4.2K are much smaller while the large angle cross-sections are significantly bigger than the corresponding cross-sections at room temperature. The observed behaviour is qualitatively in agreement with that expected from the temperature dependence of the spontaneous magnetization.

(iv) For Fe 50% Ni the cross-section dips in the forward direction as observed for other FeNi alloys containing more than about 40% Ni (435,542-4). A similar dip has also been observed for Pt 5 and 10% Fe (see section 5.3) and for PdMn alloys containing $\gtrsim$ 1% Mn (738) and has been attributed to either magnetic short range order (435, 542-4,738), which in all these systems probably duplicates the positional short range order, or to antiferromagnetic correlations between some of the constituent magnetic moments (738). Although there is yet no direct proof nevertheless, we suspect that there is a correlation between antiferromagnetic solute-solute interactions and the occurrence of short range atomic order, as in the FeNi, PtFe and PdMn systems mentioned above.

Overall the present data for the FeNi Invar alloys appear to be significantly larger than those of Men'shikov et al.(544) but the crilth forward cross-section for Fe 35% Ni is in good agreement with that determined by Komura et al. (709). However, we believe that the present data are probably more accurate than the previous results not only

because the use of long wavelength neutrons eliminates the need for multiple scattering corrections but also because an energy analysis, even if crude, ensures that only the strictly elastic (or quasi-elastic) scattering is observed. Thus there is not an additional (i.e. to the multiple scattering corrections) uncertainty about a possible contribution to the small angle cross-section from spin wave scattering.

(b) Analysis of Data

Since all the cross-sections have been obtained from difference counts (either field off-field on or field parallel and perpendicular to the scattering vector) we must rule out any contribution due to scattering from antiferromagnetic clusters (or paramagnetic voids) as given by eq.(7.6). Such scattering can only add to the small angle nuclear scattering although there could be a small magnetic contribution arising from the polarization of these paramagnetic voids when a large magnetic field is applied.

Local environment effects, which we have seen are important in this alloy system (as indeed in many other systems) would dictate the use of the Marshall model in analysing the data but we must express our reservations as to whether such a formalism which was developed strictly for strongly ferromagnetic hosts with dilute concentration of solutes can be applied to concentrated alloys in which what constituent is the host or solute is a matter of choice. Also the reported observation of critical scattering over a wide temperature range (554) makes it necessary for an allowance for it to be made especially with respect to the crilth and RTMAG data obtained at room temperature where for

$c \lesssim 35\%$ Ni $T/T_c \gtrsim 0.6$.

However, we do not completely accept the suggestion made by Men'shikov et al.(554) that the occurrence of critical scattering over a wide temperature range in some alloys is due to magnetization fluctuations caused by concentration fluctuations. In section 3.3 it was shown that

$$\frac{d\sigma}{d\Omega} = 73 \langle (\delta M)^2 \rangle$$ (eq.(3.45) and (3.48)

with $\sin\alpha = 1$) where δM is the magnetization fluctuation. This fluctuation can result from either concentration or thermal fluctuations and since these are essentially independent in origin it may be assumed, to a first approximation, that their average contributions are additive, i.e.

$$\langle (\delta M)^2 \rangle = \langle (\delta M)^2 \rangle_c + \langle (\delta M)^2 \rangle_T \qquad 7.13$$

in an obvious notation. The first term in eq.(7.13) has been considered in some detail in the preceding chapters (3,5 and 6) and, in general, for a dilute binary alloy, it is given by

$$\langle (\delta M)^2 \rangle_c = c(1-c)\Gamma^2(K) + c f_i^2(K) \langle (\delta\mu_i)^2 \rangle + (1-c) F_h^2(K) \langle (\delta\mu_h)^2 \rangle$$

(eq.(5.6)) where

$$\Gamma(K) = F_i \bar{\mu}_i - F_h \bar{\mu}_h + c F_i H(K) + (1-c) F_h G(K) \cdot$$ (eq.(5.7)).

In the ensuing discussion we shall refer to this scattering simply as the ferromagnetic scattering. In the critical concentration region for the onset of ferromagnetism the above formulae do not apply to the unpolarized neutron scattering cross-sections; instead there exist concentration-induced critical fluctuations of the long range order parameter so that

$$\langle (\delta M)^2 \rangle_{c\sim c_f} \sim c(1-c)\chi_c(\vec{K}) + c(1-c)\left\{F_i\bar{\mu}_i - F_h\bar{\mu}_h\right\}^2 + cF_i^2\langle(\delta\mu_i)^2\rangle + (1-c)F_h^2\langle(\delta\mu_h)^2\rangle$$

(eq. (3.135)) valid at T=0, with $\chi_c(0) \propto |c-c_f|^{-1}$. Thus critical scattering also occurs at this phase transition point. $\langle (\delta M)^2 \rangle_c$ may, however, be temperature dependent not because of statistical concentration fluctuations (as long as the alloy is initially as disordered as it can be made by suitable heat treatment) but because the average projection of the atomic moments in a direction (say the z-direction) specified by an applied magnetic field is temperature dependent. Thus

$$\bar{\mu} \equiv \bar{\mu}(c,T) = c\bar{\mu}_i^z(c,T) + (1-c)\bar{\mu}_h^z(c,T) \qquad 7.14$$

and

$$\frac{d\bar{\mu}}{dc} = \frac{d\bar{\mu}}{dc}(c,T). \qquad \bar{\mu}_i^z(T) \text{ and } \bar{\mu}_h^z(T)$$

may be calculated in a mean field theory as attempted by Arkhipov et al. (714) in the case of fcc FeNi alloys. This calculation showed that the forward cross-section is not necessarily monotonic in temperature and also that $\bar{\mu}_{Fe}^z$ decreases relatively rapidly with temperature, the variation resembling closely that of the spontaneous magnetization (suggesting, perhaps, that the spontaneous magnetization is almost entirely due to Fe atoms).

The "direct" contribution, $\langle (\delta M)^2 \rangle_T$, from thermal fluctuations to $\langle (\delta M)^2 \rangle$ is defined as that contribution which would still be present in a pure magnetic metal. It results from <u>thermally induced</u> spatial fluctuations of the order parameter and thus is important near T_c where

$$\langle (\delta M)^2 \rangle_{T\sim T_c} \sim K_B T \chi_T(\vec{K}) \; ; \qquad \left|\frac{T-T_c}{T_c}\right| \leq 0.02 \text{ and}$$

$\chi_{T\sim T_c}(0) \propto |T-T_c|^{-1}$ in a mean field theory. In this case, it is possible for concentration fluctuations to enhance the scattering at the transition point, T_c (717). Also if r_1^2 (defined in eq.(7.9c)) is large, i.e. the exchange interaction is long ranged, then the correlation length K_c (eq.(7.9d)) remains small over a wide temperature range which only implies that the cross-section continues to exhibit a sharp forward peak as a function of ϕ for temperatures well outside the normal critical range. This fact does not, however, affect the width of the transition as determined from a plot of the forward cross-section against T because $\left(\frac{d\sigma}{d\Omega}\right)_0 \propto \chi_T(0) \propto (K_c r_1)^{-2} = \left|\frac{T-T_c}{T_c}\right|^{-1}$, from eq.(7.9d). Thus any broadening of the critical scattering at T_c cannot be accounted for in terms of the range of the exchange interactions.

For alloys where, owing to concentration fluctuations, there exists a distribution of molecular fields especially if the exchange interactions between different atom pairs are widely different thermal fluctuations could have another important effect (i.e. apart from making $\bar{\mu}_i$ and $\bar{\mu}_h$ temperature dependent). Any local ferromagnetic regions for which the effective molecular field $B_{eff} \leq \frac{K_B T}{M_{cl}}$, where M_{cl} is the magnetic moment of the local region, would effectively decouple from the rest of the ferromagnetic matrix and behave essentially as paramagnetic units. As the temperature increases so does the concentration of these uncoupled magnetic clusters, currently referred to also as finite clusters as opposed to the infinite cluster (i.e. rest of the ferromagnetic matrix). The uncoupled clusters give

rise to paramagnetic scattering and as shown below (section 7.6) it is this scattering that is primarily responsible for the apparent broadening of the critical scattering at T_c. If, in addition, the alloy is in a concentration region where $\frac{d\bar{\mu}}{dc}$ is large then the cross-section will remain appreciable down to OK.

From the above discussion it is clear that the elastic diffuse magnetic scattering from an alloy can consist of contributions from critical fluctuations of the order parameter (near either c_f or T_c), paramagnetic scattering by finite magnetic clusters, and from concentration induced but thermally dependent fluctuations of magnetization for concentrations and temperatures outside the phase transition regions (i.e. the ferromagnetic scattering defined above). An exact analysis of such data may therefore be difficult especially if, as in the present experiments, the field geometry used cannot distinguish between paramagnetic scattering and scattering due to critical fluctuations of the order parameter. However, from both the alloy composition and the temperature range of observation it may be possible to guess which contributions that should be dominant.

As the first step in the analysis of our data it has been assumed that the observed scattering consists of the ferromagnetic scattering and, as Men'shikov et al.(554) suggest, the critical scattering at T_c which could persist to lower temperatures. Using eq.(7.10) for the critical scattering we thus have (remembering that all cross-sections are the maximum switchable) that for the crilth data

$$\left(\frac{d\sigma}{d\Omega}\right)^{crilth} = 73\, K_B T(\chi_{11}-\chi_\perp) + 73\, c(1-c)\, \Gamma^2(K) + 73\, c\langle(\delta\mu_{Ni})^2\rangle + 73(1-c)\langle(\delta\mu_{Fe})^2\rangle \qquad 7.15$$

where

$$\Gamma(K) = e^{-0.05K^2}\left\{\bar{\mu}_{Ni} - \bar{\mu}_{Fe} + c\,H(K) + (1-c)\,G(K)\right\} \qquad 7.16$$

and $F_{Ni}(K) \simeq f_{Fe}(K) \simeq e^{-0.05K^2}$. In the crilth the magnetic field is always on and it is reasonable to assume that the field ($\gtrsim$ 5KG) is sufficient to suppress the critical scattering so that

$$\left(\frac{d\sigma}{d\Omega}\right)^{crilth} \equiv \left(\frac{d\sigma}{d\Omega}\right)^{fm} \simeq 73\, c(1-c)\,\Gamma^2(K) + 73\, c\, F_{Ni}^2\langle(\delta\mu_{Ni})^2\rangle + 73(1-c)F_{Fe}^2\langle(\delta\mu_{Fe})^2\rangle. \qquad 7.17$$

Similarly for the RTMAG data

$$\left(\frac{d\sigma}{d\Omega}\right)^{RTMAG} \simeq -73K_B T(\chi_{11}-\chi_\perp) + \left(\frac{d\sigma}{d\Omega}\right)^{fm} \qquad 7.18$$

Since T_c > 300K for all the alloys investigated it is highly unlikely that the critical scattering at T_c will persist to 4.2K, at which temperature the cryostat measurements were carried out. Thus $\left(\frac{d\sigma}{d\Omega}\right)^{cryostat}$ is also given by eq.(7.17) although the parameters are expected to be temperature dependent.

Eq.(7.18) is apparently consistent with the observation that the RTMAG data agree with the crilth data at large angles but are smaller and even negative at small angles.

It is further assumed that both $\langle(\delta\mu_{Ni})^2\rangle$ and $\langle(\delta\mu_{Fe})^2\rangle$ are negligible. This assumption may be justified in the case of Ni for which $\bar{\mu}_{Ni}$ is found to be small but probably not for Fe for which $\bar{\mu}_{Fe}$ is large

and decreases rather rapidly as the temperature is increased. The $\langle(\delta\mu_{Fe})^2\rangle$ term should be more important at room temperature than at 4.2K. Also since both $\bar{\mu}_{Ni}$ and $\bar{\mu}_{Fe}$ are affected by local environment effects we have put

$$c\,H(K) + (1-c)\,G(K) \equiv \phi(K) \simeq \frac{\phi(0)\,K_0^2}{K_0^2 + K^2}$$

as in the case of NiRh (see eq.(6,6)). Thus both the crilth and cryostat data have been analysed using the equation

$$\left(\frac{d\sigma}{d\Omega}\right)^{fm} \simeq 73\,c(1-c)\,e^{-0.1K^2}\left\{\bar{\mu}_{Ni} - \bar{\mu}_{Fe} + \phi(K)\right\}^2 \qquad 7.19$$

The resulting fits are the solid lines through the data points in figs. 7.8-7.10 and the parameters $\phi(0)$, K_0 and $(\bar{\mu}_{Fe} - \bar{\mu}_{Ni})$ are shown in table 7.1. For the cryostat data (T=4.2K) the fits appear to be reasonably good but for the crilth data ($T \simeq 300K$) the fits are very unsatisfactory at large angles.

Table 7.1: Parameters obtained from fitting the crilth ($T \simeq 300K$) and cryostat (T=4.2K) data for FeNi Invar alloys to the Marshall model. The quoted errors represent the statistical and fitting errors only.

	T = 4.2 K			T ≃ 300 K		
c % Ni	$\phi(0)$ μ_B/atom	K_0 Å^{-1}	$\{\bar{\mu}_{Fe} - \bar{\mu}_{Ni}\}$ μ_B	$\phi(0)$ μ_B/atom	K_0 Å^{-1}	$\{\bar{\mu}_{Fe} - \bar{\mu}_{Ni}\}$ μ_B
32.3	=	=	=	19.6 ± 1.2	0.23 ± 0.02	−0.3 ± 0.2
35	6.7 ± 0.5	0.27 ± 0.02	2.2 ± 0.1	15.4 ± 1.6	0.21 ± 0.02	0.6 ± 0.2
38	1.9 ± 0.7	0.16 ± 0.05	2.46 ± 0.06	8.7 ± 1.5	0.19 ± 0.03	1.2 ± 0.1

There is, in fact, one other reason to doubt the applicability of the Marshall model to these data. Earlier polarized neutron measurements have shown that in the fcc FeNi system $\bar{\mu}_{Fe} > \bar{\mu}_{Ni}$ (551); since apparently $\frac{dM_{oo}}{dc} \gtrsim 0$ for $c \leq 38\%$ Ni $\phi(0)$ must be positive and hence $\frac{d\sigma}{d\Omega}$ should become zero for some value of κ, a conclusion which is not borne out by the experimental data. Therefore, too much significance should not be attached to the values of the range parameter, κ_o, in table 7.1 but the values of $\phi(0)$ give useful estimates of the forward cross-sections because the latter do not appear to depend very sensitively on the values of κ_o and $\{\bar{\mu}_{Fe} - \bar{\mu}_{Ni}\}$. For example if we simply put

$$\left(\frac{d\sigma}{d\Omega}\right)^{Critth} \simeq 73\, c(1-c)\, \Gamma^2(\kappa) \qquad 7.20$$

and assume that $\Gamma(\kappa)$ is Lorentzian we obtain $\Gamma(0) = 21.5$, 15.1 and 8.2 μ_B/atom for the 32.3, 35 and 38% Ni alloys respectively which values agree with those shown in table 7.1. The corresponding values of κ_o are 0.20, 0.24 and 0.29 Å^{-1} which shows an opposite concentration dependence. Fig. 7.12 shows the plot of $\Gamma(\kappa)^{-1}$ vs κ^2.

Individual values of $\bar{\mu}_{Fe}$ and $\bar{\mu}_{Ni}$ may be determined in the usual way by combining the values of $\{\bar{\mu}_{Fe} - \bar{\mu}_{Ni}\}$ obtained from the neutron cross-sections at sufficiently large κ with the spontaneous magnetization values. If

$$\Delta\mu(c,T) = \bar{\mu}_{Fe}(c,T) - \bar{\mu}_{Ni}(c,T)$$

and

$$M_o(c,T) = c_{Fe}\,\bar{\mu}_{Fe}(c,T) + c_{Ni}\,\bar{\mu}_{Ni}(c,T)$$

then

$$\bar{\mu}_{Fe}(c,T) = M_o(c,T) + c_{Ni}\,\Delta\mu(c,T) \qquad 7.21a$$

Fig. 7.12: $\Gamma(K)^{-1}$ vs K^2 (eq.(7.20)) for the crilth data.

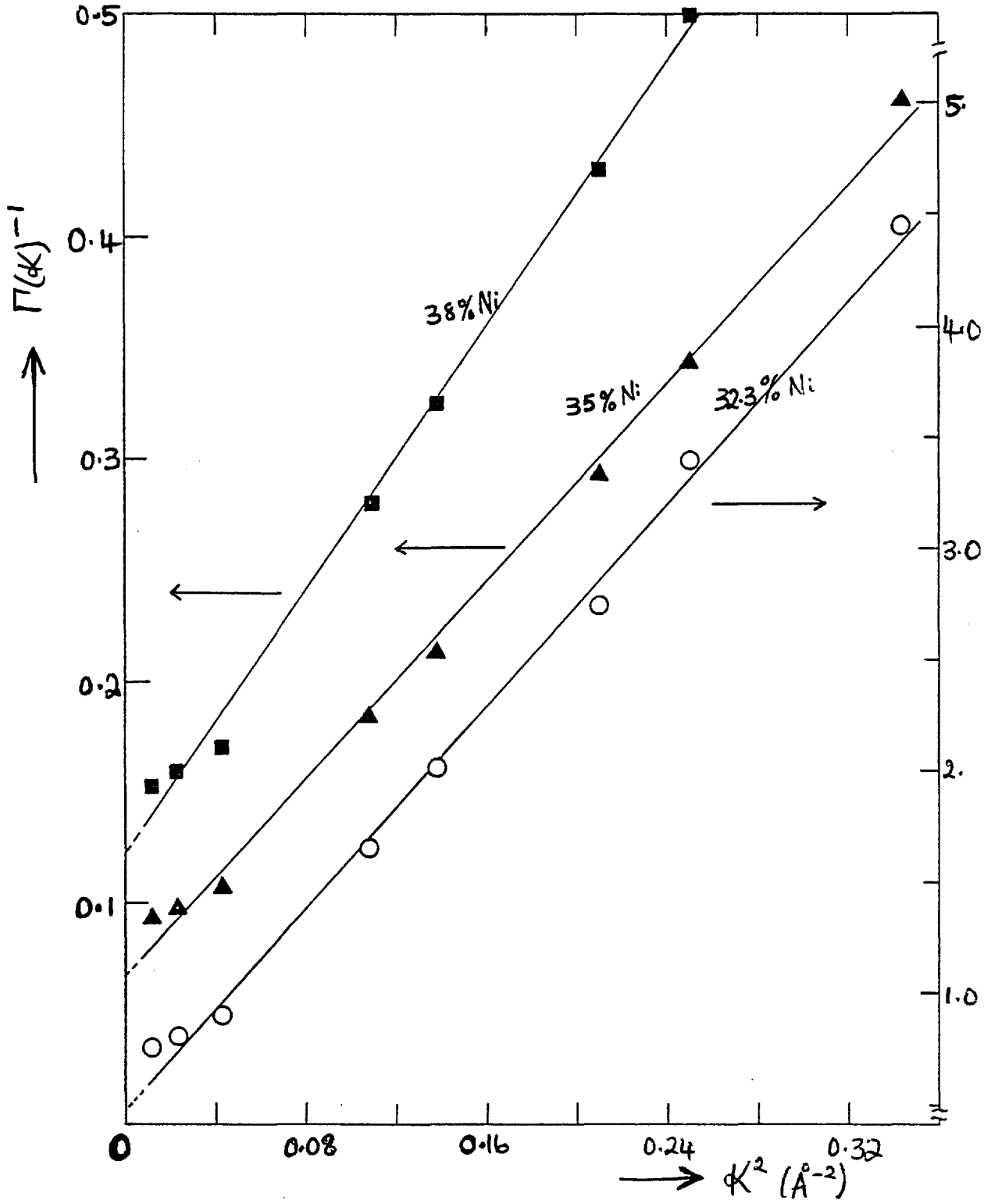

and $\bar{\mu}_{Ni}(c,T) = M_o(c,T) - c_{Fe}\,\Delta\mu(c,T)$ 7.21b

As stated above the fit of the Marshall formula (eq.(7.19)) to the crilth data is very unsatisfactory at large angles so that we do not consider the values of $\{\bar{\mu}_{Fe} - \bar{\mu}_{Ni}\}$ obtained therefrom as reliable. We have therefore used the average values of $\frac{d\sigma}{d\Omega}$ at $K = 1.42\text{Å}^{-1}$ for the crilth and RTMAG data to compute $\{\bar{\mu}_{Fe} - \bar{\mu}_{Ni}\}$ at 300 K. We have also assumed that $M_o(c, T = 4.2\,K) \simeq M_{oo}(c)$ while values of $M_o(c, T \simeq 300\,K)$ have been determined either directly (only for Fe 32.3% Ni) or indirectly by some suitable interpolation (see fig.7.13) from experimentally observed reduced equations of state (i.e. plots of (M_o/M_{oo}) vs T/T_c) obtained by Crangle and Hallam (602). The values of $\bar{\mu}_{Fe}$ and $\bar{\mu}_{Ni}$ obtained at both 4.2 and 300 K are shown in table 7.2.

Table 7.2: Concentration and Temperature Dependence of $\bar{\mu}_{Fe}$ and $\bar{\mu}_{Ni}$ for FeNi Invar Alloys. Only the statistical and fitting errors are quoted. (M_{oo}, M_o in μ_B/atom; $\Delta\mu$, $\bar{\mu}_{Fe}$ and $\bar{\mu}_{Ni}$ in μ_B)

c% Ni	T_c (K)	T=4.2 K	T=300 K
32.3	435	$M_{oo} = 1.45$ $\bar{\mu}_{Fe} = 2.14$* $\bar{\mu}_{Ni} \simeq 0$	$\Delta\mu = 1.22\pm0.07$ $M_o = 0.861$ $\bar{\mu}_{Fe} = 1.26\pm0.02$ $\bar{\mu}_{Ni} = 0.03\pm0.05$
35	512	$\Delta\mu = 2.19\pm0.12$ $M_{oo} = 1.73$ $\bar{\mu}_{Fe} = 2.50\pm0.04$ $\bar{\mu}_{Ni} = 0.31\pm0.07$	$\Delta\mu = 1.56\pm0.03$ $M_o = 1.27$ $\bar{\mu}_{Fe} = 1.82\pm0.01$ $\bar{\mu}_{Ni} = 0.26\pm0.02$
38	586	$\Delta\mu = 2.46\pm0.06$ $M_{oo} = 2.0$ $\bar{\mu}_{Fe} = 2.93\pm0.02$ $\bar{\mu}_{Ni} = 0.47\pm0.04$	$\Delta\mu = 2.02\pm0.05$ $M_o = 1.63$ $\bar{\mu}_{Fe} = 2.40\pm0.02$ $\bar{\mu}_{Ni} = 0.38\pm0.03$

*Estimated value assuming $\bar{\mu}_{Ni} \simeq 0$.

Fig. 7.13: $\frac{M_o}{M_{oo}}$ vs c for given values of T/T_c

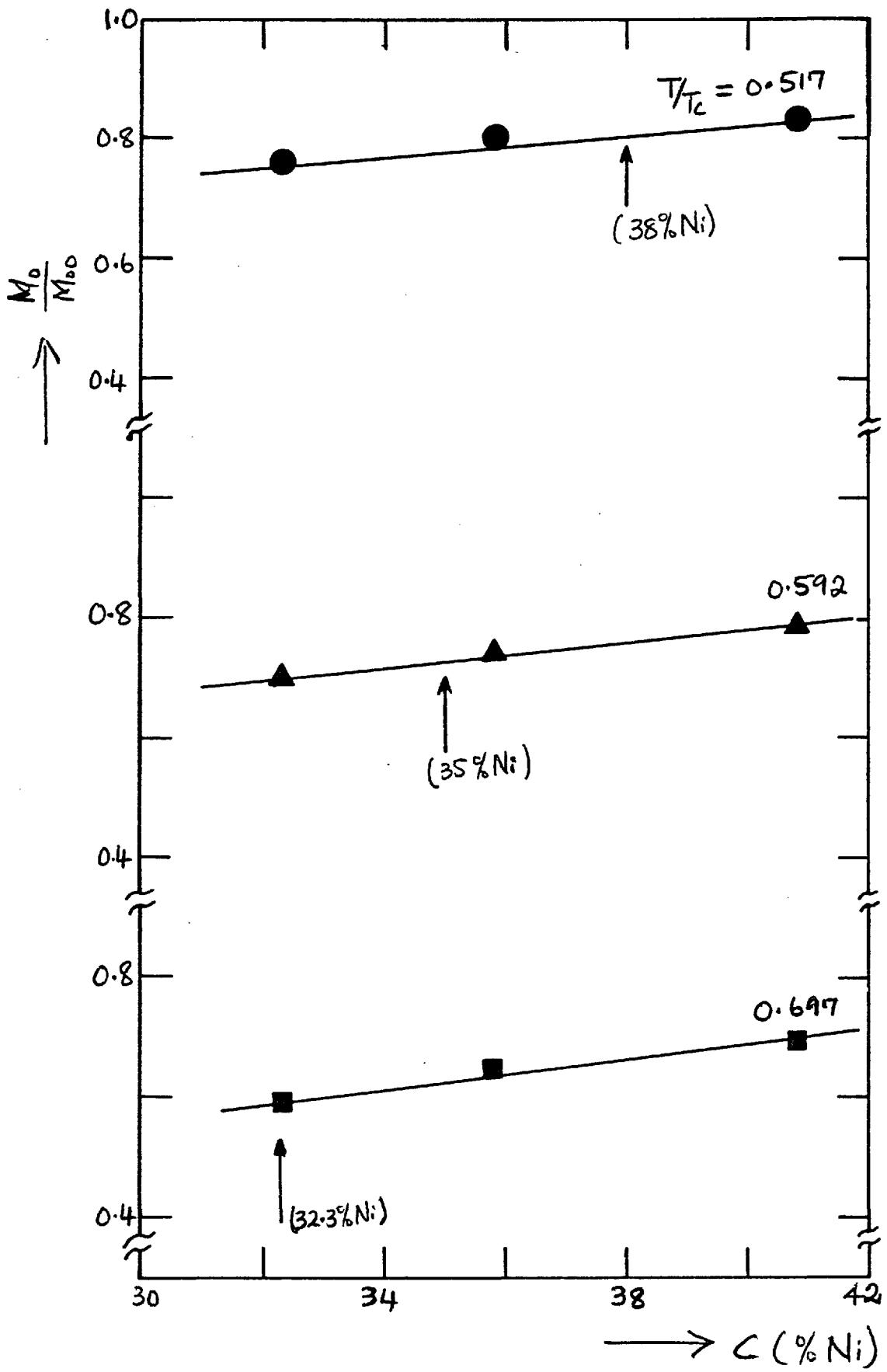

No measurements were made at 4.2K for Fe 32.3% Ni but we have estimated $\bar{\mu}_{Fe}$ at 4.2K by assuming that $\bar{\mu}_{Ni} \simeq 0$. The room temperature measurements show that $\bar{\mu}_{Ni}$ (T $\simeq$ 300K) is only $\simeq 0.03 \mu_B$ and it is unlikely that at 4.2K $\bar{\mu}_{Ni}$ can be much larger.

No analysis of the data for Fe 50% Ni and the single Rh-doped alloy has been made because the data for the 50% Ni alloy do not extend to sufficiently large K for a precise value of $\{ \bar{\mu}_{Fe} - \bar{\mu}_{Ni} \}$ to be determined while the spontaneous moment of the Rh-doped Invar alloy was not measured. It should be noted, though, that the data for the latter alloy closely resemble those for Fe 35% Ni. This is not surprising since this alloy was accidentally prepared as Ni 5% Rh but the starting "Ni" material turned out to be a bar of Fe 35% Ni Invar (see chapter 4). The dotted line through the cryostat data points is the fit of the Marshall formula to similar data for Fe 35% Ni. Thus $\bar{\mu}_{Fe}$ and $\bar{\mu}_{Ni}$ for the two alloys may be similar. Alternatively we may estimate $\bar{\mu}_{Fe}$ from the large angle scattering. For this ternary alloy this scattering is given (550, 739) by

$$\frac{d\sigma}{d\Omega} \simeq 73 C_{Ni} C_{Fe} \{F_{Fe} \bar{\mu}_{Fe} - F_{Ni} \bar{\mu}_{Ni}\}^2 + 73 C_{Fe} C_{Rh} \{F_{Fe} \bar{\mu}_{Fe} - F_{Rh} \bar{\mu}_{Rh}\}^2 + 73 C_{Ni} C_{Rh} \{F_{Ni} \bar{\mu}_{Ni} - F_{Rh} \bar{\mu}_{Rh}\}^2 \qquad 7.22$$

If $\bar{\mu}_{Rh}$ and $\bar{\mu}_{Ni}$ are negligible, which is a plausible assumption since at these compositions $\bar{\mu}_{Ni}$ has been found to be small (see table 7.2) and we have already seen in Chapter 6 that local environment effects are even more severe for Rh, then

$$\frac{d\sigma}{d\Omega} (\text{large } K) \simeq 73 \{C_{Ni} + C_{Rh}\} C_{Fe} F_{Fe}^2(K) \bar{\mu}_{Fe}^2 \qquad 7.23$$

At $\kappa = 1.199 \text{Å}^{-1}$, $\frac{d\sigma}{d\Omega} = 103.32 \pm 1.85$ mb/sr,atom thus, giving $\bar{\mu}_{Fe} \simeq 2.65 \pm 0.05\,\mu_B$ which compares favourably with the value of $2.50 \pm 0.04\,\mu_B$ for Fe 35% Ni considering the approximations made.

Finally, from eq.(7.17) and (7.18) it is expected that

$$\left(\frac{d\sigma}{d\Omega}\right)^{crilth} - \left(\frac{d\sigma}{d\Omega}\right)^{RTMAG} \equiv \Delta\frac{d\sigma}{d\Omega} \simeq 73\,K_B T\,(\chi_{11} - \chi_{\perp}) \qquad 7.24$$

The difference cross-sections are plotted in fig.7.14. If it is assumed that $\chi(\kappa)$ is Lorentzian then $\left(\Delta\frac{d\sigma}{d\Omega}\right)^{-1} \propto \kappa^2$. Instead it is found that for the three Invar alloys $\left(\Delta\frac{d\sigma}{d\Omega}\right)^{-\frac{1}{2}} \propto \kappa^2$ (see fig.7.15). One model which can account for the above observation is that of the paramagnetic scattering of neutrons by magnetic clusters. Suppose that in a ferromagnetic matrix there is a concentration, c*, of magnetic clusters of moment, M_{cl}, which are only weakly coupled to the matrix (in the sense that $B_{eff} \ll \frac{K_B T}{M_{cl}}$ as already stated above) so that they are essentially free to respond independently to external fields. We shall, however, assume that M_{cl} is sufficiently large that a moderate external field (as used in these experiments) can fully align the clusters. If, for a given field geometry, the difference count is taken in such a way that the appropriate ferromagnetic scattering is positive and using eq.(3.25) and (3.29) to obtain the paramagnetic scattering then the total unpolarized neutron cross-sections (maximum switchable) are given by

$$\left(\frac{d\sigma}{d\Omega}\right)^{crilth} \simeq -\frac{73}{2}c^* F_{cl} M_{cl} + \left(\frac{d\sigma}{d\Omega}\right)^{fm}; \qquad 7.25$$

Fig. 7.14: $\Delta \frac{d\sigma}{d\Omega} \left\{ \equiv \left(\frac{d\sigma}{d\Omega}\right)^{crilth} - \left(\frac{d\sigma}{d\Omega}\right)^{RTMAG} \right\}$ vs α.

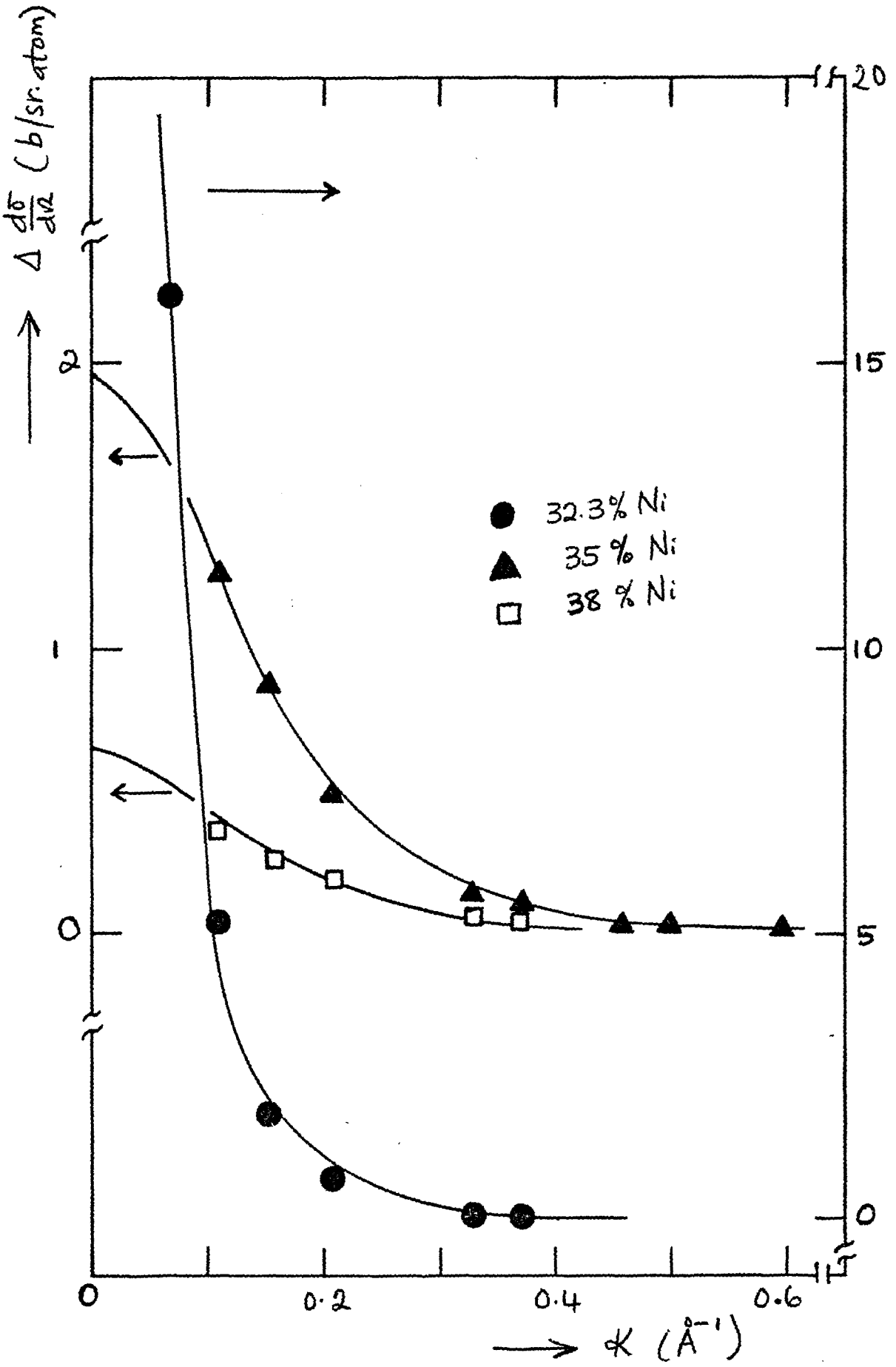

Fig. 7.15: $\left(\Delta \frac{d\sigma}{d\Omega}\right)^{-1/2}$ vs K^2 for FeNi Invar alloys.

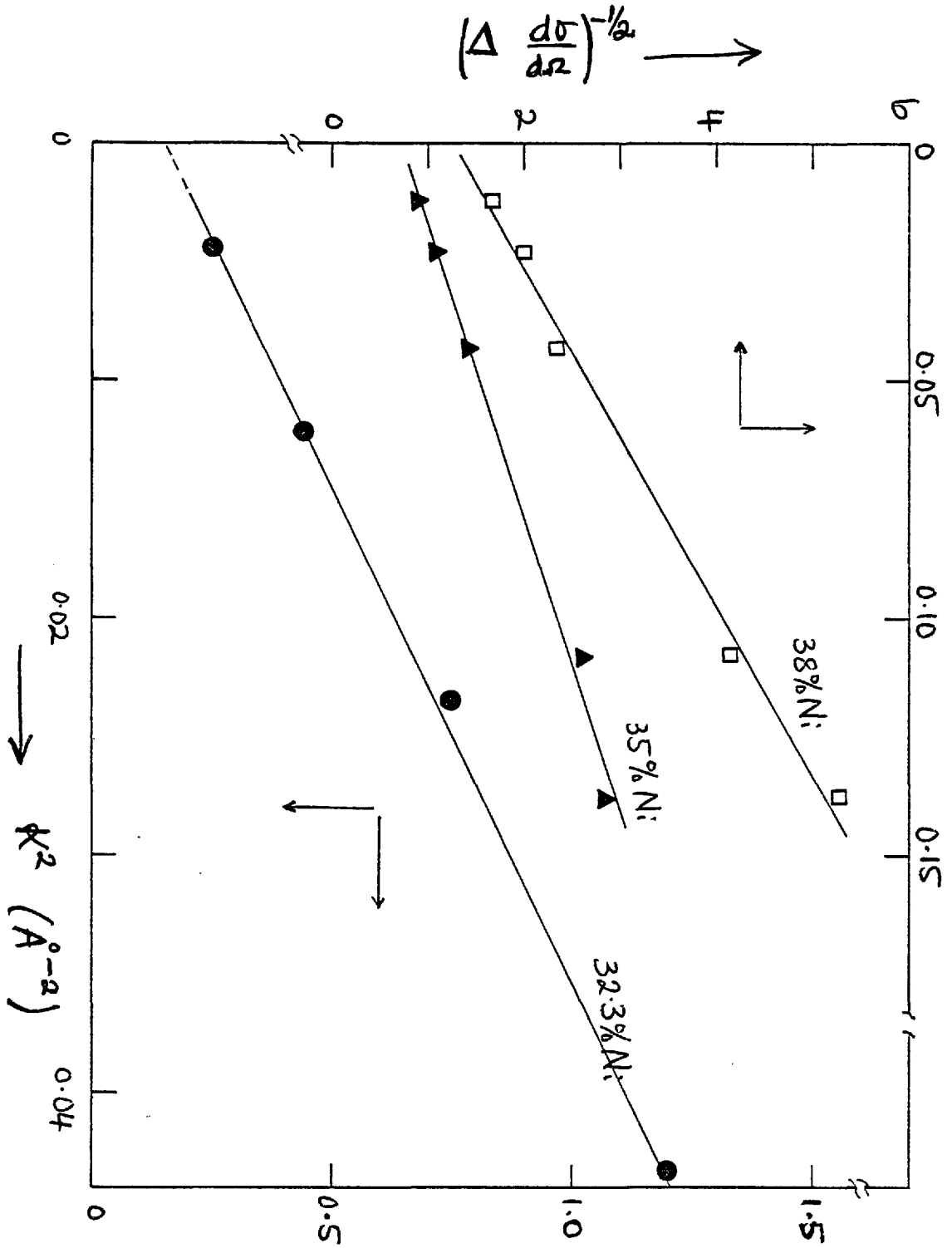

$$\left(\frac{d\sigma}{d\Omega}\right)^{RTMAG} \simeq -219c^*\left\{\frac{2}{3}F_{cl}^2 M_{cl}^2 + \frac{1}{6}F_{cl}M_{cl}\right\} + \left(\frac{d\sigma}{d\Omega}\right)^{fm}; \quad 7.26$$

$$\left(\frac{d\sigma}{d\Omega}\right)^{cryostat} \simeq 73c^*\left\{\frac{2}{3}F_{cl}^2 M_{cl}^2 - \frac{1}{3}F_{cl}M_{cl}\right\} + \left(\frac{d\sigma}{d\Omega}\right)^{fm}; \quad 7.27$$

where F_{cl} is the cluster form factor (eq.(5.16)) and $\left(\frac{d\sigma}{d\Omega}\right)^{fm}$ is given by eq.(7.17). For RTMAG the paramagnetic scattering is large and negative and probably overcomes the ferromagnetic scattering at small angles as experimentally observed. The paramagnetic scattering could also be large in the case of the cryostat and adds to the ferromagnetic scattering. However, it is obviously to be expected that c* should decrease as the temperature decreases so that the paramagnetic scattering at 4.2K may be much smaller than at 300K. For the crilth the paramagnetic scattering is relatively smaller (since it is proportional to M_{cl} and not to M_{cl}^2) but is opposed to the ferromagnetic scattering. From eq. (7.25) and (7.26)

$$\left(\Delta\frac{d\sigma}{d\Omega}\right)_{cl} \equiv \left(\frac{d\sigma}{d\Omega}\right)^{crilth} - \left(\frac{d\sigma}{d\Omega}\right)^{RTMAG} = 146c^* F_{cl}^2 M_{cl}^2 \quad 7.28a$$

$$\simeq 146c^* M_{cl}^2 \left\{\frac{\kappa_1^2}{\kappa_1^2+\kappa^2}\right\}^2 \quad 7.28b$$

where eq.(5.16) has been used in the last step. Thus $\left(\Delta\frac{d\sigma}{d\Omega}\right)_{cl}^{-1/2} \propto \kappa^2$ as shown in fig. 7.15. The solid lines in fig. 7.14 represent the fits of $\left(\Delta\frac{d\sigma}{d\Omega}\right)_{cl}$ to eq.(7.28) and the following parameters are obtained:-

c% Ni	$\left(\Delta \frac{d\sigma}{d\Omega}\right)^{o}_{cl}$ mb/sr. atom	K_1 Å^{-1}
32.3	45000	0.078
35	1950	0.21
38	650	0.21

It is seen that the paramagnetic scattering and cluster radius ($\sim K_1^{-1}$) increase very rapidly for concentrations less than 35% Ni whereas for higher Ni concentrations the cluster radius appears to be constant ($\simeq 4.76$Å, if the clusters are assumed to be spherical). It is not possible to evaluate c* and M_{cl} separately from the present data. However, an estimate of M_{cl} and hence c* may be obtained by assuming that the alloys are completely disordered, calculating the number of atoms in a cube of side $2K_1^{-1}$, and using values of $\bar{\mu}_{Fe}$ and $\bar{\mu}_{Ni}$ given in table 7.2. Thus for Fe 35% Ni with $a_o \simeq 3.59$Å (593), $M_{cl} \simeq 95 \mu_B$ and c* $\simeq$ 0.15%.

An interesting observation is that the cluster model (cf eq.(5.14) or (6.10)) appears to give a better fit, in terms of the value of the goodness of fit parameter, to the cryostat data than the Marshall model. We have not pursued this analysis any further since we do not feel it will give any more useful information.

7.6 Discussion of Results

As observed by previous authors (543-4, 671, 709) the elastic diffuse magnetic cross-sections of FeNi Invar alloys exhibit sharp forward peaks (as a function of the scattering wave vector) characteristic of magnetically

inhomogeneous systems. The forward cross-sections are both concentration and temperature dependent increasing as the temperature and/or Fe content increases. The observed scattering is not due to paramagnetic voids as assumed by Komura et al.(709) since such scattering is approximately independent of the magnitude and direction of an applied field and so cannot contribute to the difference counts.

Since both $\bar{\mu}_{Fe}$ and $\bar{\mu}_{Ni}$ are affected by local environment effects it was not possible to obtain the moment defect parameters for each atom. Instead a single parameter $\phi(\kappa)$ has been used to characterize the local environment effects for both atomic species. At room temperature $\phi(0)$ increases rapidly with decreasing Ni concentration but the range parameter, κ_o, is approximately constant (within the quoted errors) at $\sim 0.21\text{Å}^{-1}$ (see table 7.1). At 4.2K both $\phi(0)$ and κ_o increase systematically with decreasing Ni content.

The individual values of $\bar{\mu}_{Fe}$ and $\bar{\mu}_{Ni}$ at 4.2K are plotted as a function of the Ni concentration in fig.7.16 along with the values obtained by previous authors. With the exception of the measurements of Men'shikov et al.(544) which were carried out at nitrogen temperature all other previous measurements have been made at room temperature and it is not clear that such measurements have been corrected for the temperature dependence of the magnetization. Moreover, as stated earlier (section 7.5a), we believe that the present neutron data are more accurate than the previous ones. From fig.7.16 we can see that $\bar{\mu}_{Fe}$ remains essentially

Fig. 7.16: Concentration dependence of $\bar{\mu}_{Fe}$ and $\bar{\mu}_{Ni}$ for fcc FeNi alloys. The dotted lines through the data points are merely a guide to the eye.

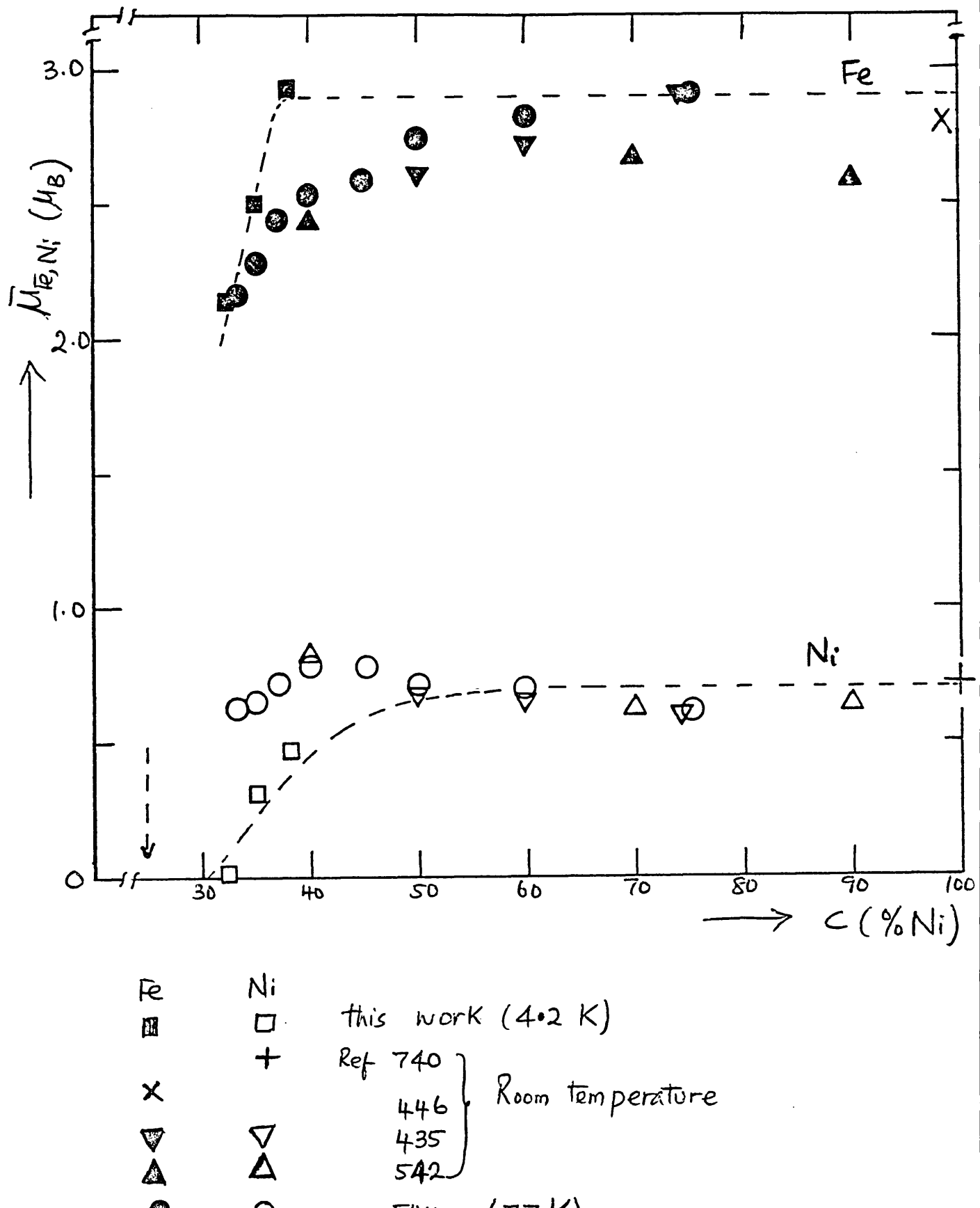

constant at $\simeq 2.9\,\mu_B$ down to $\sim 38\%$ Ni below which it decreases rapidly; but even at 32.3% Ni $\bar{\mu}_{Fe}$ is still slightly greater than $2\,\mu_B$. In contrast it appears that local environment effects are more severe for Ni because $\bar{\mu}_{Ni}$ starts to decrease at $\sim 50\%$ Ni from a nearly constant value of $\sim 0.7\,\mu_B$. The peak in $\bar{\mu}_{Ni}$ at about 40% Ni may be more apparent than real because if we use M_{oo} (instead of M_o) in conjunction with the value of $\Delta\mu$ at room temperature we obtain that $\bar{\mu}_{Ni}$ =0.75, 0.73 and 0.62 μ_B for the 38,35 and 32.3% Ni alloys respectively. These latter values would then agree with previous data (542, 544). The corresponding values of $\bar{\mu}_{Fe}$ are also larger than given in table 7.1. For example for Fe 35% Ni $\bar{\mu}_{Fe}$ would then be $2.28\pm 0.01\,\mu_B$ instead of the value given in the table. It would thus appear that the initial deviation of $M_{oo}(c)$ from a linear dependence on c results from the decrease of the Ni moment for concentrations less than about 50% Ni. The Fe moment is large and constant until the Invar region is actually reached ($\lesssim$ 36% Ni) below which it decreases rapidly. The fact that $\bar{\mu}_{Ni}$ is very small in the Invar region is shown by the fact that at 4.2K the cross-sections at large κ are almost the same for all the alloys investigated at this temperature (N.B. c_{Fe} is approximately constant, $\sim$ 63-65%). Thus the assumption, made in almost all previous theories of the Invar effect (see section 7.4) that $\bar{\mu}_{Ni}$ is independent of local environment effects does not appear to be justified.

The atomic moments are also temperature dependent, particularly that of Fe, but this is only to be expected since the observed values merely represent the average

ordered moments (i.e. μ^z_{Fe} and μ^z_{Ni}) and ideally should tend to zero at T_c with the spontaneous magnetization. What is significant, and therefore, of interest, is the fact that the value of $\bar{\mu}_{Fe}$ at 4.2K ($\simeq 2.5\,\mu_B$) is appreciably greater than its value ($\simeq 1.4\,\mu_B$) at temperatures $T \gtrsim T_c$ as measured by Collins (670). The difference is due to the existence of "critical" or "nearly magnetic" Fe atoms (662). In the ferromagnetic state below T_c such Fe atoms carry an induced moment the magnitude of which increases as the total magnetization increases (i.e. with decreasing temperature).

The occurrence of paramagnetic scattering from "nearly free" or "finite" magnetic clusters is responsible for the apparent broadening of the critical scattering at T_c. Such uncoupled clusters exist because of the existence of a distribution of molecular fields. In pure Ni or Fe a distribution of molecular fields does not occur until close to T_c where the normal critical scattering dominates any paramagnetic scattering contribution. For alloys a wide distribution of molecular fields can exist at temperatures well below T_c owing to local environment effects arising from statistical concentration fluctuations. For example Mossbauer effect spectra (650) have shown that Fe 34.5-46.9% Ni alloys have a distribution of hyperfine fields at room temperature (note that $T_c \gtrsim 498$ K); for a given concentration the distribution of internal fields becomes broader as the temperature is raised while at a given temperature the distribution broadens as the Ni concentration is decreased. Such alloys have "anomalous" M_o vs T curves

in the sense that these curves are much flatter than Brillouin functions (see section 7.2a). The paramagnetic scattering that would be observed in these alloys would make it appear as if critical scattering persisted to very low temperatures (relative to T_c). In addition if $\frac{d\bar{\mu}}{dc}$ is large then the forward cross-section will be large at very low temperatures ($\sim$ 0 K); however, such alloys invariably have a broad distribution of internal fields even at low temperatures so that the diffuse cross-sections of these alloys exhibits a broad maximum at T_c but remains substantial down to the lowest temperatures. In particular close to the critical concentration for the onset of ferromagnetism critical scattering similar to that at T_c should occur and the cross-section should then increase again as $T \longrightarrow$ OK. Unfortunately, owing to the occurrence of a martensitic transformation, the scattering measurements at 4.2K cannot be extended to sufficiently low Ni concentrations to observe the critical scattering associated with the proposed phase transition at $\sim$ 25% Ni.

7.7 Explanation of the Invar Effect

We believe that the Invar effect, as it occurs in the FeNi alloy system, can be understood on the basis of the occurrence of a magnetic phase transition as a function of concentration. The transition, which is expected to occur at $\sim$ 25% Ni, is from a ferromagnetic state to one without long range magnetic order (either paramagnetic or, more probably, some type of spin-glass state) and is driven essentially by the fact that the exchange interaction

between neighbouring Fe atoms is antiferromagnetic in this system. We have considered in some detail the onset of ferromagnetism in giant moment alloys and suggested that it is a proper cooperative magnetic phase transition (section 2.4). Using the Landau theory of phase transitions the thermodynamic properties of this phase transition have been examined (section 2.5) and it was concluded that these giant moment alloys should exhibit many of the canonical Invar characteristics. Conversely one can consider the properties of the FeNi Invar alloys as merely the thermodynamic consequences of the magnetic phase transition that would occur at $\sim$ 25% Ni. Thus the large magnetovolume effects (section 7.2b) can be readily explained.

Although the phase transition is expected to occur near 25% Ni this concentration is never reached because of the martensitic transformation that occurs in the system. The Fe 35% Ni alloy which was originally called Invar (595) is actually near the upper limit of the critical concentration region. Since the spontaneous volume magnetostriction $w \propto (c - c_f)$ (eq. (2.131)) this alloy therefore has about the largest volume magnetostriction (see fig. 7.4). However, the other physical properties such as the initial susceptibility, the forced magnetostriction coefficient, the electronic specific heat, etc, should have their maximum values at the critical concentration itself.

There is a great similarity in the behaviour of FeNi Invar and giant moment alloys. Owing to local environment effects both systems are magnetically inhomogeneous. They also contain nearly magnetic atoms or clusters on which

moments can be induced below the ferromagnetic Curie point of a given alloy. The temperature dependence of the spontaneous magnetization is also similar in both systems and is thought to be due to the existence of a distribution of molecular fields (see section 7.2a). In fact, Window's original suggestion (654) that FeNi Invars are very similar to PdFe and CuNi alloys is essentially correct. If it were possible to stabilize the fcc structure down to $\sim$25% Ni the FeNi system would be found to consist of a dilute concentration of magnetic clusters dispersed in a non-ferromagnetic matrix as in PdFe and CuNi near c_f. A similar model was proposed by Rechenberg et al. (655) for $c \lesssim 27.3\%$ Ni. At higher Ni concentrations the picture must become modified in the same way as in the giant moment alloys. Note that as long as T_c is finite both neutron diffuse scattering and Mossbauer effect measurements can only indicate that the alloys are magnetically inhomogeneous.

A fairly extensive thermodynamic treatment of various physical properties of FeNi Invars has been given (238,240, 254,395,607,631,637-8,640,730,741-5) and will be reviewed elsewhere. In particular Schlosser (745) has pointed out that if a proper, valid derivation of the two relations

$$M^2 = A + B\,\frac{B_0}{M}$$

and

$$\omega = \gamma M^2$$

where A and B are constants, can be given then the magnetovolume effects in Invar can be accounted for in a self-consistent way thermodynamically. In section 2.5 we showed that the above relations (cf eq. (2.92) and (2.128)) are valid for a cooperative magnetic phase transition to

which Landau's theory can be applied. We have already contended that Landau's theory of phase transitions can be applied to the disappearance of ferromagnetic order in FeNi alloys near ~25% Ni and, as mentioned earlier in this section, that the critical region for this transition extends up to ~36% Ni. Although the absolute values of the spontaneous magnetization for c ≳ 32% Ni are relatively large compared, for example, to that of pure Ni yet because the alloys are "unsaturated" the ratio $\frac{M_{oo}}{M_{sat}} < 1$, where M_{sat} is the saturation magnetization, and it appears that it is this condition that ensures the validity of the expansion of the thermodynamic potential of the system as a function of the relative magnetization (i.e. in terms of $\frac{M_{oo}}{M_{sat}}$). M_{sat} may be taken as lying on the extrapolation of the straight line giving the initial concentration variation of M_{oo} for small dilute additions of Fe to Ni (see fig.5 in Ref.676). Thus for Fe 35% Ni $M_{sat} \simeq 2.1$ μ_B/atom compared to $M_{oo} = 1.73$ μ_B/atom.

Although the use of Landau's theory of phase transitions to derive eq.(2.128) gives a self-consistent account of the spontaneous volume magnetostriction of Invar alloys it still does not explain the microscopic origin(s) of the magnetostriction. It would appear that the large spontaneous volume magnetostriction of FeNi Invars (and weakly ferromagnetic giant moment alloys) is due to

(i) dipolar (and/or pseudo-dipolar) interactions which are particularly large in these systems because of the non-equivalence of nearest neighbour sites (659);

(ii) The existence of nearly magnetic atoms (or

clusters) which may carry induced moments below the ferromagnetic transition temperature (662). Both Shiga (733-5) and Schlosser (746-9) have proposed empirical formulae which show that the volume of an atom is related to its magnetic moment. Shiga suggested that the lattice parameter of an alloy (or pure metal) is proportional to its average magnetic moment but noted that if such a magnetic contribution to the lattice parameter were attributable to volume magnetostriction then a quadratic dependence of this contribution on the magnetic moment should be more appropriate (735). This conclusion makes Schlosser's formula namely,

$$V_\mu = V_o + K\mu^2 \qquad 7.29$$

where V_o is the atomic volume when $\mu = 0$ and K is a universal constant (approximately), more attractive. The second term in eq.(7.29) can be considered as arising either from intra-atomic dipolar interactions (between the essentially localized magnetic d-electrons and the sp electrons) and/or from the decreased cohesion within a unit cell due to the polarization of the electrons. An interesting proposition is whether eq.(7.29) can be used to explain the central dip(at Mn) in an otherwise nearly parabolic variation of the cohesive energy of 3d transition metal series, a problem that has recently been discussed by Sayers (750) and Friedel and Sayers (751-2) but who have considered only the second of the above possibilities (i.e. electron-electron correlations). In any case what is important, from our point of view, is that there is a

positive volume magnetostriction due to the moments induced on the nearly magnetic atoms or clusters below the ferromagnetic Curie point. Since the spontaneous volume magnetostriction under consideration is that at T=0 K and is always positive, we have not included any exchange magnetostriction which, as briefly mentioned in section 2.5(iv), is only important in the temperature region near T_c and may be positive or negative depending on the variation of the exchange integral with distance.

Despite the similarity in the behaviour of FeNi Invars and giant moment alloys there are some properties that are peculiar to the former which we attribute to the tendency towards antiferromagnetism in the Fe-rich fcc FeNi alloys. For example, the FeNi Invars are structurally inhomogeneous; atomic short range order of both the $FeNi_3$ and Fe_3Ni types are known to occur (section 7.2d). The former occurs in Ni-rich regions and can be interpreted as being due to a tendency towards maximizing Fe-Ni pairs (542,732) while the latter occurs in Fe-rich regions and can be understood as being favourable to antiferromagnetic ordering. The paramagnetic-antiferromagnetic transition that occurs in Fe-rich regions at low temperatures ($\simeq$ 25K) is the cause of the relaxation effects observed in ultrasonic experiments (section 7.2j) while the concomitant exchange anisotropy is responsible for the decrease in the magneto-elastic coupling, forced magnetostriction, magnetic susceptibility and compressibility and the time dependence of some of these properties below $\sim$25K (628,732). The sensitivity of the metallurgical inhomogeneity, particularly

of the $FeNi_3$ type (732), to cold work, annealing, rolling etc, can account in a simple way for the large effect these processes can have on invar anomalies (see section 7.2i).

Another important property which is peculiar to FeNi Invars is the occurrence of the martensitic $\gamma \longrightarrow \alpha$ transformation which occurs in Fe-rich alloys. As mentioned in the introduction (section 7.1) it is also the increasing tendency towards antiferromagnetic order that drives the lattice structural change leading to soft acoustic phonon modes (allowing, of course, for the softening due to the large positive spontaneous magnetostriction). This conjecture has some theoretical backing (598). It must be emphasized that these peculiar properties of the fcc FeNi system (and the related FePd and FePt Invars) are not primarily responsible for the Invar effects although they do modify them.

Finally, it is not difficult to see how many of the previous theories of the Invar effect, with the exception of the odd few (724-8) which are based solely on the rigid band model of ferromagnetism, can be reconciled with one another. The main problem with these theories is that they attempt to use one facet of the Invar problem to construct a model to explain the whole. In trying to reconcile these models the following points must be borne in mind:

(a) In fcc FeNi alloys (and also in the corresponding FePd and FePt alloys) J_{Fe-Fe} is negative so that with increasing Fe concentration there is a tendency towards antiferromagnetic ordering which drives a magnetic phase transition expected to occur near 25% Ni but which is

interrupted by an (associated?) martensitic lattice transformation.

(b) Statistical concentration fluctuations unavoidably occur leading to a variety of local environments and hence to magnetic inhomogeneity. It is true that atomic short range order also occurs but this is not necessary and merely complicates the observed behaviour.

(c) The fraction of the intrinsic magnetic moment at an atomic site which can be observed depends on the effective molecular field acting on that site. If the effective field is small the observed moment is small and conversely. When this is taken in conjunction with the distribution of molecular fields it is no longer surprising that a given Fe or Ni atom can appear to be magnetic, nearly magnetic or non-magnetic.

(d) There is a relationship between the volume of an atom and its magnetic moment given most probably by eq.(7.29). This equation shows that a small volume is associated with a low moment state and vice-versa.

From the above points, one can now understand various aspects of the models of latent antiferromagnetism, two γ-Fe states, concentration fluctuations, etc, described in section 7.4 and see that these are not necessarily mutually exclusive but are, in fact, complementary. Also we have argued much earlier (section 2.7) that most of the theory of weak itinerant ferromagnetism is essentially a thermodynamic theory of the onset of ferromagnetism as a cooperative phase transition in transition metal alloys and hence can be applied to the Invar problem. The Bethe-Slater curve can qualitatively explain the magnitude and

sign of both $\frac{dT_c}{dP}$ and the volume magnetostriction at T_c but it is not very useful if we consider phenomena at $T \sim 0K$; moreover, as already pointed out, the curve has no rigorous theoretical backing yet. In a similar vein Zener's model explains why the exchange interaction between similar transition metal atoms is a function of their separation and can be positive or negative. Lastly, the Slater-Pauling curve must be treated with some reservation since it clearly evokes outdated rigid band concepts.

In conclusion, we believe that the ideas outlined above should be helpful in providing a suitable explanation for the Invar problem which has existed for too long a time - more than eight decades!

---oOo---

REFERENCES

1. J. Kondo: Solid State Physics 23, 183 (1969)
2. A. J. Heeger: ibid 23, 283 (1969)
3. D. L. Mills: Magnetism in Alloys (ed. P.A.Beck and J.T.Waber) AIME (1972)
4. D. K. Wohlleben and B. R. Coles: Magnetism 5, 3 (1973)
5. C. Rizzuto: Rep. Prog. Phys. 37, 147 (1974)
6. G. Gruner and A. Zawadowski: Rep. Prog. Phys. 37 1497 (1974)
7. J. Friedel: Nuovo Cimento (Suppl) 7, 287 (1958)
8. G. Boato, M. Bugo and C. Rizzuto: Nuovo Cimento 45, 226 (1966)
9. J. R. Schrieffer: J. Appl. Phys. 38, 1143 (1967)
10. J. Loram: Morgin's Conf., June 1968
11. M. D. Daybell and W. A. Steyert: J.Appl Phys. 40 1056 (1969)
12. P. W. Anderson: Phys. Rev. 124, 41 (1961)
13. P. A. Wolff: Phys. Rev. 124, 1030 (1961)
14. A. M. Clogston: Phys. Rev. 125, 439 (1962)
15. N. Rivier: Thesis, Univ. of Cambridge (1968)
16. J. R. Schrieffer and D. C. Mattis: Phys. Rev. 140, A 1412 (1965)
17. B. Kjollerstrom, D. J. Scalapino and J. R. Schrieffer: ibid 148, 665 (1966)
18. P. W. Anderson and A. M. Clogston: Bull. Am. Phys. Soc. 6, 124 (196)
19. J. R. Schrieffer and P. A. Wolff: Phys. Rev. 149, 491 (1966)
20. M. Bailyn: Advan. Phys. 15, 179 (1966)
21. S. D. Silverstein: Phys. Lett. 26A, 445 (1968)
22. C. Zener: Phys. Rev. 81, 440 (1951)
23. J. Kondo: Progr. Theor. Phys. (Kyoto) 32, 37 (1964)
24. T. Kasuya: ibid 16, 58 (1956)
25. K. Yosida: Phys. Rev. 107, 396 (1957)
26. N. E. Phillips: Critical Reviews in Solid State Science 2, 467 (1971)
27. H. Suhl: Phys. Rev. Lett. 19, 442 (1967)
28. M. J. Levine and H. Suhl: Phys. Rev. 171, 567 (1968)
29. M. J. Levine, T. V. Ramakrishnan, and R. A. Weiner: Phys. Rev. Lett. 20, 1370 (1968)
30. N. Rivier and M. J. Zuckermann: Phys. Rev. Lett. 21, 904 (1968)

31. M. J. Zuckermann, N. Rivier and M. Sunjic: Phys. Lett. 28A , 492 (1968)

32. C. M. Hurd: Electrons in Metals (J.Wiley and Sons, 1975) p.186

33. N. F. Berk and J. R. Schrieffer: Phys. Rev. Lett. 17, 433 (1966)

34. S. Doniach and S. Engelsberg: ibid 17, 750 (1966)

35. P. A. Wolff: Phys. Rev. 12D, 814 (1960)

36. J. R. Schrieffer: J. Appl. Phys. 39, 642 (1968)

37a O. K. Anderson: Phys. Rev. 82, 883 (1970)

b O. K. Anderson and A. R. Mackintosh: Solid State Comm. 6, 285 (1968)

38. A. I. Schindler and M. J. Rice: Phys. Rev. 164, 759 (1967)

39. P. Lederer and D. L. Mills: Phys. Rev. 165, 837 (1968)

40. P. Lederer and D. L. Mills: Phys. Rev. Lett. 19 1036 (1968)

41. S. Engelsberg, W. F. Brinkman and S. Doniach: ibid 19, 1040 (1968)

42. A. Schindler and C. Mackliet: ibid 20, 15 (1968)

43. G. Chouteau, R. Fourneaux, R. Tournier and P. Lederer: ibid 21, 1082 (1968)

44. K. H. Benneman: Phys. Rev. 167, 564 (1968)

45. P. Fulde and A. Luther: ibid 170, 570 (1968)

46. D. L. Mills, M. T. Beal-Monod, and P. Lederer: Magnetism 5, 89 (1973)

47. J. E. Goldman and R. Smoluchowski: Phys. Rev.75, 140 (1949)
J. E. Goldman: J. Appl. Phys. 20, 1131 (1949)
R. Smoluchowski: Phys. Rev. 84, 511 (1951)

48. L. W. McKeehan and E. M. Crabbe: Phys. Rev. 55, 505 (1939)

49. V. Jaccarino and L. R. Walker: Phys. Rev. Lett. 15, 258 (1965)

50. H. Claus, A. K. Sinha and P. A. Beck: Phys. Lett. 26A, 38 (1967)

51. L. O. Creveling, Jr., H. L. Luo and G. S. Knapp: Phys. Rev. Lett. 18, 851 (1967)
L. O. Creveling, Jr., and H. L. Luo: Phys. Rev. 176, 614 (1968)

52. L. N. Liebermann, D. R. Fredkin and H. B. Shore: Phys. Rev. Lett. 22, 539 (1969)

53. J. W. Garland and A. Gonis: Magnetism in Alloys (ed. P.A.Beck and J.T.Waber) AIME (1972)

54. D. J. Kim: Phys. Rev. 81, 3725 (1970)

55. J. Crangle and M. J. C. Martin: Phil. Mag. 4, 1006 (1959)

56. D. H. Seib and W. E. Spicer: ibid 20, 1441 (1968)

57. A. Blandin: Theory of Condensed Matter (IAEA 1968)

58. B. R. Coles: Proc. Michigan State University Summer School on Alloys (1972).

59. J. T. Waber: Magnetism in Alloys (AIME 1972)

60. T. Moriya: Progr. Theor. Phys. 34, 329 (1965)
Theory of Magnetism in Metals; Proc. of the 1966 Varena School (ed. W.Marshall) Academic Press, New York(1967)

61. H. Frolich and F. R. N. Nabarro: Proc. Roy. Soc. A175, 382 (1940)

62. M. A. Rudermann and C. Kittel: Phys. Rev. 96, 99 (1954)

63. S. V. Vonsovskii: Soviet Phys. JETP 10, 468 (1946)

64. T. Kasuya: Progr. Theor. Phys. 16, 45 (1956)

65. K. Yosida: Phys. Rev. 106, 893 (1957)

66. R. M. White: Quantum Theory of Magnetism (McGraw Hill, 1970) p.198

67. P. G. de Gennes: J. Phys. Rad. 23, 630 (1962)

68. L. M. Roth, H. J. Zeiger, and T. A. Kaplan: Phys. Rev. 149, 519 (1966)

69. A. J. Freeman: Magnetic Properties of Rare-Earth Metals (ed. R.J.Elliot) Plenum Press(1972)

70. B. Giovannini, M. Peter, and J. R. Schrieffer: Phys. Rev. Lett. 12, 736 (1964)

71. C. Zener: Phys. Rev. 82, 403 (1951)

72. C. Zener and R. R. Heikes: Rev. Mod. Phys. 25 191 (1953)

73. J. H. Van Vleck: ibid 25, 220 (1953)

74. B. R. Coles: Amorphous Magnetism (ed. H.O.Hooper and A.M. de Graaf, Plenum Press, 1973)

75. J. Mathon: Proc. Roy. Soc. A306, 355 (1968)

76. E. P. Wohlfarth: J. Phys. 32, C1-636 (1971)

77. D. M. Edwards, J. Mathon and E. P. Wohlfarth: J. Phys. F3, 161 (1973)

78. T. Kato and J. Mathon: Phys. Lett. 49A, 251 (1974)

79. D. M. Edwards, J. Mathon and E. P. Wohlfarth: J. Phys. F5, 1619 (1975)

80. J. P. Perrier and J. L. Tholence: J. Phys. 35, C4-163 (1974)

81. L. L. Hirst: Phys. Kondens. Materie 11, 255 (1970)

82a R. E. Watson: Phys. Rev. 118, 1036 (1960)

b C. Herring: Magnetism 4 (1966)

83. H. P. Meyers, L. Wallden and A. Karlson: Phil. Mag. 18, 725 (1968)

84. C. Norris and P. O. Nilsson: Solid State Comm. 6, 649 (1968)

85. M. Bassett and D. Beaglehole: J.Phys. F6, 1211 (1976)

86. K. Yosida, A. Okiji and S. Chikazumi: Progr. Theor. Phys. (Kyoto) 33, 559 (1965)

87. J. M. Ziman: Principles of the Theory of Solids (C.U.P, 2nd ed., 1972) p.342-343

88. A.Fert and O. Jaoul: Phys. Rev. Lett. 28, 303 (1972)

89. Y. Yafet: J. Appl. Phys. 42, 1564 (1971)

90. B. Carol: J. Phys. Chem. Solids 28, 1427 (1971)

91. R. F. Tournier: Proc. LT 13, Vol.2, 257 (1972)

92. A. A. Abrikosov and L. P. Gorkov: Soviet Phys. JETP 12, 1243 (1961)

93. P. J. Ford and J. A. Mydosh: J. Phys. 35, C4-241(1974)

94. N. Rivier and K. Adkins: J. Phys. F5, 1745 (1975)

95. B. V. B. Sarkissian and R. H. Taylor: ibid 4, L243 (1974)

96. E. C. Hirschkoff, O. G. Symko and J. C. Wheatley: J. Low. Temp. Phys. 5, 155 (1971)

97. M. T. Beal-Monod: Phys. Rev. 178, 874 (1969)

98. K. Matho and M. T. Beal-Monod: ibid B5, 1899 (1972)

99. Y Nagaoka: Phys. Rev. 138, A 1112 (1965)

100. D. R. Hamann: ibid 158, 570 (1967)

101. J. A. Appelbaum and J. Kondo: Phys. Rev. Lett. 19 906 (1967)

102. W. M. Star: Thesis, Leiden University (1971)

103. A. D. Caplin and C. Rizzuto: Proc. LT 11, Vol.2, 1225 (1968);Phys. Rev. Lett. 21, 746 (1968)

104. For example see E. Babic and C. Rizzuto: Proc. LT 13, Vol.2 484 (1972)

105. M. J. Zuckermann: J. Phys. F 2, L25 (1972)

106. N. Rivier and V. Zlatic: ibid 2, L87 (1972)

107. K. G. Wilson: Proc. Nobel Symp. 24, 68 (1973)

108. P. Nozieres: Phys. Bulletin 25, 457 (1974)

109. M. D. Daybell and W. A. Steyert: Phys. Rev. Lett. 20, 195 (1968)

110. G. Simmons and H. Wang: Single crystal elastic constants and calculated aggregate properties (2nd ed., M.I.I. Press, Cambridge, Mass. 1971)

111. J. A. Rowlands, D. Greig and P. Blood: J. Phys. F1, L29 (1971)

112. F. E. Hoare and J. C. Mathews: Proc. Roy. Soc. A212, 137 (1952)

113. D. W. Budworth, F. E. Hoare and J. Preston:
ibid A257, 250 (1960)

114. A. J. Manuel and J. M. P. St. Quinton:
ibid A273, 412 (1963)

115. S. Foner, R. Doclo and E. J. McNiff:
J. Appl. Phys. 39, 551 (1968)

116. H. C. Jamieson and F. D. Manchester:
J. Phys. F2, 323 (1972)

117. G. Chouteau: Thesis, University of Grenoble (1973)

118. N. F. Mott and H. Jones: The Theory of the Properties
Metals and Alloys (O.U.P. 1936, Dover
reprint) p.195
(contains even much earlier references)

119. J. Beille, D. Bloch and M. J. Besnus: J. Phys. F4
1275 (1974) (and references therein)

120. E. P. Wohlfarth: Proc. Nottingham Mag. Conference
1964 p.51

121. G. Fischer, A. Herr and A. J. Meyer:
J. Appl. Phys. 39, 545 (1968)

122. C. L. Foiles and A. I. Schindler:
Phys. Lett. 26A, 154 (1968)

123. D. Gainon and J. Sierro: ibid 26A, 601 (1968)

124. J. A. Rayne: Phys. Rev. 118, 1545 (1960)

125. B. W. Veal and J. A. Rayne: ibid 135, A 442 (1964)

126. R. E. Macfarlane and J. A. Rayne:
Phys. Lett. 18, 91 (1965)

127. G. Chouteau, R. Forneaux, K. Gobrecht and R.Tournier:
Phys. Rev. Lett. 20, 193 (1968)

128. A. T. Aldred, B. D. Rainford and M. W. Stringfellow:
Phys. Rev. Lett. 24, 897 (1970)

129. A. B. Kaiser and S. Doniach:
Int. J. Mag. 1, 11 (1970)

130. N. Rivier and V. Zlatic: J. Phys. F2, L99 (1972)

131. M. D. Sarachik: Phys. Rev. 170, 679 (1968)

132. J. W. Loram, R. J. White and A. D. C. Grassie:
Phys. Rev. B5, 3659 (1972)

133. T. Sugawara, M. Takano and S. Takayanagi:
J. Phys.Soc. Jap 36, 451 (1974)

134. R. J. White: J. Phys. F2, 503 (1972)

135. K. Yosida and Okiji: Progr. Theor. Phys. (Kyoto)
34, 505 (1965)

136. G. Iche: J. Low Temp. Phys. 11, 215 (1973)

137. N. Menyhard: Solid State Comm. 12, 215 (1973)

138. M. T. Beal-Monod, S. K. Ma and D. Fredkin:
Phys. Rev. Lett. 20, 929 (1968)

139. M. T. Beal-Monod and D. L. Mills: Solid State Comm.
14, 1157 (1974)

140. A. P. Klein: Phys. Lett. 26A, 57 (1967)
141. Y. Kurate: Progr. Theor. Phys. (Kyoto) 43, 621 (1970)
142. T. T. Hedgecock and P. L. Li: Phys. Rev. B2, 1342 (1970)
143. B. B. Triplett and N. E. Phillips: Phys. Lett. 27, 1001 (1971
144. J. E. Van Dam: Thesis, Leiden University (1973)
145. S. Misawa: Phys. Rev. Lett. 32A, 153 (1970)
146. S. Misawa: Phys. Rev. Lett. 26, 1632 (1971)
147. J. C. Ododo: Solid State Comm. 22, 585 (1977) and
Phys. Lett. A 1978 (to be published)
148. S. Misawa: Phys. Lett. 44A, 333 (1973)
149. E. Burzo and D. P. Lazar : Solid State Comm. 18, 381 (1976)
150. D. Y. Kojima and A. Isihara: ibid 18, 355 (1976)
151. H. Kojima, R. S. Tebble and D. E. G. Williams:
Proc. Roy. Soc. A260, 237 (1961)
152. E. C. Stoner: ibid A 154, 656 (1936)
153. E. W. Collings and J. C. Ito: Phys. Rev. B 2, 235 (1970)
154. J. C. Ododo: Unpublished analysis
155. J. Bardeen, L. N. Cooper and J. R. Schrieffer:
Phys. Rev. 106, 162 (1957)
ibid 108, 1175 (1957)
156. B. T. Matthias, T. H. Geballe and V. B. Compton:
Rev. Mod. Phys. 35, 1 (1963)
157. A. W. Overhauser: Phys. Rev. 128, 1437 (1962)
158. B. T. Matthias: IBM J. Res. Develop. 6, 250 (1962)
159. B. T. Matthias, V. B. Compton, H. Suhl and E. Corenzwit:
Phys. Rev. 115, 1597 (1959)
160. J. W. Garland: Phys. Rev. Lett. 11, 111 (1963)
161. ibid: 11, 114 (1963)
162. W. L. McMillan: Phys. Rev. 167, 331 (1968)
163. P. Morel and P. W. Anderson: Phys. Rev. 125, 1263 (1962
164. G. Riblet: ibid B 3, 91 (1971)
165. M. B. Maple, J. G. Huber, B. R. Coles and A. C. Lawson:
J. Low Temp. Phys. 3, 137 (1970)
166. A. B. Kaiser: J. Phys. C 3, 409 (1970)
167. M. B. Maple: Magnetism, 5, 353 (1973)
168. K. H. Bennemann and J. W. Garland: Int. J. Mag. 1, 97 (1971)
169. E. Muller-Hartmann: Magnetism 5, 353 (1973)

170. Ø. Fischer and M. Peter: ibid 5, 327 (1973)

171. For example see reference 87, p.380

172. J. Solyom and A. Zawadowski: Phys. Lett. 25A, 91 (1967)

173. C. Kittel: Introduction to Solid State Physics (J. Wiley, 4th ed. 1971) p.402

174. N. E. Alekseevskii and L. Migunov: J. Phys. (USSR) 11, 95 (1947)

175. B. R. Coles: Rev. Mod. Phys. 36, 139 (1964)

176. D. J. Kim: J. Phys. Soc. Jap. 40, 1244 (1976)

177. See for instance P. A. Beck and C. P. Flynn: Solid State Comm. 18, 127 (1976)

178a T. Moriya and A. Kawabata: J. Phys. Soc. Jap. 34, s639 (1973)

178b ibid : ibid 35, 669 (1973)

c ibid : Proc. ICM Moscow 1973

179. A. Kawabata: J. Phys. F 4, 1477 (1974)

180. T. V. Ramakrishnan: Solid State Comm. 14, 449 (1974)

181. M. Salomaa: ibid 18, 1217 (1976)

182. E. P. Wohlfarth: Comments on Solid State Phys. 6, 123 (1975)

183. G. Shirane, C. W. Chen, P. A. Flinn, and R. Nathans: Phys. Rev. 131, 183 (1963) (and references therein)

184. G. Frossati, J. L. Tholence, D. Thoulouze and R. Tournier: Proc. LT 14 Vol. 2, 370 (1975)

185. R. C. Jones: Wiss Z. Techn. Univers. Dresden 23, H.5 (1974)

186. G. Chouteau, R. Tournier and P. Mollard: J. Phys. 35, C4-185 (1974)

187. R. J. Elliott: J. Phys. Chem. Solids 16, 165 (1960)

188. A. P. Murani, S. Roth, P. Radhakrishna, B. D. Rainford B. R. Coles, K. Ibel, G. Goeltz and F. Mezei: J. Physics F. 6, 425 (1976)

189. B. Sarkissian and B. R. Coles: Communications on Physics 1, 17 (1976)

190. W. M. Lomer: Proc. Phys. Soc. (London) 80, 489 (1962)

191. F. Heiniger, E. Bucher and J. Muller: Phys. Lett. 19, 163 (1965)

192. T. Mamiya and Y. Masuda: J. Phys. Soc. Jap. 40, 390 (1976)

193. B. V. B. Sarkissian and B. R. Coles J. Less Common Metals 43, 83 (1975)

194. See for instance: J. M. D. Coey: Phys. Bulletin 27, 294 (1976)

195. A. P. Murani: J. Phys. 35, C4-181 (1974)

196. D. E. Murnick, A. T. Fiory and W. J. Kossler: Phys. Rev. Lett. 36, 100 (1976)

197. G. G. Low and T. M. Holden: Proc. Phys. Soc. 89 119 (1966)

198. T. J. Hicks, T. M. Holden and G. G. Low: J. Phys. C2, 528 (1968)

199. J. Kopp: J. Phys. F 3, 1994 (1973)

200. G. Chouteau and R. Tournier: J. Phys. 32, C1-1002 (1971)

201. C. G. Robbins, H. Claus and P. A. Beck: J. Appl. Phys. 40, 2269 (1969)

202. J. S. Kouvel and J. B. Comly: Phys. Rev. Lett. 24 598 (1970)

203. J. P. Perrier, B. Tissier and R. Tournier: ibid 24, 313 (1970)

204. T. J. Hicks, B. Rainford, J. S. Kouvel, G. G. Low and J. B. Comly: ibid 22, 531 (1969)

205. P. Panissod: J. Phys. 35, C4-173 (1974)

206. K. P. Gupta, C. H. Cheng and P. A. Beck: Phys. Rev. 133, A203 (1964)

207. R. W. Houghton, M. P. Sarachik and J. S. Kouvel: Phys. Rev. Lett 25, 238 (1970)

208. W. J. Nellis and M. B. Brodsky: J. Appl. Phys. 43, 1961 (1972)

209. H. M. Ahmad and D. Greig: Phys. Rev. Lett. 32, 833 (1974)

210. D. Sherrington and K. Mihill: J. Phys. 35, C4-199 (1974)

211. J. K. Hulm and R. D. Blaugher: Phys. Rev. 123, 1569 (1961)

212. A. Amamou, R. Caudron, P. Costa, F. Gautier and B. Loegel: Proc. LT 14, Vol.2, 254 (1975).

213. B. R. Coles, A. Tari and H. C. Jamieson: Proc. LT 13, Vol.2, 214 (1972)

214a A. Tari: Thesis, Imperial College, London (1972)

b ibid: J. Phys. F 6, 1313 (1976)

215. R. E. Walstedt, R. C. Sherwood and J. H. Wernick: J. Appl. Phys. 39, 555 (1968).

216. H. C. Jamieson: J. Phys. F 5, 1021 (1975)

217. H. Hansen: Constitution of binary alloys (McGraw Hill, New York 1958) p.495

218. H. E. N. Stone: J. Materials Science 11, L1162 (1976)

219. B. V. B. Sarkissian: Private Communication

220. F. Acker and R. Huguenin: Phys. Lett. 38A, 343 (1972)

221. M. W. Zemansky: Heat and Thermodynamics (McGraw Hill, 5th ed., 1968) p.377 et seq.

222. C. J. Adkins: Equilibrium Thermodynamics (McGraw Hill, 1st impression 1969) pp 197-201

223. See for example D. S. Rodbell and C. P. Bean: J. Appl. Phys. 33 S 1037 (1962)

224. J. S. Touger and M. P.Sarachik: Solid State Comm. 17, 1389 (1975) and reference therein.

225. M. D. Daybell and W. A. Steyert: Rev. Mod. Phys. 40, 380 (1968)

226. V. Cannella, J. A. Mydosh and J. I. Budnick: J. Appl. Phys. 42, 1689 (1971)

227. C. N. Guy: J. Phys. F 5, L 242 (1975)

228. See for instance
L. E. Wenger and P. H. Keesom: Phys. Rev. B 11 3497 (1975)

229. R. S. Preston, D. J. Lam, M. V. Nevitt, D. O. Van Ostenburg and C. W. Kimball: Phys. Rev. 149, 440 (1966)

230a S. Roth, K. Ibel and W. Just: Proc. ICM Moscow (1973)

b Ibid: J. Appl. Cryst, 7, 230 (1974)

231. L. D. Landau and E. M. Lifshitz: Statistical Physics (Pergamon Press, London, 1958) Chap. 14

232. K. P. Belov: Magnetic Transitions (Consultants Bureau, New York, 1961).

233. E. P. Wohlfarth: J. Appl. Phys. 39, 1061 (1968)

234. Ibid: J. Phys. C 2, 68 (1969)

235. D. M. Edwards and E. P. Wohlfarth: Proc. Roy. Soc. A 303 127 (1968)

236. E. P. Wohlfarth: Colloq. Int. CNRS 188, 363 (1970)

237. D. L. Mills: Solid State Comm. 9, 929 (1971)

238. L. Billard and A. Chamberod: ibid 14, 1127 (1974)

239. E. P. Wohlfarth: Proc. ICM Moscow Vol. 2, 28 (1973)

240. Ibid: I.E.E.E. Trans. Mag 11, 1638 (1975)

241. F. R. De Boer: Thesis, University of Amsterdam (1969)

242. J. Beille, D. Bloch and E. P. Wohlfarth: Phys. Lett. 43A, 207 (1973)

243. A. H. Morrish: The Physical Principles of Magnetism (J. Wiley, 1965) p. 321

244. J. Beille and G. Chouteau: J. Phys. F 5, 721 (1975)

245. N. Buis, J. J. M. Franse, J. Van Haarst, J. P. J. Kaandorp and T. Weesing: Phys. Lett. 56A, 115 (1976)

246. T. F. M. Kortekaas, J. J. M. Franse and H. Holscher: Phys. Lett. 48A, 305 (1974)

247. J. J. M. Franse, N. Buis, and T. F. M. Kortekaas: Proc. ICM Moscow Vol.1(ii), 205 (1973)

248. P. P. M. Meincke, E. Fawcett, G. S. Knapp: Solid State Comm. 7, 1643 (1969)

249. E. Fawcett, E. Bucher and W. F. Brinkman: Bull. Am. Phys. Soc. 13, 364 (1968)

250. K. Terao and A. Katsuki: J. Phys. Soc. Jap. 37 828 (1974)

251. See for example - C. J. Gorter and G. K. White: Progress in Low Temperature Physics (North Holland, 1964) Vol. IV Chapter 9.

252. E. D. Thompson, E. P. Wohlfarth and A. R. Bryan: Proc. Phys. Soc. 83, 59 (1964)

253. M. Hayase, M. Shiga and Y. Nakamura: J. Phys. Soc. Jap 30, 729 (1971)

254. E. P. Wohlfarth: Phys. Lett. 28A, 569 (1969)

255. F. R. De Boer, C. J. Schinkel, J. Biesterbos and S. Proost: J. Appl. Phys. 40, 1049 (1969)

256. T. F. M. Kortekaas, J. J. M. Franse and H. Holscher: Phys. Lett. 50A, 153 (1974)

257. C. M. Hurd: The Hall Effect in Metals and Alloys (Plenum Press, New York and London 1972) Chapter 5.

258. See for example H. H. Potter: Phil. Mag. 13, 233 (1932)

259. P. D. Hambourger, R. J. Olwert, and C. W. Chu: Phys. Rev. B11, 3501 (1975)

260. R. M. Bozorth: Phys. Rev. 70, 923 (1946)

261. See reference 257, chapter 1.

262. For a general discussion see A. Munster: Fluctuation Phenomena in Solids (ed. R. E. Burgess: Academic Press, 1965)

263a H. Palevsky and D. J. Hughes : Phys. Rev. 92 202 (1953)

b G. L. Squires: Proc. Phys. Soc. A67, 248 (1954)

c M. K. Wilkinson and C. G. Shull: Phys. Rev. 103 516 (1956)

263d R. D. Lowde: Rev. Mod. Phys. 30, 69 (1958)

264. L. Van Hove: Phys. Rev. 95, 249, 1374 (1954)

265. H. J. Zeiger and G. W. Pratt: Magnetic Interactions in Solids (O.U.P. 1973) Appendix 8.

266. W. Marshall and S. W. Lovesey: Theory of Thermal Neutron Scattering (O.U.P. 1970) Appendix 8

267. Reference 231, Chapter 12.

268. H. Thomas: Theory of Condensed Matter (IAEA Vienna 1968) p 357

269. W. Marshall and R. D. Lowde: Rep. Prog. Phys. 21 705 (1968)

270. B. D. Rainford: Lectures at the Nordic Summer School Valodalen 1971 (unpublished).

271. L. P. Kadanoff: Physics 2, 263 (1966)

272. J. E. Noakes, N. E. Tornberg and A. Arrott: J. Appl. Phys. 37, 1264 (1966)

273. J. S. Kouvel and M. E. Fisher: Phys. Rev. 136, A 1626 (1964)

274. M. E. Fisher and A. Aharony: Phys. Rev. Lett 30 559 (1973)

275. S. Arajs, B. L. Tehan, E. E. Anderson and A. A. Stelmach: Int. J. Mag. 1, 41 (1970)

276. C. Domb: Physics Today 21, 23 (1968)

277. S. Marcelja: Thesis, University of Rochester (1970) (as quoted by ref. 278)

278. P. M. Horn, Ronald Bass, and R. D. Parks: Phys. Rev. B7, 332 (1973).

279. D. L. Mills and P. Lederer: J. Phys. Chem. Solids 27, 1805 (1966)

280. B. R. Coles: Phys. Lett. 8, 243 (1964)

281. O. Laborde and P. Radhakrishna: Phys. Lett. 37A 209 (1971)

282a R. Rusby: Thesis, Imperial College London (1973) unpublished.

b Ibid: J. Phys. F 4, 1265 (1974)

283. G. K. White and S. B. Woods: Phil. Trans. Roy. Soc. A 251, 273 (1959)

284. A. H. Wilson: Proc. Roy. Soc. A 167, 580 (1938)

285. F. C. C. Kao and Gwyn Williams: J. Phys. F 4, 419 (1974)

286. J. Souletie: Proc. LT 13, Vol. 2, 479 (1972)

287. O. Laborde and J. Souletie: Proc. LT 14, 366 (1975)

288. F. J. Blatt: Phys. Rev. 108, 285 (1957)

289. B. R. Coles, S. Mozumder and R. Rusby:
Proc. LT 12 737 (1970)

290. A. P. Murani: J. Phys. F 4, 757 (1974)

291. B. R. Coles and J. C. Taylor: Proc. Roy. Soc. A267, 139 (1962)

292. F. J. Kedves, M. Hordos and L. Gergely:
Solid State Comm. 11, 1067 (1972)

293. R. W. Houghton, M. P. Sarachik and J. S. Kouvel:
Solid State Comm. 8, 943 (1970)

294. L. R. Edwards, C. W. Chen and S. Legvold: ibid 8, 1403 (1970)

295. A. P. Murani: Phys. Rev. Lett. 33, 91 (1974)

296. H. G. Purwins, Y. Talmor, J. Sierro and F. T. Hedgecock:
Solid State Comm 11, 361 (1972)

297. P. A. Beck: Bull. Am. Phys. Soc. 18, 458 (1973)

298. D. J. Gillespie, C. A. Mackliet and A. J. Schindler:
Amorphous Magnetism (Plenum Press, 1973) p. 343

299. H. Claus and J. A. Mydosh: Solid State Comm. 14,
209 (1974)

300. A. Tari and B. R. Coles: J. Phys. F 1, L 69 (1971)

301. A. Amamou, F. Gautier and B. Loegel:
J. Phys. 35, C4-217 (1974)

302. Ibid: J. Phys. F 5, 1342 (1975)

303. S. Ogawa: J. Phys. Soc. Jap. 40, 1007 (1976)

304. J. M. Ziman: Electrons and Phonons (O.U.P. 1960)
Chapter IX

305. A. I. Schindler and B. C. Laroy:
Solid State Comm. 9, 1817 (1971)

306. H. G. Purwins, H. Schulz and J. Sierro:
Int. J. Magnetism 2, 153 (1972)

307. J. Korringa and A. N. Gerritsen: Physica 19, 457 (1953)

308. See reference 87, p.244.

309. See reference 118, p.308-314

310a W. Geibel: A. anorg. Chem 69, 38 (1910)

b Ibid: ibid 70, 240 (1911)
(as quoted in reference 118)

311. J. J. Vuillemin and M. G. Priestley: Phys. Rev. Lett.
14, 307 (1965)

312. B. R. Coles: Proc. Phys. Soc. B 65, 221 (1951)
and references therein.

313. G. A. Thomas, K. Levin and R. D. Parks:
Phys. Rev. Lett. 29, 1321 (1972)

314. J. Zoric, G. A. Thomas and R. D. Parks:
ibid 30, 22 (1973)

315. S. H. Liu: J. Appl. Phys. 35, 1087 (1964)

316. K. Niira: Phys. Rev. 117, 129 (1960)

317. A. R. Mackintosh: Phys. Lett. 4, 140 (1963)

318. W. de Dood and P. F. de Chatel: J. Phys. F 3, 1039 (1973)

319. E. P. Wohlfarth: Phys. Lett. 47A, 125 (1974)

320. Ibid: Phys. Stat. Sol. A 25, 285 (1974)

321. A. Hahn and E. P. Wohlfarth: Helv. Phys. Acta 41
857 (1968)

322. D. E. Moody, M. G. Staveley and R. Kuentzler:
Phys. Lett. 33A, 244 (1970)

323. I. Mannari: Phys. Lett. 26A, 134 (1968)

324. M. E. Fisher and J. S. Langer: Phys. Rev. Lett. 20
665 (1968)

325. T. G. Richard and D. J. W. Geldart: Phys. Rev. Lett.
30, 290 (1973)

326. K. Kawasaki: Int. J. Mag. 1, 171 (1971)and refs. therein.

327. A. P. Levanyuk: Soviet Phys. JETP 22, 901 (1966)

328. P. L. Young and A. Bienenstock: J. Phys. Chem. Solids
33, 1 (1972)

329. K. P. Belov, G. I. Katayev and R. Z. Levitin: Soviet Phys. JETP 37, 670 (1960)

330. Ibid: J. Appl. Phys. 31, 153S (1960)

331. W. Doring: Ann. Phys. 32, 465 (1938)

332. E. P. Wohlfarth: Phys. Stat. Sol. (a) 10, K 39 (1972)

333. T. F. M. Kortekaas: Thesis, Univ. of Amsterdam (1975)

334. H. L. Alberts, J. Beille, D. Bloch and E. P. Wohlfarth: Phys. Rev. B 9, 2233 (1974)

335. C. H. Cheng, C. T. Wei and P. A. Beck: Phys. Rev. 120, 426 (1960)

336. K. Schröder and C. H. Cheng: J. Appl. Phys. 31, 2154 (1960)

337. E. Bucher, W. F. Brinkman, J. P. Maita and H. J. Williams: Phys. Rev. Lett. 18, 1125 (1967)

338. K. Schröder: J. Appl. Phys. 32, 880 (1961)

339. W. F. Brinkman and S. Engelsberg: Phys. Rev. 169, 417 (1968)

340. W. Proctor and R. G. Scurlock: Proc. LT 11, Vol. 2, 1320 (1968)

341. B. B. Triplett and N. E. Phillips: Phys. Lett. 37A 443 (1971)

342. E. Fawcett, J. P. Maita, E. Bucher and J. H. Wernick: Phys. Rev. B 2, 3639 (1970)

343. R. G. Scurlock and E. M. Wray: Phys. Lett. 6, 28 (1963)

344. N. M. Wolcott and R. L. Falge: J. Low Temp. Phys. 2, 329 (1970)

345. C. G. Robbins, H. Claus and P. A. Beck: Phys. Rev. Lett. 22, 1307 (1968)

346. R. L. Falge and N. M. Wolcott: J. Low Temp. Phys. 5, 617 (1971)

347. J. Beille, D. Bloch and R. Kuentzler: Solid State Comm. 14, 963 (1974)

348. W. Marshall: Phys. Rev. 118, 1519 (1960)

349. M. W. Klein and R. Brout: ibid 132, 2412 (1963)

350a M. W. Klein: ibid 136, A 1156 (1964)

b Ibid: ibid 173, 552 (1968)

351. A. P. Murani, A. Tari and B. R. Coles:
J. Phys. F 4, 1769 (1974)

352. J. Souletie and R. Tournier: J. Low Temp. Phys. 1
95 (1969)

353. P. A. Beck and H. Claus: NBS J. Res. 74A, 449 (1970)

354. L. H. Bennett, L. J. Swartzendruber and R. E. Watson:
Phys. Rev. Lett. 23, 1171 (1969)

355. J. Castaing, P. Costa, M. Heritier and P. Lederer:
J. Phys. Chem. Solids 33, 533 (1972)

356. J. Castaing, R. Caplain and P. Costa: Solid State
Comm. 9, 297 (1971)

357. B. Loegel, J. M. Friedt and R. Poinsot:
J. Phys. F 5, L54 (1975)

358. I. P. Gregory and D. E. Moody: J. Phys. F 5, 36 (1975)

359. M. Blackman: private communication.

360. C. A. Mackliet, A. I. Schindler and D. J. Gillespie:
Phys. Rev. B 1, 3283 (1970)

361. M. Dixon, F. E. Hoare and T. M. Holden: Proc. Roy. Soc.
A 303, 339 (1968)

362. W. H. Keesom and B. Kurrelmeyer: Physica 7, 1003 (1940)

363. S. A. Ahern, M. J. C. Martin and W. Sucksmith:
Proc. Roy. Soc. A 248, 145 (1958)

364. H. M. Ahmad and D. Greig: J. Phys. 35, C4-223 (1974)

365. S. Legvold, D. T. Peterson, P. Burgardt, R. J. Hofer,
B. Lundel, T. A. Vyrostek and H. Gärtner:
Phys. Rev. B 9, 2386 (1974)

366. P. Chevenard: J. Inst. Met. 36, 39 (1926)
as quoted in ref. 312.

367. M. J. Besnus, Y. Gottehrer and G. Munschy:
Phys. Stat. Sol. 49, 597 (1972)

368. B. D. Rainford, A. T. Aldred, and G. G. Low:
J. Phys. 32, C1-575 (1971)

369. H. C. Van Elst, B. Lubach and G. J. Van den Berg:
Physica 28, 1297 (1962)

370. J. W. Cable and R. A. Medina: Phys. Rev. B13, 4868 (1976)

371. V. Marian: Ann. Phys. (Paris) 7, 459 (1937)

372. C. Sadron: ibid 17, 371 (1932)

373. J. Crangle and W. R. Scott: J. Appl. Phys. 36, 921 (1965)

374. J. Crangle: Phil. Mag. 5, 335 (1960)

375. T. F. Smith, W. E. Gardner and H. Montgomery: J. Phys. C 3, S 370 (1970)

376. Gwyn Williams and J. Loram: J. Phys. Chem. Solids 30, 1827 (1969)

377. P. E. Clark and R. E. Meads: J. Phys. C 3, S 308 (1970)

378. G. Longworth and C. C. Tsuei: Phys. Lett. 27A, 258 (1968)

379. F. Bölling: Phys. Kond. Materie 7, 162 (1968)

380. J. A. Mydosh, J. I. Budnick, M. P. Kawatra and S. Skalski: Phys. Rev. Lett. 21, 1346 (1968)

381. E. Fawcett, E. Bucher, W. F. Brinkman and J. P. Maita: Phys. Rev. Lett. 21, 1183 (1968)

382. J. Beille and R. Tournier: J. Phys. F 6, 621 (1976)

383. H. Fujiwara, H. Kadomatsu and K. Ohishi: Proc. Int. Conf. on High Pressure Kyoto (1974) p275.

384. M. J. Besnus and A. Herr: Phys. Lett. 39A, 83 (1972)

385. G. Fischer and M. J. Besnus: Solid State Comm. 7, 1527 (1969)

386. A. I. Schindler and D. J. Gillespie: Proc. LT 12, 777 (1970)

387. P. Pataud, J. P. Perrier and R. Tournier: J. Phys. 35, C4-189 (1974)

388. H. Claus: Phys. Rev. Lett. 34, 26 (1975)

389. C. R. Burr, W. Zingg and M. Peter: Helv. Phys. Acta 43, 771 (1970)

390. M. V. Nevitt and A. T. Aldred: J. Appl. Phys. 34, 463 (1963)

391. J. B. Sousa, M. R. Chaves, R. S. Pinto and M. F. Pincheiro: J. Phys. F 2, L 83 (1972)

392. I. Maartense and Gwyn Williams: J. Phys. F 6, L 121 (1976)

393. C. G. Robbins and H. Claus: AIP Proc. 5, 527 (1971)

394. G. Chouteau: Physica 84B, 25 (1976)

395. J. Mathon and E. P. Wohlfarth: Phys. Stat. Sol. 30, K131 (1968)

396. G. F. Bolling, A. Arrott and R. H. Richman:
Phys. Stat. Sol. 26, 743 (1968)
397. G. Hausch: J. Phys. F 6, 1015 (1976)
398. W. F. Schlosser: Phys. Lett. 40A, 195 (1972)
399. S. Foner and E. D. Thompson: J. Appl. Phys. 30 2295 (1959)
400. E. W. Pugh and B. E. Argyle: ibid 33, S 1178 (1962)
401. N. V. Zavaristskii and V. A. Tsarev:
Soviet Phys. JETP 16, 1154 (1963)
402. B. E. Argyle, S. H. Charap and E. W. Pugh:
Phys. Rev. 132, 2051 (1963)
403. R. Kaul and E. D. Thompson: J. Appl. Phys. 40, 1383 (1969)
404. A. T. Aldred and P. H. Froehle: Int. J. Magnetism 2,
195 (1972)
405. A. T. Aldred: Phys. Rev. B 11, 2597 (1975)
406a P. C. Riedi: Phys. Rev. B 8, 5243 (1973)
406b ibid : Phys. Rev. B 16, 5197 (1977)
407. V. Cannella and J. A. Mydosh: Phys. Rev. B 6, 4220 (1972)
408. C. E. Violet and R. J. Borg: ibid 149, 540 (1966)
409. S. F. Edwards and P. W. Anderson: J. Phys. F 5, 965 (1975
410. D. Sherrington and B. W. Southern: ibid 5, L 49 (1975)
411. K. H. Fischer: Phys. Rev. Lett. 34, 1438 (1975)
412. Ibid: Solid State Comm. 18, 1515 (1976)
413. K. Adkins and N. Rivier: J. Phys. 35, C 4-237 (1974)
414. J. L. Tholence and R. Tournier: ibid C 4-229 (1974)
415. L. E. Wenger and P. H. Keesom: Proc. LT 14, 258 (1975)
416. F. W. Smith: Solid State Comm. 13, 1267 (1973)
417. J. E. Zimmerman and F. E. Hoare:
J. Phys. Chem. Solids 17, 52 (1960)
418. N. Rivier: Wiss. Z. Techn. Univ. Dresden 23, 1000 (1974)
419. J. Bonnerot, B. Caroli and B. Coqblin:
Ann. Acad. Sci. Fennicae AVI, 120 (1966)
(Proc. Helsinki LT conf.)

420. G. Chouteau, R. Fourneaux and R. Tournier: Proc. LT 12, 769 (1970)

421. J. A. Mydosh, P. J. Ford, M. P. Kawatra and T. E. Whall: Phys. Rev. B 10, 2845 (1974)

422. O. Laborde and P. Radhakrishna: J. Phys. F 3, 1731 (1973)

423. P. J. Ford, T. E. Whall and J. W. Loram: Phys. Rev. B 2, 1547 (1970)

424. E. E. Semenenko and A. I. Sudovstov: Soviet Phys. JETP 15, 708, 1033 (1962)

425. P. D. Long and R. E. Turner: J. Phys. C. 2, S127 (1970)

426. D. L. Mills, A. Fert and I. A. Campbell: Phys. Rev. B 4, 196 (1971)

427. R. J. Harrison and M. W. Klein: Phys. Rev. 154, 540 (1967)

428. M. T. Beal-Monod: Solid State Comm. 9, 401 (1971)

429. D. A. Smith: J. Phys. F 4, L 266 (1974)

430. A. A. Abrikosov: Phys. 2, 61 (1965)

431. See reference 266, chapters 5 and 14.

432. G. L. Squires: Unpublished Lectures at the Summer School on Thermal Neutron Scattering (Cambridge 1973)

433. W. Marshall and S. W. Lovesey: see ref. 266, chap. 13

434. W. Marshall: J. Phys. C 1, 88 (1968)

435. C. G. Shull and M. K. Wilkinson: Phys. Rev. 97, 304 (1955)

436. G. C. Felcher et al: Preprint

437. J. W. Cable, E. O. Wollan and H. R. Child: Phys. Rev. Lett. 22, 1256 (1969)

438. A. T. Aldred, B. D. Rainford, T. J. Hicks and J. S. Kouvel: Phys. Rev. B 7, 218 (1973)

439. Ibid: Phys. Rev. B 14, 228 (1976)

440. S. W. Lovesey and W. Marshall: Proc. Phys. Soc. (London) 89, 613 (1966)

441. S. W. Lovesey: ibid 89, 625, 893 (1966)

442. J. Gammel, W. Marshall and L. Morgan: Proc. Roy. Soc. A 275, 257 (1963)

443. E. Balcar and W. Marshall: J. Phys. C 1, 966 (1968)
444. R. Chiffey and T. J. Hicks: Phys. Lett. 34A, 267 (1971)
445. G. G. Low and M. F. Collins:
J. Appl. Phys. 34, 1195 (1963)
446. M. R. Collins and G. G. Low:
Proc. Phys. Soc. 86, 535 (1965)
447. G. G. Low: Proc. Phys. Soc. 92, 938 (1967)
448. See for instance:
G. G. Low: Adv. Phys. 18, 371 (1969)
449. A. M. Clogston: Phys. Rev. Lett. 19, 583 (1967)
450. J. B. Diamond: Intern. J. Magnetism 2, 241 (1972)
451. H. Nagasawa and N. Inoue: Proc. LT 12, 741 (1970)
452. K. V. Rao, S. Arajs, Y. D. Yao, L. Hedman,
Ch. Johannessen and H. U. Astrom:
Proc. LT 14, 399 (1975)
453. J. G. Huber, J. Brooks, D. Wohlleben and M. B. Maple:
AIP Conf. Proc. 24, 475 (1974)
454. C. J. de Pater, C. van Dijk and G. J. Nieuwenhuys:
J. Phys. F 5, L 58 (1975)
455. T. J. Hicks: J. Phys. F 7, 481 (1977)
456. H. Claus and J. S. Kouvel: Unpublished analysis quoted in ref.457
457. W. C. Muellner and J. S. Kouvel: Phys. Rev. B 11,
4552 (1975)
458. T. J. Hicks: Phys. Lett. 32A, 410 (1970)
459. H. Claus: Phys. Lett. 51A, 283 (1975)
460. J. W. Loram, G. Williams and G. A. Swallow:
Phys. Rev. B. 3, 3060 (1971)
461a M. McDougald and A. J. Manuel: J. Appl. Phys. 39,
961 (1968)
461b A. J. Manuel and M. McDougald: J. Phys. C 3, 147 (1970)
462. R. A. Medina and J. W. Cable: AIP Conf. Proc. 29, 292 (1975)
463. P. Radhakrishna, P. Pataud, W. Just and R. Tournier:
Solid State Comm. 18, 1213 (1976)
464. T. J. Hicks: Phys. Rev. Lett. 37, 719 (1976)

465. G. Felcher, J. W. Garland, J. W. Cable and R. Medina: AIP Conf. Proc. 29, 331 (1975)

466. Y. Ito and J. Akimitsu: J. Phys. Soc. Jap. 35, 1000 (1973)

467. R. M. Moon: AIP Conf. Proc. 24, 425 (1974)

468. I. A. Campbell: Proc. Phys. Soc. 89, 71 (1966)

469. J. W. Cable and H. R. Child: Phys. Rev. B 1, 3809 (1970)

470. G. G. Low: Lectures on Solid and Liquid State Physics (Atomic Energy Establishment Trombay, Bombay, India) (1964)

471. G. G. Low: Inelastic scattering of neutrons: (IAEA Symposium) Vol. 1, p.413 (1965)

472. R. A. Medina and J. W. Cable: Phys. Rev. B 15, 1539 (1977)

473. J. B. Comly, T. M. Holden and G. G. Low: J. Phys. C 1, 458 (1968)

474. B. N. Brockhouse, L. M. Corliss and J. M. Hastings: Phys. Rev. 98, 1721 (1955)

475. A. P. Murani: Ph.D Thesis, University of London (1969)

476. W. F. Brown: Phys. Rev. 60, 139 (1941)

477. F. Keffer: in "Handbuch der Physik", 18/2 (1966) (Springer-Verlag, OHG, New York) p.77

478. T. R. Mcguire and P. J. Flanders: Magnetism and Metallurgy. (ed. A. E. Berkowitz and E. Kneller. Academic Press 1969)

479. A. Arrott: Phys. Rev. 108, 1394 (1957)

480. H. C. Praddaude and S. Foner: Solid State Commun. 20, 1117 (1976)

481. I. Maartense and G. Williams: J. Phys. F 6, 2363 (1976)

482. P. J. Wojtowicz and M. Rayl: Phys. Rev. Lett. 20, 1489 (1968)

483. S. Foner, E. J. McNiff and R. P. Guertin: Phys. Lett. 31A, 466 (1970)

484. S. Foner and E. J. McNiff: Phys. Lett. 29A, 28 (1969)

485. R. M. Bozorth, D. D. Davis and J. H. Wernick: J. Phys. Soc. Jap. 17, Suppl. B-1 112 (1962)

486. R. M. Bozorth, P. A. Wolff, D. D. Davis, V. B. Compton

and J. H. Wernick: Phys. Rev. 122, 1157 (1961)

487. A. Benoit, M. Chapellier, J. Flouquet, M. Ribault, O. Taurian, J. Sanchez and J. L. Tholence: Physica 86-88B, 487 (1977)

488. L. D. Graham and O. S.Schreiber: Phys. Rev. Lett.17 650 (1966)

489. L. O. Graham, and O. S. Schreiber: Appl. Phys. 39 963 (1968)

490. J. C. Gallop and I. A. Campbell: Solid State Comm. 6, 831 (1968)

491. L. Shen, O. S. Schreiber and A. J. Arko: J. Appl. Phys. 40, 1478 (1969)

492. ibid : Phys. Rev. 179, 512 (1969)

493. J. W. Loram, A. D. C. Grassie, G. Williams, P. J. Ford, G. A. Swallow, T. E. Whall and R. J. White: Report for the U.S.Air Force (1972) unpublished.

494. G. Williams, G. A. Swallow and J. W. Loram: AIP Conf. Proc. 24, 447 (1974)

495. O. Laborde, B. Loegel and P. Radhakrishna: J. Phys. 35, C4-247 (1974)

496. G. Williams, G. A. Swallow and J. W. Loram: Phys. Rev. B11, 344 (1975)

497. B. Tissier and R. Tournier: Solid State Comm.11, 895 (1972)

498. G. A. Swallow, G. Williams and A. D. C. Grassie: Phys. Rev. B 11, 337 (1975)

499. R. Segnan: Phys. Rev. 160, 404 (1967)

500. M. P. Maley, R. D. Taylor and J. L. Thompson: J. Appl. Phys. 38, 1249 (1976)

501. J. W. Loram, R. J. White and A. D. C. Grassie: Phys. Rev. B 5, 3659 (1972)

502. G. A. Swallow, G. Williams, A. D. C. Grassie and J. W. Loram: J. Phys. F 1, 511 (1971)

503. D. K. C. MacDonald, W. B. Pearson and I. M. Templeton: Proc. Roy. Soc. A 266, 166 (1972)

504. K. V. Rao, O. Rapp, C. Johannesson, J. A. Budnick, T. J. Burch and V. Cannella: AIP Conf. Proc. 29 237 (1975)

505. F. W. Constant: Phys. Rev. 36, 1654 (1930)

506. A. W. Simpson and R. H. Tredgold: Proc. Phys. Soc. B 67, 38 (1954)

507. D. M. S. Bagguley, W. A. Crossley and J. Liesgang: Proc. Phys. Soc. 90, 1047 (1967)

508. D. M. S. Bagguley and J. A. Robertson: Phys. Lett. 27A, 516 (1968)

509. M. P. Kawatra, J. A. Mydosh, J. A. Budnick and B. Madden: Proc. LT 12 (Kyoto), 773 (1970)

510. J. Crangle: J. Phys. 20, 435 (1959)

511. G. A. Swallow and R. J. White: Phys. Lett. 44A 521 (1973)

512. N. C. Koon and D. U. Gubser: Abstract 18-3, 20th Annual Conf. on Magnetism and Magnetic Materials, AIP, 1974

513. G. E. Bacon and J. Crangle: Proc. Roy. Soc. A272, 387 (1963)

514. E. Kren, P. Szabo and T. Tarnoczi: Solid State Comm. 4, 31 (1966)

515. F. E. Hoare and J. C. G. Wheeler: Ann. Acad. Sci. Fennicae A VI 210, 158 (1966)

516. J. C. G. Wheeler: J. Phys. C.2, 135 (1969)

517. B. M. Boerstoel: Ph.D.Thesis, Leiden University (1970)

518. J. E. Van Dam and C. J. Van den Berg: Phys. Stat. Sol. 3, 11 (1970)

519. G. J. Nieuwenhuys, M. F. Pikart, J. J. Zwart, B. M. B. M. Boerstoel and C. J. Van den Berg: Physica 69, 119 (1973)

520. P. C. Ribeiro: Ph.D Thesis, University of Grenoble (1973)

521. M. Ali, W. D. Brewer, E. Klein, A. Benoit, J. Flouquet, O. Taurian and J. C. Gallop: Phys. Rev. B10, 4659 (1974)

522. O. A. Sacli, D. J. Emerson and D. F. Brewer: J. Low Temp. Phys. 17, 425 (1974)

523. C. C. Tsuei and R. Hasegawa: Solid State Comm. 7, 1581 (1969)

524. T. E. Sharon and C. C. Tsuei: Phys. Rev. B 5, 1047 (1972) and references therein.

525. E. Fawcett, D. B. McWhan, R. C. Sherwood and M. P. Sarachik: Solid State Comm. 6, 509 (1968)

526. R. D. Shull, H. Okamoto and P. A. Beck: Solid State Comm. 20, 863 (1976)

527. J. A. Budnick, V. Cannella and T. J. Burch: AIP Conf. Proc. 18, 307 (1974)

528. R. D. Shull and P. A. Beck: AIP Conf. Proc. 24,95 (1974)

529. E. F. Wasserman and J. L. Tholence: AIP Conf. Proc. 29, 237 (1975)

530. N. Rivier: J. Phys. F. Metal Phys. 4, L 249 (1974)

531. J. W. Cable, E. O. Wollan, W. C. Koehler and M. K. Wilkinson: J. Appl. Phys. 33, 1340 S (1962)

532. E. O. Wollan, J. W. Cable, W. C. Koehler and M. K. Wilkinson: J. Phys. Soc. Jap. 17, Suppl. B III, 38 (1962)

534. F. Mensinger and A. Paoletti: Phys. Rev. 143, 365 (1966)

535. B. Antonini, G. P. Felcher, G. Mazzone, F. Mensinger and A. Paoletti: Proc. Int. Conf. Mag. Nottingham (1964) p288

536. B. Van Laar: J. Phys. 25, 600 (1964)

537. B. Antonini, F. Menzinger and A. Paoletti:
Phys. Lett. 25A, 372 (1967)

538. P. C. Ling and T. J. Hicks: J. Phys. F. 3, 697 (1973)

539. J. W. Cable and H. R. Child: AIP Conf. Proc. 10, 1623 (1972)

540. J. W. Cable and H. R. Child: Proc. ICM Moscow 4, 425 (1973)

541. E. Kren and P. Szabo: Solid State Comm. 3, 371 (1965)

542. M. F. Collins, R. V. Jones and R. D. Lowde:
J. Phys. Soc. Jap. 17, Suppl. B-111, 19 (1962)

543. V. E. Arkhipov, A. Z. Men'shikov and S. K. Sidorov:
Soviet Phys. JETP Lett. 12, 243 (1970)

544. A. Z. Men'shikov, S. K. Sidorov and V. E. Arkhipov:
Soviet Phys. JETP 34, 163 (1972)

545. S. J. Pickart and R. Nathans: Phys. Rev. 123, 1163 (1961)

546. ibid : J. Appl. Phys. 33, S 1336 (1962)

547. J. W. Cable, E. O. Wollan, and W. C. Koehler:
J. Appl. Phys. 34, 1189 (1963)

548. ibid : Phys. Rev. 138, A 755 (1965)

549. W. C. Phillips: Phys. Rev. 138, A 1649 (1965)

550. J. W. Cable and E. O. Wollan: Int. J. Mag. 2, 1 (1972)

551. M. F. Collins and J. B. Forsyth:
Phil Mag. 8, 401 (1963)

552. E. F. Bertaut, A. Delapalme, F. Forrat, G. Roult,
F. de Bergevin and R. Pauthenet:
J. Appl. Phys. 33, S 1123 (1962)

553. G. Shirane, R. Nathans and C. W. Chen:
Phys. Rev. 134, A1547 (1964)

554. A. Z. Men'shikov, V. A. Shestakov, and S. K. Sidorov:
Soviet Phys. JETP 43, 85 (1976)

555. B. Dreyfus, J. C. Michel and D. Thoulouze:
J. Appl. Phys. 39, 1320 (1968)

556. B. H. Verbeek, T. Amundsen and C. Van D jik:
Physica 86-88B, 482 (1977).

557. J. van der Rest, F. Gautier and F. Brouers:
J. Phys. F. 5, 995 (1975)

558. A. Narath and H. T. Weaver: Phys. Rev. 83, 616 (1971)

559. G. Rao, E. Matthias and D. Shirley:
Phys. Rev. 184, 325 (1969)

560. R. Gersdorf and F. A. Muller: J. Phys. 32,
C1-995 (1971)

561. J. Crangle and D. Parsons: Proc. Roy. Soc.
A 255, 509 (1960)

562. H. Danan, A. Herr and A. J. P. Meyer:
J. Appl. Phys. 39, 669 (1968)

563. W. F. Brinkman, E. Bucher, H. J. Williams and
J. P. Maita: J. Appl. Phys. 39, 547 (1968)

564. H. Cottet, P. Donze, J. Ortelli, E. Walker and
M. Peter: Helv. Phys. Acta 41, 755 (1968)

565. W. C. Muellner and J. S. Kouvel:
AIP Conf. Proc. 5, 487 (1972)

566. ibid : Solid State Comm. 15, 441 (1974)

567. K. Levin, R. Bass and K. H. Bennemann:
Phys. Rev. B 6, 1865 (1972)

568. F. Brouers, F. Gautier and J. van der Rest:
J. Phys. F. 5, 975 (1975)

569. F. Brouers, F. Gautier and J. van der Rest:
J. Phys. F. 5, 975 (1975)

569. J. van der Rest: J. Phys. F. 7, 1051 (1977)

570. R. W. Houghton, M. P. Sarachik and J. S. Kouvel:
Solid State Comm. 10, 369 (1972)

571. A. Amamou and B. Loegel: J. Phys. F.3, L79 (1973)

572. A. Amamou, F. Gautier and B. Loegel:
Proc. ICM Moscow vol.6, 239 (1973)

573. F. Gautier and B. Loegel: Solid State Comm. 11,
1205 (1972)

574. G. R. Piercy and E. R. Morgan: Can. J. Phys. 31,
529 (1953) and references therein

575. J. S. Kasper and J. S. Kouvel:
J. Phys. Chem. Sol. 11, 231 (1959)

576. G. Shirane, R. Nathans and C. W. Chen:
Phys. Rev. 134, A 1547 (1964) and
references therein.

577. A Castets, D. Tochetti and B. Hennion:
Physica 86-88, 353 (1977)

578. H. Luo and P. Duwez: J. Less-Common Metals 6,
248 (1964)

579. B. R. Coles: J. Inst. Metals 84, 346 (1955)

580. P. Donze: Ph.D Thesis, University of Geneva (1969)

581. J. S. Touger and M. P. Sarachik:
Solid State Comm. 20, 1 (1976)

582. H. Fujiwara, H. Kadomatsu, K. Ohishi and Y. Yamamoto
J. Phys. Soc. Jap. 40, 1010 (1976)

583. J. W. Cable: Phys. Rev. B 15, 3477 (1977)

584. J. S. Kouvel and R. H. Wilson: J. Appl. Phys. 32,
435 (1961)

585. M. B. Stearns: AIP Conf. Proc. 24, 453 (1974)

586. For references see
F. A. Shunk: Constitution of Binary Alloys,
2nd supplement (McGraw Hill, 1969) p.551

587. S. Hirooka and M. Shimuzu: J. Phys. Soc. Jap 43,
477 (1977)

588. Y. Nakai and N.Kunitomi: J. Phys. Soc. Jap 39,
1257 (1975)

589. H. R. Child and J. W. Cable: Phys. Rev. B13, 227
(1976)

590. W. Kummerle and U. Gradmann:
Solid State Comm. 24, 33 (1977)

591. J. J. Murphy, T. J. Burch and J. I. Budnick:
AIP Conf. Proc. 10, 1627 (1972)

592. W. V. Lieres, H. Maletta, W. Potzel and
R. L. Mossbauer: Perspectives for Hyperfine
Interactions in Magnetically Ordered Systems
L'Aquila 1972. (quoted in Ref.591)

593. E. A. Owen, E. L. Yates and A. H. Sully:
Proc. Phys. Soc. 49, 315 (1937)

594. S. F. Dubinin, S. K. Sidorov and E. Z. Valiev:
Phys. Stat. Sol. (b) 46, 337 (1971)

595. C. E. Guillaume: Compt. Rend. 125, 235 (1897)

596. T. F. M. Kortekaas and J. J. M. Franse:
J. Phys. F.6, 1161 (1976)

597. S. Chikazumi, T. Mizoguchi, N. Yamaguchi and
P. Beckwith: J. Appl. Phys. 39, 939 (1968)

598. D. J. Kim: Physica 91B, 281 (1977)

599. K. Sumiyama: Ph.D Thesis, Kyoto University (1974)

600. Y. Nakamura: IEE Trans. Mag. 12, 278 (1976)

601. E. I. Kondorskii and L. N. Fedotov:
Izvest. Akad. Nauk SSR (Phys.) 16, 432 (1952)

602. J. Crangle and G. C. Hallam:
Proc. Roy. Soc. A272, 119 (1963)

603. M. Matsumoto, T. Kaneko and H. Fujimori:
J. Phys. Soc. Jap. 26, 1083 (1969)

604. R. W. Cochrane and G. M. Graham:
Can. J. Phys. 48, 264 (1970)

605. Y. Bando: J. Phys. Soc. Jap. 19, 237 (1964)

606. H. Asano: ibid 27, 542 (1969)

607. W. F. Schlosser: Int. J. Magnetism 2, 167 (1972)

608. Yamada O, Ono F and Nakai I:
Physica 86-88B, 311 (1977)

609. ibid : Physica 91B, 298 (1977)

610. M. Hennion, B. Hennion, A. Castets and D. Tocchetti:
Solid St. Commun. 17, 899 (1975)

611. M. Kohgi, V. Ishikawa and N. Wakabayashi:
Solid St. Commun 18, 509 (1976)

612. N. C. Koon and A. I. Schindler:
Phys. Rev. B8, 5257 (1973)

613. C. L. Chien and R. Hasegawa:
Phys. Rev. B 16, 3024 (1977)

614. S. K. Sidorov and A. V. Doroshenko:
Phys. Stat Sol. 16, 737 (1966)

615. Y. Tino and T. Maeda: J. Phys. Soc. Jap 24, 729 (1968)

616. E. E. Yurchikov, A. Z. Menshikov and V. A. Tzurin:
Proc. Conf. on the Application of Mossbauer Effect, Akademai Kiado, Budapest (1971)

617. L. Kaufman and M. Cohen: Pogr. Metal Phys.7, 165 (1958)

618. M. Hansen: in Constitution of Binary Alloys, 2nd ed. p682, (McGraw Hill, New York 1958).

619. J. S. Kouvel: General Electric Res. Lab. Rept. No. 67-C-393 (1967)

620. O. Yamada, R. Pauthenet and J. C. Picoche: J. Phys. 32, C1-1119 (1971)

621. H. Hiroyoshi, H. Fujimori and H. Sato: J. Phys. Soc. Jap. 31 1278 (1971

622. G. M. Graham: ibid 34, 831 (1973)

623. V. E. Rode and I. B. Krynestkaja: IEEE Trans. Mag. 10, 122 (1974)

624. S. Hatta, M. Matsui and S. Chikazumi: Physica 86-88B, 309 (1977)

625. S. Hatta, M. Hayakawa and S. Chikazumi: J. Phys. Soc. Jap. 43, 451 (1977)

626. G. K. White: Proc. Phys. Soc. 86, 159 (1965)

627. Y. Tanji: J. Phys. Soc. Jap. 31, 1366 (1971)

628. W. F. Schlosser, G. M. Graham and P. P. M. Meincke: J. Phys. Chem. Sol. 32, 927 (1971)

629. G. M. Graham and W. F. Schlosser: IEEE Trans. Mag. 8, 689 (1972)

630. M. Hayase, M. Shiga and Y. Nakamura: J. Phys. Soc. Jap. 34, 925 (1973)

631. G. Hausch: Phys. Stat. Sol.(a) 18, 735 (1973)

632. S. Kachi, H. Asano and N. Nakanishi: J. Phys. Soc. Jap. 25, 909 (1968)

633. H. Takaki, Y. Nakamura and T. Nakajima: J. Phys. Soc. Jap. 17, Suppl. B1, 349 (1962)

634. E. I. Kondorskii and V. L. Sedov: Soviet Phys. JETP 35, 586 (1959)

635. ibid : ibid 11, 561 (1960)

636. L. Patrick: Phys. Rev. 93, 384 (1954)

637. R. C. Wayne and L. C. Bartel: Phys. Lett. 28A, 196 (1968)

638. L. C. Bartel, L. R. Edwards, G. A. Samara: AIP Conf. Proc. 5, 482 (1971)

639. J. M. Leger, C. Susse and B. Vodar: Solid St. Commun 4, 503 (1966)

640. J. M. Leger and C. Susse-Loriers: Phys. Lett. 37A, 145 (1971)

641. J. M. Leger, C. Loriers-Susse and B. Vodar: Phys. Rev. B6, 4250 (1972)

642. S. Kachi, Y. Bando and S. Higuchi: Jap. J. Appl. Phys. 1, 307 (1962)

643. C E Johnson, M. S. Rideout and T. E. Cranshaw: Proc. Phys. Soc. 81, 1079 (1963)

644. Y. Nakamura, M. Shiga and N. Shikazono: J. Phys. Soc. Jap. 19, 1177 (1964)

645. Y. Nakamura, M. Shiga and Y. Endoh: Proc. Int. Conf. Mag. (IPPS, London 1964) p144

646. H. Asano: J. Phys. Soc. Jap. 25, 286 (1968)

647. Y. Nakamura, Y. Takeda and M. Shiga: ibid 25, 287 (1968)

648. U. Erich, E. Kankelelt, H. Prange and S. Hufner: J. Appl. Phys. 40, 1491 (1969)

649. Y. Nakamura, M. Shiga and Y. Takeda: J. Phys. Soc. Jap 27, 1470 (1969)

650. S. Tomiyoshi, H. Yamamoto and H. Watanabe: ibid 30, 1605 (1971)

651. Y. Tino and J. Arai: ibid 32, 941 (1972)

652. A. A. Hirsch and Z. Eliezer: IEEE Trans Mag,8 690, (1972)

653. H. N. Ok and M. S. Han: J.Appl. Phys. 44, 1932 (1973)

654. B. Window: ibid 44, 2853 (1973)

655. H. Rechenberg, L. Billard, A. Chamberod and M. Natta:
J. Phys. Chem. Sol. 34, 1251 (1973)

656. A. Chamberod, H. Rechenberg and R. Tournemine:
Proc. ICM Moscow Vol.3, 170 (1973)

657. A. Z. Menshikov and E. E. Yurchikov:
Soviet Phys. JETP 36, 100 (1973)

658. Y. Tino and J. Arai: J. Phys. Soc. Jap 36, 669 (1974)

659. B. Window: J. Phys. F.4, 329 (1974)

660. A. Ferro-Milone and I. Ortalli: IEE Trans. Mag.10,
186 (1974)

661. H. E. H. Stremme: ibid 10, 189 (1974)

662. M. Shiga, Y. Maeda and Y. Nakamura:
J. Phys. Soc. Jap. 37, 363 (1974)

663. U. Gonser, S. Nasu, W. Keune and O. Weis:
Solid St. Commun. 17, 233 (1975)

664. J. Arai: J. Phys. Soc. Jap. 39, 692 (1975)

665. J. Arai: ibid 39, 1409 (1975)

666. C. Bansal, J. Ray and G. Chandra:
J. Phys. F.5, 1663 (1975)

667. J. Hesse and J. B. Muller: Solid St. Commun. 22,
637 (1977)

668. T. Sohmura and F. E. Fujita: ibid 25, 43 (1978)

669. V. I. Gonman'kov, I M Puzei and M. N. Rukosuev:
Soviet Phys. Crystallography 13,449 (1968)

670 M. F. Collins: Proc. Phys. Soc. 86, 973 (1965)

671. V. I. Goman'kov, I. M. Puzei, V. N. Sigaer,
E. V. Kozis and E. I. Mal'tsev: JETP Lett 13, 428 (1971)

672. Y. L. Rodionov, E. S. Machurin and P. L. Gruzin:
Soviet Phys. Dokl. 20, 355 (1975)

673. P. L. Gruzin, Y. L. Rodionov, E. S. Machurin and
O. S. Sarsenbin: Soviet Phys. Dokl. 21, 278 (1976)

674. G. Hausch and H. Warlimont: Phys. Lett. 36A, 415 (1971)

675. V. G. Veeraraghavan, C. F. Eagen, H. R. Harrison and P. G. Winchell; J. Appl. Phys. 47, 4768 (1976)

676. E. I. Kondorskii and V. L. Sedov: J. Appl. Phys. 31, S331 (1960)

677. B. E. Armstrong and R. Fletcher: Can. J. Phys. 50, 244 (1972)

678. E. I. Kondorskii: Soviet Phys. JETP 10, 1284 (1960)

679. M. C. Cadeville and B. Loegel: J.Phys. F 3, L115 (1973)

680. M. C. Cadeville, R. Caudron, P. Costa and C. Lerner: J. Phys. F: 4, L 87 (1974)

681. H. Hasegawa and J. Kanamori: J. Phys. Soc. Jap. 31, 382 (1971)

682. I. A. Campbell: J. Phys. F 4, L 181 (1974)

683. Y. Shirakawa: Sci. Rep. Tohoku Univ. 27, 485 (1939)

684. V. E. Rode, A. V. Deryabin and G. Damashke: IEEE Trans. Mag. 12, 404 (1976)

685. V. E. Rode and A. V. Deryabin: Physica 86-88B, 313 (1977)

686. T. Soumura: J. Phys. Soc. Jap. 42, 826 (1977)

687. T. Soumura: ibid 40, 435 (1976)

688. V. L. Sedov: Soviet Phys. JETP Lett. 14, 341 (1971)

689. K. P. Gupta, C. H. Cheng and P. A. Beck: J. Phys. Chem. Solids 25, 73 (1964)

690. D. I. Bower, E. Claridge and I. S. T. Tsong: Phys. Stat. Sol. 29, 617 (1968)

691. S. Kawarazaki, M. Shiga and Y. Nakamura: Phys. Stat. Sol.(b) 50, 359 (1972)

692. R. Caudron, J. J. Meunier and P. Costa: Solid St. Commun. 14, 975 (1974)

693. M. Dixon, F. E. Hoare, T. M. Holden and D. E. Moody:
Proc. Roy. Soc. A 285, 561 (1965)

694. P. Zoller, P. R. Decker and J. R. Dillinger:
J. Appl. Phys. 40, 1964 (1969)

695. C. E. Guillaume: Proc. Phys. Soc. (London) 32, 374 (1920)

696. Y. Tino and T. Maeda: J. Phys. Soc. Jap. 18, 955 (1963)

697. G. Hausch and H. Warlimont: Phys. Lett. 41A, 437 (1972)

698. ibid : Z. Metallkunde 63, 547 (1972)

699. ibid : Acta Met. 21, 401 (1973)

700. G. Hausch: Phys. Stat. Sol. (a) 15, 501 (1973)

701. G. A. Alers, J. R. Neighbour and H. Sato:
J. Appl. Phys. 30, S 231 (1959)

702. G. Pupke and H. J. Bunge: Z. Metallkunde 49, 626 (1958)

703. J. Echigoya, S. Hayashi, T. Nakamichi and M. Yamamoto:
J. Phys. Soc. Jap. 30, 289 (1971)

704. J. Echigoya, S. Hayashi and M. Yamamoto:
Phys. Stat. Sol. (a) 14, 463 (1972)

705. P. P. M. Meincke and J. Litva: Phys. Lett. 29A, 390 (1969)

706. R. Fletcher: J. Phys. C. 2, 2107 (1969)

707. G. J. Johanson, H. B. McGirr and D. A. Wheeler:
Phys. Rev. B1, 3208 (1970)

708. D. L. Williamson, W. Keune and U. Gonser:
Proc. ICM Moscow Vol.1, 246 (1973)

709. S. Komura, G. Lippmann and W. Schmatz:
J. Appl. Cryst. 7, 233 (1974)

710. S. Kachi and H. Asano: J. Phys. Soc. Jap. 27, 536 (1969)

711. S. Komura, T. Takeda and M. Roth:
Phys. Lett. 62A, 365 (1977)

712. S. F. Dubinin, S. K. Sidorov, S. G. Teploukhov and V. E. Arkhipov: Soviet Phys. JETP Lett. 18, 324 (1973)

713. S. G. Teploukhov: S. F. Dubinin and S. K. Sidorov: Fiz. Metal. Metalloved. 38, 1090 (1974)

714. V. E. Arckhipov, A. Z. Men'shikov and S. K. Sidorov: Soviet Phys. JETP 34, 799 (1972)

715. S. Komura, T. Takeda and S. Ohara: J. Phys. Soc. Jap. 35, 706 (1973)

716. S. Komura, G. Lippmann and W. Schmatz: J. Mag. and Magnetic Materials 5, (1977)

717. M. A. Krivoglaz: Sov. Phys. Dokl. 3, 61 (1958)

718. M. Hatherly, K. Hirakawa, R. D. Lowde, J. F. Mallet, M. W. Stringfellow and B. H. Torrie: Proc. Phys. Soc.84, 55 (1964)

719. D. R. Rhiger and R. Ingalls: Phys. Rev. Lett. 28, 749 (1972)

720. G. Hilscher, N. Buis and J. J. M. Franse: Physica 91B, 170 (1977)

721. D. A. Colling and W. J. Carr: J. Appl. Phys. 41, 5125 (1970)

722. L. Kaufmann, E. Clougherty and R. J. Weiss: Acta Met. 11, 323 (1963)

723. R. J. Weiss: Proc. Phys. Soc. 82, 281 (1963)

724. M. Shimuzu and S. Hirooka: Phys. Lett. 27A, 530 (1968)

725. M. Shimuzu and S. Hirooka: ibid 30A, 133 (1969)

726. M. Shimuzu: J. Phys. 32, C1, 1115 (1971)

727. A. Katsuki: Brit. J. Appl. Phys. 18, 199 (1967)

728. T. Mizoguchi: J. Phys. Soc. Jap. 25, 904 (1968)

729. E. P. Wohlfarth: Phys. Lett. 31A 525 (1970)

730. E. J. Hayes and E. P. Wohlfarth: Phys. Lett. 37A, 385 (1971)

731. S. Kachi, H. Asano and N. Nakanishi:
J. Phys. Soc. Jap. 25, 285 (1968)

732. W. F. Schlosser: J. Phys. Chem. Sol. 32, 939 (1971)

733. M. Shiga: Solid St. Commun. 10, 1233 (1972)

734. M. Shiga: IEEE Trans. Mag. 8, 666 (1972)

735. M. Shiga: AIP Conf. Proc. 18, 463 (1974)

736. L. Billard and M. Natta: J. Phys. 35, C4-157 (1974)

737. M. Natta: IEEE Trans. Mag. 10, 180 (1974)

738. J. W. Cable and L. David: Phys. Rev. B 16, 297 (1977)

739. J. W. Cable, E. O. Wollan, W. C. Koehler and H. R. Child:
J. Phys. Chem. Sol. 25, 1453 (1964)

740. H. A. Mook: Phys. Rev. 148, 495 (1966)

741. G. M. Graham and R. W. Cochrane: Phys. Rev. 184, 543 (1969)

742. G. M. Graham: Phys. Lett. 39A, 325 (1972)

743. W. F. Schlosser: Int. J. Magnetism 4, 49 (1973)

744. E. P. Wohlfarth: Int. J. Magnetism 6, 89 (1974)

745. W. F. Schlosser: ibid 6, 177 (1974)

746. W. F. Schlosser: Phys. Lett. 42A, 437 (1973)

747. W. F. Schlosser: Phys. Stat. Sol. (a) 17, 199 (1973)

748. W. F. Schlosser: Phys. Stat. Sol. (a) 22, K 219 (1974)

749. W. F. Schlosser: AIP Conf. Proc. 24, 441 (1974)

750. C. M. Sayers: J. Phys. F. 7, 1157 (1977)

751. J. Friedel and C. M. Sayers: J. Phys. 38, 697 (1977)

752. J. Friedel and C. M. Sayers: J. Phys. 39, L 59 (1978)

753. S. Misawa and K. Kanematsu: J. Phys. F 6, 2119 (1976)

754. S. Misawa: Physica 86-88B, 383 (1977)

755. Y. Teraoka and J. Kanamori: Physica 86-88B, 321 (1977)

756. S. Arajs, K. V. Rao, Y. D. Yao and W. Teoh:
Phys. Rev. B 15, 2429 (1977)

757. P. Pataud: Ph.D Thesis, University of Grenoble (1976)

758. J. C. Ododo and W. Howarth: Solid St. Commun. 25, (1978)

759. J. Crangle and G. M. Goodman: Proc. Roy. Soc. London
A 321, 477 (1971)

760. M. F. Collins, V. J. Minkiewicz, R. Nathans, L. Passell and
G. Shirane: Phys. Rev. 179, 417 (1969)

761. A. Benoit, M. Chapellier, J. Flouquet, M. Ribault, O. Taurian,
J. Sanchez and J. L. Tholence: Physica 86-88B, 487 (1977)

762. ibid : Phys. Rev. Lett. 38, 81 (1977)

ACKNOWLEDGEMENTS

I am deeply grateful to my supervisor, Brian D Rainford, not only for giving me the opportunity to do some neutron work but also, and more importantly, in my view, for not attempting to put me in a strait – jacket (by not always insisting that my ideas should conform with current thinking). I am equally grateful to Prof. B R Coles for reserving a place for me in his research group in spite of a year's delay and for helping me to find my feet in the first two years of this work by patiently attempting to answer many of my questions. I have also benefited greatly from discussions with past and present members of both the Metal Physics and Solid State Theory groups here, especially Prof. N H March, Prof. M Blackman, Nick Rivier, Amir Murani, and last, but by no means the least, Howard Stone who also prepared nearly all the alloys investigated.

The neutron diffraction work could probably not have been successfully completed without the excellent back-up support provided by the Material Physics Division, UKAERE, Harwell and I will like to express my gratitude to Vic Rainey, Rusty Harris and Doug Cummings among others. A special "Thank you" also goes to Chris Sampson of the same address for help with the X-ray diffraction work.

Financial support for the first three years of this study was provided by the British Council within their Technical Assistance Aid programme to the Federal Republic of Nigeria. I am also grateful to the U.K. Science Research Council for a year's Research Assistantship and

to University of Nigeria, Nsukka, Nigeria for a leave of absence which was generously extended on request.

I am greatly indebted to Miss J C Ukaegbu for patiently typing such a long thesis without any previous experience! and yet making an excellent job of it. Finally to all my friends especially Chinyere, Chiaka and, of course, Mama, whose support in various ways in some very difficult circumstances has been unquestioningly total and invaluable, I can only say "Unu emela" - for now. Chineke gozie unu.

-----oOo-----